OSMOTIC FLOW AND VOLUME CHANGE IN CLAY SOILS

SIDNEY LEE BARBOUR

1987

OSMOTIC FLOW AND VOLUME CHANGE

IN CLAY SOILS

BY

SIDNEY LEE BARBOUR

A Thesis
submitted to the Faculty of Graduate Studies
in Partial Fulfillment of the Requirements for
the Degree of Doctor of Philosophy
in the Department of Civil Engineering
University of Saskatchewan
Saskatoon, Saskatchewan

December, 1986

ABSTRACT

The engineering profession has been called upon by the public in recent years to provide ever increasing degrees of containment for low level waste contained in shallow sub-surface waste containment facilities. To provide this protection, the use of engineered liners or barriers has become a common design feature. In many cases, these barriers are constructed out of natural clays or artificial mixtures of clay minerals.

The use of soil barriers to contain waste products consisting of strong electrolyte solutions, has met with mixed success. Clays of lowest permeability are also those whose behavior is the most influenced by the presence of salt solutions. Failures of clay liners exposed to electrolyte solutions have not been well documented. The mechanism for failure seems to be the result of shrinkage of the clay, which then leads to the development of a secondary structure of cracks and fissures. Field cases of liner failure have often been described as occurring as a result of "osmotic desiccation".

The general objective of this study was to define, and quantify, the mechanisms controlling the rate and magnitude of volume change in clay soils exposed to strong electrolyte solutions. A review of the literature presented two possible mechanisms for osmotic volume change. These were termed osmotically induced consolidation and osmotic consolidation.

Osmotically induced consolidation occurs as a result of rapid flow of water out of the sample in response to osmotic gradients. Osmotic consolidation occurs as as result of a reduction in the net electrostatic repulsive stresses between clay particles. A general theoretical description of osmotically induced consolidation and osmotic consolidation was developed. A phenomenological approach was adopted to describe fluid flow in response to osmotic

gradients. A Darcy type flow law was used to related osmotic flows to osmotic gradients through a conductivity term called the osmotic permeability. To describe osmotic consolidation, the osmotic pressure of the pore fluid was selected as a stress state variable. Volume changes were linked to the osmotic pressure of the pore fluid through a constitutive relationship. The soil property used to define changes in soil volume due to osmotic pressure changes was called the osmotic compressibility.

A numerical solution to the theoretical description of osmotic flow and volume change was developed using finite element techniques. This model was used to characterize the processes of osmotic and osmotically induced consolidation. A laboratory program was undertaken to monitor the osmotic flow and volume change in two clays; Regina Clay and an Ottawa Sand/ Na montmorillonite mixture. From the results of these tests the dominant mechanism of volume change for these clays was found to be osmotic consolidation. The test procedures developed allowed the soil properties describing osmotic flow and volume change to be evaluated.

A technique was developed by which the electrostatic repulsive stresses within a clay could be measured indirectly through laboratory testing. The results indicated that the onset of fracturing may be predicted by comparing the change in the net repulsive stress that occurs as result of changing pore fluid concentrations, to the confining stress within the soil.

ACKNOWLEDGEMENTS

It is true that no man is an island. I acknowledge the contribution of numerous individuals and institutions to the completion of this dissertation as well as to my own personal development.

The Potash Corporation of Saskatchewan provided financial support during my course work at the University of Waterloo. This support is gratefully acknowledged.

I acknowledge the support and patience provided by the faculty, students and support staff within the Department of Civil Engineering as I undertook to complete a program of doctoral studies in addition to filling a faculty position. In particular I would like to thank Mr. Alex Ho, who provided invaluable assistance in the laboratory as well as a foundation of research on which I could build, and Dr. D.G. Fredlund who acted as supervisor, advisor and mentor.

The most difficult acknowledgements to make are those which words are not able to fully express. I acknowledge my indebtedness to my parents. Any success I have experienced as an individual is founded upon values that they have built into my life. By example, they have passed to me an appreciation of the eternal as well as the temporal priorities of life.

I don't believe sacrifice is an inappropriate word to describe the contribution my family has made to the completion of this work. My daughters, Erin and Megan, have been patient and have encouraged me with the joy and love they bring into my life. I will likely not ever comprehend the full contribution that my wife Twila has made. Her support through undergraduate, masters and doctoral studies has been undiminished. She has not only sacrificed emotionally, physically and financially throughout these past eight years but has risen repeatedly to fill the gaps within our family that I have left.

Most importantly, I acknowledge the very real help I have found in my relationship with Jesus Christ. He is the cornerstone on which my life is built.

> "Surely you desire truth in the inner parts; you teach me wisdom in the inmost place." Psalm 51:6

TABLE OF CONTENTS

List of Appendices

List of Figures

List of Tables

CHAPTER 1

INTRODUCTION

1.1 General Background

Public concern regarding the protection of the environment has grown dramatically over the last two decades. Accompanying these concerns have been increasingly stringent regulatory requirements on engineering works that may have deleterious impacts on the environment. Consequently, the engineering community has been faced with ever increasing demands to provide designs that will not affect the environment in any adverse way. Geotechnical engineers responsible for the design of waste containment facilities face an extremely difficult problem in this regard.

Engineered containment facilities are required for the storage of small quantities of extremely toxic, or high level, waste as well as large volumes of low level waste, such as mine tailings. A primary focus of design has been to minimize the amount of leakage from the containment facility into the environment.

The demand for low or "zero" leakage impoundments for waste requires that barriers, or liners, of low permeability be utilized. In many cases, natural clay barriers or compacted earth liners have been relied on to provide this containment. Unfortunately, the clays that are characteristically of low permeability are also those which are the most physio-chemically active. The mechanical and hydraulic properties of these materials are strongly influenced by the chemical composition of the pore fluid.

Physio-chemical alteration of the physical and mechanical properties of clays has been of particular concern in the design of impoundments to contain strong

electrolyte solutions such as salt brines. Containment of brines in shallow surface impoundments is commonly required in many industries. Examples include the potash mining industry, the displacement storage of petroleum products in evaporite formations, oil exploration, and storage impoundments for road salt.

1.2 The Use of Clays for Brine Storage - Field Evidence

The use of clay barriers to contain salt wastes has met with varying degrees of success. Few references exist in the literature regarding the use of clays for the storage of electrolyte solutions (Ridley 1985). It is more common to find unpublished reports, or verbal communications regarding the failures as well as the successes of these designs. Several case histories will be described briefly in order to illustrate the nature of the problems that may occur in these types of installations.

Imperial Oil Brine Ponds - Redwater Alberta - FAILURE

Devenny (1978) investigated the failure of a NaCl brine pond several years after construction. The pond was lined with a compacted clay-till liner. The failure of this liner was also described by Wallace and Eigenbrod (1984) as follows:

> "The investigation concluded that the primary causes of leakage related to the operating conditions of the pond. A fractured block structure was noted to have become dominant within the liner materials, with definite vertical and horizontal fissures and fine fractures."

Hudec (1979) reported that samples of this material underwent approximately 1.5% shrinkage, accompanied by the development of "large through going cracks", when submerged in brine. Cracking of the samples was also evident in permeability tests conducted by Hudec. A 5-fold increase in the permeability of the samples occurred when the permeant was changed from freshwater to brine. This increase was

linked to the development of a secondary structure of cracks and fissures due to "osmotic desiccation cracking".

Procor Brine Ponds - Regina, Saskatchewan - SUCCESS (?)

Several unlined brine ponds have been operated by Procor in Regina over the last 14 years. The ponds are situated within a surficial deposit of highly plastic clay, approximately 7 to 8 metres thick. A investigation of leakage from these ponds was carried out by Kent and Clifton (1980) and Kent and Chursinoff (1981). They found that shallow lateral leakage from the ponds was taking place. This leakage was confined to the upper surface of the clay. The clay is fractured and fissured to a depth of approximately 3 metres due to desiccation. There was no evidence of vertical leakage deeper into the natural clay and clay till.

The author visited the site in July 1985 during rehabilitation of one of the ponds which had been operating without a liner for 6 years. Soft, saturated soil which had been eroded from the slopes of the impoundment and had settled on the base of the lagoon had been removed. The natural soil below this level was found to be very stiff and dense, with no evidence of the softening that would be expected below a surface water impoundment.

Soil extracts (2:1 water:soil) of samples taken below the base of the pond illustrate that even over 6 years of operation, brine penetration has only occurred through the upper 3 metres (Figure 1.1). It would appear that downward migration of the brine only occurred through the upper fractured material. There is no evidence that fracturing of the deeper intact clay has occurred.

Potash Tailings Ponds, Saskatchewan - SUCCESS (?)

A recent study of the waste management facilities at the ten potash mines in Saskatchewan was completed by Tallin (1984). Nine of the ten mines in Saskatchewan are located over clayey deposits. At eight of these mines there have been significant problems with shallow seepage of brine from the tailings ponds. The failure of compacted clay barriers to contain the tailings brine has generally been contributed to "construction problems".

The shallow leakage within the natural material occurs because of lenses of coarser sediments within the clayey surficial deposits, or as a result of the desiccated, fractured nature of the upper surface of the clay. There is little evidence to date that deep penetration of the brine into the natural clay deposits is occurring.

It is difficult to draw any specific conclusions from the few case histories available. As a result of failures of clay liners, there is a growing concern within the industry that compacted fresh water clay liners are ineffective as barriers. Yet, in many cases natural clay barriers at depth seem to be fairly effective.

There is little understanding of the specific mechanisms at work in either the failures or successes. Failures are often attributed to "osmotic effects", however; there is no definition of what these effects actually are.

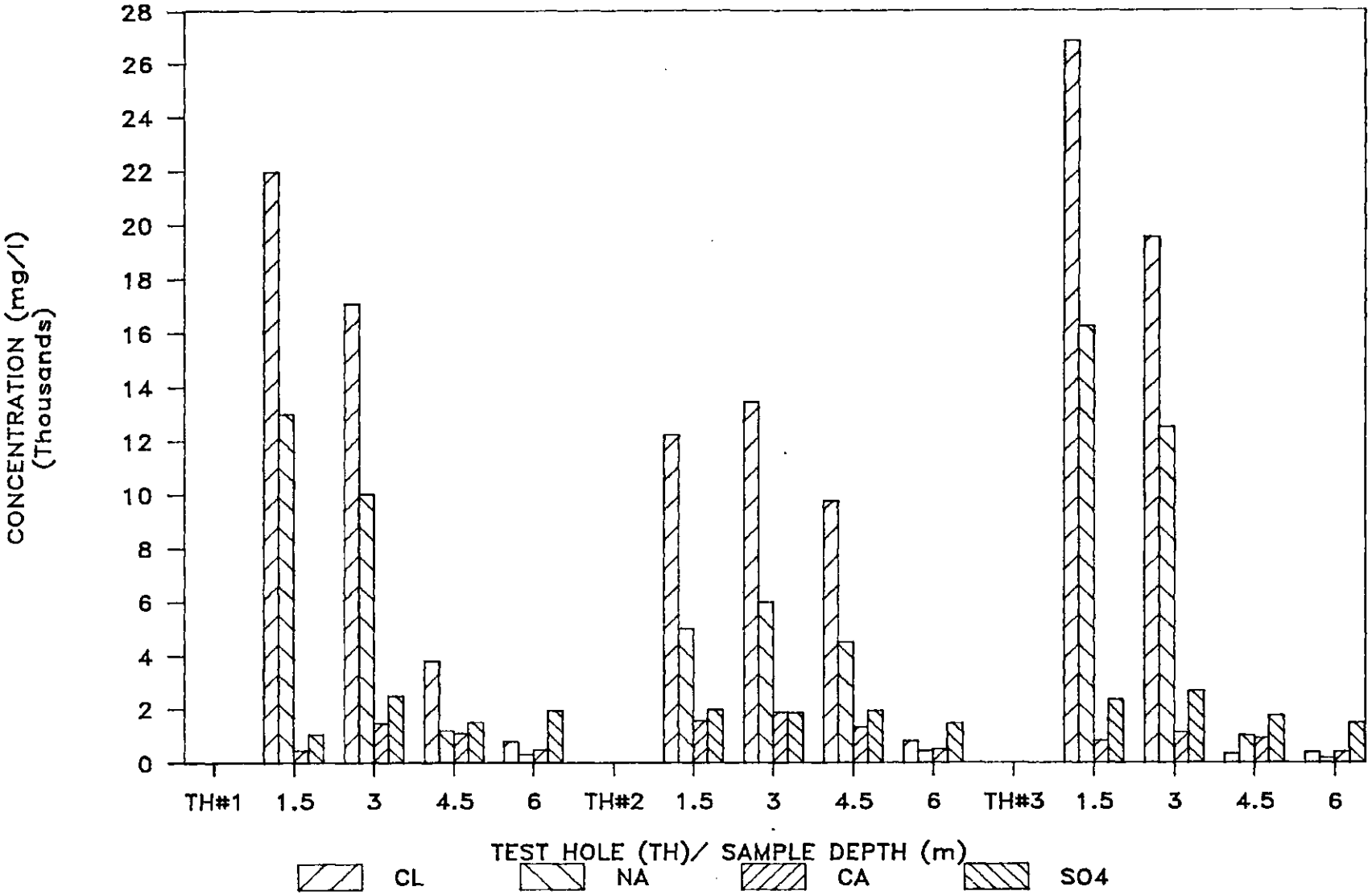

Figure 1.1 Concentration of Soil Extracts with Depth - Procor Brine Pond

1.3 Guidelines and Design

Environmental guidelines in Canada provide few special design requirements for clay barriers used to contain strong electrolyte solutions. A minimum thickness and permeability for the liner are commonly specified. If the liner is to be exposed to brine, a somewhat thicker liner is specified (Ridley 1985).

In design, there has been no attempt to predict the behavior of the liner when it is exposed to brine. Rather, a fairly empirical approach to design has been pursued. Laboratory model testing has been used to observe the changes that occur in the permeability of a particular liner material when it is exposed to the waste fluid.

It has been recognized that the permeability of a liner may change as it is permeated with a waste fluid. The specification of liner permeability in guidelines has led to a significant amount of research on the change in permeability of liners on permeation with leachate, organic fluids, or brine (Anderson 1982, Anderson and Jones 1983, Ridley 1983, Jones 1984, Buettner 1985, Zrymiak 1985). Ridley (1985) provides a detailed review of this area of study.

1.4 Possible Mechanisms for Permeability Increases

Changes in the permeability of a soil after permeation with a waste fluid are primarily a result of changes in either the macro or micro structure of the clays. Anderson and Jones (1983) suggest that changes in the micro or macro structure occur when the clay experiences either of the following:

1. Volume changes on exposure to the permeant, and
2. Piping or dissolution due to chemical reactions between the permeant and the soil solids.

Rapid, substantial, increases in the permeability of clay soils due to brine exposure can often be linked to volume changes. Shrinkage of the clay in the presence of the electrolyte solution causes the development of a secondary structure of cracks and fissures. The permeability of the fractured soil mass is significantly larger than that of the unfractured clay matrix.

Turk (1974) studied interactions between brine and unconsolidated sediments below brine ponds. He found that shrinkage and cracking occurred in these sediments that led to increased leakage from the ponds. Turk suggested that volume change may have occurred as a result of osmosis between the brine and underlying freshwater.

1.5 Study Objectives

Clay liner - leachate compatibility is an active area of study at the present time. Designs and regulatory requirements continue to be based on compatibility testing of leachate/liner combinations. There remains, however, no theoretical framework for the prediction of the volume change of clays due to exposure to electrolyte solutions.

This study is an attempt to obtain an understanding of the nature of the volume change behavior of clay soils caused by the presence of electrolyte solutions. The objectives of this study are as follows:

1. To observe the volume change behavior of clay soils on exposure to a strong electrolyte solution.

2. To identify the dominant mechanisms of osmotic volume change.

2. To develop a theoretical model to describe transient osmotic volume change, based on a phenomenological approach.

3. To evaluate the potential use of the theoretical model to predict the rate and magnitude of volume change in clay soils on exposure to NaCl brines.

Chapter 2 provides a summary of the potential mechanisms for volume change in clay soils as represented in the literature. A theoretical formulation to describe osmotic volume change and flow is developed in Chapter 3. A numerical solution for the governing equations describing osmotic volume change is presented in Chapter 4. The laboratory program used to observe the behavior of two clay soils exposed to NaCl solutions is outlined in Chapter 5, and the results from these tests are presented in Chapter 6. Analyses of the laboratory results and an evaluation of the prediction of osmotic flow and volume change is provided in Chapter 7. Final conclusions regarding this study are outlined in Chapter 8.

CHAPTER 2

LITERATURE REVIEW

2.1 Introduction

Consolidation of saturated clay soils may be described as time dependant volume change which results from a net fluid flux out of the soil mass. The soil behavior during this transient process is influenced by two separate soil properties: the resistance the soil provides to fluid flow through the pores, and the resistance of the soil structure to deformation.

Terzaghi (1925) derived a theoretical description of the consolidation of clay soils utilizing a fluid flow law and a constitutive equation for the deformation of the soil structure. Darcy's law was used to describe the movement of fluid within the soil mass. Darcy's law relates the gradient of hydraulic head to the fluid flux, through the soil property called permeability.

The constitutive equation links the deformation of the soil structure to the effective stress on the soil through the soil property called compressibility. Terzaghi defined effective stress as the difference between the total stress and the pore fluid pressure.

In evaluating the influence of pore fluid salt concentrations on the time dependant volume change of clay soils, the question arises as to the influence that the dissolved salt has on fluid flow and deformation of the soil structure. The question could be asked as to whether the energy which produces fluid flow and deformation within the soil is altered by the presence of dissolved salt.

Terzaghi (1931) described the energy within a soil fluid system as follows:

> "The energy of a two-phase system of given concentration is composed of two parts, mechanical energy and physio-chemical energy. The former represents the equivalent of previous mechanical compression of the solid phase and can be compared with the energy stored in a compressed spiral spring. The latter is the energy equivalent of the physio-chemical interaction of the solid and the liquid phase."

If the physio-chemical interaction between the solid and solution phases is unaltered, then the use of effective stress provides an adequate description of soil behavior. However, if solution concentrations vary, then changes in the physio-chemical interactions may be significant. The effects of these changes must either be incorporated into the theoretical description of the stress state within the soil mass, or they must be duplicated in laboratory testing used to define the soil properties.

In the absence of changes in the physio-chemical interactions between the solid and solution phases, the presence of salts may also alter the pore pressure distribution within the soil. These pore pressures may in turn cause changes in the mechanical energy of the system. Terzaghi (1931) stated that mechanical interactions play a dominant role in the swelling of clays. He states:

> "According to this point of view, physio-chemical interactions which take place within the systems, influence the swelling only inasmuch as they change the elastic properties in the system by altering adhesion at the points of contact, or stiffness of molecular links or by generating an additional tension in the liquid phase by an osmotic pressure effect."

In summary; to understand the consolidation behavior of clay soils in the presence of strong and varying solution concentrations, the influence of the salt on fluid flow and on the resistance of the soil structure to deformation must be understood. This chapter provides a review of osmotic

phenomena in clay soils with specific focus as to the influence that osmotic effects have on fluid flow and volume change.

2.2 Osmotic Phenomena in Soils - Overview

Soil pore fluid is made up primarily of water and various dissolved solids. These dissolved solids are commonly Na, Mg, or Ca salts. In this discussion the components of the pore fluid will be referred to as the solvent (ie.,water) and the solute (ie.,dissolved solids).

Osmosis is the term used to describe the phenomenon by which a solvent passes from a solution of lower concentration through a semi-permeable membrane into a solution of higher concentration. A membrane is described as semi-permeable if it allows the passage of solvent, but not the solute, across it. Figure 2.1 provides a simple illustration of the osmotic phenomenon. Two cells of solution are separated by a semi-permeable membrane. The solution on the left has a higher concentration of solute than that on the right; consequently the free energy, or chemical potential, of the solvent on the right is higher. The solvent diffuses through the membrane from right to left in response to this chemical potential. A similar driving force from right to left exists on the solute, however, its migration is prevented by the membrane.

Solvent flow through the membrane can be prevented if the energy of the solvent on the left is raised relative to that on the right. This may be accomplished by increasing the pressure on the solution in the left cell. When sufficient pressure is applied, the flow of solvent between the cells is prevented. The pressure at which equilibrium is attained is called the osmotic pressure. If the pressure on the left cell is higher than the osmotic pressure the solvent will be forced to flow from left to right, contrary to its concentration gradient. This phenomena is called

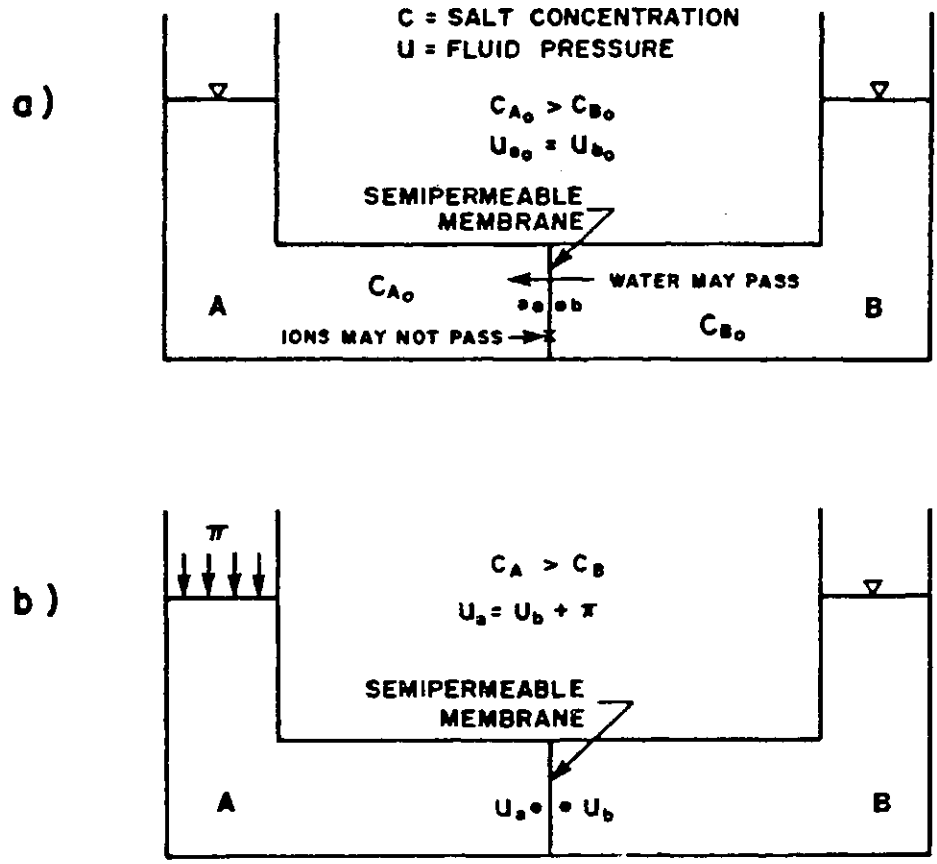

Figure 2.1 Schematic Illustration of Osmosis
a) Osmotic Flow
b) Osmotic Pressure (after Mitchell 1976)

reverse-osmosis or hyperfiltration (Spiegler and Laird 1980).

The osmotic pressure can be calculated from thermodynamic principles using the following relationship (Kemper and Rollins 1966):

$$\pi = (R\ T/V)\ \ln\ (a_w) \qquad [2.1]$$

where: π = osmotic pressure
a_w = activity of water
R = universal gas constant
T = absolute temperature
V = molar volume of solvent

The values of molar volume and activity may be obtained from chemistry handbooks such as Robinson and Stokes (1968).

The osmotic pressure can also be approximated using the van't Hoff approximation:

$$\pi = R\ T\ C \qquad [2.2]$$

where: C = sum of the molar concentrations of anions and cations in the solution.

Figure 2.2 provides a comparison of the theoretical and van't Hoff approximation of osmotic pressure for NaCl solutions.

The simple description of osmosis provided above illustrates a number of significant features of osmotic phenomena;

1. Solvent flow occurs in the presence of a osmotic gradient,
2. Solute migration is restricted by the presence of a semi-permeable membrane, and,
3. In the presence of osmotic gradients, a hydrostatic pressure imbalance is required to prevent solvent movement.

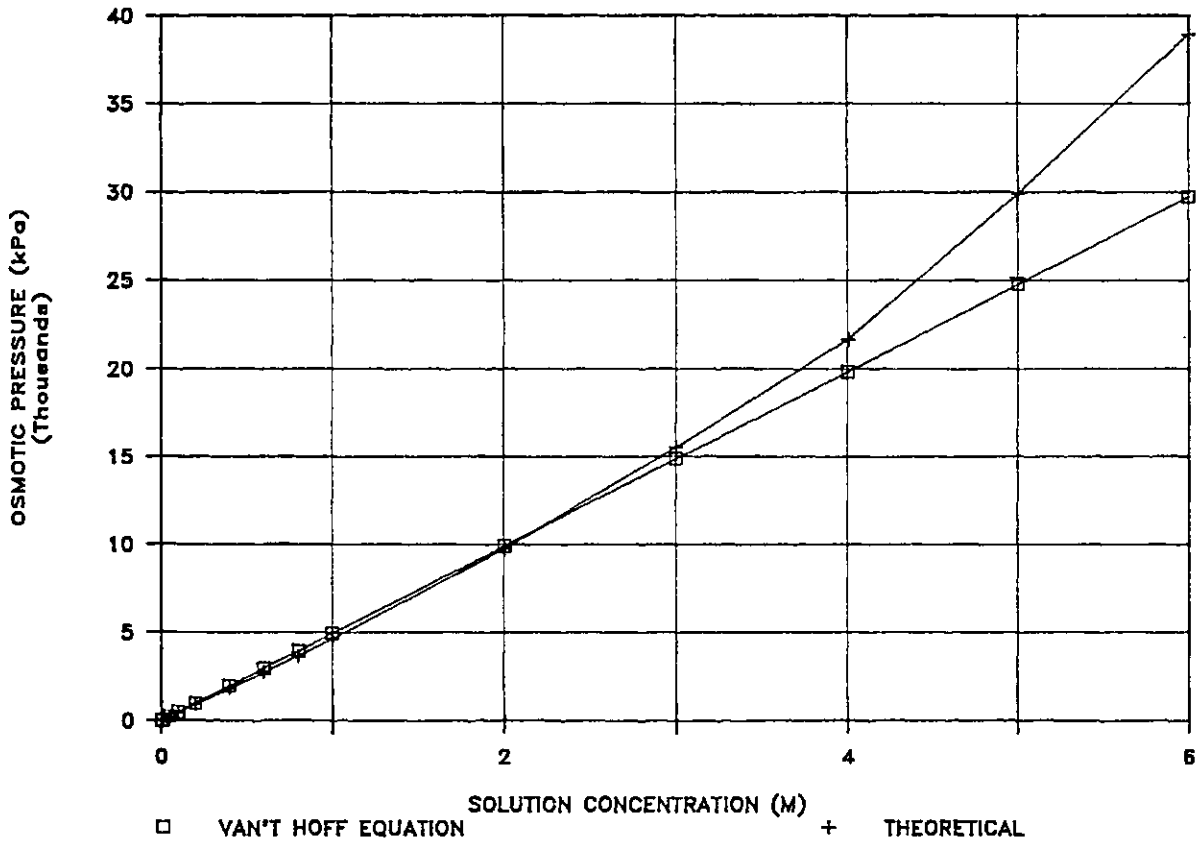

Figure 2.2 Osmotic Pressure of NaCl Solutions

These key features are reflected in studies of osmotic phenomena that have been conducted in a variety of disciplines including soil science, geology, hydrogeology, and geotechnical engineering. In soil science, osmotic phenomena have been studied in relation to the movement of water in saline soils and the diffusion of salt through clays (Low 1955, Abd-el-Aziz and Taylor 1965, Kemper and Van Schaik 1966, Kemper and Rollins 1966, Mokady and Low 1968).

Studies in geology have used osmotic phenomena to explain two similar deep groundwater conditions; the existence of excess pressure anomalies in deep saline connate waters (Hill et al 1961, Berry 1960, Hitcheon 1969, Marine and Fritz 1981, Hanshaw and Zen 1965), and the development of saline waters by ion filtration (de Sitter 1947, White 1957,1965, Bredehoeft et al 1963, Fothergill 1955, Graf 1982, Bailey 1961, Kharaka and Berry 1965). A comprehensive review of osmotic phenomena in geologic environments is provided by Neuzil (1986).

In contaminant hydrogeology there has been little direct reference to osmotic phenomena, but rather to analogous phenomena of anion exclusion and cation adsorption. In these processes, ion movement is restricted by the presence of a clay membrane (Gillham and Cherry 1982, Appelt et al 1975, Thomas and Swoboda 1972, Ridley 1985, Mckelvey and Milne 1960).

The consolidation of clays under the influence of osmotic flows has been studied by Greenberg (1971), Greenberg et al (1972, 1973) and Mitchell (1973). The effects of pore fluid composition on the compressibility and swelling of clay soils has been studied by numerous authors including; Bolt and Miller (1955), Bolt (1956), Warkentin, Bolt and Miller (1957), Olson and Mitronovas (1960), Aylmore and Quirk (1961), Blackmore and Miller (1961), Warkentin and Schofield (1962), Quirk (1963), Bailey (1965), El-Swaify and Henderson (1967), Klausner and Shainberg (1967,1971), Mesri and Olson (1971), Balasubramonian (1972), Sridharan and

Venkatappa Rao (1973), and Mitchell (1976). The literature in this area will be discussed in more detail in section 2.4.

2.3 Osmotic Flow

Osmotic flow will occur across a clay soil, in the presence of concentration gradients, if the clay exhibits the properties of a semi-permeable membrane. In the following sections the literature describing the nature of semi-permeable membranes and osmotic flow will be reviewed. A flow law for osmotic flow through clay soils is also presented.

2.3.1 Evidence of the Semi-permeable Nature of Clays

Extensive laboratory as well as field evidence exists regarding the semi-permeable nature of clays soils. The majority of the field evidence comes from studies of geologic membranes in large scale flow systems. These studies have dealt with the interaction of aquifers and confining clay layers where the clay layer separates fresh and saline groundwater.

If a saline water aquifer is confined by clay aquitards, excess pressures may develop within the saline aquifer in response to osmotic gradients. Anomalous pressures in saline aquifers have been reported by Berry (1959), Berry and Hanshaw (1960), Hill (1961), Hanshaw and Zen (1965), Van Everdingen (1968), Hitcheon (1969), Marine and Fritz (1981), and Hanshaw and Hill (1969).

The evolution of deep saline connate waters has also be attributed to osmotic phenomena. Migration of groundwater through aquifer/aquitard systems results in the development of concentrated brines within confined aquifer systems, due to ion filtration. The role of ion filtration (ie., hyperfiltration) in the evolution of subsurface brines has been discussed by de Sitter (1947), Fothergill (1955), White

(1957, 1965), Bredehoeft et al (1963), Kaharaka and Berry (1973), Graf (1982) and others.

Numerous laboratory investigations of osmotic flow have been conducted. Measurements of fluid flow in response to concentration gradients across a clay sample have been undertaken by Young and Low (1965), Kemper (1961), Kemper and Evans (1963), Kemper and van Schaik (1966), Kemper and Rollins (1966), Mokady and Low (1968), Bolt and Groenevelt (1969), and Elrick et al (1976). Figure 2.3a illustrates the simple osmometer used by Young and Low (1965) to measure osmotic flows through disks of siltstone bedrock, taken from the Viking Formation in Alberta, Canada. The osmotic flow rates measured by Young and Low are illustrated in Figure 2.3b.

Laboratory measurements have also been made of the hydraulic pressure that develops across a clay sample when osmotic flow is prevented from occurring. Tests of this type have been described by Kemper (1961), McKelvey and Milne (1963), Abd-el-aziz and Taylor (1965) and Olsen (1969, 1972, 1985). Figure 2.4 illustrates the type of apparatus used by Kemper (1961) and the test results for several clay soils.

Apparent deviations from Darcy's law have also been attributed to osmotic flow by several investigators including Kemper (1961), Low (1955) and Olsen (1985).

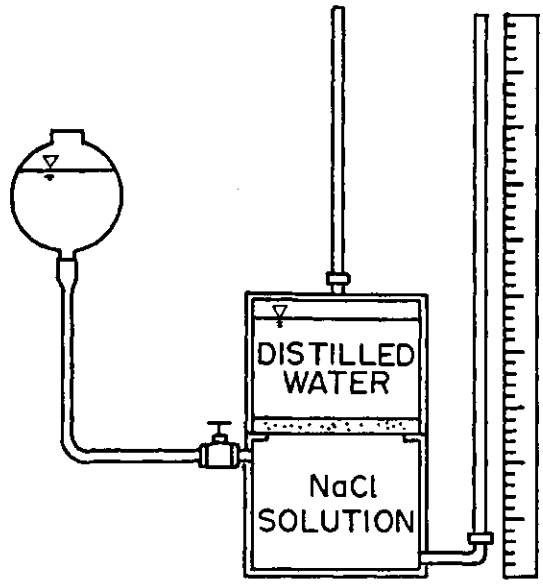

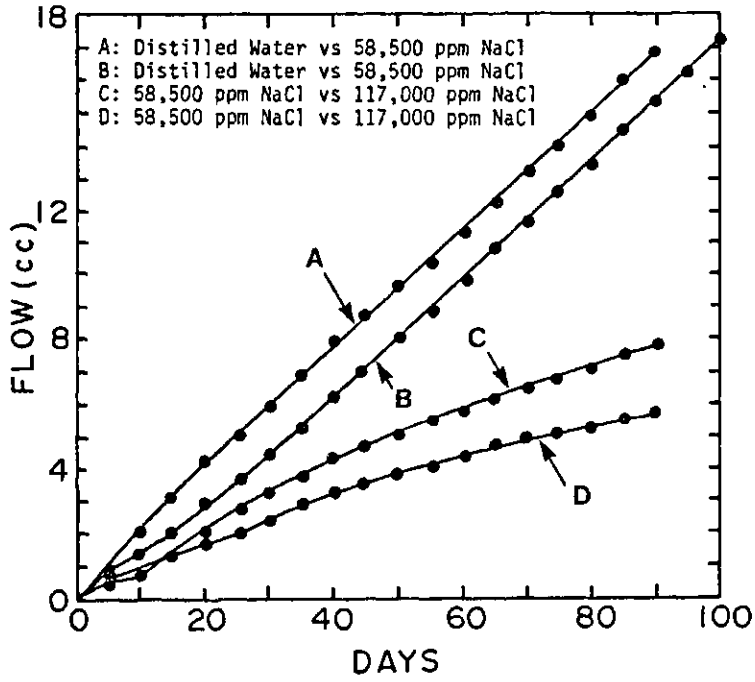

Figure 2.3 Osmotic Flow Measurements Conducted by Young and Low (1965) a) Osmometer b) Measured Osmotic Flow Rates

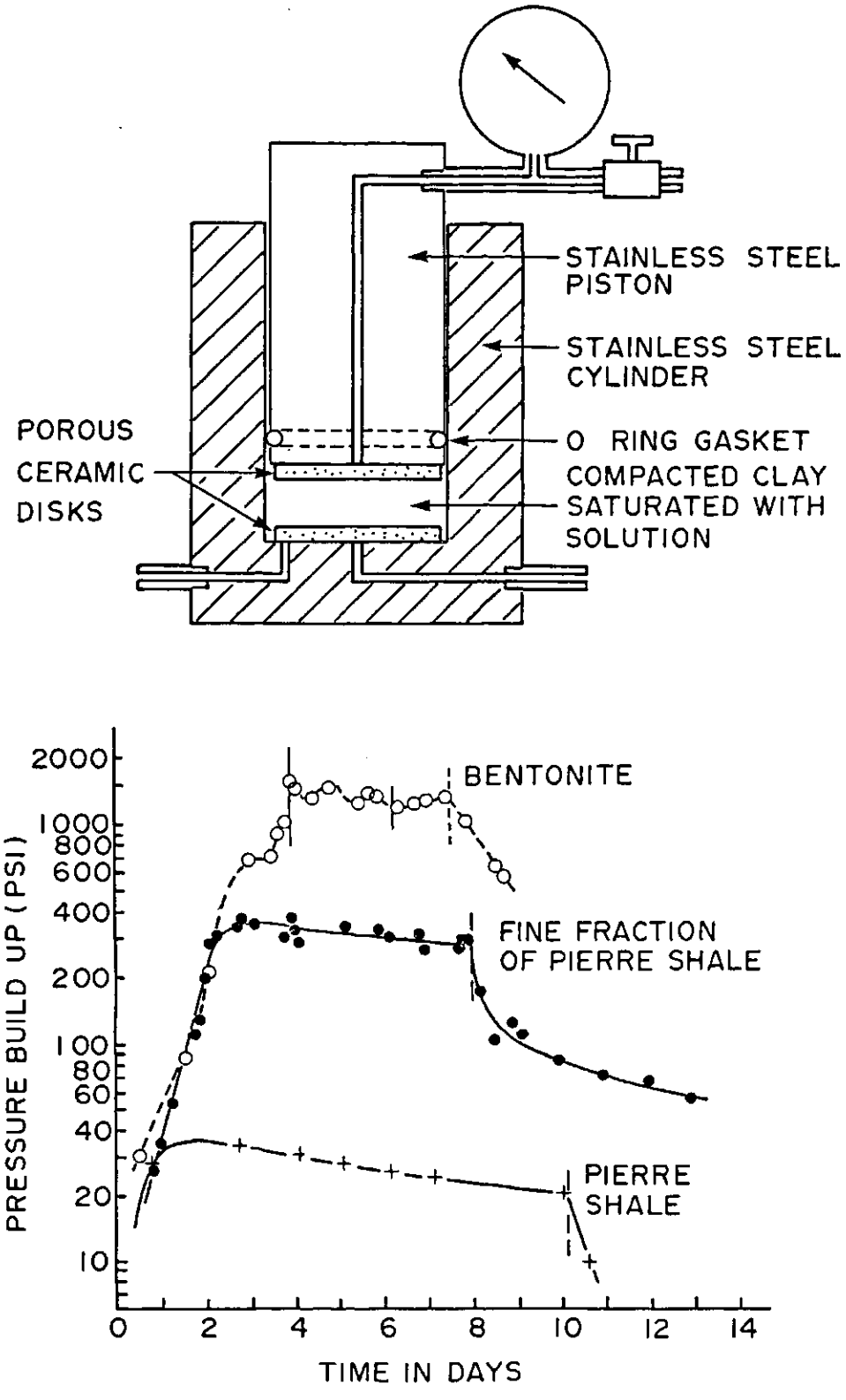

Figure 2.4 Measurement of Osmotic Pressure (Kemper 1961) a) Apparatus b) Hydraulic Pressure Response (5.4 N NaCl)

2.3.2 Mechanism for the Semi-permeable Nature of Clays

The osmotic flow of water that develops within clays which behave as semi-permeable membranes is described by Mokady and Low (1968) as follows:

> "The evidence obtained in the present study indicates that water moves through a clay in response to a salt concentration gradient by viscous or quasi-viscous flow. Usually, this kind of flow is associated with a hydraulic gradient that is measurable by tensiometers or piezometers. However, the data ... show that no hydraulic gradient, measured in the conventional way, existed in the systems under investigation. Consequently, the observed flow cannot be ascribed to a hydraulic gradient. ... Therefore, the absence of an hydraulic gradient cannot be construed as evidence for the absence of an internal pressure gradient." (p123 Mokady and Low 1968)

The potential mechanism by which viscous flow of solvent develops in response to concentration gradients is described by Kemper and van Schaik (1966) as follows:

> "Under practical conditions pressure gradients, electrostatic potential gradients, and osmotic pressure gradients may cause movement of the solution with respect to the solid matrix. the osmotic pressure gradient is always associated with a concentration gradient in the diffusion process. If the soil or clay restricts the solute components more than the water, the osmotic pressure gradient becomes a real pressure gradient causing bulk flow of the solution"(p. 535 Kemper and van Schaik 1966)

The nature of a semi-permeable membrane is that of a porous medium whose pores are continuous and which retards or hinders the flow of solute more than the flow of solvent (Greenberg 1971). A variety of mechanisms have been proposed for the semi-permeable nature of artificial membranes (Greenberg 1971, Spiegler and Laird 1980). Two mechanisms that may be applicable to natural soils are the sieving mechanism and the permselectivity or electrostatic mechanism.

Sieving, as the name implies is a mechanism by which the solute molecules are filtered out from the solvent simply on the basis of geometrical size restrictions. This mechanism has some validity for large diameter organic molecules. For salt molecules, however, the diameter of the solute is not significantly different than that of the water molecules, and is not larger than that of the soil pores. For example, an estimate of 10 Å for the diameter of the smallest clay pore is still larger than the diameter of ions such as Na+ or Cl-, which have diameters of 1 to 10 Å.

The permselectity, or electrostatic mechanism, is based on the fact that the clay particles usually contain net negative electrical charges on their surfaces. Electrolytic solutes which would pass by these charged surfaces would experience retardation due to the adsorption of the cations into the double diffuse layer surrounding the particles and the repulsion of the anions. In the absence of an electrical imbalance in the bulk solution, this mechanism would effectively restrict the migration of the solute within the soil pores. The occurrence of anion exclusion in clay has been described by Gillham and Cherry (1982), Appelt et al (1975), Thomas and Swoboda (1972), Ridley (1985), Mckelvey and Milne (1960) and others.

The viscous nature of osmotic flow has been demonstrated for artificial membranes by Mauro (1957) and Kemper and Evans (1963). The flow rates measured by these investigators were too large to be explainable on the basis of solvent diffusion alone. Mauro provides this comment on the viscous nature of osmotic flow:

"It should be emphasized that there is no kinetic theory in existence to explain the basis of the flux arising from the mole fraction effect. Unfortunately, the theory of liquids is inadequate at the present time for carrying out more than speculative analysis, but certainly, as suggested by Lars Onsager, there must be a momentum deficiency in the microdomain of the pore in the solution side of the barrier. That is, in a solid region of the barrier, the time average transfer of momentum is that prescribed by the hydrostatic pressure of the phase, but in the opening of the pore there is a deficiency since the momentum arising from the macromolecule is not transferred to the solvent species in the pore, being cut off by the finite size of the pore."

Conceptually the mechanism for sieving and permselectivity is similar. A portion of the momentum of solute and solvent molecules that might have been transferred across the soil pore is being removed due to the physical or electrical restriction provided by the particle.

2.3.3 Flow Law for the Solvent

In the presence of a perfect semi-permeable membrane solvent will flow through the membrane in response to the chemical potential difference across the membrane. The flow equation for solvent flow can be written in a form analogous to that of Darcy's law for fluid flow due to hydraulic gradients;

$$q_\pi = k_\pi \, (d\pi/dx) \qquad [2.1]$$

where: q_π = solvent flux
k_π = media conductivity for osmotic flow
x = distance
π = osmotic pressure

For thin membranes, across which a pressure difference acts, Heyer et al (1969) gave this equation the following form, called Starlings Law:

$$q = -k_h \, (\Delta P - \Delta \pi) \qquad [2.2]$$

where: P = hydraulic pressure
k_h = media conductivity to hydraulic flow

The following aspects of osmotic flow are implicit in this form of equation;

1. The solvent flow across the membrane is viscous,
2. The conductivity of the membrane is the same, regardless of whether the driving force is hydrostatic pressure on the solution, or osmotic pressure in the solvent, and
3. The solvent flux is directly proportional to the osmotic gradient.

In soil systems it has been observed that the fluxes due to osmotic gradients cannot be accounted for by diffusion of water molecules (Mokady and Low 1968, Kemper 1961, Kemper and van Schaik 1966). Describing osmotic flow as either viscous or diffusive, however, may not be so much a real physical difference as much as it is one of definition. Mokady and Low (1968) describe this as follows:

> "there may be no inherent difference other than the degree of cooperation between molecules, that is molecules probably move individually in diffusion, as clusters or domains in viscous flow".

Equation (2.1) implies that the conductivity should be simply a constant of proportionality between the flux and osmotic gradient. The proportionality between osmotic flow and osmotic gradient has been demonstrated by numerous researchers, including Heyer et al(1969), Low (1955), and Olsen (1969,1972).

The flow equation (Equation 2.1) shown above is sufficient in the case of a perfect semi-permeable membrane; however, if the membrane is "leaky" with respect to the solute, the equation is somewhat more ambiguous. In the case of a leaky membrane, the equation relates the flux of the solvent to driving forces acting on the solvent as well as the solution. To describe the flow of water through imperfect membranes, the flow equation may be modified by considering the "osmotic efficiency" of the membrane.

2.3.4 Osmotic Efficiency

Staverman (1951) coined a parameter called the reflection coefficient to handle imperfect artificial membranes. This parameter is used as an empirical constant by which the theoretical osmotic gradient is reduced so that the observed solvent fluxes are obtained. The flow equation then becomes:

$$q = -k_h(\Delta P/\Delta x - \sigma\Delta\pi/\Delta x) \qquad [2.3]$$

where: σ = reflection coefficient

The disadvantage of this approach is that it implies that the driving force is reduced, when in fact it is the ability of the membrane to promote viscous flow of the solvent which has been reduced. In the absence of any restriction to the solute the osmotic gradient is still undiminished; however, it is now dissipated by diffusion rather than viscous solute flow.

Combining the pressure and osmotic gradients is only valid if the membrane is perfect. With a leaky membrane, such as clay, the flow through the membrane due to the pressure gradient will be solution, whereas the flow due to the osmotic gradient will be solvent alone.

A preferred approach would be to use a separate conductivity for osmotic flow such that;

$$q_\pi = k_\pi(\Delta\pi/\Delta x) \qquad [2.4]$$

Solution flow due to pressure gradients is written with a separate conductivity from that of the solute flow due to osmotic gradients. The total volumetric flux may be written then as;

$$q_t = -k_h\, dP/dx + k_\pi d\pi/dx \qquad [2.5a]$$

$$\text{or} \quad q_t = -k_h\, dP/dx + \sigma k_h d\pi/dx \qquad [2.5b]$$

where: $\sigma = k_\pi / k_h$

For soils the ratio of k_π / k_h is termed the osmotic efficiency of the membrane. This a similar to the reflection coefficient described by Staverman (1951) for artificial membranes.

Kemper and Evans(1963) calculated the osmotic efficiency of synthetic membranes to various organic solutes based on the degree of exclusion of the solute molecules that occurred due to geometrical size restrictions. As described by Mauro (1957), pore fluid pressure may be described as the average change of momentum of all molecular collisions. The pressure in the solution on both sides of a semi-permeable membrane may be the same. However, in the vicinity of the pore, the impacts of the solute molecules are taken in part by the membrane itself. This results in a pressure deficiency on the solution side of the pore, and viscous flow of solvent then occurs from the inside of the pore, into the solution.

The permselective mechanism for the restriction of charged solutes from the pore spaces of charged particles may be viewed in a similar manner to that described above. Any factor which reduces the number of solute molecules impacting on solution inside the small restricting pore will cause an increase in the osmotic efficiency. In permselective membranes, the repulsion of anions from the vicinity of negatively charged clay surfaces would be such a factor (Kemper and Evans 1963).

Kemper and Rollins (1966) calculated the osmotic efficiency of clays based on a approach similar to that used for artificial membranes. The assumption was made that the "driving force on the solution (solvent) is approximately proportional to the degree to which the solute is excluded". The driving force was considered to be the osmotic pressure difference between the bulk solution and the solution within the pore. This osmotic pressure difference was calculated using the van't Hoff approximation. The concentration of the

pore fluid concentration within the pore was based on double diffuse layer theory. Experimental results obtained on samples of Wyoming bentonite gave osmotic efficiencies which agreed relatively well with calculated efficiencies (Figure 2.5).

A number of general trends in the osmotic efficiency of bentonite are observed. The osmotic efficiencies are increased by:

1. Saturating the clay with monovalent rather than divalent cations,
2. Using divalent rather than monovalent anions in the bulk solution,
3. Decreasing the water content (void ratio) of the clay, and,
4. Decreasing the average concentration of the bulk solution.

Kemper and Rollins (1966) showed that with the combination of increasing theoretical osmotic pressure and decreasing osmotic efficiency with increasing bulk solution concentration, an optimum solution concentration existed at which the maximum effective osmotic pressure would be generated (Figure 2.6).

Bresler (1973) also estimated the dependence of osmotic efficiency on soil water content and solution fluid concentration based on the work of Kemper and Rollins (1966). These estimates compared quite well with available data on clays and clay soils as illustrated in Figure 2.7.

Olsen (1972) demonstrated the strong dependence of osmotic efficiency on void ratio. For a sample of kaolinite the osmotic efficiency increased from a value of .025 at 100 kPa to 0.9 .at 70000 kPa, as illustrated in Figure 2.8.

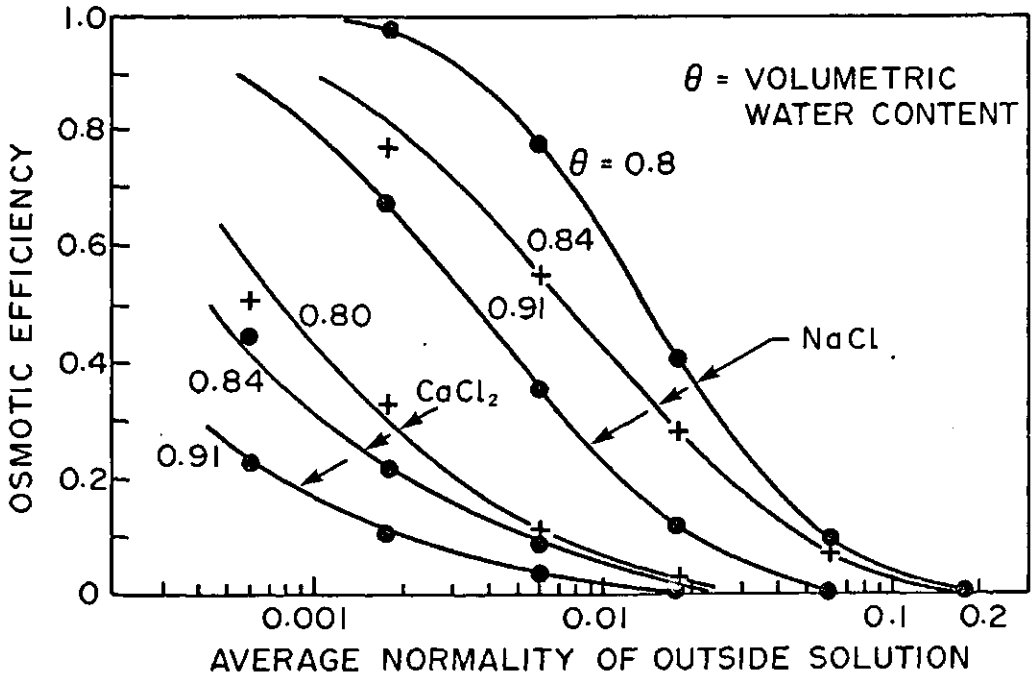

Figure 2.5 Osmotic Efficiencies of Clay at Various Moisture Contents (Kemper and Rollins 1966)

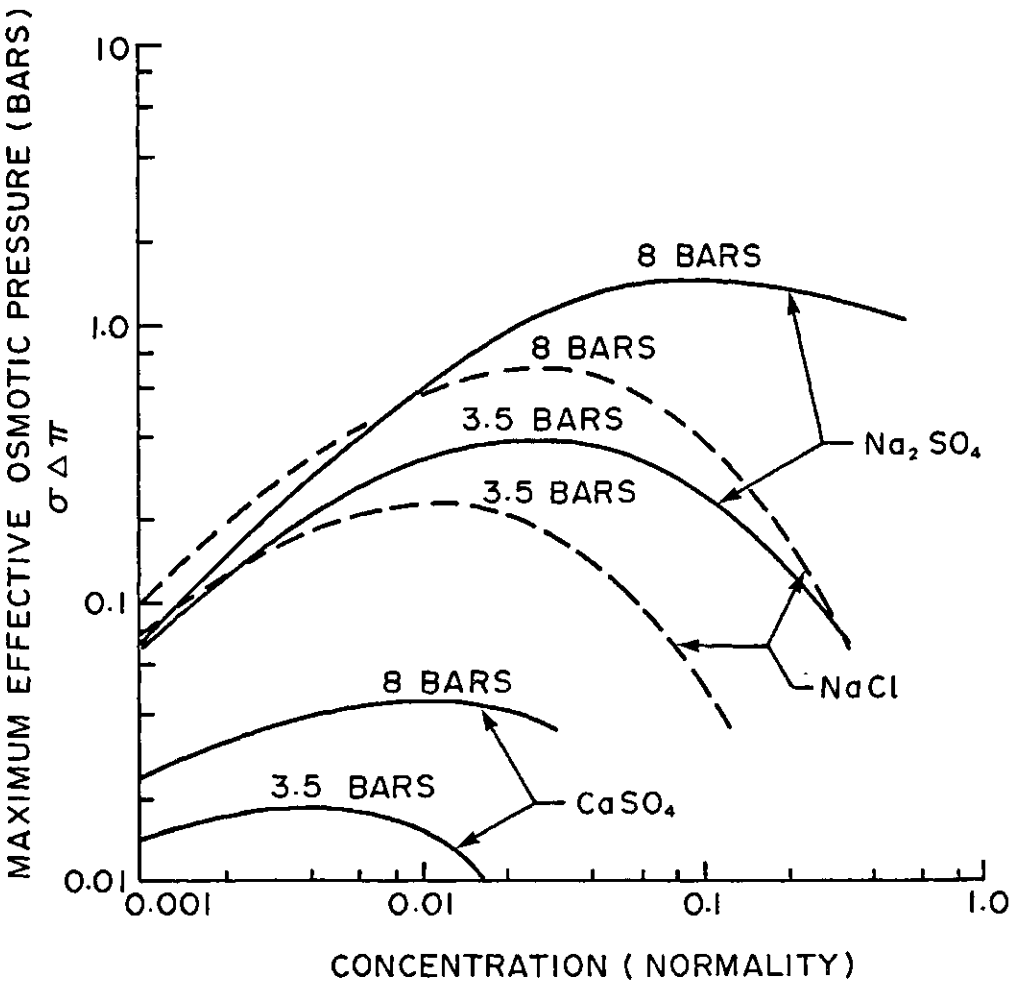

Figure 2.6 A Comparison of Maximum Effective Osmotic Pressure at 3.5 and 8.0 Bars of Soil Water Suction (Kemper and Rollins 1966)

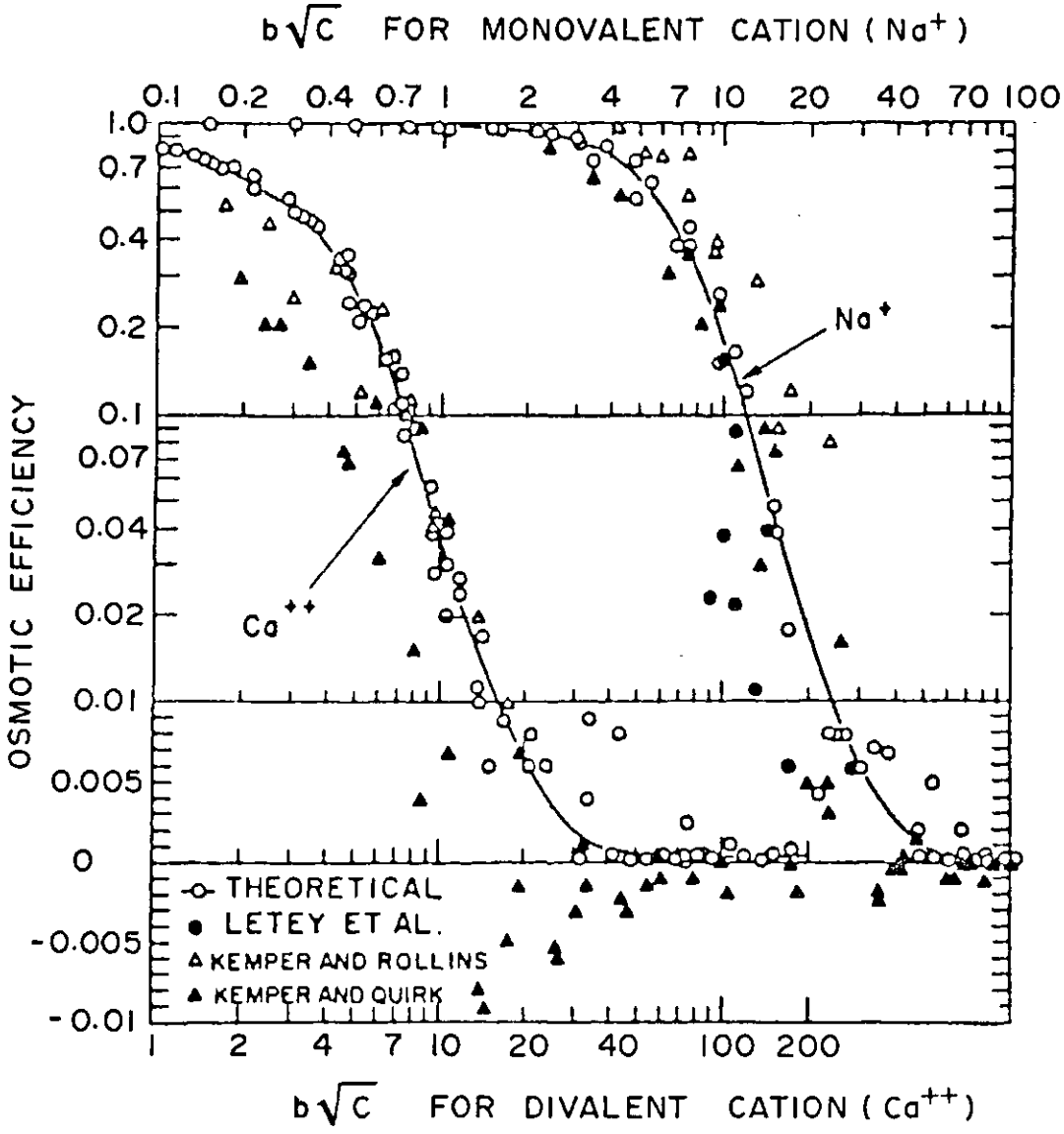

Figure 2.7 Osmotic Efficiency as a Function of $b\sqrt{C}$ (C is ion concentration in normality, 2b is film thickness in angstroms, Bresler 1973)

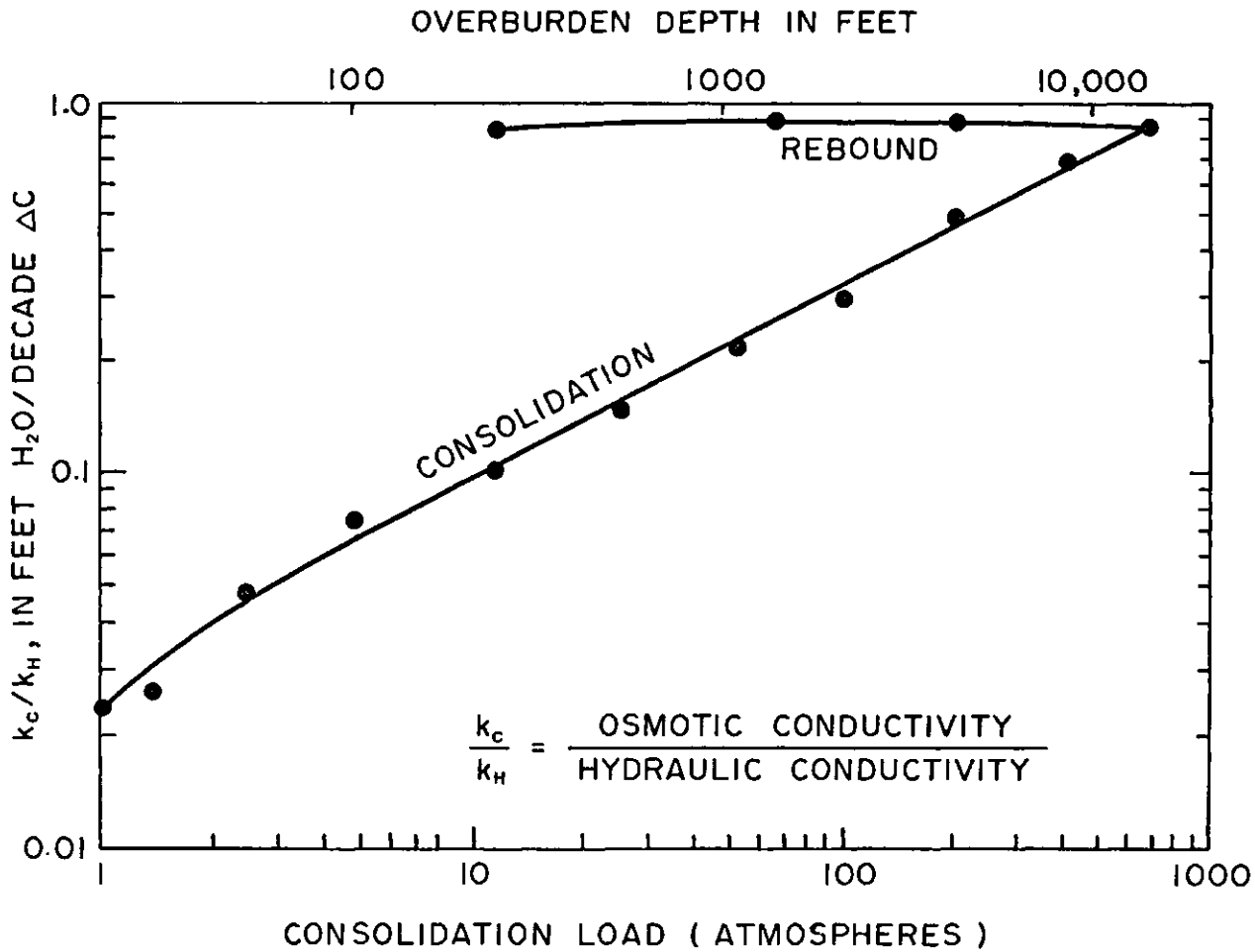

Figure 2.8 Ratio of Osmotic to Hydraulic Conductivity during Successive Increments of Consolidation and Rebound (Olsen 1972)

Boundary layer effects during testing may also produce an apparent reduction in osmotic efficiencies. This was demonstrated by Heyer et al (1969). Inadequate mixing, of the solvent flow through the membrane with the boundary solution, produces a diluted concentration in the vicinity of the membrane. This lower solution concentration results in a lower effective osmotic gradient across the membrane.

In reverse osmosis, a reduction in osmotic efficiency with increasing flow rates was noted and was attributed to "piling up" of the solute molecules at the membrane, thereby restricting the flow of solvent.

2.3.5 Theoretical Formulation for Osmotic Flow

A complete description of the osmotic flow problem involves a description of the flow of pore solution, solvent and the dissolved solute, in response to hydraulic and osmotic gradients. Two distinct approaches have been taken in the literature in addressing this problem. These are discussed as the Total Potential Approach and the Phenomenological Approach. A theoretical development of transient osmotic flow is developed in Chapter 3, based on the Phenomenological Approach.

2.3.5.1 Total Potential Approach

Potential is defined as the energy of a material phase per unit volume, mass or weight. Thermodynamically, for any spontaneous or natural process to occur there must be a net loss in energy of the phase. In other words, flow must occur from higher to lower potentials. Consequently, the total potential approach attempts to define a potential for the soil water such that water will always move from regions of higher to lower potential. If the potential is constant at all points, the water is in equilibrium (Corey and Klute 1984). The flow of pore-water is equal to a conductivity,

which is a function of the media, multiplied by the negative gradient of the potential, which is the driving force.

The Total Potential Approach to the flow of pore-water was originally developed by Buckingham (1907) and Richards (1928) for gravitational, and pressure or capillary potentials, and was extended to include osmotic pressure effects by Edlefsen and Anderson (1943), Childs and Collis-George (1943), Low and Deming (1953), and Bolt and Miller (1958). The classic work of Hubbert (1940) also provides a rigorous development of potential theory as related to groundwater flow. Mitchell (1962) utilizes the Total Potential Approach in discussing the significance of pore-water pressures to the engineering behavior of soils.

The Total Potential Approach has been applied successfully to soil water flow problems in which no significant density variations occur, and for problems in which osmotic effects are not significant. It has a number of serious shortcomings, however, when these effects are included. These limitations are discussed in detail by Corey and Kemper (1961) and Corey and Klute (1984), and are reviewed briefly here.

There are several basic difficulties with the Total Potential Approach. First, potentials such as pressure and gravitational potential, which refer to an element of solution, are intermixed with osmotic potentials which refer only to the solvent phase of the solution. Second, a constant "pore-water" conductivity is applied to the gradient of the total potential. However, as noted previously, the conductivity is really that of the pore fluid for hydraulic potential, whereas it is that of the solvent for osmotic potential. Finally, in cases in which substantial density variations occur, the use of a potential defined as energy per unit mass or weight is inappropriate. Corey and Klute (1984) state;

"a force potential for the solution, taking into account the effects of both gravity and pressure cannot be uniquely defined for a solution of varying density unless the density is a unique function of pressure.

For example, consider a case in which the total potential is defined as the sum of the gravity and pressure potentials as follows:

$$h = P/\rho g + z \qquad [2.6]$$

where: h = total potential
P = pressure
ρ = fluid density
z = elevation

The gradient of total potential would then be written as:

$$\partial h/\partial x = (1/\rho g)(\partial P/\partial x) - (P/g)(\partial \rho/\partial x) + \partial z/\partial x \qquad [2.7]$$

Unless $\partial \rho/\partial x$ can be expressed as $(\partial \rho/\partial P)(\partial P/\partial x)$, the use of a single total potential is not valid.

2.3.5.2 Phenomenological Approach

The Phenomenological Approach has been applied to coupled flow problems in which the gradient which produces one type of flux, will alter the flux of another type. Table 2.1 taken from Mitchell (1976) presents examples of several types of coupled flow systems.

Table 2.1 Coupled and Direct Flow Phenomena (Mitchell 1976)

	Gradient *X*			
Flow *J*	Hydraulic Head	Temperature	Electrical	Chemical (concentration)
Fluid	Hydraulic conduction *Darcy's law*	Thermo-osmosis	Electro-osmosis	Normal osmosis
Heat	Isothermal heat transfer	Thermal conduction *Fourier's law*	Peltier effect	Dufour effect
Current	Streaming current	Thermo-electricity	Electric conduction *Ohm's law*	Diffusion and membrane potentials
Ion	Streaming current	Soret effect—thermal diffusion of electrolyte	Electro-phoresis	Diffusion *Fick's law*

The coupled flow problem may be dealt with by two different schemes within a Phenomenological Approach. For the purpose of this discussion, these schemes are called the Irreversible Thermodynamic Approach (IRT) and the Mechanistic Approach.

The use of the term "Mechanistic" is reserved within the context of this discussion, to refer to a description of processes at a macroscopic, not a microscopic level. de Vries (1975) provides a summary of the difference between these two schemes when he contrasts his approach to the study of simultaneous flow of moisture and heat in unsaturated soil, to that conducted by Cary and Taylor (1962):

> "Macroscopic theories of combined heat and moisture transfer in soils have been developed along two different lines. In the first approach one attempts to identify separate transfer phenomena occurring in the soil and to develop equations for the macroscopic fluxes of heat and moisture on the basis of a physical model of the soil system. In the second approach one applies the formalism of Irreversible Thermodynamics to the coupled phenomena of heat and moisture transfer and attempts to identify the relevant fluxes and forces. The fluxes are then expressed as linear functions of the forces through the so called phenomenological relations. Neither approach is able to do full justice to the complexity of the system that it tries to describe."

Irreversible Thermodynamic Approach (IRT)

The basis for the IRT approach is that any spontaneous or natural process, such as flow, is accompanied by a production of entropy. For a fluid mixture, for example, water and dissolved salts, " an entropy balance equation is developed in which the time rate of production of entropy is set equal to the sum of the negative divergence of the entropy flux and an entropy source function" (Corey and Klute 1984). The source function represents the contribution to entropy production due to the transport of chemical

constituents, heat, electrical charge or the transport of the bulk fluid by viscous flow.

This source, or dissipative function is written as:

$$\phi = \Sigma J_i X_i \qquad [2.8]$$

where: ϕ = dissipative function
J_i = generalized flows
X_i = generalized forces

The flows are assumed to be linear functions of all the forces such that:

$$J_i = \Sigma L_{ik} X_k \qquad [2.9]$$

where; L_{ik} are called the transport or phenomenological coefficients. The matrix of coefficients is said to be symmetrical based on the Onsager reciprocal theorem (Onsager 1931a,b). The forces include the thermodynamic gradients on each component of flow.

This approach has been applied to the problem of simultaneous flows of water and heat, electricity, or solute by Taylor and Cary (1960) and Cary and Taylor (1962). Developments for steady state coupled chemico-osmotic and hydraulic flow have also been described by Abd-el-Aziz and Taylor (1965), Olsen (1969, 1972), Groenevelt and Elrick (1976), and Groenevelt et al (1978, 1980). Mitchell (1967) develops the IRT approach for electro-osmotic flow and consolidation. The formulation for osmotically induced consolidation, which is described in section 2.4 was also developed by Greenberg (1971) using this approach.

Greenberg (1971) utilizes the driving forces as the chemical potential of each fluid component (water and salt) and develops the following flux equation for the solvent, 1 and the solute, s:

$$J_\ell = L_{11} V_L \, \text{grad}(-U) + L_{12} RT/C_s \, \text{grad}(-C_s) \qquad [2.10a]$$

$$J_\ell = L_{21} V_L \, \text{grad}(-U) + L_{22} RT/C_s \, \text{Grad}(-C_s) \qquad [2.10b]$$

where; J = fluxes of the solute and solvent
L = phenomenological coefficients
V = partial molar volume of each component
U = hydrostatic pressure of the solution
C_s = molar concentration of the solute
R = Universal Gas Constant
T = absolute temperature

Major Difficulties of the Irreversible Thermodynamics Approach

The use of IRT has a number of significant drawbacks. Of primary concern is the validity of the assumptions regarding the phenomenological coefficients and the practical evaluation of these coefficients. Mitchell (1976) states;

> "A major problem in the quantitative description of coupled flows is in the proper representation of coefficients and gradients. Irreversible Thermodynamics provides a basis for derivation of the proper equations. The relationships are valid only if forces and fluxes are linearly related ..".

The verification of the validity of Onsagers theorem has been demonstrated by Abd-el-Aziz and Taylor (1965) and Olsen (1969). Olsen also showed that the fluid fluxes were linearly related to the driving forces; however, this was only for changes in electrical voltage and salt concentrations exterior to the sample. The results of Abd-el-Aziz and Taylor also indicated that even the coefficient relating water flow to pressure differences, in the absence of concentration gradients, was not constant but varied with both pore fluid concentrations and hydrostatic pressure. These coefficients were constant over very limited ranges of these parameters (Figure 2.9).

Mitchell(1976) noted that the assumptions regarding linearity of the phenomenological coefficients are not guaranteed by theory but must be established empirically.

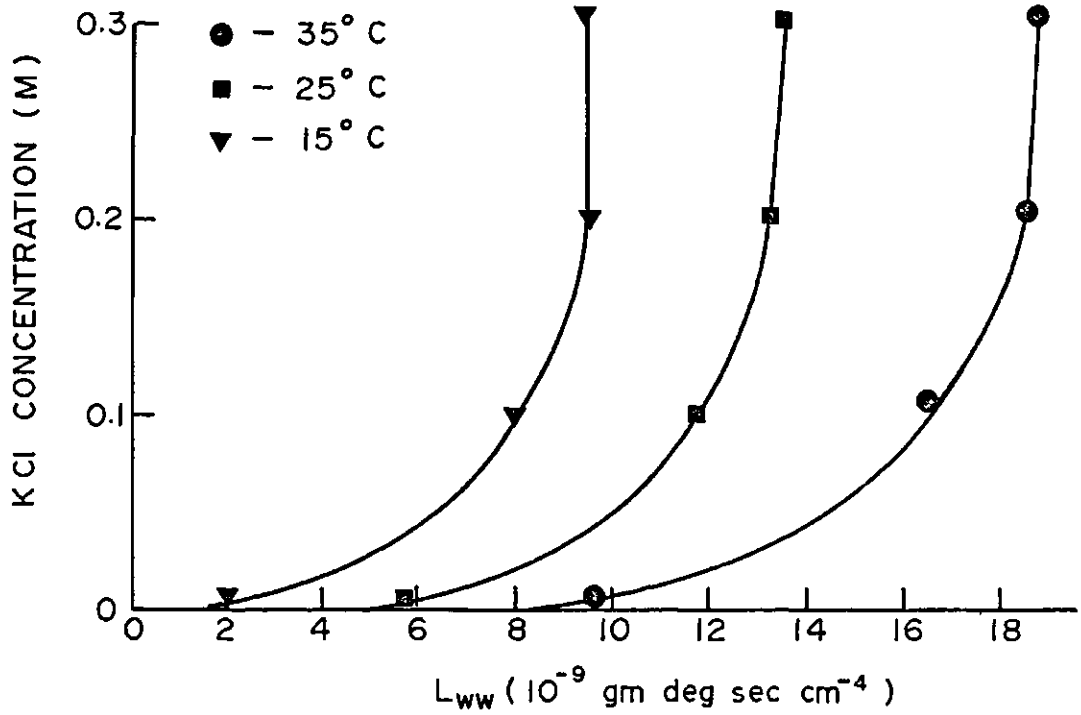

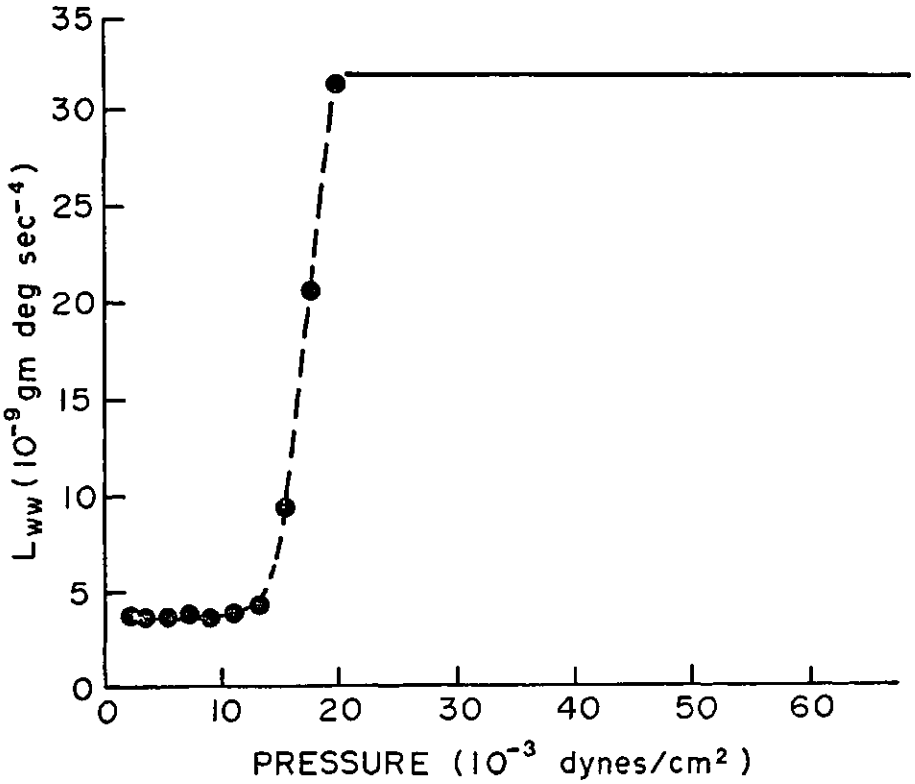

Figure 2.9 Variation of Phenomenological Coefficient, L Relating Fluid Flux to Pressure, with Solute Concentration and Pressure Difference (P) (Abd-el Aziz and Taylor 1965)

These assumptions have been verified only for carefully prepared samples, of constant composition and fabric, with either steady state or equilibrium conditions. Practical evaluation of the coefficients in general still remains a problem.

Neuzil (1986) provides this comment on the present state of the art in the study of transient, coupled osmotic flow problems:

> "Important questions also surround coupled flow behavior within the membrane medium itself, particularly when this behavior is transient. Experimental techniques utilized so far for the study of geologic membranes have been limited in this respect. Specifically, they have utilized only observations of conditions external to the membrane, and, with the exception of osmotic consolidation studies by Greenberg (1971), they have considered only steady state flow. Thus there is a dearth of direct information on transient behavior within the membrane with which to compare theoretical predictions."

Mechanistic Approach

The Irreversible Thermodynamics Approach is a formal description of energy transfer from which the relevant fluxes and forces and their interrelationship are extracted. The Mechanistic Approach, on the other hand, first observes the fluxes that occur and the forces that produce these fluxes on the basis of a physical model. The significant difference in the two approaches lies in the role of coupling. In the IRT approach coupling is "built in", so to speak, while in the Mechanistic Approach the interaction of fluxes is first observed, and then established on the basis of a separately defined mechanisms.

For example, the flow of solute due to pressure gradients in the solution phase, appears in the solute flux equation in the IRT approach. In the Mechanistic Approach the flow of solution due to pressure gradients would be viewed as a single mechanism. Flow of the solute would then

be evaluated by the separate mechanism of advection and diffusion of the solute within the bulk solution flow.

Bresler (1973) utilized the mechanistic approach when developing the description of coupled hydraulic and osmotic flows in unsaturated soil. The flow law for the solution phase was written in the same form as Darcy's Law as follows:

$$q = -K(\theta)\ (dH/dz - \sigma(\theta,C)/\rho g\ d\pi/dz) \qquad [2.11]$$

where: q = darcy fluid flux
K = permeability as function of
θ = volumetric water content
H = hydraulic head
σ = osmotic efficiency as function of
C = solute concentration
ρ = density of solution
π = osmotic pressure

This equation was then solved in a coupled manner with the salt transport equation:

$$\partial/\partial t\ (C\theta - Q(C,\theta)) = \partial/\partial z\ (D(v,\theta)\ \partial C/\partial z - q\ C) \qquad [2.12]$$

where: Q = local anion concentration in adsorbed phase
D = diffusion coefficient as a function of v,θ
v = interstitial fluid velocity

A similar approach for the flow of pore water alone was described by Corey and Kemper (1961). In that work the mass balance equations for the solution and solute phase are combined with a mechanical force balance for the solution. The mass balance equations for the solute consist of an advection-diffusion mass transfer equation, where the solute flow due to advection with the solution, and diffusion of the solute due to chemical gradients, are summed.

The Phenomenological Approach to osmotic flow and volume change is developed in the next chapter. Effects of volume change on solution flow, including the effect of fluid density variations are incorporated. This formulation

does not appear to have been developed previously in the geotechnical engineering literature.

2.4 Osmotic Volume Change

There are two forms of volume change in clay soils which have been associated with chemico-osmotic phenomena. For the purposes of this review these have been termed osmotically induced consolidation and osmotic consolidation.

2.4.1 Osmotically Induced Consolidation

Osmotically induced consolidation was addressed in a study by Greenberg (1971) and subsequently discussed by Greenberg et al (1972, 1973), Mitchell (1973), and Mitchell (1976). Flow of water out of the soil occurs due to osmotic gradients. In response to this flow, a pore fluid pressure deficiency develops within the sample. This causes increased effective stresses within the sample and results in consolidation. In the literature this process is often referred to as osmotic consolidation. However, it is clear that this is similar to conventional consolidation of the soil mass; however, it is induced by the osmotic flow process.

Greenberg (1971) developed a numerical simulation of osmotically induced consolidation by combining the flux equations [equation 2.10] with continuity equations for the salt and water components. These continuity equations were based on conventional constitutive relationships between volume change and changes in effective stress.

Examples of a numerical simulation of osmotically induced consolidation, as presented by Mitchell (1973), are illustrated in Figures 2.10 and 2.11. Mitchell suggests that the most significant results of the numerical simulation were as follows:

"1. Chemico-osmotic consolidation builds rapidly and smoothly to a maximum followed by swelling. In all cases the maximum consolidation occurred at dimensionless time, T=2.0, and real time 2.0H /Cv"

"2. The maximum amount of chemico-osmotic consolidation increases with increase in boundary salt concentration
increase and increase in soil compressibility."

"3. The time taken to reach eventual equilibrium in the diffusion of both pore water and salt increases as soil void ratio decreases and soil compressibility increases."

A series of laboratory experiments were conducted by Greenberg (1971) to establish the magnitude of osmotically induced consolidation for a variety of soil solution systems. One set of these tests used a conventional oedometer to consolidate the soil samples to an effective stress of 100 kPa prior to flushing solution through the porous stone. Only a bentonite clay sample, exposed to a solution of polyethylene glycol, exhibited a detectable amount of osmotically induced consolidation.

Mitchell(1973) concludes:

"from the results of these tests is seems reasonable to conclude that chemico-osmotic consolidation is likely to be of practical significance only in highly compressible clays of low permeability like bentonite."

2.4.2 Osmotic Consolidation

Osmotic consolidation of clays occurs as changes in the pore fluid chemistry alter the electrostatic interactions between the clay particles. These interactions are in turn influenced by the distribution of charged ions in the pore fluid adjacent to the clay particles.

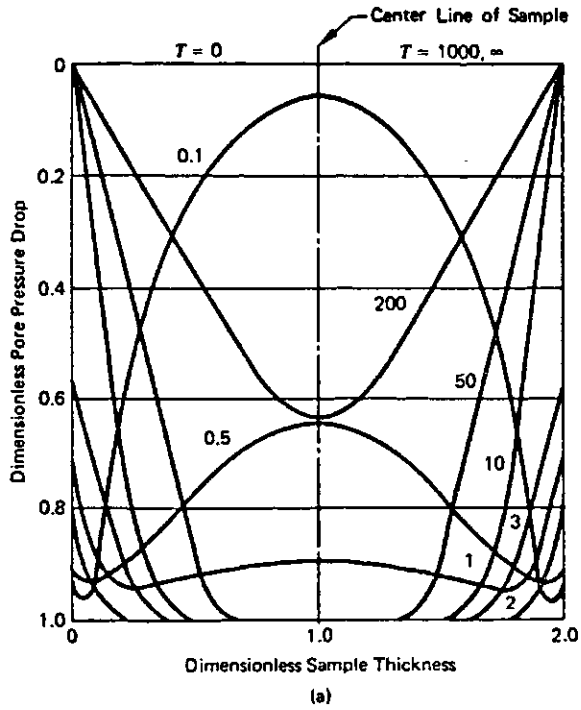

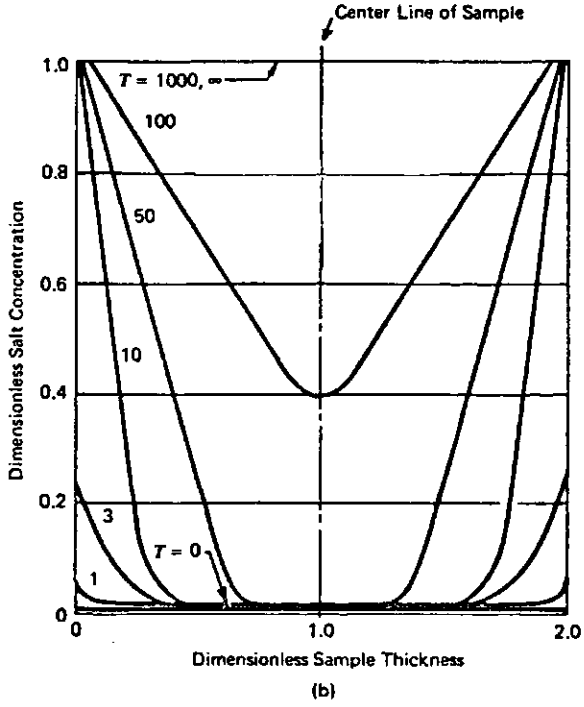

Figure 2.10 Isochrones during Osmotically Induced Consolidation a) Pore Pressure b) Salt Concentration (Mitchell 1976)

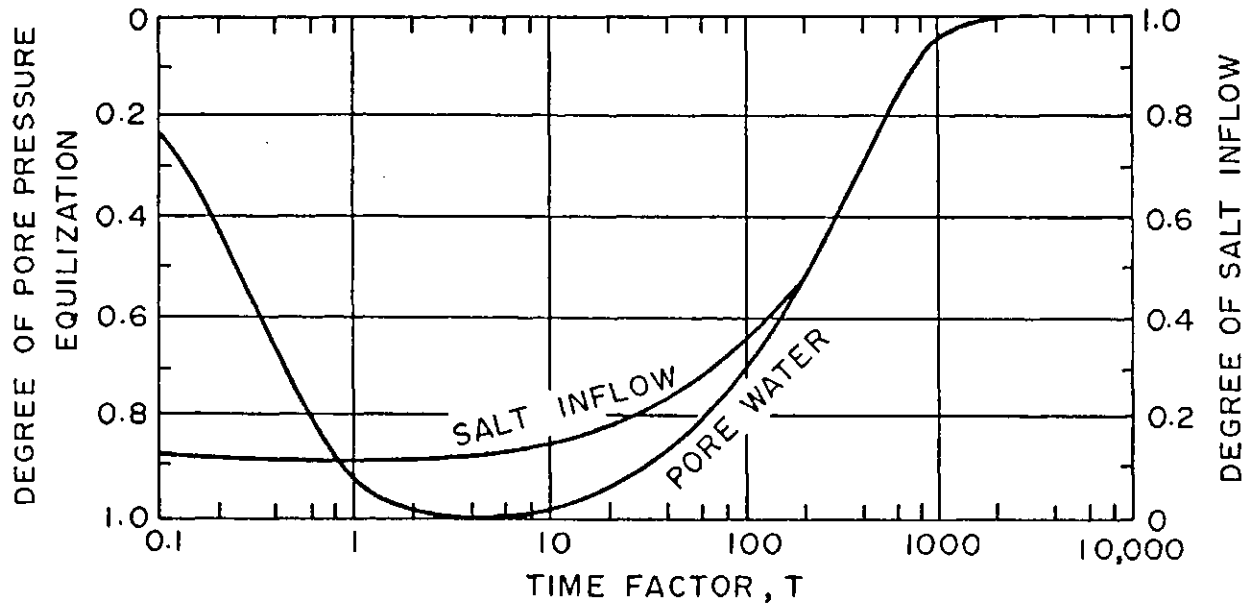

Figure 2.11 Salt Inflow and Pore Pressure Equalization during Osmotically Induced Consolidation (Mitchell 1976)

2.4.2.1 Diffuse Double Layers

Clay minerals are composed of sheets of crystals. Ideal crystals are electrically neutral; however, most clay minerals have a net negative surface charge. These negative charges may result from broken crystal bonds or maybe due to isomorphous substitution of a lower valence cation for a higher valence cation within the crystal lattice (Mitchell 1976).

In order to obtain electro-neutrality, a diffuse double layer of cations and anions within the pore fluid develops around the clay particle. The distribution of these ions around the clay particle is controlled by two opposing forces. Electrostatic attraction or repulsion of the ions develops between the clay surface and the ionic charges of the dissolved ions. This results in elevated concentrations of cations and suppressed concentrations of anions adjacent to the clay particle relative to those that exist in the bulk solution. Ionic diffusion acts to oppose the development of these concentration differences.

The negatively charged clay surface and the charge distribution adjacent to the clay particle is termed the diffuse double layer. Theoretical descriptions of the diffuse double layer were first proposed by Gouy (1910) and Chapman (1913). Stern (1924) later modified this description of the double layer to take into account the effects of a single layer of cations adsorbed directly to the particle surface. More extensive developments of diffuse double theory are provided by Mitchell (1976) and van Olphen (1977). The combined effects of electrostatic repulsion and ionic diffusion result in a distribution of charge density and electric potential described by an equation known as the Poisson-Boltzmann equation. The charge density and electric potential vary as a function of distance from the clay surface, surface charge density, surface potential,

electrolyte concentration and valence, dielectric constant of the medium and temperature.

The influence of all these factors can be seen in the equation for the distance to the center of gravity of charge density surrounding a semi-infinite negatively charged plate:

$$1/K = (D\ k\ T/8\pi no\ e^2\ v^2)^{1/2} \qquad [2.13]$$

where: $1/K$ = "thickness" of the double layer
D = dielectric constant of the medium
k = boltzmann constant
no = bulk solution electrolyte concentration
e = unit electronic charge
v = cation valence

Note that the "thickness" will vary inversely with the ion valence and the square root of concentration.

2.4.2.2 Interparticle Forces

In clay soils, particle to particle interaction is to a large degree, controlled by long range repulsive forces. The magnitude of these forces is controlled through the adsorbed cations and double diffusive layer surrounding the clay particles (Bailey 1965, Mitchell 1976).

Osmotic consolidation in clay soils occurs when changing pore fluid concentrations produce a change in long range forces and a reduction in the thickness of the double diffuse layer. One way to calculate these interparticle repulsive forces is through the osmotic pressure concept (Bolt 1956, Mitchell 1976). The clay particle system is assumed to exist as a series of parallel clay particles as shown in Figure 2.12. The Poisson-Boltzmann equation for a single particle can be integrated to obtain the mid-plane electrolyte concentration and mid-plane potential between two clay particles.

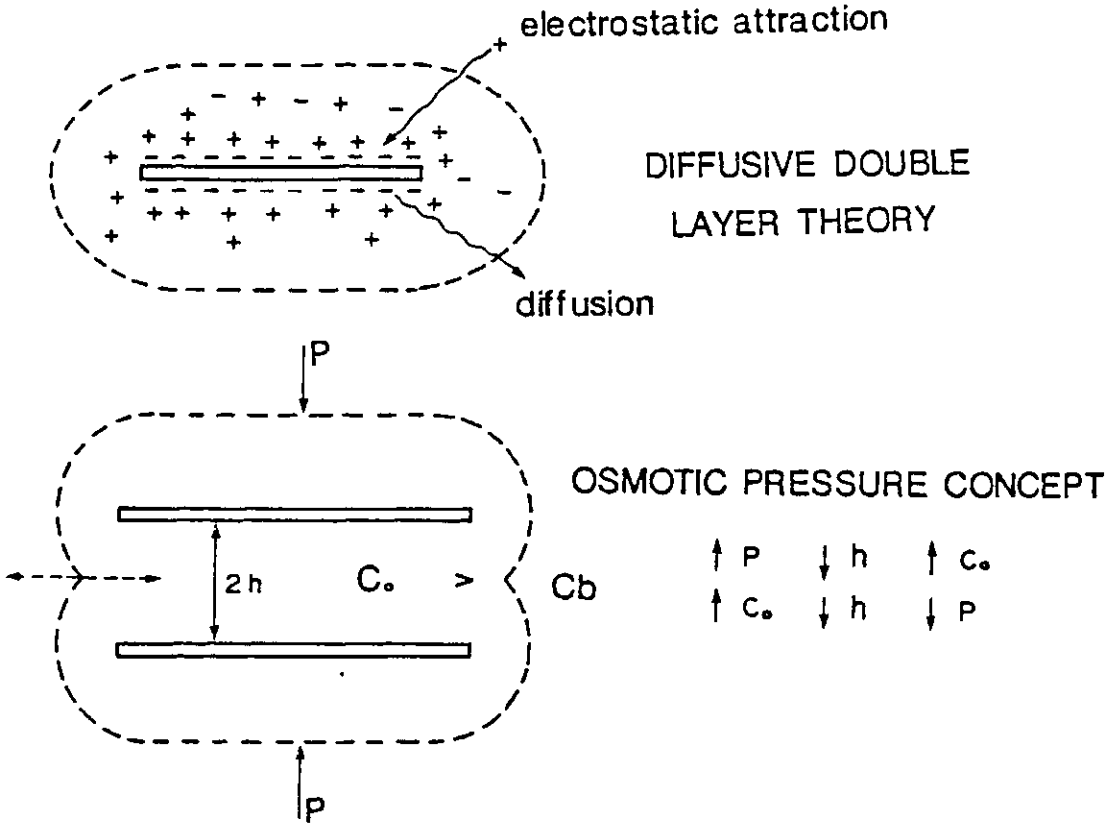

P = APPLIED STRESS

Co = INTERPARTICLE PORE
FLUID CONCENTRATION

Cb = BULK PORE FLUID
CONCENTRATION

d = INTERPARTICLE HALF SPACE

Figure 2.12 Illustration of the Osmotic Pressure Concept

The overlapping double diffuse layer also acts, however, as a semi-permeable membrane. A concentration contrast is maintained between the bulk solution and the solution midway between the clay plates. The difference in osmotic pressure between the bulk solution and that midway between the clay particles is then equivalent to the repulsive pressure or swelling pressure between the particles.

A description of the procedure to calculate the repulsive forces between clay particles using the osmotic pressure concept is presented in Appendix A.

Changing the external pressure, consequently, changes the particle spacing until a new balancing osmotic pressure difference develops. Similarly, changing the concentration (osmotic pressure) of the bulk pore fluid also changes the void ratio.

Attempts to predict compressibility and swelling pressure of clays, based on the osmotic pressure concept have met with varying degrees of success. Reviews of these efforts are provided by Mitchell (1973, 1976). A list of references for a number of these works was also given in section 2.2.

Several researchers have investigated the compressibility of clay samples premixed with solutions of varying concentration. Figures 2.13 and 2.14 show results obtained by Mesri and Olson (1971) for Ca^{2+} and Na^{+} montmorillonite. Figure 2.15 presents a comparison between measured and theoretical compression curves for Ca^{2+} and Na^{+} montmorillonite as presented by Bolt (1956). Samples premixed with the solution of interest were used in the tests of Bolt (1956), Mesri and Olson (1971) and others investigating the role of pore fluid concentration on compressibility.

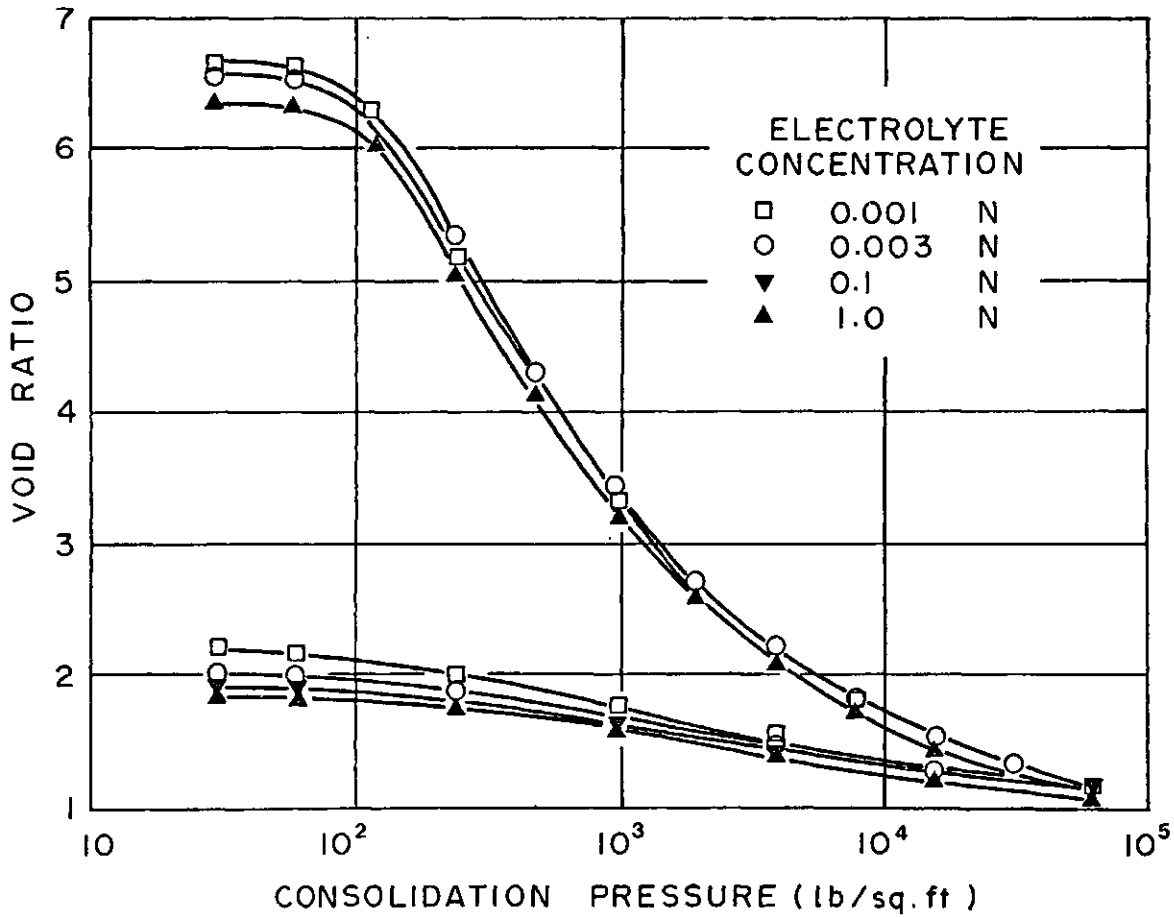

Figure 2.13 One-Dimensional Consolidation Curves for Ca2+ Montmorillonite (Mesri and Olson 1971)

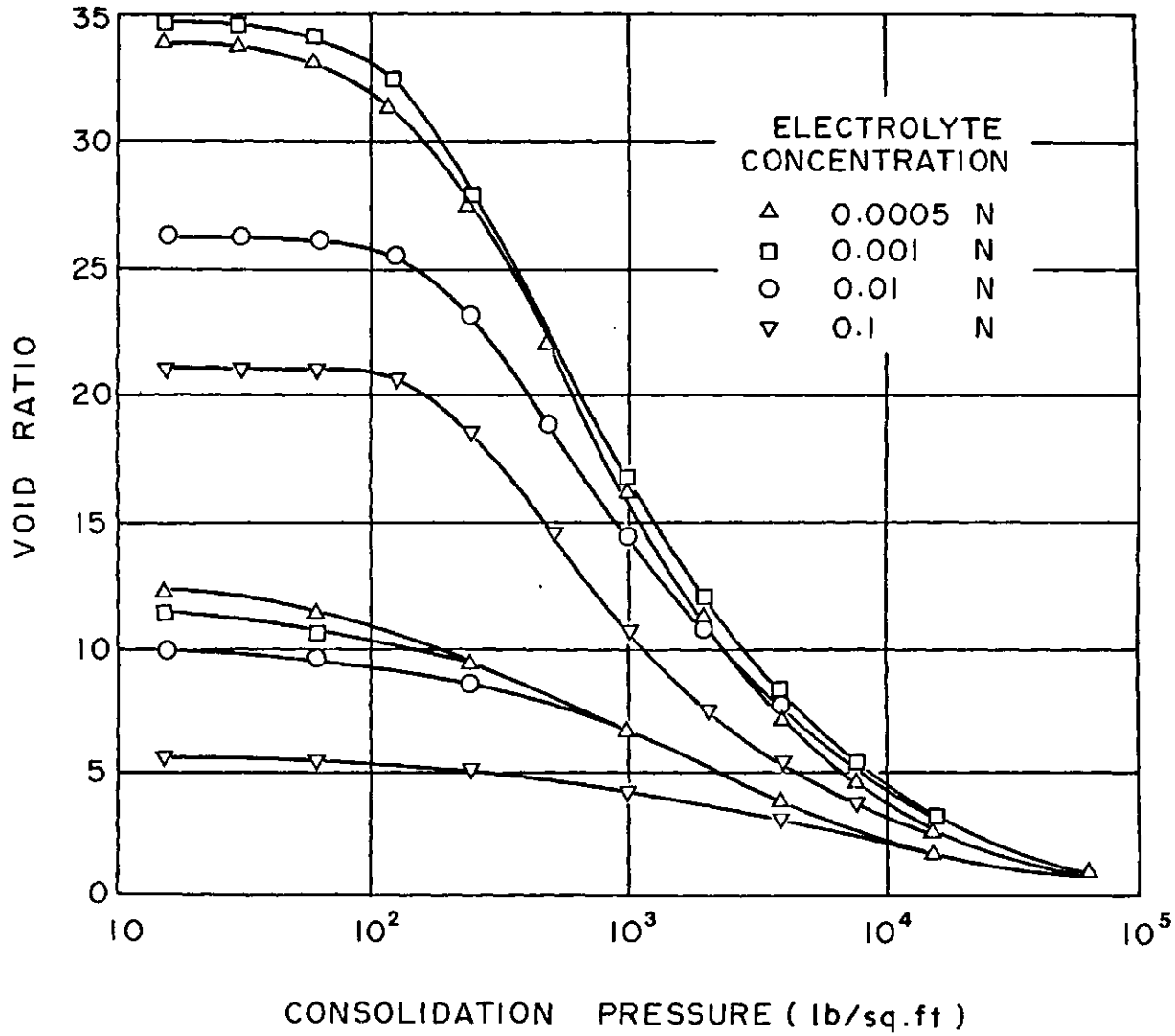

Figure 2.14 One-Dimensional Consolidation Curves for Na+ Montmorillonite (Mesri and Olson 1971)

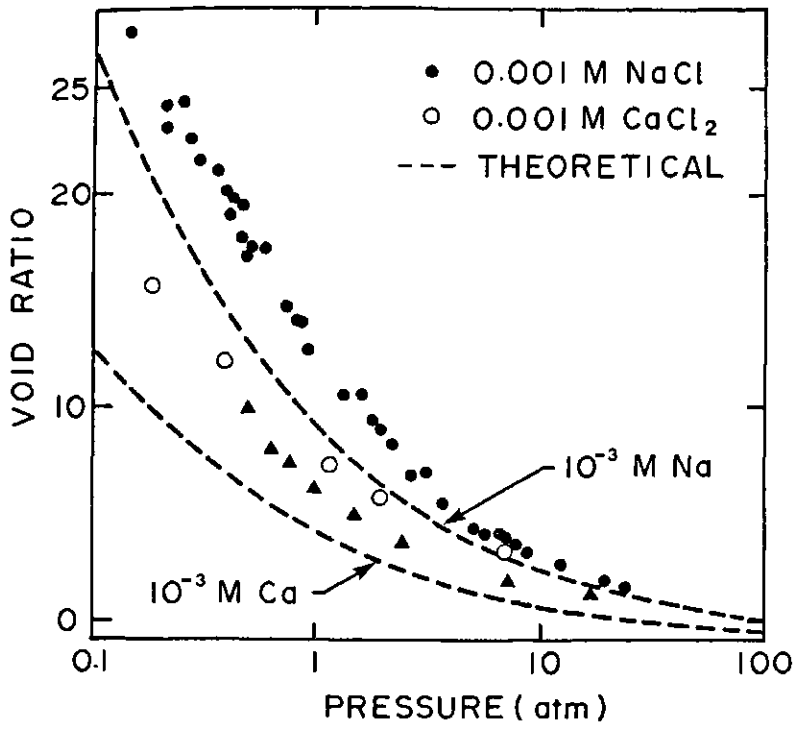

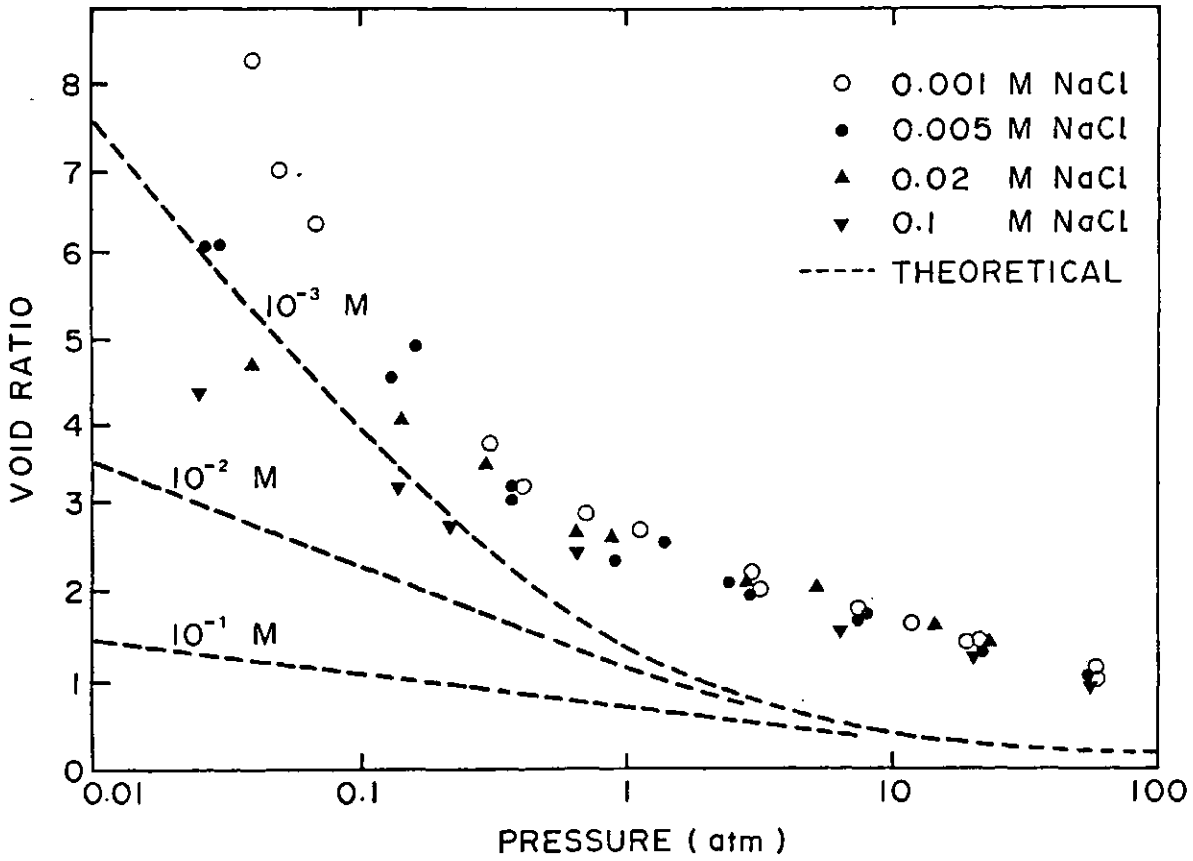

Figure 2.15 Compression Curves for a) Na+ and Ca2+ Montmorillonite b) Na+ Illite (from Bolt 1956)

Aylmore and Quirk (1962) compressed dried samples of montmorillonite and illite, and then allowed them to swell in contact with the solution of interest, under various pore-fluid suctions. The results of these tests are illustrated in Fig. 2.16 through 2.19. Figure 2.20 presents the comparison made by Aylmore and Quirk between the theoretical and measured response of Na+ Illite.

Ho (1985) consolidated reslurried samples of clay and glacial till to various confining stresses and then exposed them to various NaCl solutions. Figure 2.21 illustrates the magnitude and rate of osmotic consolidation observed for a sample of Regina Lake Clay.

2.4.2.3 Limitations of Osmotic Pressure Concept

It is evident that fairly good agreement between theory and experimental results has been obtained for homoionic clays with an ideally dispersed structure, and in the presence of homoionic solutions. Bolt(1956) stated that the major limitations in obtaining good agreement between the experimental results and the theoretical predictions is due to limitations in the following assumptions:

1. Double diffusive layer theory is applicable,
2. Clay particles are in a parallel alignment,
3. Osmotic pressure may be approximated by the van't Hoff equation, and,
4. Void ratio may be calculated from the half spacing of the clay particles.

The theoretical limitations inherent in the assumptions used for double diffuse layer theory and the van't Hoff approximation are not particularly severe (Bolt 1956). The major difficulty in the use of the osmotic pressure concept lies in the deviation of the soil structure from that of a series of perfectly parallel individual clay particles.

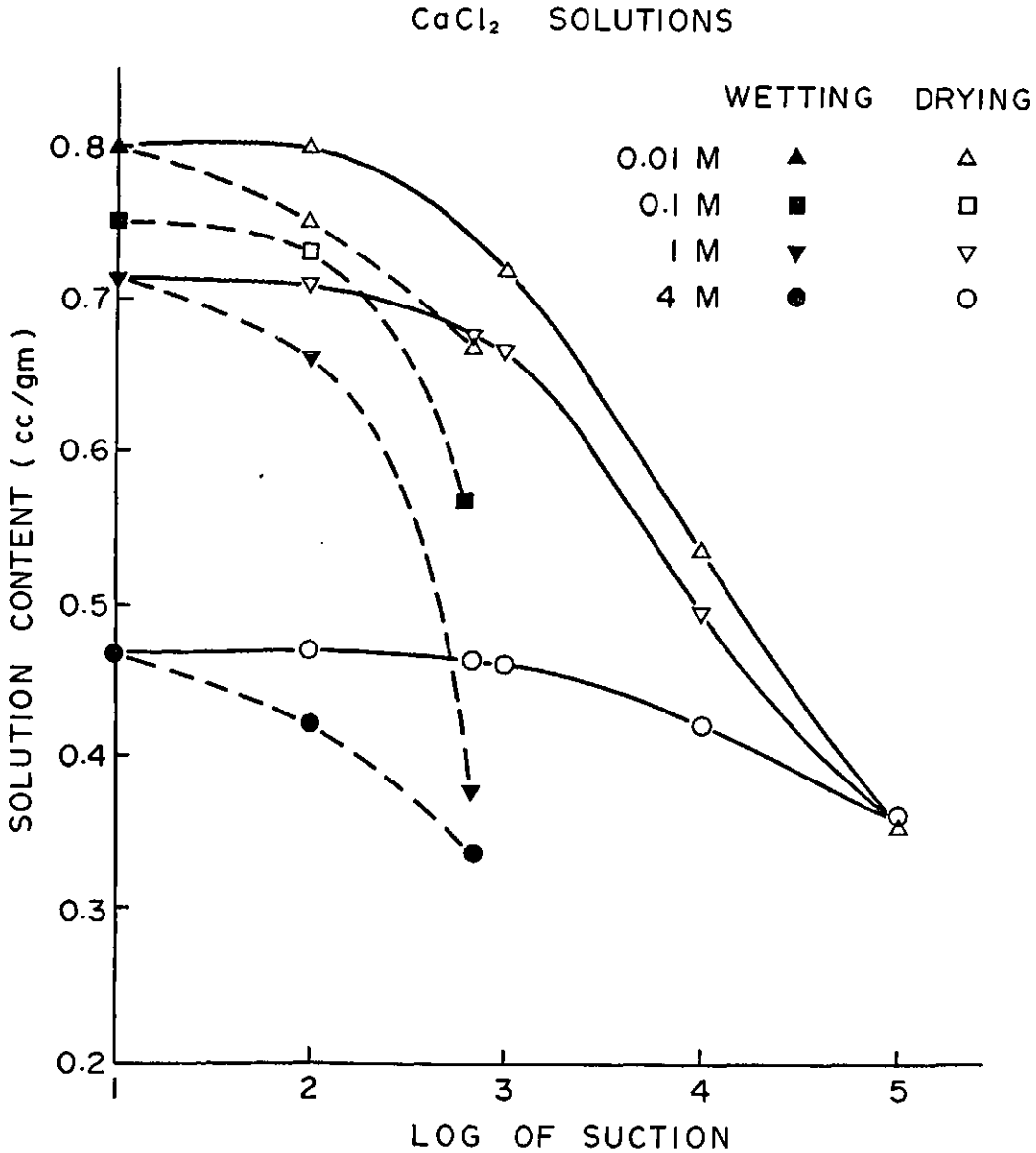

Figure 2.16 Effect of Hydrostatic Suction and CaCl Concentration on the Solution Content of Ca2+ Montmorillonite Cores (Aylmore and Quirk 1962)

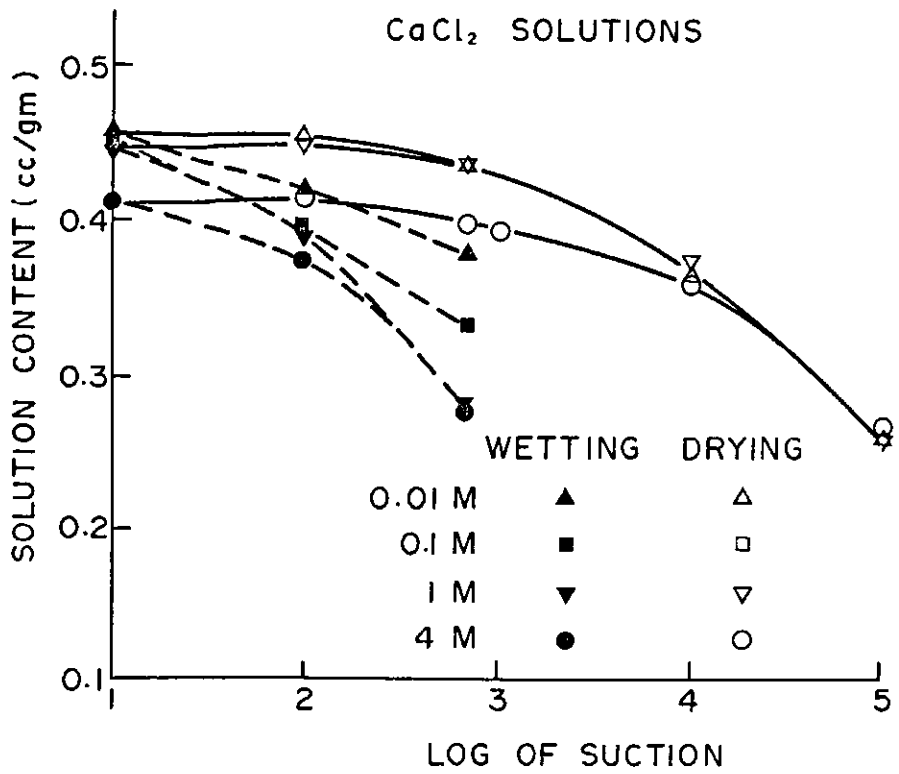

Figure 2.17 Effect of Hydrostatic Suction and CaCl Concentration on the Solution Content of Ca2+Illite Cores (Aylmore and Quirk 1962)

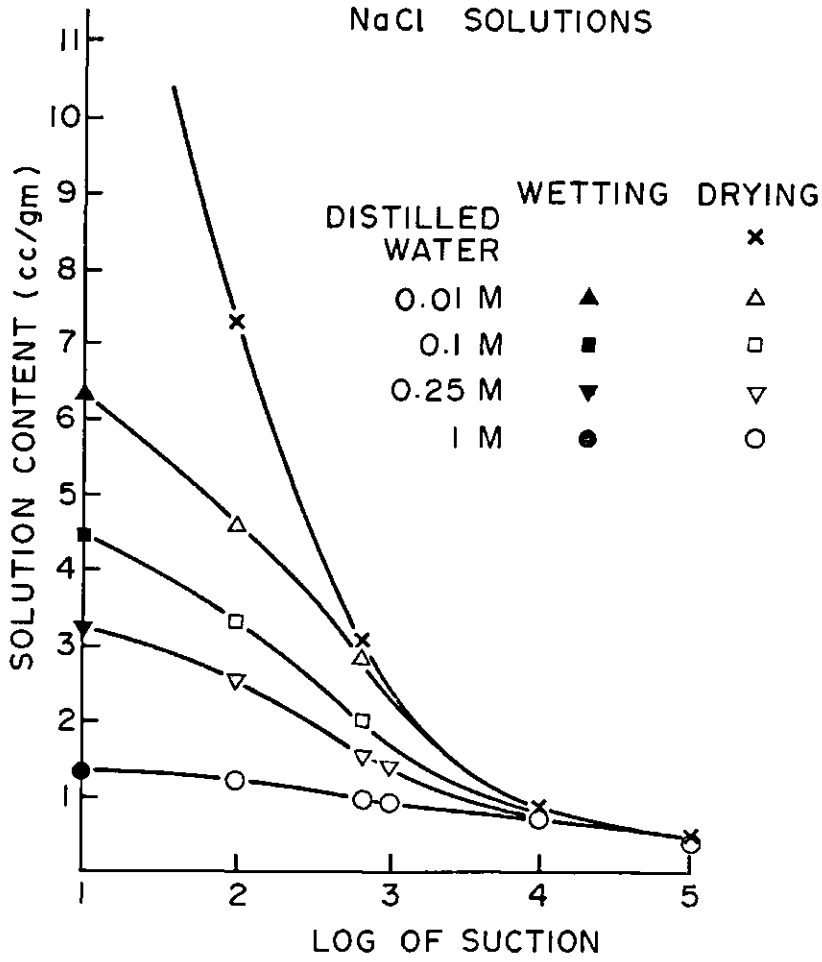

Figure 2.18 Effect of Hydrostatic Suction and NaCl Concentration on the Solution Content of Na+ Montmorillonite Cores (Aylmore and Quirk 1962).

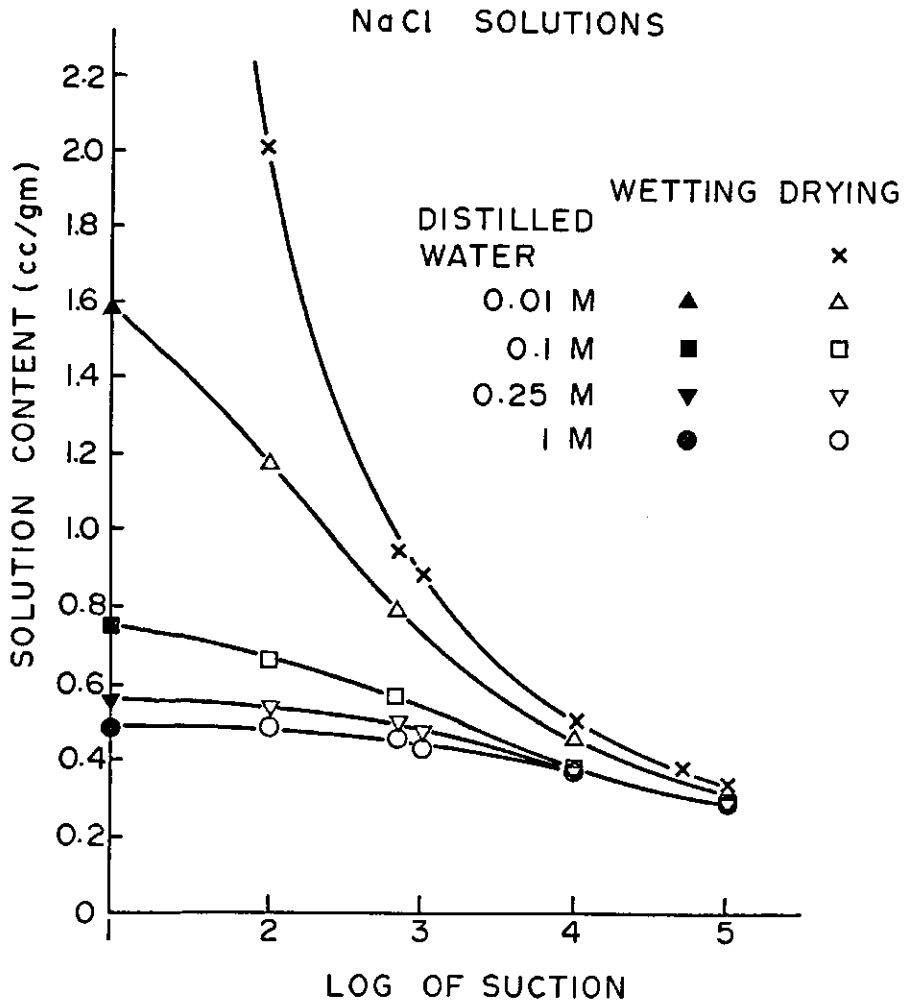

Figure 2.19 Effect of Hydrostatic Suction and NaCl Concentration on the Solution Content of Na2+ Illite Cores (Aylmore and Quirk 1962)

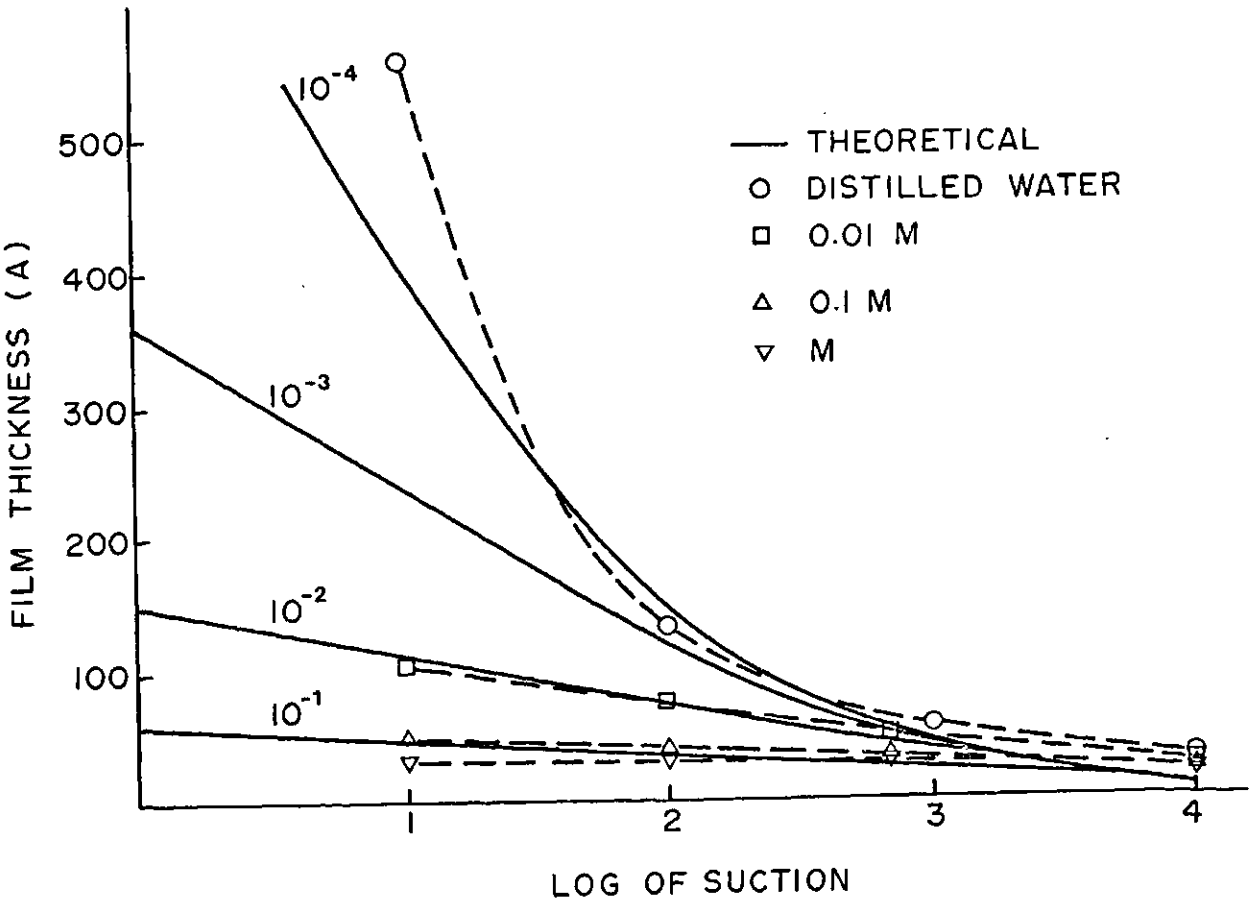

Figure 2.20 Comparison of Calculated and Theoretical Film Thicknesses for Na+ Illite Cores (Aylmore and Quirk 1962)

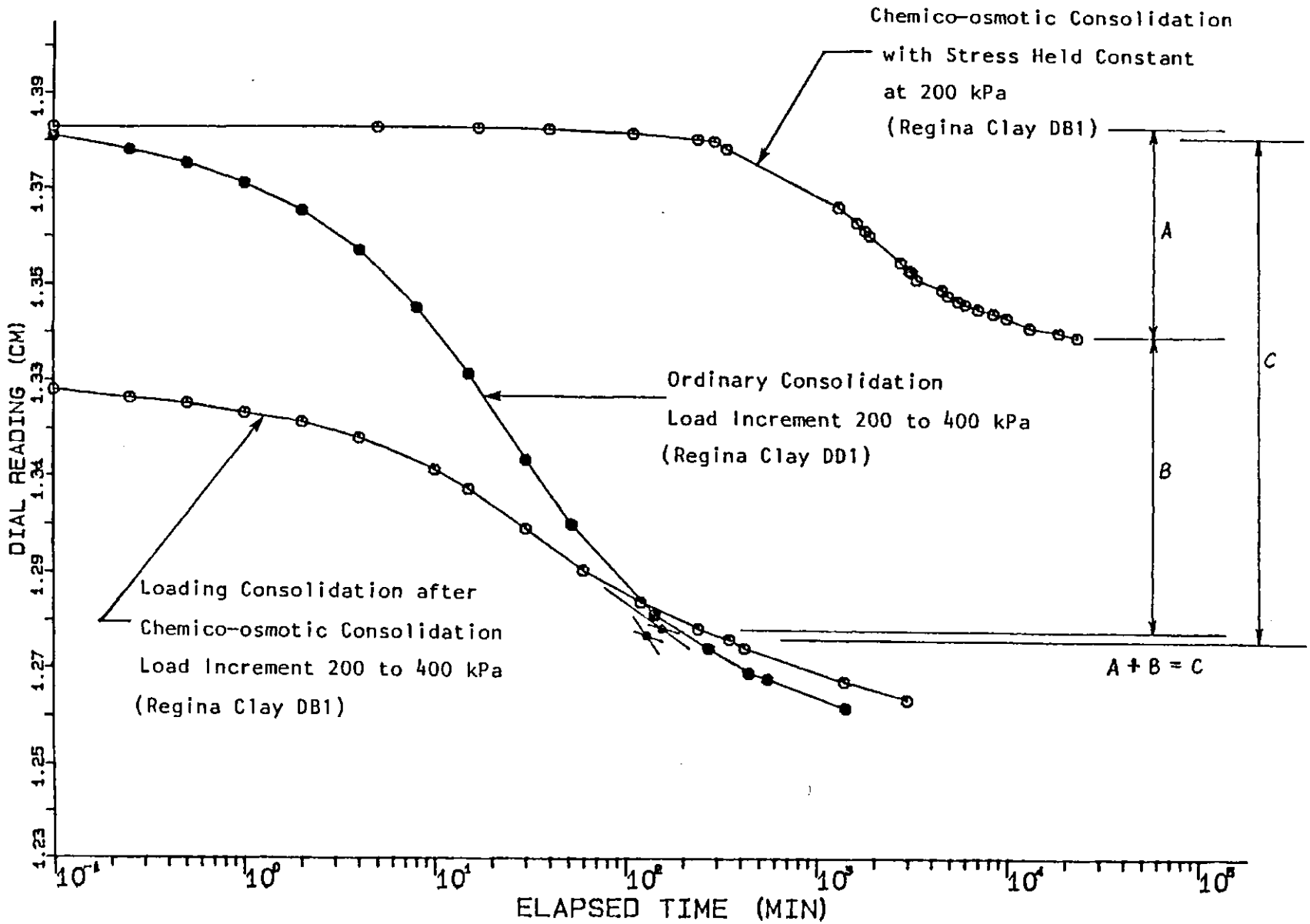

Figure 2.21 Effective Stress and Osmotic Consolidation of Regina Lake Clay (Ho 1985)

Parallel Alignment of Particles

Even in an ideally dispersed clay in which the clay particles are in parallel alignment, the individual clay particles may not be paired evenly. This results in a terraced structure of the clay particles which in turn results in "dead" pore volumes which are unaffected by the diffuse double layers. Bolt (1956) and others have suggested this as the primary source of deviations of the measured from the predicted compressibilities. Also related to this postulate is the fact that the prediction becomes poor for soil systems in which any of the larger particles sizes, 0.2 to 0.002 mm are included (Mitchell 1973).

Calculation of Void Ratio

The interparticle half-spacing, d can be related to the void ratio by the following relationship:

$$d = e / Gs\ As \qquad [2.14]$$

where; 2d = inter-particle spacing
e = void ratio
Gs = specific gravity of the solids
As = specific surface of the solids.

It has been shown by Norrish (1954) and Blackmore and Miller (1962) that in the presence of the Ca cation, montmorillonite clay particles are bound into packets. Consequently, the assumption of fully developed diffuse double layers around each individual particle is no longer valid. The influence of packet formation in producing deviations in behavior from that predicted by double diffuse layer theory has been discussed by Klausner and Shainberg (1967,1971), Quirk (1963), Aylmore and Quirk (1962) and Blackmore and Miller (1962).

Aylmore and Quirk (1962) and Quirk (1963) suggest that in the presence of high concentrations or applied stress, gel structures may be formed in clays containing divalent cations. These gel structures occur due to the dominance of attractive forces over repulsive forces. The double layer theory then plays a significant role in explaining the

behavior of monovalent but not divalent clay systems. Divalent clay systems being dominated by the influence of mechanical rather than physio-chemical forces on the gel structure.

For systems containing mixed valence cations, two models for calculating the influence of the diffuse double layer have been proposed. These are the mixed ion model and the de-mixed model (Mitchell 1973).

The mixed ion model modifies the osmotic pressure concept in light of the effect of mixed ions on the double diffuse layer. The model of Collis-George and Bozeman (1970) is an example of this approach. This model assumes that ions of all species are distributed uniformly over the individual clay surfaces, in proportion to the amounts present. The evidence for packet formation in clays, however, suggests that some cations are bound between clay particles internally within the packet. In the de-mixed model it is assumed that the Ca and Na present in the system are separated into distinct regions of the clay structure. Ca being present on the internal surfaces of the packets, and Na adsorbed onto the external surfaces. In addition, it is assumed that the external surfaces of the packets then interact according to diffuse double layer theory.

Mitchell (1976) presents a summary, as adopted from Fink, Nakayama and McNeal (1971), as to which of the two models is appropriate, based on the exchangeable sodium percentage (ESP) of the soil. This summary is shown in Table 2.2.

If the number of clay particles that are bound up within each packet can be estimated accurately, predictions of swelling pressure or compressibility of these clays can be made, based on the osmotic pressure concept (Klausner and Shainberg 1971, Balasubramonian 1972, Chattopadhyay 1972). The number of particles bound in the packet structure will change, however, with pore fluid concentration and confining stress.

Table 2.2 Classification of Mixed Cation Systems (Mitchell 1976)

ESP > 50%	Random mixing of Na+ and Ca++ unlimited swelling between all plates on water mixing
10% < ESP < 50%	De-mixing on interlayer exchange sites, with progressively more sets of plates collapsing to a 20 A repeat spacing with decrease in ESP
ESP < 10 to 15%	Interlayer exchange complex is predominantly Ca-saturated; Na ions on external planar and edge sites.

Figure 2.22 from Klausner and Shainberg (1971) illustrates the changes in compressibility that occur in a clay with varying degrees of packet formation. The inter-domain spacing can be approximated as follows (Shainberg et al 1971):

$$d' = N\,V / W\,As - do\,(N-1)/W \qquad [2.15]$$

where; $2d'$ = inter-domain spacing
N = number of particles in packet (4 to 9)
V = volume of water
W = dry weight of clay
As = specific surface
$2do$ = half spacing between platelets in packet (4.5 Angstroms)

Shainberg et al (1971) obtained good agreement between a theoretical and experimental swelling curve for a mixed ion solution when the interparticle spacing is calculated using the above equation. The best agreement was obtained when N was taken equal to 3 at low pressures and 5 at high pressures.

Predictions of the repulsive force between clay particles have also been shown to be in good agreement with experimental data when the presence of packets was taken into account.

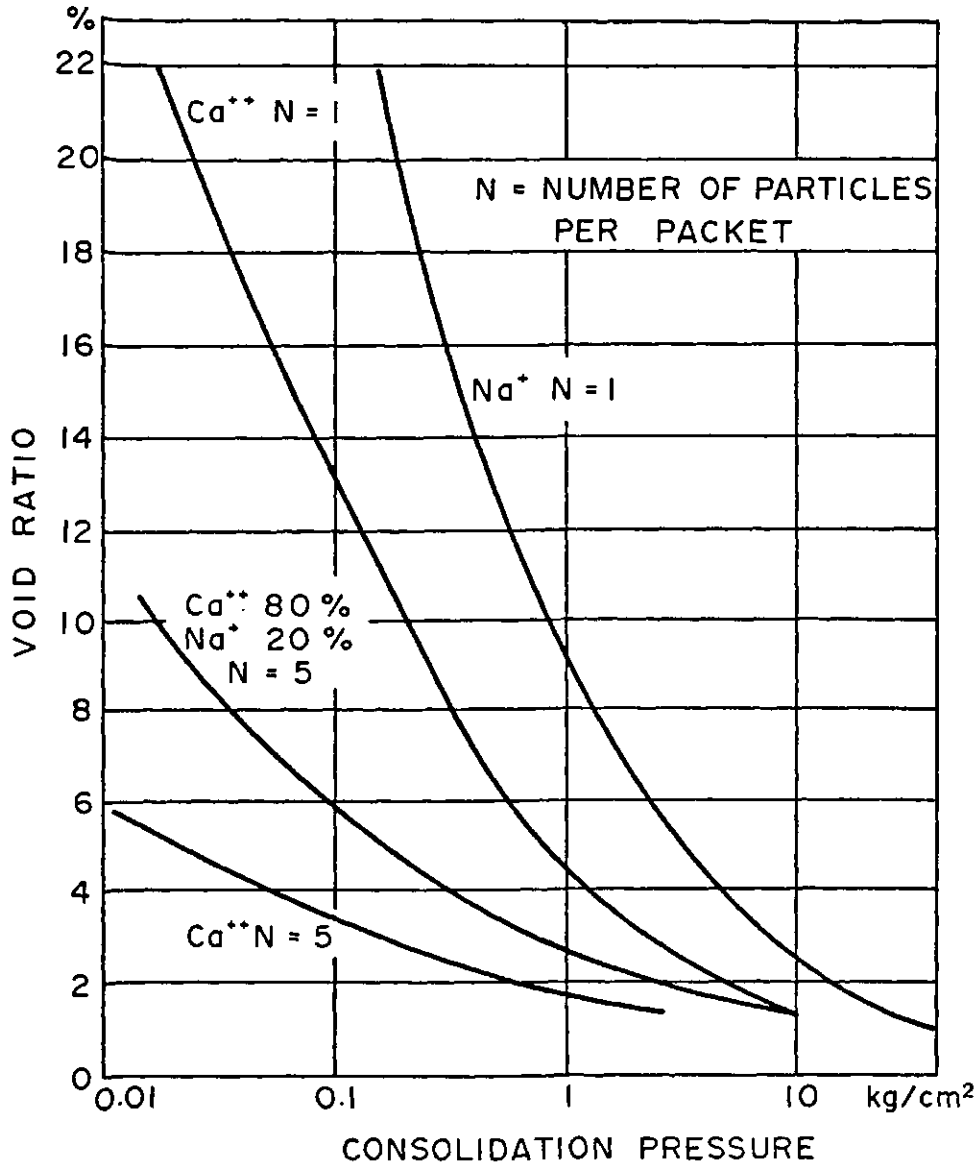

Figure 2.22 Void Ratio versus Consolidation Pressure for Montmorillonite Clay (Co = .001 M) (Klausner and Shainberg 1971)

Table 2.3 illustrates the results obtained by Morgenstern and Balasubramonian (1980) for the measured swelling pressure and the predicted interparticle repulsive force calculated after correcting the interparticle spacing for the presence of packets.

Following a comprehensive review of the influence of pore fluid chemistry and mineralogy on the swelling behavior of clays, Mitchell (1973) presents this conclusion:

> "Double layer repulsions can account reasonably well for the swelling behavior of sodium montmorillonite, and possibly also for that of calcium montmorillonite, provided account is taken of the water and area associated with the internal surfaces of multi-plate tactoids." (or packets)

In spite of the many limitations, the development set forth by the osmotic pressure concept does provide an understanding of the role of the bulk solution concentration on volume change. Chapter 3 develops this relationship further in linking changes in the osmotic pressure of the bulk solution to changes in the stress state variables controlling volume change of clays.

Table 2.3 Observed and Predicted Values of Double Layer Repulsion, Bearpaw Shale (Morgenstern and Balasubramonian 1980)

Swell %	Water Content %	$\bar{d}$ A	(R-A) Observed tsf	(MPa)	(R-A) Predicted tsf	(MPa)
0	30.5	26.3	-	-	0.70	(0.067)
2	32.3	27.8	0.66	(0.063)	0.58	(0.056
4	34.1	29.4	0.57	(0.055)	0.48	(0.046)
6	35.9	31.0	0.47	(0.045)	0.40	(0.038)
8	37.7	32.5	0.44	(0.042)	0.32	(0.031)

Notes:

Concentration of original pore water	0.13N
Concentration of cell water for 1-4-WF4-pw	0.15N
(R-A) for 1-4-WF4-pw	0
Concentration of cell water for 1-4-CH5-dw	$0.02N_o$
X_o	3.68 A
Effective specific surface	116 m^2/g

2.5 Interparticle Stresses- True Effective Stress

The behavior of a soil mass is in response to changes in stress that are transmitted directly to the particle contacts. The nature of these interparticle stresses between the grain contacts may be long range or short range. Long range stresses of repulsion and attraction include the electrostatic stresses (ie stresses resulting from double diffuse layer effects) and van der Waals stresses. Short range repulsive stresses may also include Born repulsion and surface hydration, and short range attractive stresses may include electrostatic attraction and primary valence and cementation bonds (Bailey 1965, Mitchell 1976).

From an engineering perspective it is not adequate to deal with these forces at a microscopic level. Macroscopic, measurable stresses have to be postulated in order to facilitate the development the proper relationships for volume change and shear strength. The use of a macroscopic definition of "effective stress",(i.e., equal to the difference between total stress and pore-water pressure), has been proven extremely useful in describing the stress conditions controlling the behavior of saturated soils.

For clay soils, in which physio-chemical effects may influence the interparticle contact stresses, a number of researchers have suggested incorporating the net electrostatic repulsive minus attractive stresses (i.e., R-A) between the clay particles into the definition of a true effective stress (Lambe 1958, 1960, Mitchell 1972, Bailey 1965, Balasubramonian 1972, Chattopadhyay 1972, Fredlund 1981, Sridharan and Rao 1973, 1979).

Lambe (1960) developed a stress equation based on static equilibrium of normal forces perpendicular to a wavy plane that does not pass through the soil particle.

This equation is written as follows:

$$\sigma_n = \sigma_c \, a_m + u_w \, (1 - a_m) + (R - A) \qquad [2.16]$$

where: σ_n = total normal stress
σ_c = average contact stress acting over am
a_m = ratio of mineral to mineral contact to the unit area
u_w = pore-water pressure
R-A = interparticle stress due to physio-chemical interactions

The wavey plane model of Lambe (1960) provides a statement of the equivalence of stress; however, it is not a true free body diagram. Consequently it is an inappropriate technique by which to obtain the stress state variable for the soil.

Balasubramonian (1972) and Chattopadhyay (1972) suggest that the pore-pressure should be considered to act across the entire surface of the wavy plane. The pore pressure is also to be taken to be equal to the piezometric pressure. The piezometric pressure was defined by Mitchell (1962) to be that pore-pressure measured by a piezometer containing exactly the same pore fluid as that existing within the pores. Balasubramonian (1972) and Chattopadhyay (1972) give the following equation for the true effective stress:

$$\sigma^* = \sigma_n - u_w - (R - A) \qquad [2.17]$$

where: $\sigma^* = \sigma_{n'} - (R - A)$

$$\sigma_{n'} = \sigma_n - u_w$$

Chattopadhyay (1972) demonstrated that the residual shear strength of clays is controlled by the true effective stress (σ^*). Balasubramonian (1972) showed that swelling pressures (ie., $\sigma_{n'}$), which developed in test samples in which volume change was prohibited, were equivalent to the change in (R-A). That is, when no volume change is permitted, the net change in the true effective stress is zero, although the components of effective stress and interparticle physio-chemical interactions may vary.

CHAPTER 3

THEORETICAL DEVELOPMENT

3.1 General

A complete understanding of the time dependant volume change of a clay soil when exposed to electrolyte solutions requires that a complete description of osmotic flow, salt transport, and osmotic and osmotically induced consolidation be developed. Formulations for osmotic flow combined with salt transport (section 2.3.5), and osmotically induced consolidation (section 2.4.1) have been developed in the literature. A general formulation for osmotic flow and volume change, incorporating the effects of osmotic consolidation, does not appear to have been developed previously in the geotechnical literature.

This chapter provides a theoretical description of flow and volume change in saturated clays subjected to osmotic phenomena. A continuum mechanics approach is utilized to relate volume changes in the soil to changes in stress state variables through constitutive relationships. The phenomenological approach is used to describe the coupled flow of pore fluid and dissolved salt.

In the continuum mechanics of multiphase mixtures the behavior of each phase is dictated by the forces acting on that phase. Force gradients on the solid phase produce deformation of the soil structure, whereas, force gradients acting on the liquid phase produce flow.

The continuum mechanics approach described by Fredlund (1973) consists of four steps:

1. The description of the physical element. Bear (1972) describes this as the representative elementary volume.

2. The establishment of the state variables associated with each phase.

3. The proposal of suitable constitutive relationships.

4. The formulation of the partial differential equations for the engineering problem of interest, utilizing the laws of conservation of mass and energy.

Section 3.2 provides a description of the physical element or representative elementary volume. Section 3.3 and 3.4 describe the Stress State Variables (SSV) and the Deformation State Variables (DSV). A constitutive relationship for osmotic volume change is proposed in section 3.5. The formulation of the coupled, transient flow problem is developed in section 3.6.

3.2 Description of the Elementary Volume

An element of saturated soil can be considered as a three phase system consisting of the soil particles, the pore fluid, and the diffuse double layer or adsorbed fluid hull surrounding each soil particle (Figure 3.1). The diffuse double layer includes the surface charge along the clay particles. By definition, a phase must possess differing properties from the contiguous homogeneous phases and must have a continuous bounding surface throughout the element. The unique properties of the double diffuse layer have been documented by Mitchell (1976). The existence of a distinct boundary surface is not as well defined but the extent of the adsorbed fluid phase is described by double layer theory.

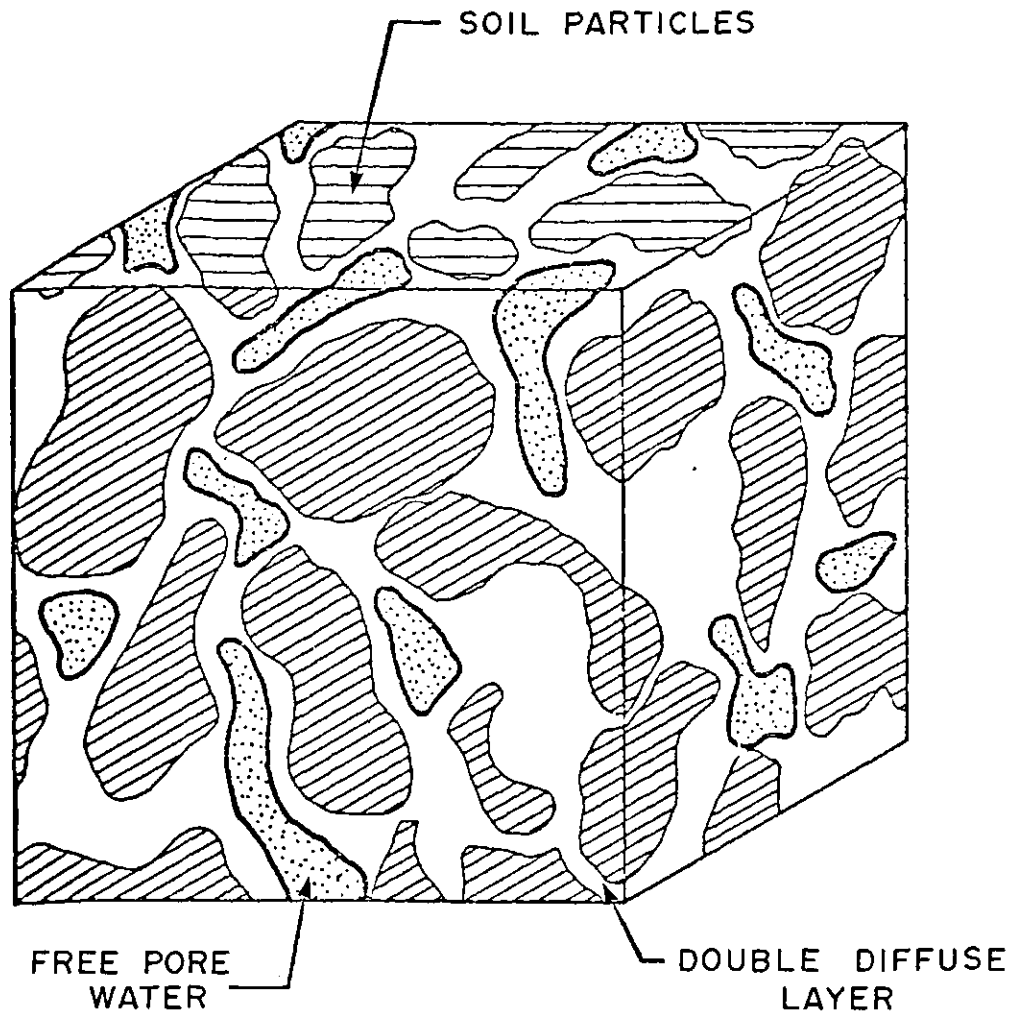

Figure 3.1 Element of Saturated Soil Illustrating the Double Diffuse Layer (after Fredlund 1973)

The porosities of each phase of the elementary volume may be defined as follows:

n_p = volume of soil particles / total volume

n_f = volume of bulk pore fluid / total volume

n_d = volume of diffuse double layer / total volume

The sum of the phase porosities is equal to unity.

3.3 Stress State Variables

Force equilibrium for the element is ensured by considering equilibrium for each phase independently. The elemental forces consist of surface tractions, gravity body forces and interaction forces between the phases. The interaction body forces between the phases are as follows:

F_f = interaction force between the double diffuse layer and pore fluid

F_d = interaction force between the soil particles and the double diffuse layer

Figures 3.2 through 3.4 illustrate the equilibrium stress systems acting on the overall element and the diffuse double layer and bulk pore fluid phases.

The assumption is made that the electrostatic interactions between particles can be described by the net repulsive minus attractive stress (R-A) acting within the double diffuse layer. A second assumption is that when (R-A) is expressed as a stress tensor (R-A) it is isotropic and does not contain shear stresses. The density of the double diffuse layer is assumed to be equal to the density of the pore fluid.

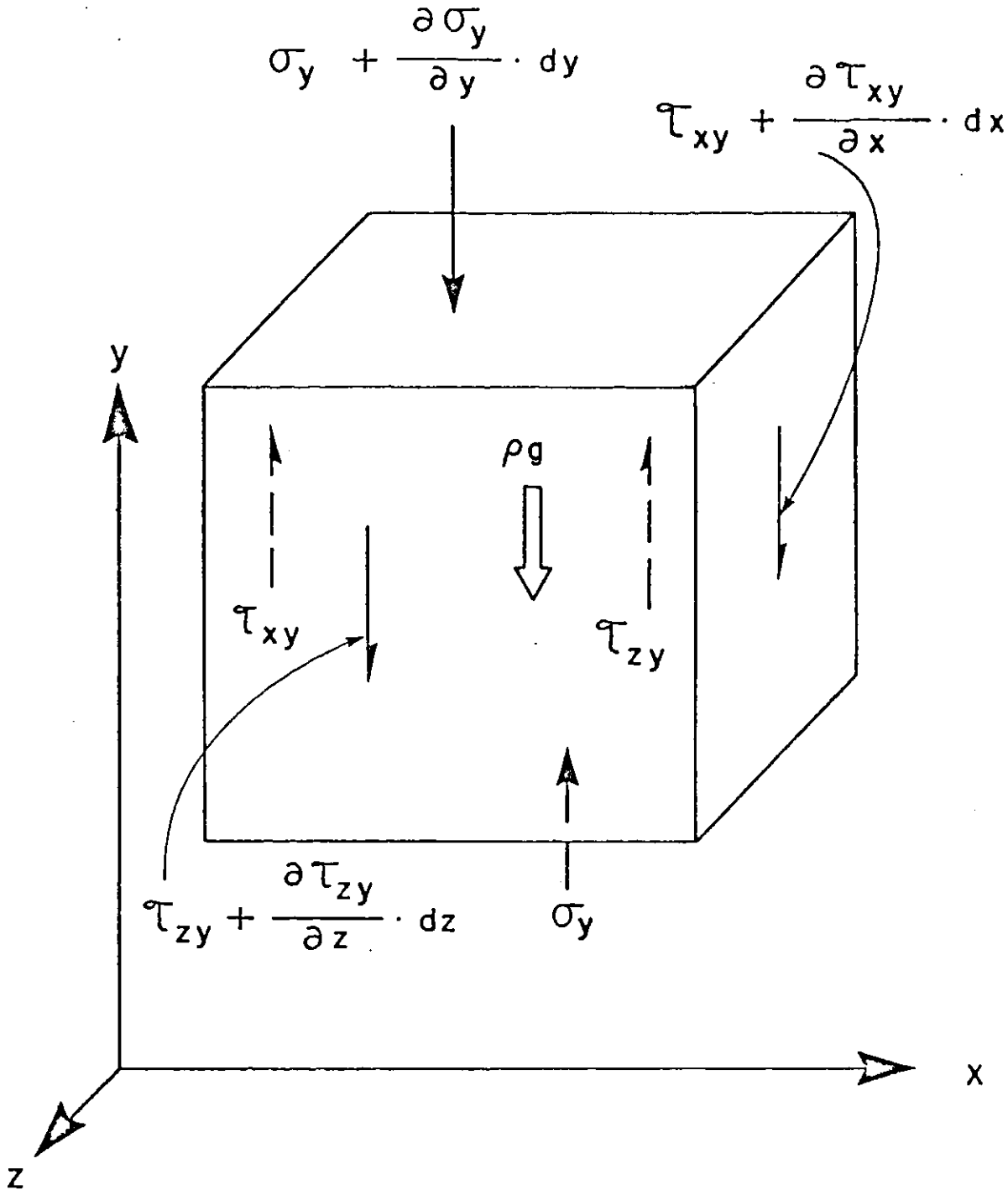

Figure 3.2 Total Stress Equilibrium for an Element of Saturated Soil

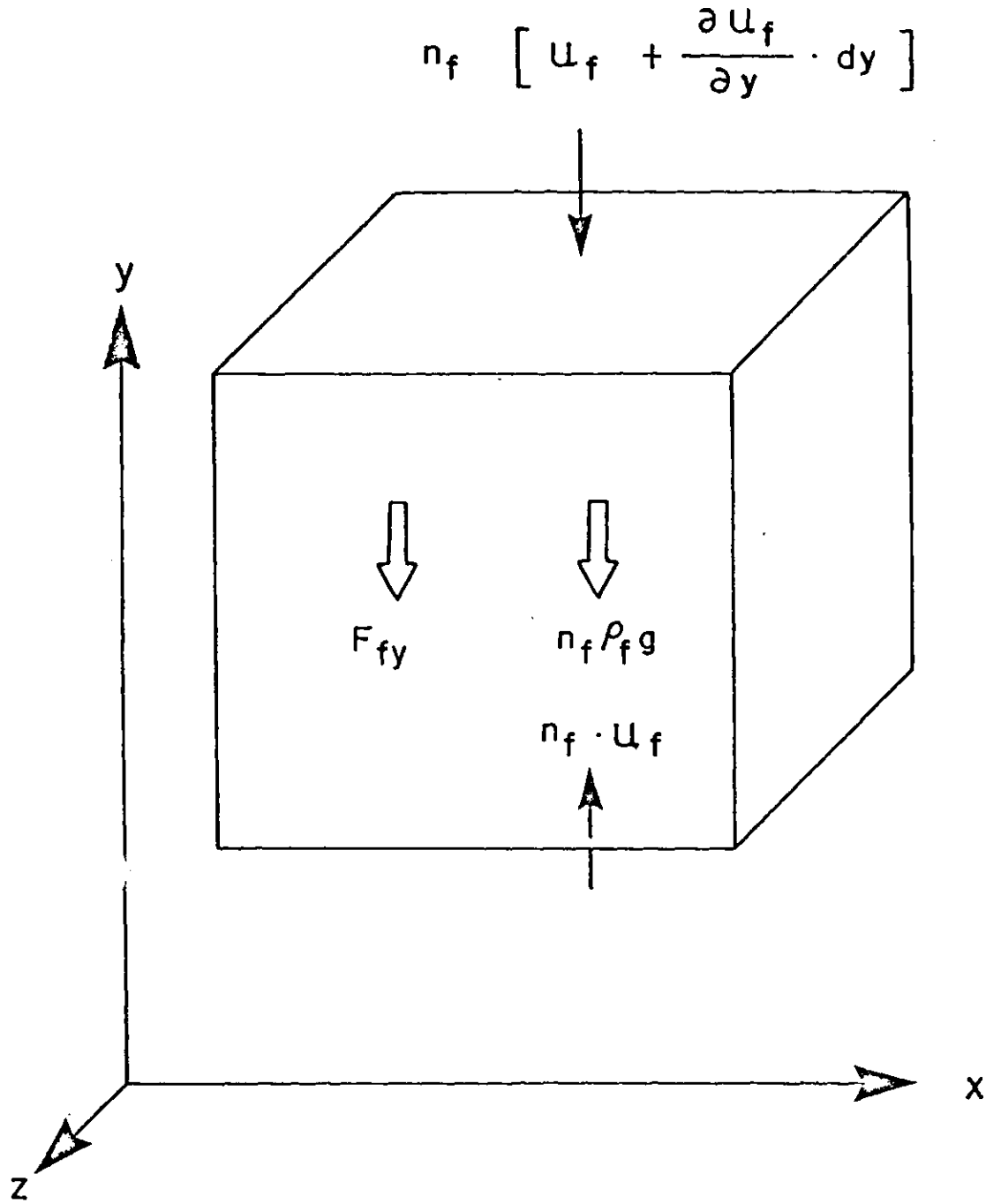

Figure 3.3 Pressure Equilibrium for the Fluid Phase

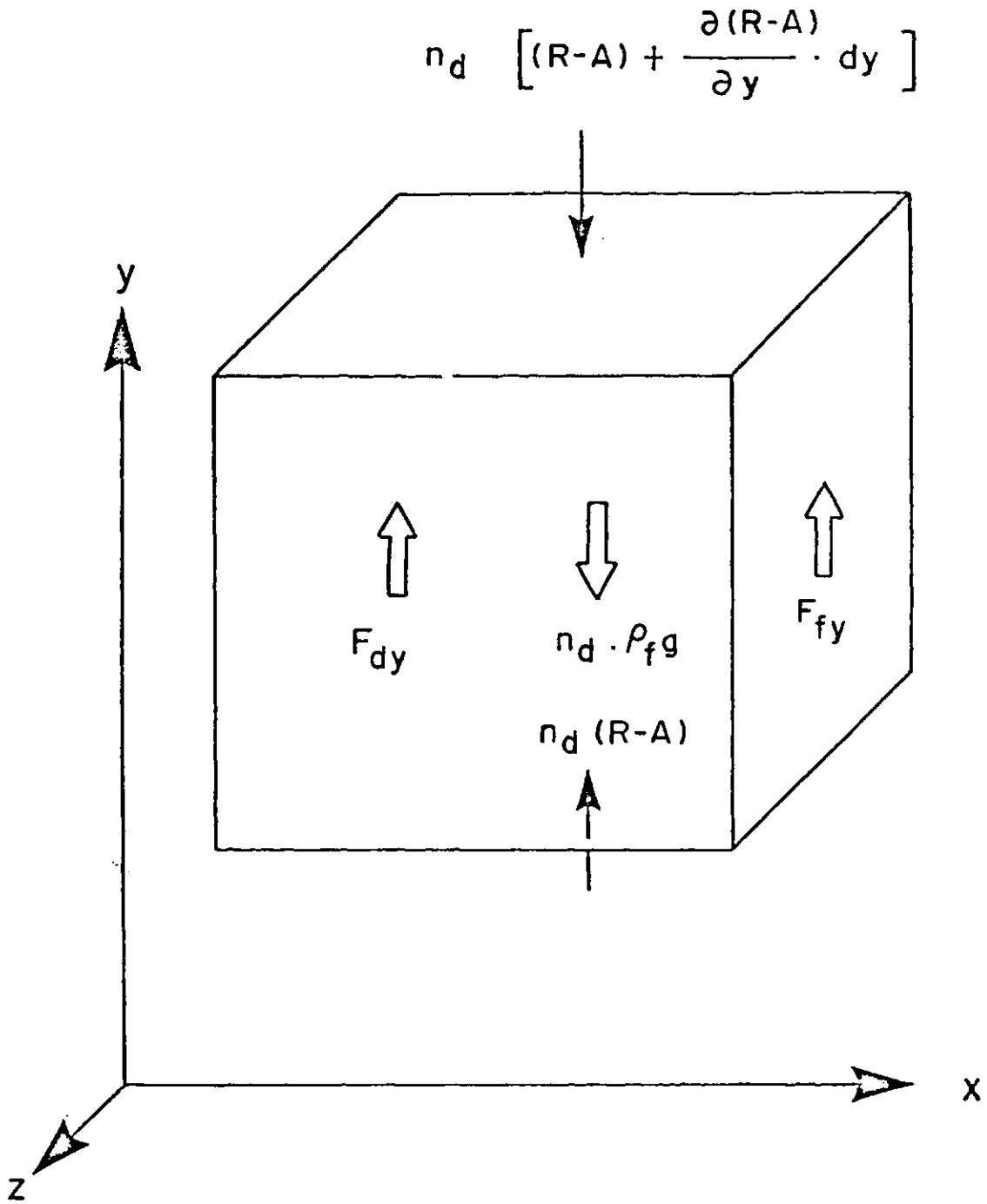

Figure 3.4 Stress Equilibrium for the Adsorbed Double Diffuse Layer

Equilibrium equations can be written for the overall soil element as well as for each phase. A one-dimensional form of these equilibrium equations are written as follows:

Overall Element:

$$\partial\tau_{xy}/\partial x + \partial\sigma_y/\partial y + \partial\tau_{zy}/\partial z + \rho_t g = 0 \qquad [3.1]$$

Pore Fluid:

$$\partial u_f/\partial y - F_f/n_f + \rho_f g = 0 \qquad [3.2]$$

Double Layer:

$$\partial(R-A)/y - F_f/n_d - F_d/n_d + \rho_f g = 0 \qquad [3.3]$$

where: σ_y = normal stress in the y-direction
τ_{xy} = shear stress on the x-plane in the y-direction
τ_{zy} = shear stress on the z-plane in the y-direction
u_f = pore fluid pressure
ρt = total density of the soil
ρf = fluid density

Equations [3.1] through [3.3] are statements of equilibrium for the overall element, the pore fluid, and the adsorbed double layer.

Volume change of the soil structure is controlled by the interparticle interactions between the soil particles, however these interactions cannot be measured directly. An equation for the effective stresses at the interparticle contacts can be written as the difference between the statement of equilibrium for the entire element, and those for the pore fluid and double layer phases. This equation is then written as follows:

$$\partial\tau_{xy}/\partial x + \partial(\sigma_y - u_f - (R-A))/\partial y + \partial\tau_{zy}/\partial z - F_f/n_f \qquad [3.4]$$

$$+Fd/n_d + F_f/n_d + \rho_t g - 2\rho_f g = 0$$

Similar expressions may be written for the other coordinate directions. From these equations the stress state variables may be selected as illustrated in matrix form below:

$$\begin{bmatrix} \sigma_x - u_f - (R-A) & \tau_{xy} & \tau_{xz} \\ \tau_{yx} & \sigma_y - u_f - (R-A) & \tau_{yz} \\ \tau_{zx} & \tau_{zy} & \sigma_z - u_f - (R-A) \end{bmatrix} \quad [3.5]$$

The stress state variable $(\sigma - u_f - (R-A))$, can be extracted from equation [3.5]. This is a similar expression to that of the "true" effective stress proposed by Balasubramonian (1972) and Chattopadhyay (1972). Alternatively, the matrix equation [3.5], could be written as two separate matrices as follows:

$$\begin{bmatrix} \sigma_x - u_f & \tau_{xy} & \tau_{xz} \\ \tau_{yx} & \sigma_y - u_f & \tau_{yz} \\ \tau_{zx} & \tau_{zy} & \sigma_z - u_f \end{bmatrix} - \begin{bmatrix} (R-A) & & \\ & (R-A) & \\ & & (R-A) \end{bmatrix} \quad [3.6]$$

From this form of equation, two separate stress state variables may be selected. The first is the effective stress for a saturated soil, $(\sigma - u_f)$. The second stress state variable is the net interparticle repulsive minus attractive force, (R-A). The use of two separate stress state variables is preferable if changes in (R-A) are not as effective in producing volume change as are changes in the effective stress.

There are two requirements which need to be met in order to accept a particular combination of stresses as a single stress state variable. One is that the elements of the stress state variable must be equally effective in

producing behavioral changes within the soil mass. Fredlund (1973) demonstrated that a null type test could be used to confirm the correct components for the stress state variables for unsaturated soils. Testing by Balasubramonian (1972) and Chattopadhyay (1972) demonstrated that if (R-A) could be estimated, the changes in the effective stress were equal to changes in (R-A), when the volume of the sample was maintained constant.

Indirect evidence of the equivalency of the effective stress and (R-A) components of true effective stress was also described for ideal clay systems in Chapter 2.

The second requirement for the stress state variable, however, is that the individual components of stress state variable can be measured. For example in saturated soils, the use of effective stress requires that both the total stress and the pore fluid pressure be measurable quantities. Although the measurement of total stress is straight forward, Mitchell(1962) suggests that the actual pore pressure between clay particles is unknown. An approximate measure of the appropriate pore fluid pressure, however, can be taken to be the piezometric pressure. The piezometric pressure is a pressure measured in a piezometer which has a reservoir of similar chemistry to that of the pore fluid, maintained at the same elevation as the soil and in equilibrium with the soil pore fluid (Mitchell 1962). In practice differences between the actual pore fluid pressure and the measured piezometric pressure have been compensated for in the material properties describing volume change or shear strength.

In the case of true effective stress, it is not possible to measure (R-A) directly. The prediction of (R-A) is possible only under ideal conditions. This is a severe restriction to the use of (R-A) as a component of the stress state variable. However, it may be possible to obtain indirect estimates of this component. Because of this, it

may be necessary that a deduced quantity, which is more easily measured than (R-A), be used.

The osmotic pressure concept relates the change in repulsive stress between clay particles, to the osmotic pressure difference between the interparticle fluid and the bulk external fluid.

Mitchell (1962) suggested that "double layer interactions and the consequent repulsion between opposing particles are reflected by the osmotic pressure". The osmotic pressure is described as having two components; one associated with the free salt in the bulk solution and the other caused by the additional ions required to satisfy double layer requirements. The osmotic pressure of the bulk solution can be readily evaluated using samples of the pore fluid, however the difference between the osmotic pressure of the bulk fluid and that between the clay particles cannot be measured directly.

In most practical problems, the change of osmotic pressure is of more interest in regard to the process of osmotic consolidation than the absolute value of the components of osmotic pressure. For problems of osmotic consolidation, changes in the osmotic pressure of the bulk solution will be large relative to the initial osmotic pressure within the sample. Consequently, it is assumed that the osmotic pressure of the bulk solution can be used as an independent stress state variable.

The osmotic pressure of the bulk solution is also the driving force for osmotic flow. Consequently, the use of osmotic pressure as a stress state variable provides for continuity of the stresses in the description of volume change within the soil structure, as well as flow of the pore fluid. The validity of assumptions described in this section are discussed more fully in Chapter 7, in light of the results of the testing program.

3.4 Deformation State Variables

Deformation state variables are required to define the movement of each phase with time. The mass of the multiphase continuum is equal to the sum of the mass of each of the component phases. In a similar manner, the volumetric requirement can be written as:

$$V = \Sigma V_i \quad \text{or} \quad \Delta V/V = \Sigma \Delta V_i/V) \qquad [3.7]$$

where: V = total initial volume of the element
V_i = volume of each phase

For the representative element in this derivation:

$$\Delta V/V = \Delta V_p/V + \Delta V_f/V + \Delta V_d/V \qquad [3.8]$$

where: V_p = volume of the particle
V_f = volume of the bulk fluid
V_d = volume of the diffuse double layer

Assuming that changes in the particle volume are small the volumetric requirement becomes:

$$\Delta V/V = \Delta V_f V + \Delta V_d/V \qquad [3.9]$$

Suitable deformation state variables can be selected as

$\Delta V/V$, $\Delta V_f /V$ and $\Delta V_d/V$. If any two are known, the third deformation state variable can be calculated.

Both ΔV_f and ΔV_d involve fluid flow. Flow from the element which produces a change in the volume of the element will only occur when there is a net difference between V_f and V_d . In engineering problems, it is the change in the volume of the element, and not necessarily the partitioning between the bulk fluid and adsorbed fluid phase, which is of interest. The net flow of fluid from the element is of interest. The net flow of fluid from the soil is measurable, whereas partitioning of fluid flow between the bulk fluid and that contained in the adsorbed layer is not. Consequently the effective deformation state variables are taken as $\Delta V/V$ and $\Delta V_f/V.$, where, ΔV_f is the net change in

fluid volume. For small changes in volume, the latter deformation state variable can be written as $d(V_f/V)$.

3.5 Constitutive Relationship for Volume Change

A general form for the relationship linking the stress state variables and the deformation state variables may be written as follows:

$$\varepsilon = -\Delta V/V = 1/V\,(\,\partial V/\,\partial(\sigma - u_f))d(\sigma - u_f) + 1/V(\partial V/\partial \pi)d\pi \qquad [3.10]$$

where: ε = volumetric strain

This equation takes the form of a three-dimensional constitutive surface as shown in Figures 3.5 and 3.6. These figures are drawn from the theoretical and experimental relationship between void ratio and swelling pressure for different pore fluid concentrations, as presented by Bolt (1956) and Mesri and Olson (1971).

The general shape of two-dimensional surfaces of volume change versus osmotic pressure, taken at various values of constant effective stress, can be visualized from the curves in Figures 3.7 through 3.11. Figures 3.8 through 3.11 are taken from the experimental data of Aylmore and Quirk (1962) presented in Figures 2.16 through 2.19.

Along a plane in which π is constant, the slope of the constitutive surface may be described by the coefficient of volume change, m_v. Along a plane in which $(\sigma - u_f)$ is constant, the slope is defined by the osmotic coefficient of volume change, m_π. The constitutive equation can then be written as:

$$\varepsilon = -dV/V = m_v\, d(\sigma - u_f) + m_\pi\, d(\pi) \qquad [3.11]$$

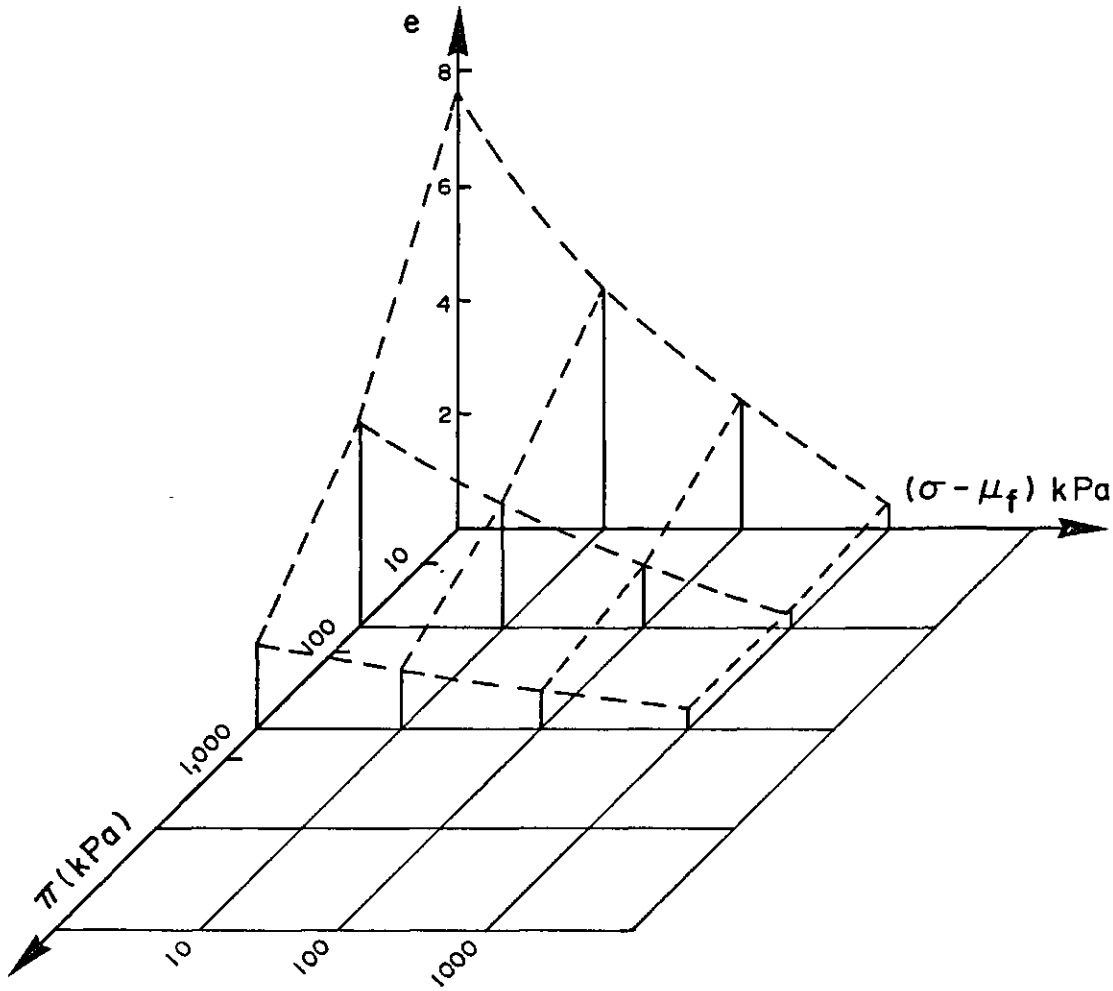

Figure 3.5 Theoretical Constitutive Surface for Na Illite (after Bolt 1956)

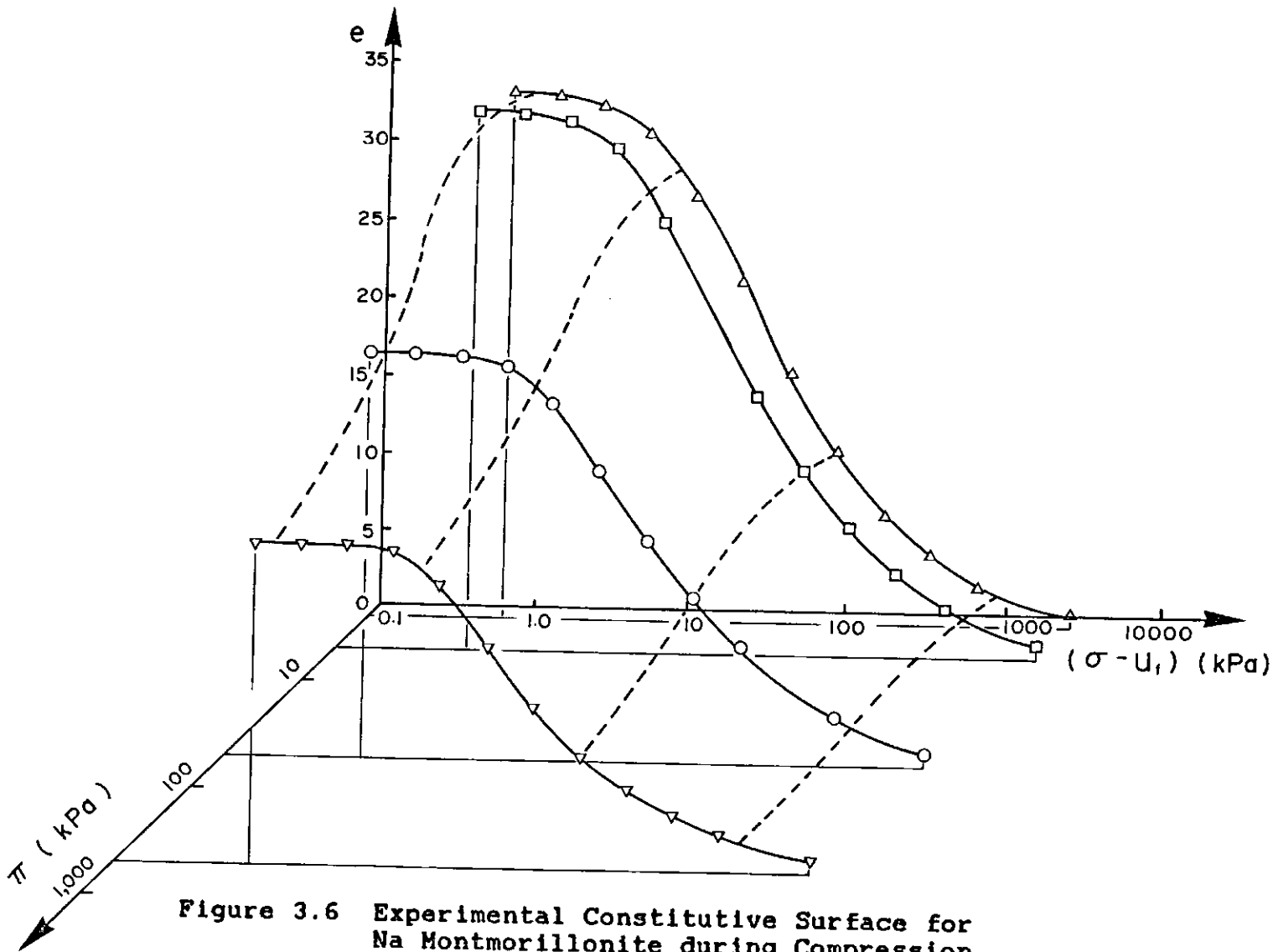

Figure 3.6 Experimental Constitutive Surface for Na Montmorillonite during Compression (after Mesri and Olson 1971)

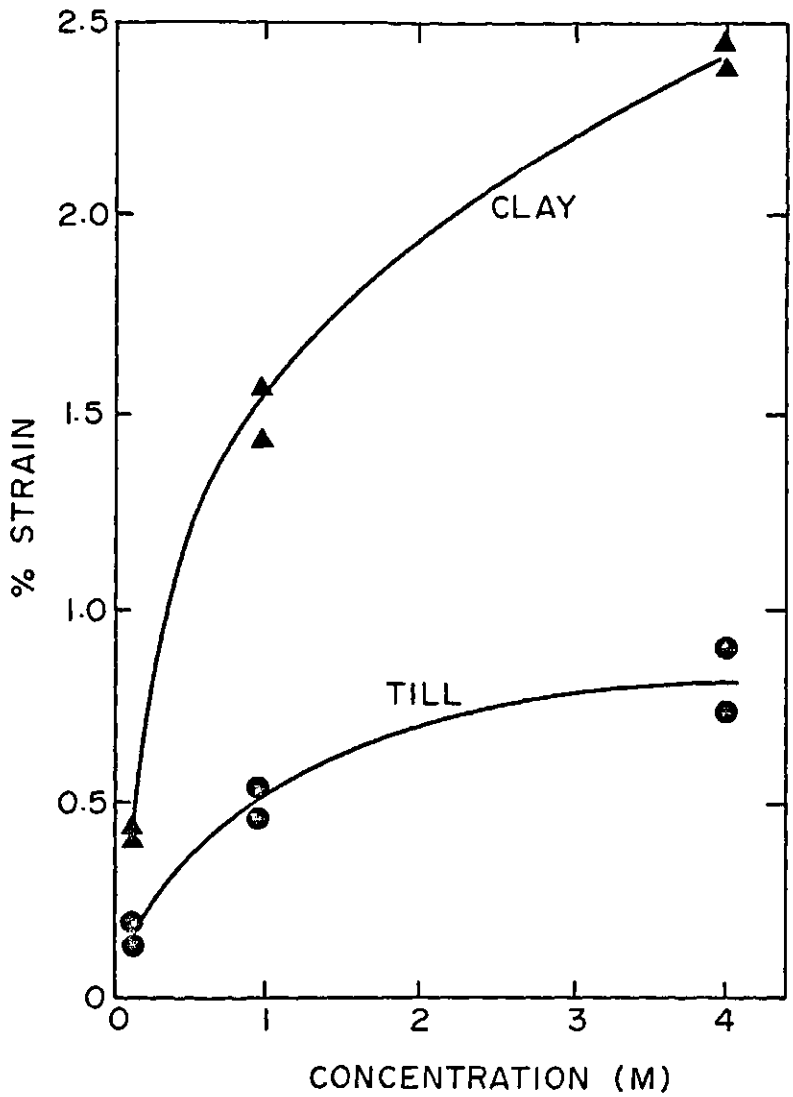

Figure 3.7 Percent Strain due to Osmotic Consolidation (after Ho 1985)

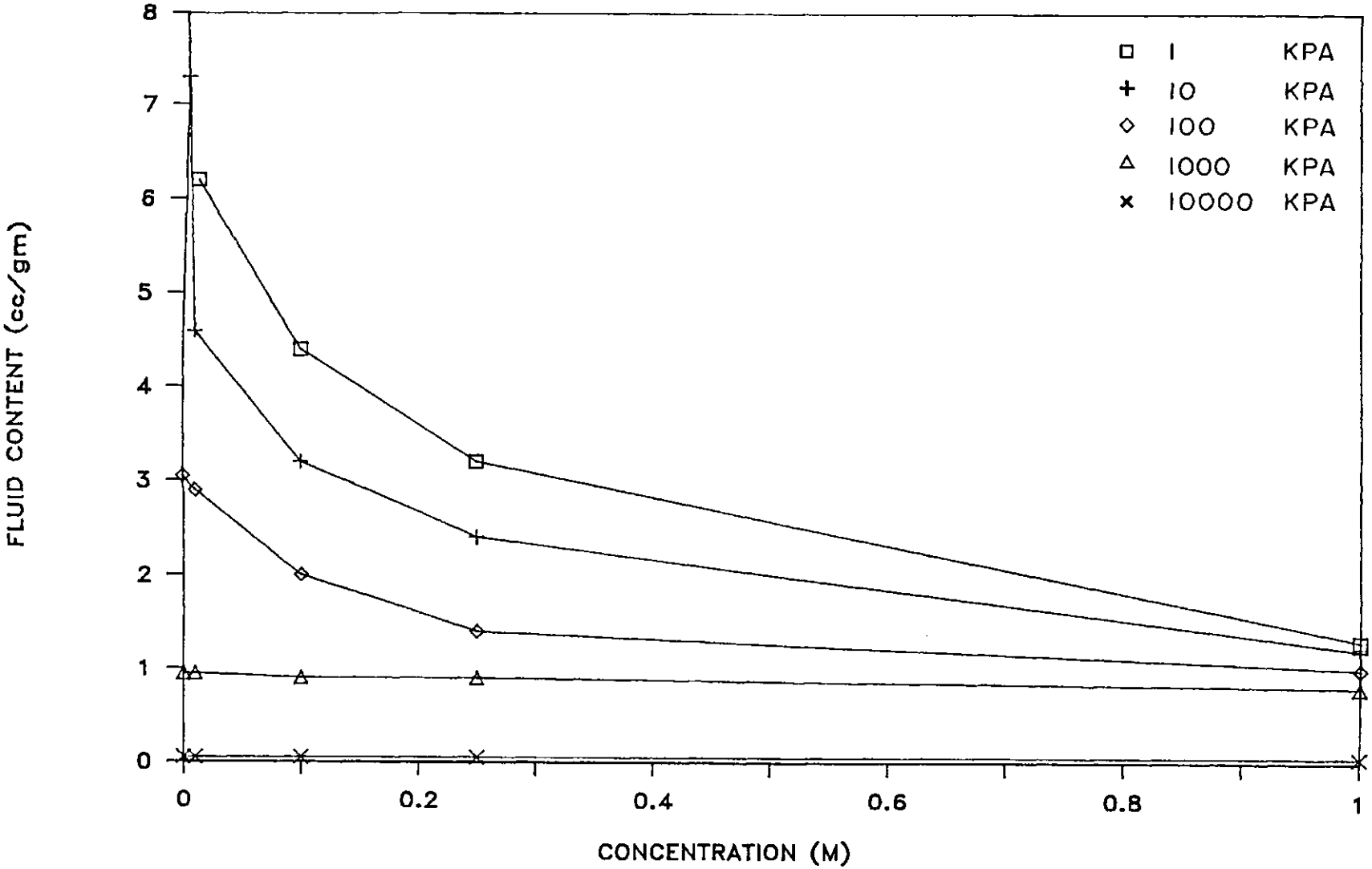

Figure 3.8 Solution Content versus Pore Fluid Concentration for Na Montmorillonite / NaCl Solution (after Aylmore and Quirk 1962)

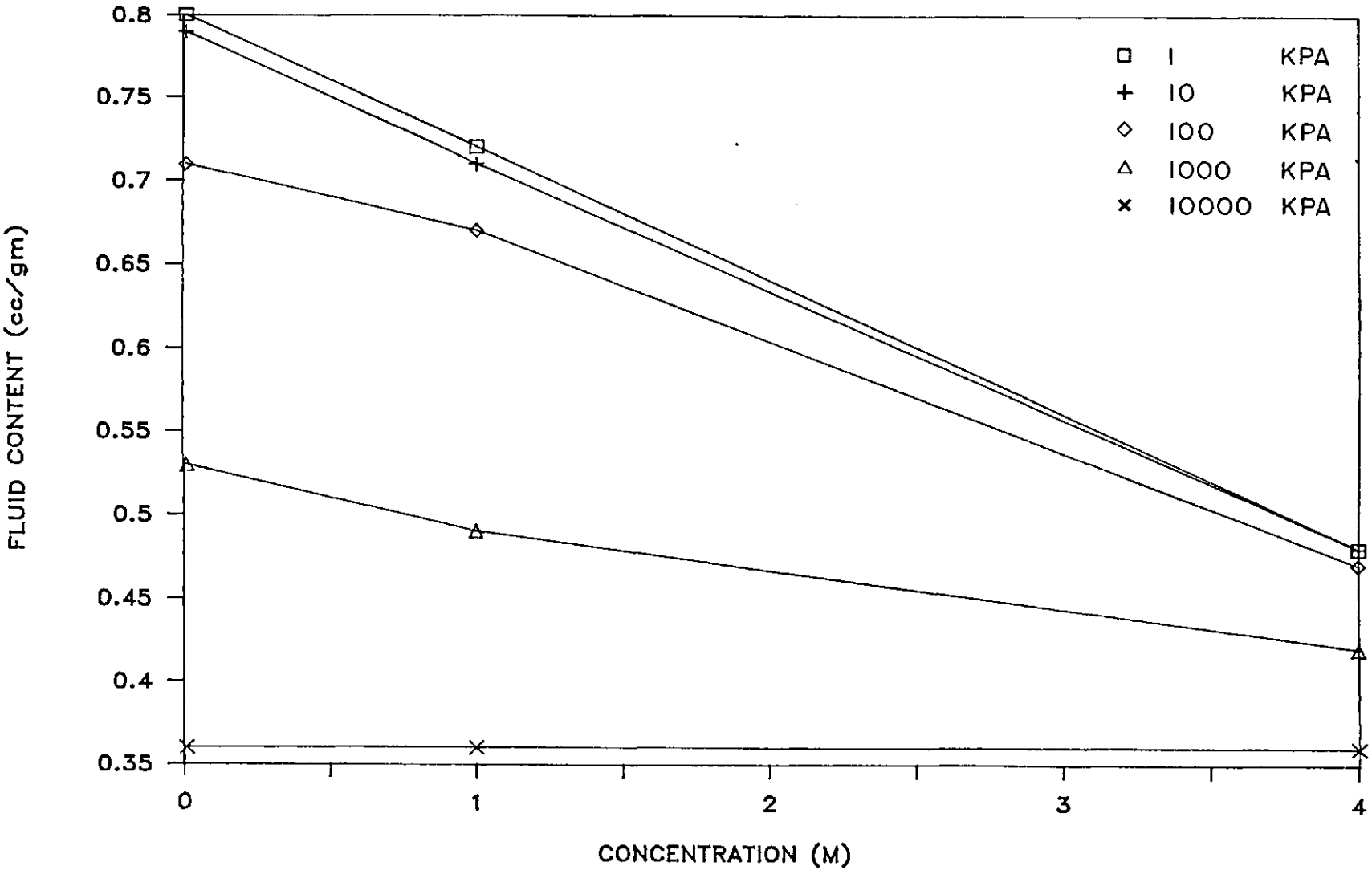

Figure 3.9 Solution Content versus Pore Fluid Concentration for Ca Montmorillonite / CaCl Solution (after Aylmore and Quirk 1962)

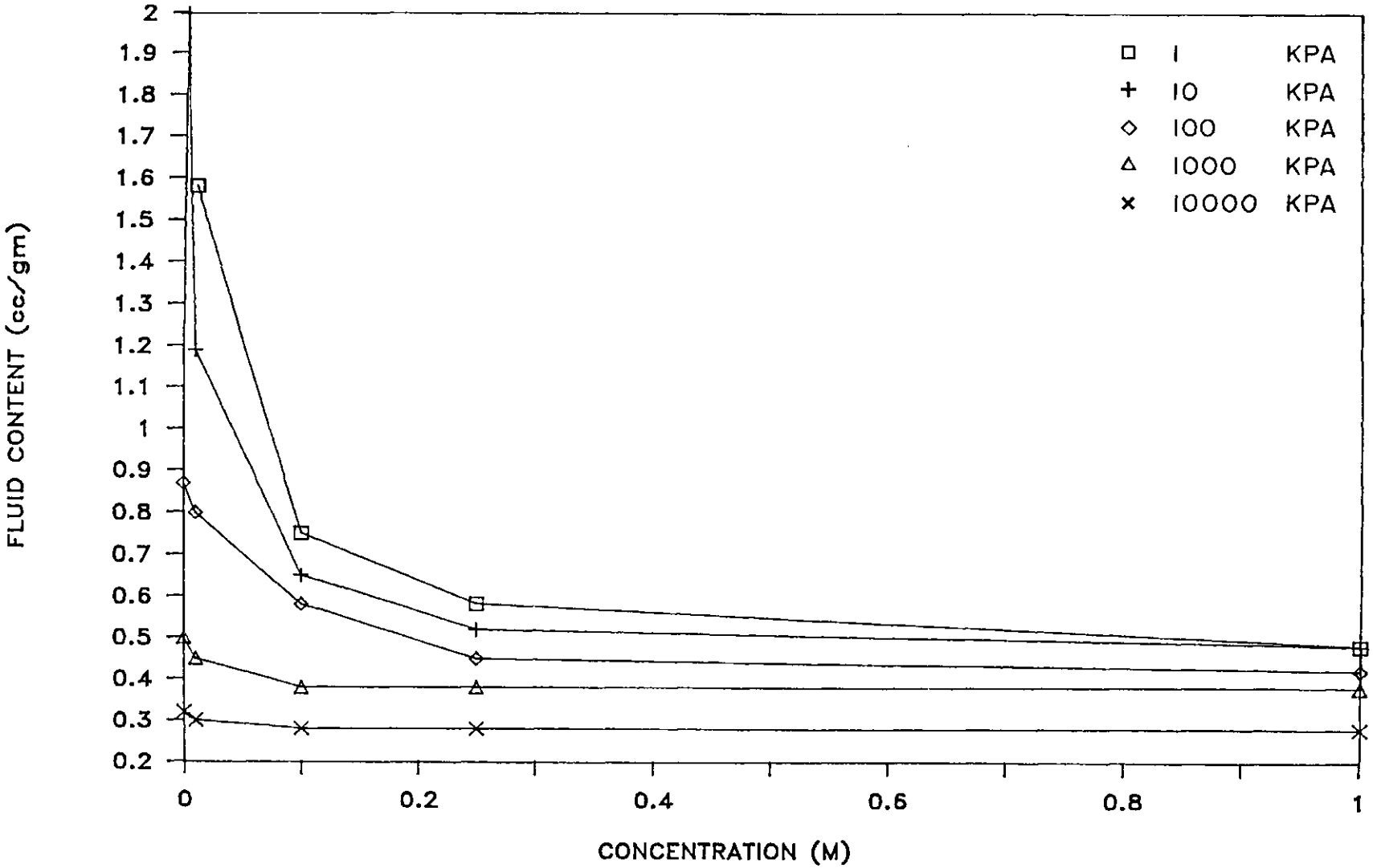

Figure 3.10 Solution Content versus Pore Fluid Concentration for Na Illite/ NaCl Solution (after Aylmore and Quirk 1962)

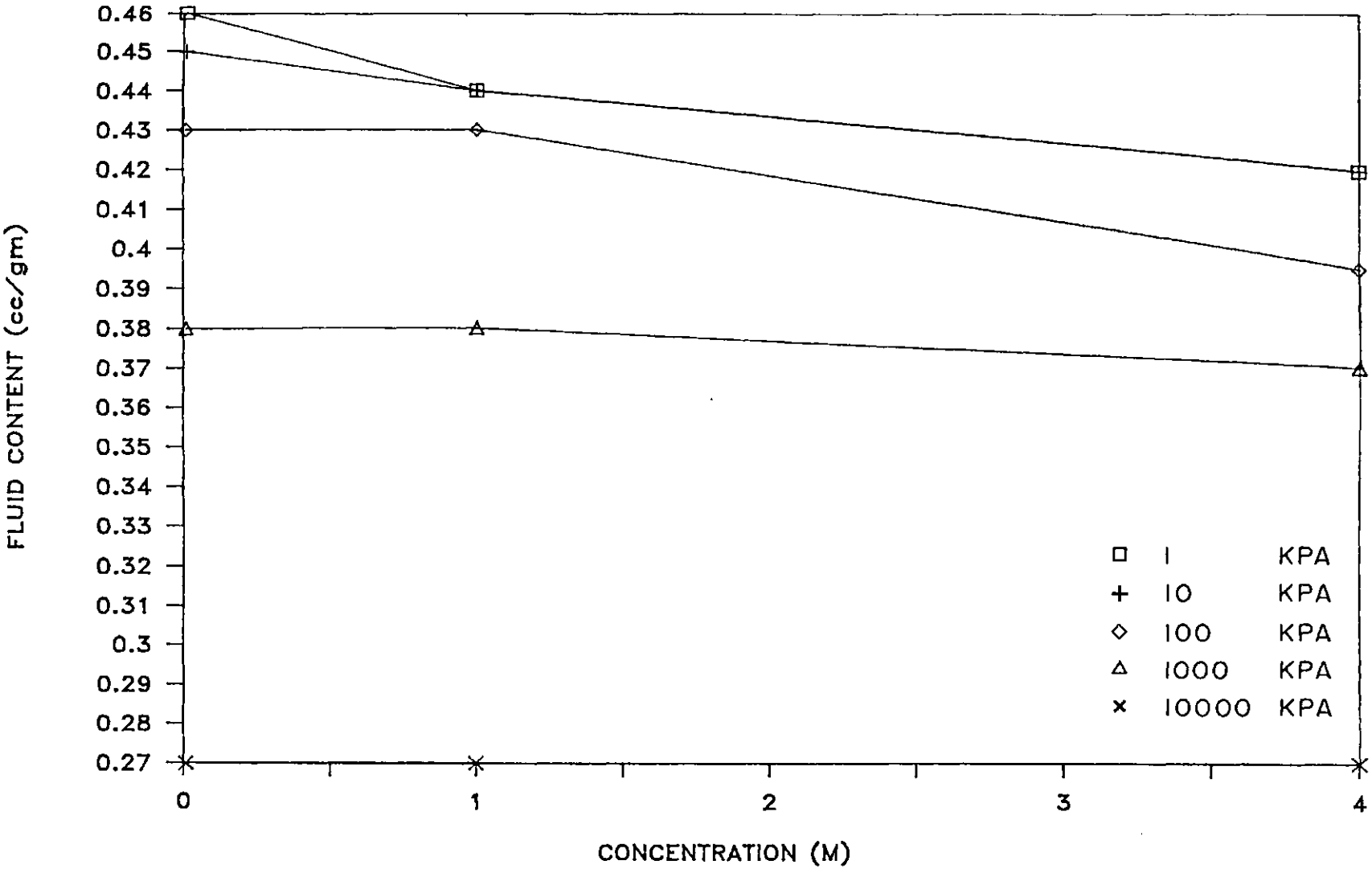

Figure 3.11 Solution Content versus Pore Fluid Concentration for Ca Illite / CaCl Solution (after Aylmore and Quirk 1962)

3.6 Formulation for One-Dimensional Consolidation and Brine Migration

The formulation for the problem of osmotic consolidation requires the prediction of the rate of change in the stress state variables with time. Changes in the stress state variables with time are related to volume change through the constitutive equation. Continuity is used to relate these volume changes to the divergence of the mass flux from the element. These mass fluxes are in turn defined by the flow laws for the individual constituents of the fluid phase. Only a one-dimensional form of the formulation is developed in this thesis.

The assumption is made that all volume change occurs as a result of deformation of the soil structure in the vertical direction. Assuming that the applied total stress is constant, force equilibrium is satisfied implicitly during changes in fluid pressures. The compressibility of the fluid phase with changes in pressure are assumed to be negligible. The continuity relationships are established by considering a fixed elemental volume in fixed coordinates. This approach is valid only if the following relationship is satisfied (Freeze and Cherry 1979):

$$v_s \, u_f << \partial u_f / \partial t \qquad [3.12]$$

where: v_s = velocity of the solid particles
u_f = fluid pressure

In general, the rate of consolidation must not exceed the rate of fluid flow for the inequality to hold.

The value for osmotic pressure within the sample can be calculated from the pore fluid concentrations using the van't Hoff approximation. Concentration changes within the sample with time can be calculated from the governing partial differential equation for salt transport through the sample.

3.6.1 Transient Salt Migration

The development of the equation for salt migration will follow the derivation by Freeze and Cherry (1979) and Bear (1972). It is assumed that the soil is saturated, homogeneous and isotropic.

The law of conservation of mass is applied to the net flux of salt through a small elemental volume. Salt is moved by the processes of advection with the solution and by hydrodynamic dispersion. The concentration of solute is defined as the mass of solute per unit volume of solution. For a unit volume of soil the mass of salt is equal to the porosity multiplied by the solution concentration (nCs). The components of salt flux are as follows:

$$\text{Transport by Advection} = q_f \, Cs \, dA \qquad [3.13a]$$

$$\text{Transport by Dispersion} = -n \, D \, (\partial Cs/ \partial y) dA \qquad [3.13b]$$

where: q_f = total fluid flux through the element
D = coefficient of hydrodynamic dispersion

The coefficient of hydrodynamic dispersion, is related to the coefficient of molecular diffusion, D*, and the dispersivity of the medium, , by (Freeze and Cherry 1979):

$$D = \alpha v + D^* \qquad [3.14]$$

where: v = seepage velocity of the pore fluid

Conservation of mass requires that the rate of change of mass within the element be equal to the divergence of the mass fluxes. This is written as follows:

$$\partial(-nCs)/ \partial t = \partial/ \partial y(-nD\partial \, Cs/ \partial y + q_f Cs \qquad [3.15a]$$

$$\partial Cs/ \partial t = D \, \partial^2 Cs/ \partial y^2 - (q_f/n) \, \partial Cs/ \partial y \qquad [3.15b]$$

Evidence of salt filtering or ion exclusion in geologic formations gives support to the potential retardation of salt migration relative to that of the solution. If streaming potentials (i.e., electric gradients) are absent, the retardation would be of both the cations and anions. If a simple ion adsorption phenomena is assumed then the

retardation factor R could be incorporated into equation [3.15] as shown below. The retardation factor is a measure of the retardation of the solute relative to the flow of solution.

$$\partial Cs/\partial t = D/R\ \partial^2 Cs/\partial y^2 - (q_f/Rn)\partial\ Cs/\partial y \qquad [3.16a]$$

$$\partial Cs/\partial t = D'\partial^2\ Cs/\partial y^2 - v'\partial Cs/\partial y \qquad [3.16b]$$

where: $D' = D/R$

$v' = q_f/Rn$

A term to describe the change in the concentration of salt that occurs as a result of decreasing void ratios could also be included in equation [3.16]. This effect was described by Greenberg (1971) as "void ratio coupling"; however, it was shown to have a negligible effect on solution concentrations during osmotically induced consolidation. This term will not be be included in this development.

3.6.2 One-Dimensional Consolidation

The total flux of water through the elemental volume is the sum of water flux due to hydraulic fluid flow and osmotic flow. The flow laws for water transport are written as follows:

due to fluid flow; $q_h = q_f C_w$ [3.17a]

due to osmotic flow; $q_\pi = k_\pi \partial\pi/\partial y$ [3.17b]

where: = concentration of water
= hydraulic conductivity
= osmotic conductivity

The concentration of water is approximately equal unity even for concentrated solutions, consequently, the total fluid flux is given as follows:

$$q_f = q_h + q_\pi \qquad [3.18]$$

Conservation of mass requires that a change in storage within the element be related to the divergence of the water flux. This can be written as:

$$-\partial V/\partial t(1/V) = \partial q_f/\partial y \qquad [3.19]$$

A decrease in the volume of the element is taken as positive volumetric strain to be consistent with geotechnical engineering convention. An assumption is made that the salt flux into the element does not represent a significant component of volume change. This should not be a severe limitation in that even for a concentrated NaCl brine, the presence of the salt accounts for only approximately 10% of the total volume of the solution.

Equation [3.11] can be differentiated with time to obtain the following constitutive relationship:

$$-\partial V/\partial t(1/V) = \partial/\partial t(m_v d(\sigma - u_f) + m_\pi d\pi) \qquad [3.20]$$

If equation [3.19] is substituted into [3.20], assuming total stress to remain constant, then equation [3.20] becomes:

$$-m_v \partial u_f/\partial t + m_\pi \partial \pi/\partial t$$

$$= \partial/\partial y(-C_w k_h(\partial u_f/\partial y + \rho_f g) + k_\pi \partial \pi/\partial y) \qquad [3.21]$$

A further simplification of equation [3.21] can be made by using two potential quantities called the equivalent freshwater hydraulic head, , and the osmotic head, . The use of a freshwater hydraulic head was suggested by Frind (1982a,b) for the solution of transient density-dependent transport problems related to coastal seawater intrusion. The principal advantages of this approach are as follows:

1) It minimizes the effect of numerically large static pressures, overshadowing dynamic pressure differences due to density effects, which may be producing flow, and,

2) It rewrites the flow equation in such a way that the conductivity term is independent of variations in fluid properties.

The equivalent freshwater hydraulic head and the osmotic head may be written as:

$$\psi = u_f/(\rho_w g) \qquad [3.22a]$$

$$\Pi = \pi/(\rho_w g) \qquad [3.22b]$$

The hydraulic and osmotic flow equations are then written as:

$$h = -K_h(\partial\psi/\partial y + \rho_r) \qquad [3.23a]$$

$$\pi = K_\pi \partial\Pi/\partial y \qquad [3.23b]$$

where: K_h = permeability = $k_h\rho_w g$
K_π = osmotic permeability = $k_\pi\rho_w g$
ρ_r = relative density = $\rho_f/\rho_w - 1$

Since $\partial u_f/\partial t = \rho_w g \partial\psi/\partial t$, the consolidation equation can be written as:

$$-m_v\rho_w g\partial\psi/\partial t + m_\pi \rho_w g \partial\Pi/\partial t = \partial/\partial y(-K_h(\partial\psi/\partial y + \rho_r) + K_\pi \partial\Pi/\partial y) \qquad [3.24]$$

In equation [3.24], m_v, K_π, and K_h may all be a function of solution concentration. As discussed in Chapter 1, when osmotic volume change results in fracture of the clay, large increases in the permeability can be expected. However, in the absence of fracture development the changes in permeability may be fairly minor. Figure 3.12 from Mesri and Olson (1971) illustrates the small changes in permeability that occur at similar void ratios, but with different concentrations of pore fluid. The numerical solution of equations [3.23] and [3.24] will utilize a constant value of permeability.

Equation [3.23] and [3.24] must solved in conjunction with the salt transport equation [3.16b]. The numerical solution used to solve this coupled problem is described in Chapter 4.

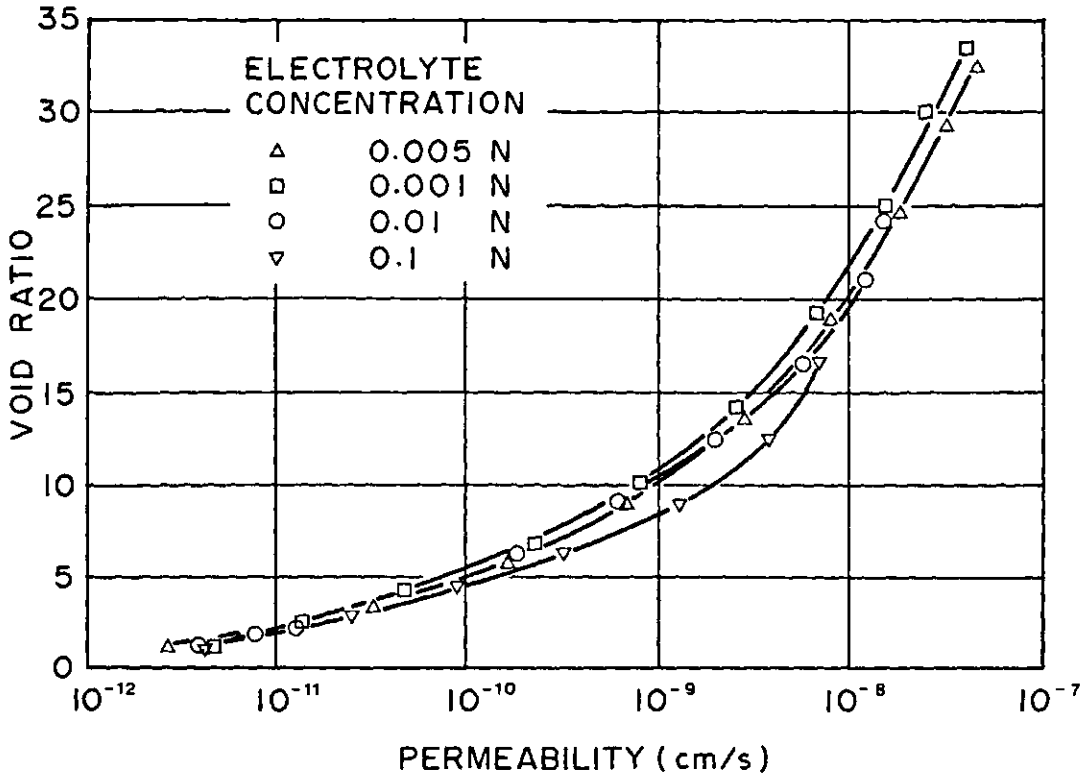

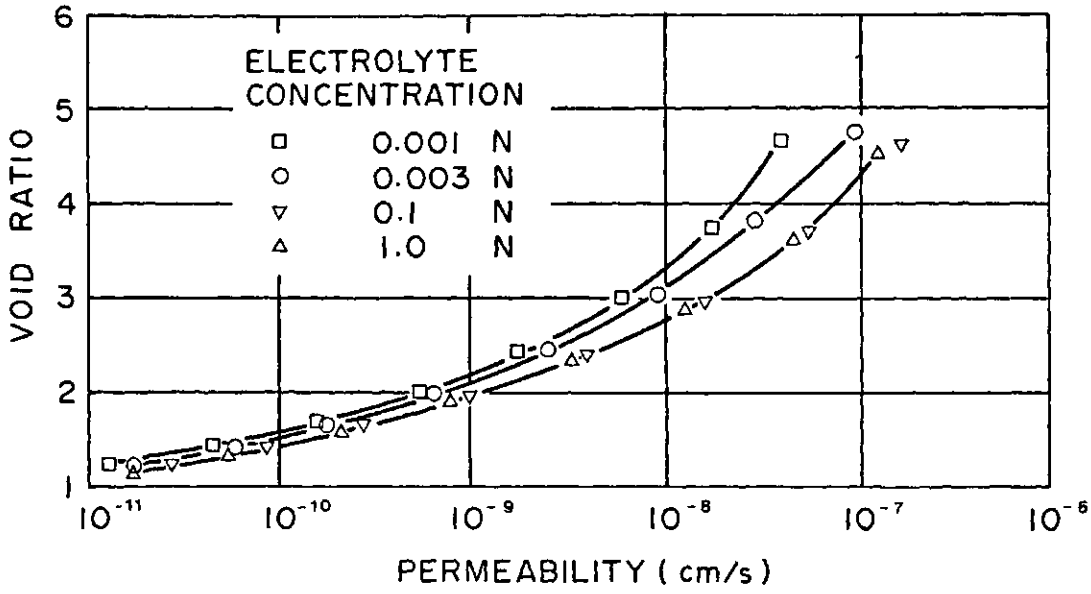

Figure 3.12 Permeability Void Ratio Curves for
a) Na-montmorillonite
b) Calcium Montmorillonite
(Mesri and Olson 1971)

CHAPTER 4

NUMERICAL SIMULATION OF ONE DIMENSIONAL OSMOTIC FLOW AND VOLUME CHANGE

4.1 General - Method of Solution

The governing partial differential equations for one-dimensional osmotic flow and volume change were developed in Chapter 3. Equation [3.24] describes the volume change that occurs within a saturated soil, as a result of changes in effective stress and osmotic pressure. This equation is coupled with equation [3.16] which describes the changes in pore fluid concentration with time. A numerical solution of these two equations can be obtained through the use of a finite element numerical model.

The numerical model developed to solve the governing equations is called OSMOPC. The model utilizes a series of one-dimensional elements to discretize the spatial domain of the problem, and a finite difference approximation of the time derivatives. The values of concentration, osmotic head and hydraulic head, are defined at the element nodal points. The distribution of these values across the element is assumed to be linear. Both a central difference and a backward difference approximation can be used for the solution of either of the transient equations.

A detailed documentation for OSMOPC is presented in Appendix B. The documentation describes the development of the finite element equations and data input formats. The flow charts for the algorithm are also presented in Appendix B. The overall structure of the model is illustrated in Figures 4.1 and 4.2.

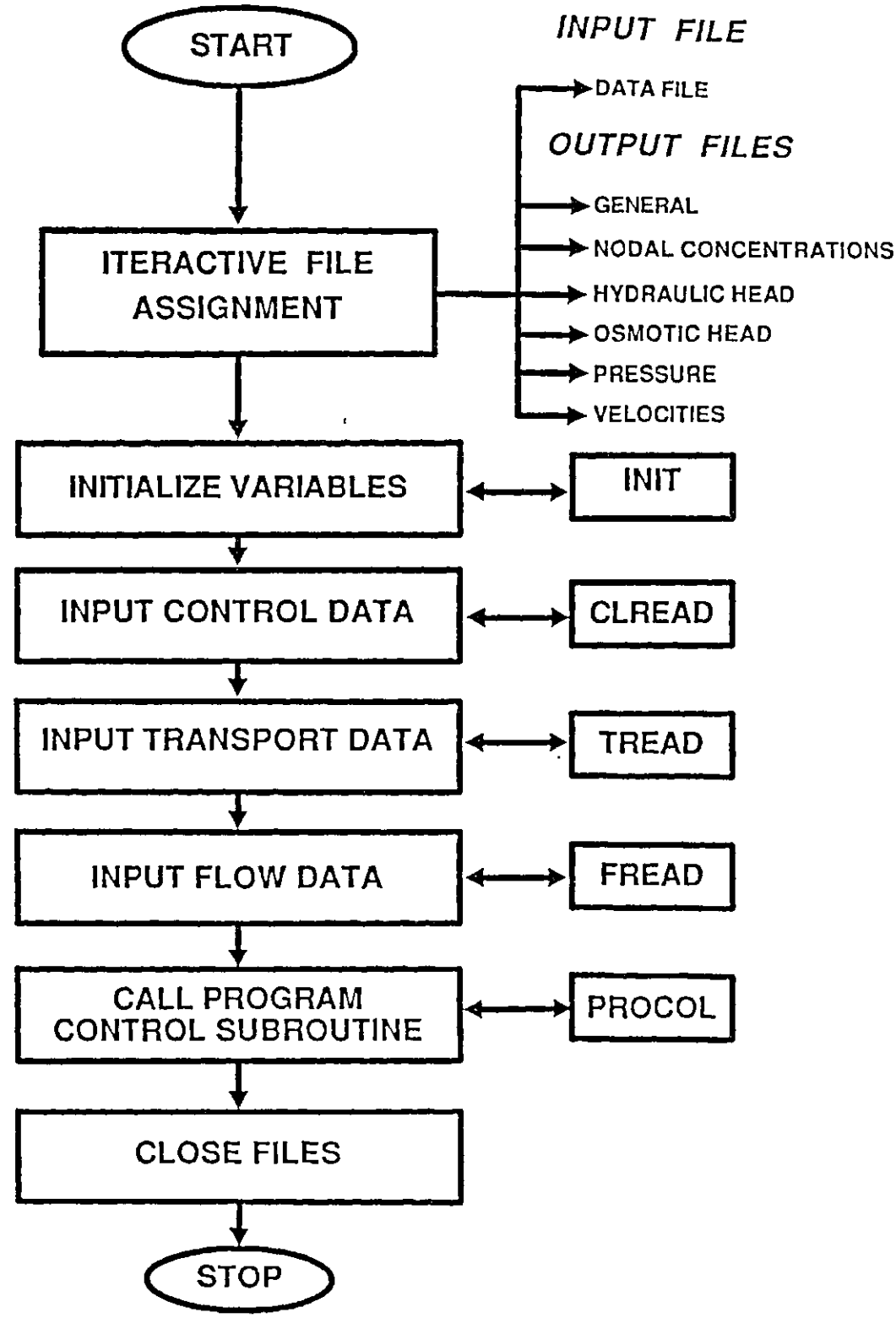

Figure 4.1 Flow Chart for OSMOPC - Subroutine MAIN

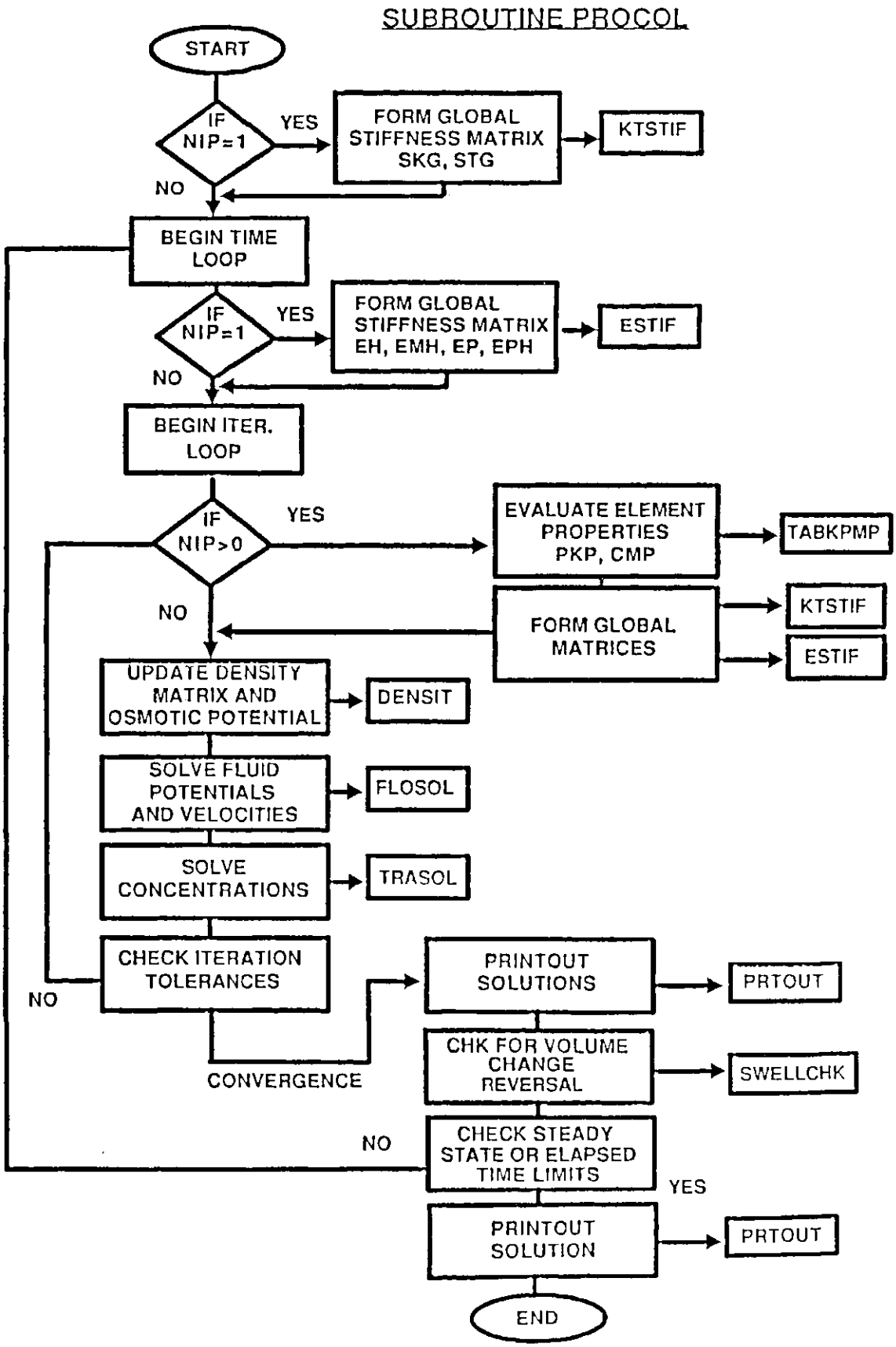

Figure 4.2 Flow Chart for OSMOPC - Subroutine PROCOL

The following steps are followed for each increment of time:

1. The consolidation equation, (equation [3.24]) is solved for the hydraulic head at the nodes, using initial estimates of the osmotic heads,

2. The pore fluid velocities are calculated using the values of hydraulic and osmotic head,

3. The salt transport equation , (equation [3.16]) is solved to obtain the concentration at each element nodal point,

4. Steps 1 through 3 are repeated until convergence for the nodal concentration is obtained,

5. Following convergence, the solution is obtained for the next time step using the final nodal concentrations from the previous step as initial conditions.

The program was originally developed in Fortran to run on a Vax 11-780 mainframe computer. It was later modified to run using Microsoft Fortran (Version 3.0) on a Commodore PC-10 microcomputer, with a 8087 coprocessor, 20 megabyte hard drive and 512 kilobytes of random access memory. The program is capable of handling any number of material types, as well as tabulated relationships for the values of K_π and m_π. Independent values of compressibility may be used if the sample changes from compression to swelling during the osmotic consolidation process (i.e., m_v to m_s).

4.2 Program Verification

The computer program solves the general problem of osmotically induced consolidation and osmotic consolidation. In this general form, there is no other analytical or numerical model with which to compare results for verification. However, the program is also capable of solving a series of simpler problems for which analytical or numerical solutions are available.

A series of simple problems were solved during development which included: steady state flow, contaminant

transport in a steady state flow regime, transient flow (one-dimensional consolidation), density dependent flow, steady state osmotic flow, and osmotically induced consolidation. A summary of these verification exercises is provided in Table 4.1.

The simple cases listed in Table 4.1 were used to "debug" the program, to provide verification of the algorithm, and also to make decisions regarding the degree of refinement of spatial and temporal discretizations required to ensure accurate solutions.

4.3 Example Simulations

OSMOCO simulates the response of a clay layer to the effects of osmotic flow and consolidation. The simulated responses of the numerical model provide insight into the types of behavior that may be characteristic of clay layers that undergo either osmotic or osmotically induced volume change.

The two potential mechanisms for osmotically related volume change in clay soils are osmotically induced consolidation and osmotic consolidation. It is anticipated that in actual testing, a clay would respond to both mechanisms of volume change to varying degrees. In this section the numerical model is used to demonstrate the characteristic behavior of a typical clay sample when its volume change is controlled by one mechanism or the other.

4.3.1 General Description of Simulations

Four simulation cases are presented in this section. The material properties, initial conditions, and boundary conditions for these simulations are presented in Figure 4.3. Two of the four cases simulate osmotic consolidation (i.e., Cases A1 and A2), and two cases simulate osmotically induced consolidation (i.e., Cases B1 and B2).

Table 4.1 OSMOCO Verification Problems

Problem Type	Case Runs	Comparative Analytical/ Numerical Solutions
Mass Transport (Steady Flow)	- 1st and 3rd Type Boundary Conditions - Condensed vs Lumped Formulation - Peclet / Courant Number Trials	Ogata Banks (1961) / Analytical Barbour (1981) / Numerical
Consolidation	- 1-way and 2-way Drainage - Constant Initial Excess Pressure - Triangular Initial Excess Pressure Distribution	Taylor (1948) / Analytical
Density - Dependent Flow	- Steady State Velocity for various Brine Density Contrasts - Transient Density Dependant Flow	van der Kamp (1984) / Analytical unpublished model - MTRADEN/ Numerical Frind (1982a,b)
Steady State Osmotic Flow	- Steady Osmotic Flow from Linear Concentration Distribution	osmotic flow law
Induced Osmotic Consolidation	- Time to 100 % Consolidation	Greenberg (1971), Mitchell (1973) / Numerical

EXAMPLE SIMULATION DATA

General Properties:

$K_h = 1 \times 10^{-10}$ m/s
$m_v = 5 \times 10^{-4}$ /kPa
$C_v = 2.03 \times 10^{-4}$ cm^2/s
$D = 5 \times 10^{-10}$ m^2/s
$n = 0.5$

Boundary Conditions:

CASE 1

Transport/ 1st type/ C = 4 M
Flow/ 1st type/ u = 0

Co = 0, t<0
uo = 0, t<0

1 cm

Transport/ 2nd type/ $\partial C / \partial x = 0$
Flow/ 2nd type/ qo = 0

CASE 2

Transport/ 1st type/ C = 4 M
Flow/ 1st type/ u = 0

Co = 0, t<0
uo = 0, t<0

Transport/ 3rd type/ qoCo =0
Flow/ 1st type/ u = 0

Cases:

Case A - Osmotic Consolidation
$K_\pi = 0$
$m_\pi = 2.5 \times 10^{-6}$ /kPa

Case B - Osmotically Induced Consolidation
$K_\pi = 5 \times 10^{-13}$ m/s, efficiency = .005
$m_\pi = 0$

Figure 4.3 Example Simulation Cases A1, A2, B1, B2.

All four cases simulate the response of a clay sample exposed at the upper surface to 4.0 M NaCl brine. Cases A1 and B1 simulate the condition where fluid flow across the base of the sample is prevented. Cases A2 and B2 are for the condition where a zero pore fluid pressure is maintained at the base, consequently flow of fluid in or out of the base of the sample is permitted.

The model output data consists of nodal concentrations, nodal osmotic and hydraulic heads, and element velocities, for each time step. The deflection of the sample with time was calculated using a utility program, VELFIL. The deflection was calculated as equal to the net total cumulative flux out of the sample. Two other utility programs, NODVAL and TELFIL, were used to reduce the output pressure and concentration files to sets of contours for plotting. A listing of each utility program is included in Appendix B.

4.3.2 Base Flow Restricted - Cases A1 and B1

Restricting the base flow during osmotic volume change, results in the development of pore-pressures along the base of the sample. Figures 4.4 and 4.5 illustrate the base pressure response with time, for Cases A1 and B1. Small positive pressures begin to build during osmotic consolidation (Case A1), reaching a maximum value of 24 cm of head at a time factor of approximately 2.

Positive pressures result from the expulsion of fluid due to osmotic consolidation at the top of the sample. In Case B1, large negative pressures develop along the base of the sample. The peak pressure again develops at approximately a time factor of 2. The maximum negative pressure head is approximately 1000 cm. Using the van't Hoff approximation, the osmotic pressure of 4 molar brine is approximately 20000 kPa. The ratio of the peak base pressure to the maximum osmotic pressure is equal to the

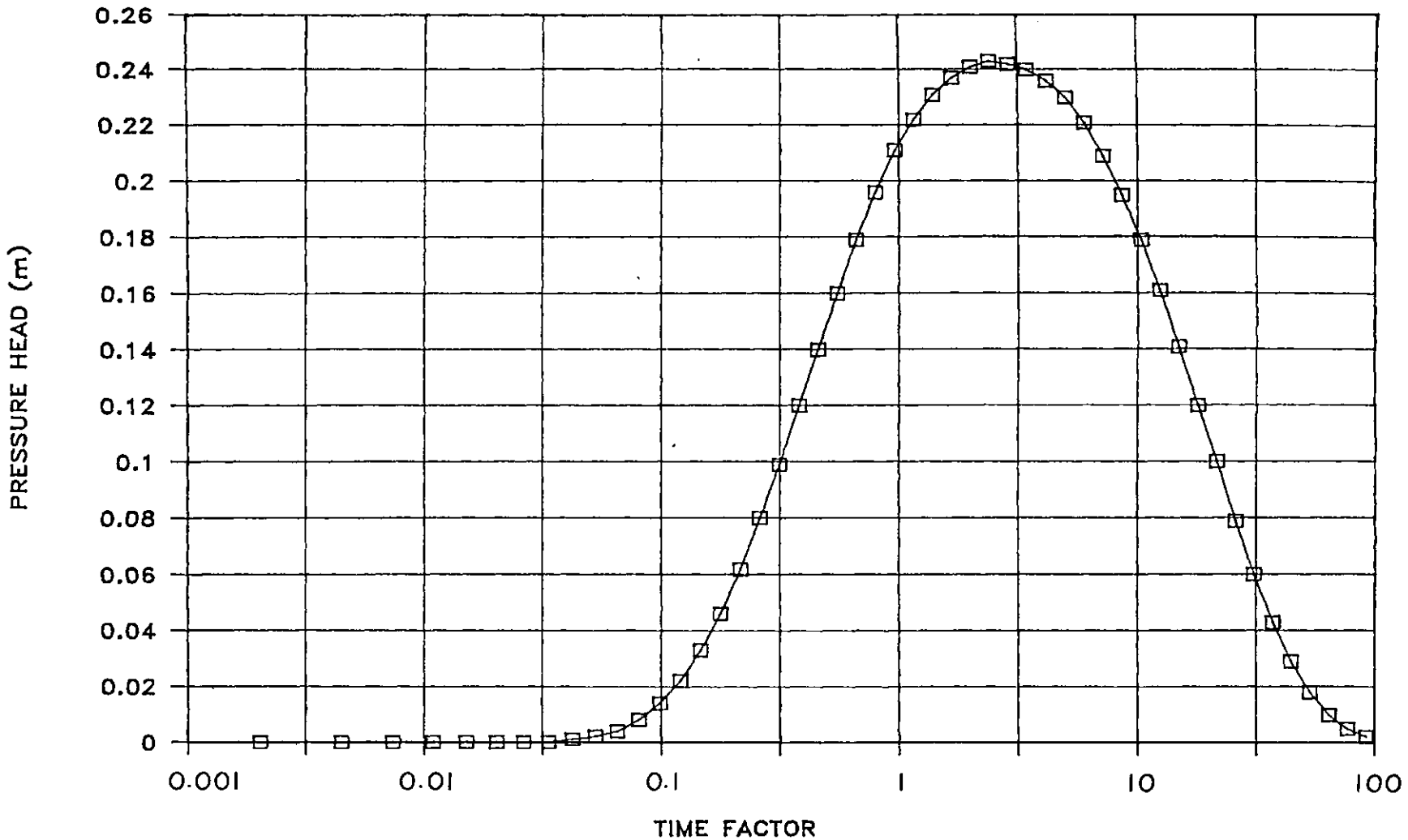

Figure 4.4 Case A1 Base Pressure versus Time Factor (Osmotic Consolidation)

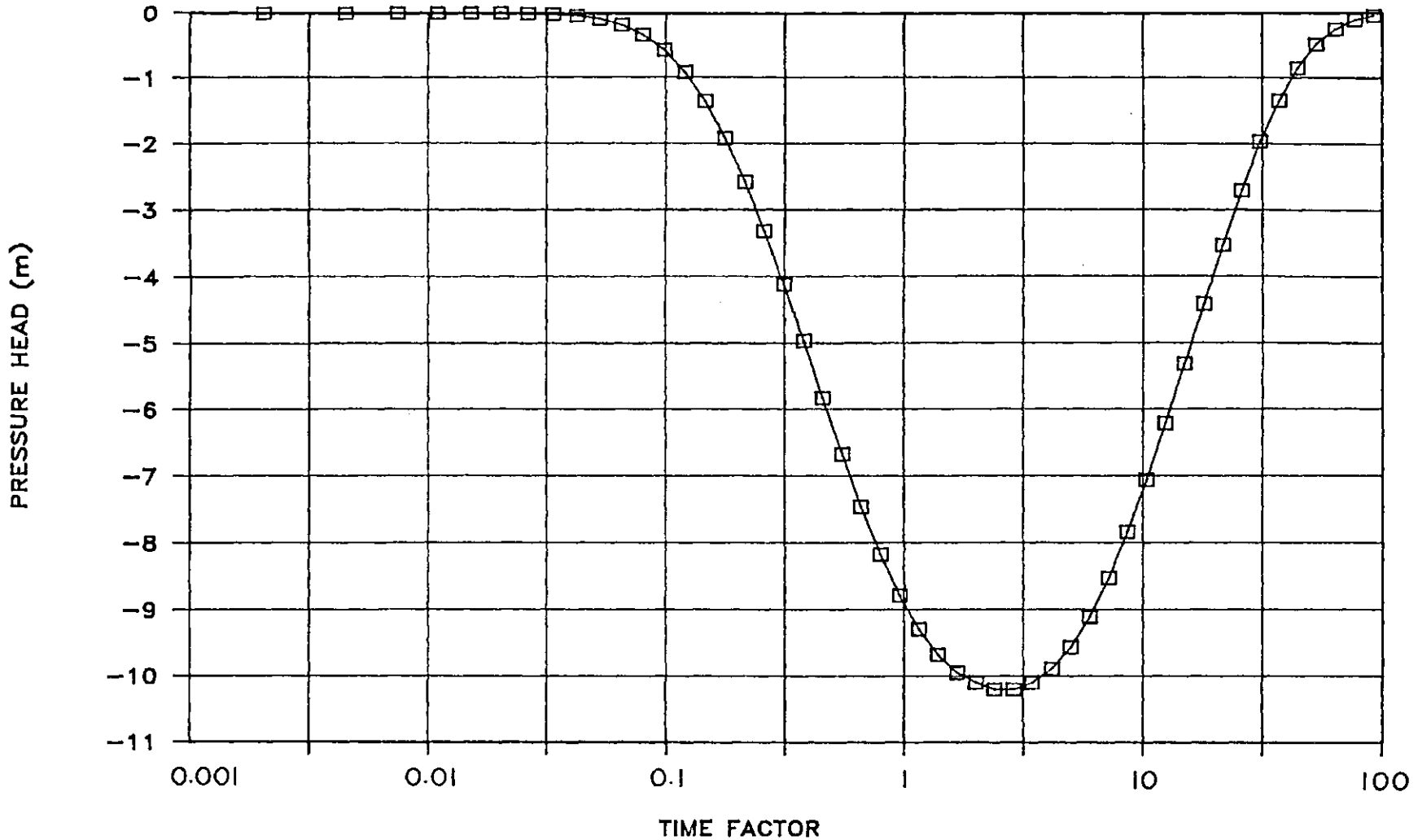

Figure 4.5 Case B1 Base pressure versus Time Factor (Osmotically Induced Consolidation)

osmotic efficiency of the clay (i.e., .005) used in the simulation.

Although the magnitudes of the pressures that develop within the sample are dramatically different, the shape of the pressure contours illustrated in Figures 4.6 and 4.7 are mirror images of each other. In the case of osmotic consolidation (Case A1) a maximum peak pressure head of 24 cm of water builds and then decays to zero as concentrations equalize throughout the sample, and osmotic consolidation is complete. In Case B1, high negative pressures develop within the sample in response to the strong osmotic gradients. A maximum negative pressure head of approximately 1000 cm develops over most of the sample, before it begins to decay as a result of the equalization of concentrations throughout the sample.

The concentration contours, illustrated in Figures 4.8 and 4.9, are essentially identical for the two cases. At an elapsed time equal to a time factor of 2 the strong osmotic flows generated in Case B1 have dissipated. After that time,the rate of salt migration is controlled by diffusion, and consequently the rate of salt migration in both cases is essentially the same.

4.3.3 Base Flow Unrestricted - Cases A2 and B2

In Cases A2 and B2, the fluid pressure at the base is maintained at atmospheric. The flow generated during the osmotic volume change process is illustrated in Figures 4.10 and 4.11. Flow out of the base (ie., negative cumulative base flow) begins at a time factor of approximately 1 for the case of osmotic consolidation (Case A2). The flow is in response to the expulsion of pore fluid due to osmotic consolidation that is occurring within the sample. Consequently, the base flow slows with time, and eventually stops when osmotic consolidation is complete.

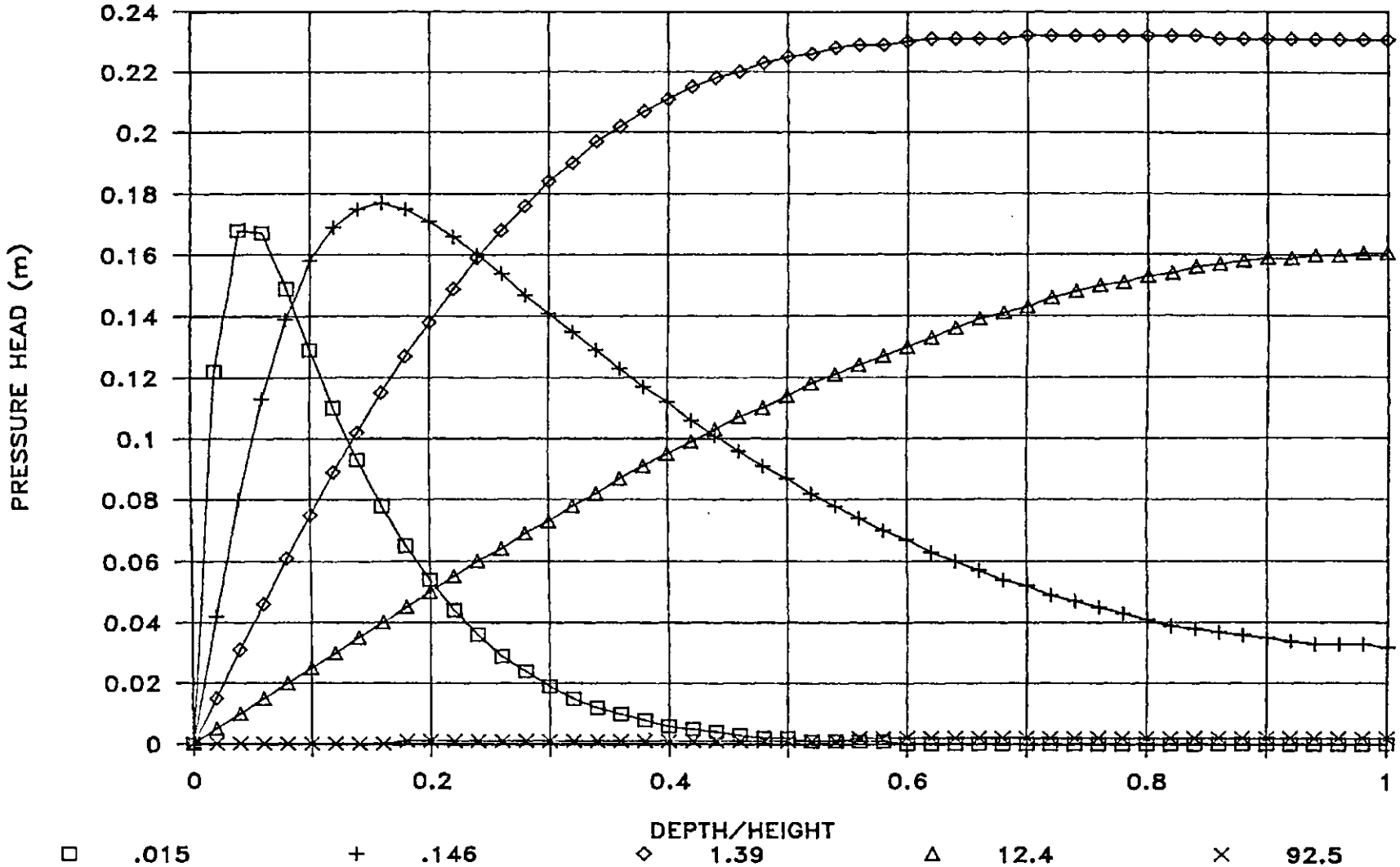

Figure 4.6 Case A1 Pressure Head Contours
(Osmotic Consolidation)

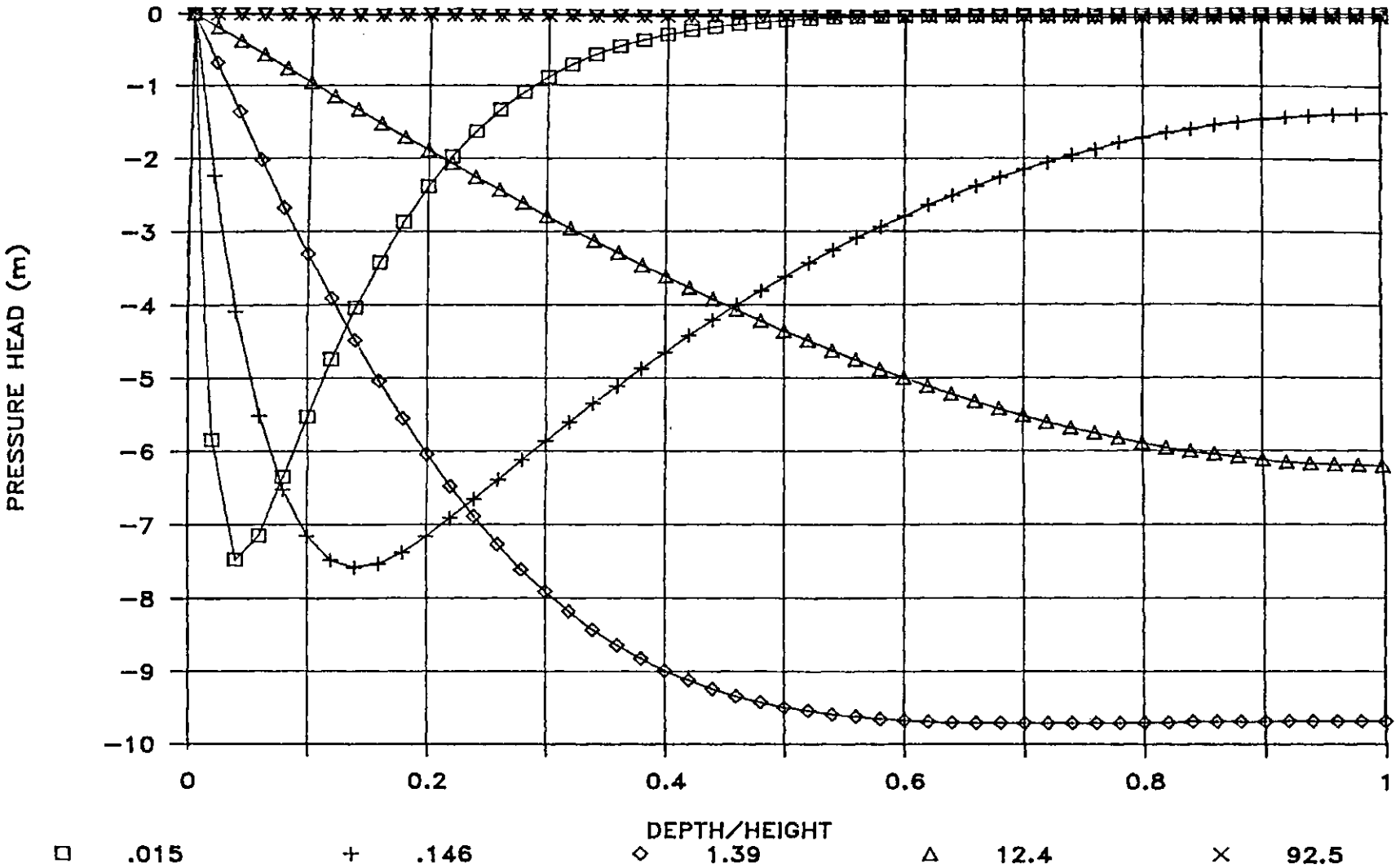

Figure 4.7 Case B1 Pressure Head Contours
(Osmotically Induced Consolidation)

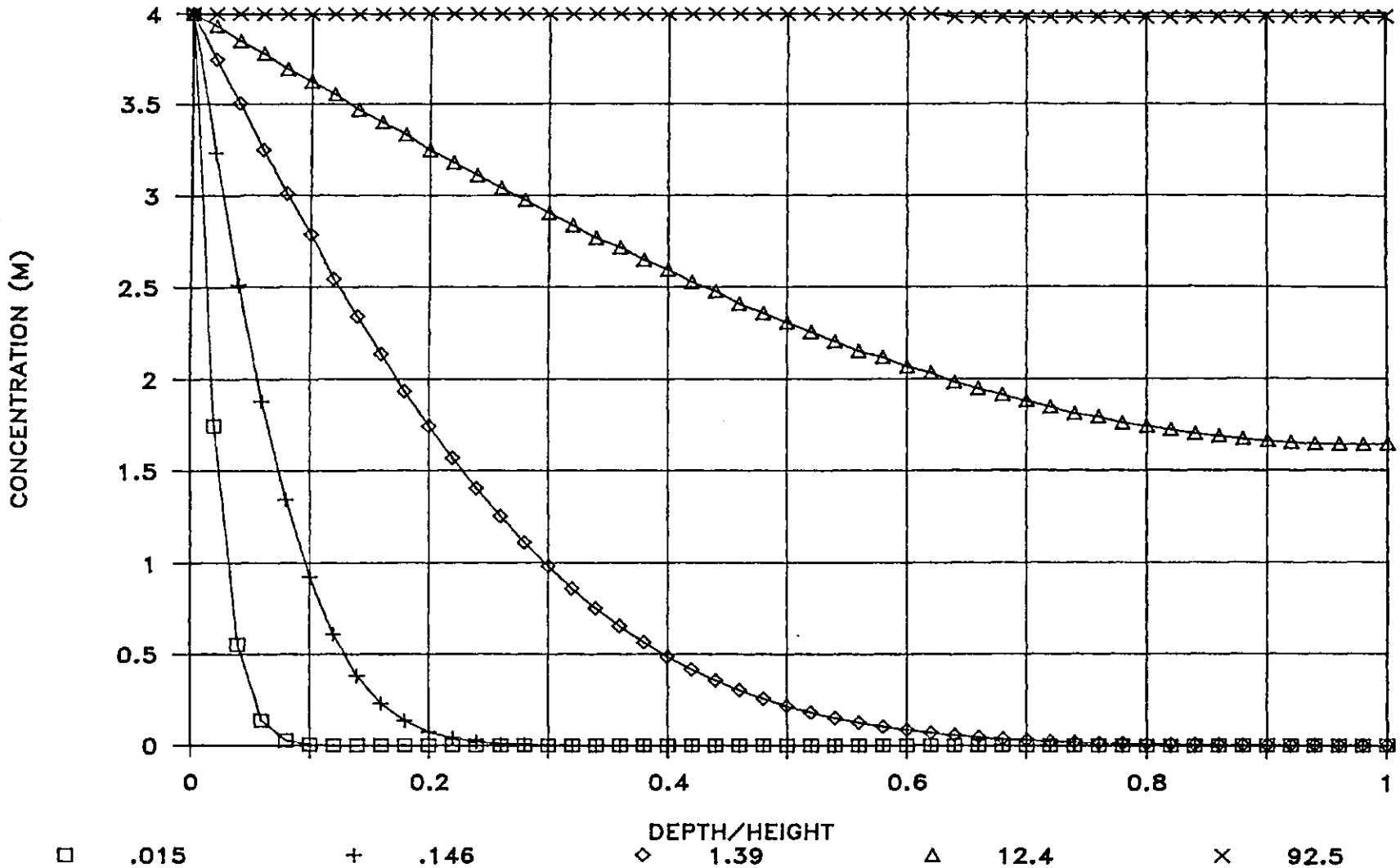

Figure 4.8 Case A1 Concentration Contours
(Osmotic Consolidation)

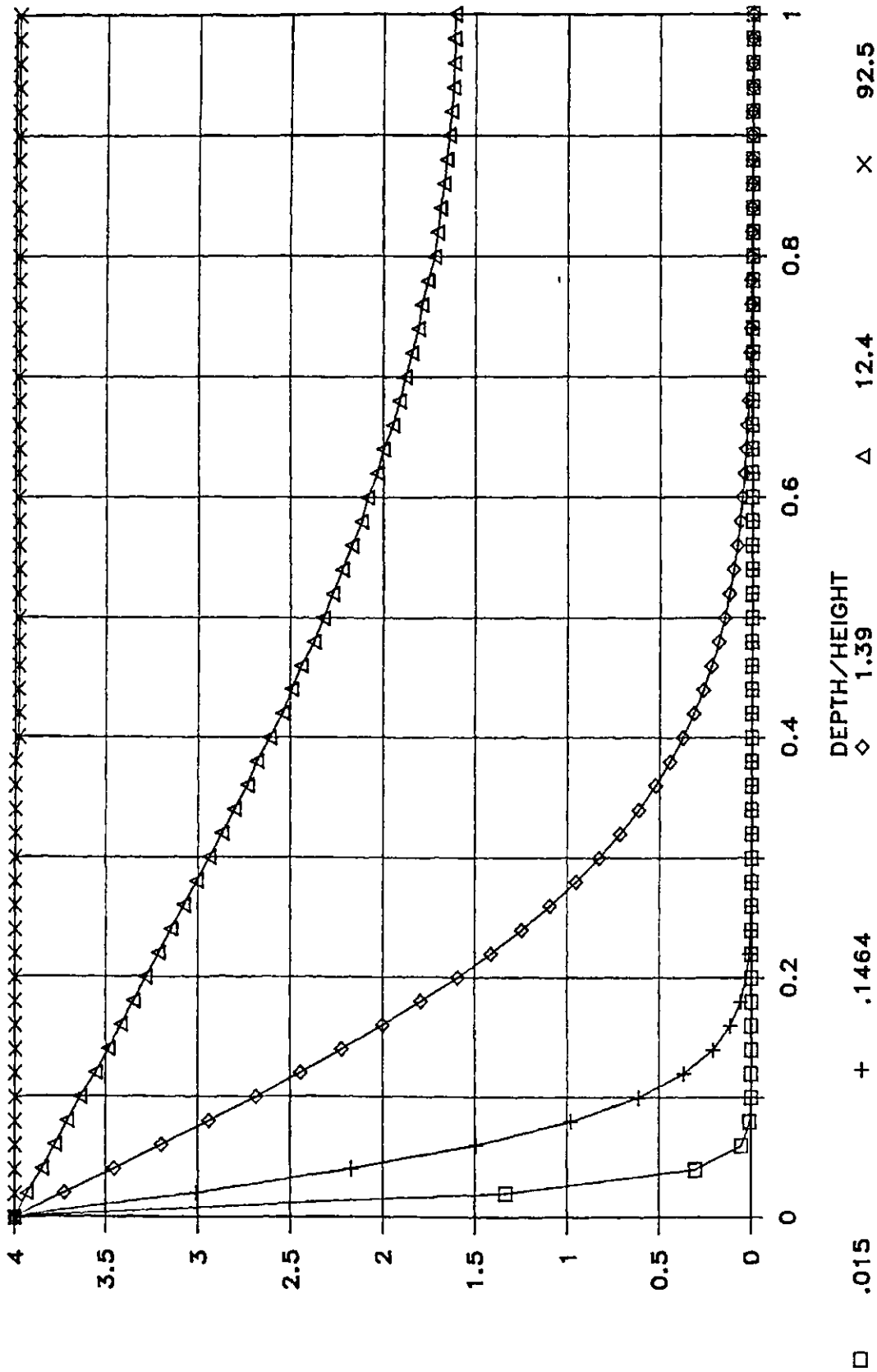

Figure 4.9 Case B1 Concentration Contours
(Osmotically Induced Consolidation)

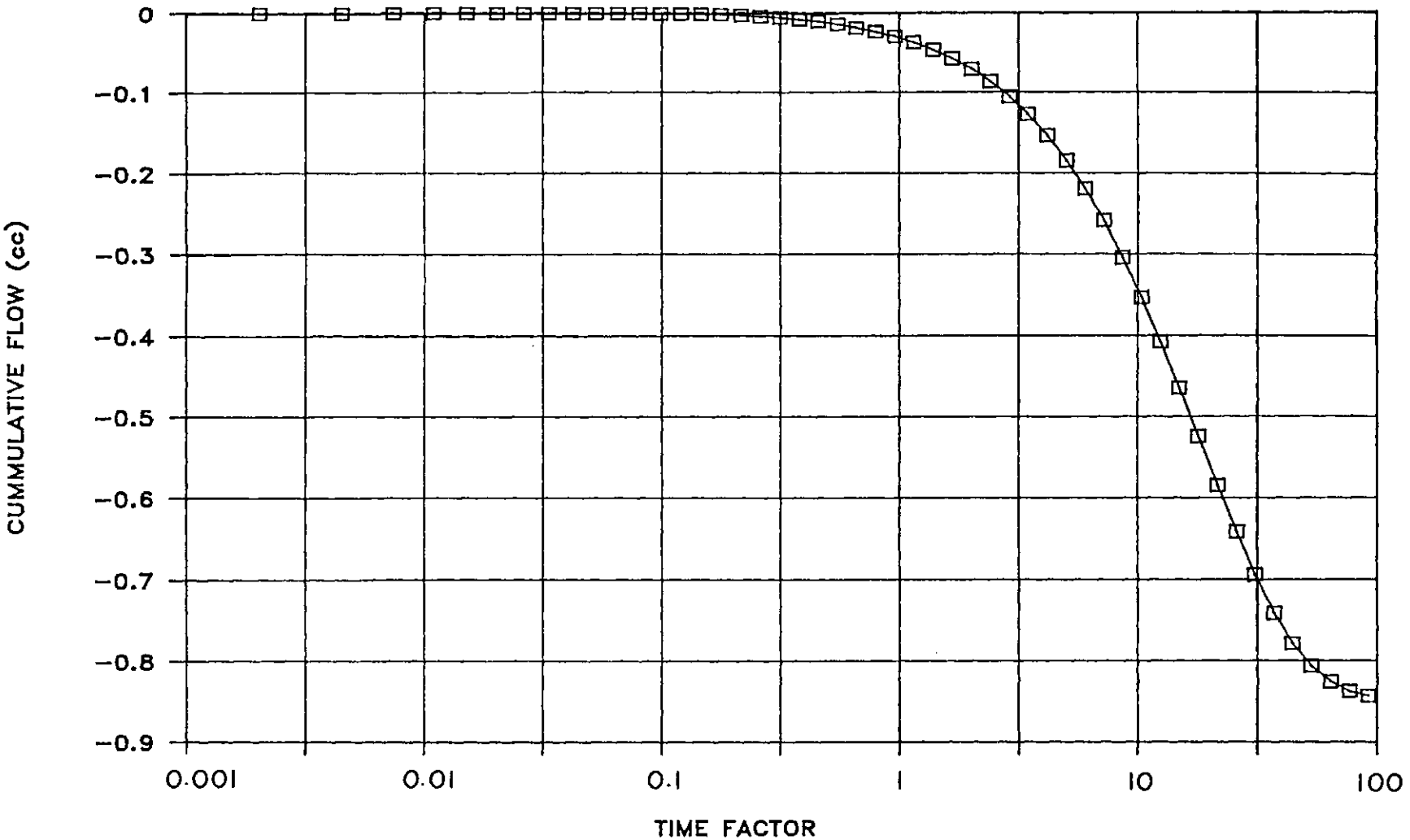

Figure 4.10 Case A2 Cumulative Base Flow versus Time Factor (Osmotic Consolidation)

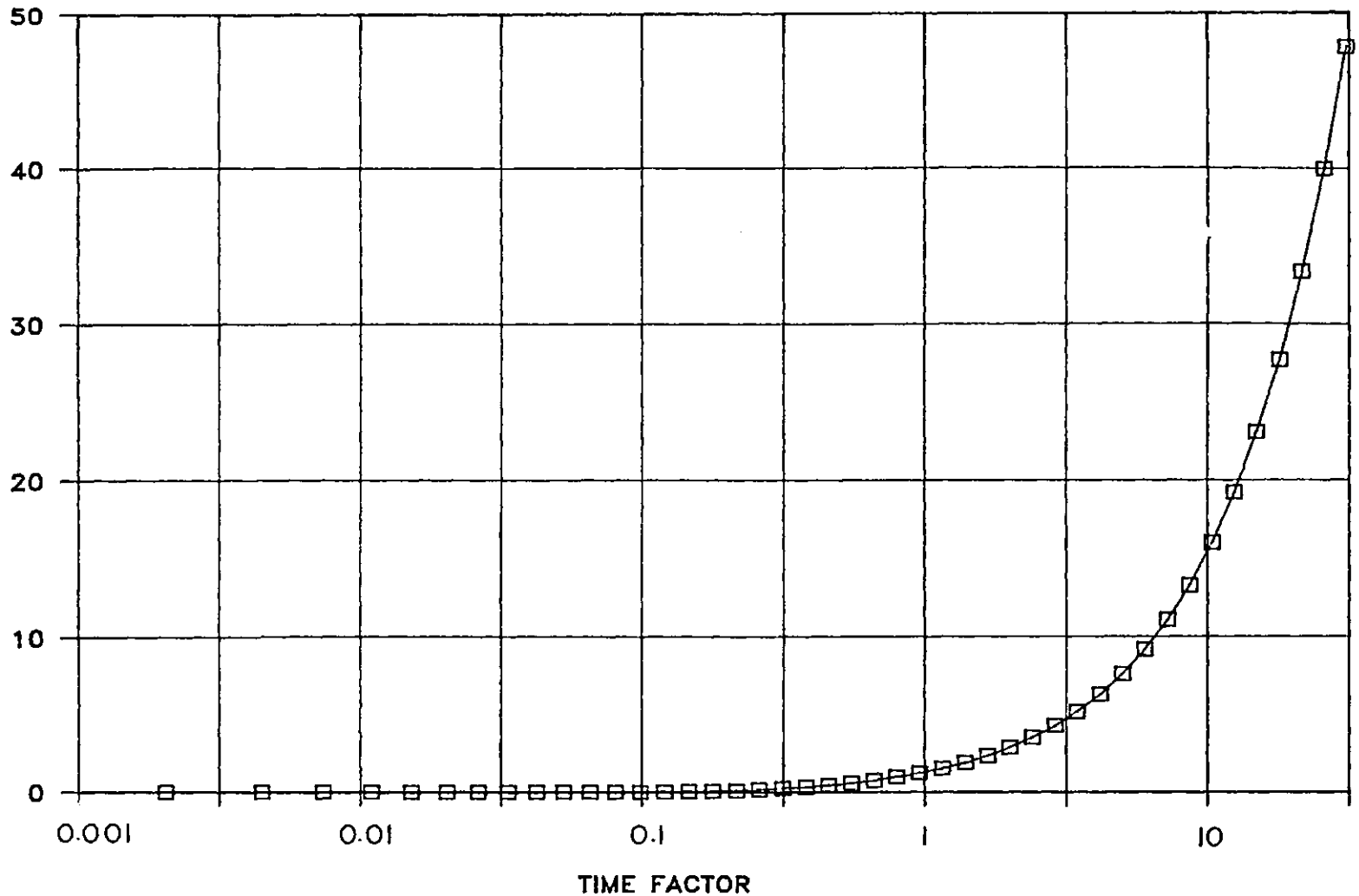

Figure 4.11 Case B2 Cumulative Base Flow versus Time Factor (Osmotically Induced Consolidation)

For the case of osmotically induced consolidation (Case B2), pore fluid pressures at the base begin to develop at a time factor approximately equal to 1. In this case, the base flow is into the base of the sample, and the flow rate continues to increase with time. Figure 4.12 illustrates the cumulative base flow on a arithmetic time scale. It is evident that the base flow reaches a steady flow rate into the sample. The flow rate produced is approximately 1.87 x 10^{-2} cm^3/min. For the sample area of 31.67 cm^2, this is equivalent to a hydraulic gradient across the sample of approximately 1000. The potential osmotic pressure gradient across the sample is approximately 20000. Consequently, the ratio of the osmotic permeability to the hydraulic permeability (i.e., the osmotic efficiency) is .005.

The pressure contours across the sample are illustrated in Figures 4.13 and 4.14. For the case of osmotic consolidation (Case A2), the maximum pressure head develops near the top of the sample at early times, and then decays to zero as the salt concentrations equalize throughout the sample. In the osmotically induced consolidation case (Case B2), large negative pressures develop near the top of the sample but then do not fully decay. A steady state negative pore pressure distribution develops within the sample after a time factor of approximately 10.

The steady state pressure distribution in Case B2 occurs in response to the distribution of concentration throughout the sample. The concentration contours are presented in Figures 4.16. The strong upward steady flows that develop through the sample prevent the concentrations from equalizing across the sample.

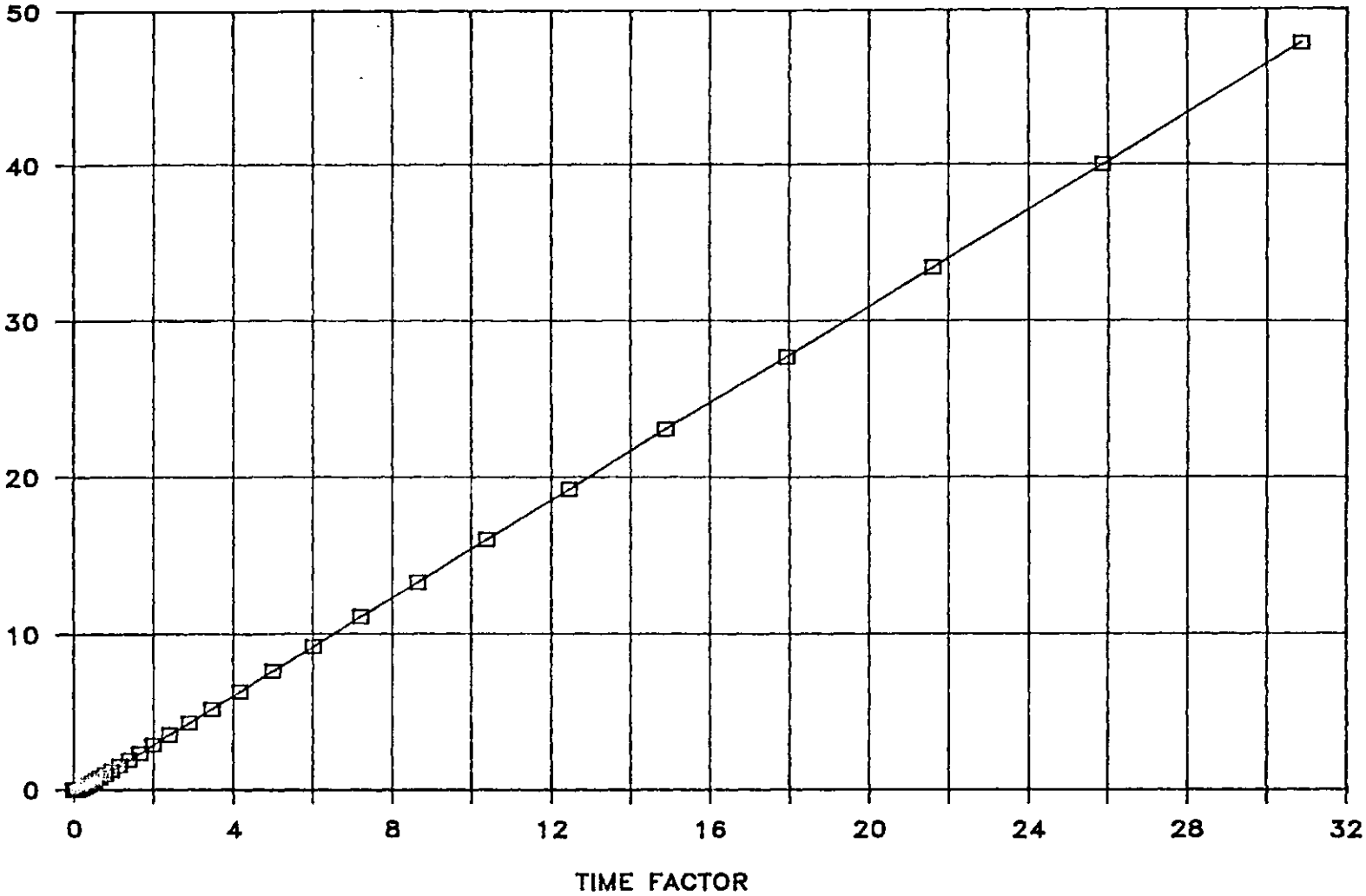

Figure 4.12 Case B2 Cumulative Base Flow versus Time Factor - Arithmetic Scale

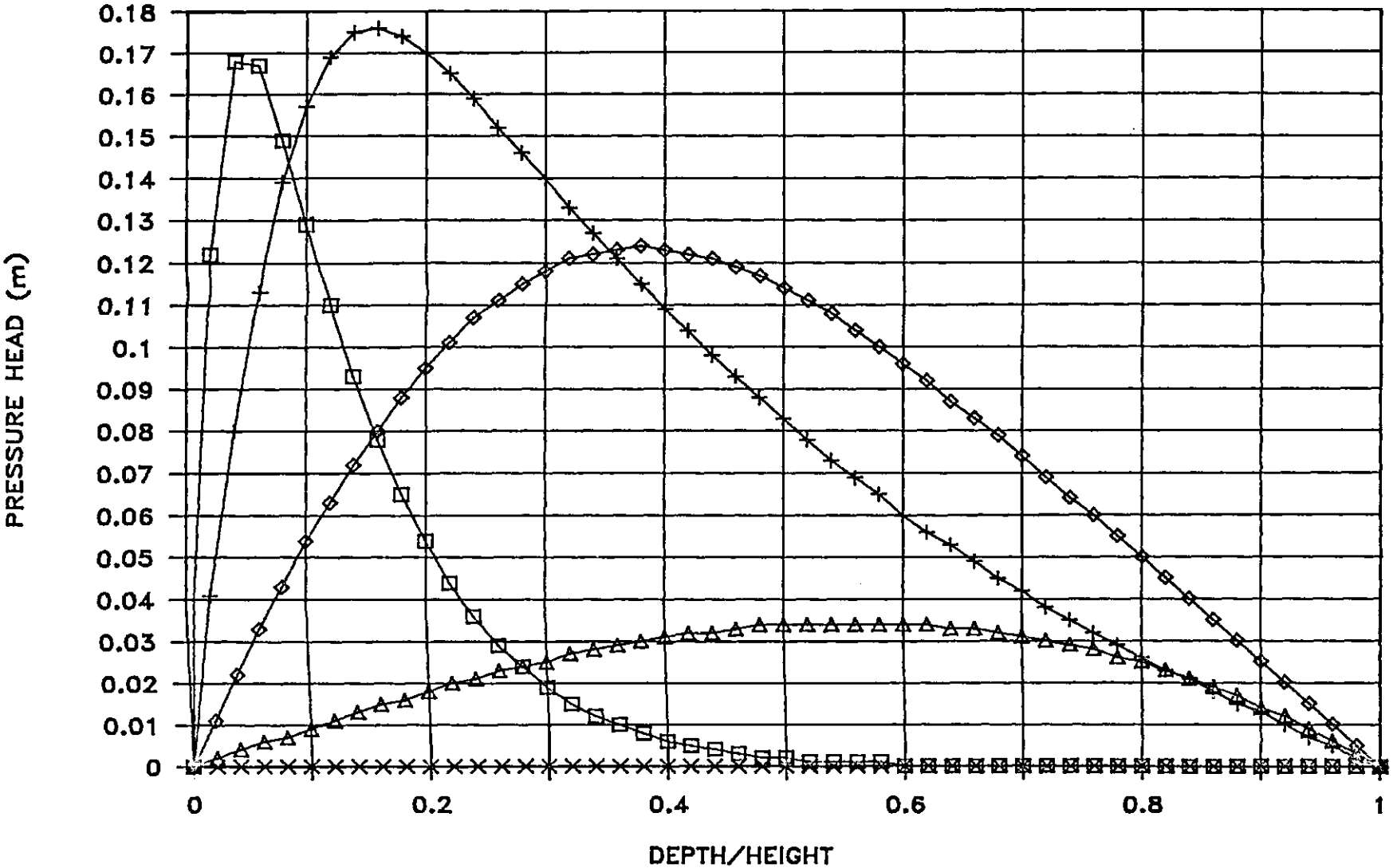

Figure 4.13 Case A2 Pressure Head Contours (Osmotic Consolidation)

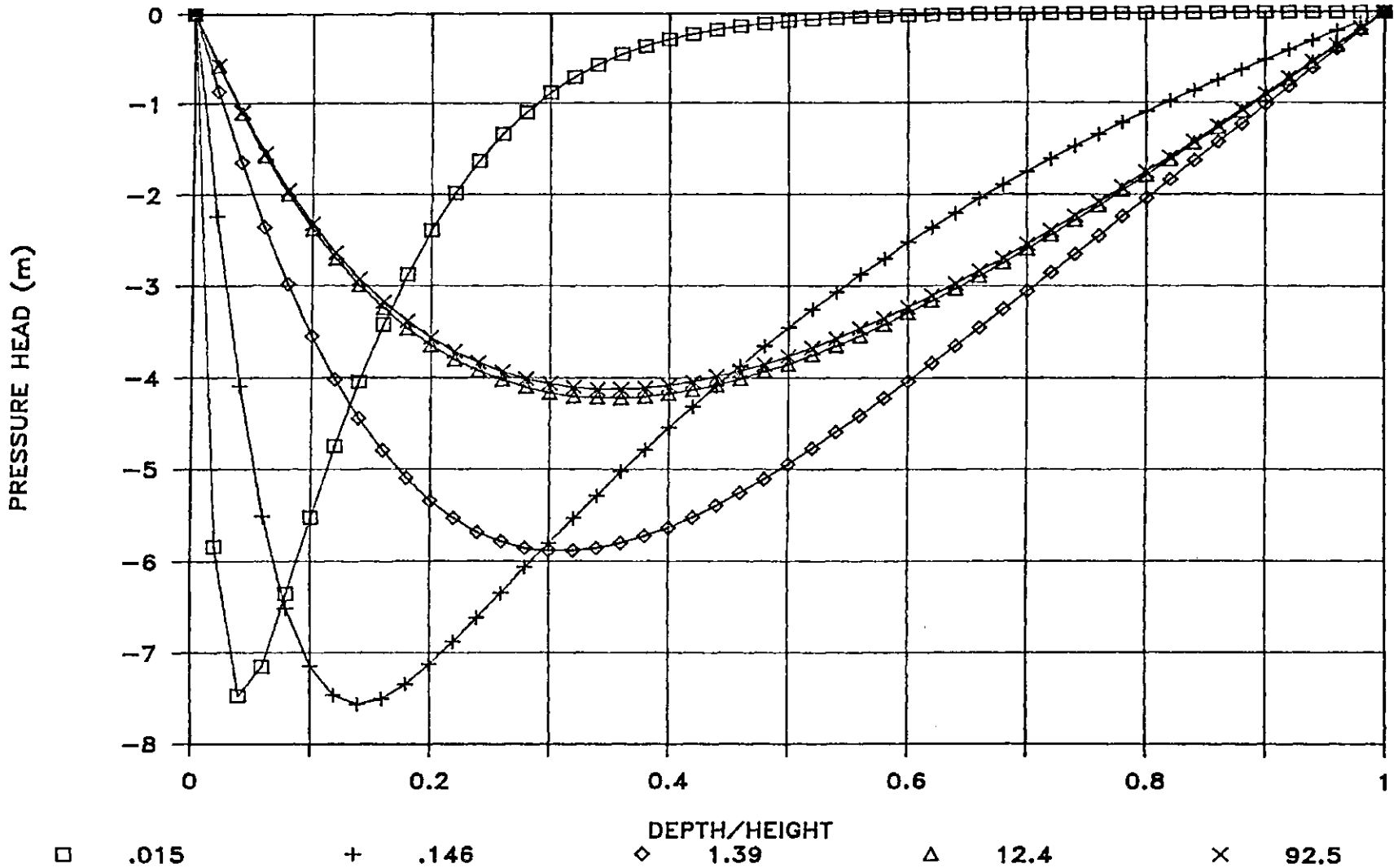

Figure 4.14 Case B2 Pressure Head Contours
(Osmotically Induced Consolidation)

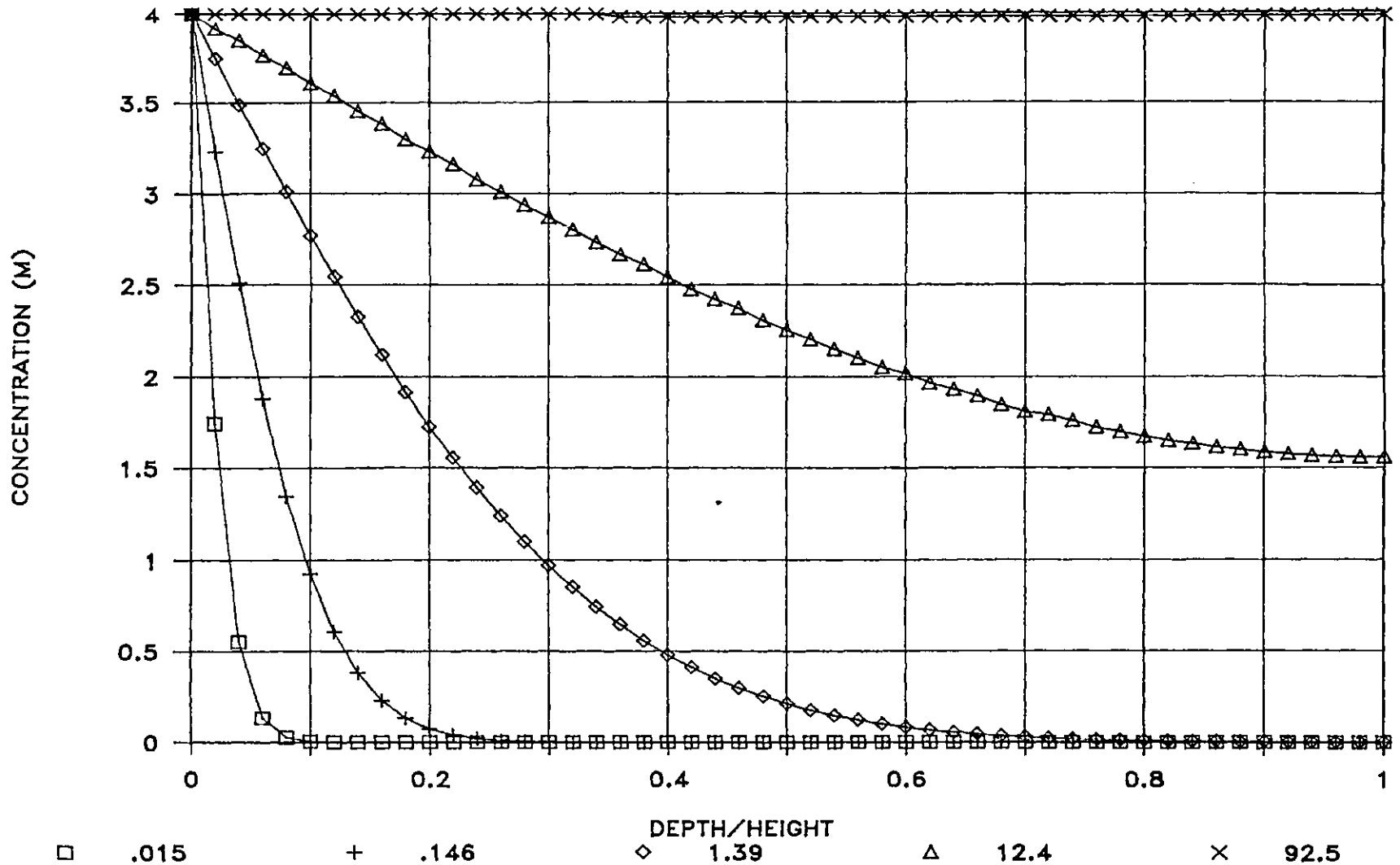

Figure 4.15 Case A2 Concentration Contours
(Osmotic Consolidation)

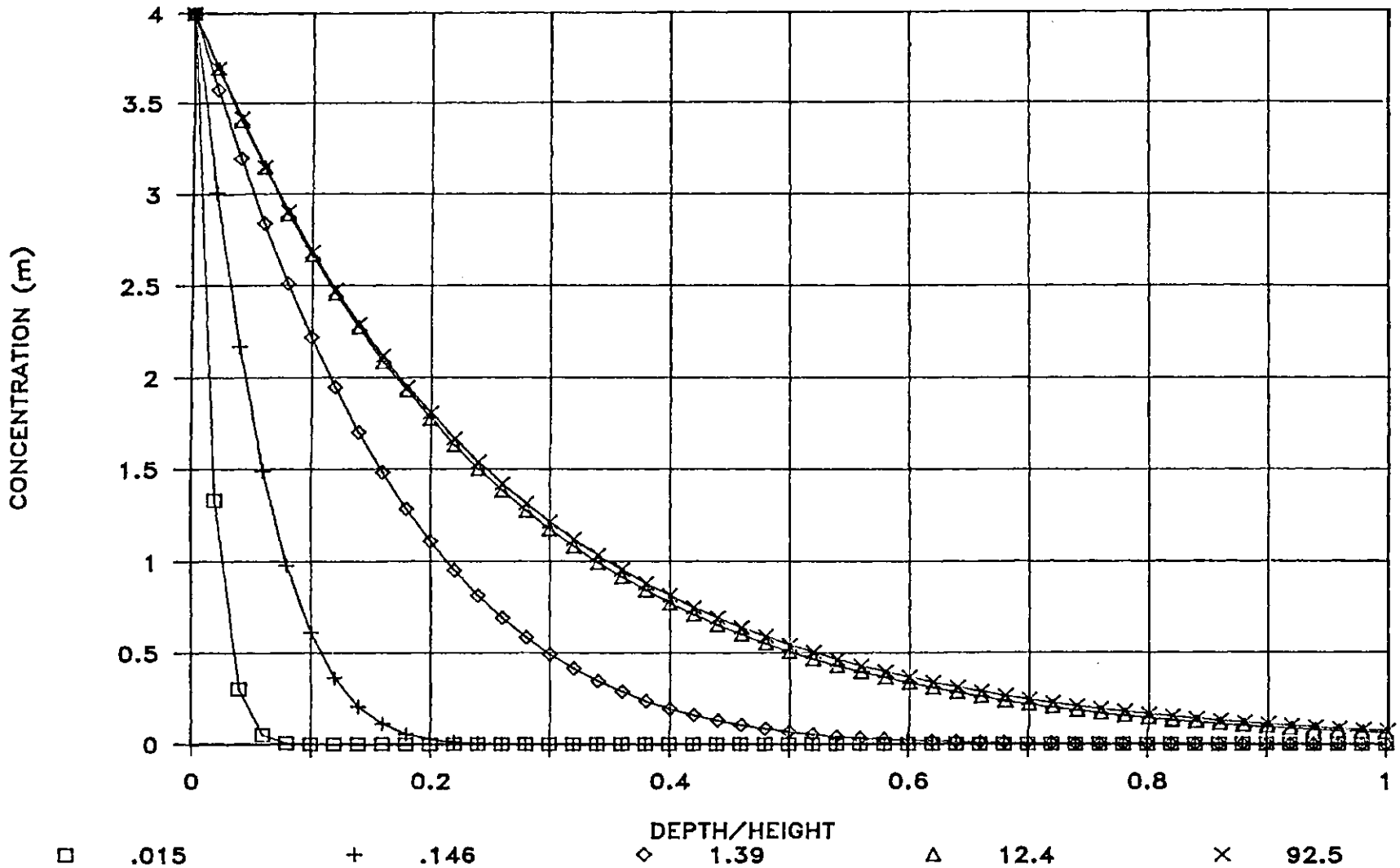

Figure 4.16 Case B2 Concentration Contours
(Osmotically Induced Consolidation)

A steady state concentration profile is reached when diffusive salt transport towards the base of the sample is offset by advective transport of the salt towards the top of the sample. Figure 4.16 demonstrates that the presence of strong osmotic flows in clay liners would prove to be an effective barrier to salt migration.

The concentration contours in Figure 4.15 are nearly identical to those illustrated for Case A1 in Figure 4.8. The small flows generated by expulsion of pore fluid during osmotic consolidation would seem to have little influence on the rate of penetration of salt into the sample.

4.3.4 Time Deflection Responses - Cases A1,B1,A2,B2

The time deflection plots for the four cases are illustrated in Figure 4.17. An additional trial (Case B1a) is also shown on this figure. A swelling index (m_s), equal to 1/10 of the compressibility (m_v) is utilized by the model when the sample swells.

Cases B1 and B1a reach a maximum deflection at a time factor of 2. This is the same value of the time factor for 100 percent osmotically induced consolidation reported by Greenberg (1971) and Mitchell (1973). After 100 percent consolidation, the sample begins to swell. Negative pore pressures which developed within the sample during consolidation, begin to dissipate, which causes relaxation of the effective stress within the sample. For Case B1a swelling occurs with a much smaller modulus and consequently full rebound of the sample is not realized.

Flow into the sample was permitted in Case B2. Consequently, large negative pressures never develop across the entire sample. As a consequence, the maximum deflection of Cases B1 and B1a is not matched by Case B2.

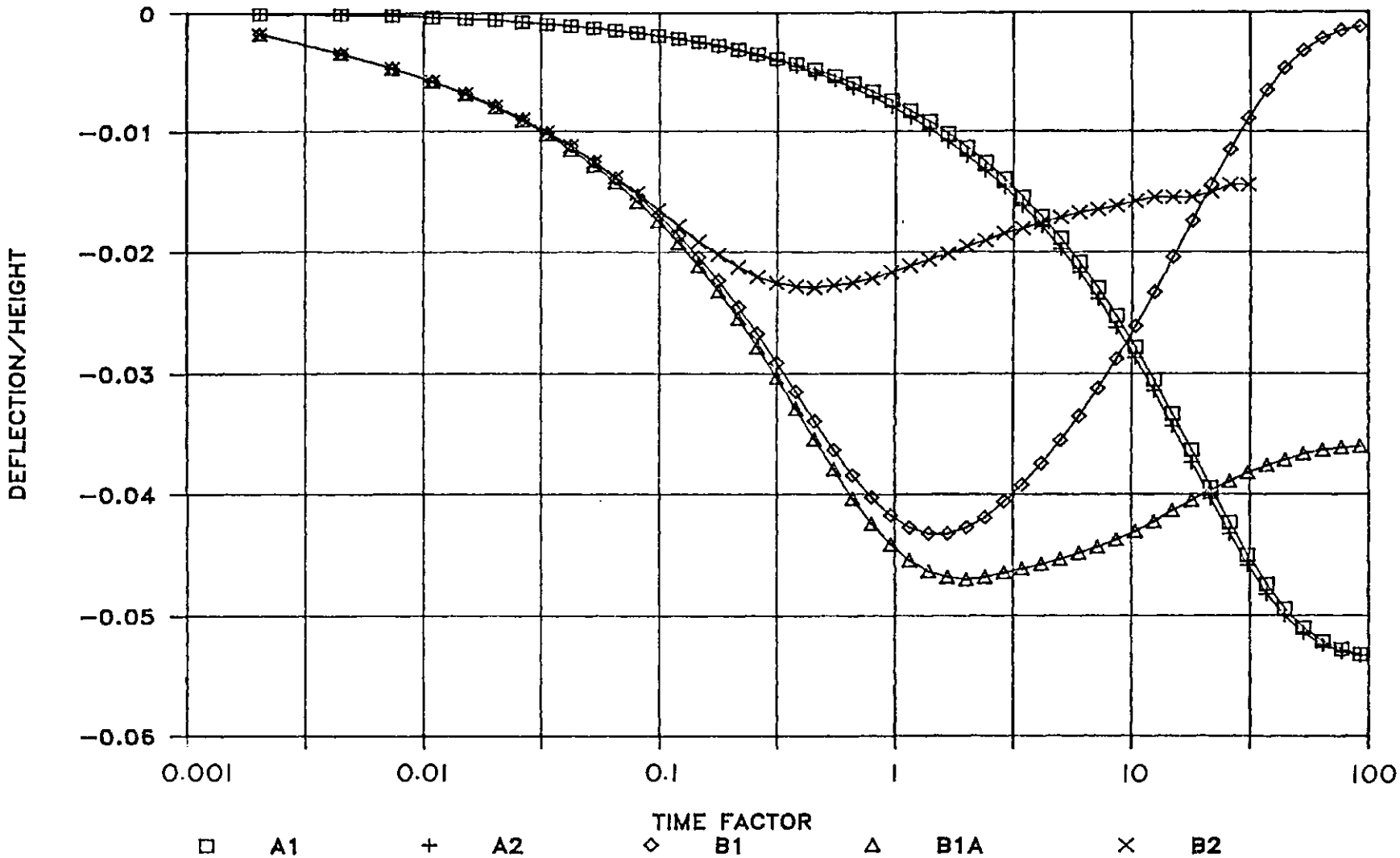

Figure 4.17 Deflection versus Time Factor - All Cases

The osmotic consolidation cases (Case A1 and A2) have nearly identical time-deflection curves. Full consolidation in these cases is reached at a time factor of 100. It was noted earlier that the small flows generated by expulsion of pore fluid during osmotic consolidation had little influence on the rate of salt migration. In both of these cases volume change was only occurring as a result of osmotic consolidation. Consequently, the time to 100 percent consolidation should also be representative of the time to 100 percent equalization of concentration.

The equation for salt transport through soil due to diffusion alone can be written as follows:

$$\partial C/\partial t = D\,\partial^2 C/\partial y^2 \qquad [4.1]$$

where; = diffusion coefficient

This equation is of the same form as that of the consolidation equation:

$$\partial u/\partial t = Cv\,\partial^2 u/\partial y^2 \qquad [4.2]$$

where; = coefficient of consolidation

The classical solution of the consolidation equation relates the degree of consolidation to the time factor, T, equal to (Cvt/h^2). The time factor for 50 percent consolidation is approximately 0.197. The ratio of Cv to D must then also be equal to the ratio of the time factors for 50 percent osmotic consolidation to 50 percent effective stress consolidation. The coefficient of diffusion calculated in this manner is in fact equal to 4.0×10^{-10} m^2/s, approximately 80% of the value input into the simulations.

4.3.5 Summary

A number of general conclusions can be drawn from the results of the simulations of osmotic and osmotically induced consolidation. For the case of osmotically induced consolidation, it is evident that the general shape of the pore pressure contours and deflection-time curves of the

sample are consistent with the responses reported by Greenberg (1971) and Mitchell (1973). The time factor for 100 percent osmotic consolidation was the same as that reported by these authors.

The base pressure response and the cumulative base flow would seem to provide reasonable estimates of the osmotic efficiency of the clay. The maximum base pressure response was equal to the maximum osmotic pressure pressure multiplied by the osmotic efficiency. An equivalent hydraulic gradient can be calculated from the maximum osmotic base flow rate. The ratio of the equivalent hydraulic gradient to the osmotic gradient, provides an accurate estimate of the osmotic efficiency.

When osmotic flows are strong, complete equalization of the pore fluid concentrations across the sample is not attained. When this occurs, the consolidation of the sample may be significantly lower.

The contrast between osmotic consolidation and osmotically induced consolidation is evident in the time-deflection curves for the sample. The osmotically induced consolidation process occurs within a time frame consistent with that of conventional consolidation. The rate of osmotic consolidation, on the other hand, is controlled by the diffusion of salts into the sample. The time to 100 percent osmotic consolidation can be related to the coefficient of diffusion for the soil.

The results of the simulation demonstrate the anticipated behavior of a clay under the two extreme cases of osmotic or osmotically induced consolidation. It would seem apparent, based on these simulations, that the relative significance of either of these two processes on the actual consolidation of a clay can be characterized by monitoring sample deflection, base flow rates, and base pressure responses with time.

CHAPTER 5

LABORATORY PROGRAM

5.1 Introduction

The primary objective of the laboratory investigation is to identify and quantify the dominant mechanisms producing volume change within clay soils exposed to concentrated electrolyte solutions. The volume change, fluid flow, and pore fluid pressure response of a sample of clay (undergoing osmotic and osmotically induced consolidation) have been demonstrated to be diagnostic of the osmotic phenomena active within the clay.

In this chapter the laboratory program used to monitor the characteristic responses of two types of clay samples is described. A review of the literature is presented to illustrate the types of experimental techniques that have been applied to date in the study of osmotic flow and volume change in clay soils. The general approach to the laboratory program is discussed, followed by a detailed description of the testing equipment. The procedure followed for each stage of testing is also described. The material properties for the soils and electrolyte solutions used in the laboratory program are given. Finally an overview of the different testing series is then described.

5.2 Laboratory Studies of Osmotic Phenomena in Clay Soils

Previous laboratory studies of osmotic phenomena in clay soils can be classified as being one of three basic types:

1. Studies of osmotic flow,

2. Studies of the effect of pore fluid concentration on compressibility and swelling, and,

3. Studies of transient volume change of clays due to osmotic phenomena.

Most studies presented in the literature have isolated particular aspects of the general mechanisms of interest in this study.

Osmotic Flow

Laboratory studies of osmotic flow were described in Section 2.3.1 of the literature review. Various forms of osmometers have been used in these studies, similar to those depicted in Figure 5.1 and 5.2. After sample of clay is placed between two porous end caps, concentration differences are applied across the sample, and measurements of fluid flow across the sample are made. No provision is made in these devices to control the confining stress on the sample.

Studies which have observed the induced pressure response, rather than the osmotic flow directly, have also been described in Section 2.3.1. Figure 2.4 illustrates the typical apparatus used in these tests. The sample is contained within a steel cylinder and confining stresses are applied to the sample through a loading piston.

Influence of Pore Fluid Chemistry on the Compressibility and Permeability of Clays

Studies which have investigated the influence of pore fluid concentrations on the compressibility or swelling of clays have been described in Section 2.2. In general, these investigations have utilized samples which have been premixed with fluids of various concentrations. These samples have then been tested in conventional consolidation apparatus.

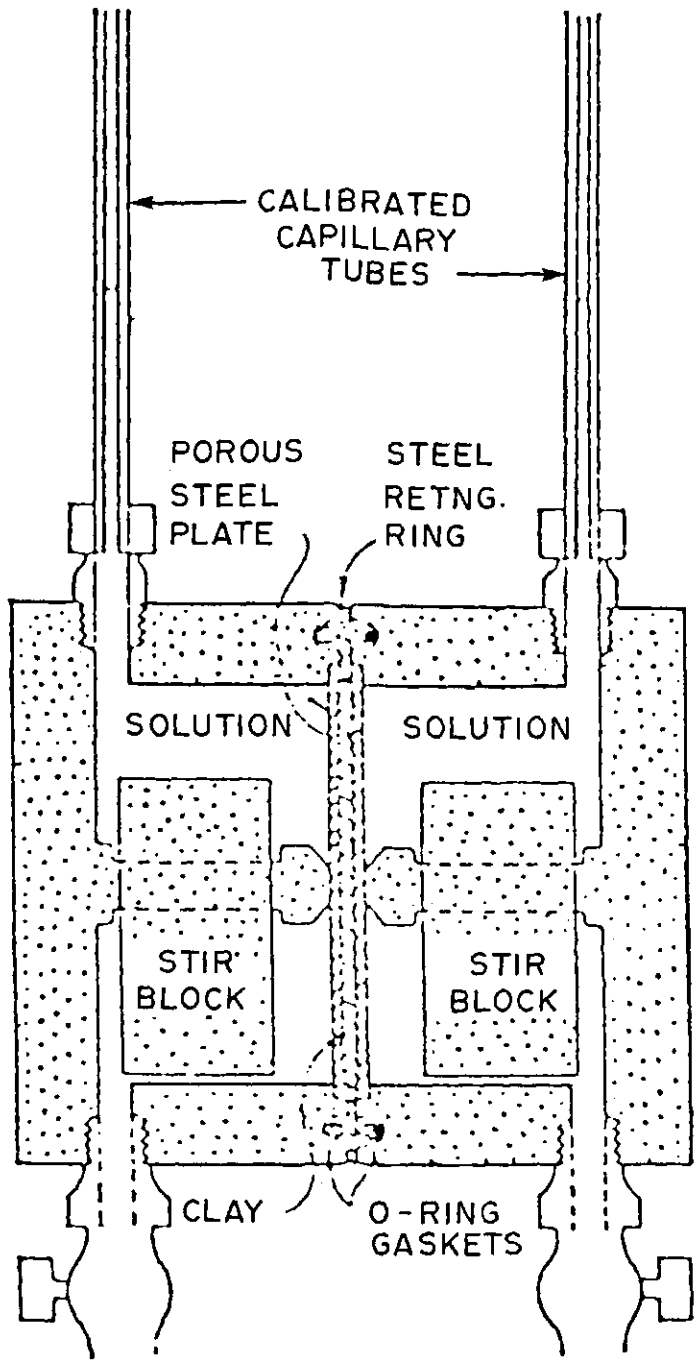

Figure 5.1 Osmometer used by Kemper and Rollins (1966) to Measure Osmotic and Hydraulic Conductivity

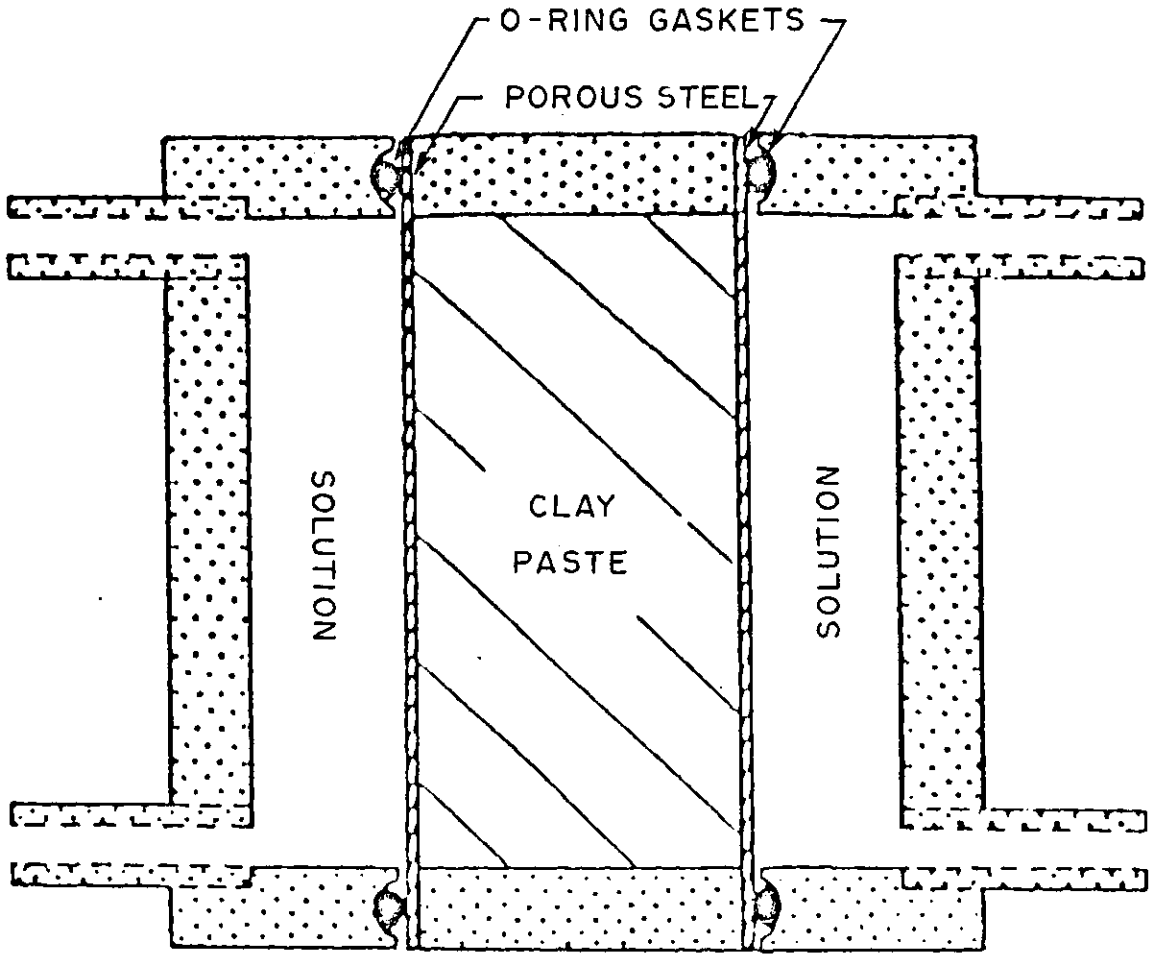

Figure 5.2 Osmometer used by Kemper and van Shaik (1966) to Measure Osmotic Pressures

A major disadvantage of this approach is that only dilute solutions can be utilized without producing significant changes in the structure of the clay. These structural changes tend to overshadow changes that occur in the alteration of the physio-chemical interactions between individual clay particles within a constant structure.

Another method of varying the pore-fluid composition has been to force a new pore fluid into the sample using high hydraulic gradients (Sridharan and Rao 1973). This approach has been used to investigate the effect of changing pore fluid composition on permeability (Buettner 1985, Zrymiak 1985, Ridley 1985,1983, Anderson and Jones 1983, Anderson et al 1984). In these studies rigid wall, or flexible wall triaxial permeameters have been used to measure changes in permeability as the pore fluid composition is changed. Reviews of the literature in this area are provided by Zrymiak (1985) and Ridley (1985). The rate and magnitude of volume change within the clay has been of secondary interest in these studies, relative to the alteration in permeability that occurs due to permeation with a new pore fluid.

Osmotic and Osmotically Induced Consolidation

The focus of studies into the changes in permeability that occur as a result of brine permeation, has been on the behavior of the clay during steady flow conditions. The transient behavior of clay soils in response to osmotic phenomena has been investigated by Greenberg (1971) and Ho (1985).

Greenberg (1971) studied the development of osmotically induced consolidation using various clays and solutions of glycol and NaCl. His experimental investigation included the measurement of the rate of one-dimensional osmotic consolidation of clay samples exposed to glycol solutions. The glycol solution was injected into the porous stone at the base of an oedometer. A schematic of his testing apparatus is depicted in Figures 5.3. Greenberg (1971) made

one attempt to measure the development of negative pressures within a sample during osmotically induced consolidation; however, he was unable to detect any change in pore fluid pressures.

Ho (1985) undertook a broad laboratory study on the influence of NaCl brine on the geotechnical properties of clay soils. In one set of tests, samples of clay were exposed to NaCl solutions by replacing the water reservoir in a standard oedometer with various NaCl solutions. Figure 5.4. illustrates the test device used by Ho. This testing provided a general characterization of the rate and magnitude of osmotic volume change; however, the study was not able to establish the magnitude of the respective mechanisms of osmotically related volume change.

5.3 Testing Methodology

The objective of this present study was to identify the mechanisms of volume change which occur in clays under relatively low confining stresses. The theoretical response of a sample undergoing either osmotically induced consolidation, or osmotic consolidation, was described in Chapter 4.

Osmotically induced consolidation occurs rapidly, within the time frame of normal consolidation, and is accompanied by strong water flow as a result of osmotic gradients. This results in the development of negative fluid pressures within the sample. Osmotic consolidation, on the other hand is characterized by slow consolidation, controlled by the diffusion of salts into the sample. Osmotic consolidation is accompanied by small volumes of fluid flow out of the sample and positive pressures changes within the sample.

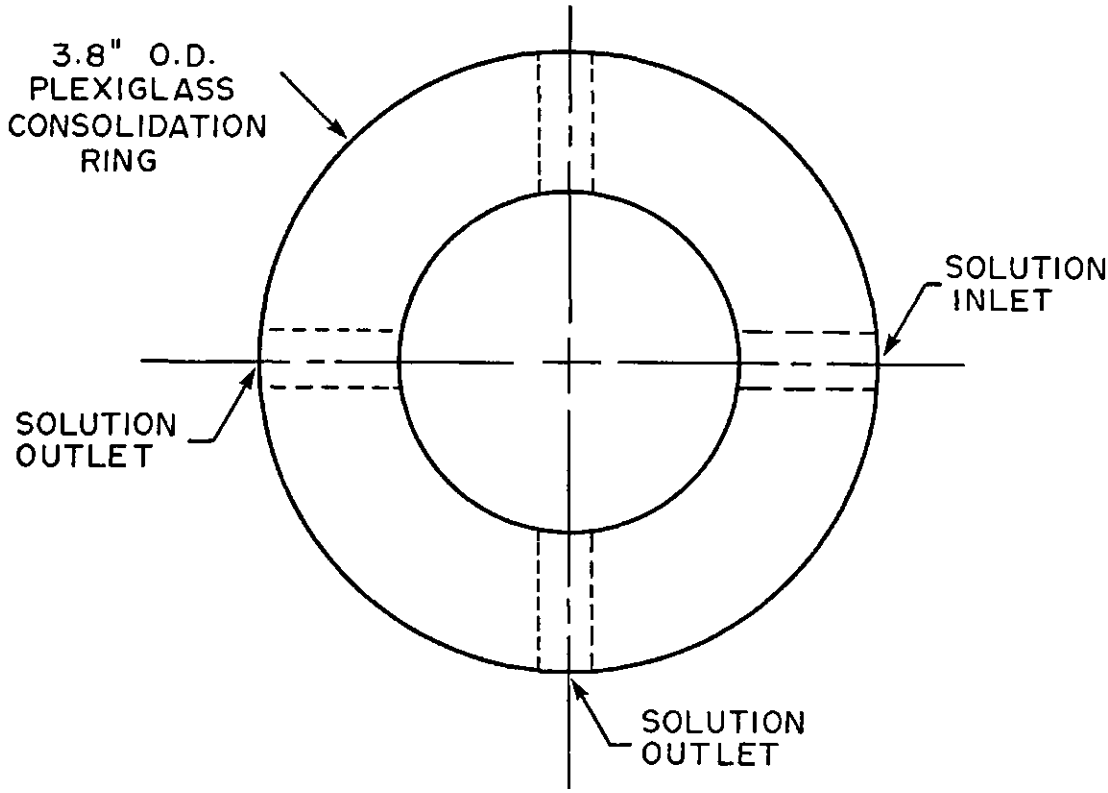

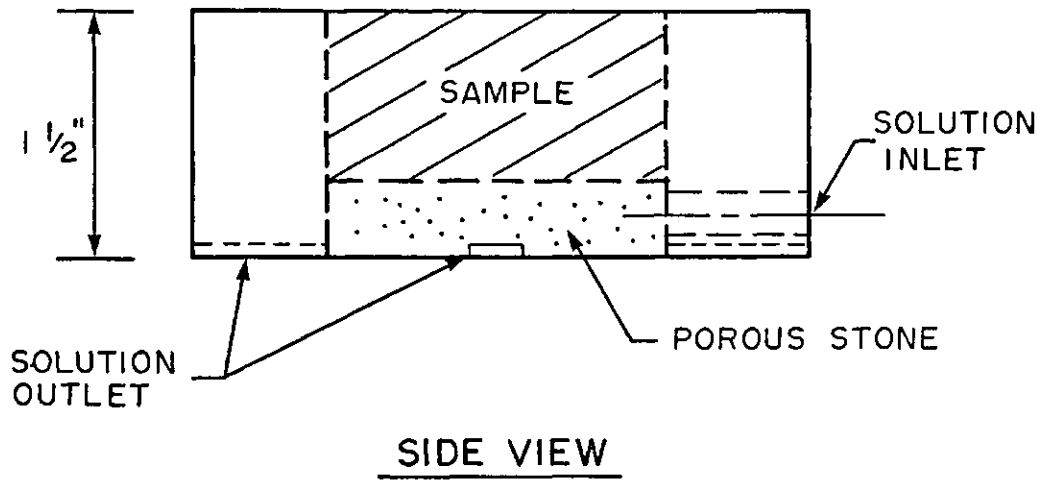

Figure 5.3 Consolidation Ring used by Greenberg (1971) to study Osmotically Induced Consolidation of Clay Soils

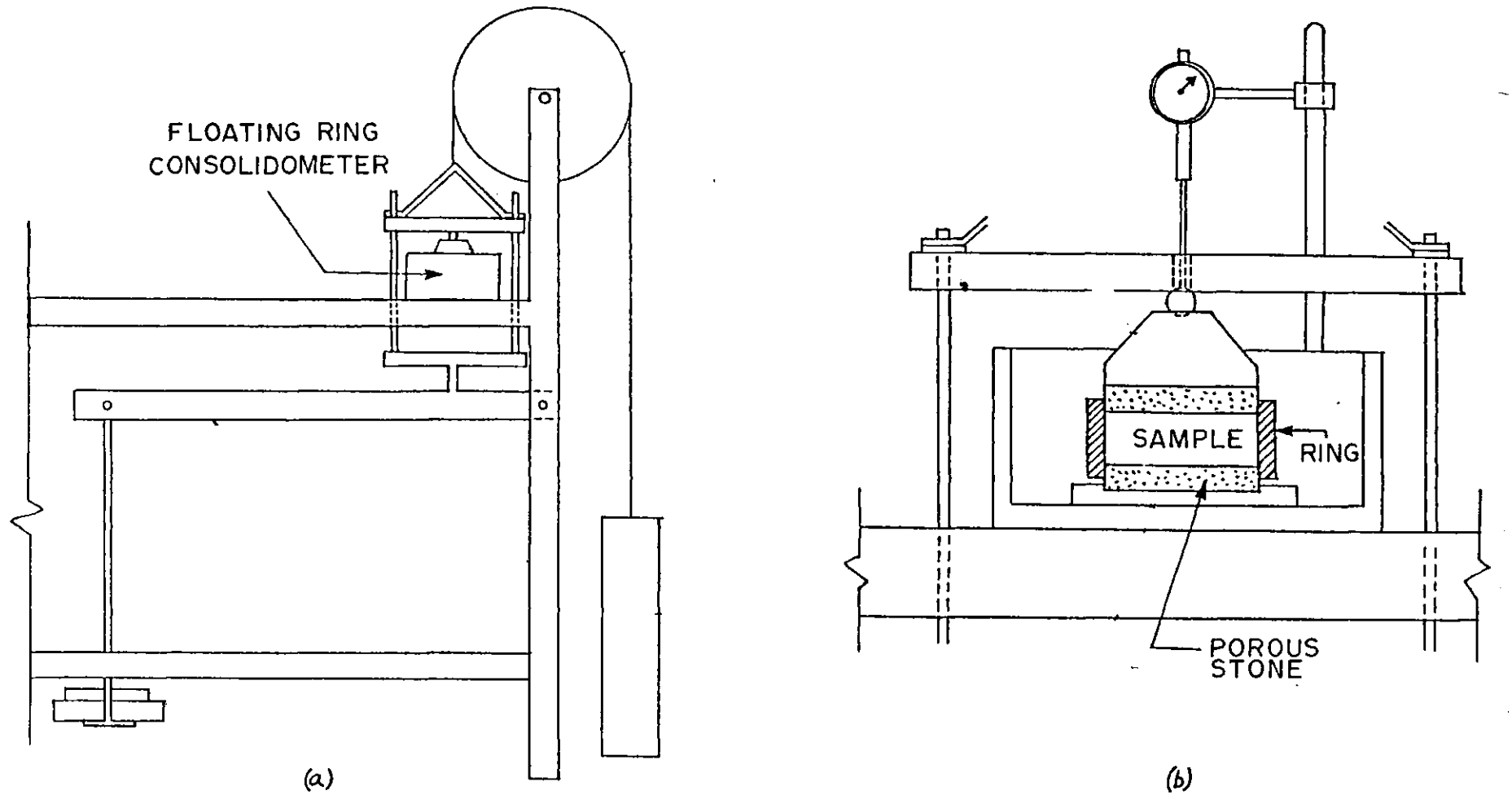

Figure 5.4 Consolidation Test Apparatus used by Ho (1985)

These characteristic responses should be readily observable if a sample of clay is exposed to the electrolyte along only one surface. Observations of volume change can be made by monitoring the deflection of the upper sample surface. Observations of flow or pressures that develop across the base of the sample with time can also be made.

The material properties required to quantify the osmotic volume change processes were developed in Chapter 3. The material properties required included osmotic compressibility, m_π ; osmotic permeability, K_π ; or efficiency K_π/K_h; compressibility, m_v; permeability, K_h; and the coefficient of diffusion, D.

Conventional one-dimensional consolidation testing of clay soils is used to evaluate the compressibility. Consolidation theory can also be utilized to obtain an indirect estimate of the permeability. Several studies have suggested, however, that considerable errors in the value of permeability may occur using this technique (Olson and Daniel 1981, Tavenas et al 1983a, Tavenas et al 1983b). A more accurate definition of the permeability of the sample can be obtained using a constant head permeability test.

Osmotic compressibility can be obtained from measurements of the magnitude of volume change that occurs in the clay with increases in the pore fluid concentration. It was illustrated in Chapter 4 that the base flow or pressure response within the sample can be used to define the osmotic permeability or efficiency of the clay.

A variety of techniques exist for the evaluation of the coefficient of diffusion (Gillham et al 1984, Robinson and Stokes 1968). One of the simplest is to measure the steady state mass flux of salt across a sample in the presence of known concentration gradients.

5.4 Equipment

The primary measurement to be made is that of the rate of osmotic volume change. Measurements of volume change

during consolidation have been made routinely for effective stress consolidation of soils using a conventional laboratory oedometer. A similar device will be used in this study. Modifications to the basic oedometer design are required to allow measurements of flow and pressure across the base of the sample to be made. In addition provisions also have to be made to expose the top of the sample to constant solution concentrations.

5.4.1 Modified Oedometer

The modified oedometer developed for this study is illustrated in Figure 5.5. Vertical loading of the sample is provided through a standard ELE loading frame. The stainless steel sample ring is sealed into the base plate using a single o-ring. The base is connected through a system of valves to calibrated burettes or a pressure transducer (Figure 5.6).

Two burettes were used during testing. Both burettes were laid horizontally at the same elevation as the top of the sample. A small glass burette is used to measure flow rates across the base of the sample during osmotic consolidation. Measurements of fluid volumes are made by monitoring the movement of an air/water meniscus within the burette. The volume of the burette is 0.052 ml of water per cm of displacement. The burette was vented to the atmosphere through a high humidity water vapor reservoir to eliminate evaporation losses.

A second, larger polyethylene burette was used during constant head permeability testing of the samples. This burette has a volume of 0.16 ml per cm of displacement of the air/water meniscus. During permeability testing the larger burettes were connected to an air pressure supply through pressure gauges. Soil Moisture Inc. pressure gauges were used which had a range of approximately 400 kPa, and an accuracy 0.25%.

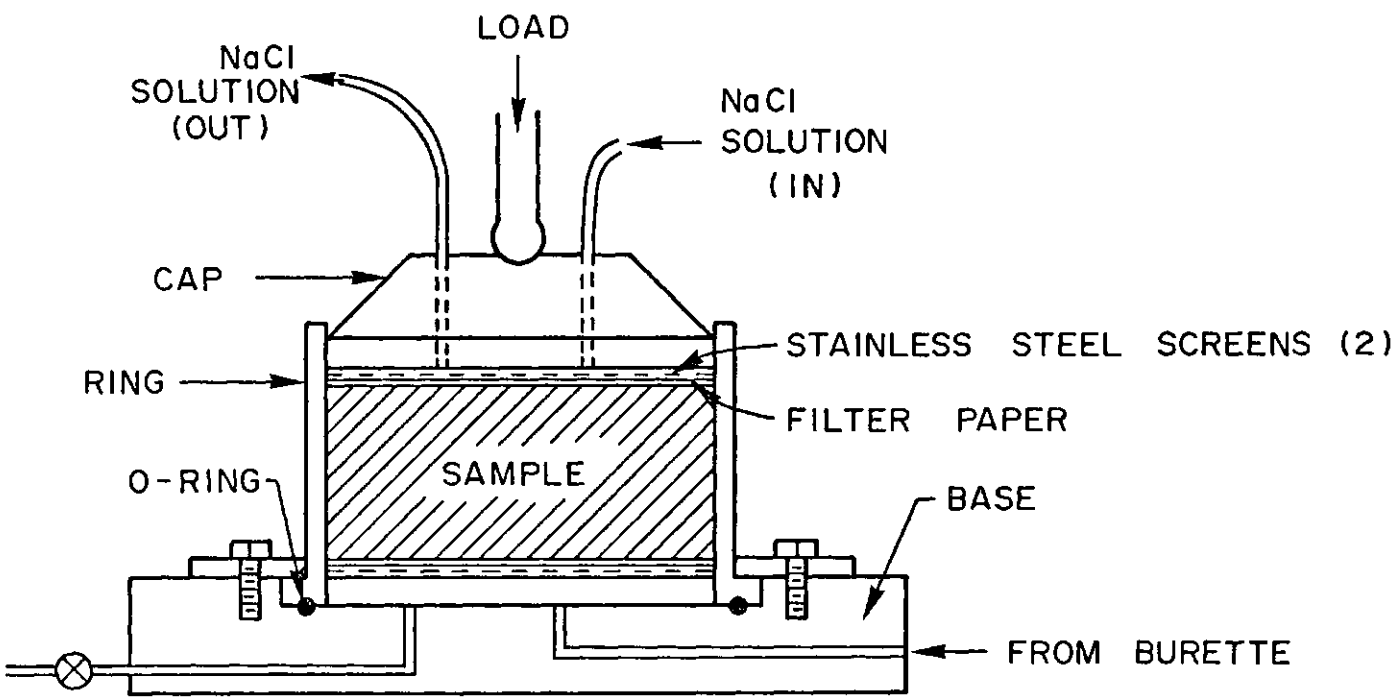

Figure 5.5 Schematic of Modified Oedometer

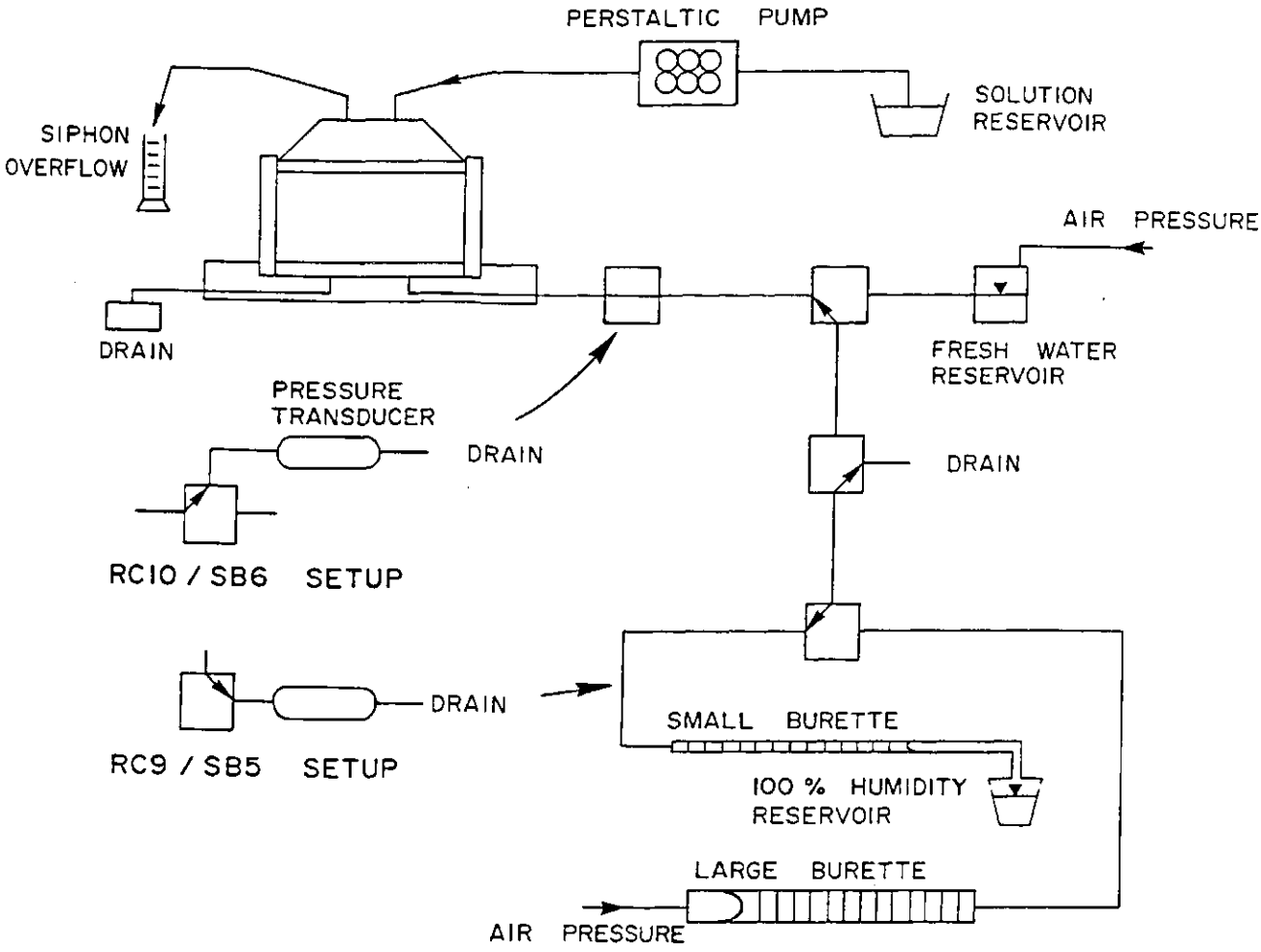

Figure 5.6 Schematic Diagram of Test Setup

Two sets of transducers connected in series to the base plate, were used for tests in which the base pressure response of the pore fluid was to be measured. The changes made in the test setup to accommodate the pressure transducers are shown in Figure 5.6. A low range (Celesco LCVR) transducer, and a high range (Celesco PLC) transducer were used for only one set of tests. The low level transducers proved to be unstable and their use was discontinued. The high range transducers had a pressure range of 100 kPa and an accuracy of 0.5%. Corrections for barometric pressure variations were made using a third Celesco PLC transducer left open to the atmosphere. Verification of the barometric pressure measurements was made periodically using a No. 1215 Sargent-Welch mercury barometer.

For the second series of pressure response tests the high level transducers were connected directly to the base plate through less than 30 cms of polyethylene tubing. The tubing length was shortened so as to minimize time lag in the pressure readings due to volume changes in the tubing. Calibration of the transducers was performed by connecting the pressure lines to standing water columns of known height. Calibration data for the pressure transducers is included in Appendix C.

Exposure of the sample to NaCl solutions was accomplished by providing a continuous siphon of solution across the top of the sample. For several initial tests, the solution supply to the samples was provided by a gravity siphon from an adjacent solution reservoir. Excess brine was then siphoned from the sample ring into a graduated cylinder. In later tests a peristaltic pump was used to ensure a constant supply of solution from the reservoir to the sample.

Two concentric grooves within the loading cap ensured an even radial flow of solution across the top of the sample from the inner ring to the outer ring. For all but two test

samples (i.e., RC1 and RC2), stainless steel screens were used at the top of the sample in place of porous stones. Porous stones or stainless steel rings were used to separate the base of the sample from the base plate.

5.4.2 Standard Oedometer

A series of tests were undertaken to observe the magnitude and rate of osmotic deformation using "two-way drainage" setups. These consisted of light loading frames with modified loading caps. In place of porous stones, pairs of fine mesh stainless steel screens were used on the top and bottom of the sample. Modifications were made to allow solution to be injected directly onto the screens. Replacement of the solution in the reservoir surrounding the sample was performed periodically in order to ensure full solution strengths adjacent to the sample. The old solution was siphoned out of the reservoir and the fresh solution was injected directly into the top and bottom screens.

5.5 General Test Procedures

For most of the tests, the clay samples were reconsolidated from a slurry. At the selected stress level, the permeability of the sample was measured. The sample was then exposed to various solution concentrations and changes in volume, and base flow or pressure, were then monitored. In the following sections each stage of this test sequence is described in detail.

5.5.1 Test and Sample Preparation

The sample ring and base plate was assembled and flushed repeatedly with distilled water prior to testing. A leakage test was performed prior to every test by filling the ring with distilled water to the same elevation as the burettes. The ring was covered with plastic wrap, and the base was opened to the small burette. In general, leakage

tests were conducted overnight and were deemed acceptable only if the leakage rate was non-detectable. For a few cases a leakage rate of less than 0.0026 ml per hour was accepted.

Samples for the tests were mixed from air-dried soil and distilled water to moisture contents approximately equal to the liquid limit for the soil plus 10%. After mixing, the samples were placed in a moisture and temperature controlled room to cure overnight. The sample was then placed in the ring with sufficient reworking so as to remove any trapped air bubbles.

5.5.2 Sample Consolidation

Following placement of the slurried sample into the test ring, filter paper, stainless steel screens and the loading cap were placed on the sample. The sample was then left to consolidate for approximately half a day. Loading of the sample to the desired confining stress was then carried out by doubling the load increments. In all but two of the tests, the samples were consolidated in a double drainage mode by leaving the sample base connected to the large burette, which was left vented to the atmosphere. For samples RC10 and SB6 pore pressure responses during consolidation were used to measure the response time of the transducers.

At the stress level at which osmotic volume changes were to be observed, the sample was left to consolidate until the rate of secondary consolidation of the sample was established. Following the completion of osmotic volume change, several samples were consolidated to higher stress levels.

5.5.3 Constant Head Permeability Tests

Constant head permeability tests were performed on all samples following consolidation. For permeability testing the base of the sample was opened to the large burette. Air

pressure was applied to the large burette, and the Darcy flux through the sample was measured by monitoring the movement of the air-water meniscus with time. A constant air pressure was maintained until a steady flow rate through the sample was achieved. For several samples the permeability test was repeated for up to three different gradients.

The maximum air pressure used was kept to a minimum in order to avoid significant changes in the effective stress within the sample. The average effective stress change within the sample was kept less than 10% of the effective stress prior to permeability testing.

Permeability testing, following the completion of osmotic volume change, was undertaken on three samples. The reservoir of fluid below the sample in the cell was contaminated with salt during the osmotic volume process. The duration of the post-osmotic permeability testing was minimized in order that fresh water from within the burette tubing would not penetrate the sample.

5.5.4 Osmotic Volume Change

The sample was left a sufficient length of time following permeability testing to dissipate any excess pressures within the sample. The small burette was then opened to the base of the sample and the top of the sample was exposed to the specified solution concentration. Deflection, and base flow or pressure measurements were then commenced. All data was recorded manually with the exception of the pressure measurements which were recorded using a data acquisition system.

Following the completion of osmotic volume change, the sample was removed, retested for permeability, and/or loaded to higher applied stress levels. The thickness and moisture content of the sample was obtained after removal of the sample from the apparatus.

The soluble salt content of the pore fluid of several samples was obtained by measuring the total dissolved salt content of extracted samples of the pore fluid. The pore fluid was extracted by the use of a soil press (Figure 5.7). This technique has been used successfully by Manheim (1966) and Balasubramonian (1972).

The press was assembled after it was washed twice with distilled water and air dried. The soil sample was placed on top of filter paper, and a clean plastic syringe was inserted into the effluent passage. Pressure was gradually applied until several mls of fluid were extracted. The mass of dissolved salt was measured gravimetrically by oven drying a known volume of the extracted fluid. The volume was measured using a volumetric pipette.

5.5.5 Diffusion Test

Direct measurements of the coefficient of diffusion were made in two separate tests (i.e., RC4 and SB3). These samples were consolidated and then tested for permeability using the above described methods. After the completion of the permeability test, the base of the sample was then opened to the large burette on one side and a drainage tube on the other. The outlet of the drainage tube was kept at the same elevation as that of the solution reservoir at the top of the sample. As the top of the sample was exposed to brine a slow siphon of distilled water was maintained across the base of the sample. This underflow was sampled periodically and tested for total dissolved solids content and conductivity. Three to 10 ml samples of the base underflow were taken.

These samples were oven-dried for a minimum of half an hour and then cooled in a desiccator for 15 minutes. The samples were then weighed to obtain the weight of the total dissolved solids within the sample.

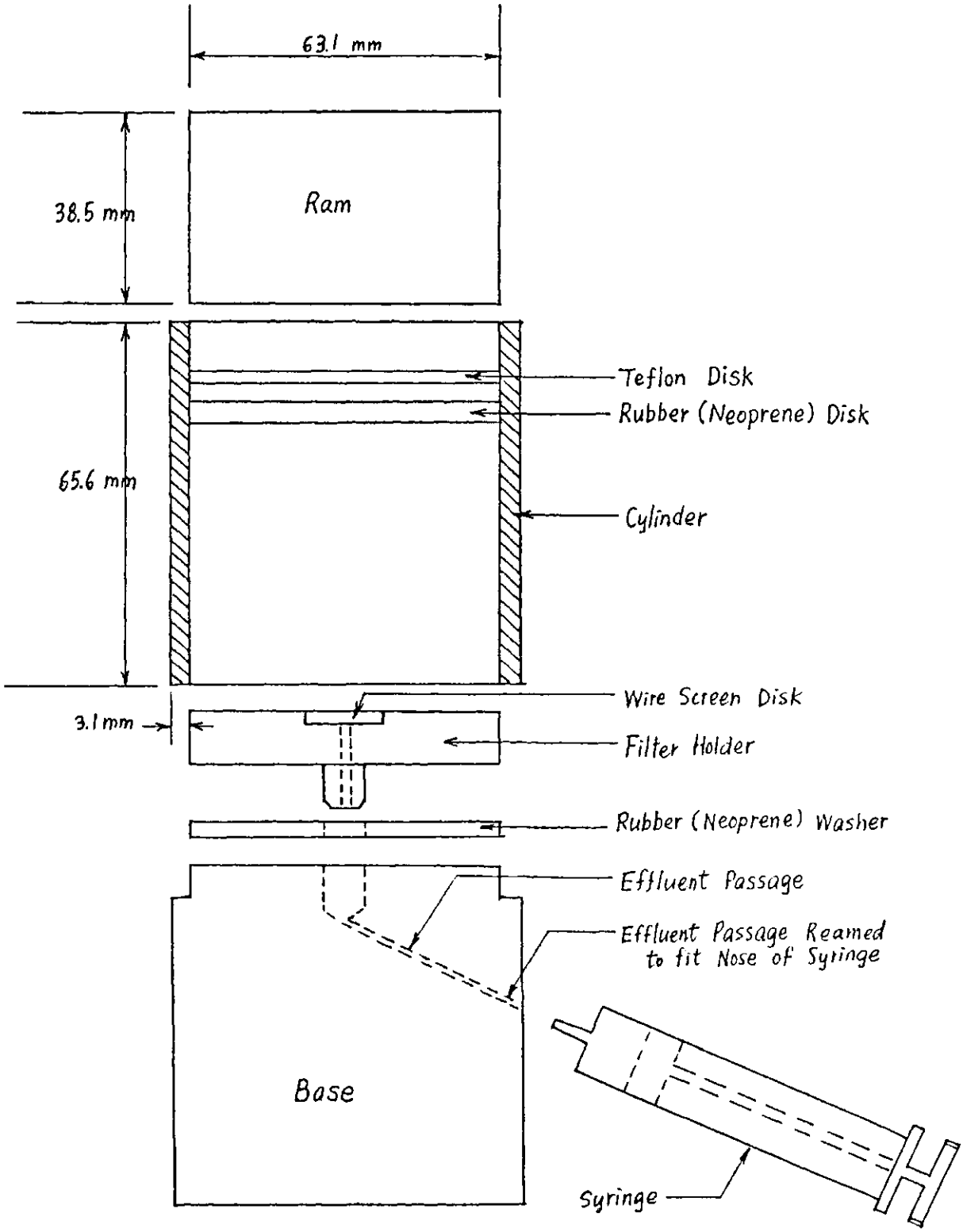

Figure 5.7 Schematic of Soil Press (after Ho 1985)

Conductivity measurements of the base underflow were taken periodically using a Industrial Instruments (Model RA-2A) conductivity meter. Sufficient flow was always provided to maintain the concentration of the underflow to a level less than 1% of that being used at the upper surface of the sample.

5.6 Description of Test Soils and Solutions

The types of soil and solution selected for this study are described in this section. Basic properties of each of these materials are also provided.

5.6.1 Description of Soil Types

Two clay soils were selected for testing. These were Lake Regina Clay and a 20% : 80% mixture of Na-montmorillonite and Ottawa sand. The selection of these soil types was made in anticipation that the two clays would exhibit different mechanisms of osmotic volume change. The properties of these two materials are discussed below.

Ho (1985) tested samples of reconsolidated Regina Clay and obtained results which were indicative of a slow volume change process similar to that envisaged for osmotic consolidation (Figure 2.19). Testing by Buettner (1985) and Zrymiak (1985) used mixtures of Na-montmorillonite and Ottawa sand to evaluate the effect of brine contamination on the permeability of clay liners. Buettner exposed a sample of approximately 17% Na-montmorillonite to a saturated NaCl brine, under a hydraulic gradient of 270. Upon brine exposure, the fluid flow at the upstream end of the sample reversed against the prevailing hydraulic gradient. This reversal in flow continued for a time factor of approximately 1 after which time, flow into the sample resumed.

5.6.1.1 Regina Clay

Two series of tests were performed on Regina clay; one on remolded samples and the other on intact samples. For the tests of slurried Regina Clay, only the material passing a No. 10 sieve was used in testing. The intact Regina Clay samples were taken during the field drilling program for a separate study (Bruch 1985). The samples were taken from a depth of up to 7.7 metres. The tests on the intact samples were to provide a qualitative indication as to whether the influence of osmotic consolidation was as significant to undisturbed specimens of Regina Clay as it appeared to be for the remolded samples.

Regina Clay has been used in a number of studies undertaken at the University of Saskatchewan including Ho (1985), Fredlund et al (1980), and Fredlund and Hasan (1979). The clay is obtained from a surficial, glacial lake deposit situated at Regina, Saskatchewan, Canada. It is grayish brown in color (2.5Y 5/2, dry) and highly plastic. A summary of index properties for Regina Clay is provided in Table 5.1. The results of an analysis of soluble salts based on a saturation extract, are given in Table 5.2.

5.6.1.2 Na Montmorillonite/ Ottawa Sand Mixture

The Na-montmorillonite (i.e.,bentonite) is a commercial product known as Avongel Sodium Bentonite. The sand used was an Ottawa sand, meeting ASTM C-190 specifications. It is a uniform fine silica sand that passes the No. 30 US sieve and is retained on the No. 100 sieve.

A summary of the general properties of the Na-montmorillonite, Ottawa sand, and the sand/bentonite mixture is given in Tables 5.1 and 5.2.

Table 5.1 Summary of Classification Tests

Test	Regina Clay	Na-Mont	Sand	Mixture
Specific Gravity	2.83	2.56	2.65	2.63
Atterberg Limits				
Liquid Limit	75.5%	-	-	62.1%
Plastic Limit	24.3%	N/A	-	np
Plasticity Index	51.2%	N/A	-	-
Grain-Size Distribution				
Sand Sizes	0%	0%	100%	80%
Silt Sizes	34%	0%	0%	0%
Clay Sizes	66%	100%	0%	20%
Mineralogical Composition - Less than 2 microns				
Montmorillonite	45.2%*	80%**	N/A	N/A
Illite	27.7%	7%	N/A	N/A
Kaolinite	17.7%	0%	N/A	N/A
Trichlorite	9.4%	0%	N/A	N/A
Quartz	0.0%	8%	N/A	N/A
Gypsum	0.0%	3%	N/A	N/A
Carbonate	0.0%	2%	N/A	N/A
Specific Surface (m /gm)	53***	700-840****	N/A	140-168
Exchange Capacity (me/100 gm)*****	31.7	80-150	N/A	N/A
Exchangeable Cations***** (me/100gm)				
Magnesium	15.3	N/A	N/A	N/A
Calcium	54.4	N/A	N/A	N/A
Potassium	0.59	N/A	N/A	N/A
Sodium	1.77	N/A	N/A	N/A

---

* Test performed by Saskatchewan Research Council
** Quigley (1984)
*** Test performed by Department of Soil Science, University of Saskatchewan by ethylene glycol sorption (Black 1965 Part 1)
**** Mitchell 1976
***** Fredlund 1975

Table 5.2 Chemical Analysis of Saturation Extract (performed by Saskatchewan Soil Testing Laboratory - after Black 1965 part II)

Test Result	Regina Clay	Bentonite
w.c. of extract	88%	550%
pH	7.4	8.8
Conductivity (mS/cm)	3.7	4.0
Ions in Extract (ug/ml)		
Na+	210	910
Ca++	546	23
Mg++	183	7
K+	35	9
Cl-	133	81
SO4--	1700	1400
Sodium Adsorption Ratio	2.0	42.2

5.6.2 Test Solution

NaCl solutions were used throughout the testing. These solutions were prepared from distilled water and dry fine granulated salt. The salt used was Windsor Fine Granulated Salt. This salt was not iodized and was composed of 99.3% NaCl. The manufacturing specifications for the dry salt is provided in Appendix C.

Solution concentrations used in testing varied from 0.01 M to 5.0 M. Fully saturated NaCl solutions were not used. It was feared that if saturated solutions were used variations in temperature might result in precipitation of the dissolved salt during testing.

5.7 Summary of Tests

Table 5.3 presents a summary of the tests completed in this study. A total of 26 tests were completed. Each test provided data on the rate and magnitude of osmotic volume change, however, each test could be monitored for only base flow or pressure. Ten samples were monitored for base flows, and 4 samples were monitored for base pressure responses. Tests RC7 and SB3 were conducted primarily to establish values for the coefficient of diffusion at different concentrations. Tests RCDD and SBDD were conducted in order to establish the shape of the virgin consolidation curve for reslurried Regina Clay and Sand/bentonite without the effect of varying solution concentrations.

Table 5.3 Summary of Laboratory Tests

Sample	Primary Purpose of Test	Base Measurements		Verticle Stress during Exposure to Brine (kPa)	Verticle Stress after Reloading (kPa)	CONCENTRATIONS OF NACL (MOLARITY)
		Flow %	Pressure %			
Remolded Regina Clay - 1 Side Exposure						
RC1	Consolidation	%	-	203	203	4.0
RC2	Consolidation	%	-	201	201	4.0
RC3	Consolidation	%	-	199	199	4.0
RC4	Consolidation	%	-	200	200	0.5 1.0 4.0 5.0
RC5	Consolidation	%	-	49	803	0.1 0.5 1.0 2.0 4.0 5.0
RC6	Consolidation	%	-	100	806	0.1 0.5 1.0 2.0 4.0 5.0
RC7	Diffusion	-	-	203	203	0.5 1.0 2.0 4.0
RC8	Base Flow	%	-	202	202	.005 .01 .05 0.1 0.5 1.0 2.0 4.0 5.0
RC9	Base Pressure	-	%	205	205	DW .01 .05 0.1 0.5 1.0 2.0 3.0 4.0 DW
RC10	Base Pressure	-	%	200	200	4.0
RCDD	Consolidation	-	%	-	207	DW
Intact Regina Clay - 2 Side Exposure						
DB1	Consolidation	-	-	300	300	4.0
DB2	Consolidation	-	-	300	1209	0.1 0.5 1.0 2.0 4.0
DB3	Consolidation	-	-	83	83	4.0
DB4	Consolidation	-	-	200	200	0.1 0.5 1.0 1.0%4.0% (% @ 390 kPa)
DB5	Consolidation	-	-	758	1229	0.1 0.5 1.0
DB6	Consolidation	-	-	518	518	4.0 DW
Sand/Bentonite - 1 Side Exposure						
SB1	Consolidation	%	-	203	203	4.0
SB2	Consolidation	%	-	205	803	4.0
SB3	Diffusion	-	-	203	203	0.5 1.0 2.0 4.0
SB4	Base Flow	%	-	202	202	DW .05 0.1 0.5 1.0 2.0
SB5	Base Pressure	-	%	205	205	DW .01 .05 0.1 0.5 1.0 2.0 3.0 4.0 DW
SB6	Base Pressure	-	%	205	1608	4.0
SBDD	Consolidation	-	%	-	1603	DW
Sand/Bentonite - 2 Side Exposure						
SBOC1	Consolidation	-	-	96	1715	.05 0.1 0.5 1.0 2.0 4.0
SBOC2	Consolidation	-	-	201	201	.05 4.0 2.0 1.0 0.5 0.1 .05 .01 DW
SBOC3	Consolidation	-	-	23.5	1598	.01 .05 0.1 0.5 1.0 2.0 4.0

The sample thicknesses prior to exposure to the NaCl solutions ranged from approximately 0.5 cm to 1.7 cm. Although the samples were extremely thin, the time for equilibrium for a single increment of concentration was several days to several weeks. Consequently, the time to complete the testing program outlined in Table 5.3 was approximately 10 months using two modified oedometer setups and up to 6 standard oedometer setups.

CHAPTER 6

PRESENTATION OF DATA

6.1 Introduction

The primary objective of the laboratory study was to identify the mechanisms producing osmotic volume change in clay soils, and to quantify these mechanisms in terms of soil properties. Based on the results of numerical simulations of osmotic consolidation and osmotically induced consolidation it was apparent that the mechanisms of osmotic volume change could be distinguished on the basis of measurements of deflection, and base flow rate or base pressure response.

The theoretical framework developed in Chapter 3 defined the process of osmotic volume change and flow in terms of the following soil properties: compressibility (m_v),osmotic compressibility (m_π), permeability (K_h), osmotic permeability (K_π), and the coefficient of diffusion, (D). Each of these properties can be deduced from the various stages of the testing procedure.

The coefficient of volume change (i.e., compressibility), at various stress levels can be determined from the volume change of the sample that takes place during reconsolidation. The values obtained in this manner are an average compressibility taken over the applied stress increment. To obtain the compressibility at the stress level at which osmotic volume change was monitored, an extrapolation of the compressibility obtained at lower stress levels will have to be used.

The permeability of each sample tested in the modified oedometer setup was measured prior to osmotic volume change, using a constant head permeability test. For three samples,

the permeability test was repeated after the completion of osmotic volume change.

A time-deflection curve is obtained for every sample that undergoes osmotic volume change. If osmotic consolidation is the dominant mechanism of volume change, these curves can be used to establish the deflection of the sample under each increment of osmotic pressure. The osmotic compressibility can then be calculated as the percent volume change divided by the osmotic pressure increment to which the sample has been exposed.

The numerical simulation in Chapter 4 illustrated that when osmotic flow occurs across the sample, the magnitude of the flow can be used to calculate an equivalent hydraulic gradient across the sample. The ratio of the equivalent hydraulic gradient to the actual osmotic gradient across the sample is the efficiency of the clay membrane. Efficiency is defined as the ratio of the osmotic permeability to the hydraulic permeability.

The coefficient of diffusion can be established from Fick's first law, which relates the concentration gradient to the mass flux. Two tests were run in which constant boundary concentrations were maintained, and the mass flux across the sample was measured.

Sections 6.2 through 6.6 provide a description of the measurements made to evaluate each of the material properties discussed above. Examples of the tests data are presented accompanied by a discussion of the significant concerns regarding each data set. The analyses of the test data, in order to evaluate the properties listed above, are presented in Chapter 7.

6.2 Consolidation Tests

Consolidation testing was undertaken on a total of 26 samples. Of these, 20 samples were reconsolidated samples of slurried material and 6 were intact samples of Regina Clay. The deflection-time plots obtained during loading were analyzed using a log-time (i.e., Casagrande) construction, to obtain the values of deflection at 100% consolidation. These deflections were corrected for the compressibility of the apparatus.

Void ratios were calculated, based on the final sample height and the final water content of the sample. The water contents were corrected for the presence of dissolved salts to obtain the weight of water alone to the weight of mineral soil solids. This correction was based on estimates of the final pore fluid concentration as obtained from the pore-fluid extractions described in section 6.4.

Summary calculations of void ratio, water content, porosity, and compressibility for each stress increment are included in Appendix D.1. Table 6.1 provides a summary of the water content, void ratio, porosity and compressibility for each sample at the load increment prior to the start of osmotic volume change.

Considerable scatter exists in the values of void ratio for different samples, at the sample stress level. For the Regina Clay samples, the void ratio at an applied stress of 200 kPa, varies by as much as 40%. For the sand/bentonite samples the void ratio varies by as much as 17%. There are several possible reasons for the variability.

The calculation of the void ratio at any stress level is obtained by back calculation from the measured sample height and water content at the completion of osmotic volume change. Errors in the measurement of the final sample height, or in the final water content or pore fluid concentrations, would result in significant variations in the calculated void ratios.

Likely of more significance is the extremely long times over which the osmotic volume change process took place. During these time periods the magnitude of secondary consolidation that took place is significant. Although corrections for secondary consolidation were incorporated into the time deflection measurements obtained during osmotic consolidation, no correction for the magnitude of secondary consolidation was made in the void ratio data presented in Table 6.1 and in Appendix D.1.

Scatter in the values of void ratio may also result from the variation in initial water contents at which the samples were slurried. Table 6.2 illustrates the fairly wide range of initial water contents used during sample preparation. Although all the samples were to be prepared at initial water contents equal to the liquid limit plus 10%, variations in the water content of the "air-dried" material produced a fairly wide range of measured initial water contents.

Samples RCDD and SBDD were not exposed to brine. Plots of void ratio versus effective stress for these samples are presented in Figures 6.1 and 6.2. These curves illustrate the general form of the consolidation curves for the reslurried Regina Clay and sand/bentonite mixture. A constant compression index of 0.67 was obtained for the Regina Clay over the stress range up to 200 kPa. A distinct break in the virgin branch of the sand/bentonite mixture takes place at approximately 200 kPa. The compression index of the sand/bentonite sample is 0.72 at stresses less than 200 kPa.

Figures 6.3 and 6.4 are a compilation of all the values of compressibility obtained during the reconsolidation of the test samples. The curves of compressibility versus stress for the different materials show little scatter. The significant decrease in the values of compressibility of the sand/bentonite mixture at stresses greater than 200 kPa is readily apparent in Figure 6.4.

Table 6.1 Sample Consolidation Summary

Sample	Stress (kPa)	Void Ratio	Water Content (%)	Porosity (%)	m_v (1/kPa)
Regina Clay Samples					
RC1	203	1.37	48.9	58	6.91×10^{-4}
RC2	201	1.54	54.8	61	6.50×10^{-4}
RC3	199	1.32	47.1	57	8.78×10^{-4}
RC4	200	1.52	60.4	54	7.19×10^{-4}
RC5	49	1.85	66.6	65	21.0×10^{-4}
RC6	100	1.58	56.4	61	12.7×10^{-4}
RC7	203	1.41	50.4	59	7.71×10^{-4}
RC8	202	1.13	40.5	53	7.25×10^{-4}
RC9	205	1.16	41.5	54	7.33×10^{-4}
RC10	200	1.30	46.5	56	8.16×10^{-4}
RCDB1	300	.79	28.2	44	1.18×10^{-4}
RCDB2	300	.89	31.9	47	1.05×10^{-4}
RCDB3	83.3	1.00	36.0	50	1.55×10^{-4}
RCDB4	200	1.05	37.5	51	1.73×10^{-4}
RCDB5	758	.925	33.0	48	1.30×10^{-4}
RCDB6	517	.938	33.5	48	1.34×10^{-4}
RCDD	207	1.26	45.2	56	7.95×10^{-4}
Sand/Bentonite Samples					
SB1	203	1.03	39.0	51	8.96×10^{-4}
SB2	205	1.07	40.6	52	9.34×10^{-4}
SB3	203	1.17	44.6	54	8.11×10^{-4}
SB4	202	0.94	35.7	48	7.27×10^{-4}
SB5	205	1.05	39.9	51	8.43×10^{-4}
SB6	205	.86	32.8	46	8.87×10^{-4}
SBDD	200	1.09	41.3	52	9.22×10^{-4}
SBOC1	96	1.06	40.2	51	15.7×10^{-4}
SBOC2	201	.91	34.6	48	6.99×10^{-4}
SBOC3	23.5	1.45	55.2	59	41.8×10^{-4}

Table 6.2 Initial Slurry Water Contents

Sample	Water Content	Sample	Water Content
RC1	N/A	SB1	70.3%
RC2	N/A	SB2	72.6%
RC3	N/A	SB3	76.4%
RC4	88.6%	SB4	78.3%
RC5	85.7%	SB5	75.3%
RC6	N/A	SB6	78.7%
RC7	84.0%	SBDD	78.2%
RC8	84.9%	SBOC1	78.3%
RC9	83.9%	SBOC2	79.0%
RC10	89.8%	SBOC3	78.6%
RCDD	87.8%		

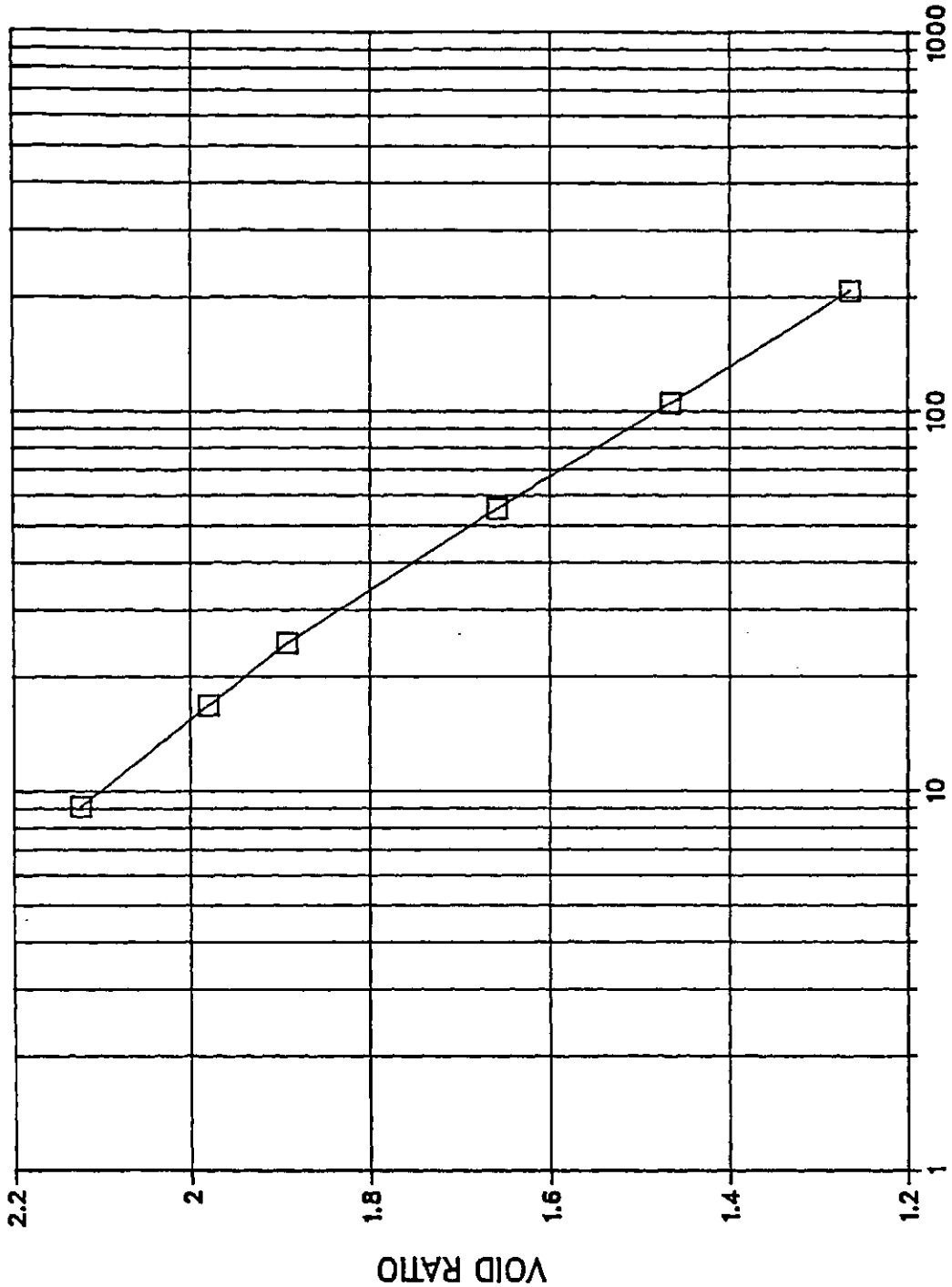

Figure 6.1 Sample RCDD - Void Ratio versus Applied Stress

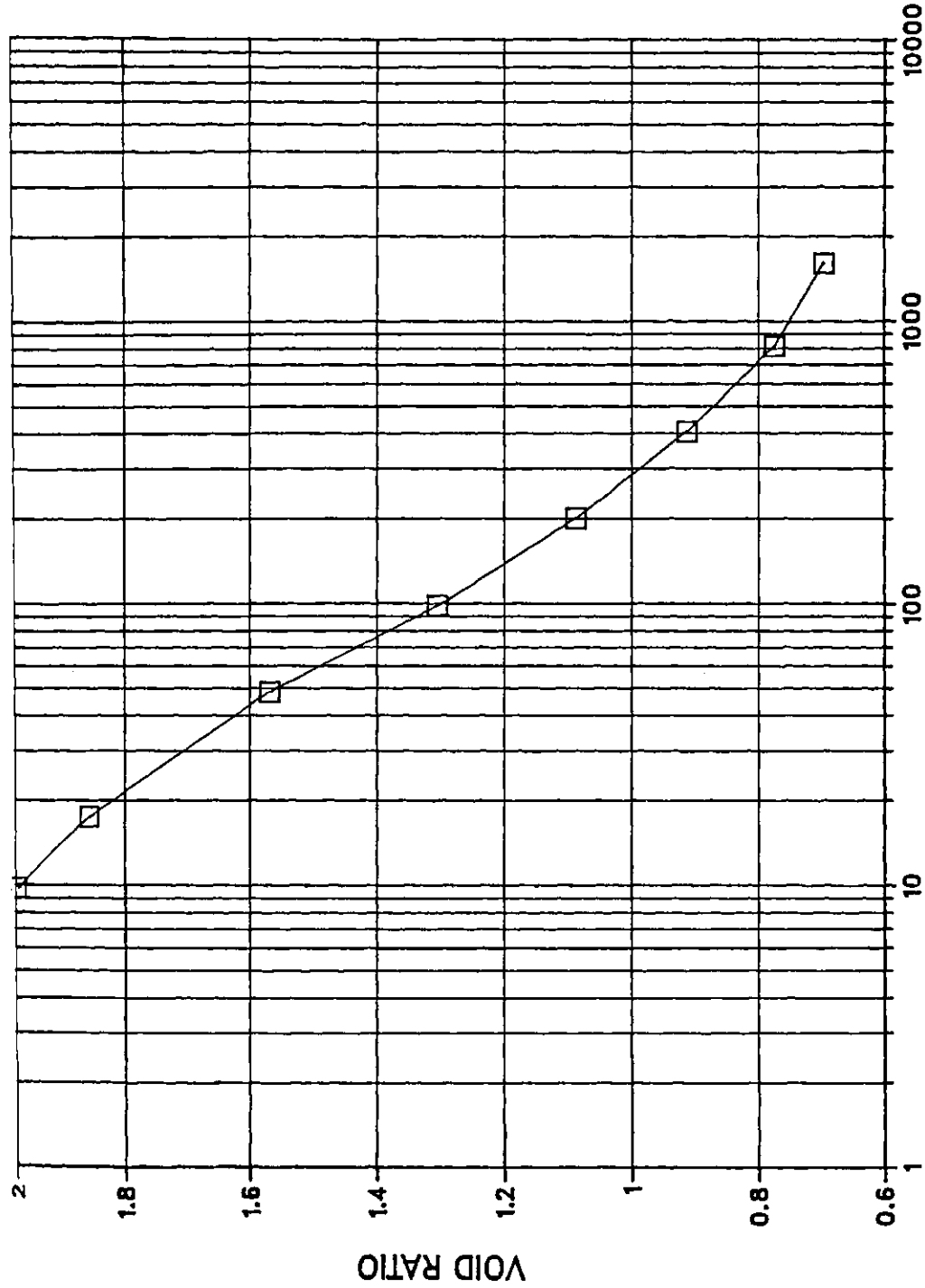

Figure 6.2 Sample SBDD - Void Ratio versus Applied Stress

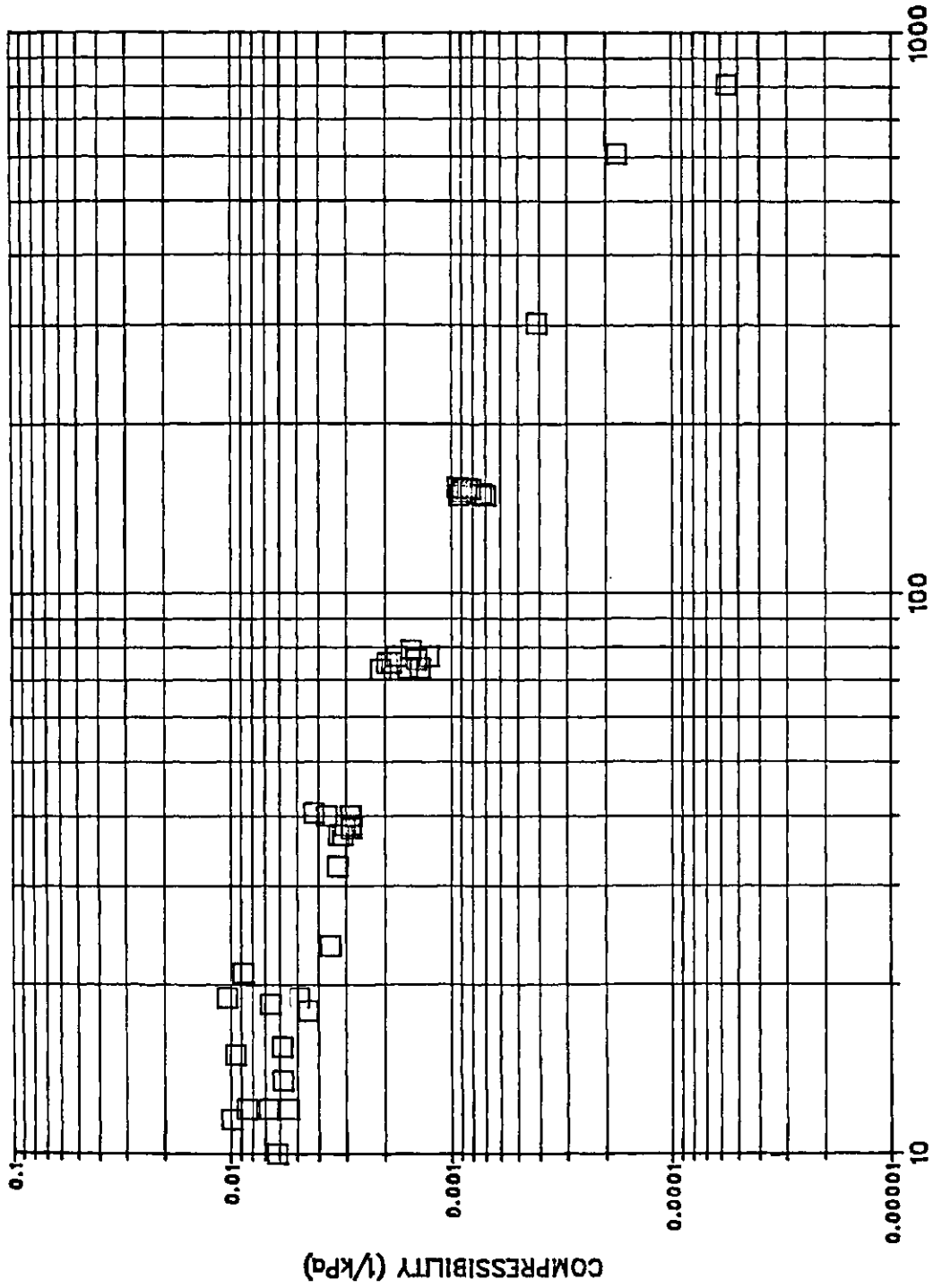

Figure 6.4 Sand/bentonite - Compressibility versus Applied Stress

6.3 Constant Head Permeability Test

Constant head permeability testing was performed on 17 samples tested in the modified oedometer setups. Three of these samples were tested for permeability after the completion of osmotic volume change. The constant head permeability tests were completed with few difficulties. Figure 6.5 illustrates a typical set of burette readings versus time for sample SB2. Similar figures for all the samples tested are presented in Appendix D.2. Steady state flow rates were well defined for all the samples tested.

Table 6.3 summarizes the results of the permeability tests. The results appear to be reasonably consistent. The permeability for the Regina Clay, at a stress of 200 kPa, is approximately $1x10^{-10}$ m/s. The permeability of the sand/bentonite mixture at the same stress level is approximately $1x10^{-11}$ m/s.

For the Regina Clay samples, RC2 and RC10, the measurements showed that little change in permeability occurred before and after exposure to NaCl solutions. For the sand bentonite sample, SB6, the permeability of sample increased by almost one order of magnitude after exposure to a 4 M NaCl solution.

6.4 Osmotic Volume Change

In order to initiate osmotic volume change, NaCl solution was flushed through the loading cap and into the porous stone or stainless steel screens. At the beginning of the test, fairly rapid flushing was used in order to ensure an instantaneous change in the concentration of the solution at the boundary of the sample. The flushing rate was reduced after the first few minutes to a rate of several mls per minute. Flushing was continued over several days until osmotic volume change of the sample was complete.

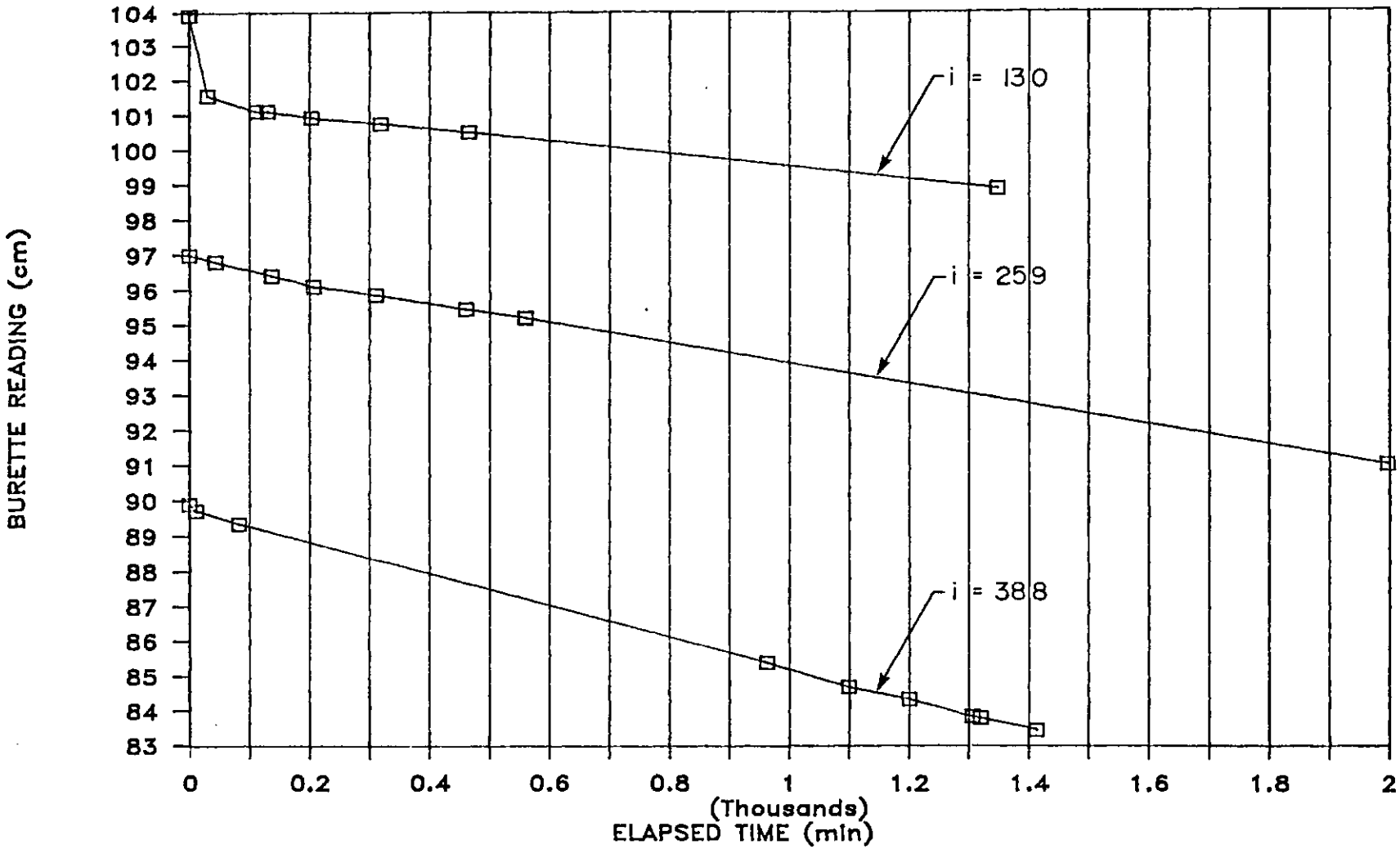

Figure 6.5 Permeability Tests Results - Sample SB2

Table 6.3 Summary of Permeability Tests

Sample	Stress (kPa)	Gradient	KH (m/s)	
RC1	203	181	7.16×10^{-11}	
		360	7.72×10^{-11}	
		544	8.20×10^{-11}	
RC2	201	195	7.98×10^{-11}	pre-osmotic
		195	7.59×10^{-11}	post-osmotic
RC3	199	85	13.46×10^{-11}	
RC4	200	103	11.20×10^{-11}	
RC5	49	122	93.0×10^{-11}	
RC6	100	129	39.5×10^{-11}	
RC7	203	171	11.2×10^{-11}	
		341	11.8×10^{-11}	
		512	12.0×10^{-11}	
RC8	202	189	8.9×10^{-11}	
RC9	205	150	7.2×10^{-11}	
RC10	200	130	10.3×10^{-11}	pre-osmotic
		130	10.3×10^{-11}	post-osmotic
SB1	203	163	1.38×10^{-11}	
		489	1.12×10^{-11}	
SB2	205	130	1.24×10^{-11}	
		259	0.93×10^{-11}	
		388	0.95×10^{-11}	
SB3	203	328	1.33×10^{-11}	
SB4	202	310	1.58×10^{-11}	
SB5	205	311	0.41×10^{-11}	
SB6	205	163	2.07×10^{-11}	pre-osmotic
		171	$14. \times 10^{-11}$	post-osmotic

In general, the osmotic volume change that occurred was fairly small and took place over extremely long lengths of time. Consequently, the measured deflections of the sample had to be corrected for secondary consolidation. Figure 6.6 compares the magnitude and rate of osmotic volume change relative to that produced by loading the sample from 100 to 200 kPa. The correction for secondary consolidation is illustrated in Figure 6.6. All of the osmotic deflection curves were corrected for secondary consolidation. A complete set of the corrected osmotic time-deflection curves are presented in Appendix D.3.

Plots of verticle strain versus time are presented in Figures 6.7 through 6.9, for slurried and intact samples of Regina Clay, and for the sand/bentonite mixture. These samples were exposed to 4.0 M NaCl solutions. These figures illustrate the fairly good reproducibility of osmotic volume change measurements obtained during testing. A porous stone on top of the sample was used for samples RC1 and RC2 (Figure 6.7). The deflection curves for these two samples are shifted to the right relative to the curves for Sample RC3 and RC10. It is likely that the porous stone prevented complete flushing of the top of the sample at the initiation of osmotic volume change. In addition, as pore fluid was expelled from the sample, the pore fluid in the porous stone was somewhat diluted. Due to these effects, it is unlikely that the full solution strength was maintained across the top of these samples at all times.

The deflection curves for the sand/bentonite samples all have similar shapes. It is not known why sample SB6 exhibited a lower deflection than the other two samples. The time to 100% osmotic volume change was of the same order of magnitude as the time to effective stress consolidation, for the 100 to 200 kPa applied stress increment.

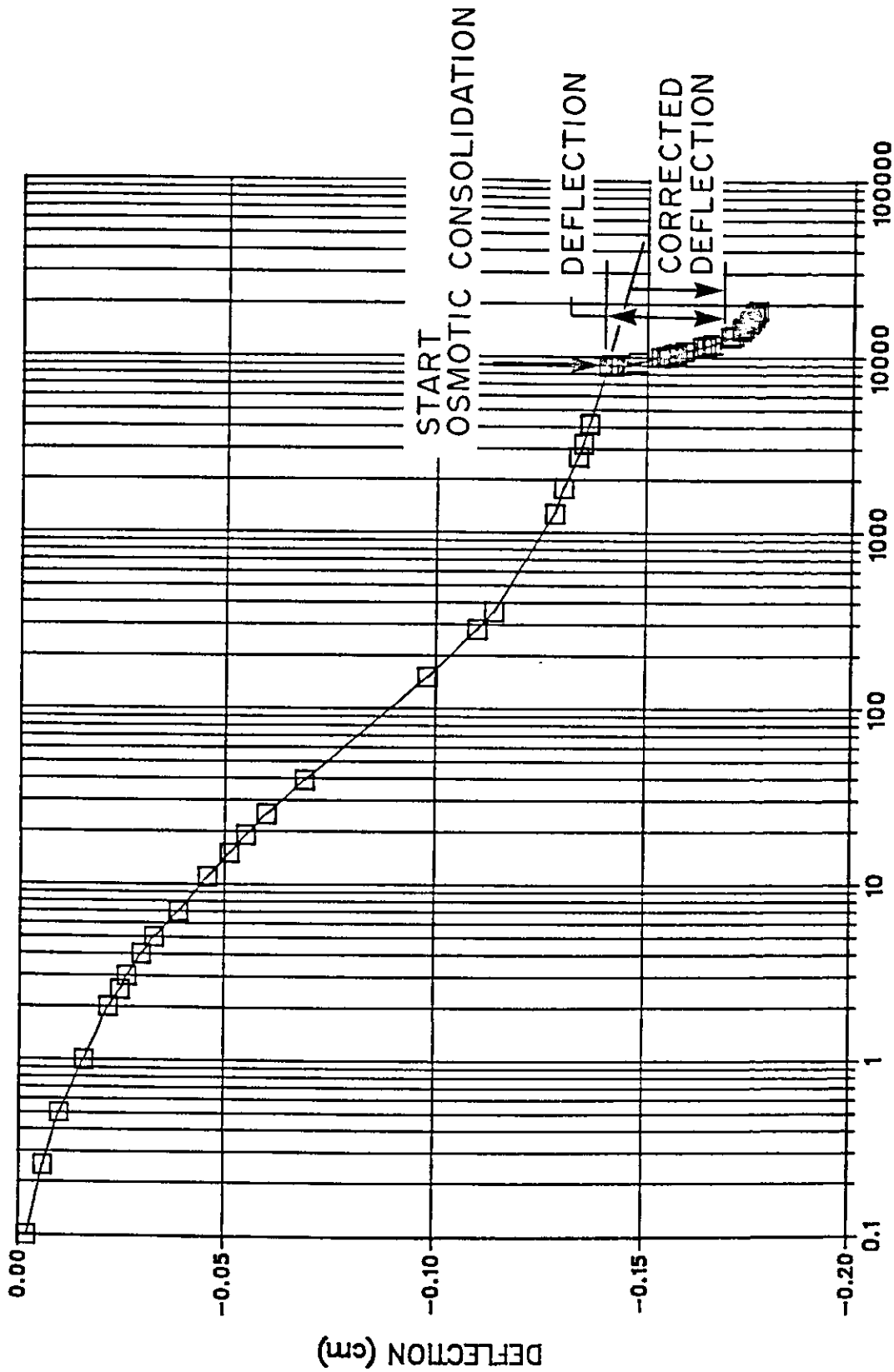

Figure 6.6 Sample RC10 - 100 to 200 kPa Effective Stress Consolidation and Osmotic Consolidation

Equalization of pore fluid concentrations at the end of testing was demonstrated by measurement of the dissolved salt contents of several samples. Table 6.4 presents the final pore fluid concentrations of several of the tests. Samples of the pore fluids were obtained by squeezing the sample in a hydraulic press. The final pore fluid concentration of sample RC2 is anomalous, and is likely due to errors in the gravimetric determination of the dissolved salt content. Overall, the samples demonstrate nearly complete equalization of pore fluid concentrations. Somewhat smaller concentrations near the base of the sample (i.e., sample RC3) are likely the result of steady upward osmotic flows through the sample.

Table 6.4 Final Pore Fluid Concentrations

Sample		Concentration (M)				
RC1	top	3.3	3.08	2.9	3.63	bottom
RC2		0.83				
RC3	top	3.88	3.72	3.38	3.26	bottom
RC4		3.91				
SB1		3.56				

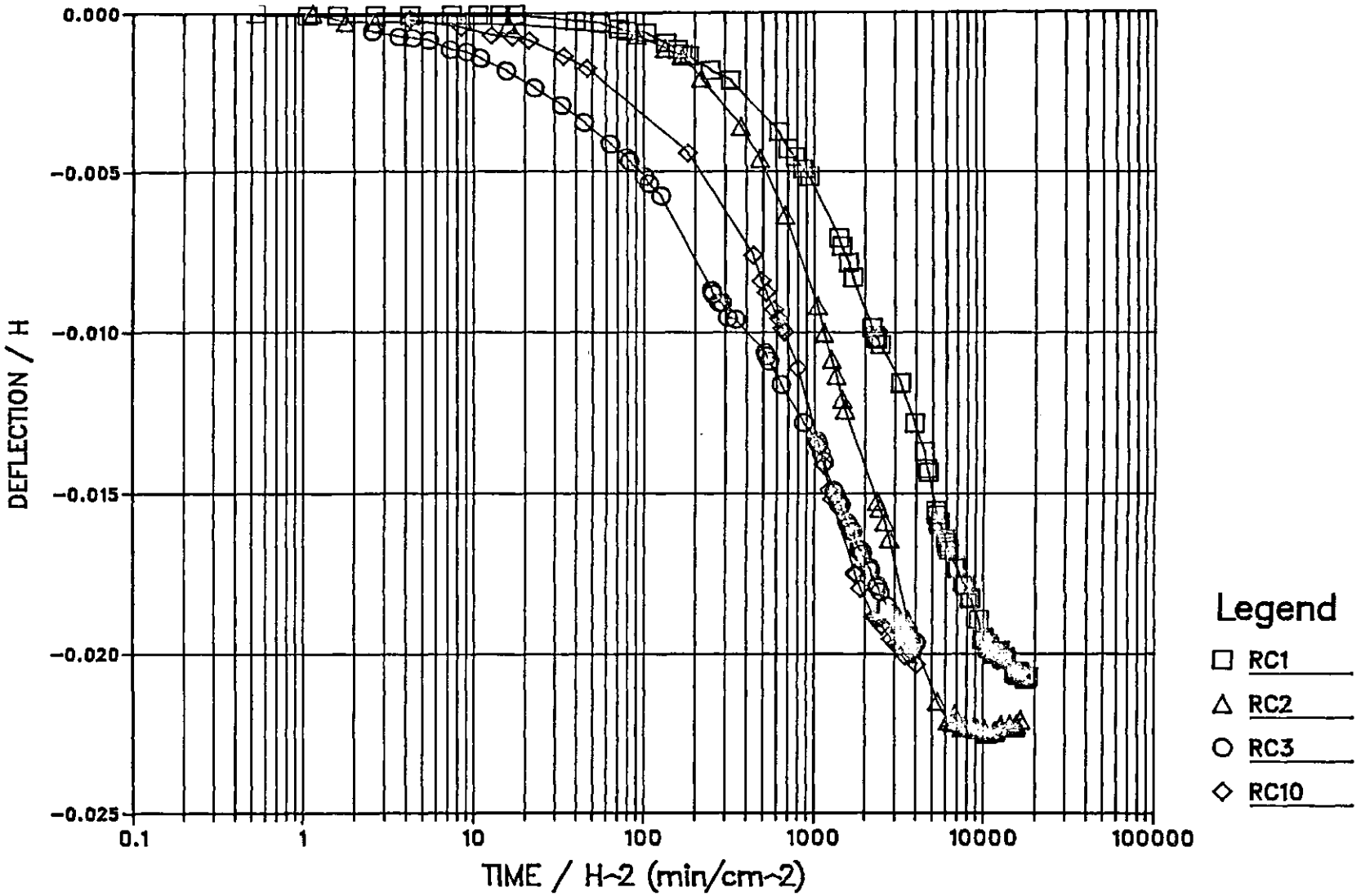

Figure 6.7 Slurried Regina Clay - Verticle Strain versus Time - 4.0 M NaCl Solution

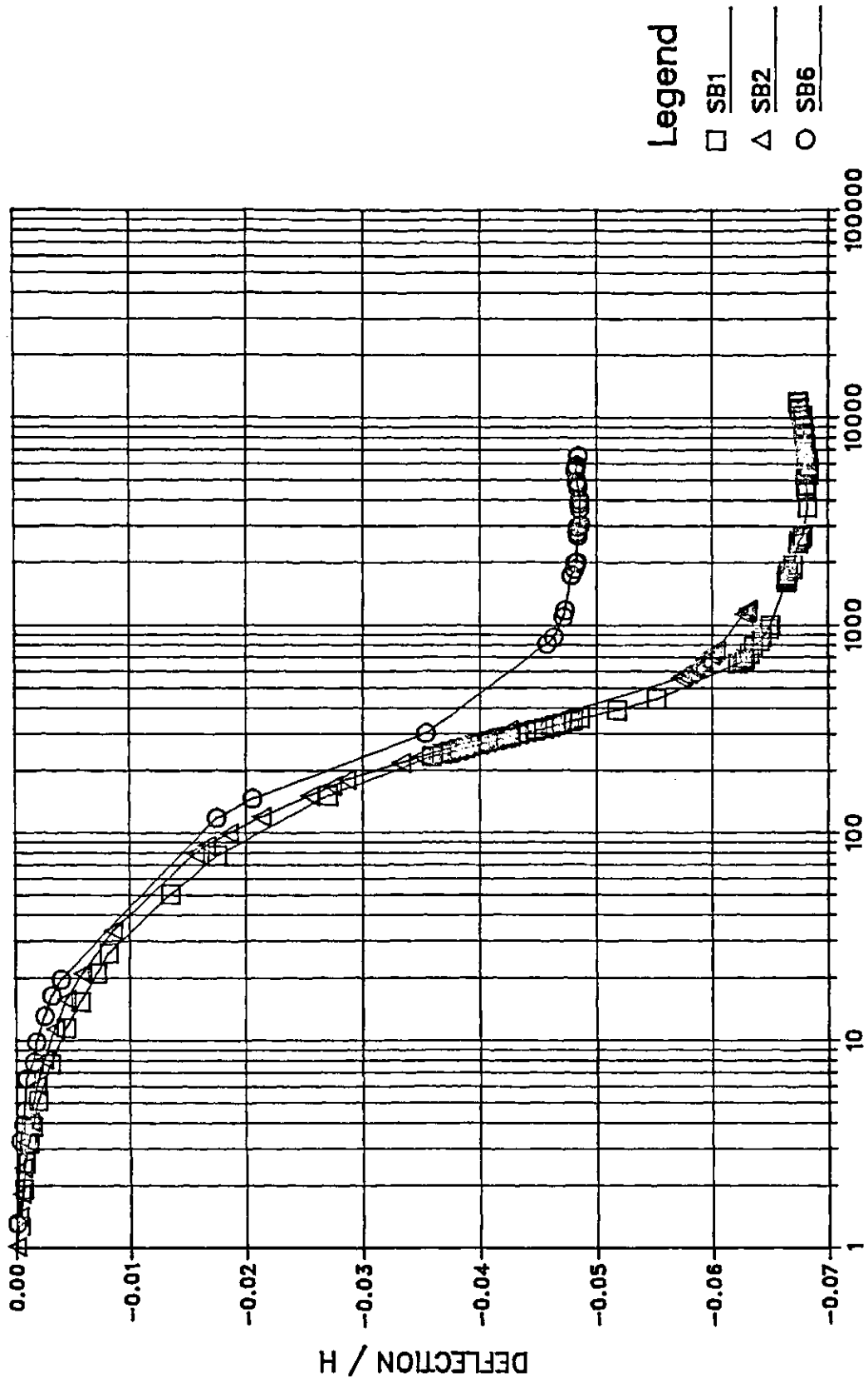

Figure 6.8 Sand/bentonite Mixture - Verticle Strain versus Time - 4.0 M NaCl Solution

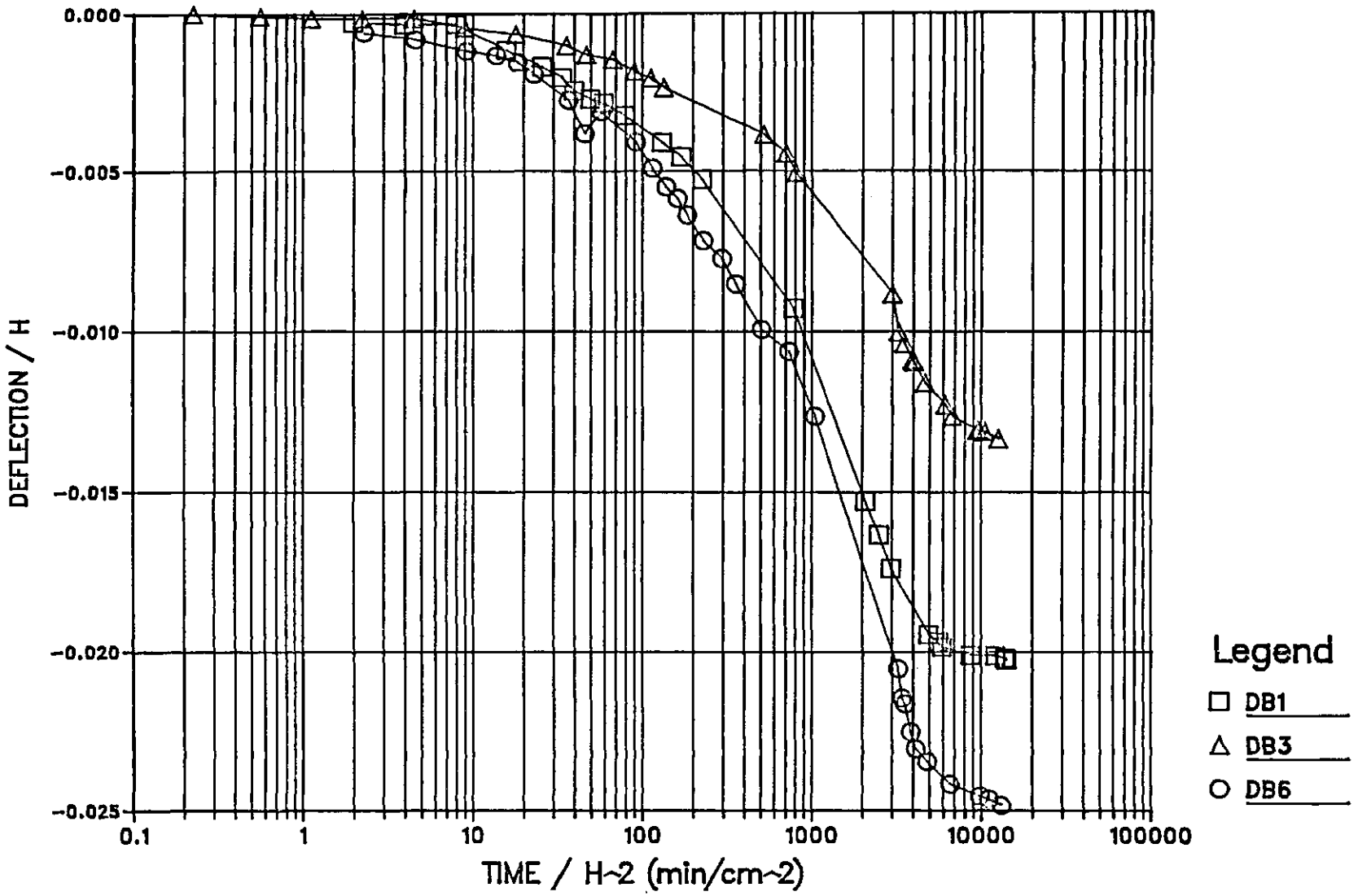

Figure 6.9 Intact Regina Clay - Verticle Strain versus Time - 4.0 M NaCl Solution

6.5 Flow and Pressure Responses at the Sample Base

Measurement of base flow rates where obtained for all samples except those used for diffusion testing (i.e., RC7,SB3) and the tests in which base pressures were monitored (i.e., RC9, RC10, SB5, SB6). Both base flow rates and the base pressure responses during osmotic volume change are used to evaluate the osmotic efficiency of the clay samples.

6.5.1 Base Flows

Measurements of flow through the base of the sample during osmotic volume change were made in all but four samples. In general, steady flow readings were obtained for all values of concentration. Figures of cumulative base flow versus elapsed time are presented in Appendix D.4.

Plots of cumulative base flow normalized with respect to initial sample thickness, versus elapsed time normalized with respect to initial sample thickness squared, for several Regina Clay and sand/bentonite samples are presented in Figures 6.10 and 6.11. The results appear to be quite reproducible. In the case of the Regina Clay samples, small flows into the sample begin at normalized times of less than 100 min/cm^2 and then build to nearly steady rates. For the sand/bentonite samples the early flows are out of the sample. These flows reverse, after a normalized time of approximately 800 min/cm^2, and again build to steady flow rates. These times are roughly equivalent to the time to 100% consolidation for the samples under the 100 to 200 kPa applied stress increment.

The steady upward flow through the sample is a result of a steady state condition in which the diffusive flux of salt to concentration gradients is opposed by the advective flux of salt due to osmotic flows in response to concentration gradients. The concentration profile for sample RC3 (Table 6.5) would support this conclusion.

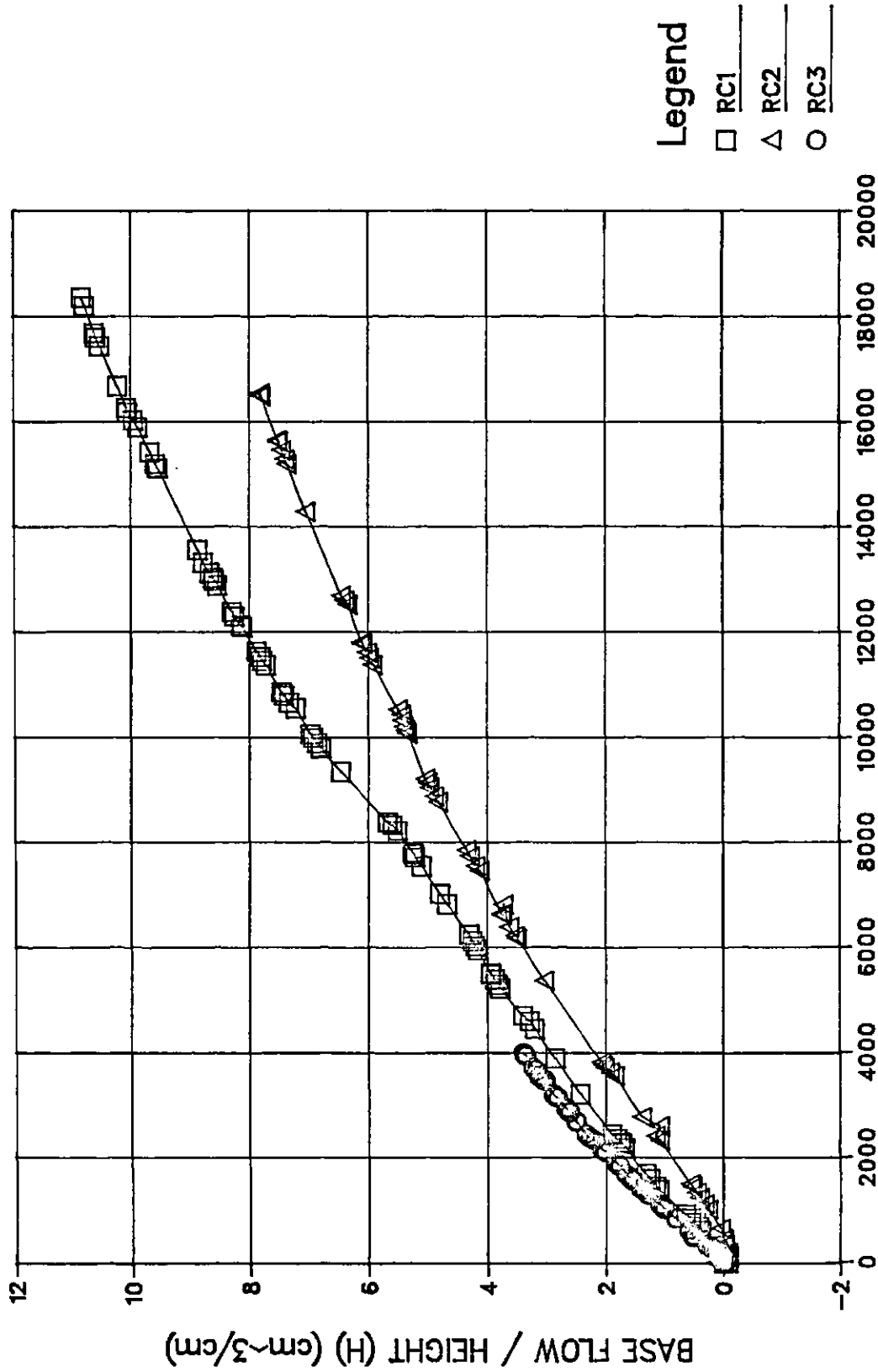

Figure 6.10a Regina Clay - Normalized Base Flows versus Normalized Time - 4.0 M NaCl Solution

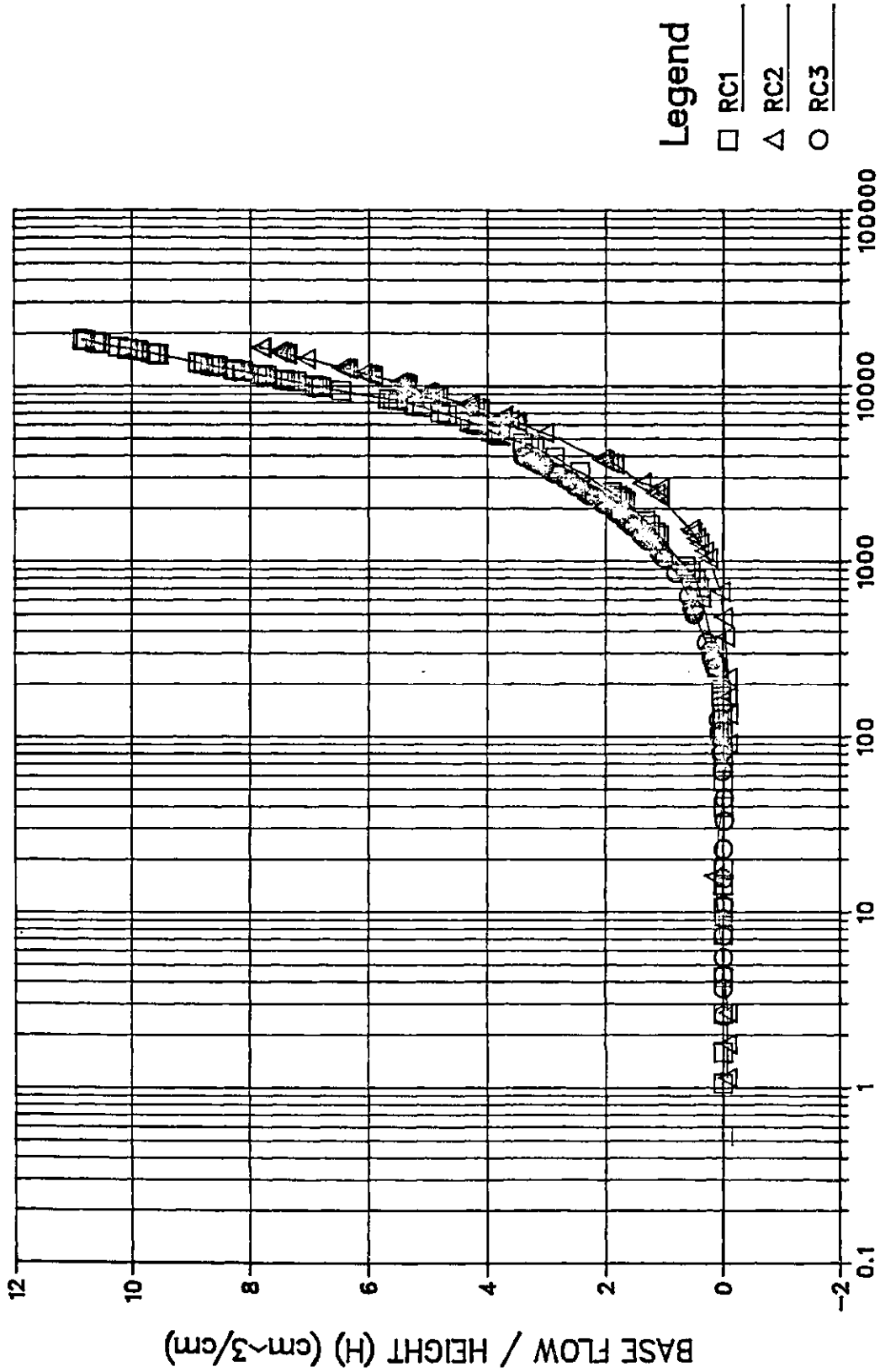

Figure 6.10b Regina Clay - Normalized Base Flows versus Normalized Time - 4.0 M NaCl Solution

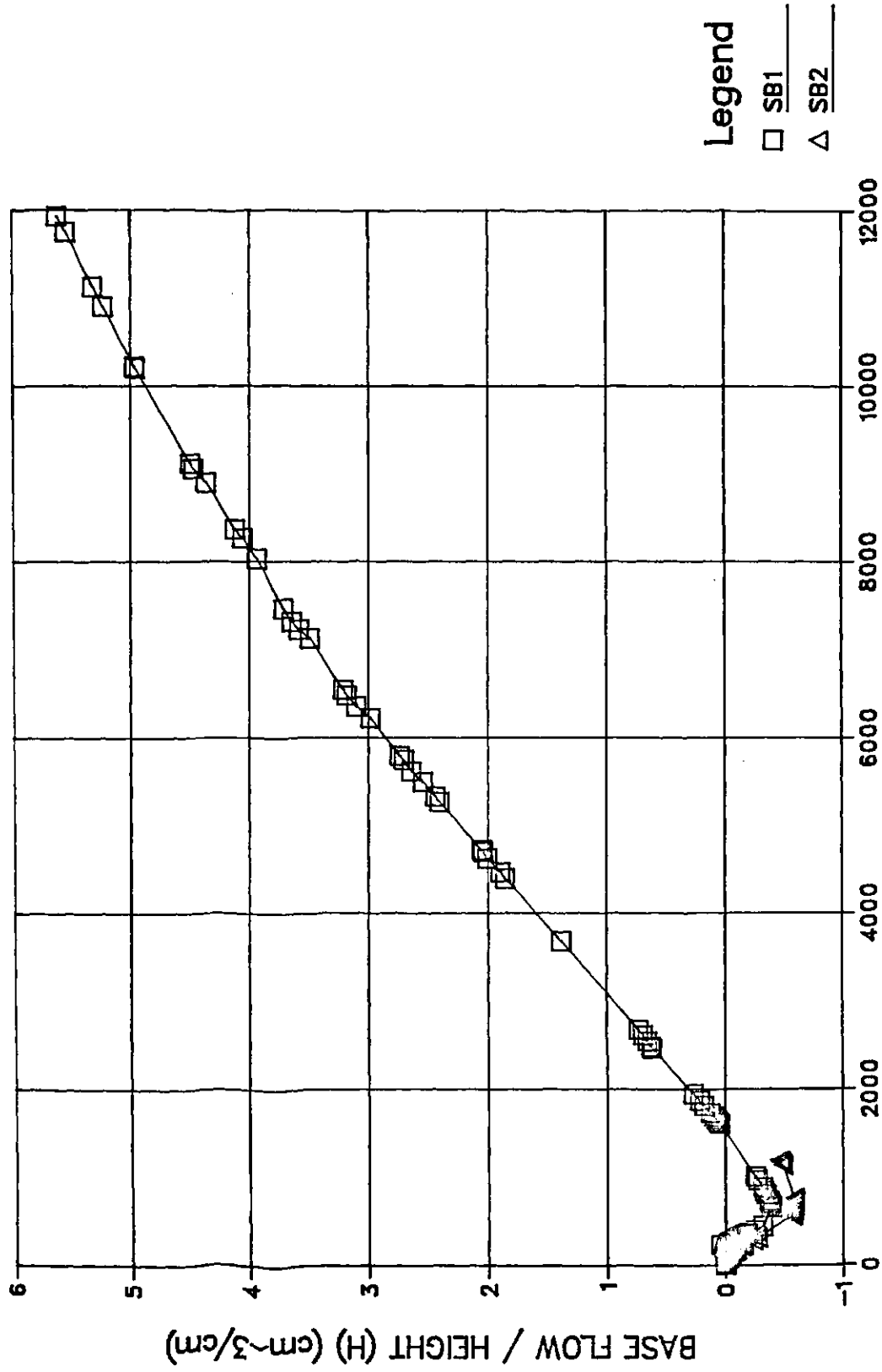

Figure 6.11a Sand/bentonite - Normalized Base Flows versus Normalized Time - 4.0 M NaCl Solution

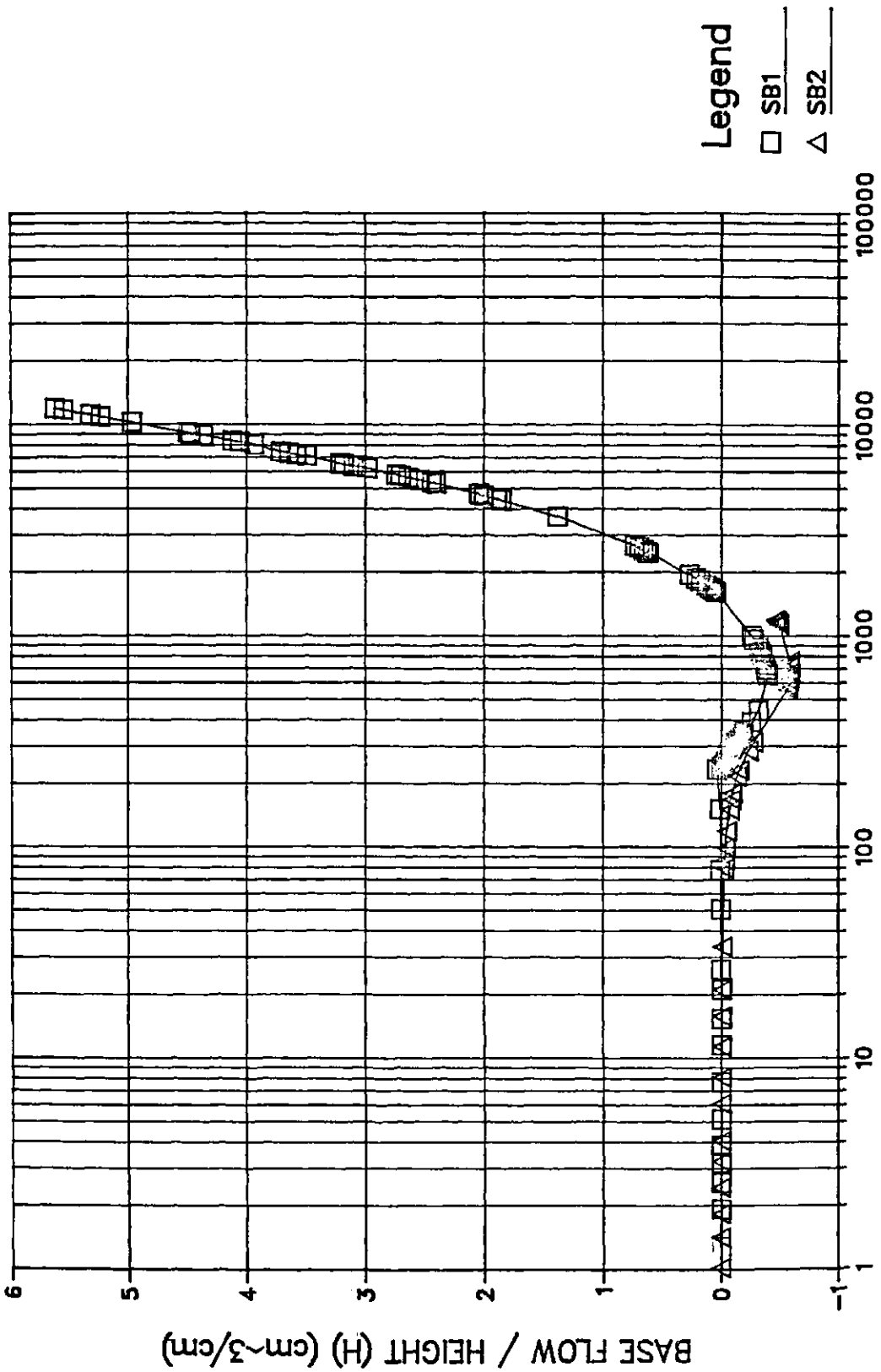

Figure 6.11b Sand/bentonite - Normalized Base Flows verus Normalized Time - 4.0 M NaCl Solution

6.5.2 Base Pressure Response

The observation that steady osmotic flows developed within the samples during osmotic volume change gave reason to believe that significant pressure responses at the base of the sample could be measured when these flows were prevented. Base pressure responses with changing solution concentrations were measured in samples RC9 and SB5. The results of these tests are presented in Appendix D.5.

Two particular concerns regarding the accuracy of these measurements arose during testing. The first concern pertained to whether a significant time lag existed between the generation of base pressures in the sample and the measurement of these pressures with the transducers. Measurements of pressure response demonstrate a slow buildup of pressure with time, followed by decay. Without the countervailing osmotic flows, equalization of concentrations across the entire sample was taking place. Consequently, only brief peaks in osmotic pressure at the base of sample were measured.

A second concern was the influence of temperature variations in the laboratory on the pressure measurements. During the period of time in which the tests for RC9 and SB5 were underway, there were difficulties encountered with the airconditioning system in the building. Temperature variations in excess of 5 to 10 °C occurred within 48 hour periods. An attempt was made to buffer these temperature variations by enclosing the test apparatus in insulated tarpaulins.

Samples RC10 and SB6 were exposed to a single solution concentrations of 4 M. The pressure response and air temperature diagrams for these tests are illustrated in Figures 6.12 and 6.13.

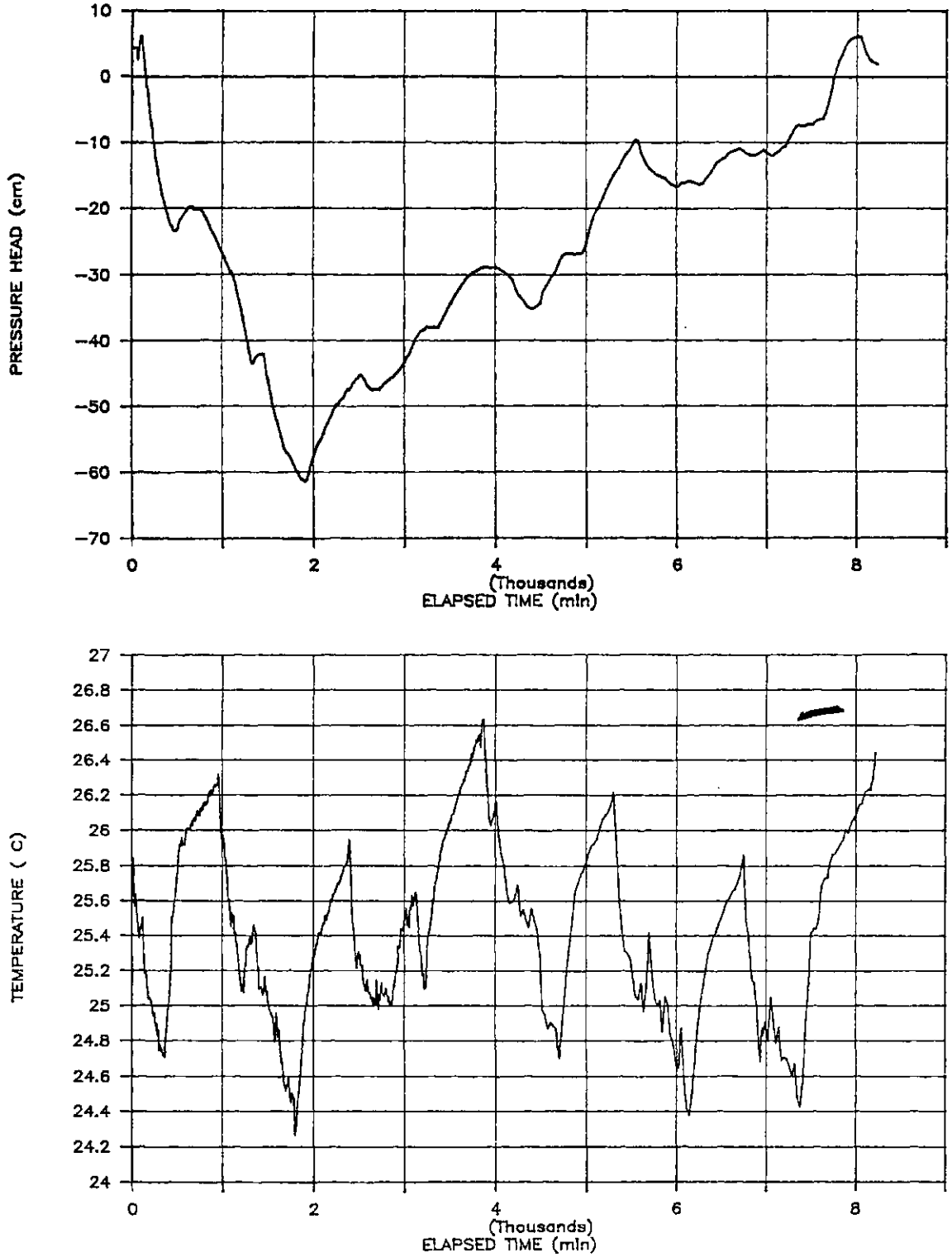

Figure 6.12 Sample RC10 a) Base Fluid Pressure b) Air Temperature versus Elapsed Time during Osmotic Volume Change

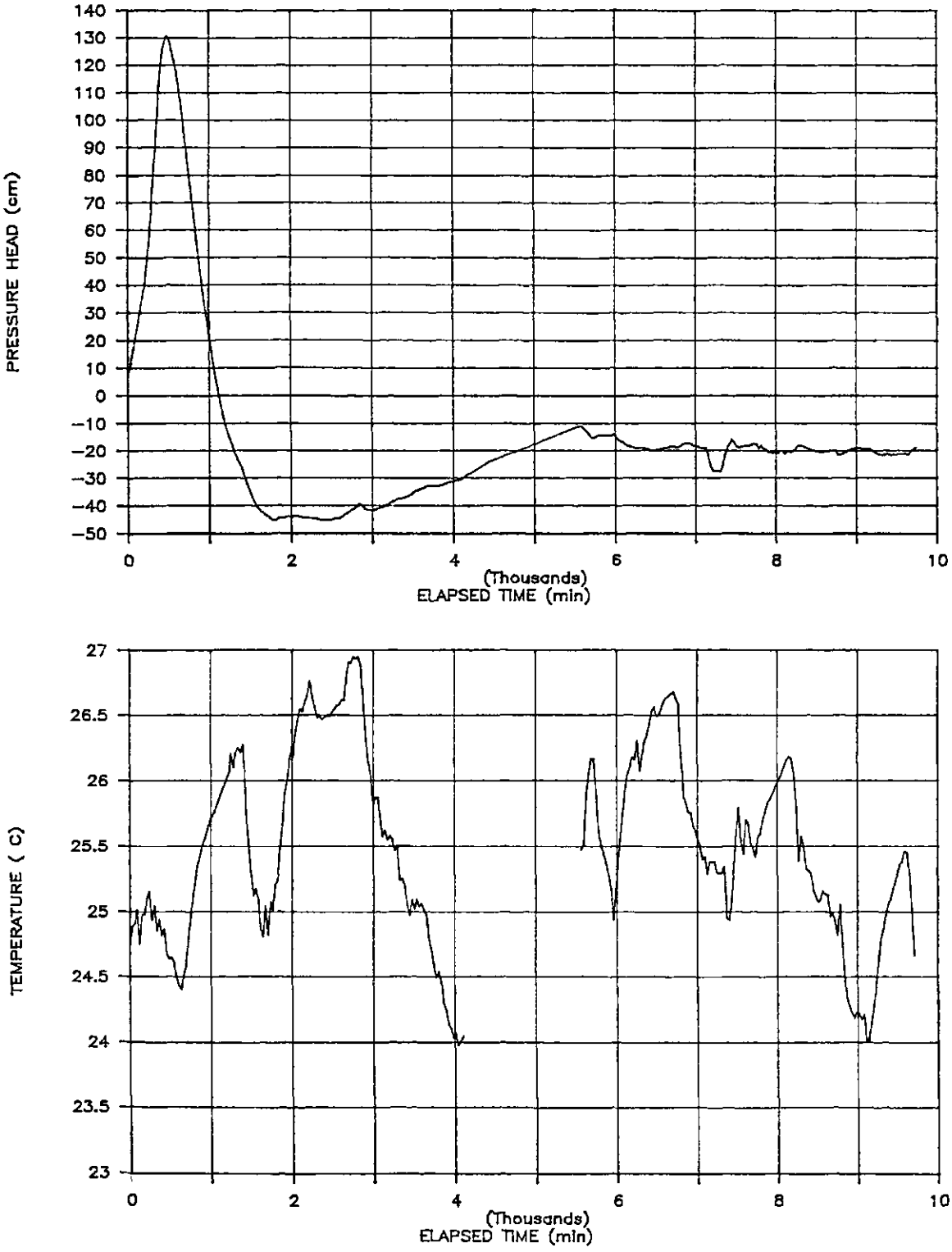

Figure 6.13 Sample SB6 a) Base Fluid Pressure b) Air Temperature versus Elapsed Time during Osmotic Volume Change

Somewhat erratic changes in pressure occurred for the Regina Clay sample, RC10. These changes occur at the same time that rapid changes in the air temperature within the testing enclosure occur. Even though the temperature variation was less than 2 °C, the rapid changes in temperature had a significant effect on pressure measurements. Due to the much stronger, positive, pressure response measured for the sand/bentonite sample the effect of temperature variations is not nearly as significant.

Expansion or contraction of the apparatus and connecting tubing occurs as a result of changes in temperature. This volume change in turn results in a change in pressure within the measuring system until sufficient flow from the sample occurs to reinstate the sample pressures.

Figure 6.12 illustrates that rapid increases in temperature correspond to drops in pressure. Similarly, rapid decreases in temperature result in increases in pressure. For most of these changes, 500 to 800 minutes of elapsed time are required to return the pressure to the trends observed prior to the change in temperature.

An indication of the response time of the pressure measurement system was obtained for sample RC10 and SB6 by measuring the pressure response at the base of the sample during loading of the sample. The base pressure response for these samples, under the 100 to 200 kPa applied stress increment, is presented in Figures 6.14 and 6.15.

The maximum pore pressure measured at the base of the samples was only 50% to 60% of the theoretical maximum induced pressure of 100 kPa. These peak pressures were reached in 20 minutes for the Regina Clay sample, and 100 minutes for the sand/bentonite sample. Even under the strong flows produced during this loading increment, a significant time lag seems to occur. No attempt was made to establish the time lag under boundary conditions similar to those that occur during osmotic volume change.

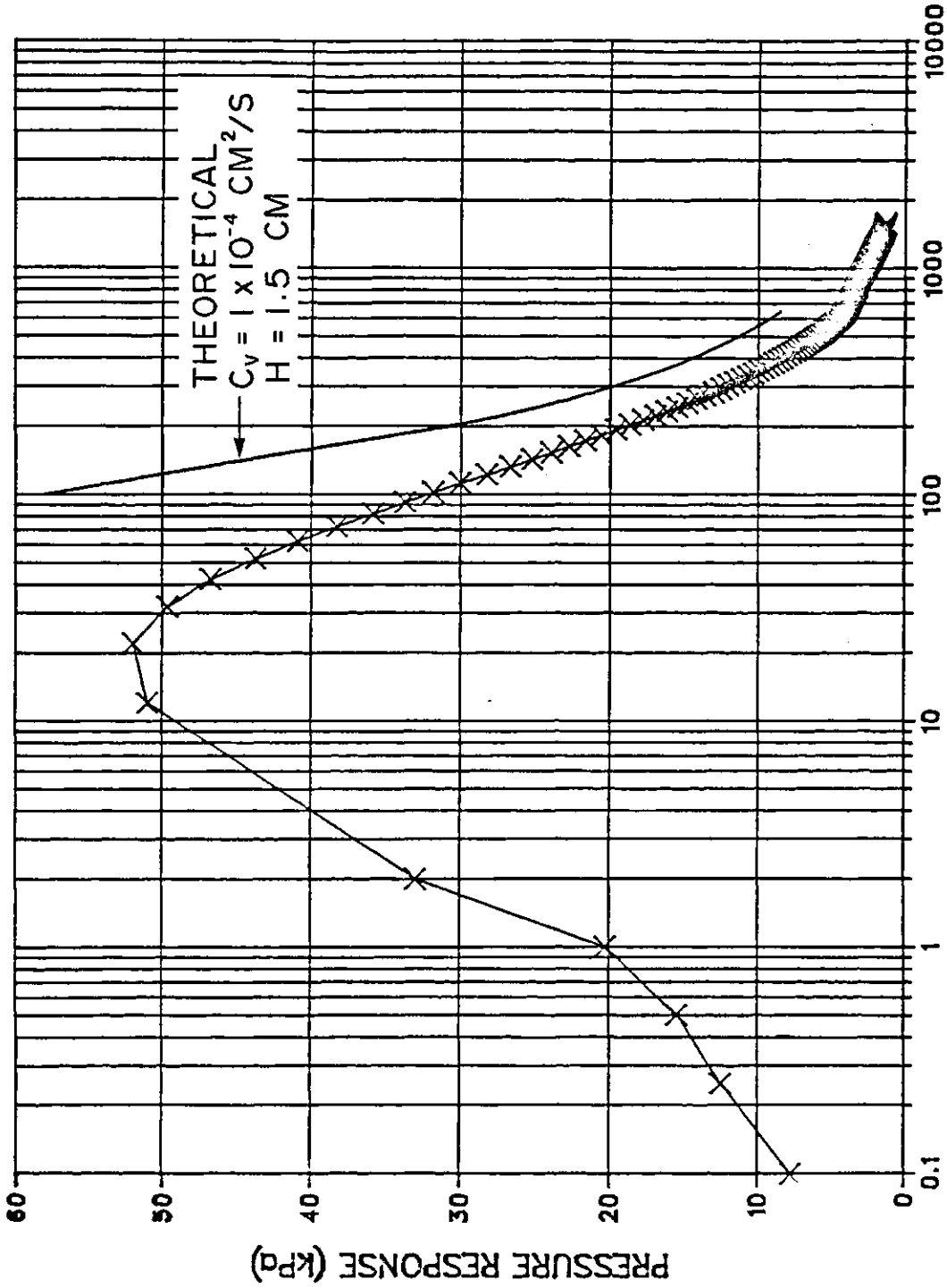

Figure 6.14 Sample RC10 - Base Pressure Response during 100 to 200 kPa Loading Increment

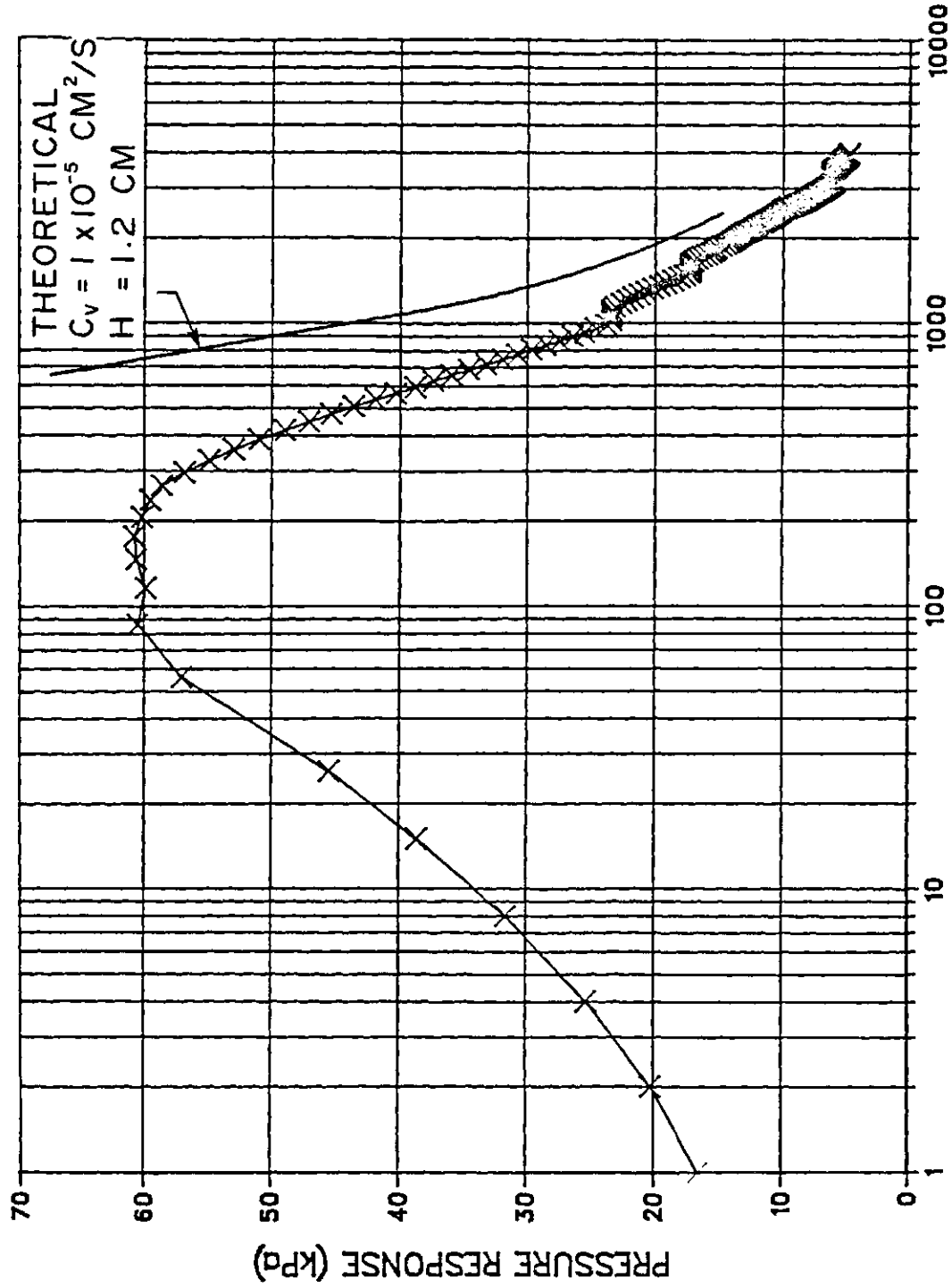

Figure 6.15 Sample SB6 - Base Pressure Response during 100 to 200 kPa Loading Increment

6.6 Diffusion Tests

The salt flux through samples RC7 and SB3 was measured in order to establish the coefficient of diffusion for the Regina Clay and sand/bentonite soils. Figures 6.16 and 6.17 illustrate a typical set of results for Regina Clay. The complete set of results are presented in Appendix D.6. Well defined curves of increasing salt flux with time were obtained in most of the tests. The measured base concentrations and sampling details are also provided in Appendix D.6.

Calculations of the salt flux were made by averaging the concentration of the underflow over sampling intervals. The concentrations were obtained from measurements of conductivity as well as by gravimetric determination of the dissolved salt content of selected samples. The two types of measurements provided somewhat different values for the base concentration, however, both methods provided consistent values for the salt flux.

One difficulty encountered in these tests was in controlling the underflow rate so that the base concentrations were always less than 1% of the concentration of solution at the surface of the sample. This test method could be improved by continuously monitoring the conductivity of the base underflow using a flow-through conductivity cell. Continuous monitoring of the underflow concentrations would allow gradual adjustments to the flow rate to be made in order to maintain a constant base concentration.

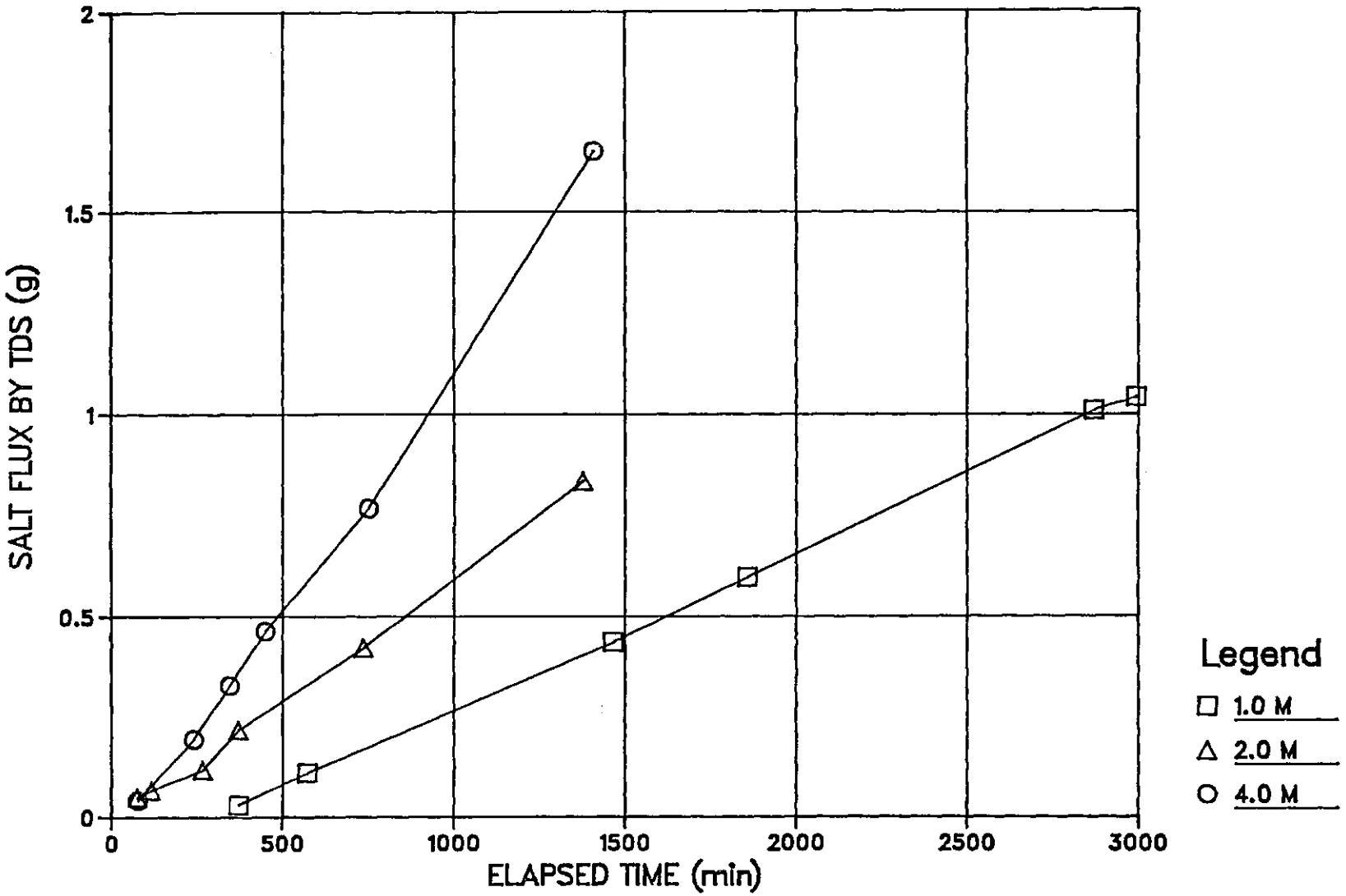

Figure 6.16 Sample RC7 - Cumulative Salt Flux versus Elapsed Time - Gravimetric Determination

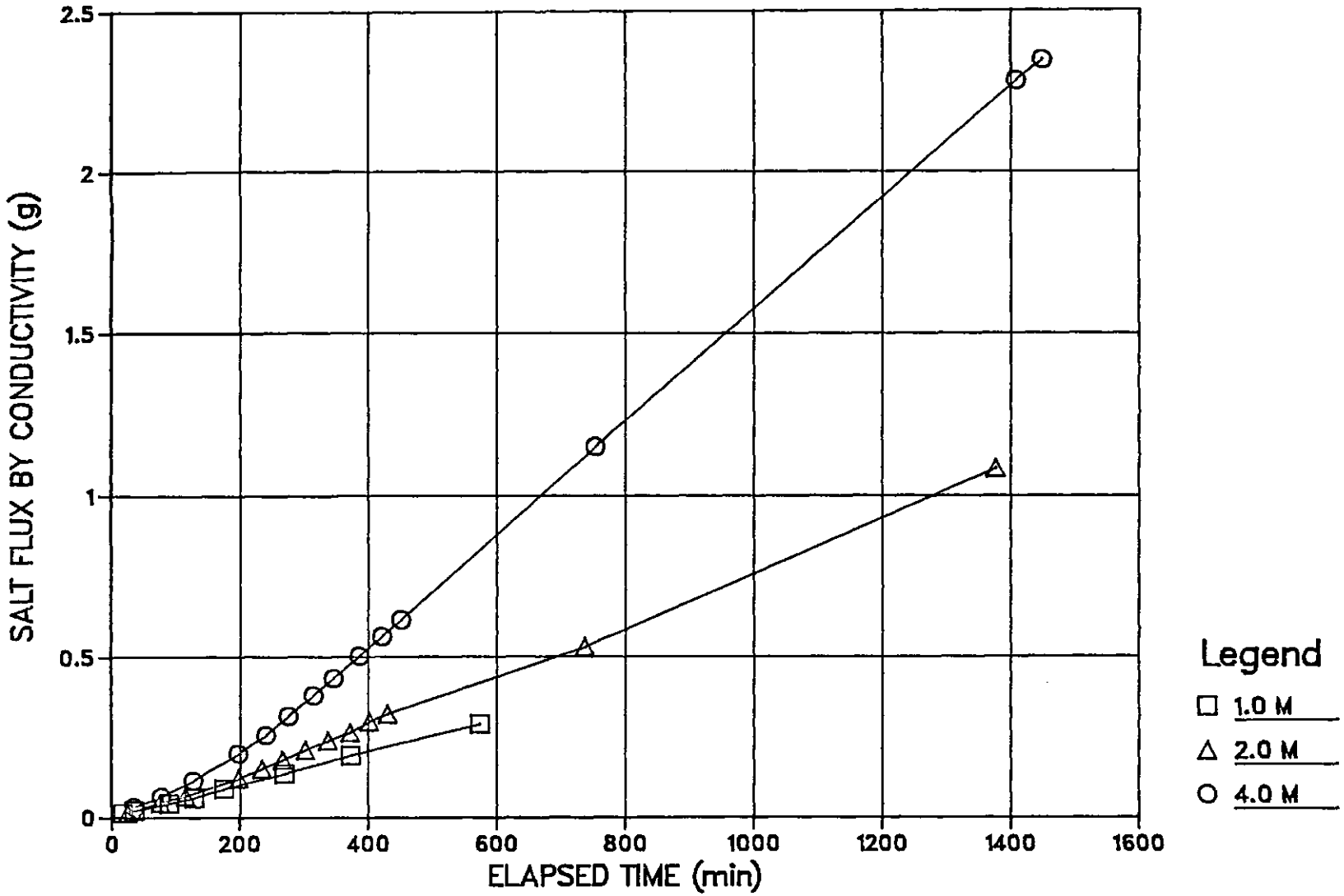

Figure 6.17 Sample RC7 - Cumulative Salt Flux versus Elapsed Time - Conductivity Determination

One other area of uncertainty in these tests was in the influence that osmotic flows might have on the rate of salt flux through the sample. Simultaneous measurements of osmotic flow and salt flux through the base of the sample could not be made. Calculations of the reduction of diffusive salt flux that may occur as a result of upward osmotic flows were made, based on previous measurements of osmotic flow rates. These calculations indicated that the measured salt flux may up to 10% less than that which occurs in the absence of osmotic flow.

CHAPTER 7

DATA ANALYSES AND DISCUSSION

7.1 Introduction

The principal objective of this research program has been to identify, describe, and quantify the processes of osmotic flow and volume change through clay soils. Two basic mechanisms of osmotic volume change were identified. These were termed osmotically induced consolidation and osmotic consolidation.

A theoretical description of these processes was developed in Chapter 3. A numerical simulation of the processes of osmotic and osmotically induced consolidation was presented in Chapter 4. Observable contrasts in the behavior of a clay sample under the influence of these two processes were noted. Observations of volume change, and of base flow or fluid pressure response of clay samples exposed to NaCl solutions were described in Chapter 6.

In this chapter, the observations presented in Chapter 6 will be interpreted in light of the descriptions provided by the literature review, the theoretical framework, and the numerical simulation. The objective of this interpretation is to evaluate:

1. The dominant mechanism of osmotic volume change for the two clay soils investigated,
2. The material properties of K_π, m_π and D which are used to characterize these processes,
3. The capability of the theoretical description, aided by numerical simulation, to predict the osmotic flow and volume change processes observed during laboratory testing, and,
4. The role of osmotic pressure as a stress state variable.

7.2 Osmotic Permeability / Membrane Efficiency

The flow rates that occurred across the base of the clay samples during testing were described in Chapter 6. Table 7.1 provides a summary of these flow rates as measured from the figures contained in Appendix D.4. Leakage testing of the test apparatus prior to each test indicated either zero leakage, or in a few cases, less than 4.3 x cm /min occurred. This is a small percentage of the flow rates listed in Table 7.1.

The negative sign for several of the flow rates indicates that flow was out of the base of the sample. Flow rates out of the samples occurred when the concentration of the solution at the top of the sample was less than that of the initial pore fluid. The initial pore fluid concentration in the samples at a stress level of 200 kPa can be calculated based on the chemical analysis of the saturation extract of air- dried sand/bentonite and Regina Clay presented in Table 5.2.

For the sand bentonite samples, the initial pore fluid concentration is approximately 0.008 M. The initial pore fluid concentration for the Regina Clay samples is approximately 0.05 M.

The equivalent hydraulic head that would be required to develop the measured flow rates across the sample, was calculated using the permeability and the height of each sample. These equivalent pressure heads are listed in Table 7.1. Figures 7.1 and 7.2 illustrate the values of equivalent head as a function of pore fluid concentration. For several samples, direct measurements were made of the pressure at the base of the sample. These direct pressure measurements are included in Figures 7.1 and 7.2.

Table 7.1 Summary of Equivalent Pressure Heads

Sample	Stress (kPa)	Permeability (cm/s)	Solution Concentration (M)	Height (cm)	Base Flow (cc/min)	Equivalent Head (cm)	Equivalent Head (kPa)
RC1	200	7.70E-09	4	1.37	7.00E-04	65.54	6.55
RC2	200	8.04E-09	4	1.07	6.50E-04	45.52	4.55
RC3	200	1.35E-08	4	2.3	4.38E-04	39.27	3.93
RC4	200	1.05E-08	0.5	0.48	2.03E-04	4.88	0.49
		1.05E-08	1	0.48	5.37E-05	1.29	0.13
		1.05E-08	4	0.48	1.55E-03	37.29	3.73
		1.05E-08	5	0.48	2.03E-03	48.84	4.88
RC5	50	9.30E-08	0.1	0.79	6.10E-03	27.27	2.73
		9.30E-08	0.5	0.79	2.15E-04	0.96	0.10
		9.30E-08	1	0.79	6.03E-04	2.70	0.27
		9.30E-08	2	0.79	0.00E+00	0.00	0.00
		9.30E-08	4	0.79	1.63E-03	7.29	0.73
		9.30E-08	5	0.79	2.10E-03	9.39	0.94
RC6	100	3.90E-08	0.1	0.75	2.57E-04	2.60	0.26
		3.90E-08	0.5	0.75	1.90E-04	1.92	0.19
		3.90E-08	1	0.75	0.00E+00	0.00	0.00
		3.90E-08	2	0.75	1.16E-04	1.17	0.12
		3.90E-08	4	0.75	1.23E-03	12.45	1.24
		3.90E-08	5	0.75	1.60E-03	16.19	1.62
RC8	200	8.00E-09	0.005	1.05	-1.02E-04	-7.05	-0.70
		8.00E-09	0.01	1.05	-8.46E-05	-5.84	-0.58
		8.00E-09	0.05	1.05	1.53E-04	10.57	1.06
		8.00E-09	0.1	1.05	2.07E-04	14.30	1.43
		8.00E-09	0.5	1.05	2.55E-04	17.61	1.76
		8.00E-09	1	1.05	0.00E+00	0.00	0.00
		8.00E-09	2	1.05	2.99E-04	20.65	2.07
		8.00E-09	4	1.05	9.58E-04	66.17	6.62
SB1	200	1.25E-09	4	1.25	5.20E-04	273.66	27.37
SB1	200	1.04E-09	4	1.57	0.00E+00	0.00	0.00
SB4	200	1.58E-09	0	1.28	-4.03E-04	-171.81	-17.18
		1.58E-09	0.05	1.28	5.60E-04	238.75	23.87
		1.58E-09	0.1	1.28	3.53E-04	150.50	15.05
		1.58E-09	0.5	1.28	0.00E+00	0.00	0.00
		1.58E-09	1	1.28	0.00E+00	0.00	0.00
		1.58E-09	2	1.28	0.00E+00	0.00	0.00

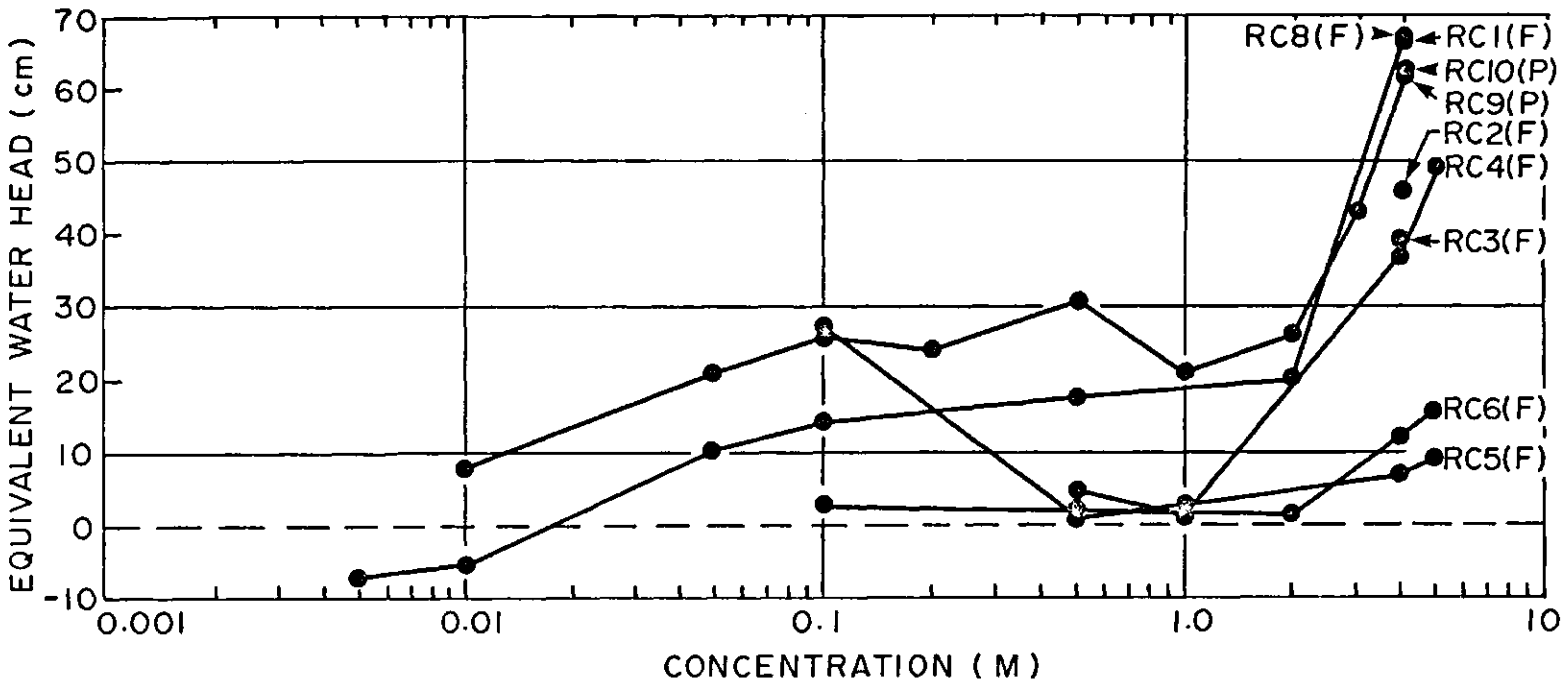

Figure 7.1 Osmotic Pressure Heads for Regina Clay

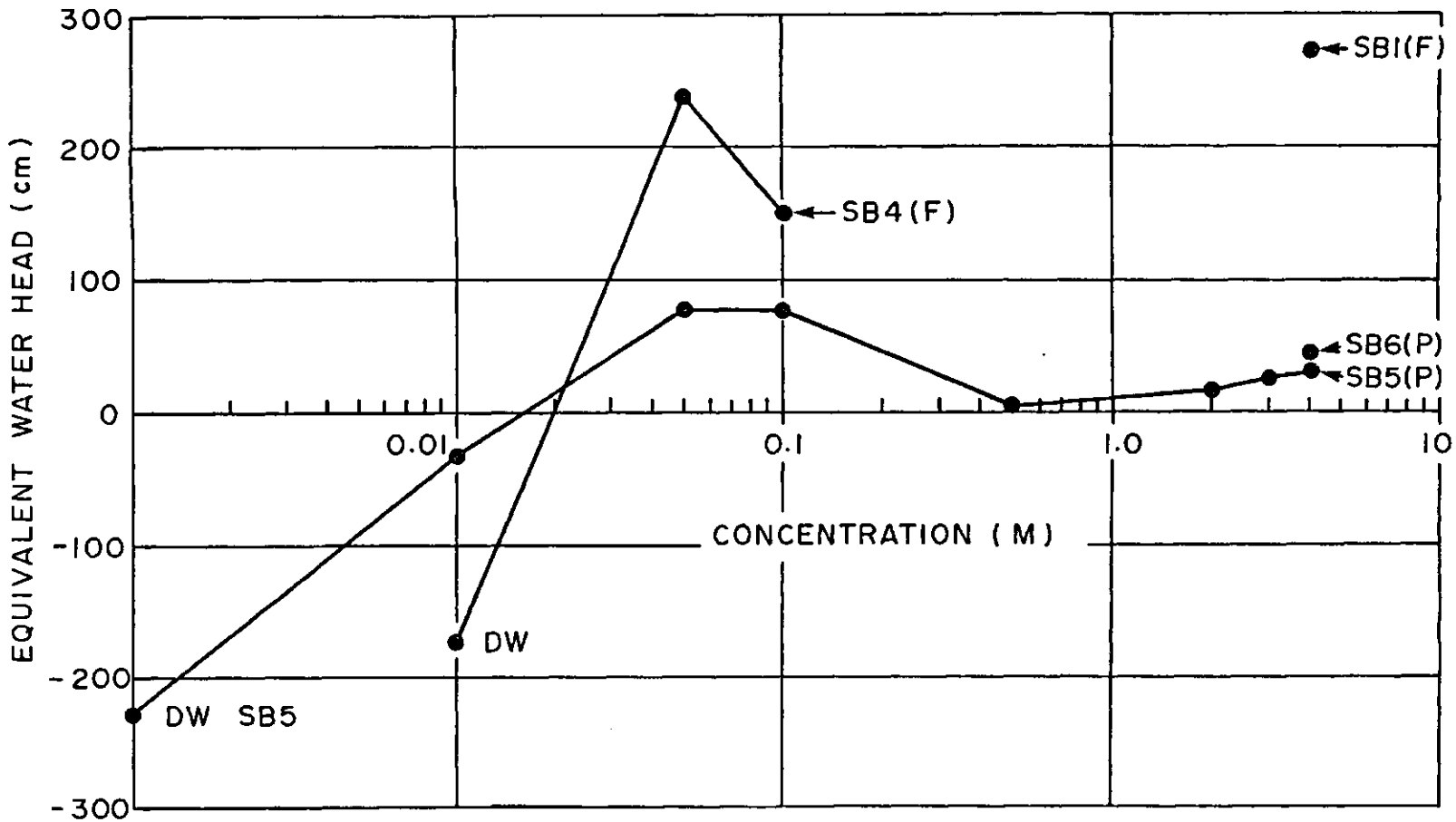

Figure 7.2 Osmotic Pressure Heads for Sand/bentonite

Fairly low pressures are developed within the samples due to osmotic gradients. In general, most samples experienced less than a 10 kPa change in the pore fluid pressure. Similar trends of equivalent head with concentration are observed in Figures 7.1 and 7.2, for both the sand/bentonite and the Regina Clay samples. A peak osmotic pressure occurs at a concentration of 0.1 M. Extremely low values of osmotic pressure are developed at a concentration of approximately 1.0 M. This observation is consistent with the description of peak osmotic pressures described by Kemper and Rollins (1966) (Figure 2.6).

Fairly good agreement between the calculated pressure heads, and those obtained by direct measurement is also apparent. Approximately 35 to 45 cm of pressure head were measured using the transducers. The one exception to the agreement obtained by indirect and direct evaluation of pressure head is Sample SB1. The calculated pressure head was approximately 270 cm. The large increase in hydraulic conductivity that occurred in the sand bentonite samples, after exposure to the NaCl solutions, was noted in Chapter 6. The equivalent head, calculated using the higher post-osmotic permeability of the sample, would be 38 cm. This value is in agreement with the heads measured with the pressure transducers.

The lower pressure heads for Samples RC5 and RC6 are likely due to the lower stress level to which these samples were consolidated. The base flow rates measured in these samples were similar to those measured at higher stress levels, however, the permeability of samples RC5 and RC6 was significantly higher.

Osmotic Efficiency

The osmotic efficiencies of the clays can be calculated as the ratio of the equivalent hydraulic head, to the osmotic head across the sample. Table 7.2 presents a summary of the osmotic efficiencies for the clays.

Table 7.2 Summary of Calculated Osmotic Efficiency

Sample	Molarity	Flow or Pressure Measurement	Equiv. Head (CM)	Osmotic Efficiency
RC1	4	flow	65.54333	3.33E-04
RC2	4	flow	45.52414	2.31E-04
RC3	4	flow	39.27072	1.99E-04
RC4	0.5	flow	4.883696	2.18E-04
	1	flow	1.291894	5.18E-05
	4	flow	37.2893	2.49E-04
	5	flow	48.83696	9.79E-04
RC5	0.1	flow	27.26934	1.09E-02
	0.5	flow	0.961132	4.82E-05
	1	flow	2.695641	1.08E-04
	2	flow		0.00E+00
	4	flow	7.286725	7.30E-05
	5	flow	9.387806	1.88E-04
RC6	0.1	flow	2.60094	1.04E-03
	0.5	flow	1.922874	9.64E-05
	1	flow		0.00E+00
	2	flow	1.173965	2.35E-05
	4	flow	12.44808	1.25E-04
	5	flow	16.19262	3.25E-04
RC8	0.005	flow	-7.04531	3.14E-03
	0.01	flow	-5.84346	2.34E-02
	0.05	flow	10.56796	5.30E-03
	0.1	flow	14.29783	5.73E-03
	0.5	flow	17.61327	8.83E-04
	1	flow	0	0.00E+00
	2	flow	20.65243	4.14E-04
	4	flow	66.17066	6.63E-04
RC9	0.01	pressure	8	4.01E-03
	0.05	pressure	21	1.05E-02
	0.1	pressure	16	6.41E-03
	0.2	pressure	24	4.81E-03
	0.5	pressure	31	2.07E-03
	1	pressure	21	8.42E-04
	2	pressure	26	5.21E-04
	3	pressure	43	8.62E-04
	4	pressure	61	1.22E-03
RC10	4	pressure	62	3.15E-04
SB1	4	flow	273.6554	1.37E-03
SB4	0	flow	-171.814	4.31E-01
	0.05	flow	238.749	9.57E-02
	0.1	flow	150.4971	6.03E-02
	0.5	flow	0	0.00E+00
	1	flow	0	0.00E+00
	2	flow	0	0.00E+00
SB5 D.W.	0.02	pressure	-228	3.81E-01
	0.01	pressure	-31	6.21E-02
	0.05	pressure	78	3.91E-02
	0.1	pressure	77	3.09E-02
	0.5	pressure	3	1.50E-04
	1	pressure		0.00E+00
	2	pressure	17	3.41E-04
	3	pressure	28	5.61E-04
	4	pressure	31	6.21E-04
SB6	4	pressure	45	2.26E-04

The osmotic head was calculated from the concentration difference across the sample, using the van't Hoff approximation of osmotic pressure. Efficiencies were taken as positive in all cases, even though the actual flow rate may have been out of the sample rather than into the sample.

The efficiencies for the sand/bentonite and Regina Clay samples are illustrated in Figures 7.3 and 7.4. In spite of a considerable amount of scatter, some significant trends can be observed. Fairly high efficiencies are obtained at low solution concentrations and low efficiencies at high solution concentrations. This is consistent with the results described by Kemper and Rollins(1966) (Figure 2.5). The higher efficiencies at concentrations of 4 to 5 M, may be due in part to an under-estimate of the osmotic pressures using the van't Hoff approximation.

The transparent overlays for Figures 7.3 and 7.4 illustrate theoretical osmotic efficiencies based on the work of Bresler (1973) (Figure 2.7). An estimate of the interparticle spacing is required in order to calculate these efficiencies. The interparticle spacings were calculated using estimates of specific surface and the equation for the interparticle spacing between packets of particles given by Shainberg et al (1971) (Equation 2.13). Table 7.3 presents the interparticle half spacings for Regina Clay and sand/bentonite calculated from typical values of void ratio, specific gravity, and specific surface. The specific surface of the sand bentonite mixture was taken as 20% of the specific surface of 570 m^2/gm for the bentonite alone.

Altering the estimate of the specific surface of the clays shifts the theoretical curves in Figures 7.3 and 7.4 to the left or right. It is of interest that in the case of the sand/bentonite samples, the efficiency follows along a curve of constant N, where N is the number of particles per packet.

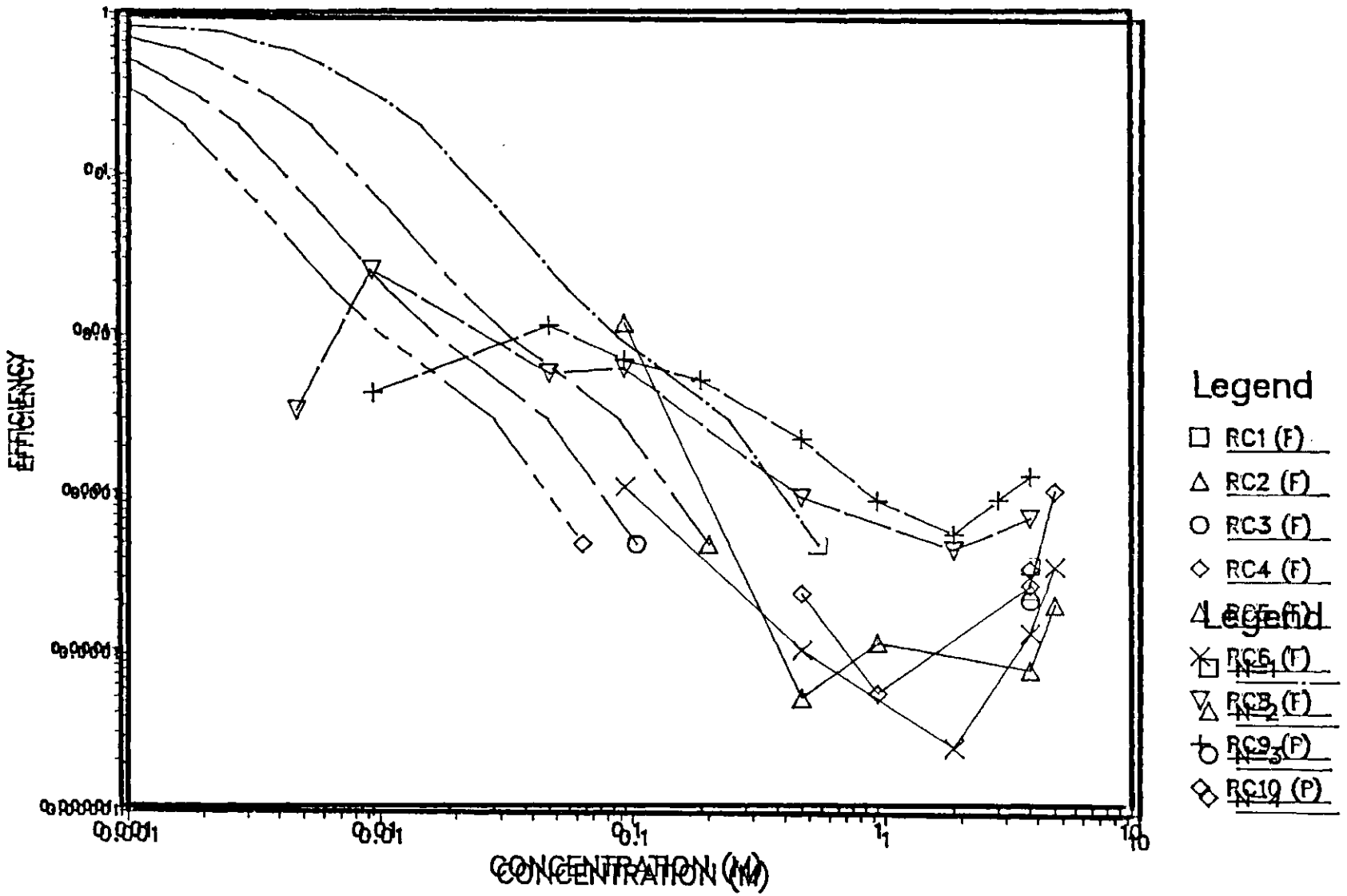

Figure 7.3 a) Experimental Osmotic Efficiencies
b) Theoretical Osmotic Efficiencies
for Regina Clay (after Bresler 1973)

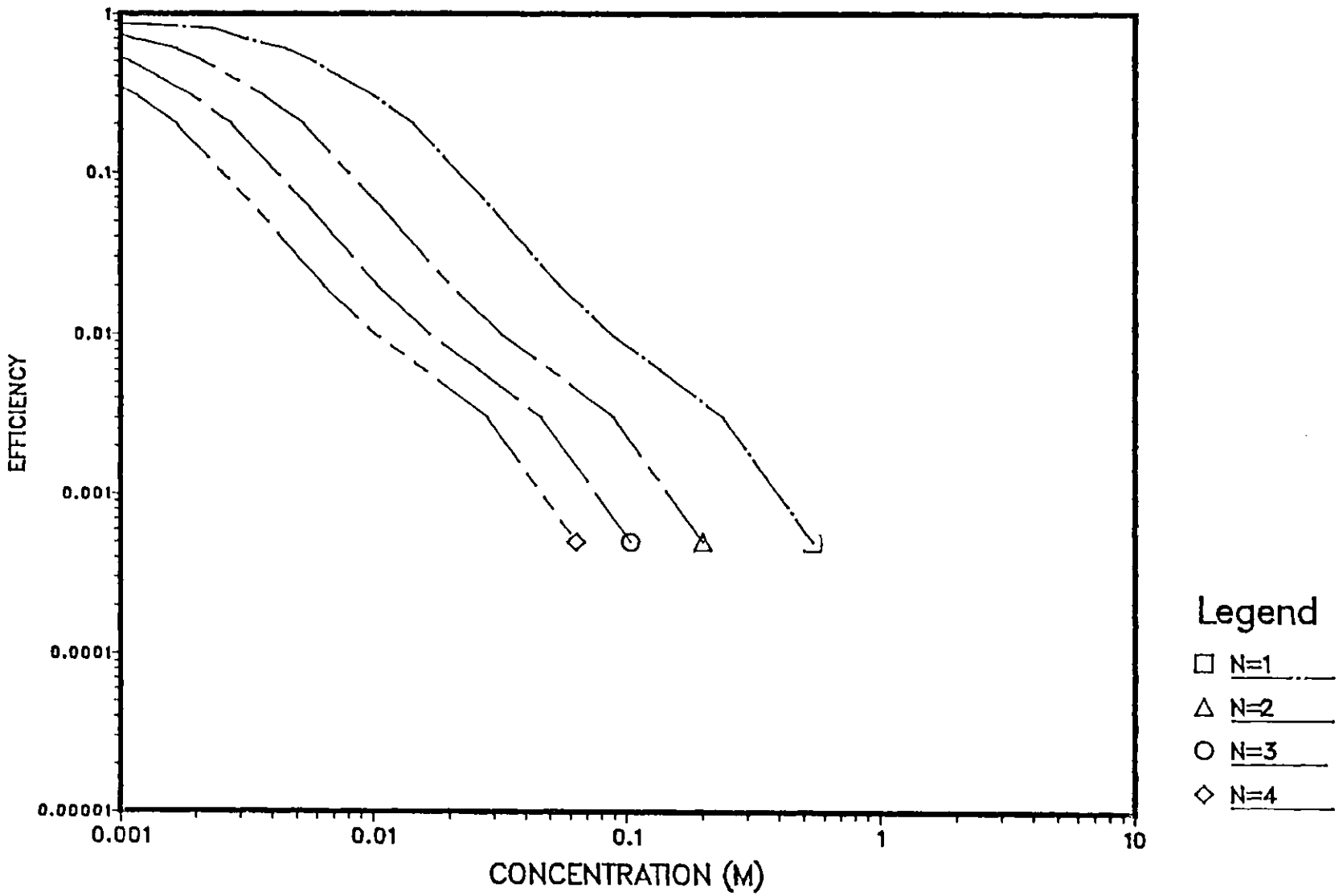

Figure 7.3 b) Theoretical Osmotic Efficiencies for Regina Clay (after Bresler 1973)

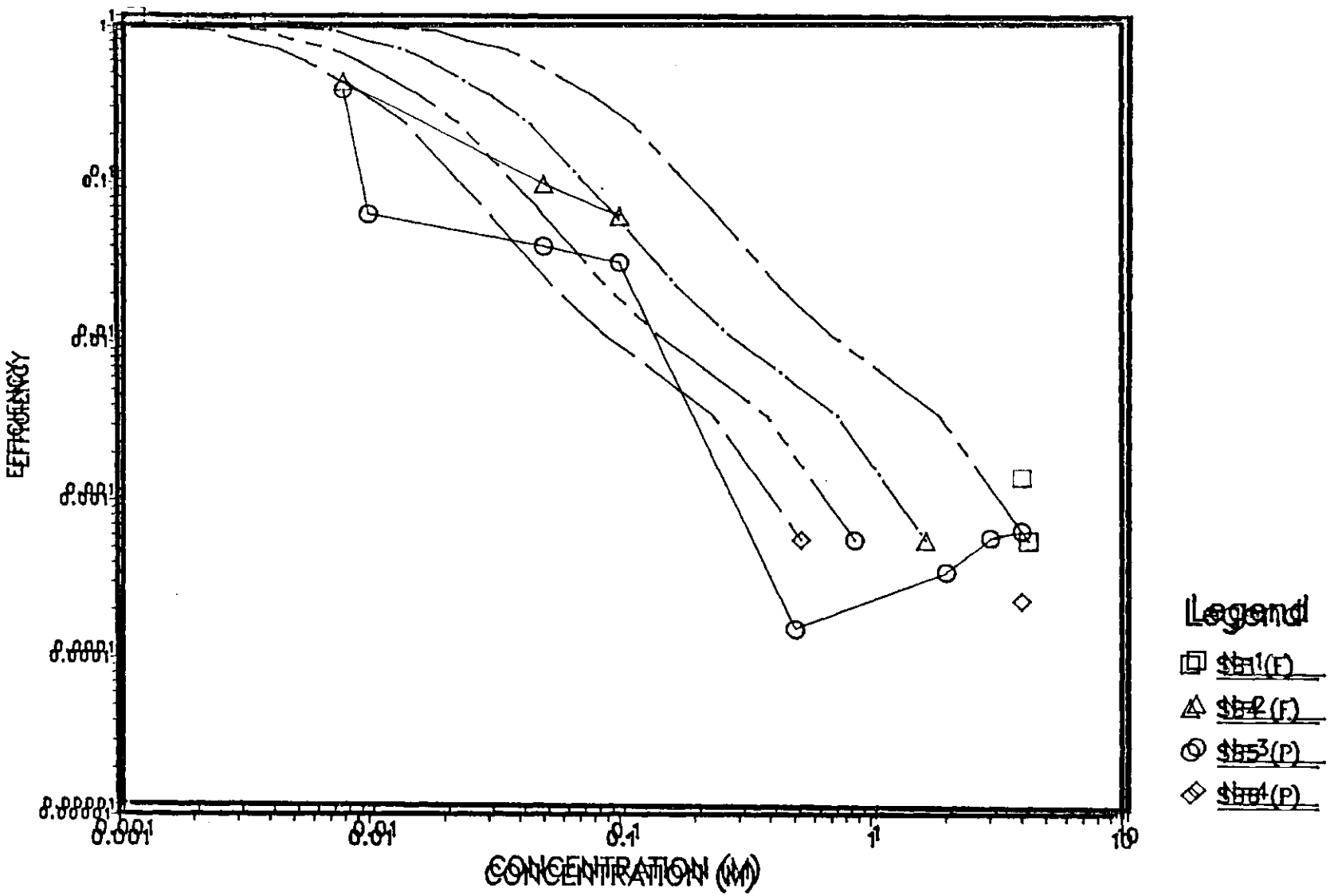

Figure 7.4a) Theoretical Osmotic Efficiencies for Sand Bentonite (after Bresler 1973)

Figure 7.4b) Experimental Osmotic Efficiencies for Sand Bentonite

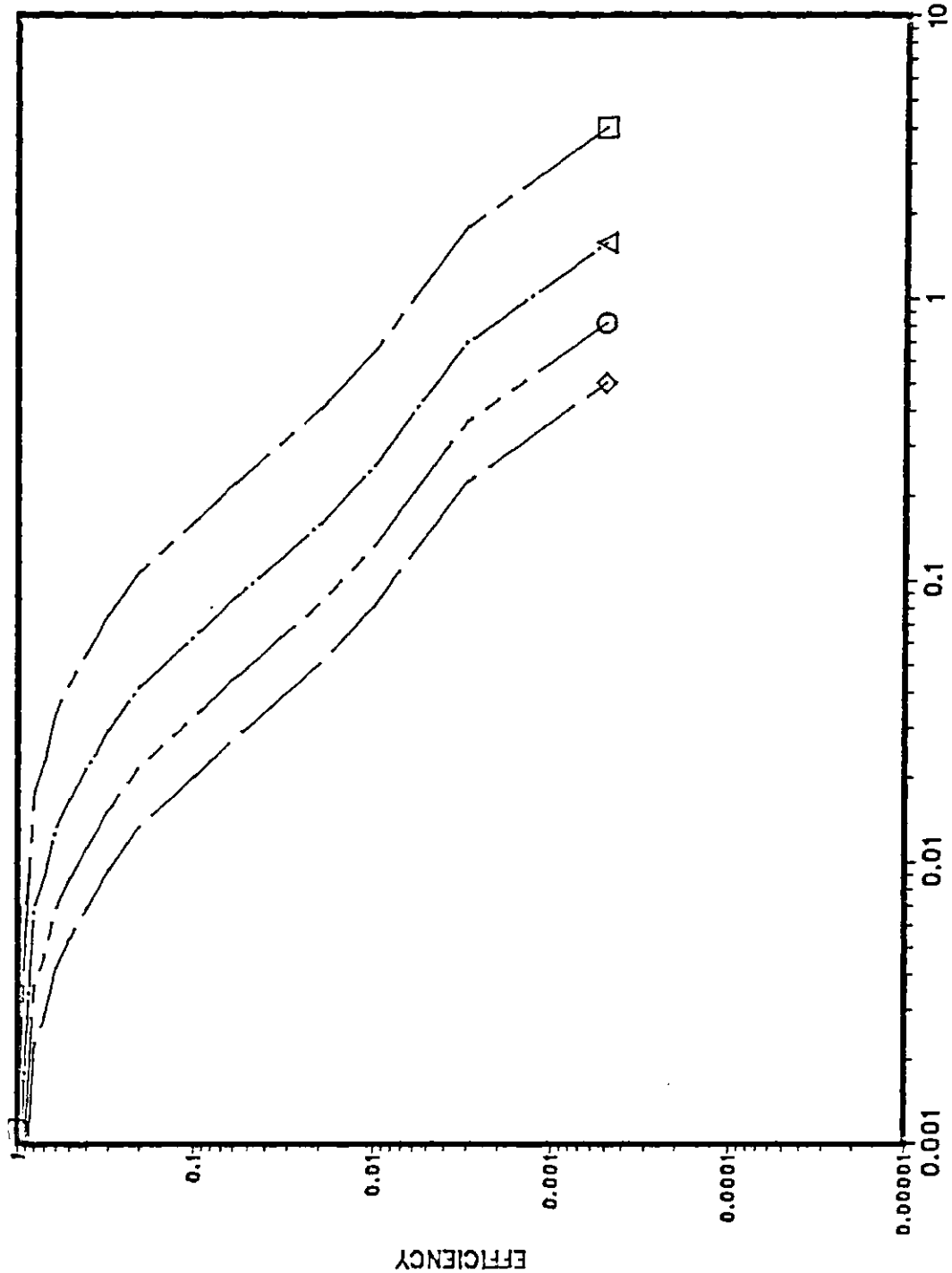

Figure 7.4 b) Theoretical Osmotic Efficiencies for Sand Bentonite (after Bresler 1973)

Table 7.3 Calculation of Particle Half Spacing

Regina Clay		Sand Bentonite	
Void Ratio =	1.2	Void Ratio =	0.9
Gs =	2.74	Gs =	2.63
Spec. Surface = (sq. m/gm)	53	Spec. Surface = (sq. m/gm)	115

Particles /domain (N)	half spacing (b)	Particles /domain (N)	half spacing (b)
1	82.6	1	29.8
2	135.1	2	48.2
3	187.6	3	66.6
4	240.1	4	85.1
5	292.5	5	103.5
6	345.0	6	122.0
7	397.5	7	140.4

In the case of Regina Clay, the efficiencies cross over the theoretical curves from values of N equal to 4 or more at low concentrations to a value of 1 at higher concentrations. This observation is consistent with the fact that Regina Clay is predominately a Ca++ Montmorillonite. Consequently, the clay would be expected to form packets of clay particles during sedimentation. However, as the pore fluid becomes concentrated these packets would begin to disperse, resulting in fewer particles per packet.

7.3 Osmotic Compressibility

The equivalent stress change that occurs during osmotic volume change of the Regina Clay and sand/bentonite samples is illustrated in the curves of void ratio versus applied stress presented in Figures 7.5 through 7.8. The changes in void ratio that occur during contamination are equivalent to those which would occur under effective stress changes of 100 kPa or more. It is obvious that the pressure changes due to osmotic flow, which were generally less than 6 kPa, could not account for these changes in volume. The dominant mechanism for volume change in these soils must be osmotic consolidation.

It has been the view of a number of researchers that the net repulsive minus attractive stress is simply a component of the "true" effective stress of the soil. If this case, the change in void ratio that occurs in Figure 7.5 through 7.8 could be taken as representative of the release of the net (R-A) stress between the clay particles. This net (R-A) stress can be evaluated as the difference in stress from the void ratio at the completion of osmotic consolidation, to the stress level along the virgin branch at the the same void ratio.

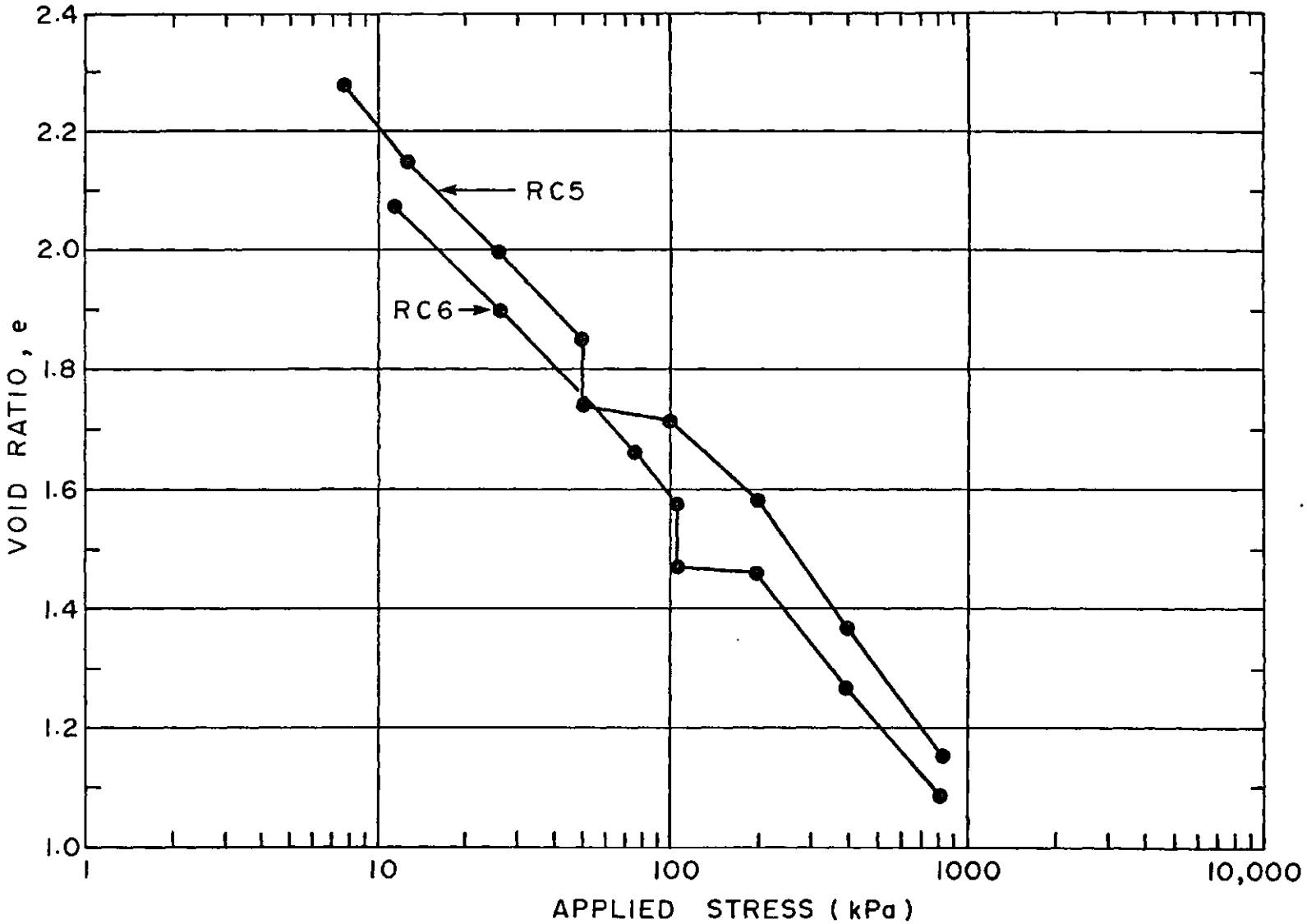

Figure 7.5 Void Ratio versus Applied Stress for Samples RC5 and RC6

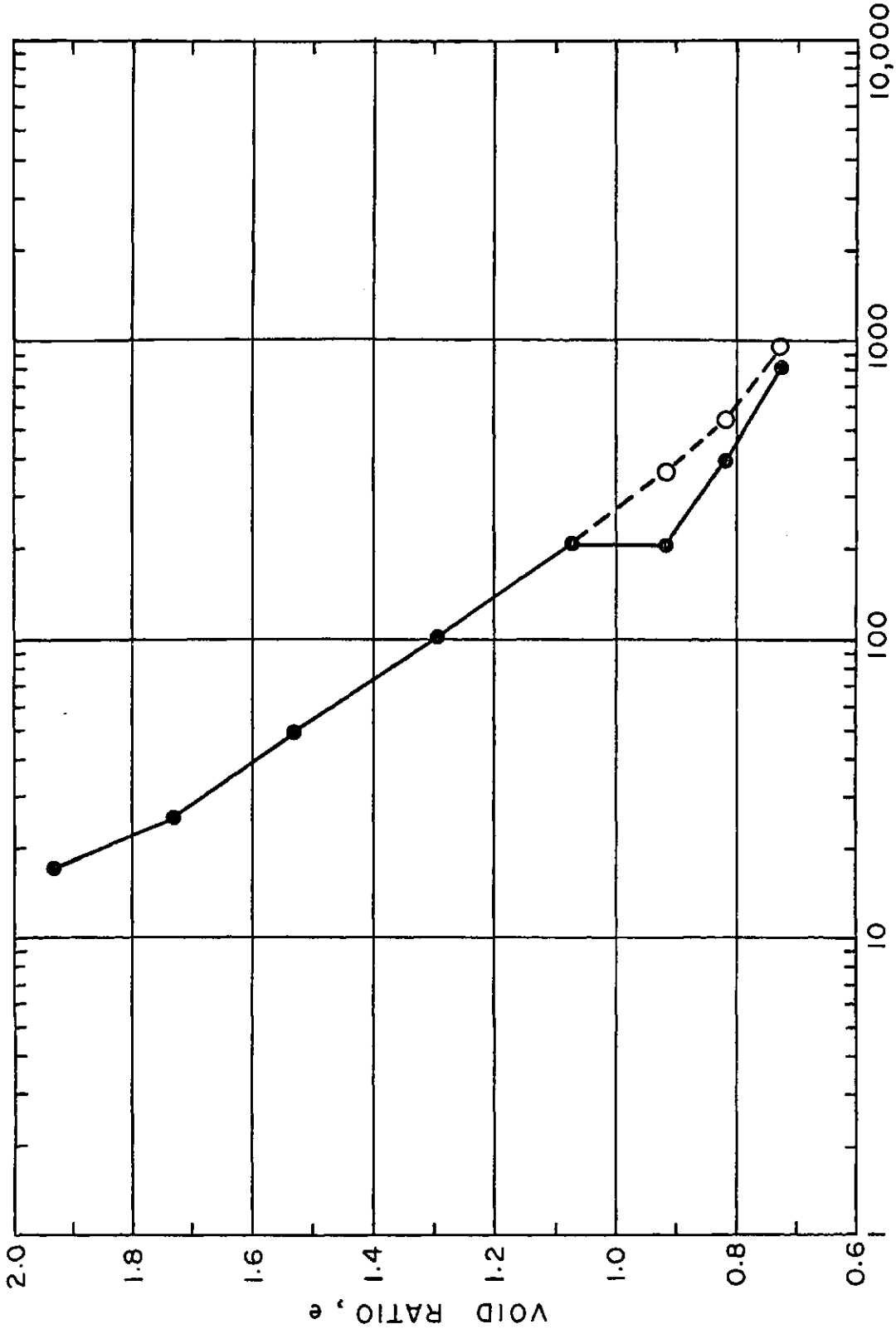

Figure 7.6 Void Ratio versus Applied Stress for Sample SB2

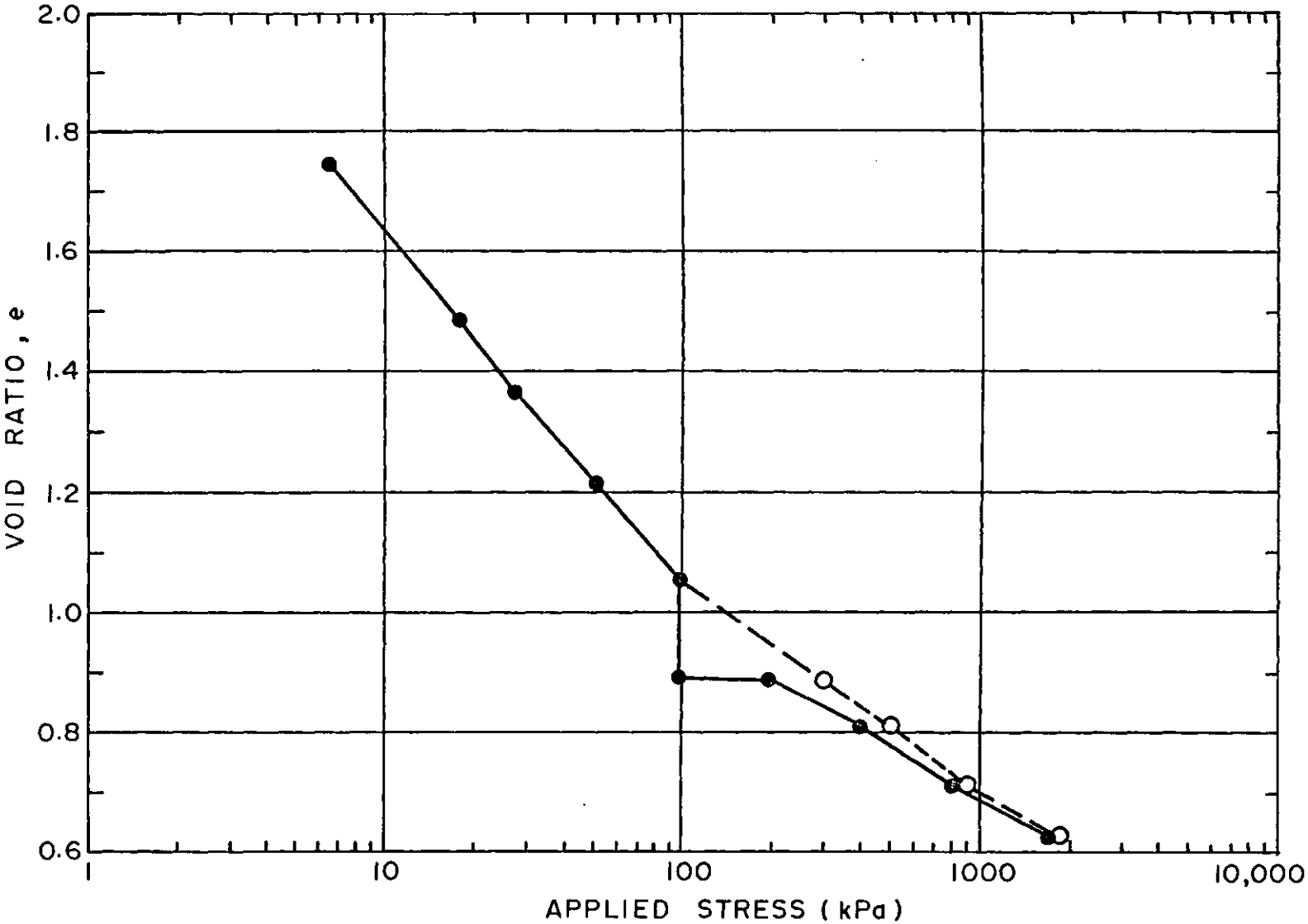

Figure 7.7 Void Ratio versus Applied Stress for Sample SBOC1

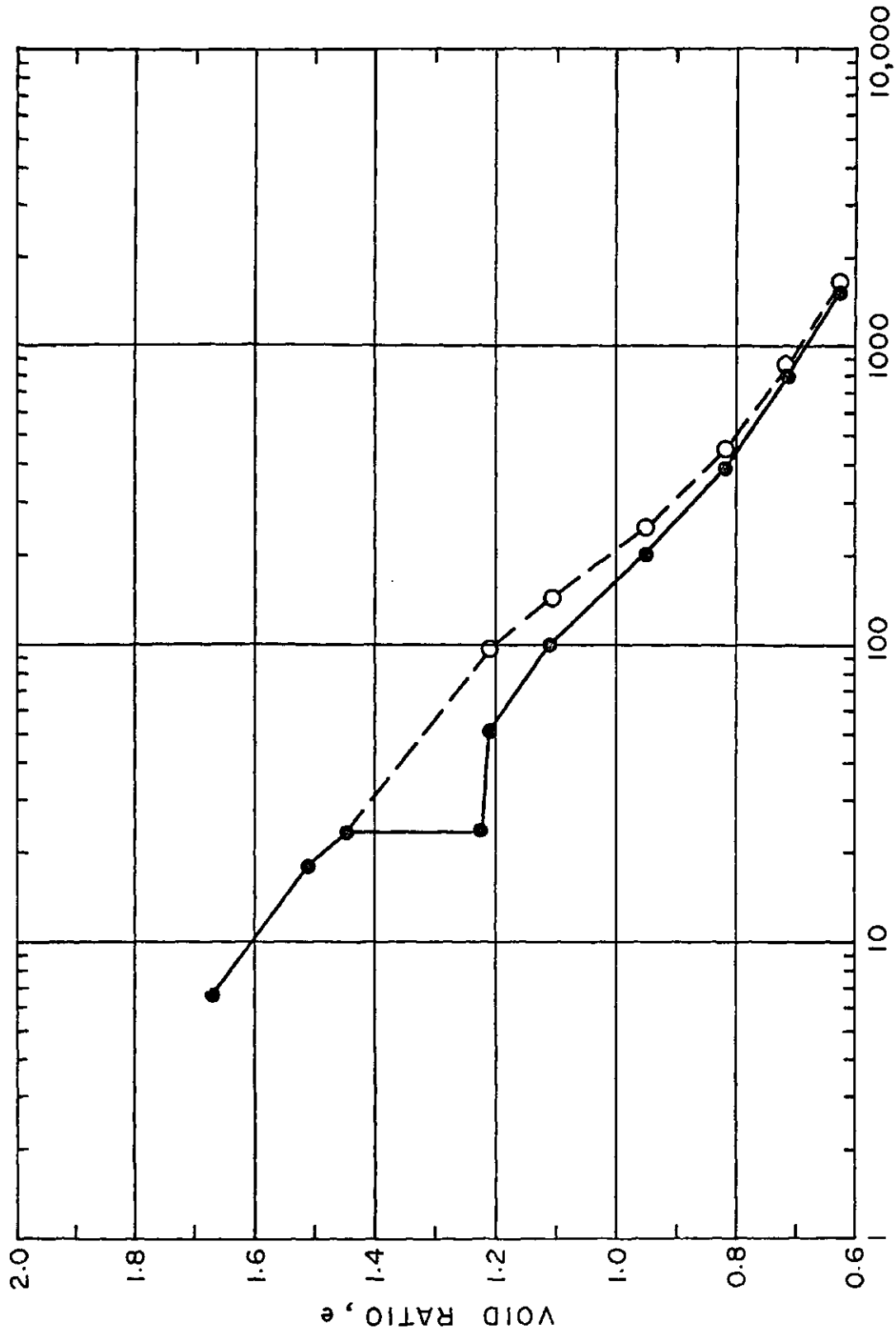

Figure 7.8 Void Ratio versus Applied Stress for Sample SBOC3

The dashed lines in Figures 7.6 through 7.8 represent the reconstruction of the virgin branch of the soil by correcting subsequent applied stress increments by the equivalent change in (R-A). The shape of the corrected curves are in good agreement with the general shape of the virgin branch illustrated in Figure 6.2.

The material appears to behave in accordance with a change in a single value of "true" effective stress during osmotic consolidation. It does not matter whether changes in this stress results from changes in total stress, pore pressure, or in this case, (R-A).

The construction described above, does not seem to apply to the Regina Clay curves. The reason for this may be the fact that the Regina Clay begins to behave as a new material following osmotic consolidation. The steepening of the virgin branch after osmotic consolidation is quite pronounced in both curves shown in Figure 7.5, and is not in agreement with the general shape of the virgin branch depicted in Figure 6.1. The increase in the compressibility of Regina Clay is consistent with a change in structure that would result from the dispersion of the clay packets. Figure 2.22 in Chapter 2 illustrates the decrease in compressibility that occurs as a clay moves from a fully dispersed structure (N=1) to one composed of packets. The destruction of clay packets in the presence of a strong NaCl solution, would account for the increased compressibility of the samples after osmotic consolidation.

Evaluation of Osmotic Compressibility

Table 7.4 provides a summary of the strain due to osmotic consolidation for each sample. The deflections were obtained from the 100 percent consolidation deflections off the osmotic consolidation curves in Appendix D.3. Figures 7.9, 7.10 and 7.11 present the values of strain as a function of pore fluid concentration for the Regina Clay, sand/bentonite, and intact Regina Clay samples.

Table 7.4a Summary of Osmotic Compressibility - Regina Clay Samples

Sample	Stress (kPa)	Conc. (M)	Initial Height (cm)	Defl. (cm)	% Strain	m_π (1/kPa)
RC1	200	4	1.37	0.0285	2.08	1.04E-06
RC2	200	4	1.07	0.0237	2.21	1.11E-06
RC3	200	4	2.3	0.0459	2.00	1.00E-06
RC4	200	0.5	0.48	0.001	0.21	8.35E-07
		1	0.48	0.0021	0.44	8.77E-07
		4	0.48	0.0105	2.19	1.10E-06
		5	0.48	0.0123	2.56	1.03E-06
RC5	50	0.1	0.79	0	0.00	0.00E+00
		0.5	0.79	0.0008	0.10	4.06E-07
		1	0.79	0.0027	0.34	6.85E-07
		2	0.79	0.0063	0.80	7.99E-07
		4	0.79	0.0152	1.92	9.64E-07
		5	0.79	0.0159	2.01	8.07E-07
RC6	100	0.1	0.75	0.0003	0.04	8.02E-07
		0.5	0.75	0.0009	0.12	4.81E-07
		1	0.75	0.0017	0.23	4.54E-07
		2	0.75	0.0065	0.87	8.69E-07
		4	0.75	0.0141	1.88	9.42E-07
		5	0.75	0.0151	2.01	8.07E-07
RC7	200	0.25	0.58	0	0.00	0.00E+00
		0.5	0.58	0.0008	0.14	5.53E-07
		1	0.58	0.0018	0.31	6.22E-07
		2	0.58	0.005	0.86	8.64E-07
RC8	200	0.005	1.05		0.00	0.00E+00
		0.01	1.05		0.00	0.00E+00
		0.05	1.05		0.00	0.00E+00
		0.1	1.05		0.00	0.00E+00
		0.5	1.05		0.00	0.00E+00
		1	1.05	0.0019	0.18	3.63E-07
		2	1.05	0.0031	0.30	2.96E-07
		4	1.05	0.022	2.10	1.05E-06
RC9	200	0.01	0.637		0.00	0.00E+00
		0.05	0.637		0.00	0.00E+00
		0.1	0.637		0.00	0.00E+00
		0.2	0.637		0.00	0.00E+00
		0.5	0.637		0.00	0.00E+00
		1	0.637		0.00	0.00E+00
		2	0.637	0.0065	1.02	1.02E-06
		3	0.637	0.0101	1.59	1.06E-06
		4	0.637	0.0135	2.12	1.06E-06
RC10	200	4	1.3	0.031	2.38	1.20E-06
DB1	300	4	1.424	0.0288	2.02	1.01E-06
DB2	300	0.1	1.6793	0.00108	0.06	1.29E-06
		0.5	1.6793	0.00268	0.16	6.40E-07
		1	1.6793	0.0117	0.70	1.40E-06
		2	1.6793	0.0279	1.66	1.67E-06
		4	1.6793	0.0318	1.89	9.49E-07
DB3	83	4	1.3367	0.0178	1.33	6.67E-07
DB4	200	0.1	1.4207		0.00	0.00E+00
		0.5	1.4207	0.00281	0.20	7.93E-07
		1	1.4207	0.01	0.70	1.41E-06
DB5	758	0.1	1.4011	0.00204	0.15	2.92E-06
		0.5	1.4011	0.0202	1.44	5.78E-06
		1	1.4011	0.022	1.57	3.15E-06
DB6	517	4	1.3204	0.0328	2.48	1.24E-06

Table 7.4b Summary of Osmotic Compressibility - Sand/bentonite Samples

Sample	Stress (kPa)	Conc. (M)	Initial Height (cm)	Defl. (cm)	% Strain	m_π (1/kPa)
SB1	200	4	1.25	0.085	6.80	3.41E-06
SB2	200	4	1.57	0.098	6.24	3.13E-06
SB3	200	0.5	0.61	0.025	4.10	1.64E-05
		1	0.61	0.029	4.75	9.53E-06
		2	0.61	0.0345	5.66	5.67E-06
		4	0.61	0.039	6.39	3.20E-06
SB4	200	0.05	1.28	0.0011	0.09	3.45E-06
		0.1	1.28	0.0018	0.14	2.82E-06
		0.5	1.28	0.0304	2.38	9.52E-06
		1	1.28	0.0355	2.77	5.56E-06
		2	1.28	0.0472	3.69	3.70E-06
SB5	200	0.01	0.63	0.0019	0.30	6.05E-05
		0.05	0.63	0.009	1.43	5.73E-05
		0.1	0.63	0.0158	2.51	5.03E-05
		0.5	0.63	0.035	5.56	2.23E-05
		1	0.63	0.0434	6.89	1.38E-05
		2	0.63	0.04508	7.16	7.17E-06
		3	0.63	0.04815	7.64	5.11E-06
		4	0.63	0.0488	7.75	3.88E-06
SB6	200	4	1.2354	0.06	4.86	2.43E-06
SBOC1	96	0.05	1.3547	0.037	2.73	1.10E-04
		0.1	1.3547	0.0524	3.87	7.75E-05
		0.5	1.3547	0.0706	5.21	2.09E-05
		1	1.3547	0.0875	6.46	1.29E-05
		2	1.3547	0.0917	6.77	6.78E-06
		4	1.3547	0.0922	6.81	3.41E-06
SBOC2	201	0.05	1.26	0.0266	2.11	8.46E-05
		4	1.26	0.0658	5.22	2.62E-06
SBOC3	23.5	0.01	1.61	0.0101	0.63	1.26E-04
		0.05	1.61	0.04137	2.57	1.03E-04
		0.1	1.61	0.0642	3.99	7.99E-05
		0.5	1.61	0.0873	5.42	2.17E-05
		1	1.61	0.123	7.64	1.53E-05
		2	1.61	0.1298	8.06	8.08E-06
		4	1.61	0.135	8.39	4.20E-06

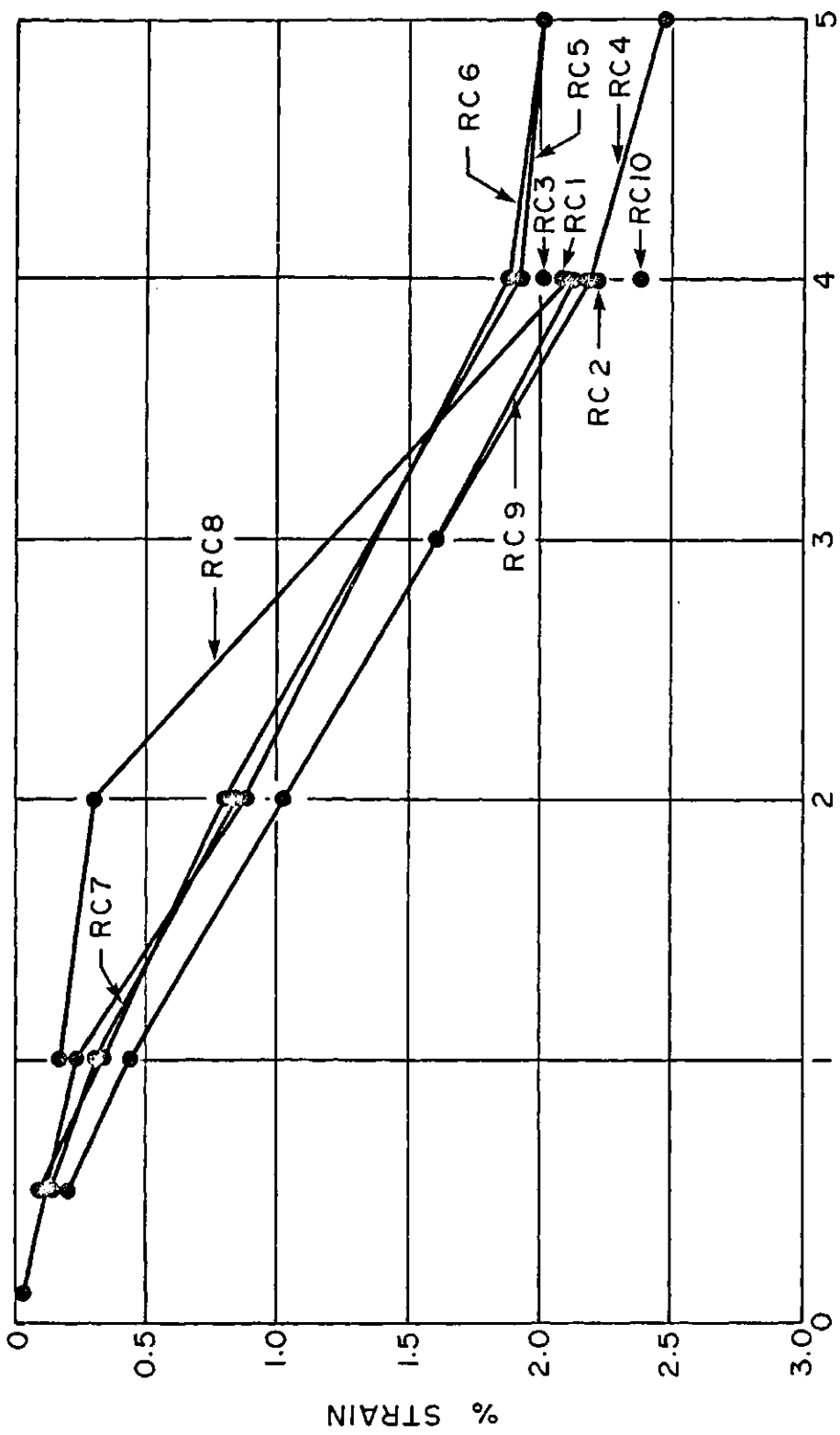

Figure 7.9 Osmotic Volumetric Strain versus Concentration for Regina Clay Samples

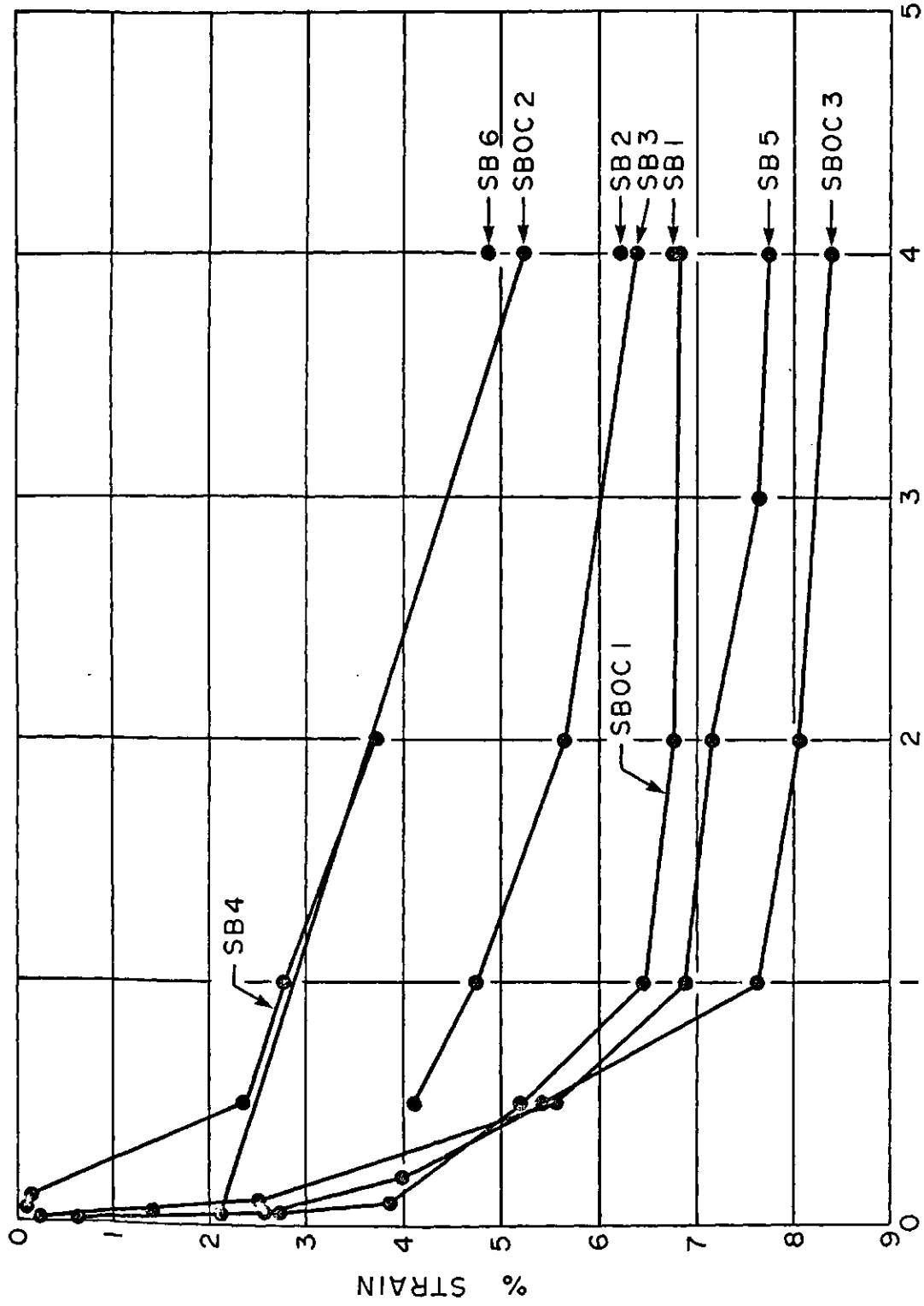

Figure 7.10 Osmotic Volumetric Strain versus Concentration for Sand/bentonite Samples

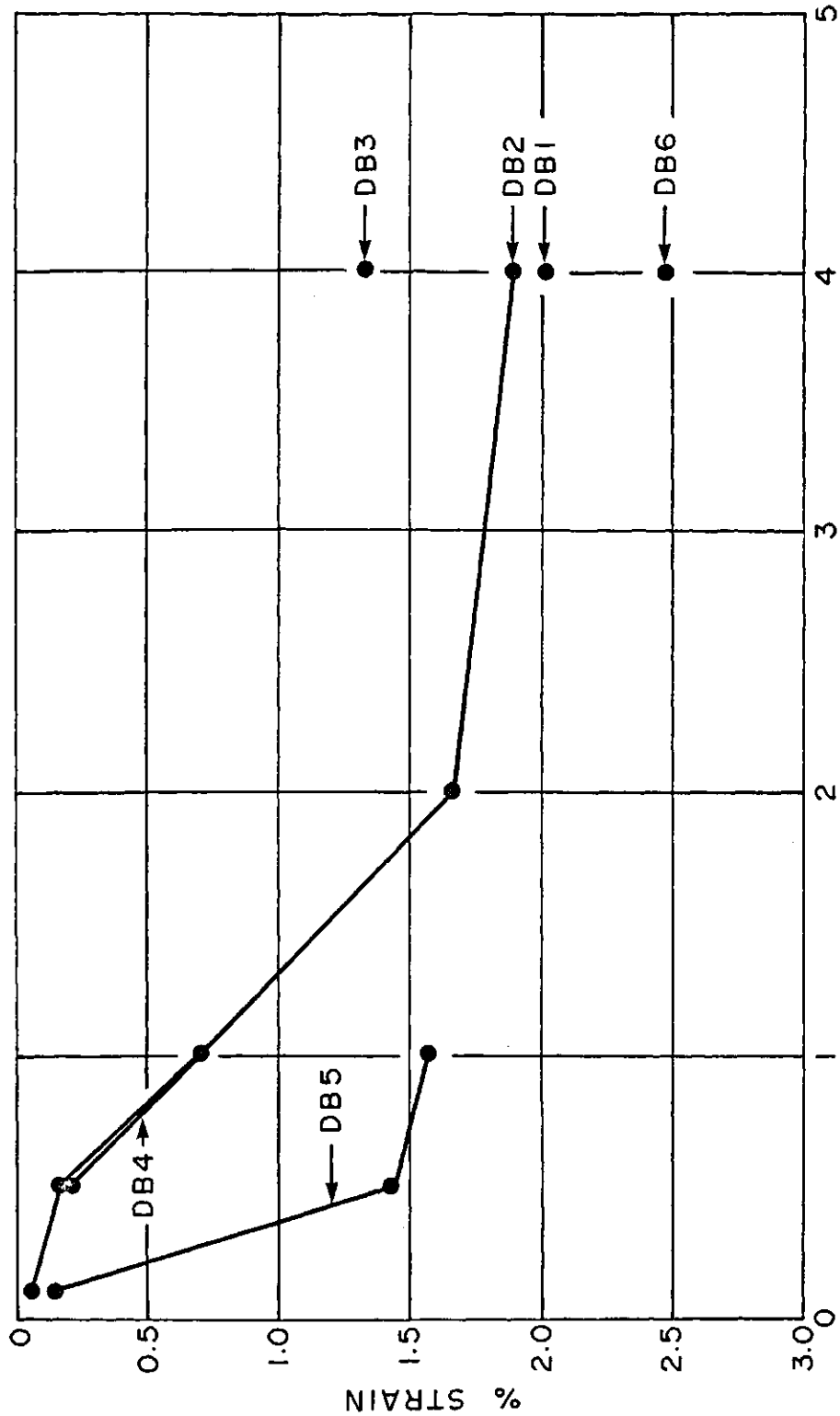

Figure 7.11 Osmotic Volumetric Strain versus Concentration for Intact Regina Clay Samples

The general shape of the curve for the sand/bentonite samples is consistent with double layer theory, in that the majority of the strain due to osmotic consolidation occurs at fairly low concentrations. Double layer calculations would indicate however, that full suppression of the diffuse double layer would occur at concentrations well below 1 M.

The nearly linear relationship between strain and concentration for the Regina Clay samples is obviously not consistent with the suppression of the diffuse double layers about individual clay platelets. Figure 7.10, has a similar shape to the curves presented in Figures 3.9 and 3.11 for Na montmorillonite and Na illite. Figure 7.9 has a similar shape to curves for Ca montmorillonite and Ca illite presented in Figures 3.10 and 3.12. Figures 3.9 through 3.12 were derived from the work of Aylmore and Quirk (1962) on the swelling of Ca and Na montmorillonite. Aylmore and Quirk attributed the anomalous behavior of the Ca montmorillonite to the presence of clay packets.

The results for the intact Regina Clay samples are more scattered. The magnitude of the osmotic strains, however, are very similar to those observed for the reslurried Regina Clay samples.

The slope of the curves in Figures 7.9 through 7.11 may be used to evaluate the osmotic compressibility. Figure 7.12 provides a summary of the values of osmotic compressibility for all of the test samples. The nonlinear nature of osmotic compressibility for the sand/bentonite samples is evident in this figure. The value of osmotic compressibility for the Regina Clay samples is nearly constant.

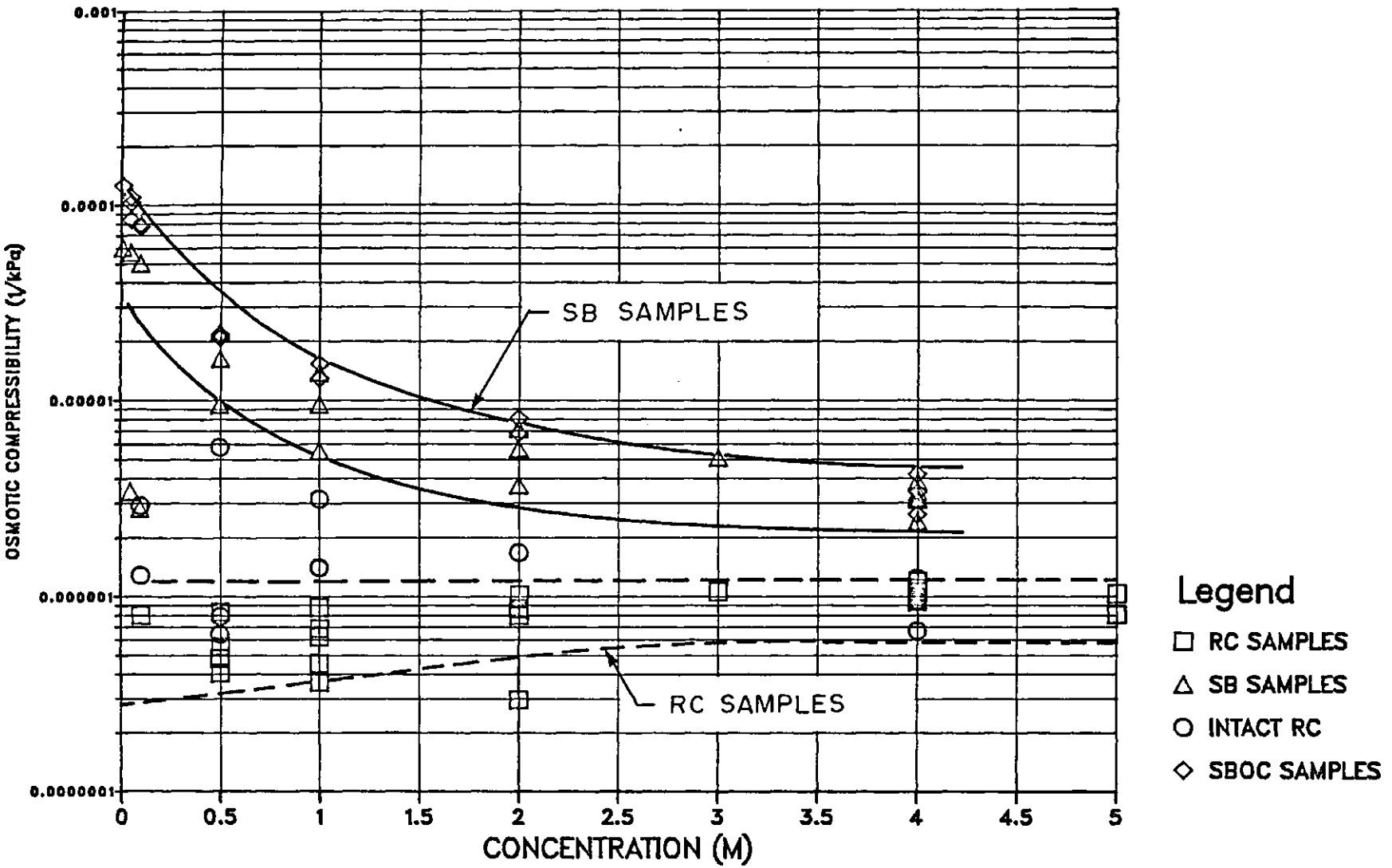

Figure 7.12 Osmotic Compressibility versus Molarity

7.4 Coefficient of Diffusion

The coefficient of diffusion for the clays was determined by measurement of the steady state salt flux through two clay samples. Fick's first law describes this mass flux rate as follows:

$$q_m = n\ D\ \partial C/\partial x \qquad [7.1]$$

where; q_m = mass flux
n = porosity
D = coefficient of diffusion
C = concentration of salt
x = distance

Table 7.5 provides a summary of the coefficients calculated for samples RC7 and SB3. The coefficients of diffusion for both the Regina Clay and sand/bentonite samples are approximately 4 x 10^{-6} cm^2/s. The concentration of the pore fluid seems to have little influence on the diffusion coefficient. Robinson and Stokes (1968) indicate that the coefficient of diffusion of NaCl in free water only varies from 1.61 to 1.474 x 10^{-5} cm^2/s over a 6 M range in concentration.

Table 7.6 provides a summary of coefficients of diffusion for porous media from the literature. Gillham et al (1984) obtained a value of 8 x 10^{-6} cm^2/s for mixtures of 20% bentonite and 80% sand, similar to the mixture used in this study.

The numerical simulation of Chapter 4 indicated that if the flows produced by osmotic effects were not particularly strong, the coefficient of diffusion could be estimated from the time to 50 percent osmotic consolidation. The value of t50 can be obtained from the osmotic consolidation curves in Appendix D.3. Figure 7.13 illustrates the coefficients of diffusion for Regina Clay obtained using this approach. Only the 4.0 M increments of osmotic consolidation were used.

Table 7.5 Summary of Diffusion Test Results

Sample	Concentration Top (M)	Concentration Base (g/l)	Sample Height (cm)	Porosity	Mass Flux (Append D) (g/min)	D (cm^2/s)
RC7						
by conductivy method	1.00	0.91	0.582	0.58	4.59E-04	4.21E-06
	2.00	0.81	0.58	0.58	7.91E-04	3.58E-06
	4.00	0.74	0.578	0.58	1.73E-03	3.89E-06
					avg. D =	3.89E-06
by gravimetric method	1.00	0.94	0.582	0.58	4.11E-04	3.77E-06
	2.00	0.73	0.58	0.58	6.57E-04	2.97E-06
	4.00	0.58	0.578	0.58	1.35E-03	3.03E-06
					avg. D =	3.26E-06
SB3						
by conductivy method	1.00	0.674	0.54	0.48	4.25E-04	4.35E-06
	2.00	0.60	0.54	0.48	8.39E-04	4.27E-06
	4.00	0.75	0.53	0.48	1.67E-03	4.16E-06
					avg. D =	4.26E-06
by gravimetric method	0.50	1.14	0.55	0.48	2.02E-04	4.33E-06
	1.00	0.91	0.54	0.48	3.21E-04	3.30E-06
	2.00	1.00	0.54	0.48	7.44E-04	3.80E-06
	4.00	1.81	0.53	0.48	1.29E-03	3.24E-06
					avg. D =	3.67E-06

Sample	Method	Average D		
RC7	cond.	3.89E-06	RC7	
RC7	grav.	3.26E-06	avg. D =	3.58E-06
SB3	cond.	4.26E-06	SB3	
SB3	grav.	3.67E-06	avg. D =	3.96E-06
	avg. D =	3.77E-06		

Table 7.6 Coefficients of Molecular Diffusion (after Barbour)

Reference	Source	Contaminant	Soil Type	Dd(cm^2/s)
de Josselin de Jong 1958	Lab Test	Saline Solution	.08 mm dia	7×10^{-5}
Simpson 1962	Lab Test	Indigo Carmine Dye	Porous Block	6×10^{-5}
Ogata 1964	Lab Test	Radioactive Phosphorous	Uniform Sand	8×10^{-6}
Manheim 1970	Lab Test reported in literature	Monovalent and Trivalent,	Fine Sands	2×10^{-6} to 6×10^{-6}
Manheim 1970		Monovalent	Free Solution	1.5×10^{-5}
Lerman and Tangiguchi 1972	Case history	Sr-90	Lake Sediment (clay & sand)	2×10^{-6} to 6 x 10-6
Goodall and Quigley 1977	Case history	Ca^+, Mg^+, k^+ and alkali	Silty Clay	2.2-13x10-7
	Literature	chlorides		$2.2\text{-}13 \times 10^{-7}$
Freeze and Cherry 1979	Literature	--	--	1×10^{-7} to 1×10^{-6} (2×10^{-5})
Lee et al. 1980	Assumption	Saline Solution	Fine Sand	7.3 x 10-6
Gillham et al. 1984	Lab test	$^{36}_{CL}$	Bentonite Sand Mixture	$8\text{-}10 \times 10^{-6}$

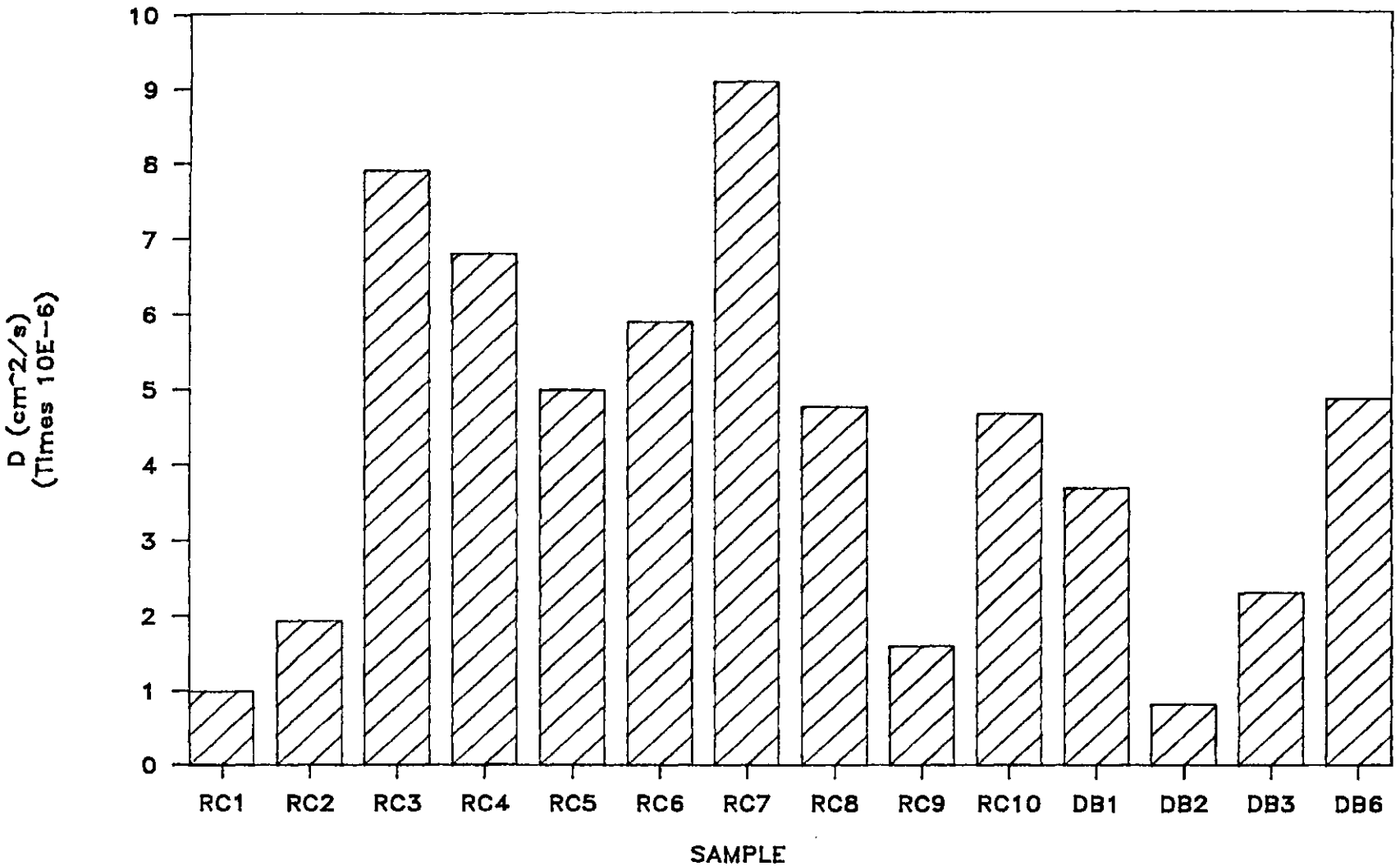

Figure 7.13 Coefficients of Diffusion Estimated from Osmotic Time-Deflection Curves

The coefficients of diffusion obtained using the indirect approach are in reasonable agreement with those obtained using the direct approach. It would appear that the intact Regina Clay samples have somewhat lower values for the coefficient of diffusion. This may be a result of the lower void ratios for these samples and the fact that these samples may not be completely saturated.

7.5 General Characterization of Osmotic Flow and Volume Change by Numerical Simulation

7.5.1 Objective

One of the objectives of this research program was to develop a complete description of osmotic flow and volume change. The individual soil properties required to describe this volume change have been evaluated in Section 7.2 through 7.4. It is of interest to see how well a numerical simulation of the response of these clays to osmotic flow and volume change agrees with the observed response. Only a general representation of the properties of each clay, based on average properties, will be used in the simulation. Consequently, only the general nature of the observed response may be used for comparison. In evaluating the usefulness of the predictive approach outlined in this study, the broader comparison should prove more significant than evaluation of the responses observed for any one particular test.

Four example simulations are presented. The response of a typical sand/bentonite sample and a Regina Clay sample will be simulated for two different sets of boundary conditions.

7.5.2 Simulation Boundary Conditions and Material Properties

The boundary conditions for all simulations are presented in Figure 7.14. Case 1 represents the case in which atmospheric pressure was maintained at the base of the sample and base flow rates were observed. Case 2 represents the case in which base flow is prevented and the pore pressure response at the base was observed. In the laboratory tests, a small reservoir existed below the base of the samples. This reservoir would tend to delay the time to full equalization of concentrations across the samples. Additional salt flux has to occur in order to raise the concentration within the reservoir to the same concentrations that exist within the sample. The presence of the reservoir was not included in these simulations.

Figure 7.15 provides a representation of the curves of osmotic volumetric strain versus concentration for the clays. These curves were used to evaluate the osmotic compressibility of each sample. The osmotic compressibilities calculated from the slope of these curves are given in Table 7.7.

Three sets of osmotic permeability, designated as Cases A,B, and C, were used for each simulation. Figures 7.16 and 7.17 illustrate the three sets of efficiencies used to calculate the osmotic permeabilities for each simulation. Table 7.7 provides a summary of the soil properties utilized in each simulation.

Boundary Conditions:

Case 1

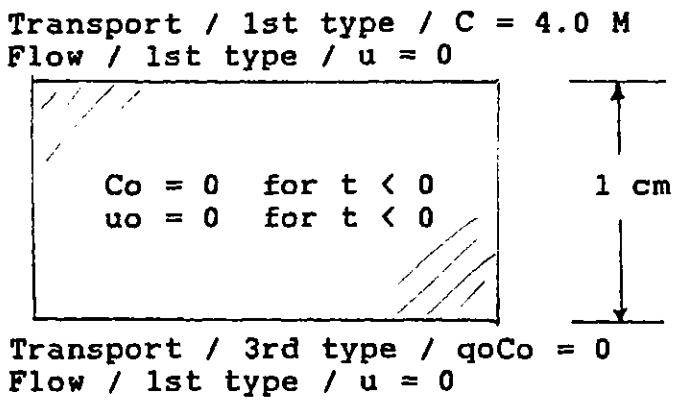

Case 2

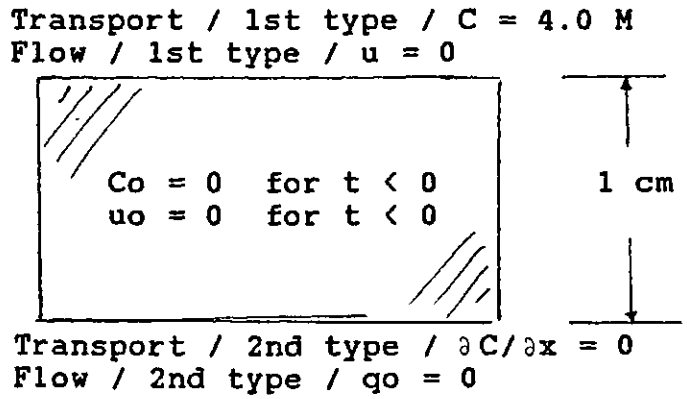

Figure 7.14 Simulation of Regina Clay and Sand Bentonite - Initial and Boundary Conditions

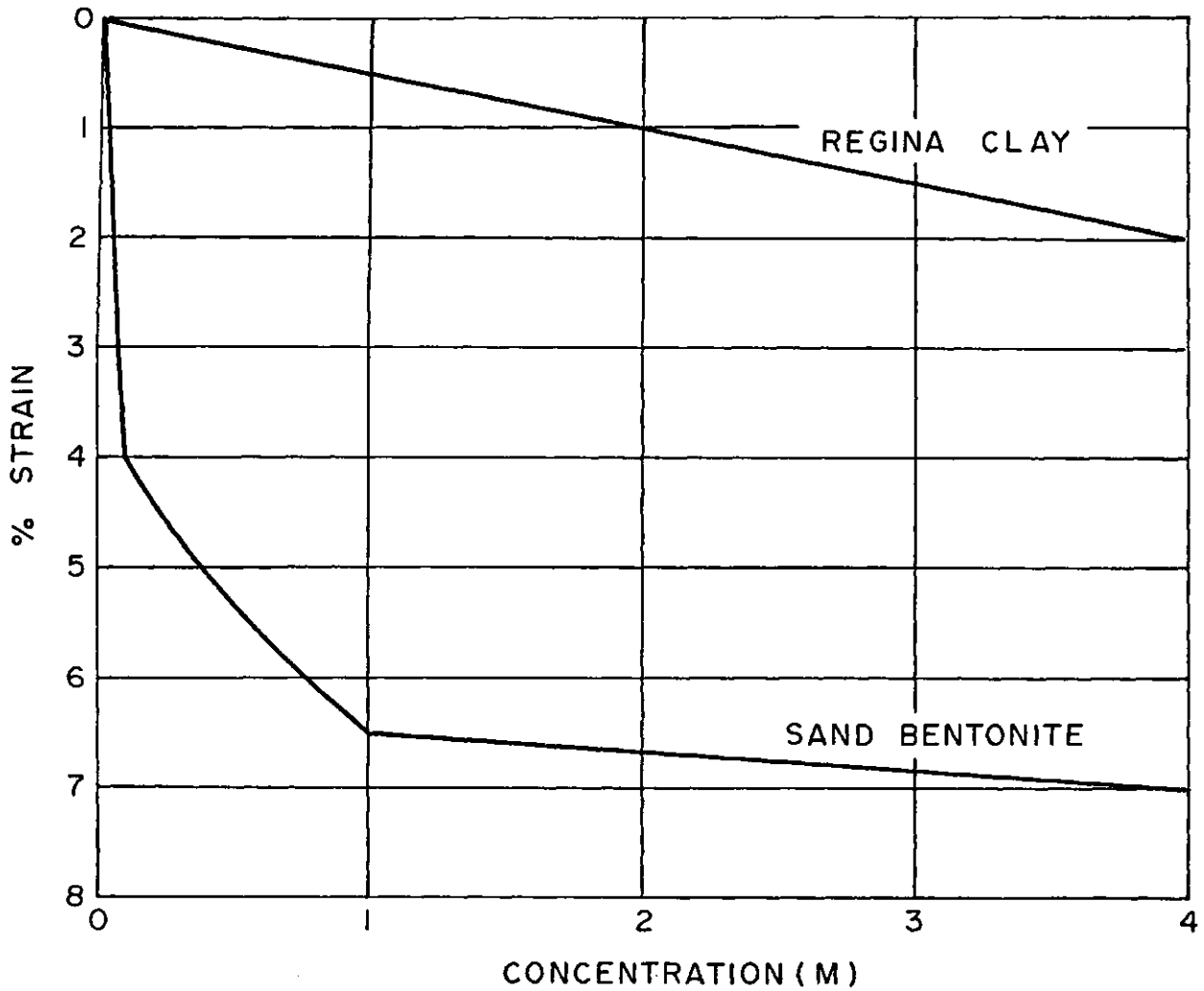

Figure 7.15 Typical Curves of Volumetric Strain versus Concentration for Regina Clay and Sand/bentonite

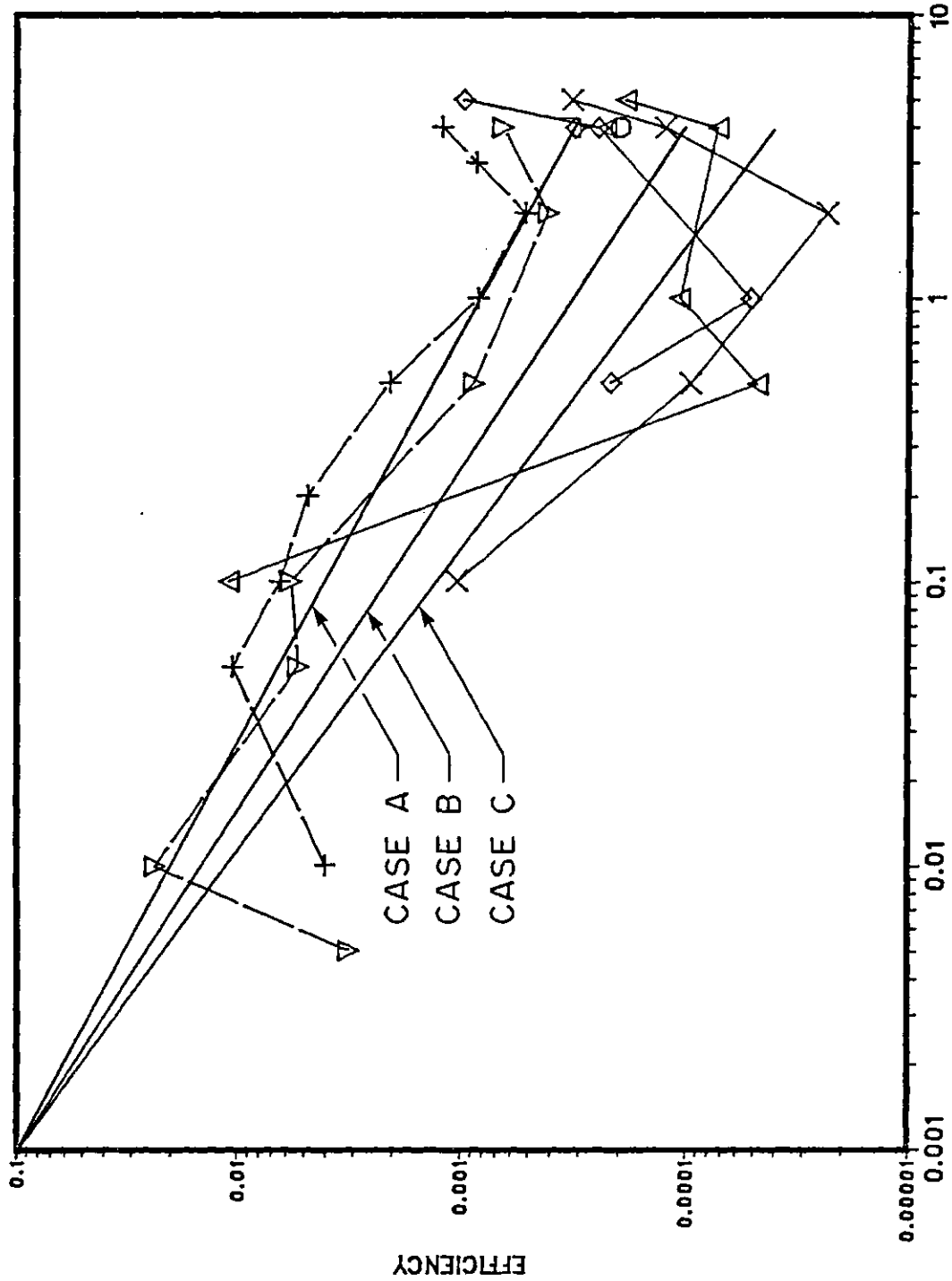

Figure 7.16 Simulation Efficiencies for Regina Clay

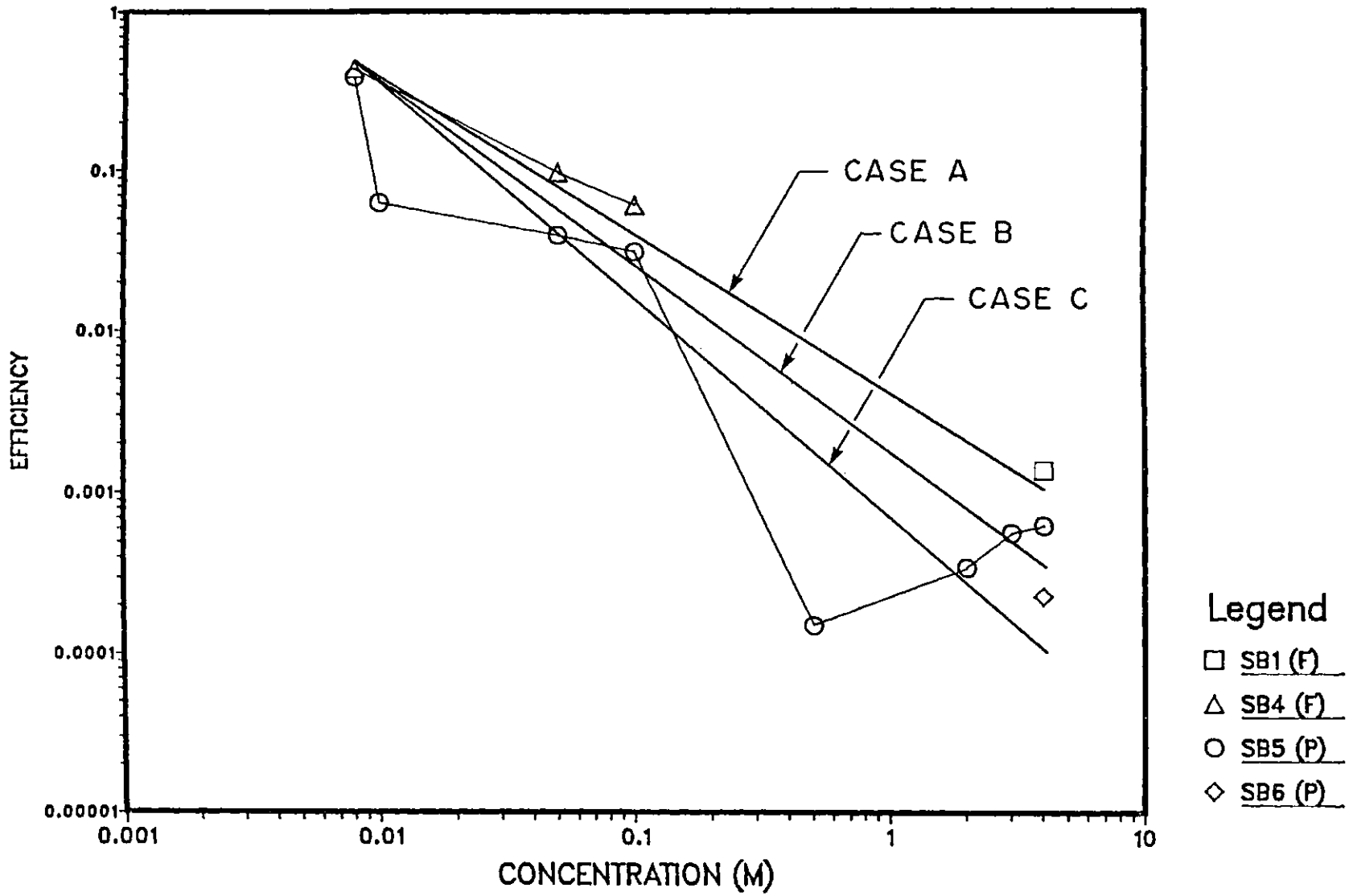

Figure 7.17 Simulation Efficiencies for Sand/bentonite

Table 7.7 Summary of Soil Properties for Numerical Simulation

a) Regina Clay

General: $m_v = 5.5 \times 10^{-4}$ /kPa $\quad k_h = 1 \times 10^{-10}$ m/s

$D = 4 \times 10^{-10}$ m^2/s $\quad n = 0.55$

$C_o = 0.05$ M = 2.925 gm/l

Concentration (M)	Concentration (gm/l)	Osmotic Permeability (m/s) Case A	Case B	Case C	Osmotic Compressibility (1/kPa)
0.05	2.925	6.5×10^{-13}	3.8×10^{-13}	2.2×10^{-13}	1.0×10^{-6}
0.1	5.85	4.0×10^{-13}	2.2×10^{-13}	1.1×10^{-13}	1.0×10^{-6}
0.2	11.7	2.4×10^{-13}	1.2×10^{-13}	0.56×10^{-13}	1.0×10^{-6}
0.3	17.55	1.8×10^{-13}	0.86×10^{-13}	0.38×10^{-13}	1.0×10^{-6}
0.4	23.4	1.5×10^{-13}	0.68×10^{-13}	0.29×10^{-13}	1.0×10^{-6}
0.5	29.25	1.3×10^{-13}	0.57×10^{-13}	0.23×10^{-13}	1.0×10^{-6}
1.0	58.5	0.79×10^{-13}	0.32×10^{-13}	0.12×10^{-13}	1.0×10^{-6}
2.0	117	0.49×10^{-13}	0.18×10^{-13}	$.059 \times 10^{-13}$	1.0×10^{-6}
4.0	234	0.30×10^{-13}	0.1×10^{-13}	$.003 \times 10^{-13}$	1.0×10^{-6}

b) Sand/bentonite

General: $m_v = 5.0 \times 10^{-4}$ /kPa $\quad kh = 1 \times 10^{-11}$ m/s

$D = 4 \times 10^{-10}$ m^2/s $\quad n = 0.5$

Co = 0.008 M = .468 gm/l

Concentration (M)	Concentration (gm/l)	Permeability (m/s) Case A	Case B	Case C	Osmotic Compressibility (1/kPa)
0.008	0.468	50.0×10^{-13}	50.0×10^{-13}	50.0×10^{-13}	80.0×10^{-6}
0.01	0.585	40.0×10^{-13}	38.0×10^{-13}	37.0×10^{-13}	80.0×10^{-6}
0.05	2.925	8.0×10^{-13}	5.6×10^{-13}	4.1×10^{-13}	80.0×10^{-6}
0.1	5.85	4.0×10^{-13}	2.5×10^{-13}	1.6×10^{-13}	80.0×10^{-6}
0.2	11.7	2.0×10^{-13}	1.1×10^{-13}	0.61×10^{-13}	7.5×10^{-6}
0.5	29.25	0.8×10^{-13}	0.36×10^{-13}	0.17×10^{-13}	5.0×10^{-6}
1.0	58.5	0.4×10^{-13}	0.16×10^{-13}	0.067×10^{-13}	5.0×10^{-6}
2.0	117	0.2×10^{-13}	0.069×10^{-13}	0.026×10^{-13}	0.335×10^{-6}
4.0	234	$.1 \times 10^{-13}$	0.03×10^{-13}	0.01×10^{-6}	0.335×10^{-6}

7.5.3 Simulation of Regina Clay

Figures 7.18 and 7.19 illustrate the simulated deflection of the Regina Clay with time. The typical ranges of observed deflection are also noted on these figures. The simulated deflection curves are all in good agreement with the observed deflection curves at times greater than 1000 minutes. At earlier times, the higher efficiencies of cases A and B produce rapid deflection of the sample up to a time of 100 minutes. This component of osmotically induced consolidation was not observed during testing of the Regina Clay.

The base flow rates and base pressure responses are illustrated in Figures 7.20 and 7.21. For these cases the observed sample responses are in better agreement with the higher estimates of efficiency. The shape of the simulated base flow curve for case B efficiencies is in excellent agreement with the laboratory observations. The diminishing flow rates present in the simulations occur because the small solution reservoir below the sample was not simulated. Consequently, equalization of concentrations and the removal of osmotic gradients across the sample occurs more quickly.

The observed base pressure response (e.g.,Sample RC10) has a similar shape to the simulated curves. It appears, however, to be skewed toward larger elapsed times. This may be due in part to time lag in the pressure readings.

Overall, it would appear that the predicted and observed responses are in good agreement. It would appear that the actual efficiencies of the membrane are lower at smaller concentrations than those simulated. This would be consistent with the fact that at low concentrations, the Regina Clay would still behave as a Ca montmorillonite clay. The efficiencies of divalent clays are lower than the efficiencies of monovalent clays (Kemper and Rollins 1966, Bresler 1973).

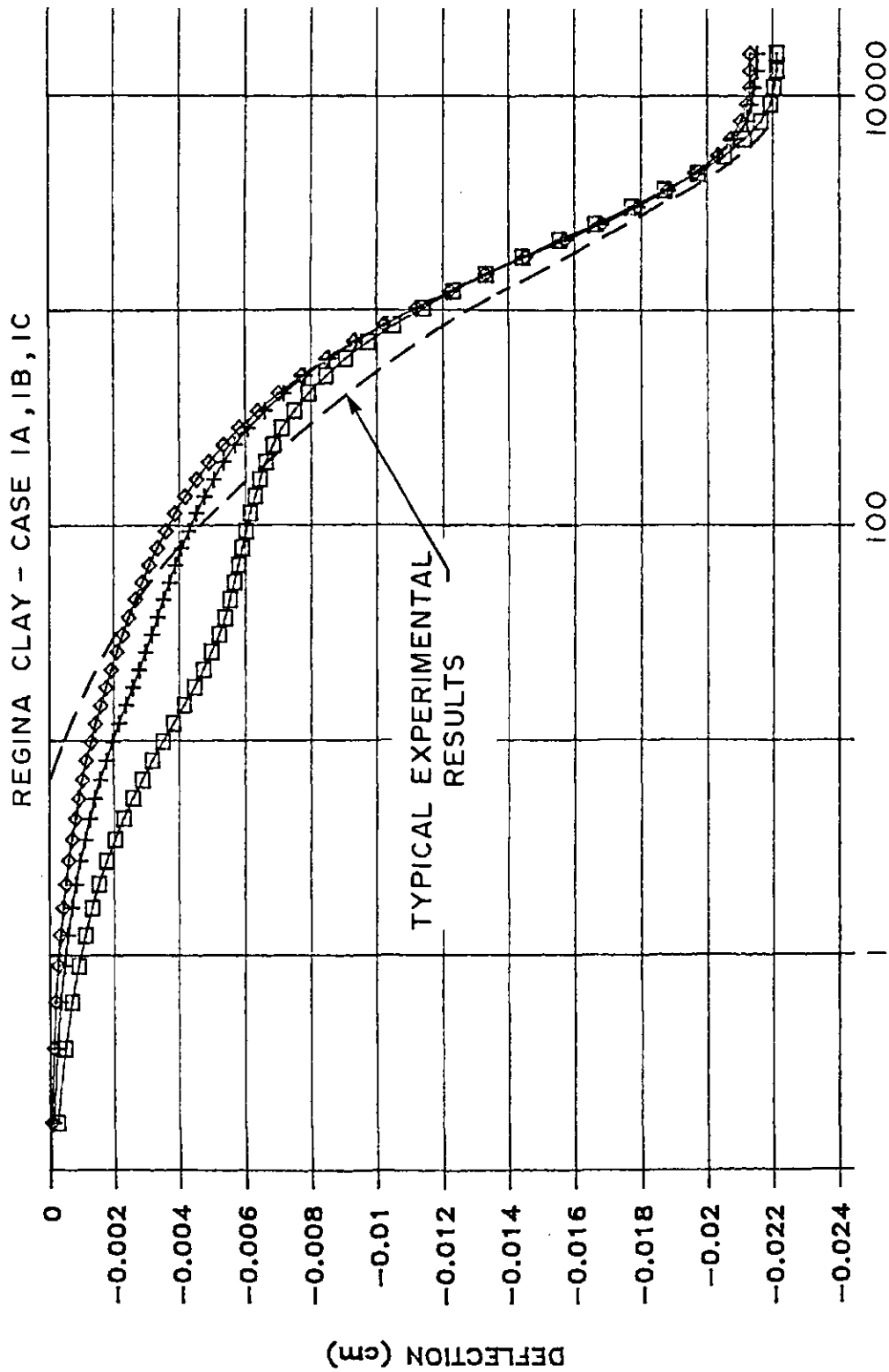

Figure 7.18 Simulated Deflections of Regina Clay - Case 1a, 1b, 1c

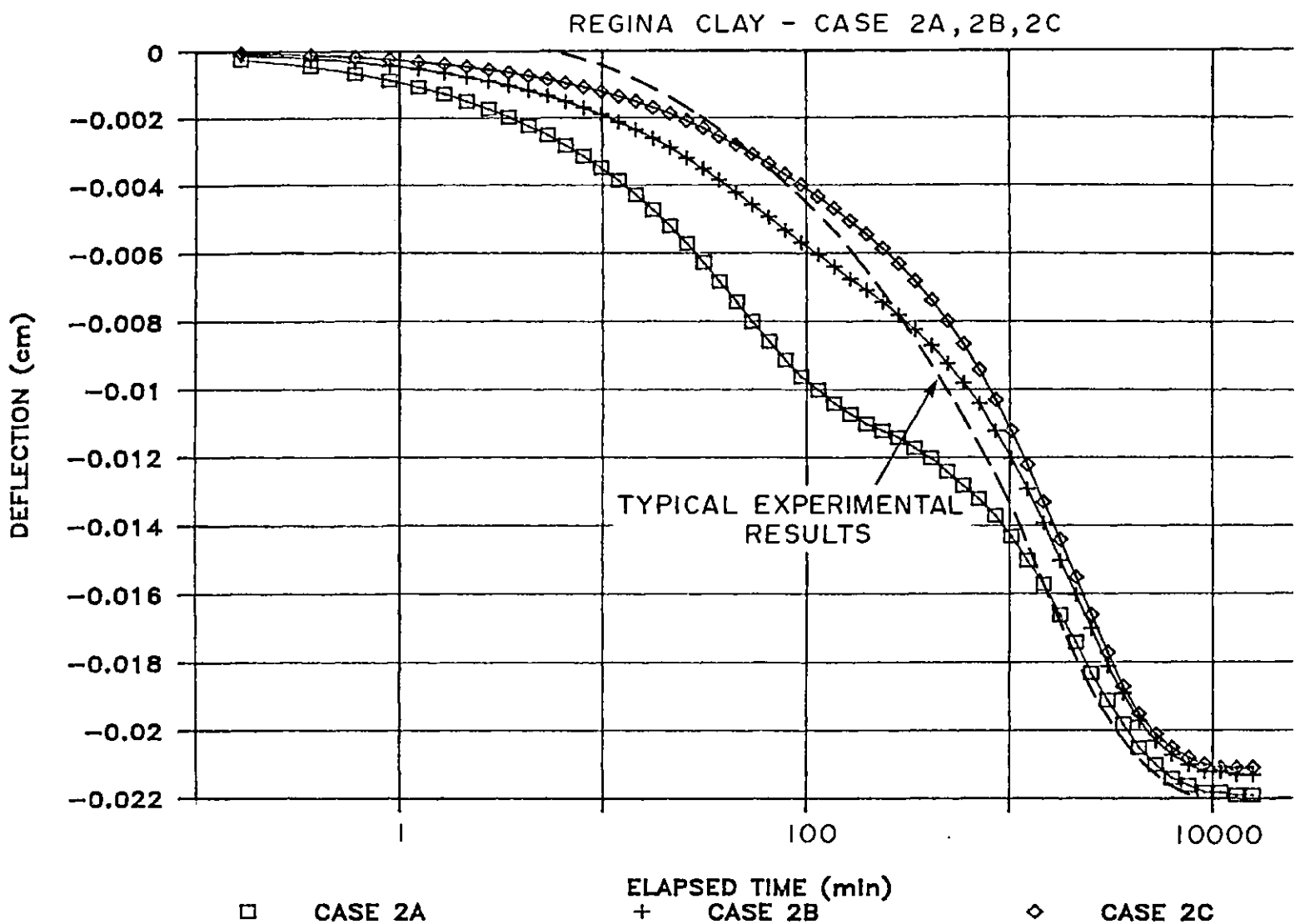

Figure 7.19 Simulation Deflections of Regina Clay - Case 2a, 2b, 2c

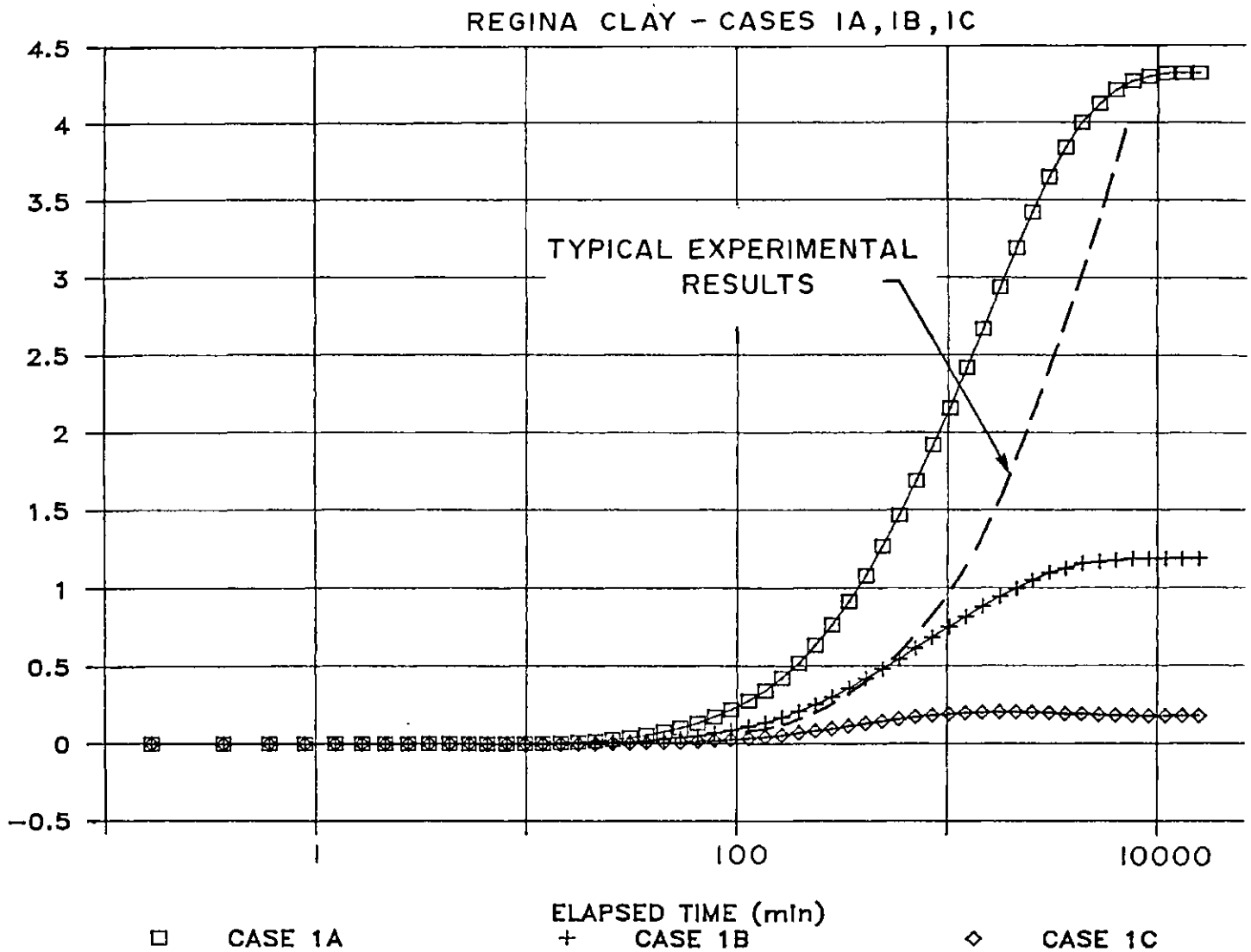

Figure 7.20 Simulated Base Flows For Regina Clay - Cases 1a, 1b, 1c

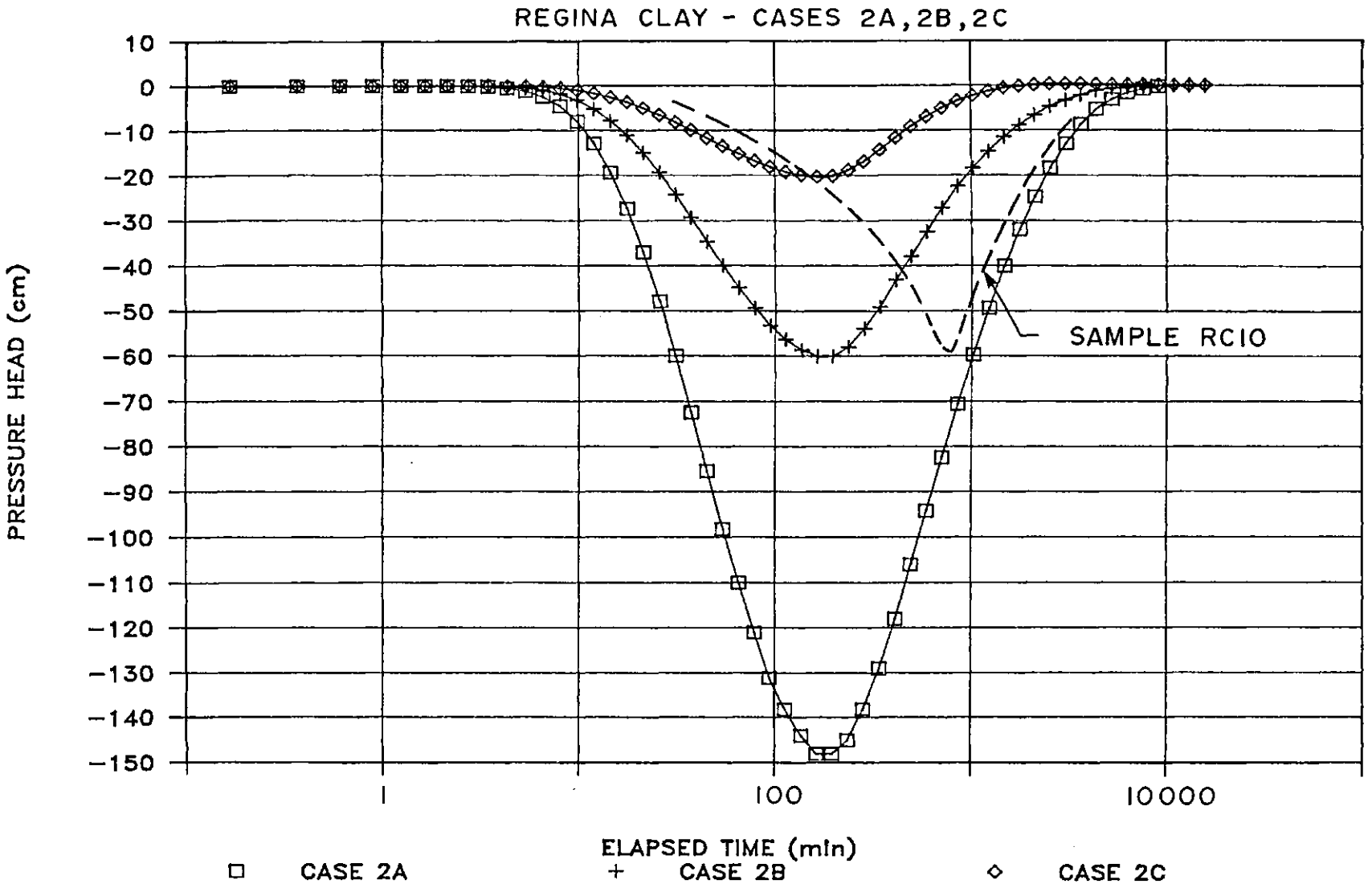

Figure 7.21 Simulated Base Pressure Response for Regina Clay - Cases 2a, 2b, 2c

7.5.4 Sand / bentonite Mixture

The simulated deflection versus time curves are presented in Figures 7.22 and 7.23. All of the curves are in good agreement with the observed range of deflections. The rapid rate of osmotic volume change would seem to indicate that the dominant volume change process was osmotically induced consolidation. The time to 100% consolidation coincides with a time factor of approximately 1 for the sample. The rapid consolidation of the sand bentonite sample, however, occurs as a result of the strong non-linearity of the osmotic compressibility with concentration, and not as a result of negative fluid pressures within the sample.

Figures 7.24 and 7.25 illustrate the base flow responses and base pressure responses for the simulations. The observed base flows are in good agreement with the lower efficiencies of case B and C. These lower efficiencies permit significant flows out of the sample to occur due to expulsion of pore fluid.

The reversal of flow that was observed in Sample SB2 was not apparent in the simulations because of the complete equalization of concentrations that occurs in the simulation. This equalization does not occur so readily in the laboratory samples because of the small reservoir of water that exists below the sample.

The general shape of the simulated base pore pressure responses are in agreement with the observed response for sample SB6. The observed response seems to somewhat smoothed relative to the simulated responses. This again may be a result of time lag in the pressure transducer readings.

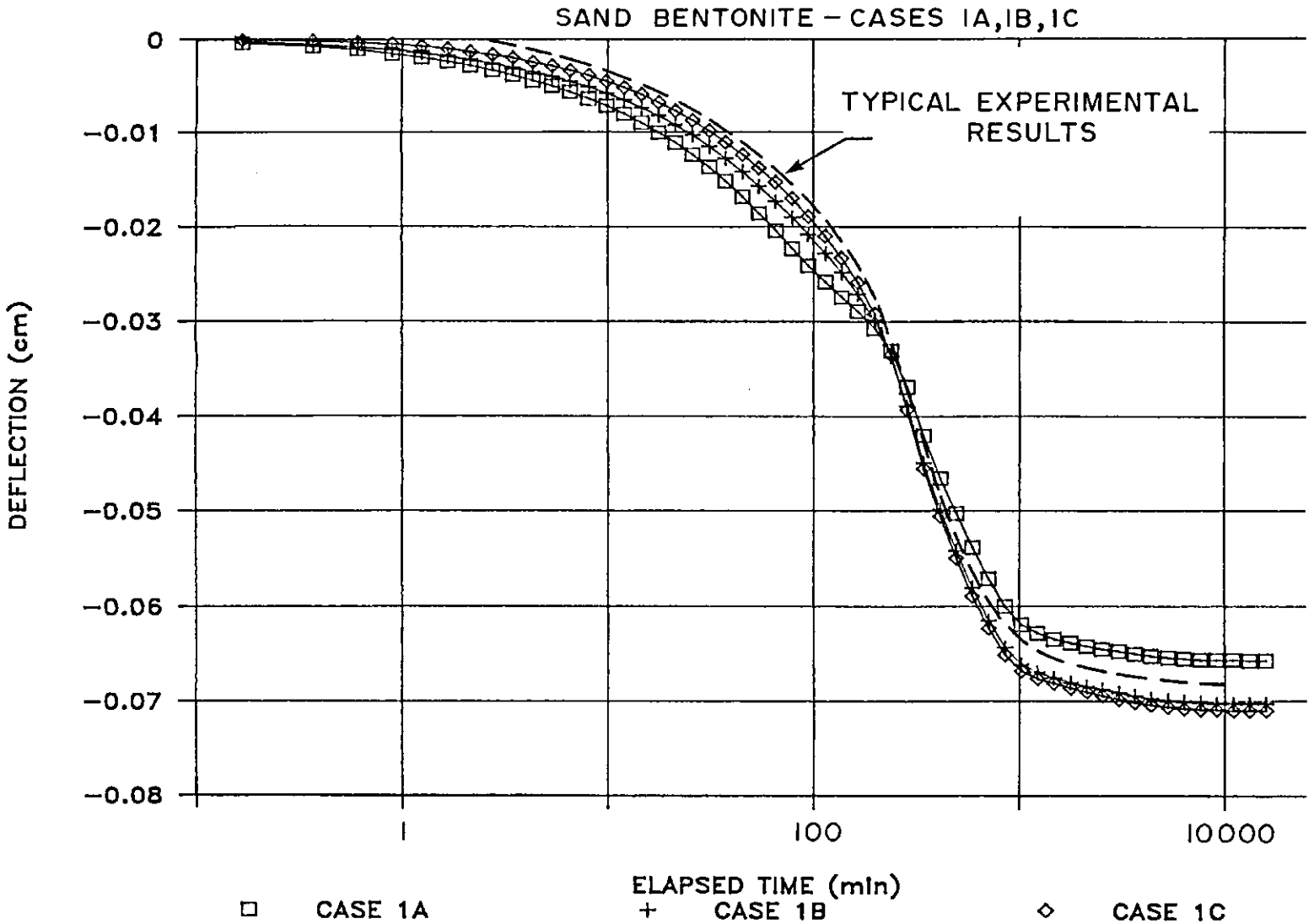

Figure 7.22 Simulated Deflection of Sand/bentonite – Cases 1a, 1b, 1c

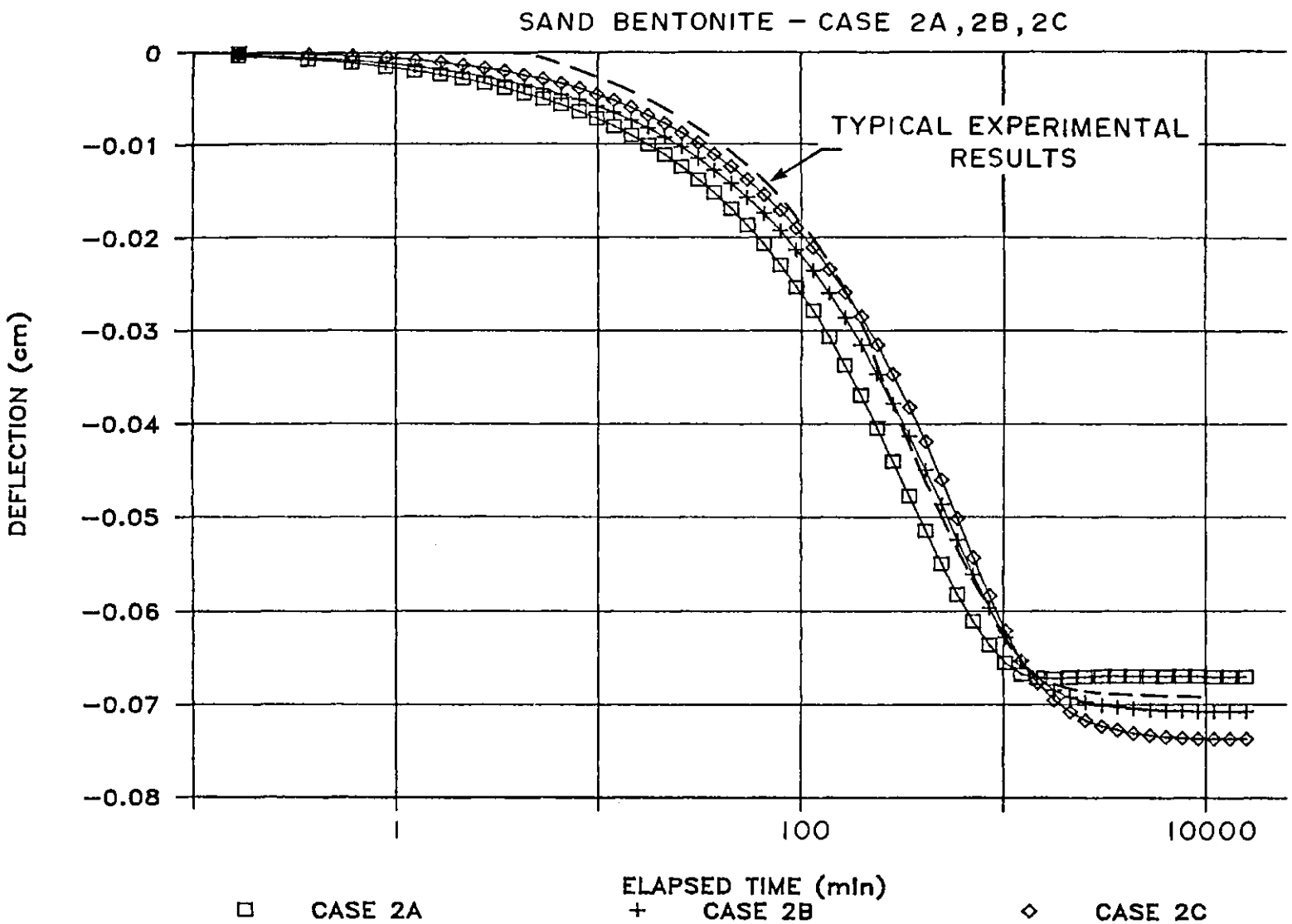

Figure 7.23 Simulated Deflection of Sand/bentonite – Cases 2a, 2b, 2c

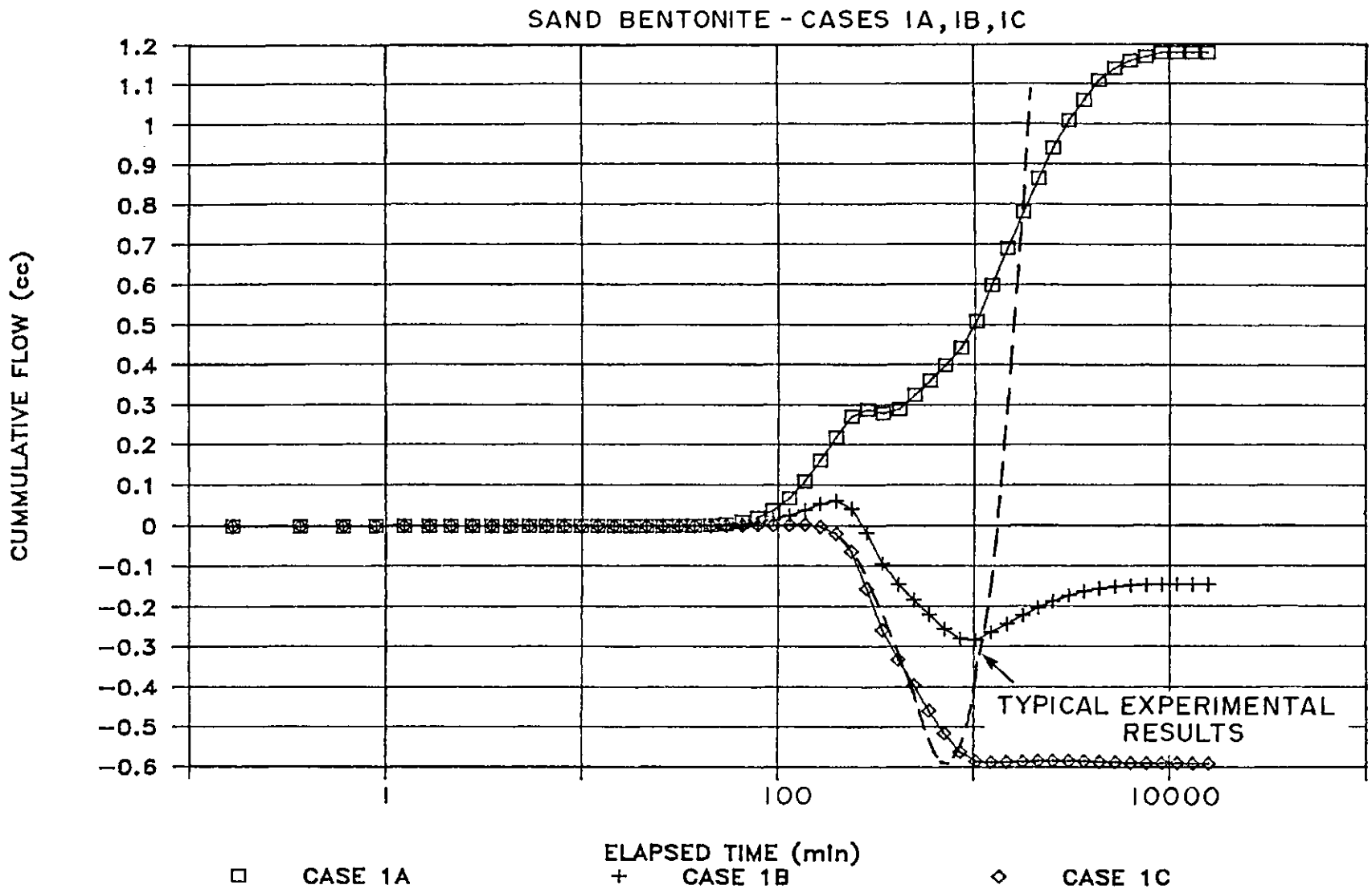

Figure 7.24 Simulated Base Flows for Sand/bentonite - Cases 1a, 1b, 1c

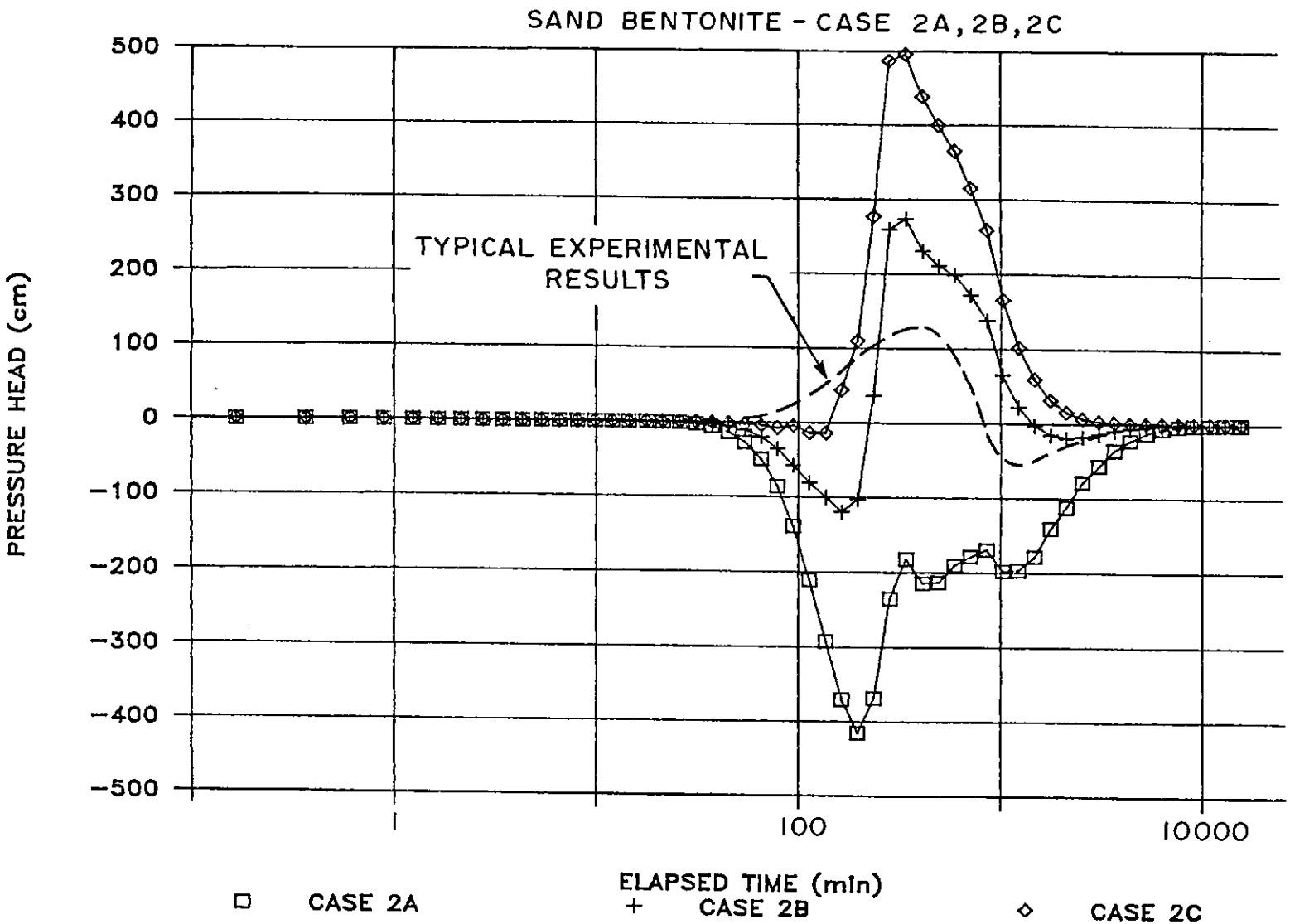

Figure 7.25 Simulated Base Pressure Response for Sand/bentonite - Cases 2a, 2b, 2c

7.5.5 Summary

The simulations support the conclusion that the controlling mechanism for osmotic volume change is osmotic consolidation. The simulations also illustrate that the rate at which osmotic consolidation takes place may be altered as a result of osmotic flows.

Good agreement was obtained between the simulated and observed osmotic time deflection curves. Due to the low osmotic efficiencies of the samples, the development of base flow and pressure are secondary responses relative to that of deflection. Consequently, obtaining a good match of the simulated and observed flow and pressure responses would not be expected. In spite of this, fairly good agreement was obtained between the simulated and the observed base flow rates. The comparison of the simulated and measured base pressures would seem to indicate that significant time lag existed in the pressure measurement system. Only the general shape of the pressure responses can be compared.

7.6 Osmotic Pressure versus (R-A) as a Stress State Variable

The final objective of the data analyses was to establish the validity of using the osmotic pressure of the bulk solution as a true representation of the stress state within the double diffuse layer. In Chapter 3 two stress state variables were selected to describe the volume change behavior of a soil in which physio-chemical effects are significant. These components were effective stress $(\sigma - u_f)$, and the net electrostatic repulsive minus attractive stress (R-A).

The value of the electrostatic repulsive stress can only be predicted accurately for idealized soil systems, using double diffuse layer theory. No known techniques exist for direct measurement of this stress. Because of these limitations, changes in the osmotic pressure of the bulk solution were selected to represent the effect of changes in the value of (R-A).

In this section the choice of osmotic pressure as a stress state variable is evaluated. The changes in "true" effective stress that must take place during osmotic consolidation are also described. A technique is proposed to evaluate the (R-A) component of the "true" effective stress.

7.6.1 Consolidation Stress Paths

In the selection of osmotic pressure as a stress state variable it was not assumed that changes in the bulk osmotic pressure would be equally effective as changes in the net repulsive stress, (R-A), in promoting volume change. It was accepted that the difference in the effectiveness of osmotic pressure changes and changes in the value of (R-A) would have to be accommodated in the evaluation of the modulus m_{π}.

A principal difficulty that arises with the use of osmotic pressure lies in the description of the theoretical, monotonic stress path followed during laboratory testing. Figure 7.26a presents a schematic representation of the three dimensional constitutive surface described in Chapter 3. The stress path followed during testing is illustrated. If a continuous constitutive surface exists, then the projection of this stress path along the effective stress axis should appear as illustrated in Figure 7.26b. The actual observed behavior illustrated on Figure 7.26b is significantly different.

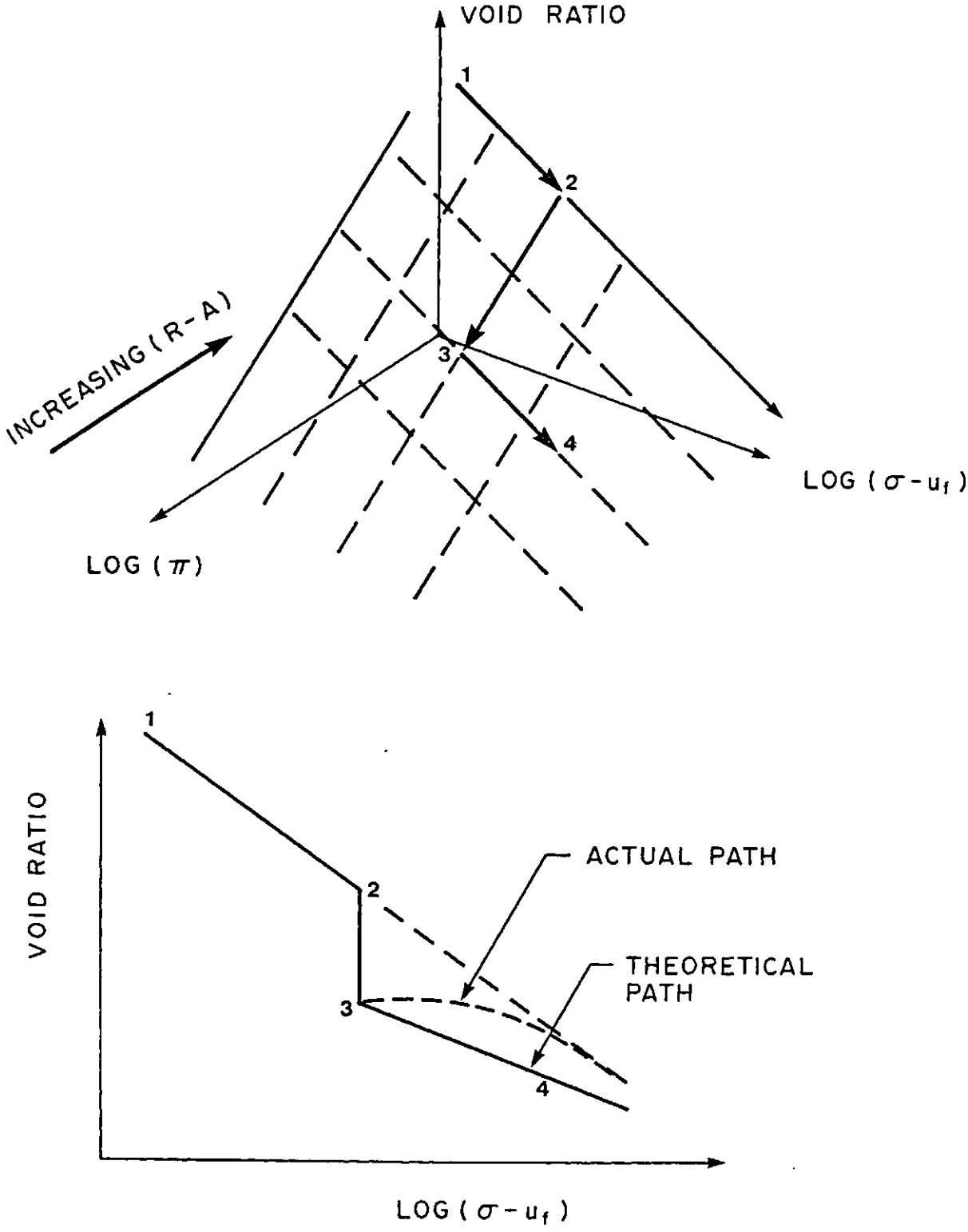

Figure 7.26 Stress Paths during Effective Stress and Osmotic Consolidation a) Three Dimensional Constitutive Surface b) Projection onto Effective Stress Axis

Reloading of the sample after osmotic consolidation should result in continuing deformation of the sample. In the test results the sample behaved as if it had been preconsolidated to somewhat higher pressures. A flat surface back towards the virgin branch develops, which becomes asymptotic to the virgin branch with increasing stress. This stress path can only be shown to be consistent with that described by the theoretical surface if osmotic pressure of the bulk fluid is decreasing during reloading.

This behavior could be rationalized, if (R-A) was considered to be the stress state variable. Following osmotic consolidation further loading would tend to produce small decreases in void ratio, which in turn would result in increases in (R-A). This is consistent with the stress path illustrated in Figure 7.26a.

The requirement that the osmotic pressure must also be decreasing during reloading could be rationalized, if the definition of the stress state variable was taken to be the difference in osmotic pressure between the bulk solution and that existing between the clay particles. Further loading after the completion of osmotic consolidation would result in a reduction of the interparticle spacing. Although the concentration of the bulk solution was unchanged, the concentration of the interparticle solution would be altered. Even if this rationalization is valid, it still leaves unanswered the question of how the physio-chemical stress state variable can be measured.

7.6.2 Indirect Evaluation of (R-A)

In section 7.3 the curves of void ratio versus applied stress for the sand/bentonite samples were viewed in terms of a single "true" effective stress. The discussion in section 7.6.1 raises the question of how an evaluation of the true physio-chemical stress state variable might be

obtained. In this section, a technique is proposed to evaluate the magnitude of (R-A) indirectly.

The changes in void ratio that occur during changes in effective stress or osmotic loading are described by a three dimensional constitutive surface. The changes in the stress state variable along one axis can be viewed in terms of equivalent changes in stress viewed along the other axis. These equivalent stresses can be obtained by projecting the three dimensional stress path onto the axis of a single stress state variable. A technique similar to this was used by Fredlund et al (1980) to predict heave in unsaturated soils. For unsaturated soils, stress state variables of total stress minus pore air pressure, $(\sigma-u_a)$, and matric suction, (u_a-u_w), are used. The insitu, equivalent matric suction for a soil can be obtained by projecting the stress path followed during a constant volume swelling test, onto the plane of void ratio versus $(\sigma-u_a)$.

The virgin curves for the Regina Clay and sand/bentonite samples are represented by the curves of void ratio versus applied stress for samples RCDD and SBDD. The volumetric strain due to osmotic consolidation from samples RC4, RC5, and RC6, and SB2, SBOC1, and SBOC3 are superimposed on these curves. A second curve can then be drawn through the series of void ratios which represent the end of osmotic consolidation. This construction is illustrated in Figures 7.27 and 7.28.

The lower curve in Figures 7.27 and 7.28 represents the virgin branch of the clays with the (R-A) component of stress removed. At any void ratio, the difference in stress between the two curves can be taken as a measure of the equivalent value of (R-A) at that void ratio. Figure 7.29 illustrates how the value of (R-A), obtained in this manner, varies with vertical effective stress.

Theoretical calculations for the electrostatic repulsive stress within the samples were also made using the

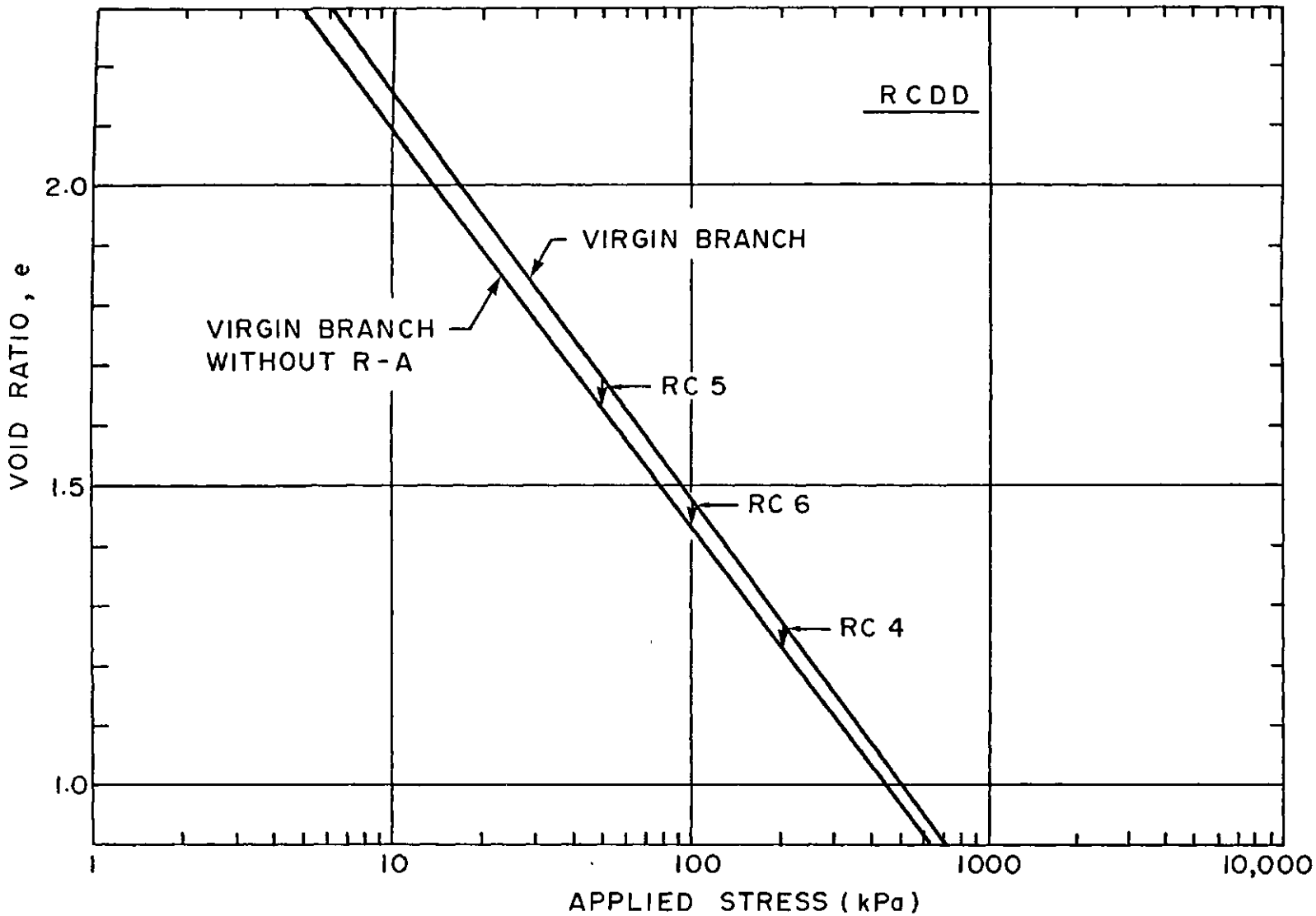

Figure 7.27 Indirect Evaluation of (R-A) from the Virgin Curve of reslurried Regina Clay

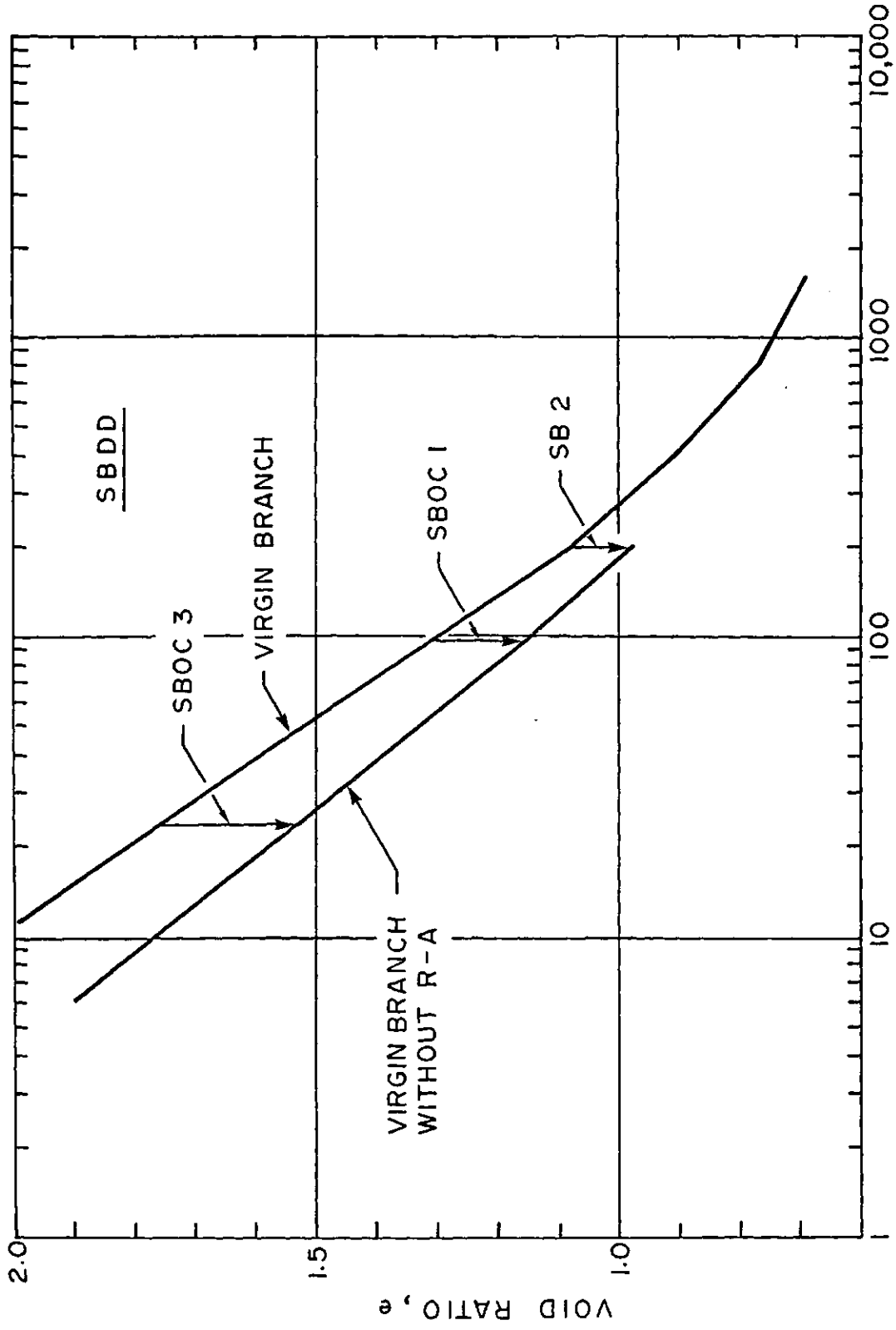

Figure 7.28 Indirect Evaluation of (R-A) from the Virgin Curve of the Sand/bentonite Mixture

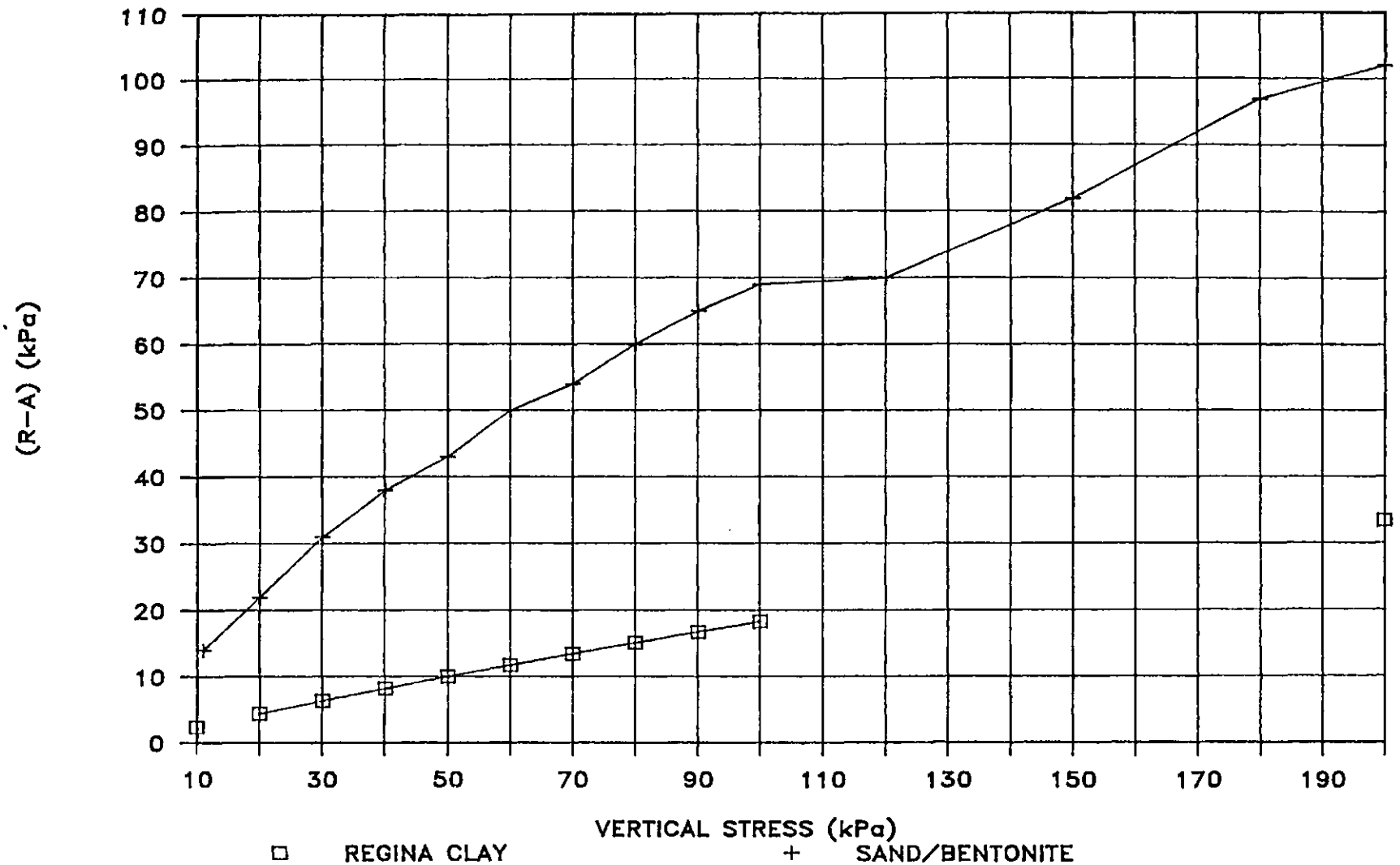

Figure 7.29 R-A versus Vertical Stress for Regina Clay and Sand/bentonite Mixture

osmotic pressure concept. The calculation method follows that described by Balasubramonian (1972). An example calculation is presented in Appendix A. For the Regina Clay samples, the theoretical electrostatic repulsive stresses were extremely small even with the assumption of a fully dispersed structure. For the sand/bentonite samples, however, the calculated values of (R-A) agreed closely with the theoretical values of the electrostatic repulsive stress. The specific surface of bentonite is assumed to be approximately 580 m^2/gm. A graphical comparison of the calculated and theoretical values is illustrated in Figure 7.30.

The variation of net repulsive stress with concentration of the pore fluid was also calculated and is presented in Figure 7.31. The agreement between the theoretical electrostatic repulsive stress and the calculated values of (R-A) is poor.

Figures 7.32 and 7.33 illustrate the ratio of the magnitude of (R-A) to the vertical effective stress for the Regina Clay and sand/bentonite samples. For the case of Regina Clay, (R-A) never exceeds a value of 30% of the vertical stress. For the sand /bentonite samples, (R-A) varies from a value of 50 % of the vertical stress at 200 kPa, to over 130% of the vertical stress at a stress level of 10 kPa.

Fracturing of the sample may occur if the confining stress on the sample goes into tension. The horizontal confining stresses can be obtained from an estimate of Ko, which is the ratio of the horizontal to the vertical effective stress. For normally consolidated soils K_o is equal to $(1-\sin \phi')$. If a friction angle of 30° is assumed for these clays, the value of Ko would be 0.5. For the sand bentonite samples, osmotic consolidation would result in a reduction in the horizontal stresses greater than the horizontal confining stress calculated using Ko.

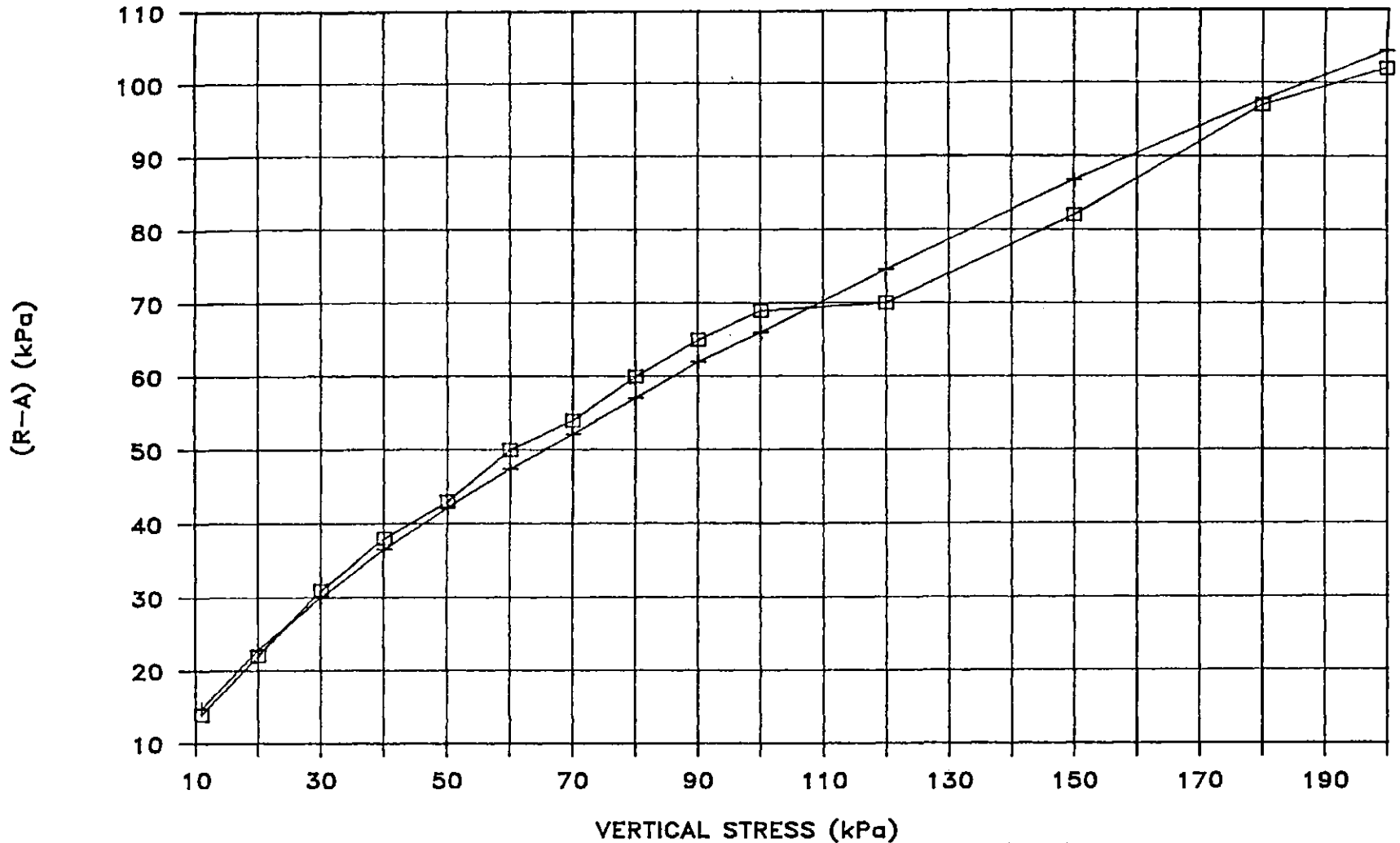

Figure 7.30 Comparison of Experimental Evaluations of (R-A) and Theoretical Electrostatic Repulsive Stress for Sand/bentonite

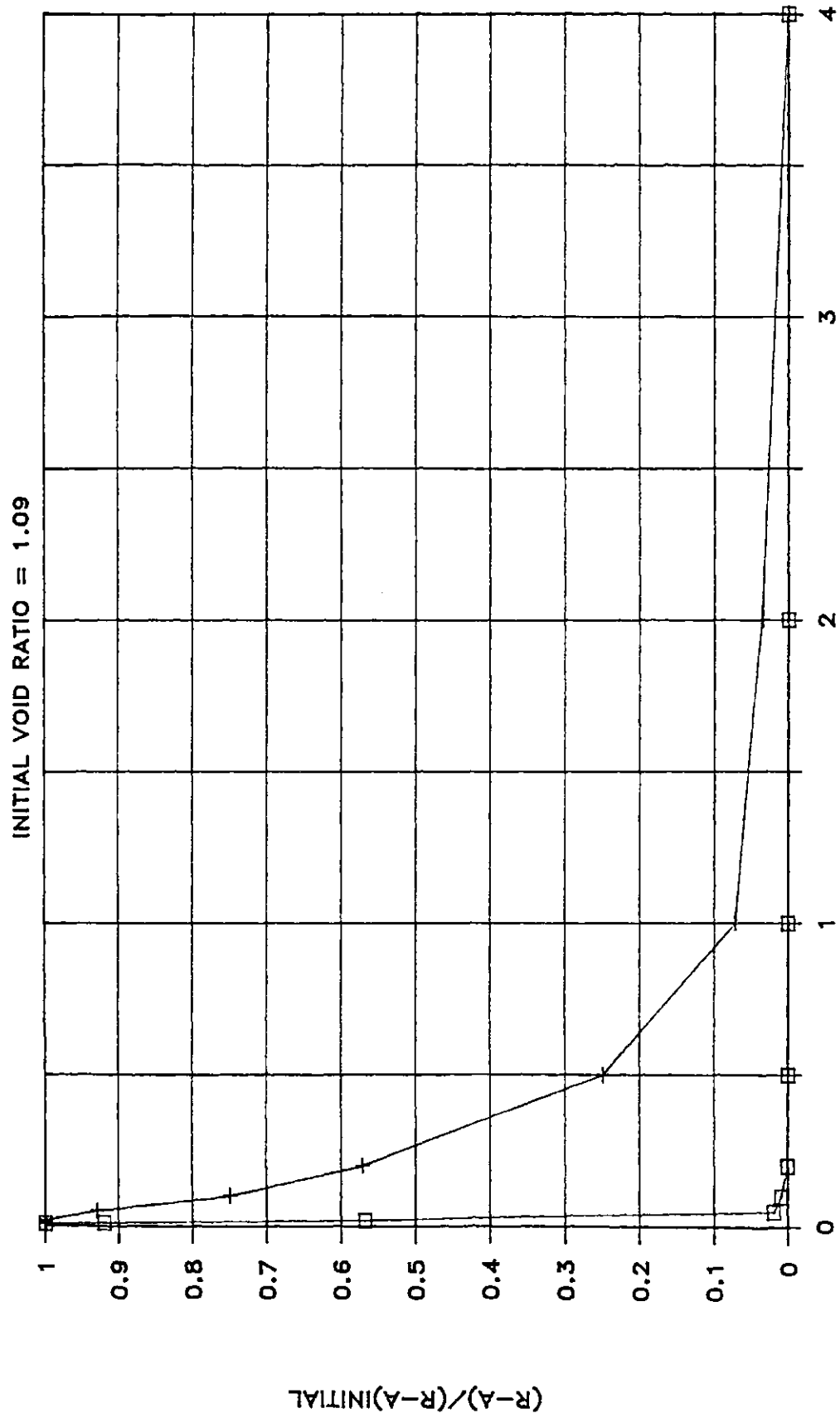

Figure 7.31 Theoretical Electrostatic Repulsive Stress and Experimental Values of R-A versus Concentration for Sand/bentonite

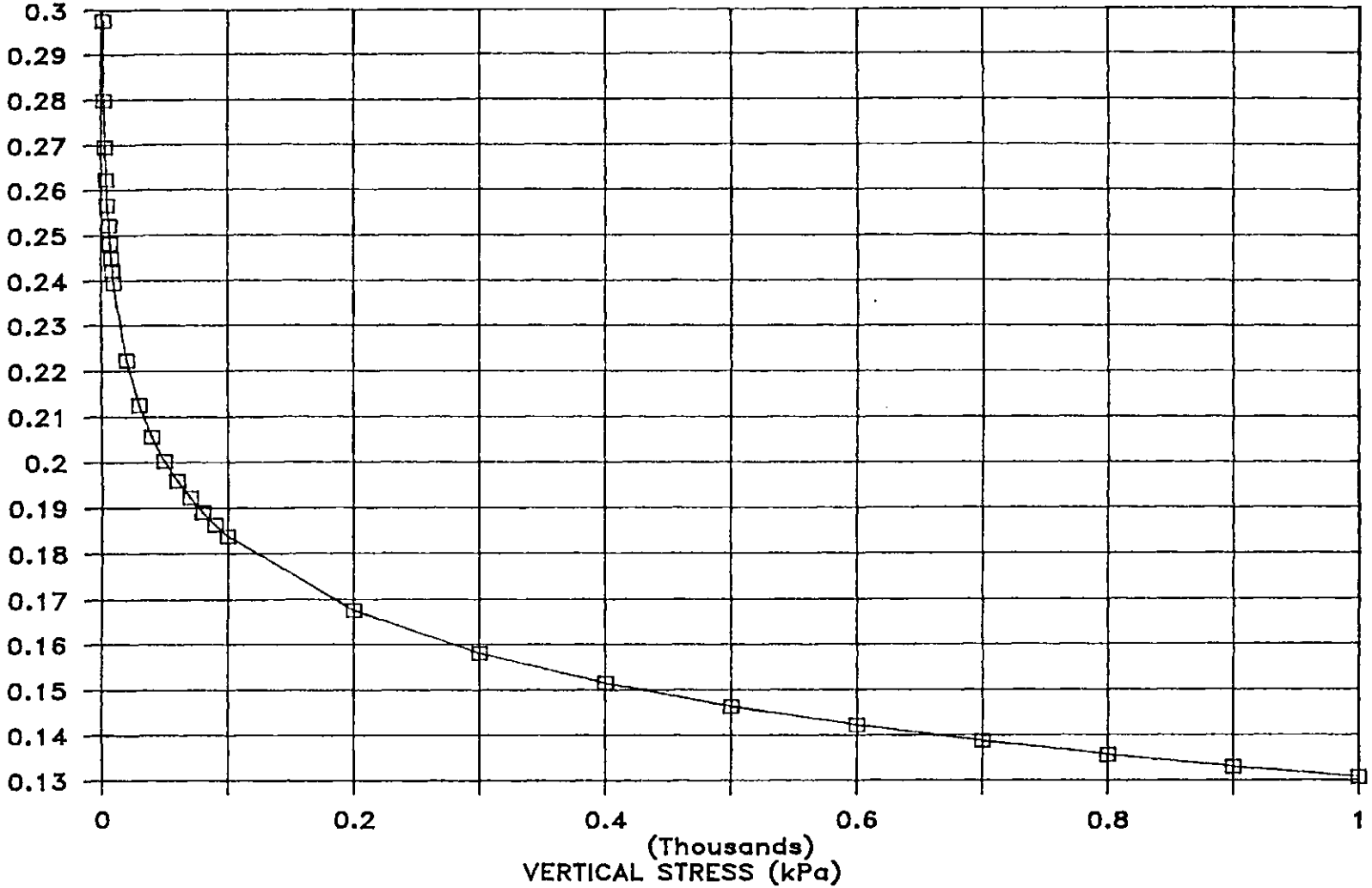

Figure 7.32 R-A as a Percentage of Vertical Stress - Regina Clay

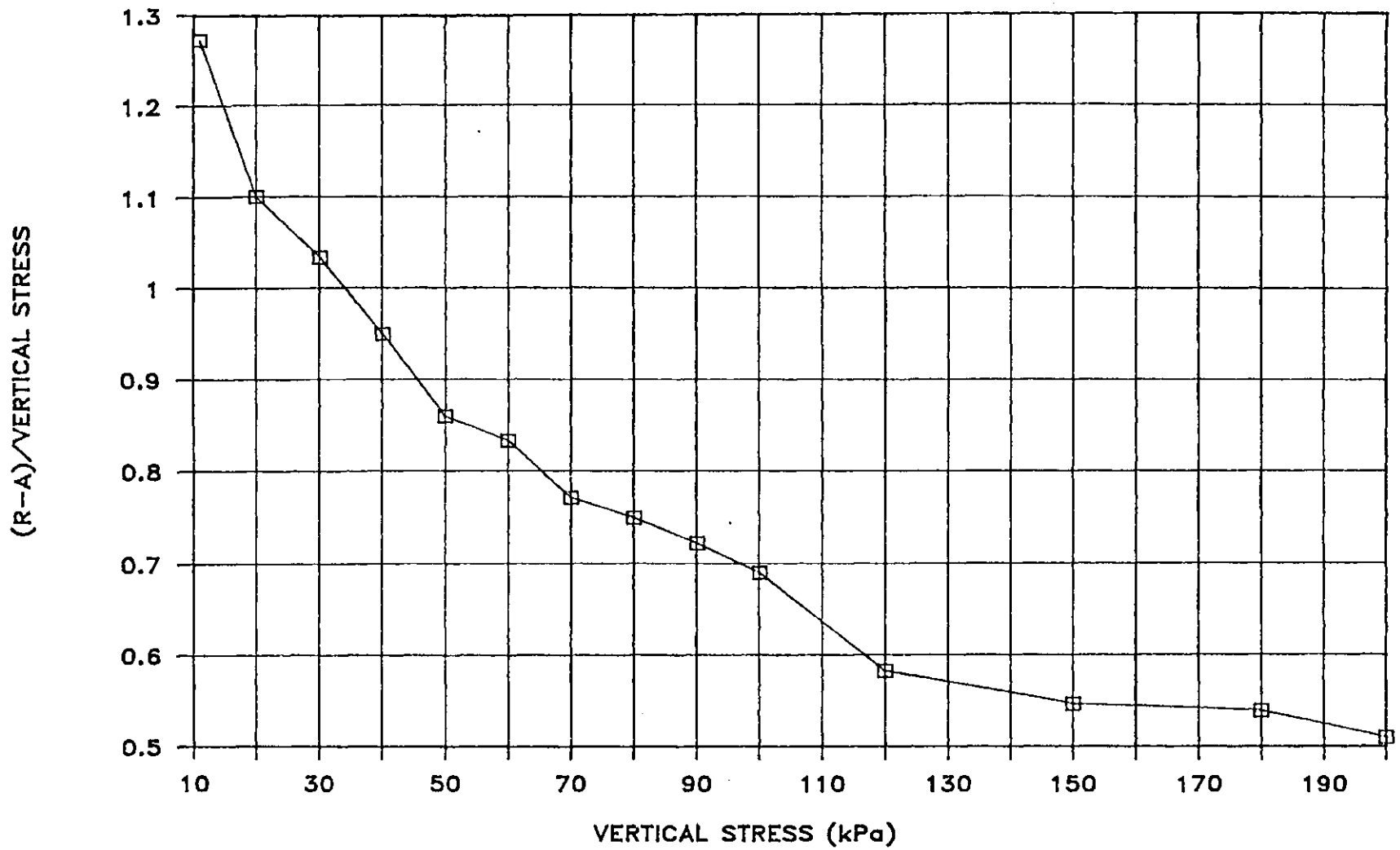

Figure 7.33 R-A as a Percentage of Vertical Stress - Sand/bentonite

Using this criterion, fracturing of the sand/bentonite should occur at all stress levels tested. For the Regina Clay fracturing might only occur at extremely low vertical stresses.

Permeability testing before and after osmotic consolidation indicated that no significant change in the permeability of the Regina Clay samples occurred. However the permeability of the sand/bentonite sample changed by almost one order of magnitude. It is not known, however, whether this permeability increase was indeed as a result of fracturing.

Ho (1985) measured the permeability of unconfined samples of Regina Clay exposed to various concentrations of NaCl solutions. Significant increases in permeability occurred in samples exposed to 4.0 M NaCl solution. Ho attributed the increases in permeability to shrinking of the sample away from the sides of the rigid wall permeameter.

The potential for these clays to undergo fracturing at low confining stresses is also consistent with the few existing case histories. Failure of sand/bentonite and compacted clay liners have occurred. These liners exist under fairly low confining stresses, consequently changes in (R-A) may lead to fracture formation. Deeper, natural clay deposits do not seem to undergo the increases in permeability that accompany osmotic consolidation in the surficial liners. Increasing confining stresses with depth seem to ensure that the development of tensile stresses due to osmotic consolidation never occur.

The above discussion is somewhat speculative. The results do suggest, however, that an indirect evaluation of the "equivalent" effective stress changes that occur within a sample during osmotic consolidation might be possible. The prediction of sample fracturing based on measured changes in (R-A), using this technique, still remains to be investigated.

CHAPTER 8

CONCLUSIONS AND RECOMMENDATIONS

8.1 Study Methodology and Objectives

The objectives of this research program were outlined in Chapter 1 as follows:

1. To observe the volume change behavior of clay soils on exposure to strong electrolyte solution.
2. To identify the dominant mechanisms of osmotic volume change.
3. To develop a theoretical model to describe transient osmotic volume change, based on a phenomenological approach.
4. To evaluate the potential use of the theoretical model to predict the rate and magnitude of volume change in clay soils on exposure to to NaCl brines.

These objectives were met through a program of literature review, theoretical formulation, numerical simulation and laboratory testing.

A review of the existing literature on osmotic flow and volume change was presented in Chapter 2. Based on the results of this review, a theoretical formulation for the general problem of transient osmotic volume change was developed in Chapter 3. The solution of the governing equations describing osmotic volume change and flow was obtained through the use of a numerical model. Example simulations, described in Chapter 4, were used to delineate the behavior of clay during osmotic flow and volume change. The laboratory testing program, described in Chapter 5, was used to observe the response of clay samples exposed to NaCl solutions. The results of the laboratory study were outlined in Chapter 6. In Chapter 7 the test results were

analyzed and discussed in light of the theoretical framework laid out in the previous chapters.

The principal conclusions that can be drawn from this study are outlined in section 8.2. Recommendations for further study are enumerated in section 8.3

8.2 Study Conclusions

The behavior of a soil undergoing effective stress consolidation was described in Chapter 3 as being the synthesis of the two soil properties; permeability and compressibility. Similarly, osmotic volume change phenomena in clay soils occur as a result of the influence that pore fluid concentrations have on fluid flow and volume change. The following conclusions focus on these influences:

1) Osmotic volume change of clay soils may take place as a result of one of the following mechanisms:
   (i) Osmotically Induced Consolidation
   (ii) Osmotic Consolidation.

   Both of these processes may be active to varying degrees within a particular soil/solution system.
2) Osmotically induced consolidation occurs as a result the rapid flow of water out of the sample in response to osmotic gradients. It is characterized by the development of large negative pressures within the sample. The consolidation process is complete at a time factor of 2.0. Volume change takes place as a result of increases in the effective stress within the sample. The sample must be fairly compressible, and also exhibit significant osmotic efficiency.

3) Osmotic Consolidation occurs as a result of a reduction in the net electrostatic repulsive forces, (R-A), between clay particles. The rate of consolidation is controlled by the rate of migration of the dissolved salt into the samples. In the absence of hydraulic flows this rate is controlled by the diffusion of salt into the sample. Under these conditions the time to 100% consolidation occurs at a diffusion time factor, T_d , equal to 1, where $T_d = D(t)/H^2$. Osmotic volume change can be calculated if the osmotic compressibility, and the change in osmotic pressure within the soil are known.

4) The magnitude of osmotic or osmotically induced consolidation is characterized by the soil properties; m_π , osmotic compressibility; K_π , osmotic permeability; and D, the coefficient of diffusion. The ratio of K_π/K_h is called the osmotic efficiency, and is a measure of the semi-permeable nature of the clay.

5) The dominant mechanism of osmotic volume change in reslurried samples of Regina Clay and a 80%:20% sand/bentonite mixture was osmotic consolidation. Under the influence of 4 M NaCl solution, the osmotic volume change for samples of Regina Clay and sand/bentonite were approximately 2% and 7% respectively.

7) The osmotic efficiencies of the soils tested were a function of the pore fluid concentration. For the sand/bentonite samples, the osmotic efficiencies ranged from 0.5 at the initial pore fluid concentrations of .008 M, to 0.001 at concentrations of 4.0 M. The osmotic efficiencies of the Regina Clay samples ranged from 0.05 at concentrations of 0.05 M to 0.0001 at concentrations of 4.0 M.

8) The osmotic compressibility of Regina Clay appears to be independent of applied stress level and pore-fluid concentrations. The osmotic compressibility for Regina Clay was approximately 1 x 10^{-6}/kPa. This is approximately 0.2% of the effective stress compressibility of Regina Clay at an applied stress of 200 kPa. The osmotic compressibility of the sand/bentonite was strongly dependent on pore fluid concentrations. The osmotic compressibility of the sand/bentonite varied from 100% of the effective stress compressibility at low concentrations, to approximately .5% of the effective stress compressibility at high pore fluid concentrations.

9) The coefficient of diffusion for the Regina Clay and sand/bentonite samples, obtained by direct measurement, was approximately 4.0 x 10^{-6} cm^2/s. Back-calculation of the coefficient of diffusion using the diffusion time factor and the time to 50% osmotic consolidation gave similar values for Regina Clay.

10) Numerical simulations of the osmotic volume change, base flow, or base pressure response of both the Regina Clay and sand/bentonite samples were in agreement with monitored sample behavior. It would appear that the osmotic flow and volume change behavior of clay soils can be predicted using the theoretical/numerical solutions presented in this study.

11) The use of the osmotic pressure of the bulk fluid as a stress state variable was shown to be adequate only in predicting volume changes during increases in pore fluid concentration. If increases in applied stress occur following the completion of osmotic consolidation, the use of the net electrostatic interparticle force (R-A) is more appropriate.

12) An indirect evaluation of (R-A) can be obtained using a series of one-dimensional osmotic consolidation tests. Fairly good agreement occurs between the value of the electrostatic repulsive stress obtained by the osmotic pressure concept, and the value of (R-A) obtained from experimental data, for the sand/bentonite samples. The presence of packets of clay particles in the Regina Clay samples prevented an adequate prediction of the magnitude of the electrostatic repulsive stress to made using the osmotic pressure concept.

13) The magnitude of the changes in (R-A) for sand/bentonite indicated that fracturing might have occurred during testing. The magnitude of (R-A) for the Regina Clay indicated that fracturing would only occur if the sample was not confined. The permeability tests carried out following osmotic volume change of the samples, confirmed that significant increases in the permeability of the sand/bentonite had occurred. No increase occurred in the permeability of Regina Clay following osmotic consolidation.

8.3 Recommendations for Further Study

The primary objective of this thesis has been the general characterization of osmotic volume change and flow through clay soils. Further studies will be required to corroborate the observations and conclusions presented in this thesis. In addition, some of the observations made in this study lead naturally to other areas of study that should be pursued. A number of suggestions for further study are as follows:

1) The dominant mechanism for volume change was determined to be osmotic consolidation. Osmotic flow, however, may influence the rate and magnitude at which osmotic consolidation occurs. It is recommended consequently that the existing test apparatus be upgraded so that steady state osmotic permeability testing of samples can be undertaken. This testing would allow a more accurate evaluation of osmotic permeability and efficiency to be obtained. The variations of efficiency with confining stress and pore fluid chemistry are of primary interest in this regard.

2) The potential for indirect evaluation of the magnitude of (R-A) should be studied further. If the magnitude of (R-A) can be evaluated, it is the preferred stress state variable to represent the influence of stresses arising from physio-chemical effects. The use of osmotic pressure is limited in that it does not describe a continuous constitutive surface during osmotic and applied stress loading. In addition, the osmotic pressure does not account for the effects of changing pore fluid chemistry, only for the effect of changing concentrations of a particular pore fluid composition.

3) The feasibility of predicting the onset of fracturing, based on an understanding of the

magnitude of (R-A) as a function of confining stress, should be investigated. A suggested test program would be to use the indirect evaluation technique described in this thesis to establish the changes in (R-A) that occur within a sample at different stress levels. The onset of fracturing during osmotic consolidation could be established by monitoring the changes in permeability that occur within the sample. A confirmation of the presence of fractures could be obtained using tracer displacement techniques or by dye injection.

4) The focus of the present study was on the magnitude of volume change and osmotic flow. Future studies should begin to focus on how the rate of migration of the dissolved salts is influenced by these processes. A technique for monitoring pore fluid concentration changes across the sample during osmotic consolidation should be developed.

5) The conclusions drawn from the laboratory studies need to evaluated against field conditions or at least a prototype of field conditions. A case history or laboratory prototype of a liner should be studied in order to evaluate the application of the results of this study to insitu conditions.

This thesis began with a description of the present dilemma being faced by geotechnical engineers, in the design of waste containment facilities for the storage of strong electrolyte solutions. Advances in engineering design can only take place when mechanism is properly understood. Design methods based on empiricism and model testing are far too restrictive and will not allow the engineer to meet the challenges being faced in the design of containment systems. This thesis provides some insight into the mechanisms by which osmotic volume change and flow through clay soils takes place.

REFERENCES

Abd-el-Aziz, M.H., and S.A. Taylor. 1965. Simultaneous flow of water and salt through unsaturated porous media: I. Rate equations. Soil Sci. Soc. Amer. Proc., 29, pp. 141-143.

Aylmore, L.A.G. and J.P. Quirk. 1962. The structural status of clay systems. Clays and Clay Minerology, 9, pp. 104-130.

Anderson, D.C. 1982. Does landfill leachate make clay liners more permeable?. ASCE Civil Engineering, 52(9),pp. 66-69.

Anderson, D.C. and S.G. Jones. 1983. Clay barrier-leachate interaction. Barriers, K.W. Brown and Associates, Inc., College Station, Texas, pp. 154-160.

Anderson, D.C., Brown, K.W. and J. Green. 1984. Effect of organic fluids on the permeability of clay soil liners, Proc. ,Denver, Colorado, 11 p.

Appelt,H., Holtzclaw, K. and Pratt, P.F. 1975. Effect of ion exclusion on the movement of chloride through soils. Soil Sci. Soc. Amer. Proc., 39, pp. 264-267.

Bailey, W.A. 1965. The effect of salt content on the consolidation behavior of saturated remoulded clays. USAE Waterways Experimental Station, Vicksburg, Contract Rpt 3-101, 162 p.

Balasubramonian, B.I. 1972. Swelling of Compaction Shale. Ph.D. Dissertation, Department of Civil Engineering, University of Alberta, Edmonton, 236 p.

Balasubramonian, B.I. and N. Morgenstern. 1980. Effects of pore fluid on the swelling of clay-shale. Proc. 4th Int. Conf. on Expansive Soils, Denver, pp. 190-205.

Barbour, 1981. A Review of the Contaminant Transport Phenomenon and Its Application to Geotechnical Engineering. M.Sc. Thesis, Department of Civil Engineering, University of Saskatchewan, Saskatoon,.

Bear, J. 1972. Dynamics of Fluids in Porous Media. American Elsevier, New York.

Berkeley, Earl of and E.G.J. Hartley, 1909. Dynamic osmotic pressures, Proc. Roy. Soc.(B), pp. 271-275.

Berry, F.A.F. 1959. Hydrodynamics and geochemistry of the Jurassic and Cretaceous systems in the San Juan Basin, northwestern New Mexico and southwestern Colorado. Ph.D. Dissertation, Stanford University, Stanford, California, 213 p.

Berry, F.A. and B.B. Hanshaw. 1960. Geologic evidence suggesting membrane properties of shales (abstract). Int. Geol. Congr Rep. Sess. Norden, 21, pp. 209.

Black, C.A. ed. 1965. Methods of Soil Analysis, Part 1 and 2. No. 9 in the Series Agronomy, American Society of Agronomy, Inc., Madison, Wisconsin.

Blackmore, A.V., and R.D. Miller. 1962. Tactoid size and osmotic swelling in calcium montmorillonite. Soil Sci. Soc. Amer. Proc., 25, pp. 169-173.

Bolt, G.H. and R.d. Miller. 1955. Compression studies of Illite suspensions. Soil Sci. Soc. Amer. Proc., 19 pp. 285-288.

Bolt, G.H. 1956. Physico-chemical analyses of the compressibility of pure clay. Geotechnique, 6(2), pp. 86-93.

Bolt, G.H. and R.D. Miller. 1958. Calculation of total and component potentials of water in soil. Trans. Am. Geophys. Union, 39, pp. 917-928.

Bolt, G.H. and P.H. Groenevelt. 1969. Coupling Phenomena as a possible cause of "non-darcian" behavior of water in soil. Bull. Int. Assoc. Sci. Hydrol., XIV, 2, pp. 17-28.

Bredehoeft, J.D., Blyth, C.R., White, W.A. and G.B. Maxey. 1963. Possible mechanism for concentration of brines in subsurface formations. Am. Assoc. Petro. Geol. Bull., 47(2), pp. 257-269.

Bresler, E. 1973. Anion exclusion and coupling effects in nonsteady transport through unsaturated soils: I. Theory. Soil Sci. Amer. Proc., 37(5), pp. 663-669.

Bruch, P. 1985. An Examination of the CME Continuous Sample Tube System. B.Sc. Thesis, Department of Civil Engineering, University of Saskatchewan, Saskatoon. 52 p.

Buettner, W.G. 1985. Permeability Testing of Soils with Low Hydraulic Conductivities. M.Sc. Thesis, Department of Civil Engineering, University of Saskatchewan, Saskatoon, 203 p.

Buckingham, E. 1907. Studies of the movement of soil moisture. U.S.D.A Bur. Soils Bull. no. 38.

Chapman, D.L. 1913. A contribution to the theory of electrocapillarity. Philosophical Magazine, 25(6), pp. 475-481.

Cary, J.W. and S.A. Taylor. 1962. The interaction of the simultaneous diffusion of heat and water vapour. Soil Sci. Soc. Amer. Proc., 26, pp. 413-416.

Chattopadhyay, P.K., 1972. Residual Shear Strength of Some Pure Clay Minerals. Ph.D. Dissertation, Department of Civil Engineering, University of Alberta, Edmonton, 340 p.

Childs, E.C. and N. Collis George. 1948. Soil geometry and soil-water equilibria. Disc. Faraday Soc., no. 3, pp. 73-85.

Collis-George, N. and J.M. Bozeman. 1970. A double layer theory for mixed ion systems as applied to the moisture content of clays under restraint. Australian Journal of Soil Research, 8(3), pp. 239-258.

Corey, A.T. and Kemper, W.D. 1961. Concept of total potential in water and its limitations. Soil Science., 91, pp. 99-305.

Corey, A.T. and Klute, A. 1984. Application of the potential concept to soil water equilibrium and transport. A paper by the Rocky Mountain Area Agricultural Research Service, U.S.D.A. in cooperation with the Colorado State University Agriculture Experimental Station, 31 p.

Devenny, D.W. and L. Balanko. 1978. Investigation of the Clay Lining of the IOL Brine Pond, Redwater, Alberta. EBA Engineering Consoluting Ltd., submitted to Imperial Oil Ltd.

Edlefsen, N.E. and A.B.C. Anderson. 1943. Thermodynamics of soil moisture. Hilgardia, 15, pp. 31-298.

Elrick, D.E., Smiles, D.E., Baumgartner, N., and P.H. Groenevelt. 1976. Coupling phenomena in saturated homo-ionic montmorillonite: I. Experimental. Soil Sci. Soc. Amer. Jour., 40, pp. 490-491.

El Swaify, S.A. and Henderson, D.W. 1967. Water retention by osmotic swelling of certain colloidal clays with varying ionic composition. Soil Science, 18(2), pp. 223-232.

Fink, D.H., Nakayama, F.S. and B.L. McNeal. 1971. Demixing of exchangeable cations in free swelling bentonite clay. Soil Sci. Soc. Amer. Proc., 35, pp. 552-555.

Folkes, D.J. 1981. Control of contaminant migration by use of liners. Canadian Geotechnical Journal, 19(3), pp.320-344.

Fothergill, L.A. 1955. The cementation of oil reservoir sands and its origin. Proc. 4th World Petroleum Congr., 13, pp. 301-314.

Fredlund, D.G. 1973. Volume Change of Unsaturated Soils. Ph.D. Dissertation, Department of Civil Engineering, University of Alberta, Edmonton, 490 p.

Fredlund, D.G. 1973. The effect of salt content on stress state variables. Internal Report, Geotechnical Group, Department of Civil Engineering, University of Saskatchewan, Saskatoon, 8 p.

Fredlund, D.G., and J.U. Hasan. 1979. Statistical geotechnical properties of Lake Regina sediments. Transportation and Geotechnical Group, Report IR-9, University of Saskatchewan, Saskatoon, 102 p.

Fredlund, D.G., Krahn, J. and J.U. Hasan. 1980. Variability of an expansive clay deposit. Proc. 4th Int. Conf. on Expansive Soils, Denver, Colorado, pp. 332-339.

Fredlund, D.G. 1981. The Behavior of Unsaturated Soils. Unpublished Lecture Notes. Department of Civil Engineering, University of Saskatchewan.

Freeze, R.A. and J.A. Cherry. 1979. Groundwater. Prentice-Hall, Englewood Cliffs, N.J.

Frind, E.O. 1982a. Simulation of long-term transient density-dependant transport in groundwater. Adv. Water Res., 5, pp. 73-88.

Frind, E.O. 1982b. Seawater intrusion in continuous coastal aquifer-aquitard systems. Adv. Water Res., 5, pp. 89-97.

Gillham, R.W., Robin, M.J.L., Dytynyshyn, D.G. and H.M. Johnston. 1984. Diffusion of non-reactive and reactive solutes through fine-grained barrier materials. Canadian Geotechnical Journal, 21(3), pp. 541-550.

Gillham,R.W. and Cherry, J.A. 1982. Contaminant migration in saturated unconsolidated geologic deposits. Geological Society of America, Special Paper 189, pp. 31-62.

Gouy, G. 1910. Sur la constitution de la charge electrique a la surface d'un electrolyte. Anniue Physique (Paris), 9(4), pp. 457-468.

Graf, D.L. 1982. Chemical osmosis, reverse chemical osmosis, and the origin of subsurface brines. Geochim. Cosmochim., Acta., 46, pp. 1431-1448.

Greenberg, J.A. 1971. Diffusional flow of salt and water in soils. Ph.D. Dissertation, Department of Civil Engineering, University of California, Berkeley, 231 p.

Greenberg, J.A., Mitchell, J.K. and P.A. Witherspoon. 1973. Coupled salt and water flows in a groundwater basin. Journal of Geophysical Research, 78(27), pp. 6341-6353.

Groenevelt, P.H., Elrick, D.E. 1976. Coupling phenomena in saturated homo-ionic montmorillonite: II. Theoretical. Soil Sci. Amer. Jour., 40, pp. 820-823.

Groenevelt, P.H., Elrick, D.E. and T.J.M. Blom. 1978. Coupling phenomena in saturated homo-ionic montmorillonite: III Analysis. Soil Sci. Soc. Amer. Jour., 42(5), pp. 671-674.

Groenevelt, P.H., Elrick, D.E. and K.B. Laryea. 1980. Coupling phenomena in saturated homo-ionic montmorillonite: IV The dispersion coefficient. Soil Sci. Soc. Amer. Jour., 44, pp. 1168-1173.

Hanshaw, B.B. and G.A. Hill. 1969. Geochemistry and hydrodynamics of the Paradox Basin region, Utah, Colorado and New Mexico. Chem. Geol., 4(1/2), pp. 263-294.

Hanshaw, B.B. and E. Zen. 1965. Osmotic equilibrium and overthrust faulting. Bull. Geol. Soc. Amer., 76, pp. 1379-1386.

Heyer, E., Cass, A. and A. Mauro. 1969. A demonstration of the effect of permeant and impermeant solutes, and unstirred boundary layers on osmotic flow. Yale Journal of Biology and Medicine, pp. 139-153.

Hill, G.A., Colburn, W.A., and J.W. Knight. 1961. Reducing oil finding costs by use of hydrodynamic evalutation, In Economics of Petroleum Exploration, Development and Property Evaluation, Proc., 1961 Institute of the International Oil and Gas Education Center, Prentice-Hall, Englewood Cliffs, New Jersey, pp. 38-69.

Hitcheon, B. 1969. Fluid flow in the western Canada sedimentary basin. 2. Effect of geology. Water Resources Research, 5(2), pp. 460-469.

Ho, Y.A. 1985. The Effects of Brine Contaminantion on the Properties of Soils. M.Sc. Thesis, Department of Civil Engineering, University of Saskatchewan, Saskatoon, 215 p.

Hubbert, M.K. 1940. The theory of ground-water motion. Journal of Geology, 68(6), pp. 785-944.

Hudec, P.P. 1979. Effect of Brine on Clay Liner Material from the IOL Brine Pond, Redwater, Alberta. University of Windsor, Windsor, Ontario, 30 p.

Jones, C.W. 1984. Effects of brine on the soil lining of an evaporation pond. In Hydraulic Barriers in Soil and Rock, ASTM Special Publication Code Number 04-874000-38, ASTM Philadelphia, Pa., pp. 213-228.

Kemper, W.D. 1961. Movement of water as affected by free energy and pressure gradients: I. Application of classic equations for viscous and diffusive movements to the liquid phase in finely porous media. Soil Sci. Soc. Amer. Proc., 25, pp. 255-260.

Kemper, W.D. and N.A. Evans. 1963. Movement of water as affected by free energy and pressure gradients III. Restriction of solutes by membranes. Soil Sci. Soc. Amer. Proc., 27, pp. 485-490.

Kemper, W.D. and J.B. Rollins. 1966. Osmostic efficiency coefficients across compacted clays. Soil Sci. Soc. Amer. Proc.,30, pp. 529 - 534.

Kemper, W.D. and J.C. van Schaik. 1966. Diffusion of salts in clay-water systems. Soil Sci. Soc. Amer. Proc., 30, pp. 534-540.

Kent, D.K. and A.W. Clifton. 1980. Assessment of Dyke Integrity, report for Procor Limited. Clifton Associates Limited, Regina, Saskatchewan, 19 p.

Kent, D.K. and R.W. Chursinoff. 1981. Geotechnical Investigation of Existing Brine Storage Lagoons, Regina, Saskatchewan, report for Procor Limited. Clifton Associates Limited, Regina, Saskatchewan, 31 p.

Kharaka, Y.K., and F.A.F. Berry. 1973. Simultaneous flow of water and solutes through geological membranes, I. Experimental investigation. Geochim. Cosochim. Acta, 37(12), pp. 2577-2603.

Klausner, Y., and I. Shainberg. 1967. Consolidation properties of arid-region soils. Proc. 3rd Asian Regional Conf. on Soil Mech. and Found. Eng., Haifa, pp. 17-19.

Klausner, Y., and I. Shainberg. 1971. Consolidation properties of Na+ and Ca++ adsorbed montmorillonites. Proc. 4th Asian Regional Conf. on Soil Mech. and Found. Eng., Bangkok, pp. 373-378.

Lamb, T.W. 1958. The engineering behavior of compacted clay. ASCE Jour. of Soil Mech. and Found. Div., 84, SM2, paper no. 1655, 35 p.

Lamb, T.W. 1960. A mechanistic picture of shear strength in clay. Proc. A.S.C.E. Research Conference on the Shear Strength of Cohesive Soil, Colo., pp. 555-580.

Low, P.F., and J.M. Deming. 1953. Movement and equilibrium of water in heterogeneous systems with special reference to soils. Soil Science, 75, pp. 187-202.

Low, P.F. 1955. The effect of osmotic pressure on diffusion rate of water. Soil Science, 80, pp. 95-100.

Maathuis, H. and G. van der Kamp. 1984. Theory of groundwater movement in the vicinity of brine ponds and salt tailings piles. Saskatchewan Research Council Technical Report no. 152, 39 p.

Manheim, F.T. 1966. A hydraulic squeezer for obtaining interstitial water from consolidated and unconsolidated sediments. U.S. Geol. Surv. Prof. Paper 550-e, Washington, D.C, pp. 256-261.

Marine, I.W. and S.J. Fritz. 1981. Osmotic model to explain anomalous hydraulic heads, Water Resources Research, 17(1), pp. 73-82.

Mauro, A. 1957. Nature of solvent transfer in osmosis. Science, 126, pp. 252-253.

Mauro, A. 1965. Osmotic flow in a rigid porous membrane. Science, 149, pp. 867-869.

Metten, U. 1966. Desalination by Reverse Osmosis. M.I.T. Press, Cambridge, Massachusetts.

McKelvey, J.G., and I.H. Milne. 1960. The flow of salt solutions through compacted clay. Clays and Clay Minerals, 9, pp. 248-259.

Mesri, G. and R.E. Olson. 1971. Consolidation characteristics of montmorillonite. Geotechnique, 21(4), pp. 341-352.

Mitchell, J.K. 1962. Components of pore water pressure and their engineering significance. Clays and Clay Minerals, pp. 162-184.

Mitchell, J.K. 1973. Recent advances in the understanding of the of the influences of minerology and pore solution chemistry on the swelling and stability of clays. Third Int. Conf. on Expansive Soils, II, pp. 11-25.

Mitchell, J.K. 1973. Chemico-Osmotic effects in fine grained soils. Journal of the Soil Mechanics and Foundation Division, ASCE, SM4, pp. 307-322.

Mitchell, J.K. 1976. Fundamentals of Soil Behavior. John Wiley and Sons, New York.

Mokady, R.S. and P.F. Low. 1966. Electrochemical determination of diffusion coefficients in clay-water systems. Soil Sci. Soc. Amer. Proc.,30, pp. 438-442.

Mokady, R.S. and P.F. Low. 1968. Simultaneous transport of water and salt through clays: I. Transport mechanisms. Soil Science, 105(2), pp. 112-131.

Neuzil, C.E. 1986. Groundwater flow in low-permeability environments. Water Resources Research, 22(8) pp. 1163-1195.

Norrish, K. 1954. The swelling of montmorillonite. Faraday Society, London, Discussions, no. 18, pp. 120-134.

Ogata, A. and R.B. Banks. 1961. A solution of the differential equation of longitudinal dispersion in porous media. U.S. Geol. Surv. Prof. Paper 411-A.

Olsen, H. 1969. Simultaneous fluxes of liquid and charge in saturated kaolinite. Soil Sci. Soc. Am. Proc., 33(3), pp. 338-344.

Olsen,H. 1972. Liquid movement through kaolinite under hydraulic, electric, and osmotic gradients. Bull. Amer. Assoc. Petr. Geol., 56(10), pp. 2022-2028.

Olsen, H. 1985. Osmosis: a cause of apparent deviations from Darcy's law. Can. Geot. Jour., 22(2), pp. 238-240.

Olson, R.E., and F. Mitronovas. 1962. Shear strength and consolidation characteristics of calcium and magnesium illite. Clays and Clay Minerals, 11, pp. 185-209.

Olson, R.E., and D.E. Daniel. 1981. Measurement of the hydraulic conductivity of fine-grained soils. ASTM Special Technical Report, STP 746, pp. 18-64.

Onsager, L. 1931a. Reciprocal relations in irreversible processes I. Phys. Rev., 37, pp. 405-426.

Onsager, L. 1931b. Reciprocal relations in irreversible processes II. Phys. Rev., 38, pp. 2265-2279.

Perry, R.H. and C.H. Chilton. 1973. Chemical Engineers Handbook. Fifth Edition, McGraw-Hill.

Quigley, R.M. 1984. Quantitative minerology and preliminary pore-water chemistry of candidate buffer and backfill materials for a nuclear fuel waste disposal vault. Atomic Energy of Canada Ltd., Whiteshell Nuclear Research Establishment, Pinawa, Manitoba.

Quirk, J.P. 1963. The role of suface forces in determining the physical behavior of soils and clays. Proc. 4th Australian-New Zealand Conf. Soil Mech., pp. 205-212.

Richards, L.A. 1928. The usefulness of capillary potential to soil moisture and plant investigations. J. Agr. Res., 37, pp. 719-742.

Ridley, K.J.D. 1985. The Impact of NaCl Brine on the Behavior of Compacted Fine Grained Soil - a Laboratory Study. Ph.D. Dissertion, Department of Civil Engineering, University of Windsor, Windsor, Ontario, 360 p.

Ridley,K.J.D., Bewtra, J.K., and J.A. McCorquodale. 1983. Behavior of compacted fine-grained soil in a brine environment. Can. Jour. Civil Eng., 11, pp. 196-203.

Robinson, R.A. and R.H. Stokes. 1968. Electrolyte Solutions. second edition, Butterworths, London, England.

Shainberg, I., Bresler, E., and Y. Klausner. 1971. Studies on Na/Ca montmorillonite systems I. the swelling pressure. Soil Science, 3(4), pp. 214-219.

de Sitter, L.U. 1947. Diagenesis of oil-field brines: Am. Assoc. Petr. Geol. Bull., 31(11), pp. 2030-2040.

Spiegler, K.S. and A.D.K. Laird. 1980. Principles of Desalination. Academic Press, Inc., New York, N.Y.

Sridharan, A. and G. Venkatappa Rao. 1973. Mechanisms controlling volume change of saturated clays and the role of the effective stress concept. Geotechnique, 23(3), pp. 359-382.

Sridharan, A. and G. Venkatappa Rao. 1979. Shear strength behavior of saturated clays and the role of the effective stress concept. Geotechnique, 29(2), pp. 177-193.

Sridharan, A. and M.S. Jayadeva. 1982. Double layer theory and compressiblity of clays. Geotechnique, 32(2), pp. 133-144.

Staverman, A.J. 1951. The theory of measurement of osotic pressure. Recueil des Travaux Chimiques des Pays-Bas, 70, pp. 344-352.

Stern, O. 1924. Zur Theorie der elktrolytischen Doppelschriht. Zeitschrift Electrochem, 30, pp. 508-516.

Tallin, J.E. 1984. Waste Management Schemes of Potash Mines in Saskatchewan. M.Sc. Thesis, Department of Civil Engineering, University of Saskatchewan, Saskatoon, 308 p.

Tavenas, F., Leblond, P., Jean, P., and Leroueil, S. 1983a. The permeability of natural soft clays, Part I. Method of laboratory measurement. Can. Geot. Jour., 20, pp. 629-644.

Tavenas, F., Leblond, P., Jean, P., and Leroueil, S. 1983b. The permeability of natural soft clays, Part II. Permeability characteristics. Can. Geot. Jour., 20, pp. 645-660.

Taylor, D.W. 1948. Fundamentals of Soil Mechanics. John Wiley and Sons, Inc.

Taylor, S.A. and J.W. Cary. 1960. Analysis of the simultaneous flow of water and heat or electricity with the thermodynamics of irreversible processes. Int. Congr. Soil Sci., Trans., 7th, 1, pp. 80-90.

Terzaghi, K. 1925. Erdbaumechanik auf Bodenphysikalischer Grundlage, Deuticke, Vienna, 399 p.

Terzaghi, K. 1931. The influence of elasticity and permeability on the swelling of two-phase systems. Colloid Chemistry, (J. Alexander, ed.), Vol. III, Chemical Catalog Co., New York, pp. 65-88.

Thomas, G.W. and Swoboda, A.R. 1970. Anion exclusion effects on chloride movement in soils. Soil Sci., 110, pp. 163-166.

Turk, L.J. 1974. Leakage from solar evaporation ponds associated with sediment-brine interactions. In proceedings, Fourth Symposium on Salt, Northern Ohio Geological Society, pp. 403-406.

van Everdingen, R.O. 1968. Studies of formation water in Western Canada: Geochemistry and hydrodynamics. Canadian Journal of Earth Sciences, 5, pp. 523-543.

van Olphen, H. 1977. An Introduction to Clay Colloid Chemistry. John Wiley and Sons, New York.

de Vries, D.A. 1975. Heat transfer in soils. in Heat and Mass Transfer in the Biosphere Part I Transfer Processes in the Plant Environment, D.A. de Vries and N. H. Afgan ed., John Wiley and Sons, New York, pp. 1-28.

Wallace, R.B., and K.D. Eigenbrod. 1984. An unprotected HDPE liner in a subartic environment. Int. Conf. on Geomembranes, Denver, Colorado, Technical Paper no. 84-1, 6 p.

Warkentin, B.P., Bolt, G.H., and R.D.Miller. 1957. Swelling pressure of montmorillonite. Soil Sci. Soc. Amer. Proc., 21, pp. 495-497.

Warkentin, and Schofield. 1962. Swelling pressures of Na-Montmorillonite. Soil Science, 13, p. 98.

White, D.E. 1957. Magmatic, connate, and metamorphic waters. Bull. Geol. Soc. Amer., 68, pp. 1659-1682.

White, D.E. 1965. Saline waters in sedimentary basins. In Fluids in subsurface environments. Amer. Assoc. Petr. Geol., Memoir 4, pp. 342-366.

Young, A. and P.F. Low. 1965. Osmosis in argillaceous rocks. Bull. Am. Assoc. Petr. Geol., 49, pp. 1004-1007.

Zrymiak, P. 1985. Effects of Brine on the Measured Hydraulic Conductivity and Volume Change of a Compacted Sand-Bentonite Mixture. M.Sc. Thesis, Department of Civil Engineering, University of Saskatchewan, Saskatoon, 141 p.

APPENDIX A

Appendix A outines the method used to calculate the electrostatic repulsive stress between clay particles or packets of clay particles. The method of calculation described follows closely to the methods layed out by Balasubramonian (1972-Appendix A), Bolt (1956), and Mitchell (1976). Detailed developments of the method of calculation are given by Mitchell (1976) and van Olphen (1977). A tabulated set of calculations for the sand/bentonite mixture are included.

A.1 Calculation of (R-A)

The net repulsive force between two clay particles may be calculated from the following equations:

$$R = 2\,C_o\,R\,T\,(\cosh y_c - 1) \qquad [A.1]$$

$$y_c = 2\,\ln\,(\cosh \Delta + 1)/(\cosh \Delta - 1) \quad \text{for } y_c < 1 \qquad [A.2]$$

$$y_c = 2\,\ln\,(\pi/\Delta) \quad \text{for } y_c > 1 \qquad [A.3]$$

$$\Delta = \kappa\,(x_o + d) \qquad [A.4]$$

$$\kappa = (8\pi e_c^{\,2}\,z^2\,n/\varepsilon k\,T)^{1/2} \qquad [A.5]$$

where;
- R = repulsive force between particles
- C_o = ion concentration of bulk solution, equal to the molar concentration X 10-3
- R = Universal Gas Constant (85 kg-cm/mol/0K)
- T = absolute temperature (^oK)
- d = interparticle half space
  - = e/AsG
- e = void ratio
- A_s = specific surface
- G_s = specific gravity of particle
- e_c = electric charge on an electron (4.8×10^{-10}) esu)
- z = valency of the ions
- n = volume concentration of cations and anions in bulk solution (ions/cc, equal to molarity x NA x 10^{-3})
- ε = dielectric constant of the pore fluid
- NA = Avogadro's number (6.0232×10^{23} mol/gm mole)
- k = Boltzman's constant

The Boltzman equation used in the derivation of equation [A.1] requires a boundary condition of infinite charge density at the particle surface. As this is unrealistic, a correction factor x_o, is introduced. x_o is the distance from the surface of infinte charge density, to a surface at which the charge density is equal to that of the soil of interest. Balasubramonian (1972) provides a method by which x_o can be

calculated. Mitchell (1976) suggests that it can be estimated as equal to; 1/v for illite, 2/v for kaolinite, and 4/v for montmorillonite, where v is the valence of the cation of interest.

Sample Calculation - Sand Bentonite Mixture

$e = 1.09$

$C_o = 0.008$ M

$1/\kappa = 33.91$

$A_s = 575\ m^2/gm * 20\%$ bentonite $= 115\ m^2/gm$

$d = e/G\ As = 1.09/(2.63 \cdot 115) = 36$ Å

$\Delta = k(x_o + d) = (1/33.91)\ (4 + 36) = 1.18$

$y_c = 2\ ln\ (\pi/\Delta) = 1.958$

$R = 2\ C_o\ R\ T\ (\cosh y_c - 1) = 104$ kPa

A.2 Calculation of (R-A)

SAND BENTONITE

SPECFIC SURFACE = 115 CM2/GM
GS= 2.632
Xo= 4 A Co=.008 M

STRESS (kPa)	STRESS (kPa)	VOID RATIO	HALF SP (A)	R-A (kPa)	1/K=33.91 DELTA	y_c
11	11	2	66.08	14.840965	2.0665403	0.8377126
20	20	1.812	59.87	22.784081	1.8833737	1.0233350
30	30	1.683	55.60	30.082688	1.7576902	1.1614632
40	40	1.591	52.56	36.496641	1.6680555	1.2661472
50	50	1.521	50.25	42.209130	1.5998552	1.3496381
60	60	1.465	48.40	47.391334	1.5452949	1.4190348
70	70	1.419	46.88	52.115536	1.5004775	1.4778975
80	80	1.375	45.43	57.079927	1.4576087	1.5358698
90	90	1.335	44.11	62.015962	1.4186371	1.5900711
100	100	1.305	43.11	66.010422	1.3894084	1.6317082
120	120	1.247	41.20	74.532694	1.3328996	1.7147510
150	150	1.175	38.82	86.822431	1.2627506	1.8228795
180	180	1.12	37.00	97.743902	1.2091647	1.9096048
200	200	1.09	36.01	104.35856	1.1799359	1.9585440

APPENDIX B

Appendix B contains the documentation of the numerical simulation OSMOPC and the listings of utility programs VELFIL, TELFIL, and NODVAL.

B.1 FINITE ELEMENT FORMULATION FOR 1-D OSMOTIC FLOW AND VOLUME CHANGE

B.1.1. Governing Equations:

$$m_v \rho_f g \frac{\partial \psi}{\partial t} - m_\pi \rho_w g \frac{\partial \Pi}{\partial t} = \frac{\partial}{\partial y} \left(K_h \left(\frac{\partial \psi}{\partial y} + \rho_r \hat{i} \right) - K_\pi \frac{\partial \Pi}{\partial y} \right)$$

$$\frac{\partial C_s}{\partial t} = \frac{D}{R} \frac{\partial^2 C_s}{\partial y^2} - \frac{v}{R} \frac{\partial C_s}{\partial y}$$

$$v = \frac{-K_h}{n} \left(\frac{\partial \psi}{\partial y} + \rho_r \hat{i} \right) + \frac{K_\pi}{n} \frac{\partial \Pi}{\partial y}$$

$$\Pi = \frac{2RT\, C_s}{\rho w g m}$$

$$\psi = \left(\frac{u_f}{\rho_w g} + \rho_r \hat{i} \right)$$

R = Gas constant

T = Absolute temperature

C_s = Concentration of salt (gm/ℓ)

m = molecular weight of salt

ρ_w = Density of water

m_v = Compressibility (1/kPa)

m_π = Osmotic compressibility (1/kPa)

K_h = Permeability

K_π = Osmotic permeabilty

$\rho_r = \rho_f / \rho_w - 1$

R = Retardation factor

D = Diffusion coefficient (m^2/S), $D' = D/R$

v = Water velocity $v' = v/R$

B.1.2. Finite Element Equation for Salt Transport:

2.1 Galerkin technique of weighted residuals, residual R;

$$R = D' \frac{\partial^2 C}{\partial y^2} - v' \frac{\partial C}{\partial y} - \frac{\partial C}{\partial t} = 0$$

2.2 Utilize linear, one-dimensional elements with a local coordinate system:

y_2

$\ell = y_2 - y_1$

y_1

local coordinates; $w_1 = 1 - y/\ell$

$w_2 = y/\ell$

2.3 Trial function;

$$C = \hat{C} = \sum_{j=j_1}^{N} C_j(t)\, w_j(y)$$ where N is no. of nodes

In matrix force the elemental trial function becomes

$$C = [w_1 \; w_2] \begin{Bmatrix} C_1 \\ C_2 \end{Bmatrix}$$

2.4 Write the Galerkin equation using trial functions; and remove second derivatives by Green's theorum.

$$\int R \cdot \phi_i \, d\ell = 0 \qquad i = 1 \ldots N$$

$$\int_\ell \left(D' \frac{\partial^2 C}{\partial y^2} - v' \frac{\partial C}{\partial y} - \frac{\partial C}{\partial t} \right) w_i \, d\ell = 0 \qquad i = 1 \ldots N$$

$$-\int_\ell D' \frac{\partial C}{\partial y} \frac{\partial w_i}{\partial y} \, d\ell + \int_s D' \frac{\partial C}{\partial y} \ell_y w_i \, ds - \int_\ell v' \frac{\partial C}{\partial t} w_i \, d\ell$$

$$-\int \ell \frac{\partial C}{\partial t} w_i \, d\ell = 0$$

Note:

$\int_s D' \frac{\partial C}{\partial y} \ell_y w_i ds$ forms third type boundary

$$D' \frac{\partial C}{\partial n} = - \frac{q_o C_o}{n} + vC$$ where q_o, C_o are specified third type boundary conditions

2.5 Substitute in trial function and third type boundary condition;

$$\int_\ell \left(D' \frac{\partial \Sigma C_j w_j}{\partial y} \frac{\partial w_j}{\partial y} + v' \frac{\partial \Sigma C_j w_j}{\partial y} w_i\right) d\ell + \int_s \left(\frac{q_o C_o}{n} - vC\right)$$

$$+ \int_\ell \frac{\partial \Sigma C_j w_j}{\partial t} w_i \, d\ell = 0 \qquad i = 1...N$$

remove summation from integral

$$\sum_{j=1}^{N} C_j \left[\int_\ell \left(D' \frac{\partial w_j}{\partial y} \frac{\partial w_i}{\partial y} + v' \frac{\partial w_j}{\partial y} w_i\right) d\ell\right] + \int_s \left(\frac{q_o C_o}{n} - vC_s\right)$$

$$+ \Sigma \frac{\partial C_j}{\partial t} \int w_i w_j d\ell = 0 \qquad i = 1...N$$

in matrix form;

$$[R + R_b] \{C\} + [T] \left\{\frac{\partial C}{\partial t}\right\} + \{Q\} = 0$$

2.6 Apply finite difference approximation of time derivative;

$$\frac{\partial C}{\partial t} = \frac{(C_j)_{t+\Delta t} - (C_j)_t}{\Delta t}$$

$$C_j = \varepsilon (C_j)_{t+\Delta t} + (1 - \varepsilon) (C_j)_t$$

where $\varepsilon = 1$ for backward difference approximation (BDA)
$\varepsilon = 1/2$ for central difference approximation (CDA)

now;

$$[R] \left(\varepsilon \{C\}_{t+\Delta t} + (1 - \varepsilon) \{C\}_t\right) + [T] \left(\frac{\{C\}_{t+\Delta t} - \{C\}_t}{\Delta t}\right) = 0$$

2.7 Evaluation of element matrices;

$$[R]_e = \int_\ell \left(D' \frac{\partial w_j}{\partial y} \frac{\partial w_i}{\partial y}\right) d_\ell + \int_\ell \left(v' \frac{\partial w_j}{\partial y} w_i\right) d\ell$$

$$= \frac{D'}{\ell} \begin{bmatrix} 1 & -1 \\ -1 & 1 \end{bmatrix} + \frac{v'}{2} \begin{bmatrix} -1 & 1 \\ -1 & 1 \end{bmatrix}$$

$$[R_b]_e = \int_s v ds = \begin{bmatrix} v & o \\ o & o \end{bmatrix}$$

$$[T]_e = \int w_j w_i = \frac{\ell}{6} \begin{bmatrix} 2 & 1 \\ 1 & 2 \end{bmatrix} \qquad \text{consistent form}$$

$$\text{or} = \frac{\ell}{2} \begin{bmatrix} 1 & 0 \\ 0 & 1 \end{bmatrix} \text{ lumped form}$$

B.1.3. Finite Element Equation for Hydraulic and Osmotic Flow

3.1 Galerkin Technique of weighted residuals, residual R;

$$R = m_v \rho g \frac{\partial \psi}{\partial t} - m_\pi \rho g \frac{\partial \Pi}{\partial t} - \frac{\partial}{\partial y}\left(K_h \left(\frac{\partial \Pi}{\partial y} - \rho_r \hat{i}\right) - K_\pi \frac{\partial \Pi}{\partial y}\right) = 0$$

$$\lambda_h = m_v \rho_w g \quad \lambda_\pi = m_\pi \rho_w g$$

$$R = \frac{\partial}{\partial y}\left[K_H \left(\frac{\partial \psi}{\partial y}\right) + K_H \rho_r - K_\pi \frac{\partial \Pi}{\partial y}\right] - \lambda_h \frac{\partial \psi}{\partial t} + \lambda_\pi \frac{\partial \Pi}{\partial t} = 0$$

3.2 Utilize linear, one-dimensional elements with a local coordinate system;

3.3 Trial Functions;

$$\psi = \hat{\psi} = \sum_{j=1}^{N} \psi_j (t)\, w_j(y) \quad \text{where N is no. of nodes}$$

$$\text{and } \Pi = \hat{\Pi} = \sum_{j=1}^{N} \Pi_j (t)\, w_j(y)$$

3.4 Write Galerkin equation using trial functions and remove second derivatives by Green's theorum.

$$\int_\ell R \cdot \phi_i \, d\ell = 0 \qquad i = 1 \ldots N$$

$$\int_\ell \left[\frac{\partial}{\partial y}\left(K_h \frac{\partial \psi}{\partial y} + K_h \rho_r + K_\pi \frac{\partial \Pi}{\partial y}\right) - \lambda_h \frac{\partial \psi}{\partial t} - \lambda_\pi \frac{\partial \Pi}{\partial t}\right) . w_i \, d\ell = 0 \quad i = 1..N$$

application of Green's theorum: in general

$$\int_A \frac{\partial}{\partial y}\left(K \frac{\partial \phi}{\partial y}\right) w_i dA = \int_s K \frac{\partial \phi}{\partial y} \ell_n w_i \, ds - \int_A K \frac{\partial w_i}{\partial y} \frac{\partial v}{\partial y} dA$$

therefore;

$$\int_s \left(K_h \frac{\partial \psi}{\partial y} + K_h \rho_r - K_\pi \frac{\partial \Pi}{\partial y}\right) . w_i ds - \int_\ell \left(K_h \frac{\partial \psi}{\partial y} \frac{\partial w_i}{\partial y} + K_h \rho_r \frac{\partial w_i}{\partial y} - \frac{K\pi}{\partial y} \frac{\partial \Pi}{\partial y} \frac{\partial w_i}{\partial y}\right) d\ell$$

$$- \int_\ell \left(\lambda_h \frac{\partial \psi}{\partial t} w_i + \lambda_\pi \frac{\partial \Pi}{\partial t} w_i\right) d\ell = 0 \qquad i = 1 \ldots N$$

<u>rewrite</u>

$$\int_\ell \left(K_h \frac{\partial \psi}{\partial y} \frac{\partial w_i}{\partial y} + K_h \rho_r \frac{\partial w_i}{\partial y} - K_\pi \frac{\partial \Pi}{\partial y} \frac{\partial w_i}{\partial y}\right) d\ell - Q_i - \int_s K_h \rho_r w_i ds$$

$$+ \int_\ell \left(\lambda_h \frac{\partial \psi}{\partial t} w_i - \lambda_\pi \frac{\partial \Pi}{\partial t} w_i\right) d\ell = 0 \qquad i = 1 \ldots N$$

where {Q} are boundary fluxes

3.5 Substitute in trial functions and remove Σ from integral;

$$\sum_j \psi_j \int_\ell K_h \frac{\partial w_i}{\partial y} \frac{\partial w_j}{\partial y} d\ell - \sum_j \Pi_j \int_\ell K_\pi \frac{\partial w_j}{\partial y} \frac{\partial w_i}{\partial y} d\ell$$

$$+ \sum_\ell \frac{\partial \psi_j}{\partial t} \int_\ell \lambda_h w_j w_i d\ell - \sum_j \frac{\partial \Pi_j}{\partial t} \int_\ell \lambda_\pi w_j w_i d\ell$$

$$+ \int \ell K_h \rho_r \frac{\partial w_i}{\partial y} d\ell - Q - Q_D = 0 \qquad i = 1 \ldots N$$

where; Q is applied fluxes,
Q_D is boundary density flux = $\int s \, K_h w_i \rho_r ds$

in matrix form;

$$[K_h] \{\psi_j\} - [K_\pi] \{\pi_j\} + [T_h] \left\{\frac{\partial \psi}{\partial t}\right\} - [T_\pi] \left\{\frac{\partial \Pi}{\partial t}\right\}$$

$$+ \{D\} - \{Q\} - \{Q_D\} = 0$$

3.6 Apply finite difference approximation of the time derivative;

$$\frac{\partial \psi}{\partial t} = \frac{\psi_{t+\Delta t} - \psi_t}{\Delta t} \qquad \frac{\partial \Pi}{\partial t} = \frac{\Pi_{t+\Delta t} - \Pi_t}{\Delta t}$$

$$\psi = (\varepsilon)\ \psi_{t+\Delta t} + (1-\varepsilon)\ \psi_t$$
$$\Pi = (\varepsilon)\ \pi_{t+\Delta t} + (1-\varepsilon)\ \pi_t$$

$$(\varepsilon[K_h] + \frac{1}{\Delta t}\,[T_h])\ \{\psi\}_{t+\Delta t} = (-(1-\varepsilon)[K_h] + \frac{1}{\Delta t}\,[T_h])\{\psi\}_t$$

$$+ (\varepsilon[K_\pi] + \frac{1}{\Delta t}\,[T_\pi])\{\Pi\}_{t+\Delta t} - (-(1-\varepsilon)[K_\pi] + \frac{1}{\Delta t}\,[T_\pi]\{\pi\}_t$$

$$- \varepsilon\ \{D\}_{t+\Delta t} - (1-\varepsilon)\{D\}_t + \{Q\} + \varepsilon\{Q_D\}_t + (1-\varepsilon)\{Q_D\}_{t+\Delta t}$$

with {Q} constant with time

3.7 Evaluation of element matrices

$$[K_h] = \int_\ell K_h \frac{\partial w_i}{\partial y} \frac{\partial w_i}{\partial y}\, d\ell = \frac{K_h}{\ell} \begin{bmatrix} 1 & -1 \\ -1 & 1 \end{bmatrix}$$

similarly $[K_\pi] = \frac{K_\pi}{\ell} \begin{bmatrix} 1 & -1 \\ -1 & 1 \end{bmatrix}$

$$[T_h] = \int_\ell \lambda_h\, w_j w_i\, d\ell = \frac{\ell \lambda_h}{6} \begin{bmatrix} 2 & 1 \\ 1 & 2 \end{bmatrix} \quad \text{consistent form}$$

$$\text{or} = \frac{\ell \lambda_h}{2} \begin{bmatrix} 1 & 0 \\ 0 & 1 \end{bmatrix} \quad \text{lumped form}$$

similarly $[T_\pi] = \frac{\lambda_\pi \ell}{6} \begin{bmatrix} 2 & 1 \\ 1 & 2 \end{bmatrix}$

$$\text{or} = \frac{\lambda_\pi \ell}{2} \begin{bmatrix} 1 & 0 \\ 0 & 1 \end{bmatrix}$$

$$\{D\} = \int_\ell K_h\, \rho_r \frac{\partial w_i}{\partial y}\, d\ell = K_h\, \rho_r \begin{bmatrix} -1 \\ 1 \end{bmatrix}$$

$$\{Q_D\} = \int_s K_h\, \rho_r w_i = K_h\, \rho_r \begin{bmatrix} 1 \\ 0 \end{bmatrix} \text{ or } K_h\, \rho_r \begin{bmatrix} 0 \\ 1 \end{bmatrix}$$

3.8 Calculation of Elemental velocities

$$\Sigma = - K_h \left(\frac{\partial \psi}{\partial y} + \rho_r\right) + K_\pi \left(\frac{\partial \Pi}{\partial y}\right)$$

$$\therefore q_c = -\Sigma \psi_j \left(K_h \frac{\partial w_j}{\partial y} + K_h \rho_r\right) + \Sigma \Pi_j K_\pi \frac{\partial w_j}{\partial y}$$

in matrix form

$$q_c = \frac{K_h}{\ell} [1 \ -1] \begin{bmatrix} \psi_1 \\ \psi_2 \end{bmatrix} - K_h \rho r + \frac{K_\pi}{\ell} [-1 \ +1] \begin{bmatrix} \Pi_1 \\ \Pi_2 \end{bmatrix}$$

B.2 Flow Charts for OSMOPC

B.2.1 Description of Subroutines

MAIN - file assignments
opens/closes - input/output files

CLREAD - input/output of control data

DENSIT - update iterative osmotic potentials and average element relative densities

DTSTIF - form density matrix, DT2

ESTIF - form flow equation matrices;
EH, EMH, EP, EMP

FLOSOL - form flow equation, modifiy for boundary conditions, solve for hydraulic heads

FREAD - input/output flow data

INIT - initialize variables and matrices

KTSTIF - form general form of K,R, and T matrices

MODIFY - modify a triadiagonal coefficient matrix for first type boundary conditions

PROCOL - main control subroutine, contains iterative and time loops

PRTOUT - solution output to files

RSTIF - form global R matrix for transport equation

SWELLCHK - check for reversal of volume change direction in each element, assign appropriate value of compressibility

TABKPMP - define element osmotic permeability and compressiblity based on tabulated input data and element concentrations

TRASOL - form transport equation, modify for boundary conditions, solve for concentrations

TREAD - input/output transport properties

TSOLVE - Thomas algorithm for solving triadiagonal symmetric or non-symmetric matrices

B.2.2 Flow Chart for MAIN

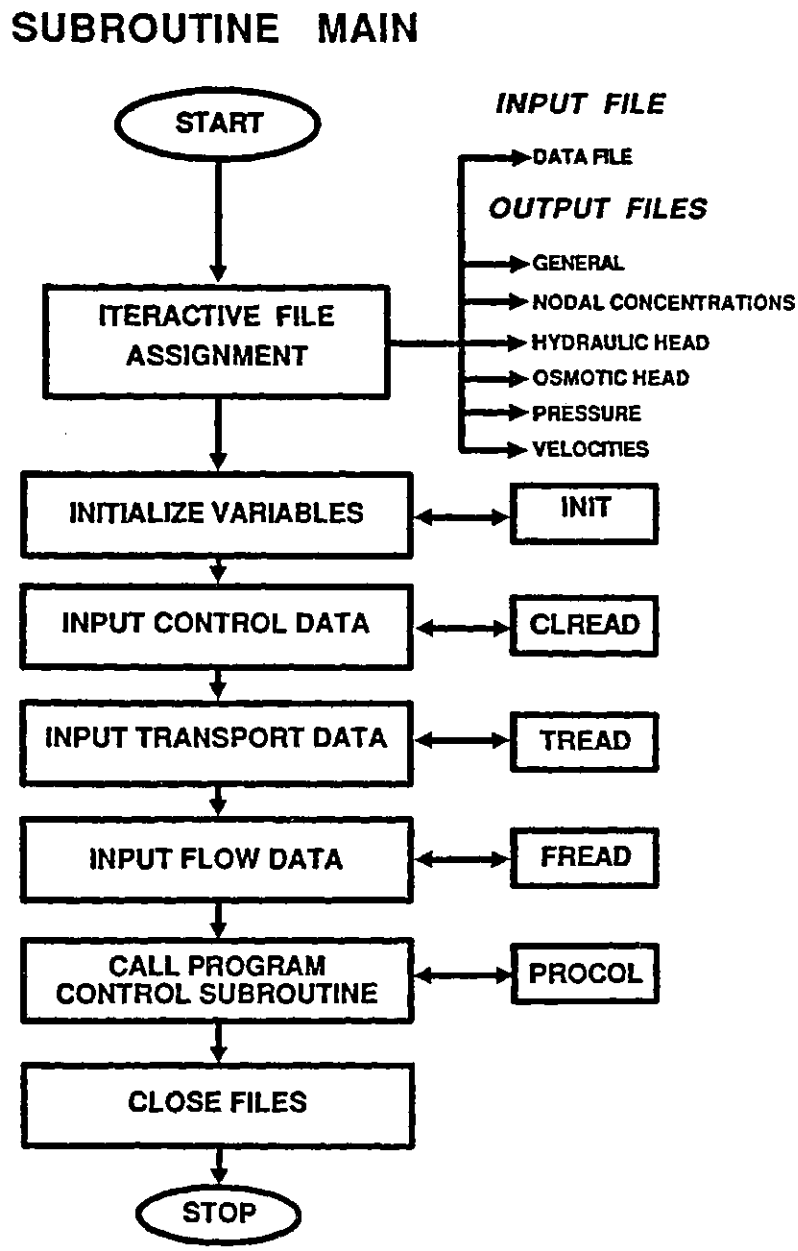

B.2.3 Flow Chart for PROCOL

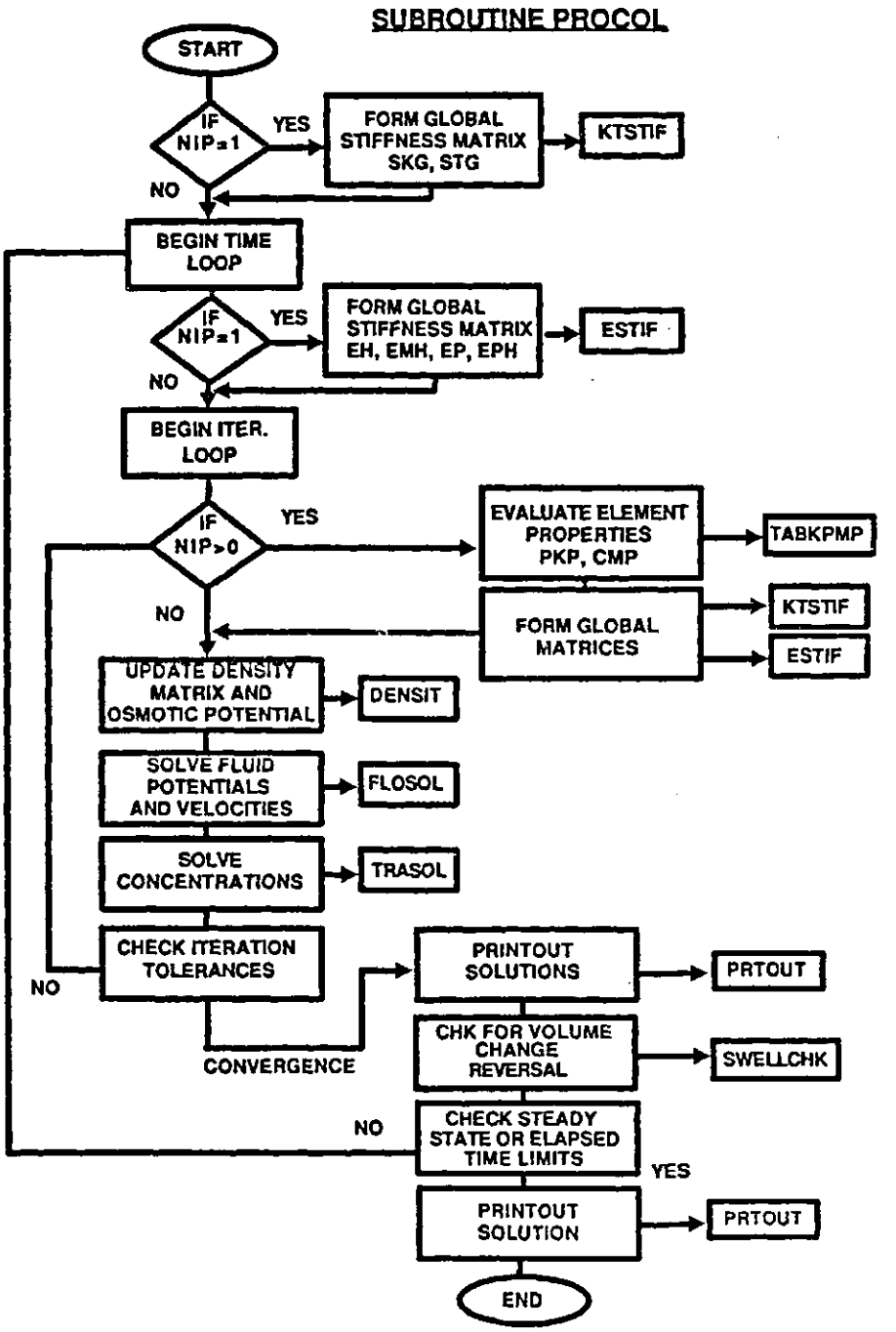

B.2.4 Flow Chart for FLOSOL

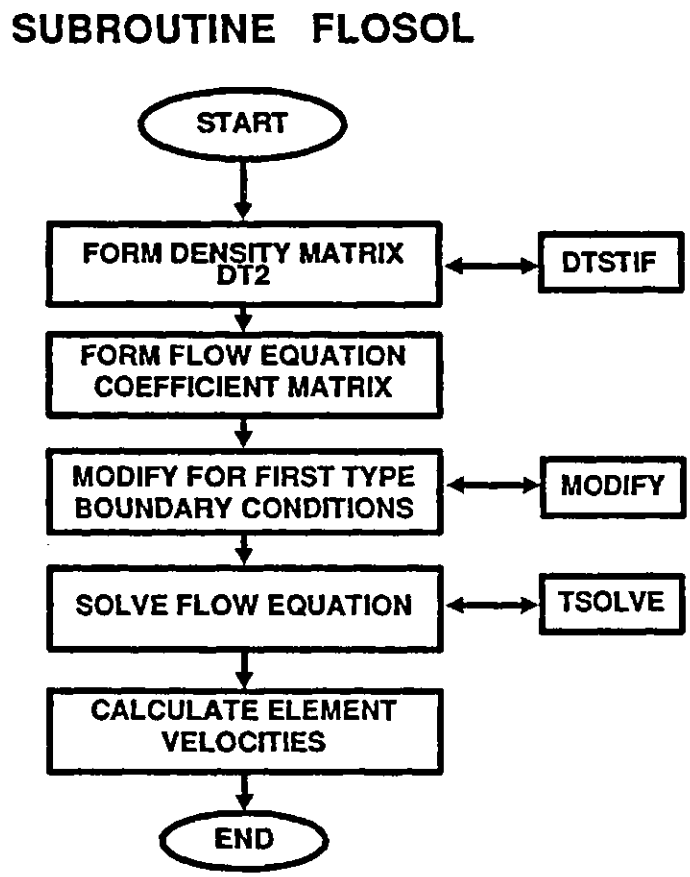

B.2.5 Flow Chart for TRASOL

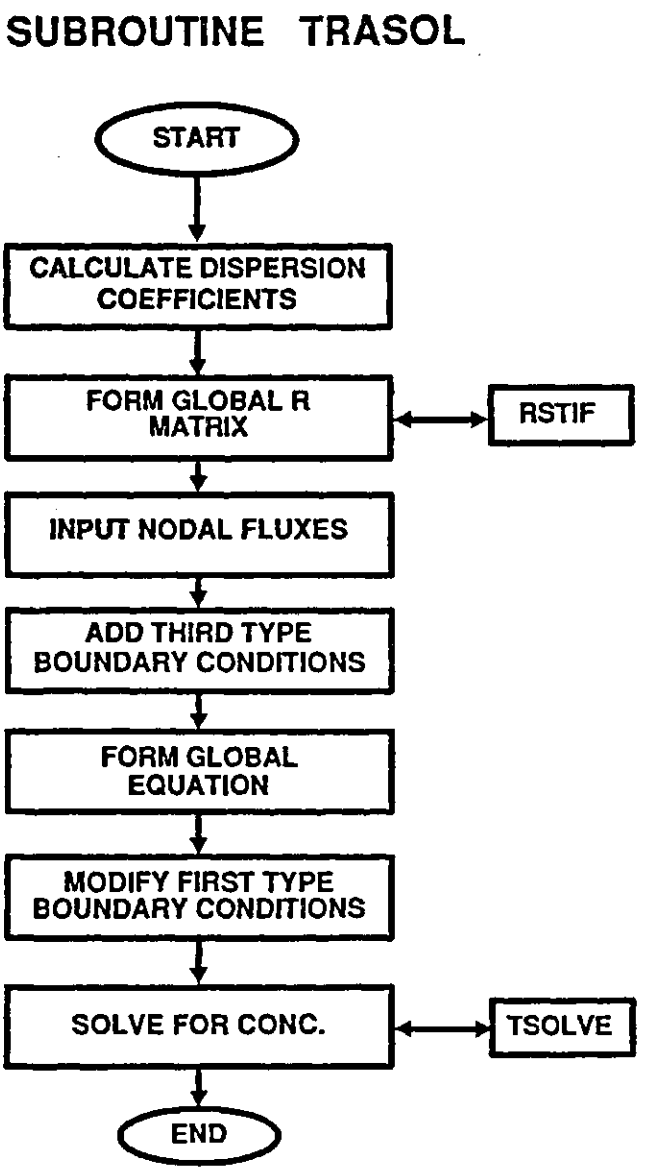

B.3 List of Primary Variables

Control and Common Variables

A(201,3) - coefficient matrix in Thomas solver
B(201) - column matrix in Thomas solver
DT - time increment
EF - time weighting factor / flow equation
ET - time weighting factor / transport equation
G - gravitational accerleration (m/s2)
ITMAX - maximum number of iterations
KF1 - flow boundary condition code, node 1; first type (1), second type (0)
KFN - flow boundary condition code, node NUMNP; first type (1), second type (0)
KT1 - transport boundary condition code, node NUMNP; first type (1), second type (0)
KTN - transport boundary condition code, node NUMNP; first type (1), second type (0)
KTF - consistent (0) or lumped (1) formulation code for flow equation
KTF - consistent (0) or lumped (1) formulation code for transport equation
MAT(200) - matrix of element material numbers
NIT - iteration number
NUMAT - number of materials
NUMEL - number of elements
NUMNP - number of nodal points
ROW - density of fluid (kN/M3)
STOL - convergence tolerance on steady state
TFAC - time increment multiplier
TIME - total elapsed time
TOL - iteration convergence tolerance
TOTIM - maximum simulation time
VEL(200) - element velocities
Y(201) - nodal coordinates

Flow Equation Variables

CLH(5) - CMV*ROW*G
CMP(200) - elemental osmotic compressibility
CMS(5) - material compressibility during swelling
CMV(5) - material compressibility
CTAB(5,20)- tabulated concentrations for TABKP, TABMP
DT1(201) - initial relative density coefficient matrix
DT2(201) - final relative density coefficient matrix
EH(201,3) - global sub-matrix for hydraulic flow
EMH(201,3)- global sub-matrix for hydraulic flow
EP(201,3) - global sub-matrix for osmotic flow
EMP(201,3)- global sub-matrix for osmotic flow
FH1(201) - initial hydraulic heads
FH2(201) - final hydraulic heads
GAMMA - relative density - concentration constant (maximum fluid density/water density -1)
NIP - number of tabulated data points for TABKP, TABMP, CTAB
OP1(201) - initial osmotic heads
OP2(201) - final hydraulic heads
OPIT(201) - osmotic heads during iteration
PKH(5) - material permeability
PKP(200) - element osmotic permeability
QF(201) - matrix of nodal flows
QF1(201) - matrix of intial nodal flows
RDEN(200) - element relative densities
RGAS - universal gas constant (8.314 kPa/mole/K)
SKH(201,3)- global conductivity matrix for hydraulic flow
SKP(201,3)- global conductivity matrix for osmotic flow
STH(201,3)- global storage matrix for hydraulic flow
STP(201,3)- global storage matrix for osmotic flow
TABKP(5,20)-tabulated osmotic permeability
TABMP(5,20)-tabulated osmotic compressibility
TEM - absolute temperature (298 0K)

Transport Equation Variables

AL(5) - material dispersivity
CT1(201) - initial nodal concentrations
CT2(201) - final nodal concentrations
CIT(201) - iterative nodal concentrations
D(201) - element coefficients of dispersion
DD(5) - material diffusion coefficient
POR(5) - material porosity
QT(201) - transport flux matrix
R(201,3) - global coefficient matrix
STT(201,3)- global storage coefficient matrix
RTRD(5) - material retardation

B.4 Input Formats for OSMOPC

```
Line: 1
Variables: HED
Format: 18A4
Description: problem description

Line: 2
Variables: NUMNP, NUMAT, EF, ET, KTF, KTT
Format: 2I5, 2F5.1, 2I5
Description: see B.3

Line: 3
Variables: I, MAT(I), J, MAT(J)
Format: 4I5
Description: element no./material type match
             - intermediate values generated as first

Line: 4
Variables: I, Y(I), J, Y(J)
Format: 2(I5, F5.3)
Description: nodal no./coordinate match
             - intermediate values generated

Line: 5
Variables: KF1, KFN, KT1, KTN
Format: 4I5
Description: see B.3

Line: 6
Variables: DT, TFAC, TOTIM
Format: E10.3, F10.3, E10.3
Description: see B.3

Line: 7
Variables: TOL, STOL, ITMAX
Format: 2F5.3, I5
Description: see B.3

Line: 8
Variables: POR(I), AL(I), RTRD(I), DD(I), I=1,NUMAT
Format: 3F10.2, E10.2
Description: see B.3

Line: 9
Variables: I, CT1(I), QT(I), I = 1,NUMNP
Format: 15, 2F10.2
Description: intermediate values between successive
             lines are generated
```

```
Line: 10
Variables: PKH(I), CMV(I), CMS(I), I = 1,NUMAT
Format: 3E10.2
Description: see B.3

Line: 11
Variables: NIP
Format: I5
Description: see B.3

Line: 12
Variables: CTAB(I,J), TABKP(I,J), TABMP(I,J),
           I=1,NUMAT, J=1,NIP
Format: F10.3, 2E10.2
Description: repeat for NIP lines, enter table of
             concentration, KP, MP / repeat for each
             material type

Line: 13
Variables: GAMMA
Format: F10.2
Description: see B.3

Line: 14
Variables: I, FH1(I), QF(I), QF1(I), I = 1,NUMNP
Format: I5, 3F10.2
Description: initial nodal head, 3rd type boundary
             nodal flux, and initial fluxes /
             intermediate values between successive
             lines - generated
```

B.5 Program Listings

B.5.1 OSMOPC

```
**********************************************************************
C
      SUBROUTINE CLREAD
C
C **********************************************************************
C
C THIS SUBROUTINE READS FROM A GENERAL INPUT FILE CONTROL DATA SUCH AS
C GRID GEOMETRY, TITLE, TIME STEP DATA, WEIGHTING FACTOR, BOUNDARY
C CONDITION CODES AND THEN ECHOS THIS DATA TO THE GENERAL OUTPUT FILE
C
$INCLUDE:'CPARM.TXT'
; IN FIRST TIME STEP CIT=CT1, IN SUBSEQUENT TIME STEPS CT1 DENSITY
C ALREADY CALCUATED
C
$INCLUDE:'CPARM.TXT'
$INCLUDE:'TPARM.TXT'
$INCLUDE:'FPARM.TXT'
C
C CACLULATE THE ELEMENT RELATIVE DENSITES. THE RELATIONSHIP USED IS A
C STRAIGHT LINE RELATIONSHIP BETWEEN S.G. OF SOLUTION AND THE
C CONCENTRATION IN GMS/CUBIC METRES
      DO 10 M=1,NUMEL
      M1=M+1
      CAVG=(CIT(M)+CIT(M1))/2.
      SG=1.+GAMMA*CAVG
      RDEN(M)=SG-1.0
   10 CONTINUE
C
C CALCULATE THE OSMOTIC POTENTIALS - VAN'T HOFF RELATIONSHIP IS USED AT
C THIS PRELIMINARY STAGE - CONC IN GM/L IS CONVERTED TO MOLE/L BY DIVIDING
C BY 58.45 THEN RELATION SHIP R*T*2*C IS USED
C
      DO 20 I=1,NUMNP
      PRESS=RGAS*TEM*2.0*CIT(I)/58.45
      OPIT(I)=PRESS/(ROW*G)
   20 CONTINUE
C
      RETURN
      END
```

```
C ***********************************************************************
C
      SUBROUTINE DTSTIF(II)
C
C ***********************************************************************
C
C THIS SUBROUTINE FORMS THE DENSITY MATRICES (DT2). FOR THE FIRST TIME
C TIME STEP DT2 IS EQUAL TO DT1
C
$INCLUDE :'CPARM.TXT'
$INCLUDE:'TPARM.TXT'
$INCLUDE:'FPARM.TXT'
C
      DO 10 I=1,NUMNP
      DT2(I)=0.0
   10 CONTINUE
C
      DO 20 M=1,NUMEL
      NM=MAT(M)
      M1=M+1
      DT2(M)=DT2(M)-PKH(NM)*RDEN(M)
      DT2(M1)=DT2(M1)+PKH(NM)*RDEN(M)
   20 CONTINUE
C
C FOR FIRST TIME STEP SET DT1=DT2
      IF(TIME.LE.DT)THEN
      DO 30 I=1,NUMNP
      DT1(I)=DT2(I)
   30 CONTINUE
      END IF
C
      RETURN
      END
```

```
C ***********************************************************************
C
      SUBROUTINE ESTIF
C
C ***********************************************************************
C
C THIS SUBROUTINE FORMS THE EH,EMH,EP,EMP MATRICES OF THE FLOW EQUATION
C WHICH ARE CONSTANT DURING EACH TIME STEP AS KP,KH,MP,MV ARE NOT A
C FUNCTION OF CONC.
C
$INCLUDE:'CPARM.TXT'
$INCLUDE:'TPARM.TXT'
$INCLUDE:'FPARM.TXT'
C
      DO 10 J=1,3
      DO 10 I=1,NUMNP
      EH(I,J)=EF*SKH(I,J)+STH(I,J)/DT
      EMH(I,J)=-(1.-EF)*SKH(I,J)+STH(I,J)/DT
      EP(I,J)=EF*SKP(I,J)+STP(I,J)/DT
      EMP(I,J)=-(1.-EF)*SKP(I,J)+STP(I,J)/DT
   10 CONTINUE
C
      RETURN
      END
```

```
C ***********************************************************************
C
      SUBROUTINE FLOSOL
C
C ***********************************************************************
C
C THIS SUBROUTINE FORMS THE DENSITY MATRIX, COMBINES THE MATRICES TO
C OBTAIN THE RIGHT AND LEFT SIDE COEFFICIENT MATRICES, MODIFIES FOR
C BOUNDARY CONDITIONS AND THEN SOLVES FOR FLUID HEADS AND VELOCITES
C USING THE THOMAS ALGORITHM  AX=B
C
$INCLUDE:'CPARM.TXT'
$INCLUDE:'TPARM.TXT'
$INCLUDE:'FPARM.TXT'
C
C FORM DENSITY MATRIX
      CALL DTSTIF
C
C INITIALIZE A,B
      DO 5 I=1,NUMNP
      B(I)=0.0
      DO 5 J=1,3
      A(I,J)=0.0
    5 CONTINUE
C
C ADD FLUX MATRIX INTO RIGHT SIDE B MATRIX, FOR FIRST TIME STEP FLUX
C IS EF*QF + (1-EF)*QF1. FOR REMAINING TIME QF IS CONSTANT
      IF (TIME.GT.DT)THEN
      DO 10 I=1,NUMNP
      B(I)=QF(I)
   10 CONTINUE
      ELSE
      DO 20 I=1,NUMNP
      B(I)=EF*QF(I)+(1.-EF)*QF1(I)
   20 CONTINUE
      END IF
C
C FORM FLOW EQUATION RIGHT SIDE COEFFICIENT MATRIX
      DO 30 I=1,NUMNP
      B(I)=B(I)-EF*DT2(I)-(1.-EF)*DT1(I)
      DO 30 JJ=1,3
      J=I-2+JJ
      IF((J.GT.0).AND.(J.LE.NUMNP)) THEN
      B(I)=B(I)+EMH(I,JJ)*FH1(J)+EP(I,JJ)*OPIT(J)-EMP(I,JJ)*OP1(J)
      A(I,JJ)=EH(I,JJ)
      END IF
   30 CONTINUE
```

```
C
C BOUNDARY FLUXES DUE TO DENISTY GRADIENTS HAVE TO BE ADDED INTO
C BOUNDARY NODES
      NM1=MAT(1)
      CONS1=GAMMA*PKH(NM1)
      NM2=MAT(NUMEL)
      CONS2=GAMMA*PKH(NM2)
      B(1)=B(1)+EF*(-CIT(1)*CONS1)+(1.-EF)*(-CT1(1)*CONS1)
      B(NUMNP)=B(NUMNP)+EF*CIT(NUMNP)*CONS2+(1.-EF)*CT1(NUMNP)*CONS2
C
C MODIFY THE MATRIX EQUATION AX=B FOR FIRST TYPE BOUNDARY CONDITIONS
      IF(KF1.EQ.1)THEN
      CALL MODIFY(1,QF(1))
      END IF
      IF(KFN.EQ.1) THEN
      CALL MODIFY(NUMNP,QF(NUMNP))
      END IF
C
C SOLVE
      CALL TSOLVE(1)
C
C STORE SOLUTION IN FH2
      DO 40 I=1,NUMNP
      FH2(I)=B(I)
   40 CONTINUE
C
C CALCULATE VELOCITES, DUE TO HYDRAULIC,OSMOTIC AND DENSITY GRADIENTS
      DO 50 M=1,NUMEL
      NM=MAT(M)
      M1=M+1
      RL=ABS(Y(M)-Y(M+1))
      FHD=FH2(M)-FH2(M1)
      OPD=OPIT(M)-OPIT(M1)
      VEL(M)=PKH(NM)/POR(NM)*(FHD/RL-RDEN(M))-PKP(M)/POR(NM)*OPD/RL
   50 CONTINUE
C
      RETURN
      END
```

```
C ***********************************************************************
C
      SUBROUTINE FREAD
C
C ***********************************************************************
C
C THIS SUBROUTINE READS IN THE MATERIAL PROPERTIES AND BOUNDARY CONDITONS
C REQUIRED TO SOLVE THE FLOW EQUATION
C
$INCLUDE:'CPARM.TXT'
$INCLUDE:'TPARM.TXT'
$INCLUDE:'FPARM.TXT'
C
C READ/WRITE FLOW/CONSOLIDATION MATERIAL PROPERTIES
      WRITE(16,200)
      DO 8 I=1,NUMAT
      READ(17,100)PKH(I),CMV(I),CMS(I)
      WRITE(16,202)PKH(I),CMV(I),CMS(I)
    8 CONTINUE
C
C FORM THE MATRIX CLH - THIS MATRIX IS MODIFIED IF SWELLING OCCURS BY SWELLCHK
      DO 9 I=1,NUMEL
      NM=MAT(I)
      CLH(I)=CMV(NM)
    9 CONTINUE
C
C READ IN OSMOTIC PERMEABILTIY AND COMPRESSIBLITY IN TABLULAR DATA POINT
C TYPE FORMAT
      READ(17,101)NIP
      DO 11 I=1,NUMAT
      WRITE(16,203)I
      READ(17,102)(CTAB(I,J),TABKP(I,J),TABMP(I,J),J=1,NIP)
      WRITE(16,204)(CTAB(I,J),TABKP(I,J),TABMP(I,J),J=1,NIP)
   11 CONTINUE
C
C READ/WRITE CONCENTRATION-RELATIVE DENSITY CONSTANT
      READ(17,107)GAMMA
      WRITE(16,207)GAMMA
C
C READ INITIAL AND BOUNDARY FRESHWATER HEADS/FLUXES AND INITAL FLUXES(TIME=0)
      READ(17,110)I,FH1(I),QF(I),QF1(I)
    5 READ(17,110)J,FH1(J),QF(J),QF1(J)
      IF((J-I).GT.1) THEN
      IP=I+1
      JM=J-1
      DN=J-I
      FD=(FH1(J)-FH1(I))/DN
      QFD=(QF(J)-QF(I))/DN
      QF1D=(QF1(J)-QF1(I))/DN
      DO 10 K=IP,JM
      FH1(K)=FH1(K-1)+FD
      QF(K)=QF(K-1)+QFD
      QF1(K)=QF1(K-1)+QF1D
   10 CONTINUE
      ELSE
      END IF
      I=J
      IF(I.LT.NUMNP)THEN
      GO TO 5
      END IF
      WRITE(16,210)(I,FH1(I),QF(I),QF1(I),I=1,NUMNP)
C
C CALCULATE INITAL OSMOTIC PRESSURES FORM CT1
      DO 30 I=1,NUMNP
      PRESS=2*RGAS*TEM*CT1(I)/58.45
      OP1(I)=PRESS/(ROW*G)
   30 CONTINUE
C
C WRITE INITIAL OSMOTIC POTENTIALS
      WRITE(16,220)(I,OP1(I),I=1,NUMNP)
C
```

```
C ***************************************************************************
C FORMAT
  100 FORMAT(3E10.2)
  101 FORMAT(I5)
  102 FORMAT(F10.3,2E10.2)
  107 FORMAT(F10.2)
  110 FORMAT(I5,3E10.2)
C
  200 FORMAT(//,33H HYDRAULIC K AND COMPRESSIBLITY: ,/27(1H*),//
     134H       PKH          CMV          CMS,
     2/34(1H*),//)
  202 FORMAT(3(2X,E10.2))
  203 FORMAT(//,40H CONC.  OSMOTIC K  COMPRESS FOR MAT NO: ,I5,
     1/40(1H*))
  204 FORMAT(/,F10.3,2X,E10.2,2X,E10.2)
  207 FORMAT(//,'CONCENTRATION - RELATIVE DENSITY CONSTANT =',F10.2)
  210 FORMAT(//,35H INITIAL FRESHWATER HEADS AND B.C ,/35(1H*),
     1/,5X,'(NODE,INITIAL HEAD,B.C,INITAL FLUXES)'//,2(I5,3E10.2,5X))
  220 FORMAT(//28H INITIAL OSMOTIC POTENTIALS ,/28(1H*),/5X,
     1'(NODE,POTENTIAL)',//,5(I5,F10.2))
C
 2001 FORMAT('FREAD',E10.2)
      RETURN
      END



C ***************************************************************************
C
      SUBROUTINE INIT
C
C ***************************************************************************
C
C THIS SUBROUTINE INITIALIZES THE MATRICES TO BE USED IN THE SOLUTION
C AS WELL AS ESTABLISHES A NUMBER OF CONSTANTS
C
$INCLUDE:'CPARM.TXT'
$INCLUDE:'TPARM.TXT'
$INCLUDE:'FPARM.TXT'
C
      DO 10 J=1,3
      DO 10 I=1,NUMNP
      R(I,J)=0.0
      SKH(I,J)=0.0
      STH(I,J)=0.0
      SKP(I,J)=0.0
      STP(I,J)=0.0
      EH(I,J)=0.0
      EMH(I,J)=0.0
      EP(I,J)=0.0
      EMP(I,J)=0.0
10    CONTINUE
C
      DO 20 N=1,NUMNP
      VEL(N)=0.0
      CT2(N)=0.0
      DT1(N)=0.0
      DT2(N)=0.0
      FH2(N)=0.0
      OP2(N)=0.0
      OPIT(N)=0.0
   20 CONTINUE
C
C SET INITIAL CONSTANTS
      ROW=1.0
      G=9.81
C R IS THE UNIVERSAL GAS CONSTANT, TEM IS ABSOLUTE TEMPERATURE
C THE WILL BE USED TO CALCULATE OSMOTIC PRESSURE IN KPA FROM
C THE EXPRESSION , OSMOTIC PRESS=RTC, C IN MOLES/L
      RGAS=8.314
      TEM=298.
C
      RETURN
      END
```

```
C
      SUBROUTINE KTSTIF
C
C ***************************************************************
C
C THIS SUBROUTINE FORMS THE GENERAL FORM OF THE K (OR R) AND T MATRICES
C THE T MATRICES DEVELOPED IN THE CONSISTENT FORM AND THEN LUMPED FOR
C THE TRANSPORT OR FLOW EQUATION IF KTF OR KTT IS '1'.
C
C THIS SUBROUTINE IS ONLY REQUIRED TO RUN ONCE FOR CONSTANT MATERIAL
C PROPERTIES.  IT IS RUN A SECOND TIME IF A SWELLING INDEX IS USED
C IT IS THEN CALLED FROM SUBROUTINE SWELLCHK
C IT IS RUN EVERY ITERATION IF VALUES OF KP AND MP ARE USED AS A FUNCTION
C OF CONCENTRATION (IE. NIP GT 1)
C
$INCLUDE:'CPARM.TXT'
$INCLUDE:'TPARM.TXT'
$INCLUDE:'FPARM.TXT'
C
      DIMENSION STE(2,2),SKE(2,2)
C
C INITIALIZE STH,STP,SKH,SKP
      DO 5 J=1,3
      DO 5 I=1,NUMNP
      STH(I,J)=0.0
      STP(I,J)=0.0
      SKH(I,J)=0.0
      SKP(I,J)=0.0
      STT(I,J)=0.0
    5 CONTINUE
C
C SET ELEMENT MATRIX VALUES
      STE(1,1)=2.
      STE(1,2)=1.
      STE(2,1)=1.
      STE(2,2)=2.
      SKE(1,1)=1.
      SKE(1,2)=-1.
      SKE(2,1)=-1.
      SKE(2,2)=1.
C

      DO 10 M=1,NUMEL
      NM=MAT(M)
      M1=M+1
      RL=ABS(Y(M)-Y(M1))
      PKHRL=PKH(NM)/RL
      PKPRL=PKP(M)/RL
C NOTE: CLH HAS ALREADY BEEN SET = CMV OR CMS FOR EACH ELEMENT
      CMVRL=CLH(M)*RL/6.*ROW*G
      CMPRL=CMP(M)*RL/6.*ROW*G
      DO 20 II=1,2
      I=II+M-1
      DO 20 JJ=1,2
      J=JJ-II+2
      STH(I,J)=STH(I,J)+STE(II,JJ)*CMVRL
      STP(I,J)=STP(I,J)+STE(II,JJ)*CMPRL
      SKH(I,J)=SKH(I,J)+SKE(II,JJ)*PKHRL
      SKP(I,J)=SKP(I,J)+SKE(II,JJ)*PKPRL
      STT(I,J)=STT(I,J)+STE(II,JJ)*RL/6.
   20 CONTINUE
   10 CONTINUE
C
C CONDENSE TO TIME MATRICES STH,STP,STT
      IF(KTT.EQ.1)THEN
      DO 30 I=1,NUMNP
      STT(I,2)=STT(I,1)+STT(I,2)+STT(I,3)
      STT(I,1)=0.0
      STT(I,3)=0.0
   30 CONTINUE
      ELSE
      END IF
```

```
      IF(KTF.EQ.1)THEN
      DO 50 I=1,NUMNP
      STH(I,2)=STH(I,1)+STH(I,2)+STH(I,3)
      STP(I,2)=STP(I,1)+STP(I,2)+STP(I,3)
      STP(I,1)=0.0
      STP(I,3)=0.0
      STH(I,1)=0.0
      STH(I,3)=0.0
   50 CONTINUE
      ELSE
      END IF
C
C
      RETURN
      END



#DEBUG
#NOFLOATCALLS
C  ***********************************************************************
C
C                            O S M O 4
C
C ***********************************************************************
C
C     THIS PROGRAM SOLVES THE FINITE ELEMENT EQUATION FOR OSMOTIC FLOW
C IN ONE DIMENSION.  THE FORMULATION WAS DEVELOPED BY S.L. BARBOUR AND
C INCLUDES THE EFFECT OF OSMOTIC FLOW, SALT ADVECTION-DISPERSION, AND
C DENSITY INDUCED FLUID FLOW.
C
C     THE PROGRAM ALSO ASSUMES AT THIS STAGE OF DEVELOPMENT, THAT
C VAN'T HOFF APPROXIMATION OF OSMOTIC PRESSURE APPLIES.
C
C  THE SECOND VERSION INCLUDED THE CAPABILITY OF A NUMBER OF DIFFERENT
C  MATERIALS AS WELL AS A SWELLING CHECK FOR CHANGING MV TO MS
C
C  THIS FOURTH VERSION (JUNE 23 ,1986) ALLOWS THE VALUES OF KP AND MP
C  TO BE INPUT AS A FUNCTION OF CONCENTRATION THROUGH A SERIES OF TABULATED
C  VALUES OF  CTAB(NM,NIP), TABKP(NM,NIP), TABMP(NM,NIP)
C
C  THE PC VERSION WAS BEGUN MODIFICATION ON JUNE 24,1986
C
      IMPLICIT REAL*8(A-H,O-Z)
$INCLUDE:'CPARM.TXT'
$INCLUDE:'TPARM.TXT'
$INCLUDE:'FPARM.TXT'
C
C OPEN INPUT/OUTPUT FILES
      CHARACTER*10 INFIL,OUTFIL,CONC,FHEAD,OHEAD,PHEAD,VELFIL
      CHARACTER*20 HED
C
      WRITE(*,1110)
      READ(*,1111)INFIL
      WRITE(*,1112)
      READ(*,1111)OUTFIL
      WRITE(*,1113)
      READ(*,1111)CONC
      WRITE(*,1114)
      READ(*,1111)FHEAD
      WRITE(*,1115)
      READ(*,1111)OHEAD
      WRITE(*,1116)
      READ(*,1111)PHEAD
      WRITE(*,1117)
      READ(*,1111)VELFIL
C
      OPEN (UNIT=17,FILE=INFIL,STATUS='OLD')
      OPEN (UNIT=16,FILE=OUTFIL,STATUS='NEW')
      OPEN (UNIT=19,FILE=CONC,STATUS='NEW')
      OPEN (UNIT=20,FILE=FHEAD,STATUS='NEW')
      OPEN (UNIT=23,FILE=OHEAD,STATUS='NEW')
      OPEN (UNIT=24,FILE=PHEAD,STATUS='NEW')
      OPEN (UNIT=25,FILE=VELFIL,STATUS='NEW')
```

```
C
 1110 FORMAT(5X,24HENTER INPUT FILE NAME:  ,$)
 1111 FORMAT(A10)
 1112 FORMAT(5X,24HENTER OUTPUT FILE NAME: ,$)
 1113 FORMAT(5X,38HENTER CONCENTRATION OUTPUT FILE NAME: ,$)
 1114 FORMAT(5X,41HENTER FRESH WATER HEAD OUTPUT FILE NAME: ,$)
 1115 FORMAT(5X,42HENTER OSMOTIC POTENTIAL OUTPUT FILE NAME: ,$)
 1116 FORMAT(5X,33HENTER PRESSURE OUTPUT FILE NAME: ,$)
 1117 FORMAT(5X,33HENTER VELOCITY OUTPUT FILE NAME: ,$)
C
C INITIALIZE ALL ARRAYS
      CALL INIT
C
C CALL CONTROL DATA READ/WRITE
      CALL CLREAD
C
C CALL TRANSPORT DATA READ/WRITE
      CALL TREAD
C
C CALL FLOW DATA READ/WRITE
      CALL FREAD
C
C CALL PROGRAM CONTROL PROTOCOL
      CALL PROCOL
C
C CLOSE FILES
      CLOSE (UNIT=1)
      CLOSE (UNIT=2)
      CLOSE (UNIT=17)
      CLOSE (UNIT=16)
      CLOSE (UNIT=19)
      CLOSE (UNIT=20)
      CLOSE (UNIT=23)
      CLOSE (UNIT=24)
      CLOSE (UNIT=25)
C
      STOP
      END
C
```

```
C ***************************************************************************
C
      SUBROUTINE MODIFY(N,BC)
C
C ***************************************************************************
C
C THIS SUBROUTINE MODIFIES THE TRIDIAGONAL COEFFICIENT MATRIX (A) FOR
C FIRST TYPE BOUNDARY CONDITIONS, ALTERING THE MATRIX (B)
C
$INCLUDE :'CPARM.TXT'
$INCLUDE :'TPARM.TXT'
$INCLUDE :'FPARM.TXT'
C
      B(N)=BC
      A(N,2)=1.0
C
      IF(N.EQ.1)THEN
      B(2)=B(2)-BC*A(2,1)
      A(1,3)=0.0
      A(2,1)=0.0
      END IF
C
      IF(N.EQ.NUMNP)THEN
      B(N-1)=B(N-1)-BC*A(N-1,3)
      A(N-1,3)=0.0
      A(N,1)=0.0
      END IF
C
      IF(N.GT.0.AND.N.LT.NUMNP)THEN
      N1=N+1
      NM1=N-1
      IF(NM1.GT.0) THEN
      B(NM1)=B(NM1)-BC*A(NM1,3)
      A(NM1,3)=0.0
      END IF
      B(N1)=B(N1)-BC*A(N1,1)
      A(N,1)=0.0
      A(N,3)=0.0
      A(N1,1)=0.0
      END IF
C
      RETURN
      END
```

```
C ***********************************************************************
C
      SUBROUTINE PROCOL
C
C ***********************************************************************
C
C THIS SUBROUTINE CONTROLS THE CALLING OF SUBROUTINES AND THE TIME
C AND ITERATIVE LOOPS TO SOLVE FOR CONCENTRATIONS AND FLUID PRESSURES
C AND OSMOTIC POTENTIALS WITH TIME.
C
$INCLUDE :'CPARM.TXT'
$INCLUDE :'TPARM.TXT'
$INCLUDE :'FPARM.TXT'
C
C SET THE ELEMENT VALUES OF KP AND MP TO CONSTANTS IF NIP=1
      IF(NIP.EQ.1)THEN
      DO 6 M=1,NUMEL
      NM=MAT(M)
      PKP(M)=TABKP(NM,1)
      CMP(M)=TABMP(NM,1)
    6 CONTINUE
      END IF
C
C TWO BASIC FORMS OF THE GLOBAL MATRICES OCCUR IN THE F.E. EQUATIONS
C THESE BASIC FORMS (SKG,STG) ARE FORMED BY CALLING KTSTIF
C THESE CAN ONLY BE FORMED OUTSIDE THE INTERATIVE LOOP IF THE MATERIAL
C PROPERTIES ARE CONSTANT IE NIP=1
      IF(NIP.EQ.1)THEN
      CALL KTSTIF
      END IF
C
C SET ITERATIVE CONCENTRATIONS AND OSMOTIC POTENTIALS TO INTIAL VALUES
      DO 5 I=1,NUMNP
      CIT(I)=CI1(I)
      OPIT(I)=OPI(I)
    5 CONTINUE
C
      II=0
      TIME=0.0
C BEGIN TIME LOOP
   10 TIME=DT+TIME
      II=II+1
C
C ALTHOUGH SOME GLOBAL MATRICES THAT ARE INDEPENDANT OF THE ITERATION LOOP ---
C EH,EMH,EP,EPH (NOTE: THIS ONLY SO IF KH,KP,MV,MP ARE TAKEN AS INDEPENDANT
C OF CONCENTRATION, IE NIP =1) AND COULD ONLY NEED TO BE FORMED
C ONCE AS LONG AS DT IS CONSTANT, ESTIF WILL BE CALLED EVERY TIME IN CASE
C SOME OF THE GLOBAL MATRICES HAVE BEEN ALTERED BY CHANGES IN COMPRESSIBLITY
C OF ELEMENTS INVOKED BY SWELLCHK
C
      IF(NIP.EQ.1)THEN
      CALL ESTIF
      END IF
```

```
C
C THE ELEMENT AND GLOBAL STIFFNESS MATRICES MUST BE BUILT EVERY ITERATION
C IF NIP IS NOT EQUAL TO 1
      IF(NIP.GT.1)THEN
      CALL TABKPMP
      CALL KTSTIF
      CALL ESTIF
      END IF
C
C UPDATE DENSITY MATRIX AND OSMOTIC POTENTIALS FOR NEW CONCENTRATIONS
      CALL DENSIT
C
C SOLVE FOR FLUID POTENTIALS AND VELOCITES
      CALL FLOSOL
C
C SOLVE FOR CONCENTRATIONS
      CALL TRASOL
C
C CHECK TOLERANCES
      IF(NIT.EQ.1)GO TO 50
      BIG=-999.
      CHECK=-999.
      DO 30 I=1,NUMNP
      TEMP=CT2(I)
      IF(TEMP.GT.(0.00001))THEN
      CHECK=ABS((CT2(I)-CIT(I))/TEMP)
      END IF
      IF(CHECK.GT.BIG)THEN
      BIG=CHECK
      END IF
   30 CONTINUE
C
      WRITE(*,40)II,NIT,BIG
      WRITE(16,40)II,NIT,BIG
   40 FORMAT(/,' TIME STEP',I3,'  ITERATION',I3,'  MAX. DIFFERENCE'
     1,F10.4)
C
      IF(BIG.LT.TOL)GO TO 80
C
C CHECK MAXIMUM NO. OF ITERATIONS LIMIT
      IF(NIT.GE.ITMAX) THEN
      WRITE(16,70) NIT
      WRITE(*,70)NIT
   70 FORMAT(' SOLUTION DID NOT COVERGE AFTER',I3,'ITERATIONS')
C
      CALL PRTOUT(II)
      GO TO 101
      END IF
C
C UPDATE TRIAL CONCENTRATIONS
   50 DO 60 I=1,NUMNP
      CIT(I)=CT2(I)
   60 CONTINUE
C
C RETURN FOR NEXT ITERATION
C
C OUTPUT CHECK
C      CALL PRTOUT(II)
      GO TO 20
C
C **** SOLUTION CONVERGES ****
   80 CONTINUE
```

```
C   CHV.  AFTER SWELLCHK THE GLOBAL MATRICES ARE RECOMPILED BY CALLING KTSTIF.
      CALL SWELLCHK
C
C PRINT RESULTS FOR THIS TIME STEP
      CALL PRTOUT(II)
C
C CHECK IF STEADY STATE HAS BEEN REACHED
      BIG2=-999.
      DO 90 N=1,NUMNP
      TEMP=CT2(N)
      IF(TEMP.GT.(.00001))THEN
      DIFF=ABS((CT2(N)-CT1(N))/TEMP)
      END IF
      IF(DIFF.GT.BIG2)BIG2=DIFF
   90 CONTINUE
C
      IF(BIG2.LT.STOL)THEN
      WRITE(*,2000)
      WRITE(16,2000)
 2000 FORMAT(///,' ******* STEADY STATE ACHEIVED *******')
      GO TO 200
      END IF
C
C UPDATE CONCENTRATION GUESS AND UPDATE OSMOTIC AND HYDRAULIC POTENTIALS
      DO 100 N=1,NUMNP
      CIT(N)=CT2(N)+((CT2(N)-CT1(N))/2.)
      CT1(N)=CT2(N)
      DT1(N)=DT2(N)
      OP1(N)=OPIT(N)
      FH1(N)=FH2(N)
  100 CONTINUE
  101 CONTINUE
C
C CHECK TOTAL ELAPSED TIME
      IF(TIME.LT.TOTIM)THEN
      DT=DT*TFAC
      GO TO 10
      END IF
C
  200 RETURN
      END
```

```
C ***********************************************************************
C
      SUBROUTINE PRTOUT
C
C ***********************************************************************
C
C THIS SUBROUTINE PRINTS NODAL CONCENTRATIONS TO THE GENERAL OUTPUT FILE
C AND CONCENTRATION, FLUID HEADS, OSMOTIC POTENTIALS, AND FLUID PRESSURE
C TO SPECIFIC OUTPUT FILES FOR EACH TIME STEP
C
$INCLUDE :'CPARM.TXT'
$INCLUDE :'TPARM.TXT'
$INCLUDE :'FPARM.TXT'
C
      DIMENSION PRESS(200)
C CALCULATION OF CONTAMINANT MASS SUM
      SUM=0.0
      DO 10 M=1,NUMEL
      NM=MAT(M)
      M1=M+1
      CAVG=(CT2(M)+CT2(M1))/2.
      RL=ABS(Y(M)-Y(M1))
      SUM=SUM+CAVG*RL*POR(NM)
   10 CONTINUE
C
C CALCULATION OF EXCESS PWP, PRESSURE HEAD
      DO 20 N=1,NUMNP
      PRESS(N)= FH2(N)-Y(N)
   20 CONTINUE
C
C OUPUT
      WRITE(16,100)TIME
C      WRITE(16,110)SUM,(CT2(I),I=1,NUMNP)
Cc       WRITE(16,120)(PRESS(I),I=1,NUMNP)
Cc       WRITE(16,130)(VEL(I),I=1,NUMEL)
      WRITE(19,140)TIME,(CT2(I),I=1,NUMNP)
      WRITE(20,140)TIME,(FH2(I),I=1,NUMNP)
C      WRITE(23,140)TIME,(OPIT(I),I=1,NUMNP)
C      WRITE(24,140)TIME,(PRESS(I),I=1,NUMNP)
      WRITE(25,150)TIME,(VEL(I),I=1,NUMEL)
C
  100 FORMAT(//,16H ELAPSED TIME = ,E10.3,'SEC',/40(1H*))
  110 FORMAT(/,' NODAL CONCENTRATIONS:',/,20(1H*),/
     1' (TOTAL CONTAMINANT MASS =',E10.3,')'/,5(F10.3))
  120 FORMAT(//,' NODAL PRESSURES:'/,16(1H*)/,5(F10.3))
  130 FORMAT(//,' ELEMENT VELOCITES:'/,18(1H*)/,5(E10.3))
  140 FORMAT(//E10.3,/5(E10.3))
  150 FORMAT(//E10.3,/5(E10.3))
C
      RETURN
      END
```

```
C ***************************************************************************
C
      SUBROUTINE RSTIF
C
C ***************************************************************************
C
C THIS SUBROUTINE FORMS THE R GLOBAL MATRIX FOR THE TRANSPORT EQUATION
C
$INCLUDE :'CPARM.TXT'
$INCLUDE :'TPARM.TXT'
$INCLUDE :'FPARM.TXT'
C
      DIMENSION RE(2,2),RTE(2,2),VE(2,2)
C
C SET ELEMENT MATRIX VALUES
      RTE(1,1)=1.
      RTE(1,2)=-1.
      RTE(2,1)=-1.
      RTE(2,2)=1.
      VE(1,1)=-1.
      VE(1,2)=1.
      VE(2,1)=-1.
      VE(2,2)=1.
C
C INTIALIZE R MATRIX
      DO 10 J=1,3
      DO 10 I=1,NUMNP
      R(I,J)=0.0
   10 CONTINUE
C
      DO 20 M=1,NUMEL
      M1=M+1
      NM=MAT(M)
      RL=ABS(Y(M)-Y(M1))
      DR=D(M)/(RTRD(NM)*RL)
      VR=VEL(M)/(RTRD(NM)*2.)
C
C FORM ELEM MATRIX
      DO 30 I=1,2
      DO 30 J=1,2
      RE(I,J)=RTE(I,J)*DR+VE(I,J)*VR
   30 CONTINUE
C
C ADD ELEMENT MATRIX INTO GLOBAL R MATRIX
      DO 40 II=1,2
      I=II+M-1
      DO 40 JJ=1,2
      J=JJ-II+2
      R(I,J)=R(I,J)+RE(II,JJ)
   40 CONTINUE
   20 CONTINUE
C
      RETURN
      END
```

```
C ***********************************************************************
C
      SUBROUTINE SWELLCHK
C
C ***********************************************************************
C
C THIS SUBROUTINE CHECKS FOR EVERY ELEMENT WHETHER THE NET FLOW OUT OFF THE
C ELEMENT IS POSTIVE (CONSOLIDATION) OR NEGATIVE (SWELLING).  IF IT IS
C NEGATIVE THEN THE VALUE OF THE SWELLING COEFFICIENT CMS IS STORED IN THE
C THE ELEMENT MATRIX CLH IN PLACE OF THE COMPRESSIBLITY CMS FOR THAT ELEMENT.
C THE STIFFNESS MATRICES ARE THEN REFORMED BY CALLING KTSTIF.
C
$INCLUDE :'CPARM.TXT'
$INCLUDE :'TPARM.TXT'
$INCLUDE :'FPARM.TXT'
C
C  CHECK TO TOP AND BOTTOM ELEMENTS SEPARATELY
      NM=MAT(1)
      IF((VEL(2)-VEL(1)).LT.0)THEN
      CLH(1)=CMS(NM)
      ELSE
      CLH(1)=CMV(NM)
      END IF
C
      NM1=NUMEL-1
      NM=MAT(NUMEL)
      IF((VEL(NUMEL)-VEL(NM1)).LT.0)THEN
      CLH(NUMEL)=CMS(NM)
      ELSE
      CLH(NUMEL)=CMV(NM)
      END IF
C
C  CHECK ELEMENTS 2 TO NUMEL-1
      NM1=NUMEL-1
      DO 10 I=2,NM1
      NM=MAT(I)
      IP1=I+1
      IM1=I-1
      IF((VEL(IP1)-VEL(IM1)).LT.0)THEN
      CLH(I)=CMS(NM)
      ELSE
      CLH(I)=CMV(NM)
      END IF
   10 CONTINUE
C
      CALL KTSTIF
C
      RETURN
      END
```

```
C ***************************************************************************
C
      SUBROUTINE TABKPMP
C
C ***************************************************************************
C
C THIS SUBROUTINE DEFINES THE ELEMENT OSMOTIC PERMEABILITIES AND
C COMPRESSIBILITES BASED ON A TABLE FORM OF CONCENTRATION VS THESE VALUES
C FOR EACH MATERIAL.  IT LOCATES THE INTERVAL OF CONENTRATION IN THE
C TABLE WHICH BORDERS THE AVERAGE ELEMENTAL CONCENTRATION.  THE VALUE OF
C KP IS THEN INTERPOLATED. THE VALUE OF MP IS TAKEN AS THE VALUE AT THE
C LOWER END OF THE INTERVAL
C
$INCLUDE :'CPARM.TXT'
$INCLUDE :'TPARM.TXT'
$INCLUDE :'FPARM.TXT'
C
      DIMENSION CAVG(100)
C
C CALCULATE THE AVGERAGE ELEMENTAL CONCENTRATIONS
      DO 10 I=1,NUMEL
      CAVG(I)=(CIT(I)+CIT(I+1))/2.
   10 CONTINUE
C
C INTERPOLATE THE ELEMENTAL PKP AND CMP VALUES
C
      DO 100 M=1,NUMEL
      NM=MAT(M)
C   FIND THE APPROPRIATE CONCENTRATION INTERVAL
      DO 20 N=2,NIP
      IF(CAVG(M).LT.CTAB(NM,N))THEN
      K=N-1
      PK=TABKP(NM,K)
      PN=TABKP(NM,N)
      RATIO=(CAVG(M)-CTAB(NM,K))/(CTAB(NM,N)-CTAB(NM,K))
      PKP(M)=PK+RATIO*(PN-PK)
      CMP(M)=TABMP(NM,K)
      GO TO 100
      END IF
   20 CONTINUE
  100 CONTINUE
C
      RETURN
      END
```

```
C ***********************************************************************
C
      SUBROUTINE TRASOL
C
C ***********************************************************************
C
C THIS SUBROUTINE UPDATES THE CACULATION OF THE ELEMENTAL DIFFUSION
C COEFFICIENT, THEN FORMS THE GLOBAL R MATRIX, COMBINES THE RIGHT AND
C LEFT SIDES OF THE TRANSPORT EQUATION, ADDING IN THIRD TYPE B.C OR
C MODIFYING FOR FIRST TYPE B.C. AND THEN SOLVING FOR CONCENTRATIONS
C
$INCLUDE :'CPARM.TXT'
$INCLUDE :'TPARM.TXT'
$INCLUDE :'FPARM.TXT'
C
C CALCULATE THE NEW ELEMENTAL DIFFUSION COEFFICIENT
      DO 10 M=1,NUMEL
      NM=MAT(M)
      AVEL=ABS(VEL(M))
      D(M)=AL(NM)*AVEL+DD(NM)
   10 CONTINUE
C
C INITIALIZE A AND B MATRICES
      DO 15 I=1,NUMNP
      B(I)=0.0
      DO 15 J=1,3
      A(I,J)=0.0
   15 CONTINUE
C
C FORM GLOBAL R MATRIX
      CALL RSTIF
C
C SET INTO B MATRIX ALL CONTAMINANT FLUXES QT THESE ARE MODIFIED
C FOR B.C
      DO 8 I=1,NUMNP
      B(I)=QT(I)
    8 CONTINUE
```

```
C ADD IN THIRD TYPE BOUNDARY CONDITIONS
      IF(KT1.EQ.0)THEN
      R(1,2)=R(1,2)+VEL(1)
      NM1=MAT(1)
      B(1)=QF(1)*QT(1)/POR(NM1)
      END IF
      IF(KTN.EQ.0)THEN
      R(NUMNP,2)=R(NUMNP,2)+VEL(NUMEL)
      NM2=MAT(NUMEL)
      B(NUMNP)=QF(NUMNP)*QT(NUMNP)/POR(NM2)
      END IF
C
C FORM RIGHT SIDE (A) AND LEFT SIDE (B) GLOBAL COEFF MATRICES
      DO 20 I=1,NUMNP
      DO 20 JJ=1,3
      J=I-2+JJ
      IF(J.GT.0)THEN
      B(I)=B(I)+((-1.+ET)*R(I,JJ)+STT(I,JJ)/DT)*CT1(J)
      A(I,JJ)=ET*R(I,JJ)+STT(I,JJ)/DT
      END IF
   20 CONTINUE
C
C MODIFY
      IF(KT1.EQ.1)THEN
      CALL MODIFY(1,QT(1))
      END IF
      IF(KTN.EQ.1)THEN
      CALL MODIFY(NUMNP,QT(NUMNP))
      END IF
C
C SOLVE FOR CONCENTRATIONS
      CALL TSOLVE(0)
C
      DO 30 I=1,NUMNP
      CT2(I)=B(I)
   30 CONTINUE
C
      RETURN
      END
```

```
C ***********************************************************************
C
      SUBROUTINE TSOLVE(KS)
C
C ***********************************************************************
C
C THE SOLUTION IS OBTAINED IN THIS ROUTINE BY THE THOMAS METHOD FOR A
C TRIDIAGONAL SYMMETRIC OF NON-SYMMETRIC MATRIX EQUATION OF THE FORM
C A X = B. FOR THE SOLUTION OF THE FLOW EQUATION, DECOMPOSITION OF
C THE A MATRIX IS ONLY REQUIRED ONE PER TIME STEP IF KH AND KP ARE
C INDEPENDANT OF CONCENTRATION
C
$INCLUDE :'CPARM.TXT'
$INCLUDE :'TPARM.TXT'
$INCLUDE :'FPARM.TXT'
C
      DIMENSION DECA(201,3)
C
C DECOMPOSITION
      IF(KS.EQ.1.AND.NIT.GT.1) THEN
      DO 10 J=1,3
      DO 10 I=1,NUMNP
      A(I,J)=DECA(I,J)
   10 CONTINUE
      GO TO 40
      END IF
C
      DO 20 I=2,NUMNP
      A(I,1)=A(I,1)/A(I-1,2)
      A(I,2)=A(I,2)-(A(I,1)*A(I-1,3))
   20 CONTINUE
C
      IF(KS.EQ.1.AND.NIT.EQ.1)THEN
      DO 30 J=1,3
      DO 30 I=1,NUMNP
      DECA(I,J)=A(I,J)
   30 CONTINUE
      END IF
C
C SOLVE
C FORWARD SUBSTITUTION
   40 DO 50 I=2,NUMNP
      B(I)=B(I)-(A(I,1)*B(I-1))
   50 CONTINUE
C
C BACKWARD SUBSTITUTION
      B(NUMNP)=B(NUMNP)/A(NUMNP,2)
      DO 60 I=2,NUMNP
      J=NUMNP-I+1
      B(J)=(B(J)-(A(J,3)*B(J+1)))/A(J,2)
   60 CONTINUE
C
      RETURN
      END
```

```
C ***********************************************************************
C
      SUBROUTINE TREAD
C
C ***********************************************************************
C
C THIS SUBROUTINE READS IN THE MATERIAL PROPERTIES AND INTIAL AND
C BOUNDARY CONCENTRATION AND FLUXES FOR THE SOLUTION OF THE TRANSPORT
C EQUATION
C
$INCLUDE :'CPARM.TXT'
$INCLUDE :'TPARM.TXT'
$INCLUDE :'FPARM.TXT'
C
C MATERIAL PROPERTIES FOR POR,AL,RTRD,DD ARE READ IN FREAD.FOR
C
      WRITE(16,200)
      DO 3 I=1,NUMAT
      READ(17,100)POR(I),AL(I),RTRD(I),DD(I)
      WRITE(16,202)POR(I),AL(I),RTRD(I),DD(I)
    3 CONTINUE
C
C READ IN INITIAL CONCENTRATION AND BOUNDARY CONCENTRATIONS
      READ(17,120)I,CT1(I),QT(I)
    5 READ(17,120)J,CT1(J),QT(J)
      IF((J-I).GT.1)THEN
      IP=I+1
      DN=J-I
      DC=(CT1(J)-CT1(I))/DN
      DQ=(QT(J)-QT(I))/DN
      JM=J-1
      DO 10 K=IP,JM
      CT1(K)=CT1(K-1)+DC
      QT(K)=QT(K-1)+DQ
   10 CONTINUE
      ELSE
      END IF
      I=J
      IF(I.LT.NUMNP)THEN
      GO TO 5
      END IF
C
      WRITE(16,210)(I,CT1(I),QT(I),I=1,NUMNP)
C
C ######################################################################
C FORMAT
  100 FORMAT(3F10.2,E10.2)
  120 FORMAT(I5,2F10.2)
C
  200 FORMAT(//,32H TRANSPORT MATERIAL PROPERTIES: ,/,32(1H#),//
     133H    POR       AL     RTRD        DD    ,/33(1H-))
  202 FORMAT(3(2X,F5.2),E10.2)
  210 FORMAT(//,39H INITAL NODAL CONCENTRATIONS AND B.C.: ,/39(1H*),/5X
     1'(NODE,INIT. CONC.,B.C)'//,2(I5,2F10.2))
C
      RETURN
      END
```

B.5.2 VELFIL

```
#nofloatcalls
C  ********************************************************************
C                          V E L F I L
C  VELFIL IS A DATA MANIPULATION PROGRAM. IT TAKES THE ELEMENT VELOCITY
C  FILE (INTERSTITIAL VELOCIIES) FROM THE OSMO2 SIMULATION AND TRANSFORMS
C  THEM INO ONE OF THE FOLLOWING FORMS: - DISPLACEMENT(CM) VS TIME (MIN)
C                                       - CUMMULATIVE BASE FLOW (CM3) VS TIME
C                                       - BASE AND TOP VELOCITIES VS TIME
C  THE REQUIRED INPUT DATA IS THE NAME OF INPUT AND OUTPUT FILES, THE
C  NUMBER OF TIME GROUPS, ELEMENTS AND THE POROSITY OF THE FIRST AND LAST
C  ELEMENTS
C
C ***** TIME IS OUTPUT IN MINUTES TO COMPARE WITH TEST DATA****
C ***** DEFLECTION IS OUTPUT IN CM TO COMPARE WITH TEST DATA **
C
      IMPLICIT REAL*8 (A-H,O-Z)
      DIMENSION V(310),V1(105),VN(105),T(105),QBTOT(105)
      DIMENSION DISP(105)
C
C ##########################################################################
C  OPEN FILES FOR INPUT OF INTERSTITIAL VELOCITIES, AND OUTPUT OF DEFLECTIONS
C  AND FLOW
      CHARACTER*12 INFIL,FLOFIL,DEFFIL,TITLE
      WRITE(*,111)
      READ(*,1111)INFIL
      WRITE(*,112)
      READ(*,1111)FLOFIL
      WRITE(*,113)
      READ(*,1111)DEFFIL
C
      OPEN(UNIT=20,FILE=INFIL,STATUS='OLD')
      OPEN(UNIT=21,FILE=FLOFIL,STATUS='NEW')
      OPEN(UNIT=22,FILE=DEFFIL,STATUS='NEW')
C
  111 FORMAT(5X,32HENTER INPUT VELOCITY FILE NAME:  ,$)
 1111 FORMAT(A12)
  112 FORMAT(5X,34HENTER OUTPUT BASE FLOW FILE NAME: ,$)
  113 FORMAT(5X,35HENTER OUTPUT DEFLECTION FILE NAME: ,$)

C ##########################################################################
C
C READ NUMBER OF DATA GROUPS TO ALTER,NUMBER OF NODES,SOIL POROSITY
C READ TITLE
      WRITE(*,4)
    4 FORMAT('TYPE IN TITLE OF SIMULATION')
      READ(*,1111)TITLE
      WRITE(21,98)TITLE
   98 FORMAT(A12)
      WRITE(22,98)TITLE
      WRITE(*,5)
    5 FORMAT('TYPE IN NO.OF GROUPS,NUMEL,SOIL POROSITY: ELEM 1 AND N')
      READ(*,*)NG,NUMEL,POR1,PORN
      WRITE(*,6)
    6 FORMAT('TYPE IN AREA OF SAMPLE (CM2)')
      READ(*,*)AS
C
      WRITE(*,15)NG,NUMEL,POR1,PORN
   15 FORMAT('NO OF GROUPS=',I5,'NUMEL =',I5,'SOIL POROSITY:',
     1' ELEM 1 =',F5.2,'ELEM N =',F5.2)
C     READ GROUPS OF DATA AND OUTPUT THEM TO OUTFIL
      DO 20 I=1,NG
      READ(20,19)T(I)
   19 FORMAT(//E10.3)
      READ(20,30)(V(J),J=1,NUMEL)
   30 FORMAT(5(F10.3))
      VN(I)=V(NUMEL)
      V1(I)=V(1)
   20 CONTINUE
```

```
C WRITE VELOCITIES, FLUXES AND TOTOL FLUXES
C      WRITE(21,45)
C   45 FORMAT(1H ,//,'   TIME      N1 VEL       DQ         Q1       NN VEL
C     1    DQ        QN     ',//,80(1H*))
       V1I=0.0
       VNI=0.0
       TI=0.0
       Q1=0.0
       QN=0.0
       DO 40 I=1,NG
       DT=T(I)-TI
       D1Q=(V1I+V1(I))/2.*DT*POR1
       DNQ=(VNI+VN(I))/2.*DT*PORN
C FOR FIRST TIME INCREMENT USE FULL VELOCITY OVER FIRST DT
       IF(I.EQ.1)THEN
       D1Q=D1Q*2.
       DNQ=DNQ*2.
       ELSE
       END IF
       Q1=Q1+D1Q
       QN=QN+DNQ
       DISP(I)=(Q1-QN)
C  KEEP TOTAL OF BASE FLUX TOTAL (CM3/CM2)
       QBTOT(I)=Q1
C
C      WRITE(21,50)T(I),V1(I),D1Q,Q1,VN(I),DNQ,QN
C   50 FORMAT(E10.3,2(E10.3,2F10.5))
       V1I=V1(I)
       VNI=VN(I)
       TI=T(I)
   40 CONTINUE
C
C PRINT OUT VELOCITY TIME
C REDUCE TIME TO MINUTES AND DEFL TO CM., AND BASE FLOW TO CM3
       DO 43 I=1,NG
       QBTOT(I)=QBTOT(I)*100*AS
       DISP(I)=DISP(I)*100.
       T(I)=T(I)/60.
   43 CONTINUE
C
C      WRITE(21,60)(T(I),V1(I),I=1,NG)
C   60 FORMAT(1H ,'"BOTTOM VELOCITIES".',/,5(1X,E10.3,',',E10.3))
C      WRITE(21,61)(T(I),VN(I),I=1,NG)
C   61 FORMAT(1H ,'"TOP VELOCITES".',/,5(1X,E10.3,',',E10.3))
C ##################################
C PRINT OUT TIME VS DISPLACEMENT
       WRITE(22,58)
   58 FORMAT(1H ,'X LABEL "TIME (MIN)".',/,' Y LABEL "DEFLECTION (CM)".'
     1/,' X AXIS IS LOG.',/,' INPUT DATA.')
       WRITE(22,70)(T(I),DISP(I),I=1,NG)
C ######################################
C WRITE OUT CUMMULATIVE BASE FLOW VS TIME
       WRITE(21,59)
   59 FORMAT('CUMMULATIVE BASE FLOW VS TIME')
       WRITE(21,71)(T(I),QBTOT(I),I=1,NG)
   71 FORMAT(E10.3,',',E10.3)
   70 FORMAT(E10.3,',',E10.3)
C
       WRITE(21,101)
       WRITE(22,101)
  101 FORMAT(1H ,'END OF DATA.')
       CLOSE(UNIT=20)
       CLOSE(UNIT=21)
       CLOSE(UNIT=22)
       END
```

B.5.3 TELFIL

```
      DIMENSION C(200),X(200)
C
      CHARACTER*12 INFIL,OUTFIL
      WRITE(*,111)
      READ(*,1111)INFIL
      WRITE(*,112)
      READ(*,1111)OUTFIL
C
      OPEN(UNIT=20,FILE=INFIL,STATUS='OLD')
      OPEN(UNIT=21,FILE=OUTFIL,STATUS='NEW')
C
  111 FORMAT(5X,24HENTER INPUT FILE NAME: ,$)
 1111 FORMAT(A12)
  112 FORMAT(5X,24HENTER OUTPUT FILE NAME: ,$)
C
C READ NUMBER OF DATA GROUPS TO ALTER,NUMBER OF NODES, DX
      WRITE(*,5)
    5 FORMAT('TYPE IN NO.OF GROUPS,NUMNP,DX')
      READ(*,*)NG,NUMNP,DX
C   10 FORMAT(I5,I5,F5.2)
C
      WRITE(*,15)NG,NUMNP,DX
   15 FORMAT('NO OF GROUPS=',I5,'NUMNP =',I5,'DX =',F5.2)
C     READ GROUPS OF DATA AND OUTPUT THEM TO OUTFIL IN TELAGRAPH
C     FORMAT
C PRINT INPUT DATA. STATEMENT
      WRITE(21,39)
   39 FORMAT(12HINPUT DATA. )
      ISS=0
      DO 20 I=1,NG
      READ(20,19)TIME
   19 FORMAT(//E10.3)
      TIME=TIME/60.
      READ(20,30)(C(J),J=1,NUMNP)
C INTERACTIVE SELECTION OF TIMES TO PLOT( LAST IS MANDATORY)
      IF(I.EQ.NG) GO TO 31
      WRITE(*,34)TIME
   34 FORMAT('DO YOU WANT TIME = ',E10.3,' (MIN)? (1=Y,0=NO,2=SS)')
C ISS IS CONTROL FOR STEADY STATE VALUES ONLY
      IF(ISS.EQ.1)GO TO 20
      READ(*,33)IQ1
   33 FORMAT(I5)
      IF(IQ1.EQ.2) THEN
      ISS=1
      GO TO 20
      END IF
      IF(IQ1.EQ.0) GO TO 20
   30 FORMAT(5(F10.3))
   31 CONTINUE
C
C OUTPUT TO TEL FILE
      DO 40 N=1,NUMNP
      X(N)=(N-1)*DX
   40 CONTINUE
      WRITE(21,49)TIME
   49 FORMAT( '"T =  ',E10.3,'(MIN)"')
      WRITE(21,50)(X(N),C(N),N=1,NUMNP)
   50 FORMAT(F7.3,',',F7.3)
C
   20 CONTINUE

C WRITE END OF DATA.
      WRITE(21,60)
   60 FORMAT('END OF DATA.')
      CLOSE(UNIT=20)
      CLOSE(UNIT=21)
      END
```

B.5.4 NODVAL

```
C  ***********************************************************************
C                              N O D V A L
C  NODVALIS A DATA MANIPULATION PROGRAM. IT TAKES ANY OUTPUT FILE AND
C  ASSEMBLES THE VALUE OF A PARTICULAR NODE WITH TIME
C
      IMPLICIT REAL*8 (A-H,O-Z)
      DIMENSION NODES(10),VALNOD(100,10),V(100),T(100)
C
C ######################################################################
C  OPEN FILES FOR INPUT OF INTERSTITIAL VELOCITIES, AND OUTPUT OF DEFLECTIONS
C  AND FLOW
      CHARACTER*12 INFIL,OUTFIL,TITLE
      WRITE(*,111)
      READ(*,1111)INFIL
      WRITE(*,112)
      READ(*,1111)OUTFIL
C
      OPEN(UNIT=20,FILE=INFIL,STATUS='OLD')
      OPEN(UNIT=21,FILE=OUTFIL,STATUS='NEW')
C
  111 FORMAT(5X,'ENTER INPUT FILE NAME: ',$)
 1111 FORMAT(A12)
  112 FORMAT(5X,'ENTER OUTPUT FILE NAME: ',$)
C
C ######################################################################
C
C READ NUMBER OF DATA GROUPS TO ALTER,NUMBER OF NODES
C READ TITLE
      WRITE(*,4)
    4 FORMAT('TYPE IN TITLE OF SIMULATION')
      READ(*,1111)TITLE
      WRITE(21,98)TITLE
   98 FORMAT(A12)
      WRITE(*,5)
    5 FORMAT('TYPE IN NO.OF GROUPS,NUMNP')
      READ(*,*)NG,NUMNP
C READ IN NODES FOR WHICH VALUES TO BE ASSEBLED
      WRITE(*,6)
    6 FORMAT('NO. OF NODES TO ASSEMBLE VALUES FOR?')
      READ(*,*)NN
      WRITE(*,7)
    7 FORMAT('TYPE IN NODES FOR WHICH VALUES WITH TIME TO BE ASSEMBLED')
      DO 8 I=1,NN
      READ(*,*)NODES(I)
    8 CONTINUE
C
C     READ GROUPS OF DATA AND OUTPUT THEM TO OUTFIL
      DO 15 I = 1,NG
      READ(20,19) T(I)
   19 FORMAT(//E10.3)
      READ(20,30) (V(J),J=1,NUMNP)
   30 FORMAT(5F10.3)
      DO 16 NI = 1,NN
      NOD=NODES(NI)
      VALNOD(I,NI)=V(NOD)
   16 CONTINUE
   15 CONTINUE
C
C PRINT OUT TIME VS NODAL VALUES
      WRITE(21,58) TITLE
   58 FORMAT(1H ,A12)
      WRITE(21,59) (NODES(N),N=1,NN)
   59 FORMAT(1H ,'OUTPUT NODES:',/,10X,10(I5,5X))
      DO 61 I=1,NG
      WRITE(21,60) T(I),(VALNOD(I,N),N=1,NN)
   60 FORMAT(E10.3,10F10.3)
   61 CONTINUE
C
      CLOSE(UNIT=20)
      CLOSE(UNIT=21)
      STOP
      END
```

APPENDIX C

C.1 Calibration of Soil Moisture Pressure Gauges

DATE: APRIL 17, 1986
DEAD LOAD TESTER - PRESUREMENTS LTD, BROOKMANS PARK, EN

APPLIED PRESSURE (KPA)	SETUP 1 GAUGE (BAR)	SETUP 2 GAUGE (BAR)	SETUP 2 ADJUSTED (BAR)
0	0	0.02	0
10	0.095	0.12	0.1
20	0.198	0.22	
30	0.3	0.32	0.298
40	0.4	0.418	
50	0.5	0.51	
60	0.6	0.618	
70	0.7	0.71	0.695
80	0.8	0.815	

C.3 Calibration of Celesco PLC Pressure Transducers

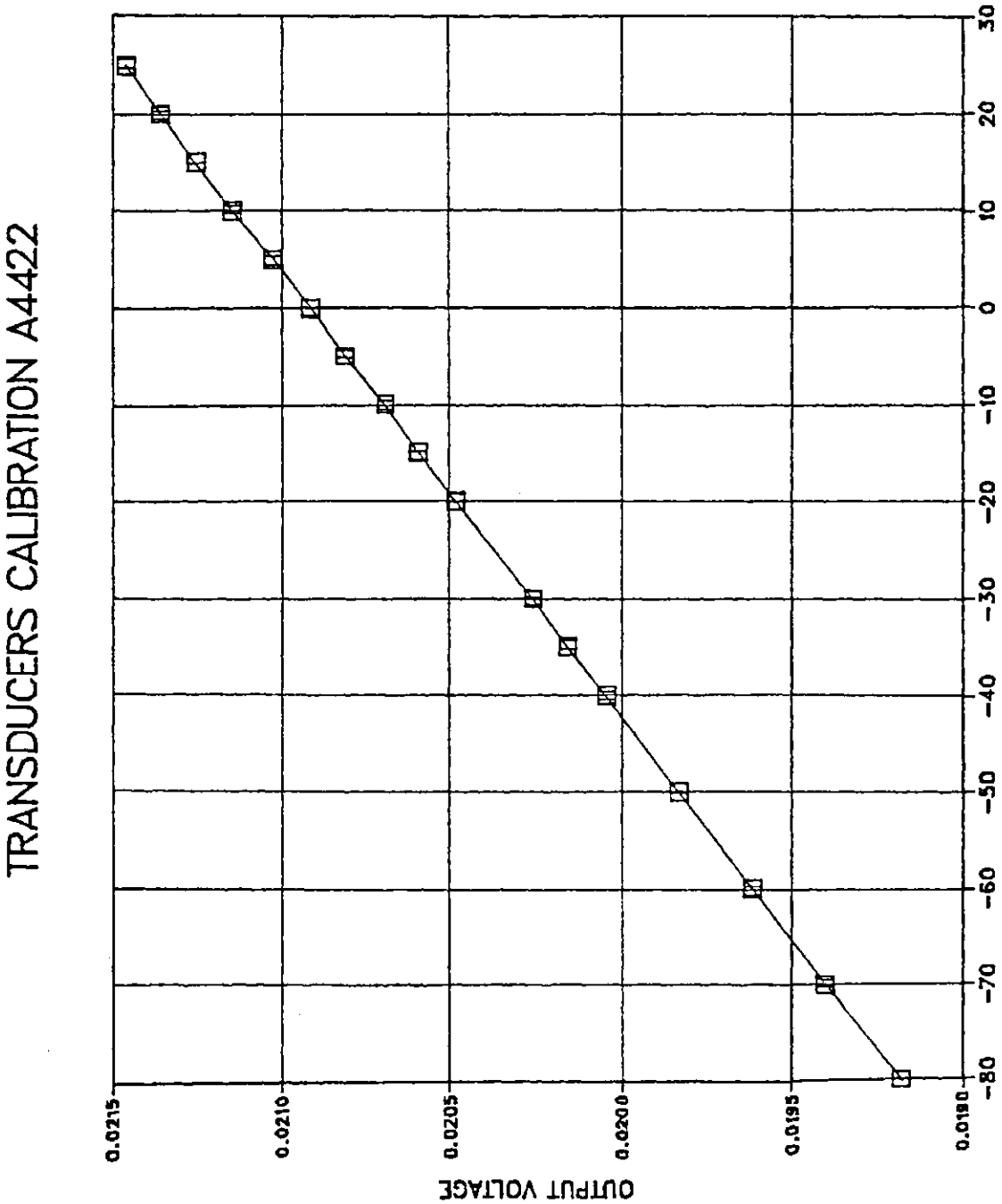

Figure C.1 Transducer A4422 Calibration

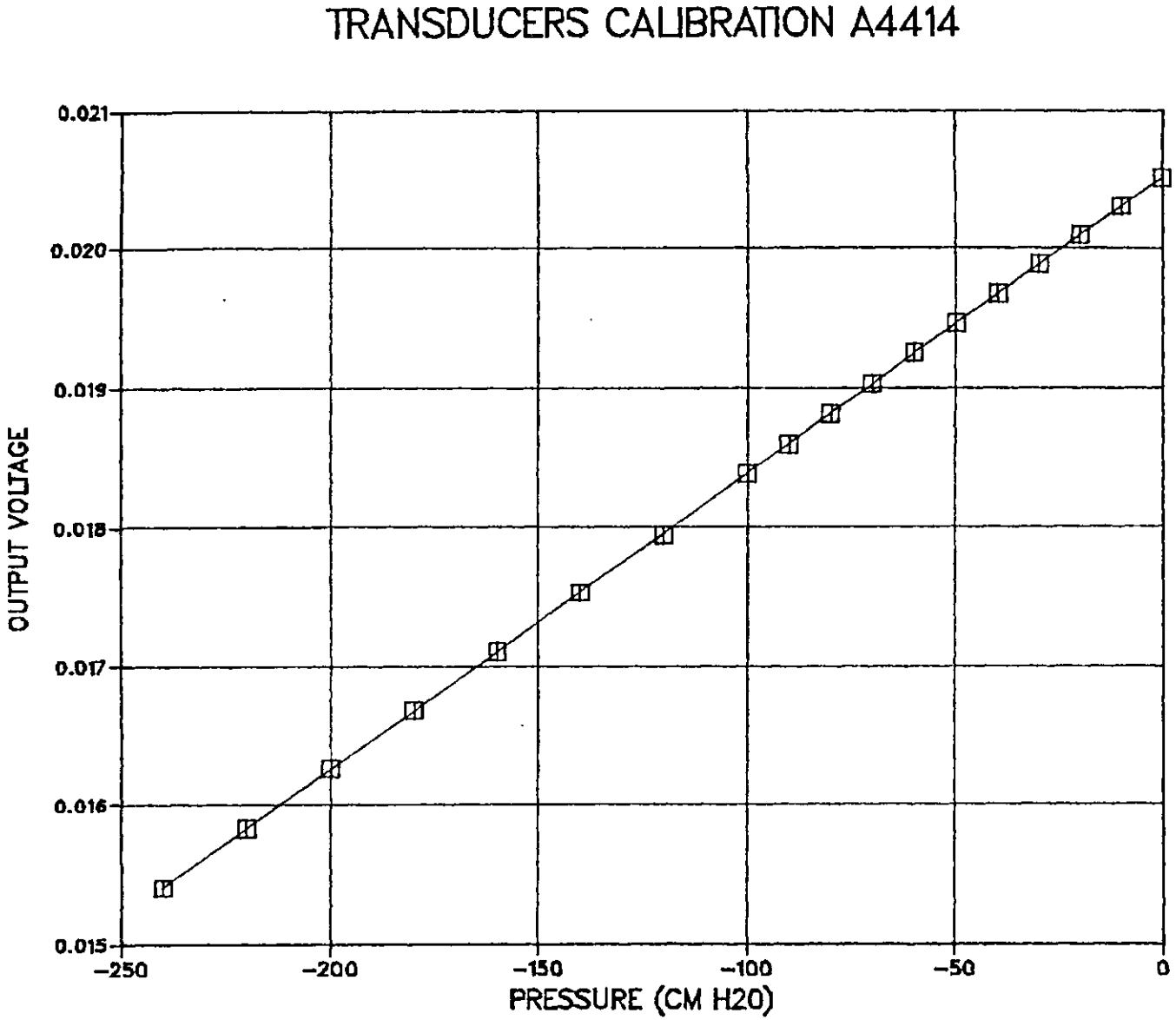

Figure C.2 Transducer A4414 Calibration

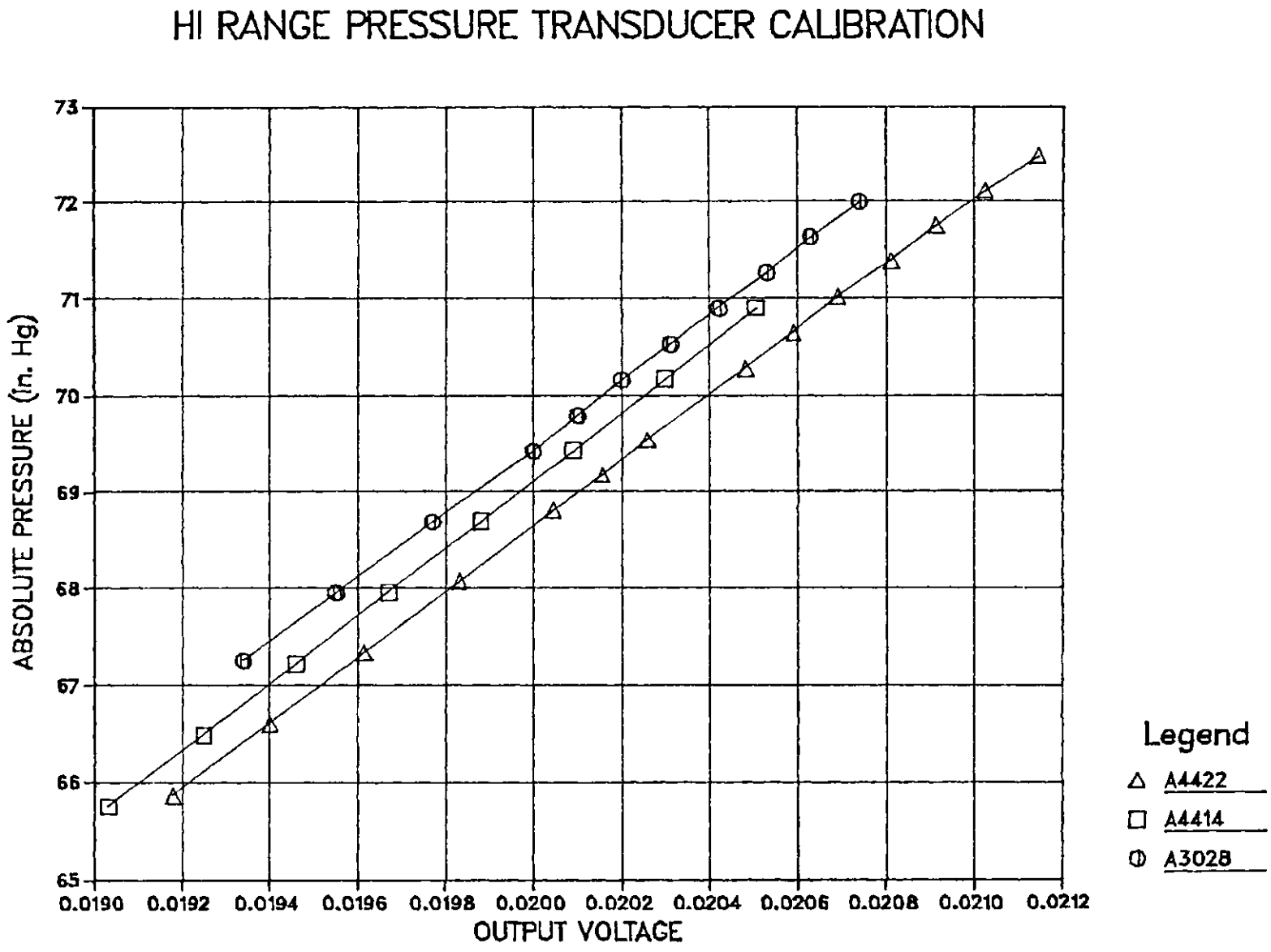

Figure C.3 Hi Range Pressure Transducer Calibration

Table C.1 Specifications Sheet for Windsor Fine Granulated Salt

TECHNICAL DATA SHEET IV-1(c)
EX: Regina
802 - 20 kg
801 - 40 kg
#2302 - Tote
#2002 - Bulk
#2010 - Bulk

Table C.1 FINE GRANULATED SALT

Chemical Analysis		Typical	Limits
Calcium Sulphate	$CaSO_4$	0.03 %	
Calcium Chloride	$CaCl_2$	0.04 %	
Magnesium Chloride	$MgCl_2$	0.02 %	
Potassium Chloride	KCl	0.6 %	
Filter Pad - APHA Test		0.20 mg	
Iron	Fe	0.4 ppm	
Copper	Cu	0.3 ppm	
Moisture	H_2O	0.03 %	
Net Salt - Dry Basis	NaCl	99.30 %	99.2 % min
Added: anti-caking agent			
Yellow prussiate of soda		3.0 ppm	13.0 ppm max

Screen Analysis

	U.S. Standard	Opening mu	Typical %	Limits %
On Mesh	20	850	0	2 max
	30	600	0 - 5	
	40	425	30 - 50	
	50	300	35 - 55	
	60	250	5 - 20	
Pass Mesh	60	250	0 - 15	20 max

Other Data

1. A screened, vacuum-evaporated cube salt. Particular suitable for use in automatic brinemaker systems. Available on special order, without YPS, #800 - 40 kg, #2301 - tote and #2001 - bulk.
2. Bulk Density - Packed: 1220 to 1300 kg/m^3 (76 to 81 lb/ft^3).
3. Crystal Surface Area per kg (est.) 7.7 m^2 - (84 ft^2).
4. Rate of solution (Swift Test) 55 to 75 %.
5. Morton name of equivalent grade - Purex Salt.
6. Available in 20 & 40 kg bags, tote and bulk.
7. This is our general purpose evaporated salt.
8. #800, #801 & #802 are approved for Kosher and supervised for Passover, Kashruth registration COR 92-P.
9. Conforms to Canada Food & Drug Regulations, and Food Chemicals Codex.

March 1985

APPENDIX D

D.1 Consolidation Summary Sheets

CONSOLIDATION SUMMARY SHEET

SAMPLE: REGINA CLAY 1

BASE DATA:

		END OF TEST DATA:	
SAMPLE AREA:	31.67		
RELATIVE DENSITY:	2.8	WEIGHT TOTAL:	87.98
FINAL CONC(M) SOL'N:	3.5	WEIGHT DRY:	58.65
CONC. WATER (GM/L):	927.8	FINAL SAMPLE HEIGHT:	1.3392

CALCULATED DATA:

WEIGHT WATER:	29.33	TRUE WEIGHT SOLIDS:	52.17735
APPARENT W/C:	50.01%	HEIGHT SOLIDS:	0.588404
VOLUME SOL'N:	31.61241	HEIGHT SOL'N:	0.750795
WEIGHT SALT:	6.472642	FINAL VOID RATIO:	1.275985
TRUE W/C:	56.21%	FINAL W/C:	42.28%

APPLIED STRESS	D100 READING CM	CORRECTED READING CM	DEFLECTION	VOID RATIO	WATER CONTENT %	POROSITY
0						
7.9	1.643	1.6435	0.46577	2.067566	73.84	0.674008
23.3	1.556	1.5645	0.38677	1.933305	69.05	0.659087
54.3	1.429	1.443	0.26527	1.726814	61.67	0.633271
103.8	1.3415	1.3345	0.15677	1.542417	55.09	0.606673
202.9	1.206	1.232	0.05427	1.368217	48.86	0.577741
202.9	1.1513	1.17773	0	1.275985	42.28	0.560629
					0.038945	

CONSOLIDATION SUMMARY SHEET

SAMPLE: REGINA CLAY 1

BASE DATA:

SAMPLE AREA:	31.67	END OF TEST DATA:	
RELATIVE DENSITY:	2.8	WEIGHT TOTAL:	87.98
FINAL CONC(M) SOL'N:	3.5	WEIGHT DRY:	58.65
CONC. WATER (GM/L):	927.8	FINAL SAMPLE HEIGHT:	1.3392

CALCULATED DATA:

WEIGHT WATER:	29.33	TRUE WEIGHT SOLIDS:	52.17735
APPARENT W/C:	50.01%	HEIGHT SOLIDS:	0.588404
VOLUME SOL'N:	31.61241	HEIGHT SOL'N:	0.750795
WEIGHT SALT:	6.472642	FINAL VOID RATIO:	1.275985
TRUE W/C:	56.21%	FINAL W/C:	42.28%

APPLIED STRESS	D100 READING CM	CORRECTED READING CM	DEFLECTION	VOID RATIO	WATER CONTENT %	POROSITY	mv /kPa
0							
7.9	1.643	1.6435	0.46577	2.067566	73.84	0.674008	
23.3	1.556	1.5645	0.38677	1.933305	69.05	0.659087	2.84E-03
54.3	1.429	1.443	0.26527	1.726814	61.67	0.633271	2.27E-03
103.8	1.3415	1.3345	0.15677	1.542417	55.09	0.606673	1.37E-03
202.9	1.206	1.232	0.05427	1.368217	48.86	0.577741	6.91E-04
202.9	1.1513	1.17773	0	1.275985	42.28	0.560629	
					0.038945		

CONSOLIDATION SUMMARY SHEET

SAMPLE: REGINA CLAY 2

BASE DATA:

SAMPLE AREA:	31.67	END OF TEST DATA:	
RELATIVE DENSITY:	2.8	WEIGHT TOTAL:	58.52
FINAL CONC(M) SOL'N:	3.5	WEIGHT DRY:	41.51
CONC. WATER (GM/L):	927.8	FINAL SAMPLE HEIGHT:	1.0297

CALCULATED DATA:

WEIGHT WATER:	17.01	TRUE WEIGHT SOLIDS:	37.75617
APPARENT W/C:	40.98%	HEIGHT SOLIDS:	0.425776
VOLUME SOL'N:	18.33369	HEIGHT SOL'N:	0.603923
WEIGHT SALT:	3.753823	FINAL VOID RATIO:	1.418403
TRUE W/C:	45.05%	FINAL W/C:	47.00%

APPLIED STRESS	D100 READING CM	CORRECTED READING CM	DEFLECTION	VOID RATIO	WATER CONTENT %	POROSITY	mv /kPa
0							
7.75	2.0775	2.0834	0.3747	2.298442	82.09	0.696826	
15.5	2.0275	2.0365	0.3278	2.188290	78.15	0.686352	4.31E-03
23.25	1.986	1.9991	0.2904	2.100451	75.02	0.677466	3.55E-03
52	1.8902	1.9117	0.203	1.895179	67.68	0.654598	2.30E-03
101.6	1.8035	1.833	0.1243	1.710340	61.08	0.631042	1.29E-03
200.7	1.72	1.7587	0.05	1.535836	54.85	0.605652	6.50E-04
200.7	1.67	1.7087	0	1.418403	47.00	0.586504	
				0.046309			

CONSOLIDATION SUMMARY SHEET

SAMPLE: REGINA CLAY 3

BASE DATA:

SAMPLE AREA:	31.67	END OF TEST DATA:	
RELATIVE DENSITY:	2.8	WEIGHT TOTAL:	131.65
FINAL CONC(M) SOL'N:	3.5	WEIGHT DRY:	95.49
CONC. WATER (GM/L):	927.8	FINAL SAMPLE HEIGHT:	2.28

CALCULATED DATA:

WEIGHT WATER:	36.16	TRUE WEIGHT SOLIDS:	87.51009
APPARENT W/C:	37.87%	HEIGHT SOLIDS:	0.986852
VOLUME SOL'N:	38.97391	HEIGHT SOL'N:	1.293147
WEIGHT SALT:	7.979909	FINAL VOID RATIO:	1.310376
TRUE W/C:	41.32%	FINAL W/C:	43.42%

APPLIED STRESS	D100 READING CM	CORRECTED READING CM	DEFLECTION	VOID RATIO	WATER CONTENT %	POROSITY	av /kPa
0							
7.75	1.712	1.7443	0.7995	2.120528	75.73	0.679541	
23.23	1.483	1.5153	0.5705	1.888477	67.45	0.653796	4.80E-03
46.5	1.281	1.3209	0.3761	1.691487	60.41	0.628458	2.93E-03
108	1.102	1.1527	0.2079	1.521046	54.32	0.603339	1.03E-03
199.4	0.894	0.9531	0.0083	1.318787	47.10	0.568740	8.78E-04
199.4	0.8857	0.9448	0	1.310376	43.42	0.567170	
					0.003627		

RC4VOID.WK1

CONSOLIDATION SUMMARY SHEET

SAMPLE: REGINA CLAY 4

BASE DATA:

SAMPLE AREA:	31.67	END OF TEST DATA:	
RELATIVE DENSITY:	2.8	WEIGHT TOTAL:	26.12
FINAL CONC(M) SOL'N:	4.5	WEIGHT DRY:	19.11
CONC. WATER (GM/L):	905.2	FINAL SAMPLE HEIGHT:	0.46

CALCULATED DATA:

WEIGHT WATER:	7.01	TRUE WEIGHT SOLIDS:	17.07135
APPARENT W/C:	36.68%	HEIGHT SOLIDS:	0.192513
VOLUME SOL'N:	7.744144	HEIGHT SOL'N:	0.267486
WEIGHT SALT:	2.038646	FINAL VOID RATIO:	1.389439
TRUE W/C:	41.06%	FINAL W/C:	44.92%

APPLIED STRESS	D100 READING CM	CORRECTED READING CM	DEFLECTION	VOID RATIO	POROSITY	av /kPa
0						
11.2	1.5419	1.5419	0.176	2.303659	0.697305	
26.7	1.4848	1.4955	0.1296	2.062637	0.673484	4.71E-03
50	1.444	1.463	0.0971	1.893818	0.654435	2.37E-03
96.4	1.403	1.431	0.0651	1.727596	0.633376	1.24E-03
200	1.355	1.3919	0.026	1.524494	0.603881	7.19E-04
200	1.329	1.3659	0	1.389439	0.581491	
				0.053497		

CONSOLIDATION SUMMARY SHEET

SAMPLE: REGINA CLAY 5

BASE DATA:

SAMPLE AREA:	31.67	END OF TEST DATA:	
RELATIVE DENSITY:	2.8	WEIGHT TOTAL:	35.94
FINAL CONC(M) SOL'N:	4.5	WEIGHT DRY:	27.21
CONC. WATER (GM/L):	905.2	FINAL SAMPLE HEIGHT:	0.6

CALCULATED DATA:

WEIGHT WATER:	8.73	TRUE WEIGHT SOLIDS:	24.67114
APPARENT W/C:	32.08%	HEIGHT SOLIDS:	0.278216
VOLUME SOL'N:	9.644277	HEIGHT SOL'N:	0.321783
WEIGHT SALT:	2.538856	FINAL VOID RATIO:	1.156592
TRUE W/C:	35.39%	FINAL W/C:	37.39%

APPLIED STRESS	D100 READING CM	CORRECTED READING CM	DEFLECTION	VOID RATIO	WATER CONTENT %	POROSITY	av /kPa
0							
7.74	3.267	3.2949	0.3119	2.277660	81.35	0.694904	
12.67	3.23	3.2613	0.2783	2.156891	77.03	0.683232	7.47E-03
25.9	3.1755	3.2174	0.2344	1.999101	71.40	0.666566	3.78E-03
49.2	3.122	3.1766	0.1936	1.852452	66.16	0.649424	2.10E-03
49.2	3.0832	3.1476	0.1646	1.748217	56.52	0.636127	
98.7	3.0658	3.1394	0.1564	1.718744	55.56	0.632183	2.17E-04
197.9	3.0185	3.1024	0.1194	1.585754	51.27	0.613265	4.93E-04
399.1	2.9515	3.0435	0.0605	1.374048	44.42	0.578778	4.07E-04
802.8	2.891	2.983	0	1.156592	37.39	0.536305	2.27E-04
				0.036542			

CONSOLIDATION SUMMARY SHEET

SAMPLE: REGINA CLAY RC6

BASE DATA:

SAMPLE AREA (CM2):	31.67	END OF TEST DATA:	
RELATIVE DENSITY:	2.8	WEIGHT TOTAL(GM):	36.89
FINAL CONC(M) SOL'N:	4.5	WEIGHT DRY(GM):	28.01
CONC. WATER (GM/L):	905.2	FINAL SAMPLE HT(CM):	0.6

CALCULATED DATA:

WEIGHT WATER(GM):	8.88	CORR. SOLIDS WT(GM):	25.42752
APPARENT W/C:	31.70%	HEIGHT SOLIDS(CM):	0.286746
VOLUME SOL'N(CM3):	9.809986	HEIGHT SOL'N(CM):	0.313253
WEIGHT SALT(GM):	2.582479	FINAL VOID RATIO:	1.092441
TRUE W/C:	34.92%	FINAL W/C:	35.32%

APPLIED STRESS (kPa)	D100 READING (CM)	CORRECTED READING (CM)	DEFLECTION (CM)	VOID RATIO	WATER CONTENT %	POROSITY	av /kPa
0							
11.25	1.815	1.815	0.2818	2.075191	74.11	0.674817	
26.7	1.753	1.7637	0.2305	1.896287	67.72	0.654730	3.77E-03
49.9	1.706	1.725	0.1918	1.761325	62.90	0.637855	2.01E-03
75.7	1.673	1.697	0.1638	1.663678	59.42	0.624579	1.37E-03
100.4	1.645	1.673	0.1398	1.579980	56.43	0.612400	1.27E-03
100.4	1.6139	1.6419	0.1087	1.471522	47.57	0.595391	
199.52	1.593	1.6399	0.1067	1.464547	47.35	0.594245	2.85E-05
397.6	1.5395	1.5846	0.0514	1.271693	41.11	0.559799	3.95E-04
806.4	1.48	1.5332	0	1.092441	35.32	0.522089	1.93E-04
				0.042038			

CONSOLIDATION SUMMARY SHEET

SAMPLE: REGINA CLAY 7

BASE DATA:

SAMPLE AREA (CM2):	31.67	END OF TEST DATA:	
RELATIVE DENSITY:	2.8	WEIGHT TOTAL(GM):	
FINAL CONC(M) SOL'N:	2	WEIGHT DRY(GM):	
CONC. WATER (GM/L):	960.1	FINAL SAMPLE HT(CM):	0.5763

CALCULATED DATA:

WEIGHT WATER(GM):	0	CORR. SOLIDS WT(GM):	-1.22389
APPARENT W/C:	-	HEIGHT SOLIDS(CM):	0.246
VOLUME SOL'N(CM3):	10.46060	HEIGHT SOL'N(CM):	0.3303
WEIGHT SALT(GM):	1.223890	FINAL VOID RATIO:	1.342682
TRUE W/C:	-	FINAL W/C:	46.04%

APPLIED STRESS (kPa)	D100 READING (CM)	CORRECTED READING (CM)	DEFLECTION (CM)	VOID RATIO	WATER CONTENT %	POROSITY	av /kPa
0							
7.73	1.2086	1.2648	0.2943	2.539024	90.68	0.717436	
15.5	1.1664	1.2373	0.2668	2.427235	86.69	0.708219	4.07E-03
23.25	1.1434	1.221	0.2505	2.360975	84.32	0.702467	2.49E-03
54.1	0.9835	1.0775	0.107	1.777642	63.49	0.639982	5.63E-03
103.7	0.9345	1.0361	0.0656	1.609349	57.48	0.616762	1.22E-03
202.7	0.8772	0.9871	0.0166	1.410162	50.36	0.585090	7.71E-04
202.9	0.8606	0.9705	0	1.342682	46.04	0.573138	
				0.027997			

CONSOLIDATION SUMMARY SHEET

SAMPLE: REGINA CLAY B

BASE DATA:

SAMPLE AREA (CM2):	31.67	END OF TEST DATA:	
RELATIVE DENSITY:	2.8	WEIGHT TOTAL(GM):	
FINAL CONC(M) SOL'N:	3.5	WEIGHT DRY(GM):	
CONC. WATER (GM/L):	927.8	FINAL SAMPLE HT(CM):	1.02

CALCULATED DATA:

WEIGHT WATER(GM):	0	CORR. SOLIDS WT(GM):	-3.25583
APPARENT W/C:	ERR	HEIGHT SOLIDS(CM):	0.5179
VOLUME SOL'N(CM3):	15.90150	HEIGHT SOL'N(CM):	0.5021
WEIGHT SALT(GM):	3.255833	FINAL VOID RATIO:	0.969492
TRUE W/C:	0.00%	FINAL W/C:	32.12%

APPLIED STRESS (kPa)	D100 READING (CM)	CORRECTED READING (CM)	DEFLECTION (CM)	VOID RATIO	WATER CONTENT %	POROSITY	av /kPa
0							
7.74	3.396	3.42	0.4882	1.912145	68.29	0.656610	
12.68	3.33	3.3583	0.4265	1.793010	64.04	0.641963	8.28E-03
24.6	3.255	3.2873	0.3555	1.655918	59.14	0.623482	4.12E-03
48.5	3.16	3.1999	0.2681	1.487159	53.11	0.597934	2.66E-03
102.6	3.052	3.1027	0.1709	1.299478	46.41	0.565118	1.39E-03
201.7	2.958	3.0171	0.0853	1.134195	40.51	0.531439	7.25E-04
202.9	2.9163	2.9318	0	0.969492	32.12	0.492254	
				0.077173			

CONSOLIDATION SUMMARY SHEET

SAMPLE: REGINA CLAY 9

BASE DATA:

		END OF TEST DATA:	
SAMPLE AREA (CM2):	31.67		
RELATIVE DENSITY:	2.8	WEIGHT TOTAL(GM):	35.59
FINAL CONC(M) SOL'N:	0	WEIGHT DRY(GM):	26.2
CONC. WATER (GM/L):	1000	FINAL SAMPLE HT(CM):	0.67

CALCULATED DATA:

WEIGHT WATER(GM):	9.39	CORR. SOLIDS WT(GM):	26.2
APPARENT W/C:	35.84%	HEIGHT SOLIDS(CM):	0.295457
VOLUME SOL'N(CM3):	9.39	HEIGHT SOL'N(CM):	0.374542
WEIGHT SALT(GM):	0	FINAL VOID RATIO:	1.267668
TRUE W/C:	35.84%	FINAL W/C:	45.27%

APPLIED STRESS (kPa)	D100 READING (CM)	CORRECTED READING (CM)	DEFLECTION (CM)	VOID RATIO	WATER CONTENT %	POROSITY	mv /kPa
0							
4.15	3.6248	3.681	0.3419	2.424856	86.60	0.708016	
11.91	3.564	3.6349	0.2958	2.268827	81.03	0.694079	5.87E-03
24.66	3.523	3.6017	0.2626	2.156459	77.02	0.683189	2.70E-03
52.2	3.458	3.488	0.1489	1.771632	63.27	0.639201	4.43E-03
106	3.394	3.3956	0.0565	1.458897	52.10	0.593313	2.10E-03
205	3.333	3.3429	0.0038	1.280530	45.73	0.561505	7.33E-04
205	3.2981	3.3081	-0.031	1.162746	41.53	0.537625	
205	3.3392	3.3391	0	1.267668	45.27	0.559018	
				0.051647			

CONSOLIDATION SUMMARY SHEET

SAMPLE: REGINA CLAY 10

BASE DATA:

		END OF TEST DATA:	
SAMPLE AREA (CM2):	31.67		
RELATIVE DENSITY:	2.8	WEIGHT TOTAL(GM):	87.27
FINAL CONC(M) SOL'N:	3.5	WEIGHT DRY(GM):	64.84
CONC. WATER (GM/L):	927.8	FINAL SAMPLE HT(CM):	1.5

CALCULATED DATA:

WEIGHT WATER(GM):	22.43	CORR. SOLIDS WT(GM):	59.89007
APPARENT W/C:	34.59%	HEIGHT SOLIDS(CM):	0.675380
VOLUME SOL'N(CM3):	24.17546	HEIGHT SOL'N(CM):	0.824619
WEIGHT SALT(GM):	4.949927	FINAL VOID RATIO:	1.220969
TRUE W/C:	37.45%	FINAL W/C:	40.46%

APPLIED STRESS (kPa)	D100 READING (CM)	CORRECTED READING (CM)	DEFLECTION (CM)	VOID RATIO	WATER CONTENT %	POROSITY	mv /kPa
0							
12.6	1.41	1.4809	0.5499	2.035176	72.68	0.670529	
28.1	1.268	1.3467	0.4157	1.836473	65.59	0.647449	4.22E-03
51.4	1.15	1.244	0.313	1.684411	60.16	0.627478	2.30E-03
101	1.02	1.1216	0.1906	1.503180	53.69	0.600508	1.36E-03
200.1	0.875	0.9849	0.0539	1.300775	46.46	0.565364	8.16E-04
200.1	0.8212	0.931	0	1.220969	40.46	0.549746	
				0.034686			

CONSOLIDATION SUMMARY SHEET

SAMPLE: REGINA CLAY (DD)

BASE DATA:

SAMPLE AREA (CM2):	31.67	END OF TEST DATA:	
RELATIVE DENSITY:	2.8	WEIGHT TOTAL(GM):	84.63
FINAL CONC(M) SOL'N:	0	WEIGHT DRY(GM):	59.11
CONC. WATER (GM/L):	1000	FINAL SAMPLE HT(CM):	1.51

CALCULATED DATA:

WEIGHT WATER(GM):	25.52	CORR. SOLIDS WT(GM):	59.11
APPARENT W/C:	43.17%	HEIGHT SOLIDS(CM):	0.666583
VOLUME SOL'N(CM3):	25.52	HEIGHT SOL'N(CM):	0.843416
WEIGHT SALT(GM):	0	FINAL VOID RATIO:	1.265281
TRUE W/C:	43.17%	FINAL W/C:	45.19%

APPLIED STRESS (kPa)	D100 READING (CM)	CORRECTED READING (CM)	DEFLECTION (CM)	VOID RATIO	WATER CONTENT %	POROSITY	mv /kPa
0							
9.1	4.104	4.1077	0.5721	2.123537	75.84	0.679850	
16.8	4.0075	4.012	0.4764	1.979969	70.71	0.664426	5.97E-03
24.5	3.9482	3.9533	0.4177	1.891908	67.57	0.654207	3.84E-03
55.4	3.79	3.798	0.2624	1.658929	59.25	0.623908	2.61E-03
105	3.656	3.6692	0.1336	1.465705	52.35	0.594436	1.47E-03
207.2	3.511	3.5356	0	1.265281	45.19	0.558553	7.95E-04

CONSOLIDATION SUMMARY SHEET

SAMPLE: SAND BENTONTITE 1

BASE DATA:

SAMPLE AREA (CM2):	31.67	END OF TEST DATA:	
RELATIVE DENSITY:	2.632	WEIGHT TOTAL(GM):	72.56
FINAL CONC(M) SOL'N:	3.5	WEIGHT DRY(GM):	56.15
CONC. WATER (GM/L):	927.8	FINAL SAMPLE HT(CM):	1.18

CALCULATED DATA:

WEIGHT WATER(GM):	16.41	CORR. SOLIDS WT(GM):	52.52858
APPARENT W/C:	29.23%	HEIGHT SOLIDS(CM):	0.630175
VOLUME SOL'N(CM3):	17.68700	HEIGHT SOL'N(CM):	0.549824
WEIGHT SALT(GM):	3.621413	FINAL VOID RATIO:	0.872493
TRUE W/C:	31.24%	FINAL W/C:	30.76%

APPLIED STRESS (kPa)	D100 READING (CM)	CORRECTED READING (CM)	DEFLECTION (CM)	VOID RATIO	WATER CONTENT %	POROSITY	av /kPa
3.51	1.83	1.83					
11.24	1.67	1.6842	0.6148	1.848093	70.22	0.648887	
26.7	1.5225	1.5484	0.479	1.632598	62.03	0.620147	4.89E-03
49.9	1.405	1.4393	0.3699	1.459472	55.45	0.593408	2.83E-03
99.44	1.2535	1.2964	0.227	1.232710	46.84	0.552113	1.86E-03
203.1	1.1164	1.1657	0.0963	1.025307	38.96	0.506247	8.96E-04
203.1	1.0201	1.0694	0	0.872493	30.76	0.465952	
				0.075452			

CONSOLIDATION SUMMARY SHEET

SAMPLE: SAND BENTONTITE 2

BASE DATA:

SAMPLE AREA (CM2):	31.67	END OF TEST DATA:	
RELATIVE DENSITY:	2.632	WEIGHT TOTAL(GM):	83.75
FINAL CONC(M) SOL'N:	3.5	WEIGHT DRY(GM):	67.33
CONC. WATER (GM/L):	927.8	FINAL SAMPLE HT(CM):	1.32

CALCULATED DATA:

WEIGHT WATER(GM):	16.42	CORR. SOLIDS WT(GM):	63.70637
APPARENT W/C:	24.39%	HEIGHT SOLIDS(CM):	0.764273
VOLUME SOL'N(CM3):	17.69777	HEIGHT SOL'N(CM):	0.555726
WEIGHT SALT(GM):	3.623620	FINAL VOID RATIO:	0.727129
TRUE W/C:	25.77%	FINAL W/C:	25.63%

APPLIED STRESS (kPa)	D100 READING (CM)	CORRECTED READING (CM)	DEFLECTION (CM)	VOID RATIO	WATER CONTENT %	POROSITY	av /kPa
0							
17.56	2.97	2.9842	0.9182	1.928531	73.27	0.658531	
25.3	2.824	2.8323	0.7663	1.729780	65.72	0.633670	8.77E-03
48.9	2.664	2.6799	0.6139	1.530375	58.14	0.604801	3.10E-03
103.1	2.468	2.4947	0.4287	1.288054	48.94	0.562947	1.77E-03
205.4	2.2935	2.3276	0.2616	1.069415	40.63	0.516771	9.34E-04
205.4	2.176	2.2111	0.1451	0.916983	32.32	0.478347	
398.95	2.089	2.134	0.068	0.816103	28.77	0.449370	2.72E-04
803.08	2.012	2.066	0	0.727129	25.63	0.421004	1.21E-04
				0.165402			

CONSOLIDATION SUMMARY SHEET

SAMPLE: SAND BENTONITE 3

BASE DATA:

SAMPLE AREA (CM2):	31.67	END OF TEST DATA:	
RELATIVE DENSITY:	2.632	WEIGHT TOTAL(GM):	
FINAL CONC(M) SOL'N:	2	WEIGHT DRY(GM):	
CONC. WATER (GM/L):	960.1	FINAL SAMPLE HT(CM):	0.57

CALCULATED DATA:

WEIGHT WATER(GM):	0	CORR. SOLIDS WT(GM):	-0.98303
APPARENT W/C:	ERR	HEIGHT SOLIDS(CM):	0.3047
VOLUME SOL'N(CM3):	8.402051	HEIGHT SOL'N(CM):	0.2653
WEIGHT SALT(GM):	0.983039	FINAL VOID RATIO:	0.870692
TRUE W/C:	0.00%	FINAL W/C:	31.76%

APPLIED STRESS (kPa)	D100 READING (CM)	CORRECTED READING (CM)	DEFLECTION (CM)	VOID RATIO	WATER CONTENT %	POROSITY	av /kPa
0							
7.73	3.28	3.336	0.4349	2.297998	87.31	0.696785	
15.5	3.2426	3.2586	0.3575	2.043977	77.66	0.671482	9.91E-03
23.2	3.168	3.1846	0.2835	1.801115	68.43	0.642999	1.04E-02
54	3.075	3.1099	0.2088	1.555956	59.12	0.608757	2.84E-03
103.7	3.0076	3.0511	0.15	1.362979	51.78	0.576805	1.52E-03
202.9	2.9401	2.9932	0.0921	1.172957	44.57	0.539797	8.11E-04
202.9	2.848	2.9011	0	0.870692	31.76	0.465438	
				0.139102			

CONSOLIDATION SUMMARY SHEET

SAMPLE: SAND BENTONITE 4

BASE DATA:

SAMPLE AREA (CM2):	31.67	END OF TEST DATA:	
RELATIVE DENSITY:	2.632	WEIGHT TOTAL(GM):	70.45
FINAL CONC(M) SOL'N:	2	WEIGHT DRY(GM):	55.26
CONC. WATER (GM/L):	960.1	FINAL SAMPLE HT(CM):	1.18

CALCULATED DATA:

WEIGHT WATER(GM):	15.19	CORR. SOLIDS WT(GM):	53.40891
APPARENT W/C:	27.49%	HEIGHT SOLIDS(CM):	0.640736
VOLUME SOL'N(CM3):	15.82126	HEIGHT SOL'N(CM):	0.539263
WEIGHT SALT(GM):	1.851088	FINAL VOID RATIO:	0.841629
TRUE W/C:	28.44%	FINAL W/C:	30.70%

APPLIED STRESS (kPa)	D100 READING (CM)	CORRECTED READING (CM)	DEFLECTION (CM)	VOID RATIO	WATER CONTENT %	POROSITY	av /kPa
0							
7.74	1.094	1.1047	0.5458	1.693460	64.34	0.628730	
23.2	0.93	0.949	0.3901	1.450459	55.11	0.591913	5.84E-03
54.1	0.783	0.802	0.2431	1.221036	46.39	0.549759	3.03E-03
93.4	0.6928	0.7208	0.1619	1.094307	41.58	0.522515	1.26E-03
201.65	0.5842	0.6211	0.0622	0.938705	35.67	0.484191	7.27E-04
201.65	0.522	0.5589	0	0.841629	30.70	0.457002	
				0.050072			

CONSOLIDATION SUMMARY SHEET

SAMPLE: SB5

BASE DATA:

		END OF TEST DATA:	
SAMPLE AREA (CM2):	31.67		
RELATIVE DENSITY:	2.632	WEIGHT TOTAL(GM):	
FINAL CONC(M) SOL'N:	0	WEIGHT DRY(GM):	
CONC. WATER (GM/L):	1000	FINAL SAMPLE HT(CM):	0.6

CALCULATED DATA:

WEIGHT WATER(GM):	0	CORR. SOLIDS WT(GM):	0
APPARENT W/C:	ERR	HEIGHT SOLIDS(CM):	0.315
VOLUME SOL'N(CM3):	0	HEIGHT SOL'N(CM):	0.285
WEIGHT SALT(GM):	0	FINAL VOID RATIO:	0.904761
TRUE W/C:	ERR	FINAL W/C:	34.38%

APPLIED STRESS (kPa)	D100 READING (CM)	CORRECTED READING (CM)	DEFLECTION (CM)	VOID RATIO	WATER CONTENT %	POROSITY	av /kPa
0							
7.75	0.6368	0.693	0.3611	2.051111	77.93	0.672250	
12.35	0.5949	0.6658	0.3339	1.964761	74.65	0.662704	6.15E-03
25.25	0.5076	0.5863	0.2544	1.712380	65.06	0.631320	6.60E-03
48.5	0.4285	0.5222	0.1903	1.508888	57.33	0.601417	3.23E-03
102.7	0.3372	0.4388	0.1069	1.244126	47.27	0.554392	1.95E-03
204.9	0.268	0.3779	0.046	1.050793	39.92	0.512383	8.43E-04
(4.0 M) 204.9	0.2104	0.3203	-0.0116	0.867936	32.98	0.464649	
(D.W.) 204.9	0.222	0.3319	0	0.904761	34.38	0.475	

CONSOLIDATION SUMMARY SHEET

SAMPLE: SAND BENTONITE 6

BASE DATA:

SAMPLE AREA (CM2):	31.67	END OF TEST DATA:	
RELATIVE DENSITY:	2.632	WEIGHT TOTAL(GM):	68.8
FINAL CONC(M) SOL'N:	3.5	WEIGHT DRY(GM):	57.14
CONC. WATER (GM/L):	927.8	FINAL SAMPLE HT(CM):	1.03375

CALCULATED DATA:

WEIGHT WATER(GM):	11.66	CORR. SOLIDS WT(GM):	54.56683
APPARENT W/C:	20.41%	HEIGHT SOLIDS(CM):	0.654628
VOLUME SOL'N(CM3):	12.56736	HEIGHT SOL'N(CM):	0.379121
WEIGHT SALT(GM):	2.573167	FINAL VOID RATIO:	0.579140
TRUE W/C:	21.37%	FINAL W/C:	20.42%

APPLIED STRESS (kPa)	D100 READING (CM)	CORRECTED READING (CM)	DEFLECTION (CM)	VOID RATIO	WATER CONTENT %	POROSITY	av /kPa
0							
12.8	3.703	3.7316	0.817	1.827176	69.42	0.646290	
28.3	3.4176	3.4595	0.5449	1.411521	53.63	0.585323	9.49E-03
51.5	3.271	3.3256	0.411	1.206977	45.86	0.546891	3.66E-03
101	3.159	3.2234	0.3088	1.050858	39.93	0.512399	1.43E-03
204.6	3.0264	3.1	0.1854	0.862354	32.76	0.463045	8.87E-04
204.6	2.951	3.0246	0.11	0.747174	28.39	0.427647	
408.9	2.9354	3.0193	0.1047	0.739078	28.08	0.424982	2.27E-05
817.5	2.8718	2.9633	0.0487	0.653533	24.83	0.395234	1.20E-04
1608.34	2.815	2.9146	0	0.579140	20.42	0.366744	5.69E-05
				0.152073			

CONSOLIDATION SUMMARY SHEET

SAMPLE: SAND BENTONITE (DD)

BASE DATA:

		END OF TEST DATA:	
SAMPLE AREA (CM2):	31.67		
RELATIVE DENSITY:	2.632	WEIGHT TOTAL(GM):	56.23
FINAL CONC(M) SOL'N:	0	WEIGHT DRY(GM):	44.47
CONC. WATER (GM/L):	1000	FINAL SAMPLE HT(CM):	0.905

CALCULATED DATA:

WEIGHT WATER(GM):	11.76	CORR. SOLIDS WT(GM):	44.47
APPARENT W/C:	26.44%	HEIGHT SOLIDS(CM):	0.533498
VOLUME SOL'N(CM3):	11.76	HEIGHT SOL'N(CM):	0.371501
WEIGHT SALT(GM):	0	FINAL VOID RATIO:	0.696349
TRUE W/C:	26.44%	FINAL W/C:	26.46%

APPLIED STRESS (kPa)	D100 READING (CM)	CORRECTED READING (CM)	DEFLECTION (CM)	VOID RATIO	WATER CONTENT %	POROSITY	av /kPA
0							
9.74	3.531	3.5329	0.6921	1.993635	75.75	0.665958	
17.47	3.4586	3.4614	0.6206	1.859614	70.65	0.650302	5.79E-03
48.4	3.302	3.3065	0.4657	1.569266	59.62	0.610783	3.28E-03
98	3.158	3.1654	0.3246	1.304786	49.57	0.566120	2.08E-03
200.2	3.038	3.0495	0.2087	1.087541	41.32	0.520967	9.22E-04
404.6	2.938	2.9563	0.1155	0.912845	34.68	0.477218	4.09E-04
813.4	2.852	2.8826	0.0418	0.774700	29.43	0.436524	1.77E-04
1603.8	2.7918	2.8408	0	0.696349	26.46	0.410498	5.53E-05
				0.187393			

CONSOLIDATION SUMMARY SHEET

SAMPLE: SAND BENTONITE - 2 WAY DRAINAGE (SBDC1)

BASE DATA:

SAMPLE AREA (CM2):	31.67	END OF TEST DATA:	
RELATIVE DENSITY:	2.632	WEIGHT TOTAL(GM):	68.84
FINAL CONC(M) SOL'N:	3.5	WEIGHT DRY(GM):	54.2
CONC. WATER (GM/L):	927.8	FINAL SAMPLE HT(CM):	1.05625

CALCULATED DATA:

WEIGHT WATER(GM):	14.64	CORR. SOLIDS WT(GM):	50.96919
APPARENT W/C:	27.01%	HEIGHT SOLIDS(CM):	0.65
VOLUME SOL'N(CM3):	15.77926	HEIGHT SOL'N(CM):	0.40625
WEIGHT SALT(GM):	3.230804	FINAL VOID RATIO:	0.625
TRUE W/C:	28.72%	FINAL W/C:	22.03%

APPLIED STRESS (kPa)	D100 READING (CM)	CORRECTED READING (CM)	DEFLECTION (CM)	VOID RATIO	WATER CONTENT %	POROSITY	av /kPa
0							
6.7	1.377	1.3773	0.7278	1.744692	66.29	0.635660	
17.9	1.195	1.2085	0.559	1.485	56.42	0.597585	8.45E-03
28.7	1.1105	1.1309	0.4814	1.365615	51.89	0.577277	4.45E-03
51.2	1.002	1.0328	0.3833	1.214692	46.15	0.548470	2.84E-03
96.2	0.884	0.9309	0.2814	1.057923	40.19	0.514073	1.57E-03
96.2	0.775	0.8219	0.1724	0.890230	33.82	0.470964	
198.2	0.756	0.8208	0.1713	0.888538	33.76	0.470490	8.78E-06
396.3	0.692	0.7706	0.1211	0.811307	30.82	0.447912	2.06E-04
807.8	0.6142	0.7063	0.0568	0.712384	27.07	0.416019	1.33E-04
1715.2	0.5439	0.6495	0	0.625	22.03	0.384615	5.62E-05
				0.081486			

CONSOLIDATION SUMMARY SHEET

SAMPLE: SAND BENTONITE 2-WAY DRAINGAE (SBDC2)

BASE DATA:

		END OF TEST DATA:	
SAMPLE AREA (CM2):	31.67		
RELATIVE DENSITY:	2.632	WEIGHT TOTAL(GM):	
FINAL CONC(M) SOL'N:	0	WEIGHT DRY(GM):	
CONC. WATER (GM/L):	1000	FINAL SAMPLE HT(CM):	1.2125

CALCULATED DATA:

WEIGHT WATER(GM):	0	CORR. SOLIDS WT(GM):	0
APPARENT W/C:	ERR	HEIGHT SOLIDS(CM):	0.6785
VOLUME SOL'N(CM3):	16.91178	HEIGHT SOL'N(CM):	0.534
WEIGHT SALT(GM):	0	FINAL VOID RATIO:	0.787030
TRUE W/C:	ERR	FINAL W/C:	29.90%

APPLIED STRESS (kPa)	D100 READING (CM)	CORRECTED READING (CM)	DEFLECTION (CM)	VOID RATIO	WATER CONTENT %	POROSITY	av /kPa
0							
6.7	1.135	1.1623	0.5795	1.641120	62.35	0.621372	
17.9	0.984	1.0279	0.4451	1.443036	54.83	0.590673	6.70E-03
29.1	0.9102	0.9624	0.3796	1.346499	51.16	0.573833	3.53E-03
51.4	0.795	0.861	0.2782	1.197052	45.48	0.544844	2.86E-03
96.4	0.688	0.7686	0.1858	1.060869	40.31	0.514767	1.38E-03
201.4	0.571	0.666	0.0832	0.909653	34.56	0.476344	6.99E-04
(4.0 M) 201.4	0.4868	0.5827	-0.0001	0.786882	29.90	0.440366	
(D.W.) 201.4	0.4869	0.5828	0	0.787030	29.90	0.440412	
				0.064289			

CONSOLIDATION SUMMARY SHEET

SAMPLE: SAND BENTONITE - 2 WAY DRAINAGE (SBOC3)

BASE DATA:

SAMPLE AREA (CM2):	31.67	END OF TEST DATA:	
RELATIVE DENSITY:	2.632	WEIGHT TOTAL(GM):	
FINAL CONC(M) SOL'N:	3.5	WEIGHT DRY(GM):	
CONC. WATER (GM/L):	927.8	FINAL SAMPLE HT(CM):	1.09

CALCULATED DATA:

WEIGHT WATER(GM):	0	CORR. SOLIDS WT(GM):	-2.74291
APPARENT W/C:	ERR	HEIGHT SOLIDS(CM):	0.667
VOLUME SOL'N(CM3):	13.39641	HEIGHT SOL'N(CM):	0.423
WEIGHT SALT(GM):	2.742914	FINAL VOID RATIO:	0.634182
TRUE W/C:	0.00%	FINAL W/C:	22.36%

APPLIED STRESS (kPa)	D100 READING (CM)	CORRECTED READING (CM)	DEFLECTION (CM)	VOID RATIO	WATER CONTENT %	POROSITY	mv /kPa
0							
6.7	1.288	1.313	0.6936	1.674062	63.60	0.626037	
17.9	1.16	1.204	0.5846	1.510644	57.40	0.601695	5.46E-03
23.5	1.1006	1.1648	0.5454	1.451874	55.16	0.592148	4.18E-03
23.5	0.9507	1.0149	0.3955	1.227136	46.62	0.550992	
51.7	0.932	1.0064	0.387	1.214392	46.14	0.548408	2.03E-04
101.5	0.852	0.9373	0.3179	1.110794	42.20	0.526244	9.39E-04
205.2	0.732	0.8314	0.212	0.952023	36.17	0.487711	7.25E-04
393.6	0.634	0.7444	0.125	0.821589	31.22	0.451028	3.55E-04
805.3	0.544	0.6762	0.0568	0.719340	27.33	0.418381	1.36E-04
1598	0.489	0.6194	0	0.634182	22.36	0.388073	6.25E-05
				0.091659			

CONSOLIDATION SUMMARY SHEET

SAMPLE ---- REGINA CLAY HOLE 1 SAMPLE DB1 WITH 4.0 M

SAMPLE X-S AREA =	32.1700	SQ CM
RELATIVE DENSITY OF SOIL =	2.8000	
INITIAL SAMPLE HEIGHT =	1.6000	CM
TOTAL DEFLECTION AT END OF TEST =	0.1287	CM
MASS OF SOIL SOLIDS =	75.8184	GM
MASS OF SODIUM CHLORIDE =	3.1516	GM
INITIAL MASS OF WATER =	18.3500	GM
FINAL MASS OF WATER =	20.6800	GM
HEIGHT OF SOIL SOLIDS =	0.8417	CM
INITIAL DEGREE OF SATURATION =	75.2234	%
FINAL DEGREE OF SATURATION =	102.1047	%
INITIAL UNIT WEIGHT =	18.5419	MN/CU M
FINAL UNIT WEIGHT =	20.6466	MN/CU M

APPLIED STRESS KPA	D100 READING CM	CORRECTED D100 READING CM	DEFL. CM	VOID RATIO	WATER CONTENT %
0.00	1.6101	1.6101	0.0000	0.9009	32.17
33.20	1.5579	1.5841	0.0260	0.8700	31.07
49.80	1.5450	1.5832	0.0269	0.8689	31.03
100.00	1.5068	1.5623	0.0478	0.8441	30.15
200.00	1.4634	1.5349	0.0752	0.8115	28.98
300.00	1.4358	1.5168	0.0933	0.7900	28.22
300.00	1.4004	1.4814	0.1287	0.7480	26.71

APPLIED STRESS KPA	AVERAGE STRESS KPA	CV SQ CM/S	AV SQ M/KN	MV SQ M/KN	K CM/S
0.00 - 33.20	16.60	0.2067E-02	0.9301E-03	0.4895E-03	0.1144E-06
33.20 - 49.80	41.50	0.2032E-03	0.6441E-04	0.3445E-04	0.7912E-09
49.80 - 100.00	74.90	0.2227E-03	0.4946E-03	0.2647E-03	0.6661E-08
100.00 - 200.00	150.00	0.1943E-03	0.3255E-03	0.1765E-03	0.3876E-08
200.00 - 300.00	250.00	0.1886E-03	0.2150E-03	0.1187E-03	0.2530E-08

SUB. LIQUID CHANGED TO THE DESIRED ONE WITH STRESS HELD CONSTANT

CONSOLIDATION SUMMARY SHEET

SAMPLE ---- INTACT REGINA CLAY DB2

SAMPLE X-S AREA =	31.5700	SQ CM
RELATIVE DENSITY OF SOIL =	2.8000	
INITIAL SAMPLE HEIGHT =	1.7700	CM
TOTAL DEFLECTION AT END OF TEST =	0.0418	CM
MASS OF SOIL SOLIDS =	82.2548	GM
MASS OF SODIUM CHLORIDE =	4.2352	GM
INITIAL MASS OF WATER =	25.4000	GM
FINAL MASS OF WATER =	27.7900	GM
HEIGHT OF SOIL SOLIDS =	0.9305	CM
INITIAL DEGREE OF SATURATION =	95.8412	%
FINAL DEGREE OF SATURATION =	110.3542	%
INITIAL UNIT WEIGHT =	19.6366	MN/CU M
FINAL UNIT WEIGHT =	20.5411	MN/CU M

APPLIED STRESS KPA	D100 READING CM	CORRECTED D100 READING CM	DEFL. CM	VOID RATIO	WATER CONTENT %
0.00	1.3970	1.3970	0.0000	0.9021	32.22
50.70	1.3895	1.4277	-0.0307	0.9351	33.40
101.50	1.3715	1.4270	-0.0300	0.9344	33.37
300.30	1.3084	1.3894	0.0076	0.8940	31.93
300.30	1.3008	1.3818	0.0152	0.8858	31.64
300.30	1.2980	1.3790	0.0180	0.8828	31.53
300.30	1.2876	1.3686	0.0284	0.8716	31.13
300.30	1.2705	1.3515	0.0455	0.8533	30.47
300.30	1.2657	1.3467	0.0503	0.8481	30.29
629.40	1.2652	1.3552	0.0418	0.8572	30.62
1209.10	1.2652	1.3552	0.0418	0.8572	30.62

APPLIED STRESS KPA	AVERAGE STRESS KPA	CV SQ CM/S	AV SQ M/KN	MV SQ M/KN	K CM/S
0.00 - 50.70	25.35	0.5233E-04	-.6507E-03	-.3421E-03	-.2023E-08
50.70 - 101.50	76.10	0.2956E-03	0.1481E-04	0.7652E-05	0.2557E-09
101.50 - 300.30	200.90	0.4269E-03	0.2033E-03	0.1051E-03	0.5070E-08
SUB. LIQUID CHANGED TO THE DESIRED ONE WITH STRESS HELD CONSTANT					
SUB. LIQUID CHANGED TO THE DESIRED ONE WITH STRESS HELD CONSTANT					
SUB. LIQUID CHANGED TO THE DESIRED ONE WITH STRESS HELD CONSTANT					
SUB. LIQUID CHANGED TO THE DESIRED ONE WITH STRESS HELD CONSTANT					
SUB. LIQUID CHANGED TO THE DESIRED ONE WITH STRESS HELD CONSTANT					
300.30 - 629.40	464.85	0.2440E-02	-.2776E-04	-.1502E-04	-.4141E-08
629.40 - 1209.10	919.25	0.2452E-02	0.0000E+00	0.0000E+00	0.0000E+00

CONSOLIDATION SUMMARY SHEET

SAMPLE ---- INTACT REGINA CLAY DB3

SAMPLE X-S AREA =	32.0700	SQ CM
RELATIVE DENSITY OF SOIL =	2.8000	
INITIAL SAMPLE HEIGHT =	1.3619	CM
TOTAL DEFLECTION AT END OF TEST =	0.0345	CM
MASS OF SOIL SOLIDS =	60.3628	GM
MASS OF SODIUM CHLORIDE =	3.2172	GM
INITIAL MASS OF WATER =	17.1600	GM
FINAL MASS OF WATER =	21.1100	GM
HEIGHT OF SOIL SOLIDS =	0.6722	CM
INITIAL DEGREE OF SATURATION =	77.5840	%
FINAL DEGREE OF SATURATION =	100.4685	%
INITIAL UNIT WEIGHT =	18.1287	MN/CU M
FINAL UNIT WEIGHT =	19.5099	MN/CU M

APPLIED STRESS KPA	D100 READING CM	CORRECTED D100 READING CM	DEFL. CM	VOID RATIO	WATER CONTENT %
0.00	1.2160	1.2160	0.0000	1.0260	36.64
38.84	1.2131	1.2131	0.0029	1.0217	36.49
83.30	1.1945	1.2037	0.0123	1.0077	35.99
83.30	1.1723	1.1815	0.0345	0.9746	34.81

APPLIED STRESS KPA	AVERAGE STRESS KPA	CV SQ CM/S	AV SQ M/KN	MV SQ M/KN	K CM/S
0.00 - 38.84	19.42	0.1519E-02	0.1111E-03	0.5482E-04	0.9413E-08
38.84 - 83.30	61.07	0.3628E-03	0.3145E-03	0.1556E-03	0.6378E-08

SUB. LIQUID CHANGED TO THE DESIRED ONE WITH STRESS HELD CONSTANT

CONSOLIDATION SUMMARY SHEET

SAMPLE ---- INTACT REGINA CLAY DB4

SAMPLE X-S AREA =	31.4700 SQ CM
RELATIVE DENSITY OF SOIL =	2.8000
INITIAL SAMPLE HEIGHT =	1.4919 CM
TOTAL DEFLECTION AT END OF TEST =	0.1985 CM
MASS OF SOIL SOLIDS =	61.8840 GM
MASS OF SODIUM CHLORIDE =	3.3360 GM
INITIAL MASS OF WATER =	22.6600 GM
FINAL MASS OF WATER =	21.8900 GM
HEIGHT OF SOIL SOLIDS =	0.7023 CM
INITIAL DEGREE OF SATURATION =	91.1920 %
FINAL DEGREE OF SATURATION =	117.6763 %
INITIAL UNIT WEIGHT =	18.3559 KN/CU M
FINAL UNIT WEIGHT =	20.9875 KN/CU M

APPLIED STRESS KPA	D100 READING CM	CORRECTED D100 READING CM	DEFL. CM	VOID RATIO	WATER CONTENT %
0.00	1.2705	1.2705	0.0000	1.1243	40.15
22.64	1.2700	1.2705	0.0000	1.1243	40.15
47.57	1.2621	1.2687	0.0018	1.1217	40.06
104.20	1.2324	1.2435	0.0270	1.0859	38.78
200.00	1.2022	1.2192	0.0513	1.0513	37.54
200.00	1.1939	1.2109	0.0596	1.0394	37.12
200.00	1.1890	1.2060	0.0645	1.0325	36.87
200.00	1.1800	1.1970	0.0735	1.0196	36.42
389.70	1.1514	1.1751	0.0954	0.9885	35.30
389.70	1.1239	1.1476	0.1229	0.9493	33.90
802.40	1.0907	1.1245	0.1460	0.9164	32.73
1600.20	1.0240	1.0720	0.1985	0.8417	30.06

APPLIED STRESS KPA	AVERAGE STRESS KPA	CV SQ CM/S	AV SQ M/KN	MV SQ M/KN	K CM/S
0.00 - 22.64	11.32	0.1827E-02	0.0000E+00	0.0000E+00	0.0000E+00
22.64 - 47.57	35.10	0.5214E-03	0.1028E-03	0.4839E-04	0.2851E-08
47.57 - 104.20	75.89	0.3200E-03	0.6336E-03	0.2986E-03	0.1080E-07
104.20 - 200.00	152.10	0.3397E-03	0.3612E-03	0.1732E-03	0.6647E-08
SUB. LIQUID CHANGED TO THE DESIRED ONE WITH STRESS HELD CONSTANT					
SUB. LIQUID CHANGED TO THE DESIRED ONE WITH STRESS HELD CONSTANT					
SUB. LIQUID CHANGED TO THE DESIRED ONE WITH STRESS HELD CONSTANT					
200.00 - 389.70	294.85	0.2168E-03	0.1644E-03	0.8139E-04	0.1994E-08
SUB. LIQUID CHANGED TO THE DESIRED ONE WITH STRESS HELD CONSTANT					
389.70 - 802.40	596.05	0.2224E-03	0.7970E-04	0.4089E-04	0.1028E-08
802.40 - 1600.20	1201.30	0.1191E-03	0.9370E-04	0.4889E-04	0.6582E-09

CONSOLIDATION SUMMARY SHEET

SAMPLE ---- INTACT REGINA CLAY DB5

SAMPLE X-S AREA =	31.5700	SQ CM
RELATIVE DENSITY OF SOIL =	2.8000	
INITIAL SAMPLE HEIGHT =	1.4919	CM
TOTAL DEFLECTION AT END OF TEST =	0.1688	CM
MASS OF SOIL SOLIDS =	62.2185	GM
MASS OF SODIUM CHLORIDE =	0.8815	GM
INITIAL MASS OF WATER =	23.5900	GM
FINAL MASS OF WATER =	21.8200	GM
HEIGHT OF SOIL SOLIDS =	0.7039	CM
INITIAL DEGREE OF SATURATION =	94.8212	%
FINAL DEGREE OF SATURATION =	111.6148	%
INITIAL UNIT WEIGHT =	18.0500	MN/CU M
FINAL UNIT WEIGHT =	19.9373	MN/CU M

APPLIED STRESS KPA	D100 READING CM	CORRECTED D100 READING CM	DEFL. CM	VOID RATIO	WATER CONTENT %
0.00	1.5626	1.5628	0.0000	1.1196	39.99
22.56	1.5626	1.5626	0.0002	1.1193	39.98
47.41	1.5451	1.5461	0.0167	1.0959	39.14
98.20	1.5123	1.5373	0.0255	1.0834	38.69
263.70	1.4586	1.5050	0.0578	1.0375	37.05
510.30	1.4114	1.4714	0.0914	0.9897	35.35
758.80	1.3761	1.4261	0.1367	0.9254	33.05
758.80	1.3680	1.4180	0.1448	0.9139	32.64
758.80	1.3473	1.3973	0.1655	0.8845	31.59
758.80	1.3439	1.3938	0.1690	0.8795	31.41
1529.20	1.3439	1.3938	0.1690	0.8795	31.41

APPLIED STRESS KPA	AVERAGE STRESS KPA	CV SQ CM/S	AV SQ M/KN	MV SQ M/KN	K CM/S
0.00 - 22.56	11.28	0.1827E-02	0.1260E-04	0.5943E-05	0.1108E-08
22.56 - 47.41	34.99	0.9032E-03	0.9433E-03	0.4451E-03	0.4102E-07
47.41 - 98.20	72.81	0.2690E-03	0.2462E-03	0.1175E-03	0.3224E-08
98.20 - 263.70	180.95	0.3753E-03	0.2773E-03	0.1331E-03	0.5096E-08
263.70 - 510.30	387.00	0.1940E-03	0.1936E-03	0.9501E-04	0.1880E-08
510.30 - 758.80	634.55	0.9444E-04	0.2590E-03	0.1302E-03	0.1254E-08
SUB. LIQUID CHANGED TO THE DESIRED ONE WITH STRESS HELD CONSTANT					
SUB. LIQUID CHANGED TO THE DESIRED ONE WITH STRESS HELD CONSTANT					
SUB. LIQUID CHANGED TO THE DESIRED ONE WITH STRESS HELD CONSTANT					
758.80 - 1529.20	1144.00	0.1437E-02	0.0000E+00	0.0000E+00	0.0000E+00

CONSOLIDATION SUMMARY SHEET

SAMPLE ---- INTACT REGINA CLAY DB6

SAMPLE X-S AREA =	31.3700	SQ CM
RELATIVE DENSITY OF SOIL =	2.8000	
INITIAL SAMPLE HEIGHT =	1.5019	CM
TOTAL DEFLECTION AT END OF TEST =	0.1442	CM
MASS OF SOIL SOLIDS =	62.8900	GM
MASS OF SODIUM CHLORIDE =	0.0000	GM
INITIAL MASS OF WATER =	23.5100	GM
FINAL MASS OF WATER =	22.1600	GM
HEIGHT OF SOIL SOLIDS =	0.7160	CM
INITIAL DEGREE OF SATURATION =	95.3602	%
FINAL DEGREE OF SATURATION =	110.0826	%
INITIAL UNIT WEIGHT =	17.9838	MN/CU M
FINAL UNIT WEIGHT =	19.5830	MN/CU M

APPLIED STRESS KPA	D100 READING CM	CORRECTED D100 READING CM	DEFL. CM	VOID RATIO	WATER CONTENT %
0.00	1.7221	1.7221	0.0000	1.0976	39.20
17.03	1.7221	1.7221	0.0000	1.0976	39.20
47.70	1.6990	1.7186	0.0035	1.0928	39.03
104.50	1.6656	1.7000	0.0221	1.0668	38.10
209.70	1.6212	1.6676	0.0545	1.0215	36.48
517.80	1.5480	1.6080	0.1141	0.9383	33.51
517.80	1.5030	1.5630	0.1591	0.8754	31.27
517.80	1.5179	1.5779	0.1442	0.8962	32.01

APPLIED STRESS KPA	AVERAGE STRESS KPA	CV SQ CM/S	AV SQ M/KN	MV SQ M/KN	K CM/S
0.00 - 17.03	8.52	0.1852E-02	0.0000E+00	0.0000E+00	0.0000E+00
17.03 - 47.70	32.37	0.7389E-03	0.1594E-03	0.7598E-04	0.5506E-08
47.70 - 104.50	76.10	0.4550E-03	0.4574E-03	0.2185E-03	0.9752E-08
104.50 - 209.70	157.10	0.2705E-03	0.4302E-03	0.2081E-03	0.5521E-08
209.70 - 517.80	363.75	0.1736E-03	0.2702E-03	0.1336E-03	0.2276E-08

SUB. LIQUID CHANGED TO THE DESIRED ONE WITH STRESS HELD CONSTANT
SUB. LIQUID CHANGED TO THE DESIRED ONE WITH STRESS HELD CONSTANT

D.2 Constant Head Permeability Test Data

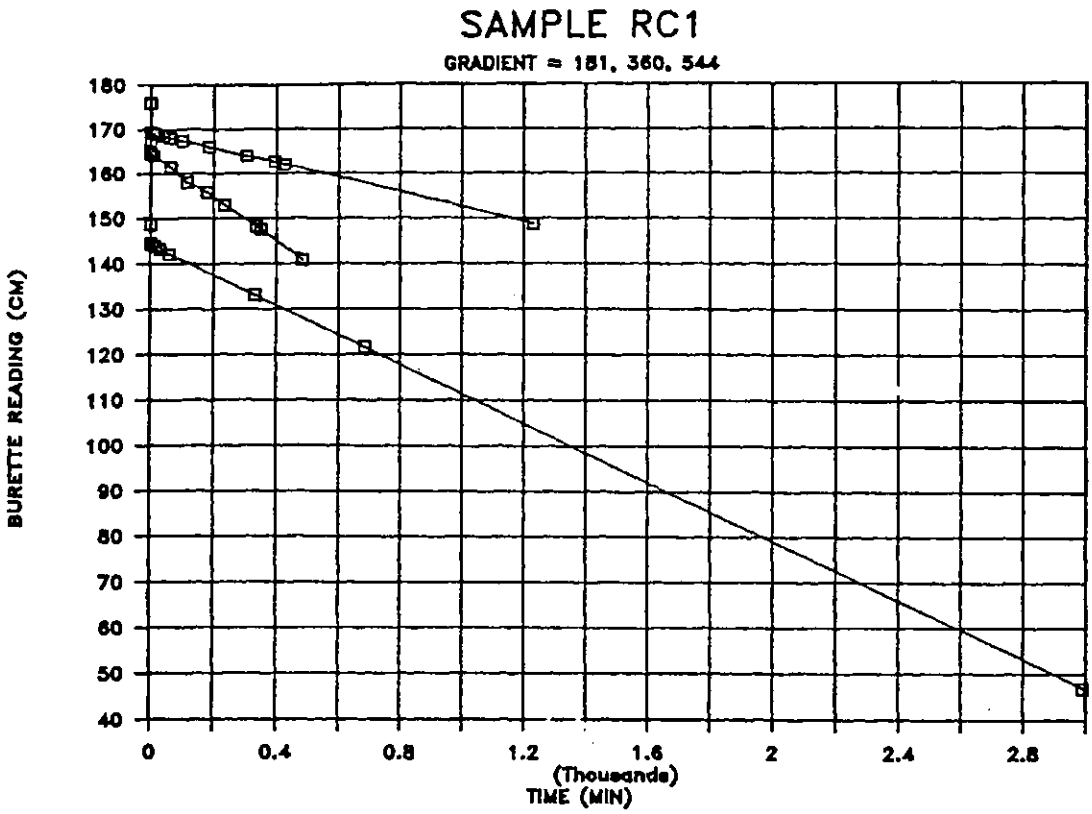

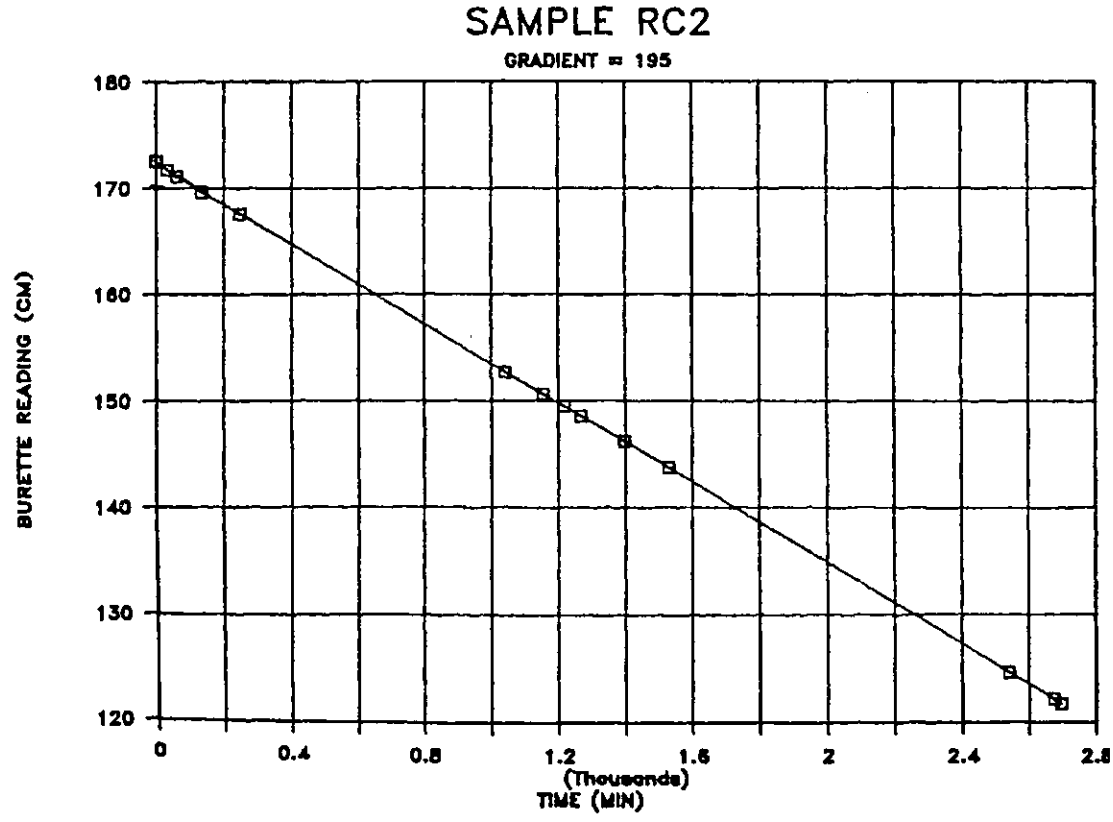

SAMPLE RC2 (POST OSMOTIC CONSOLIDATION)

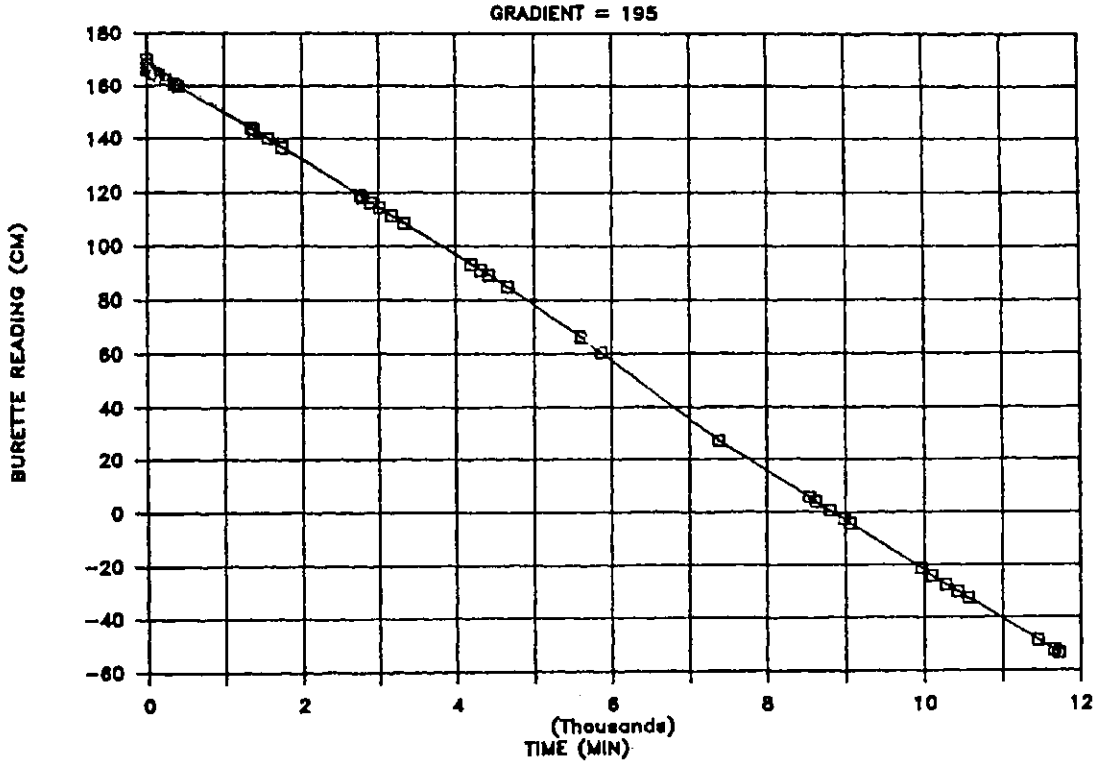

SAMPLE RC3

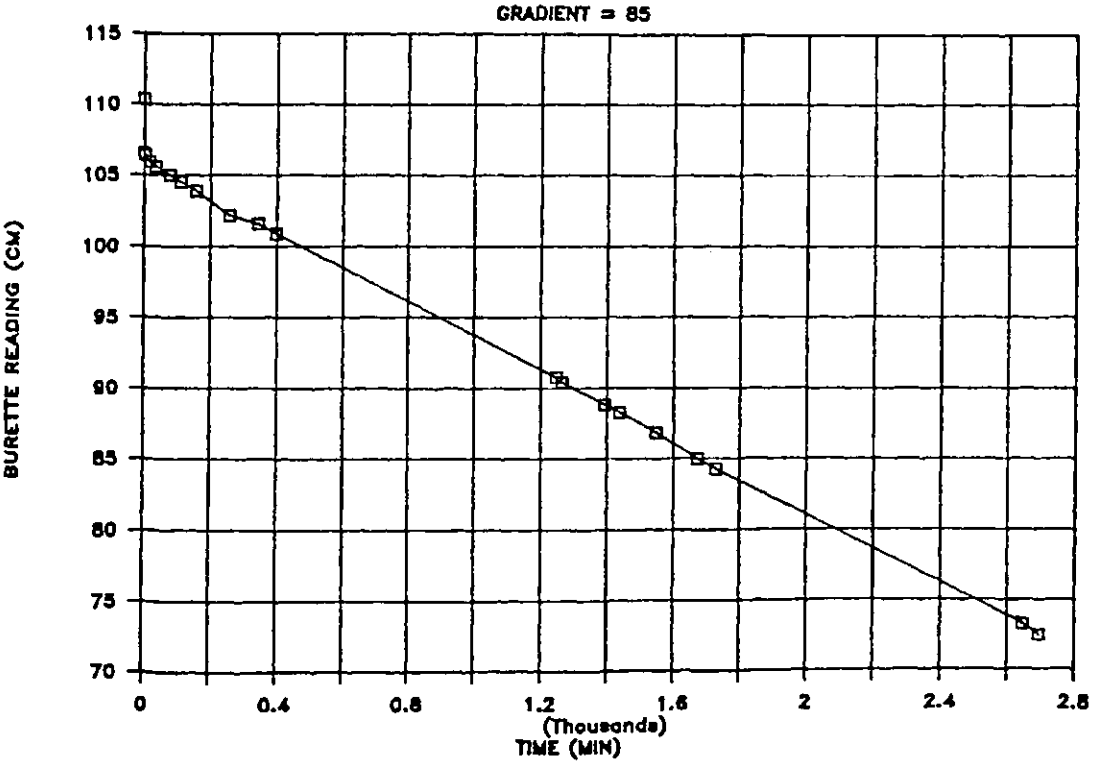

SAMPLE RC4

GRADIENT = 103, 208

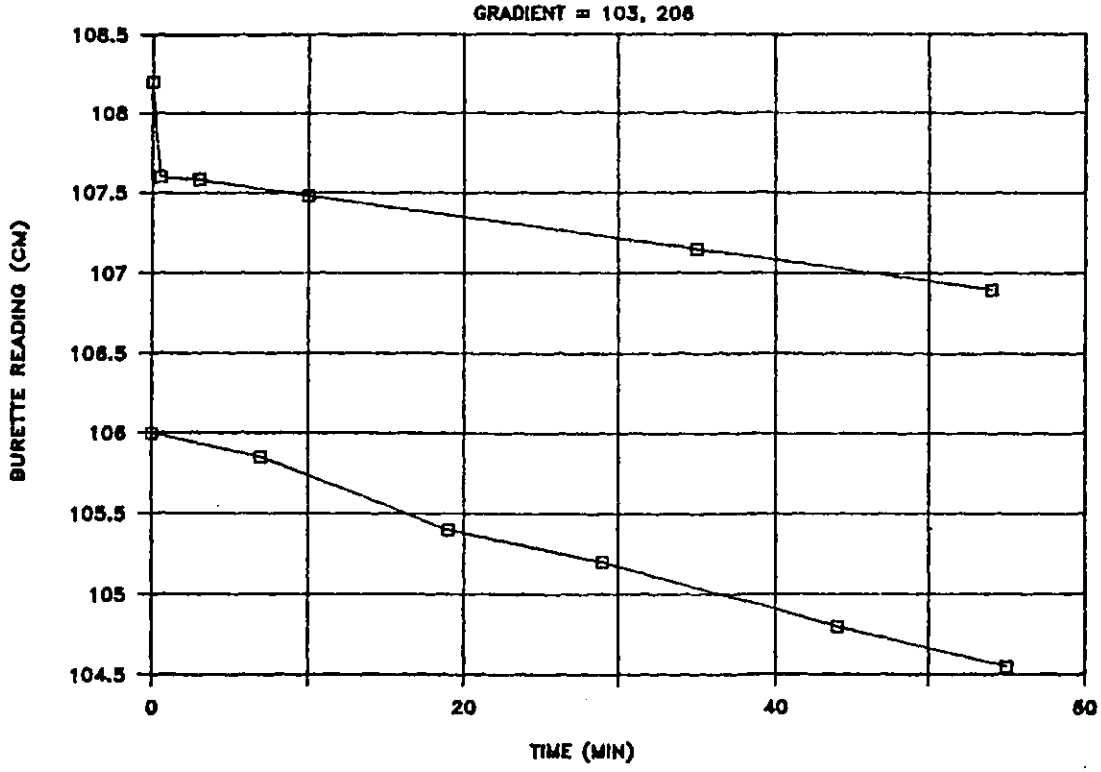

SAMPLE RC5

GRADIENT = 126

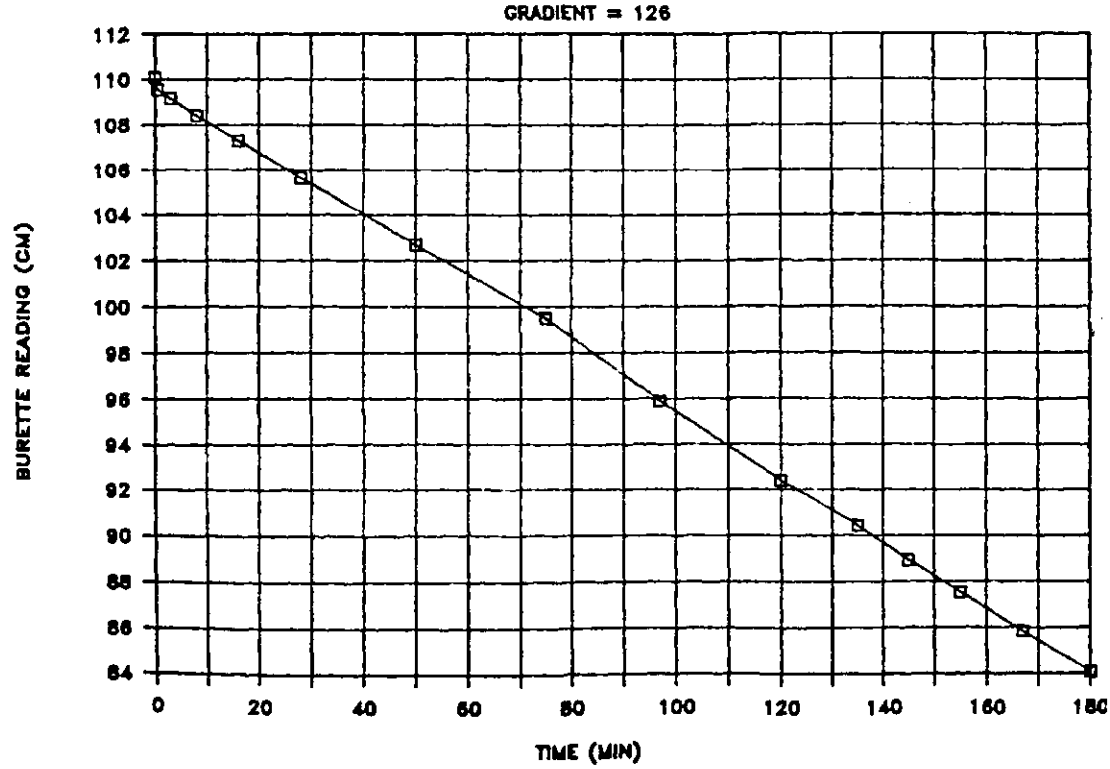

SAMPLE RC6

GRADIENT = 133

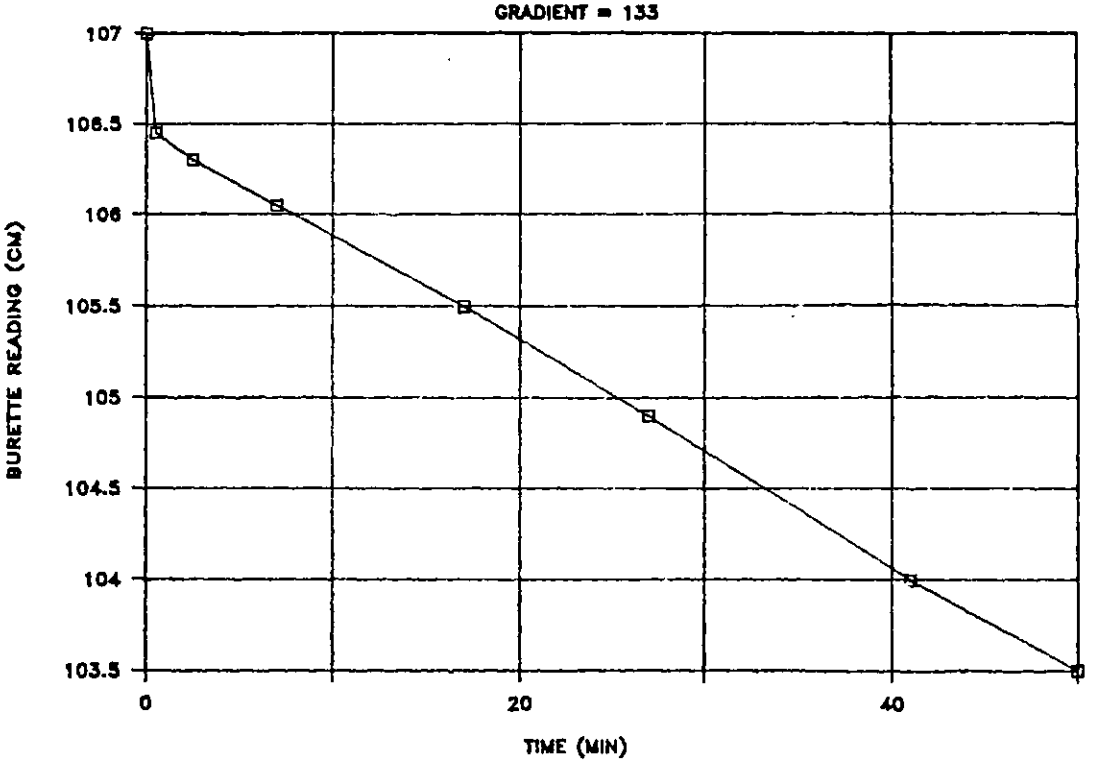

SAMPLE RC7

GRADIENT = 171, 341, 512

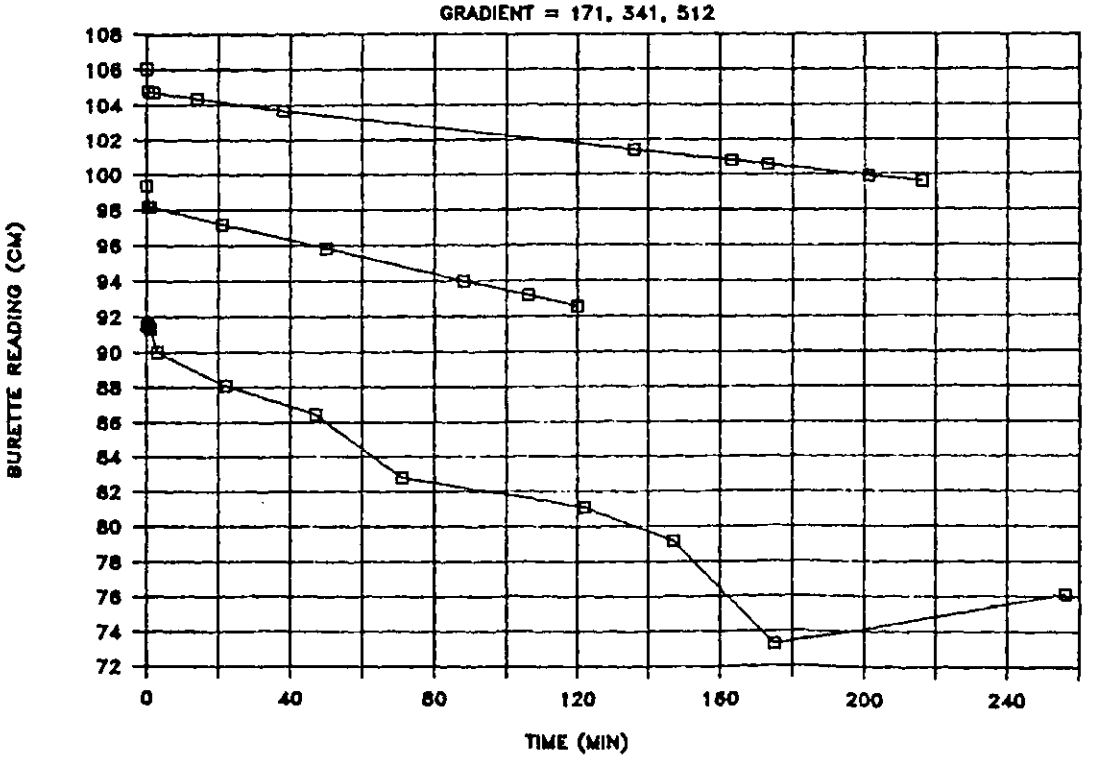

SAMPLE RC8

GRADIENT = 189

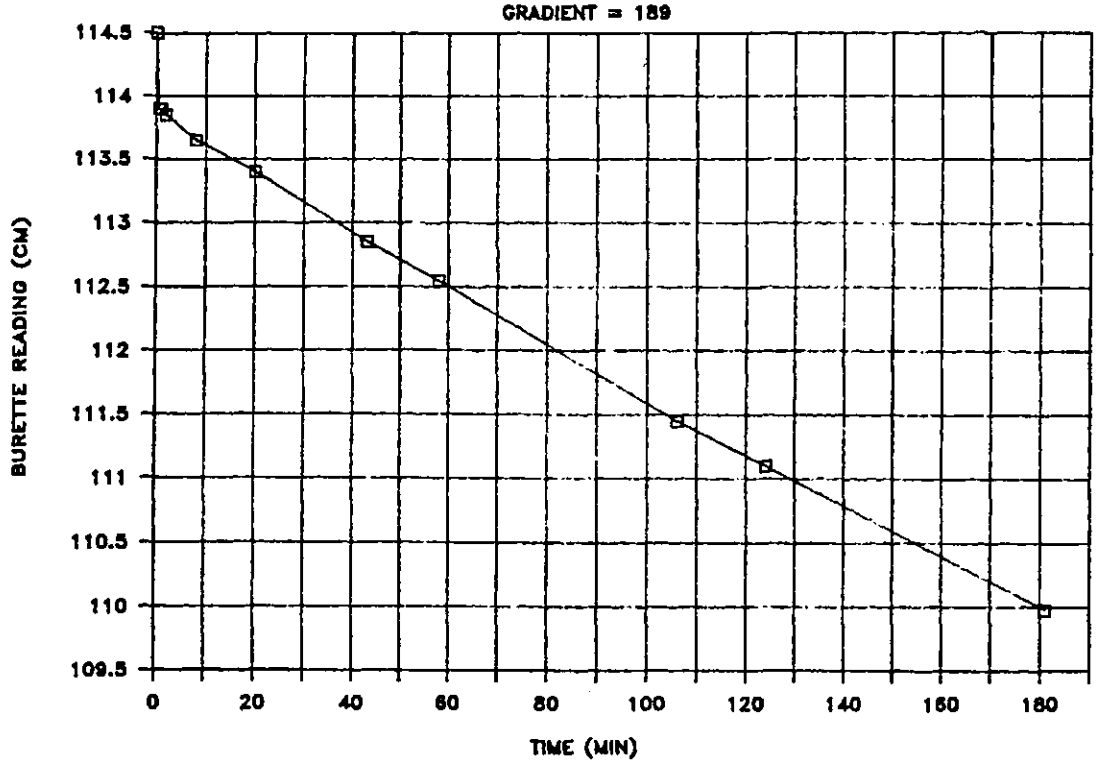

SAMPLE RC9

GRADIENT = 149.5

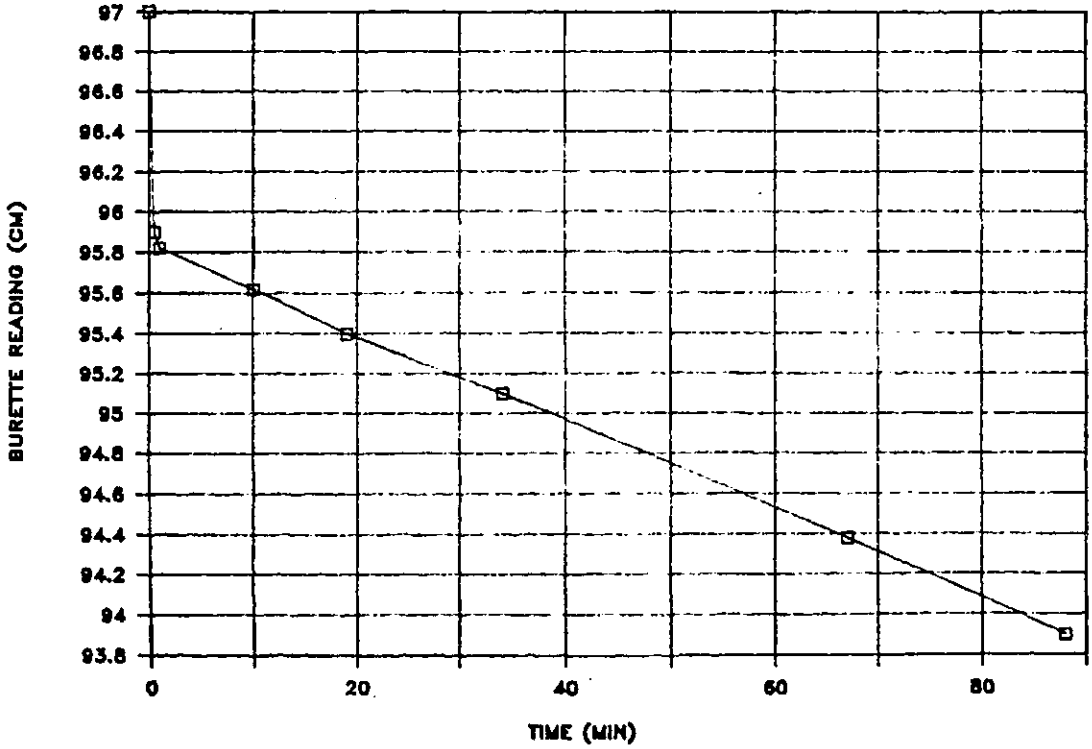

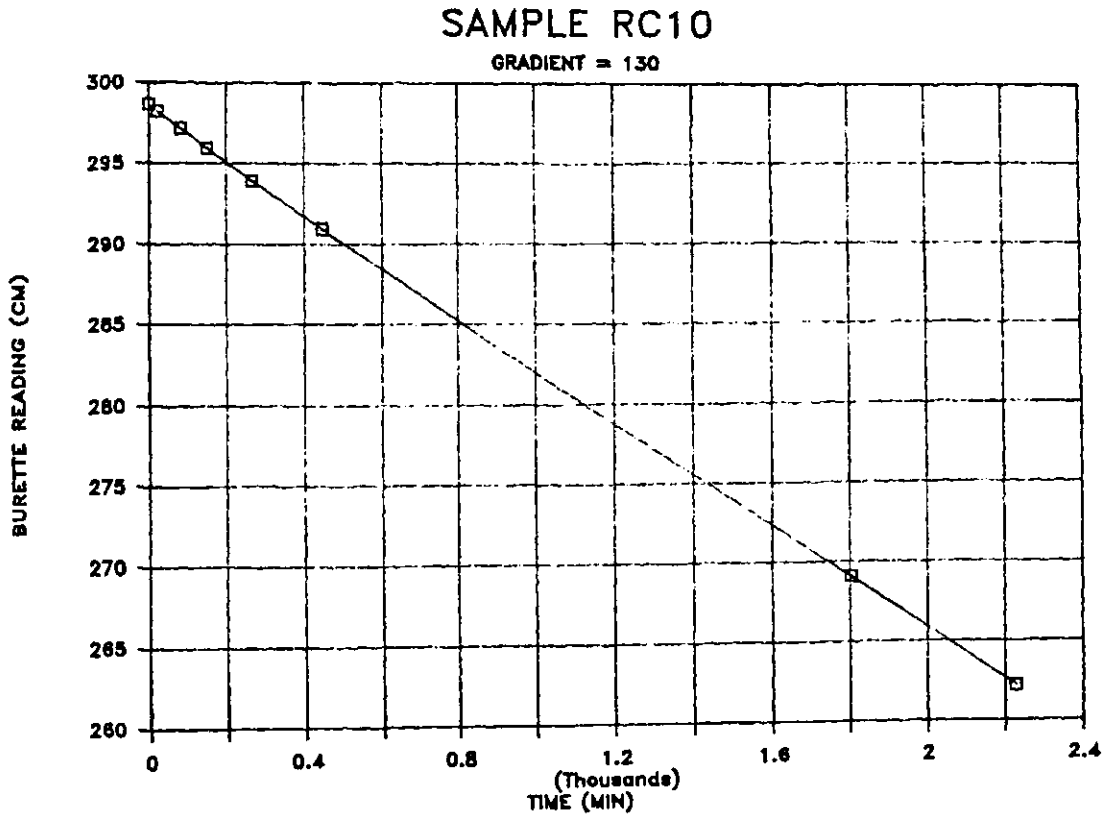
SAMPLE RC10
GRADIENT = 130
BURETTE READING (CM)
300
295
290
285
280
275
270
265
260
0
0.4
0.8
1.2
1.6
2
2.4
(Thousands)
TIME (MIN)

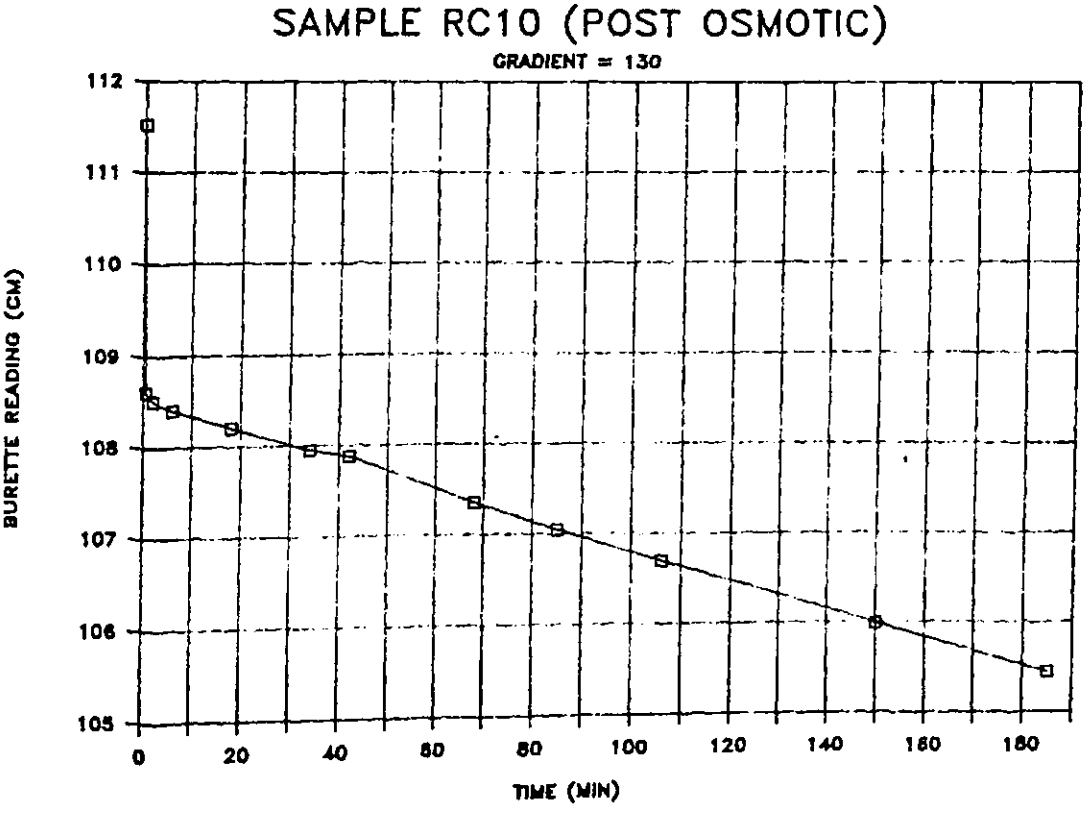
SAMPLE RC10 (POST OSMOTIC)
GRADIENT = 130
BURETTE READING (CM)
112
111
110
109
108
107
106
105
0
20
40
60
80
100
120
140
160
180
TIME (MIN)

SAMPLE SB1

GRADIENT = 163, 489

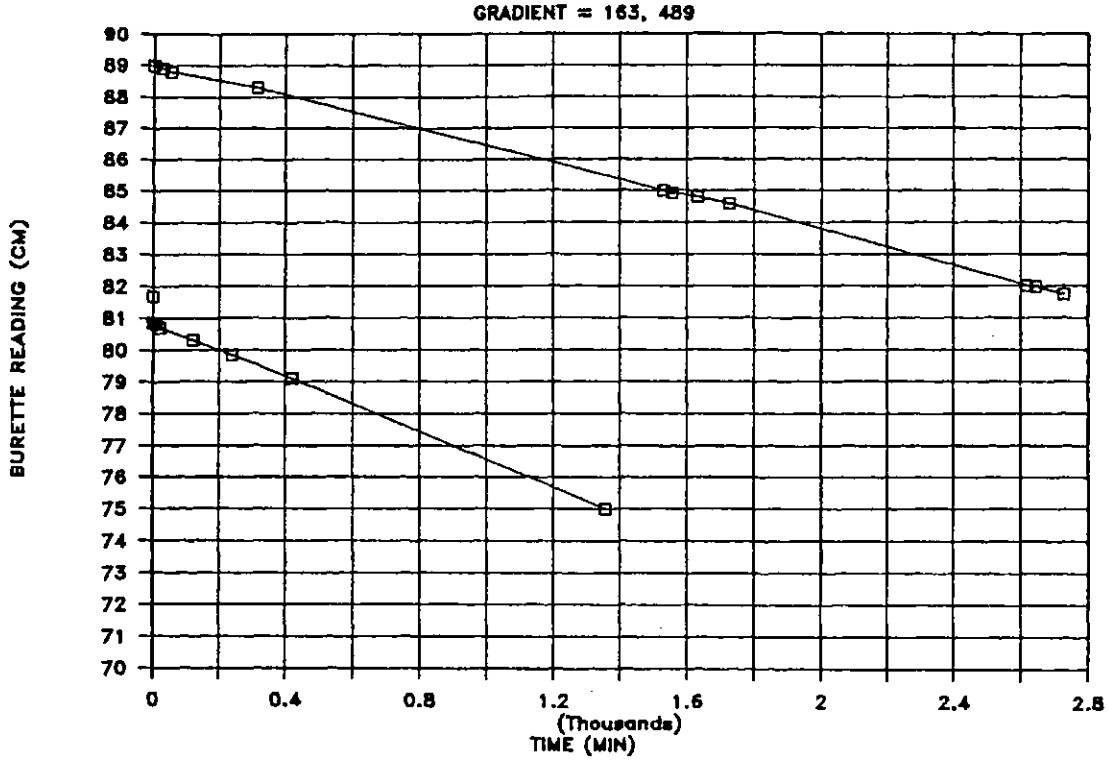

SAMPLE SB2

GRADIENT = 130, 259, 388

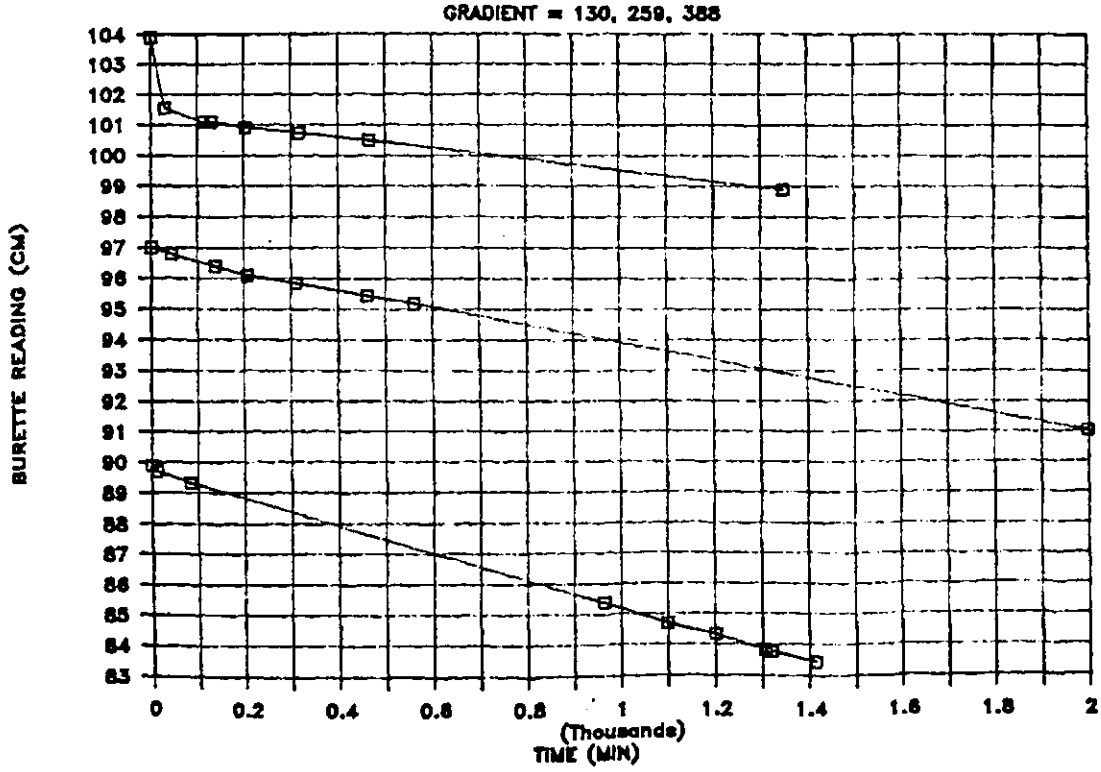

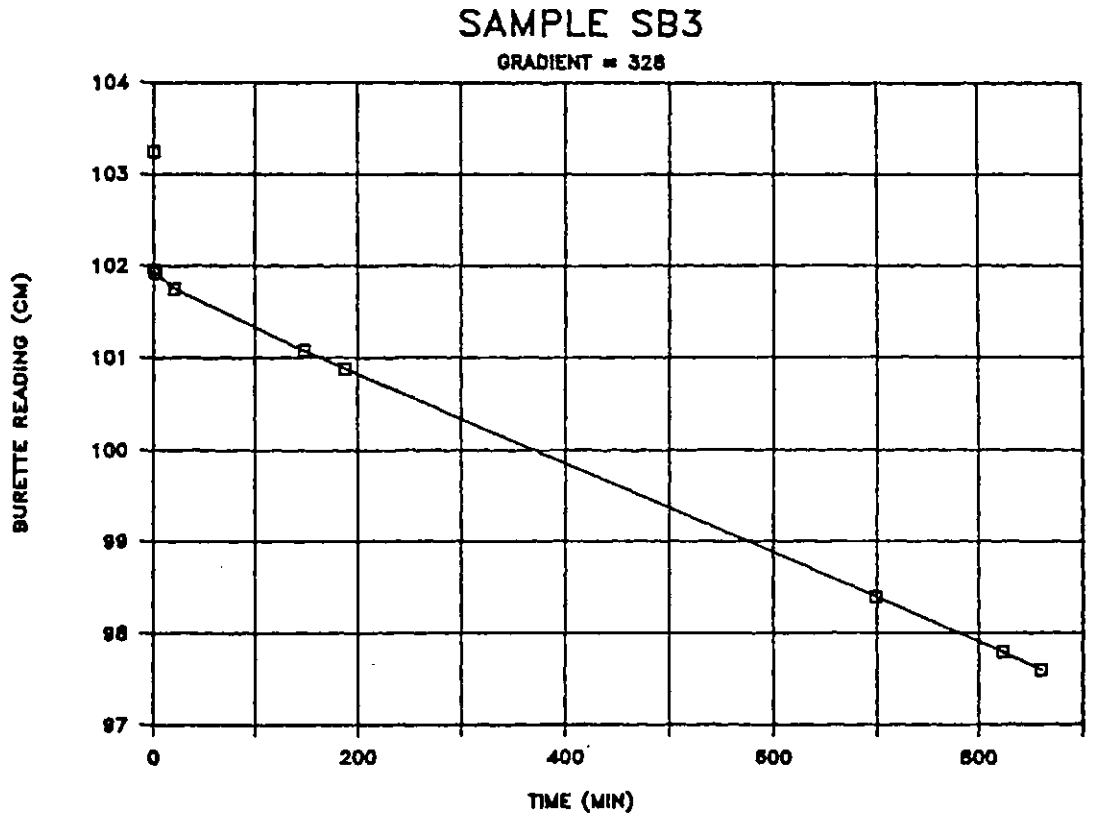
SAMPLE SB3
GRADIENT = 328
BURETTE READING (CM)
104
103
102
101
100
99
98
97
0
200
400
600
800
TIME (MIN)

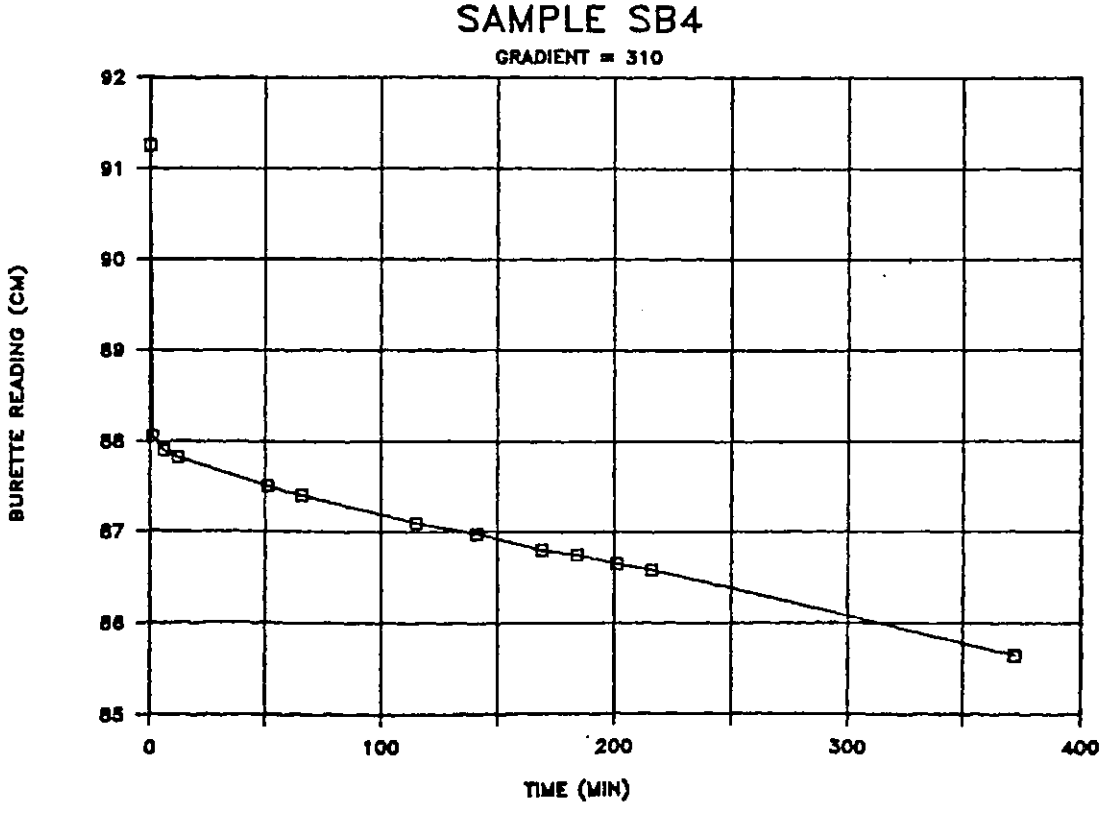
SAMPLE SB4
GRADIENT = 310
BURETTE READING (CM)
92
91
90
89
88
87
86
85
0
100
200
300
400
TIME (MIN)

SAMPLE SB5

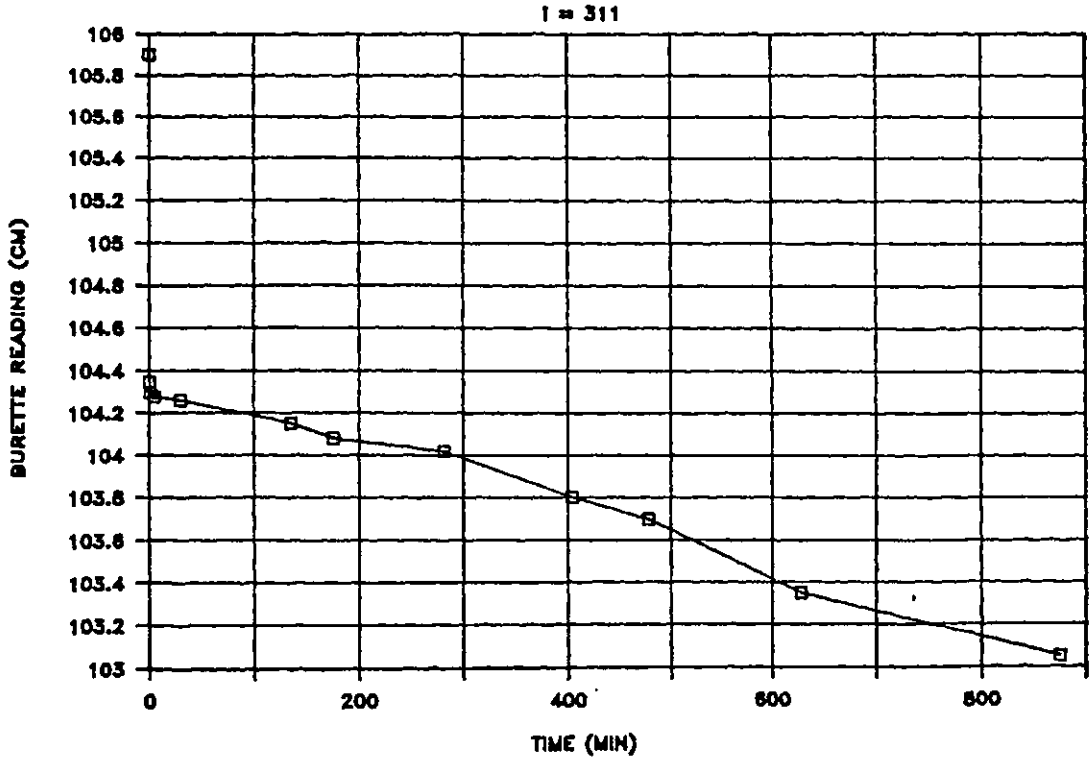

SAMPLE SB6

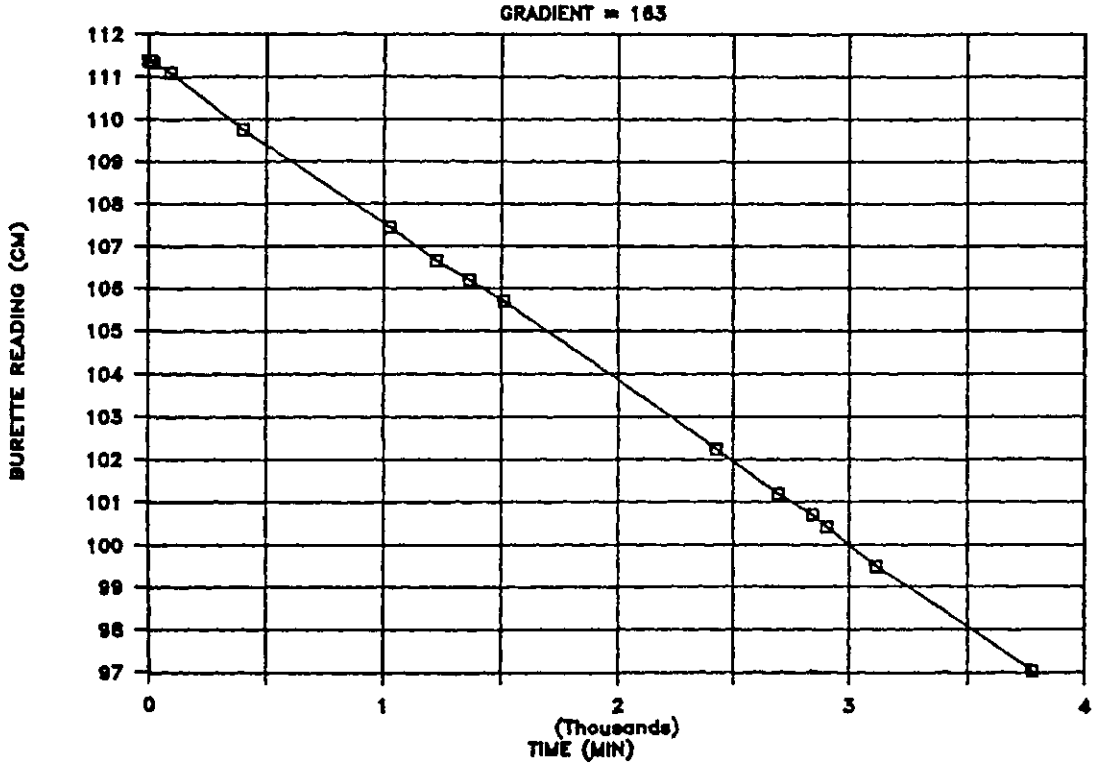

SAMPLE SB6 (POST OSMOTIC)

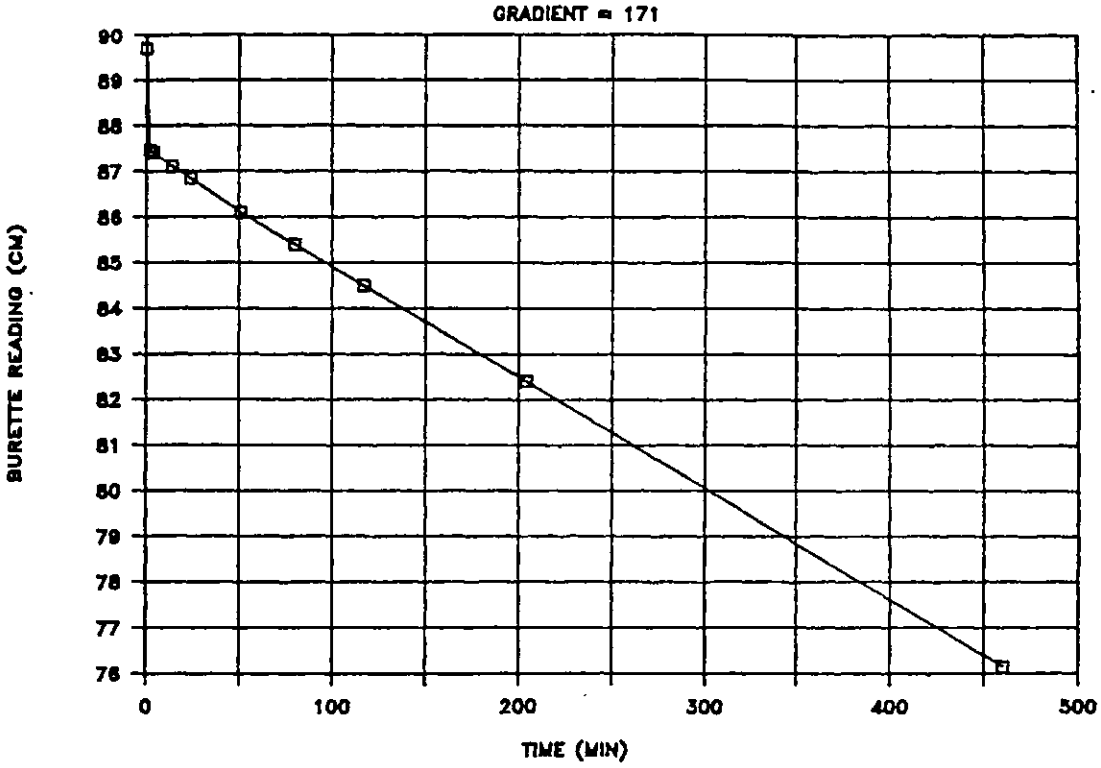

D.3 Osmotic Consolidation Time Deflection Curves

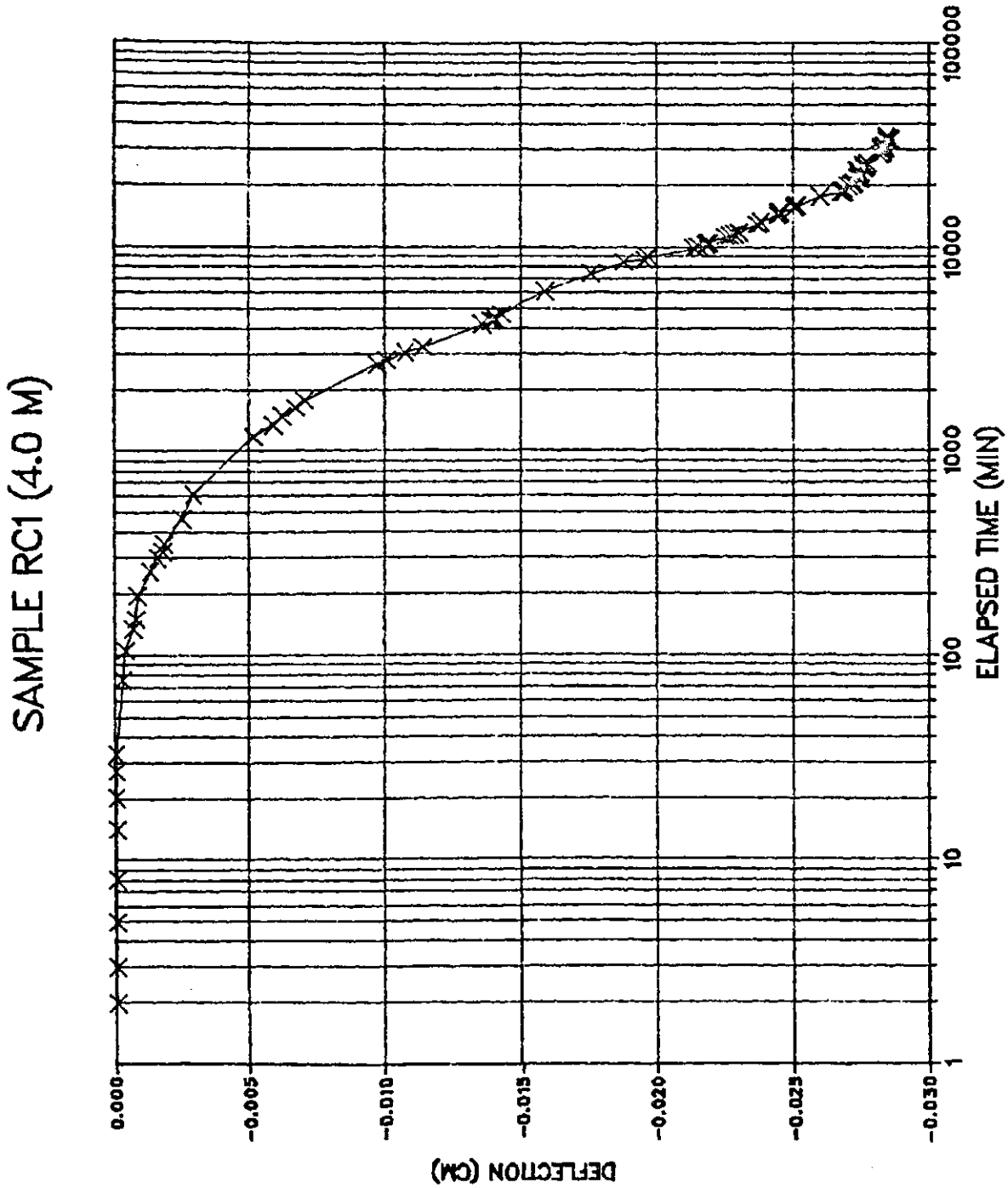

SAMPLE RC2 (4.0 M)

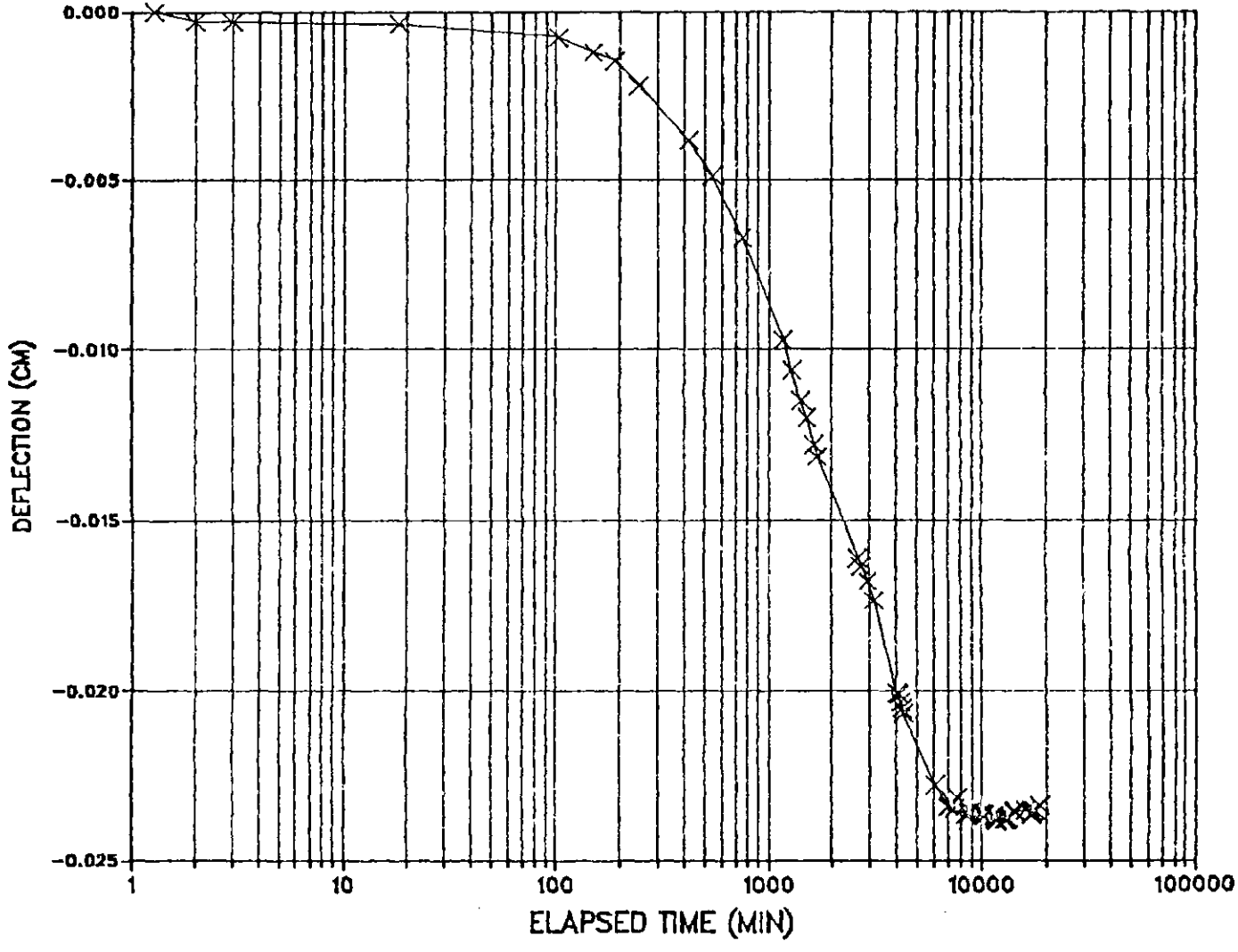

SAMPLE RC3 (4.0 M)

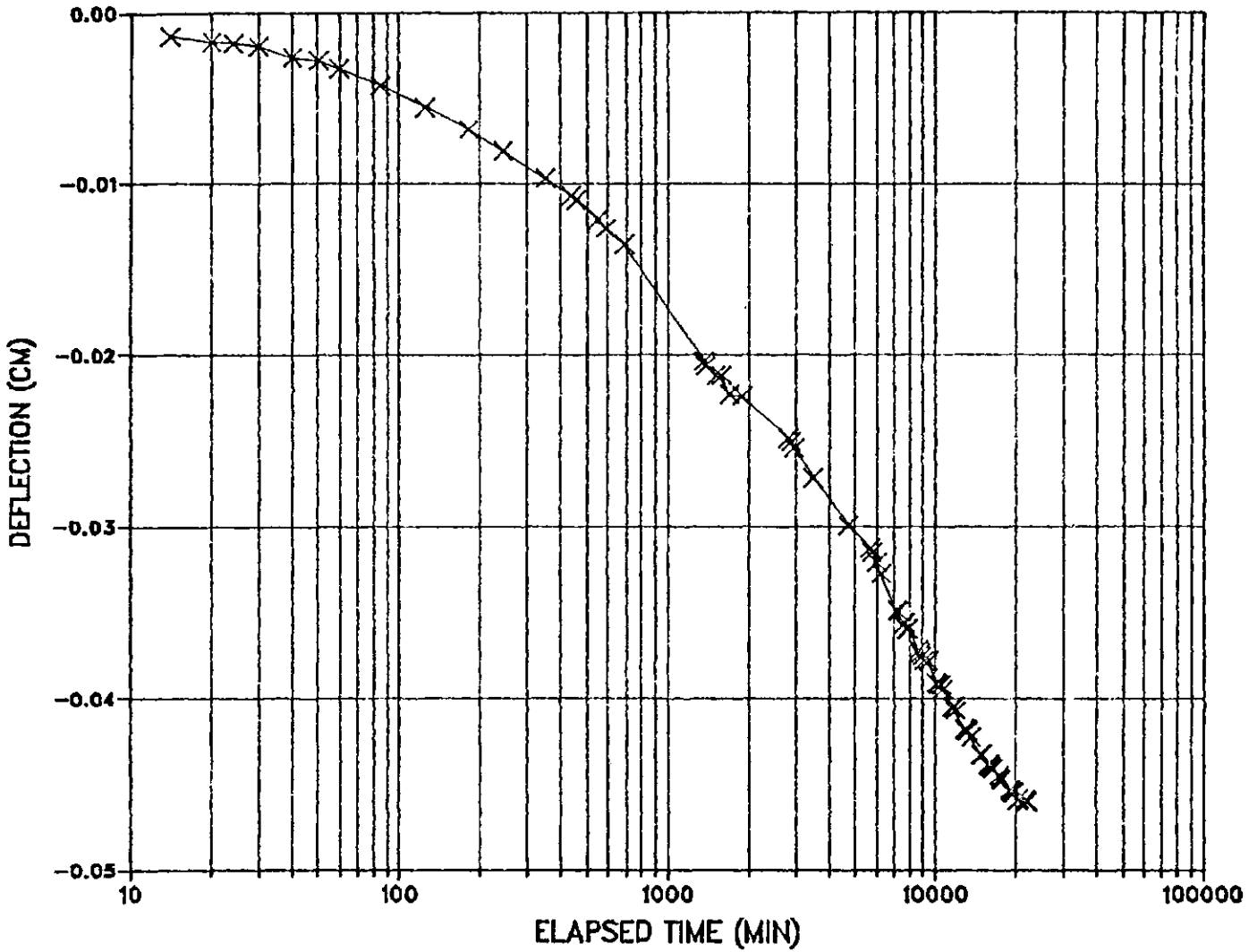

SAMPLE RC4

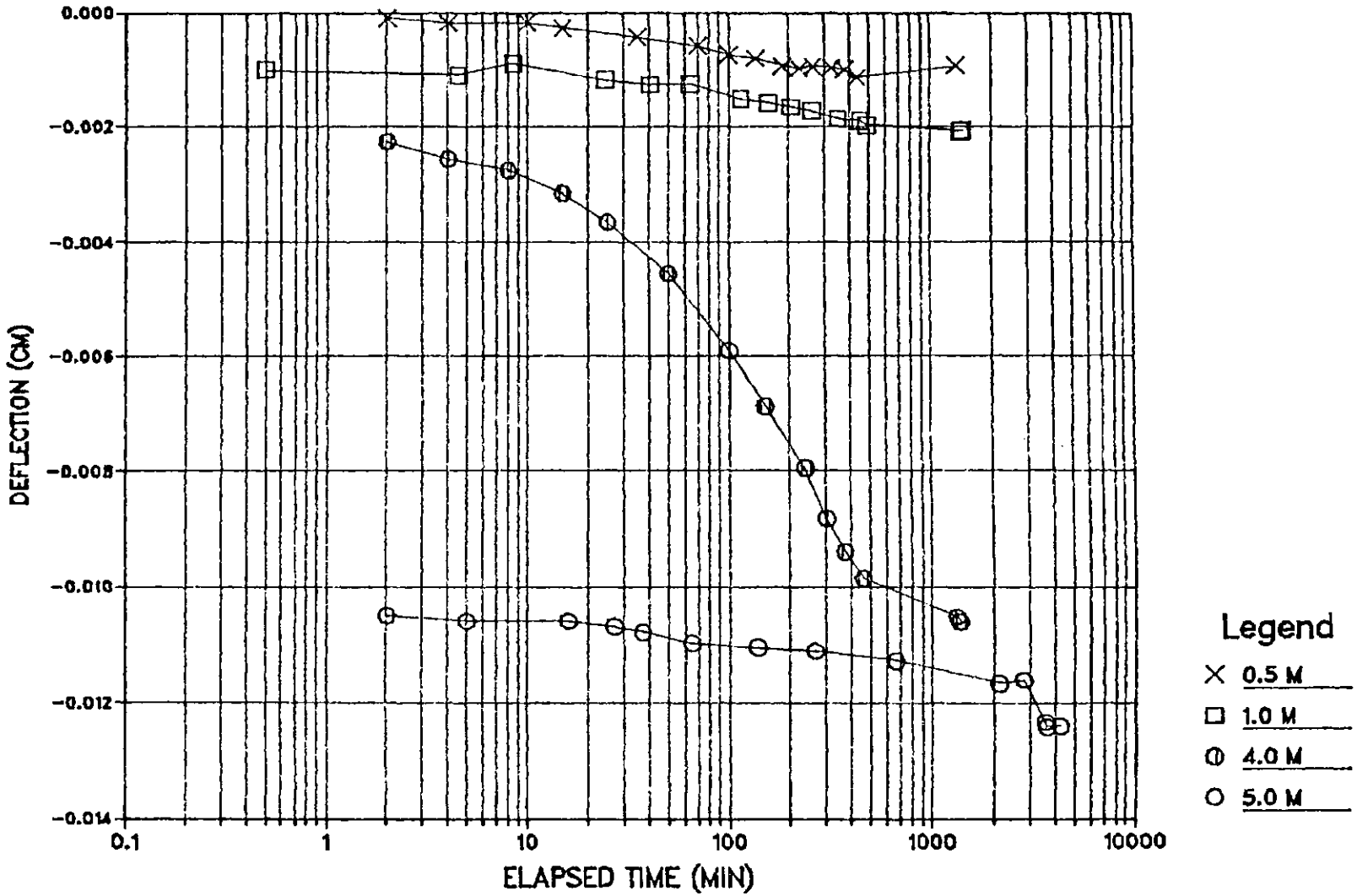
0.000
-0.002
-0.004
-0.006
-0.008
-0.010
-0.012
-0.014
DEFLECTION (CM)
0.1
1
10
100
1000
10000
ELAPSED TIME (MIN)
Legend
0.5 M
1.0 M
4.0 M
5.0 M

SAMPLE RC5

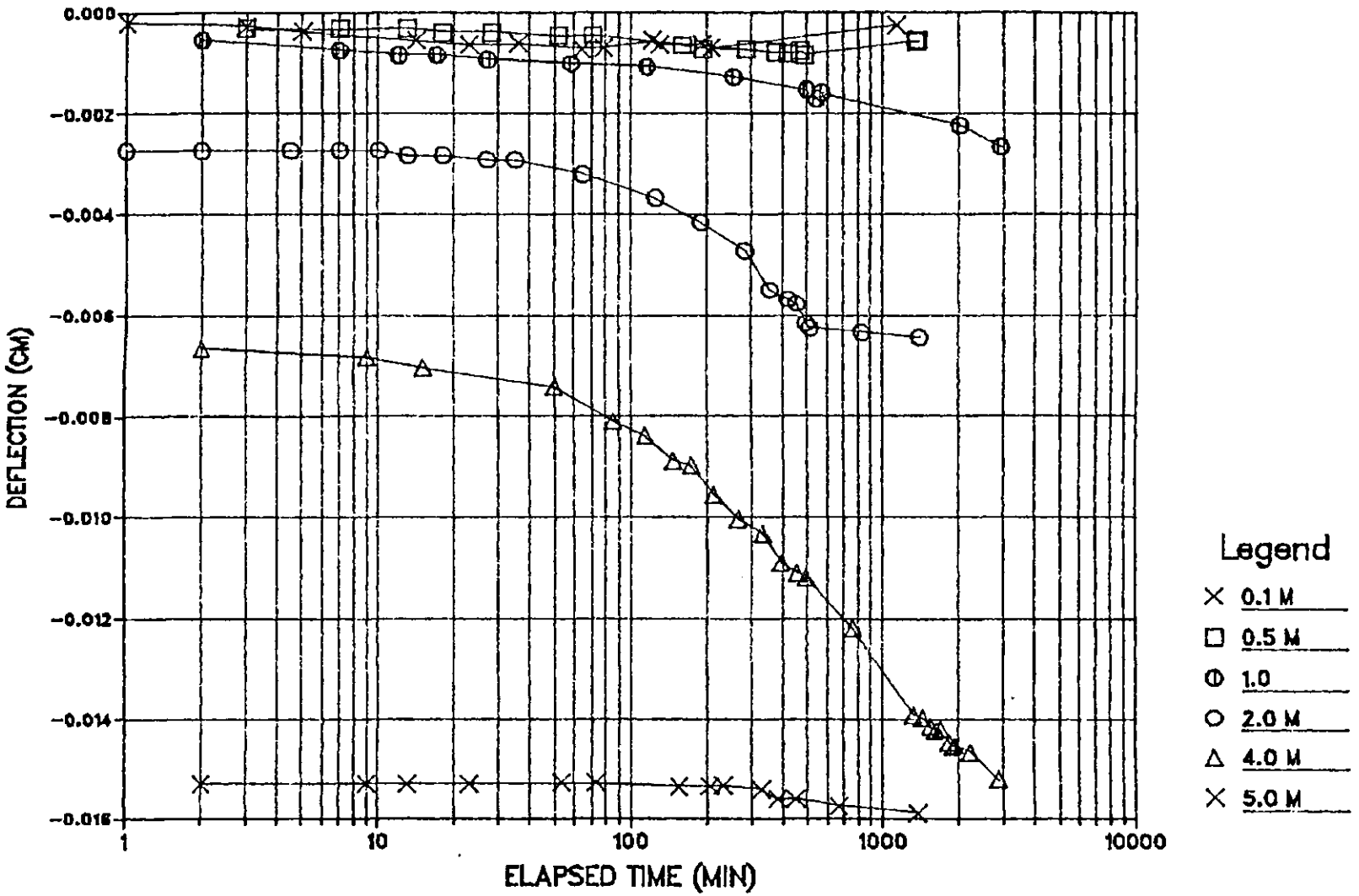
0.000
-0.002
-0.004
-0.006
-0.008
-0.010
-0.012
-0.014
-0.016
DEFLECTION (CM)
1
10
100
1000
10000
ELAPSED TIME (MIN)
Legend
0.1 M
0.5 M
1.0
2.0 M
4.0 M
5.0 M

SAMPLE RC6

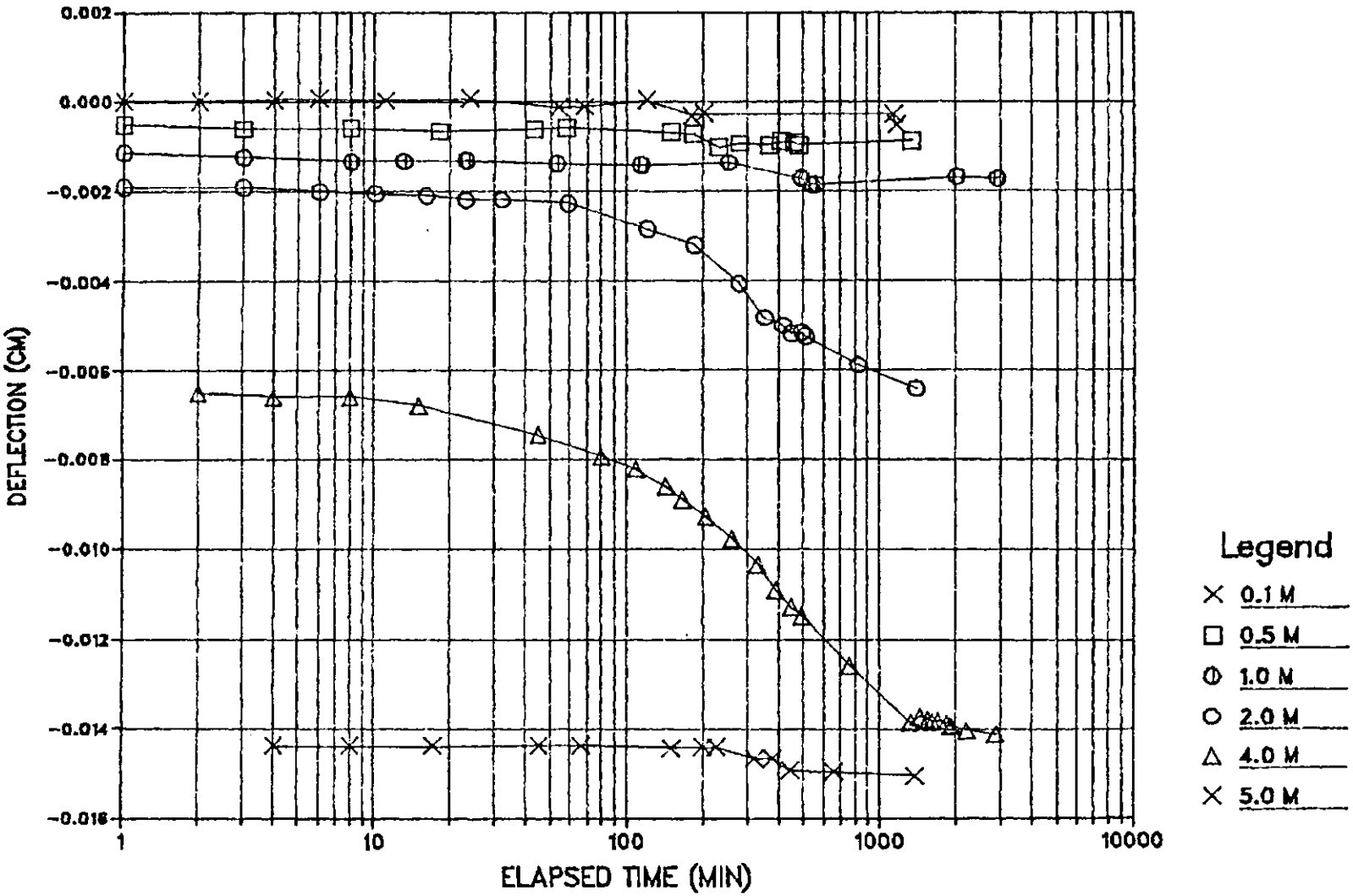
0.002
0.000
-0.002
-0.004
-0.006
-0.008
-0.010
-0.012
-0.014
-0.016
DEFLECTION (CM)
1
10
100
1000
10000
ELAPSED TIME (MIN)
Legend
0.1 M
0.5 M
1.0 M
2.0 M
4.0 M
5.0 M

SAMPLE RC7

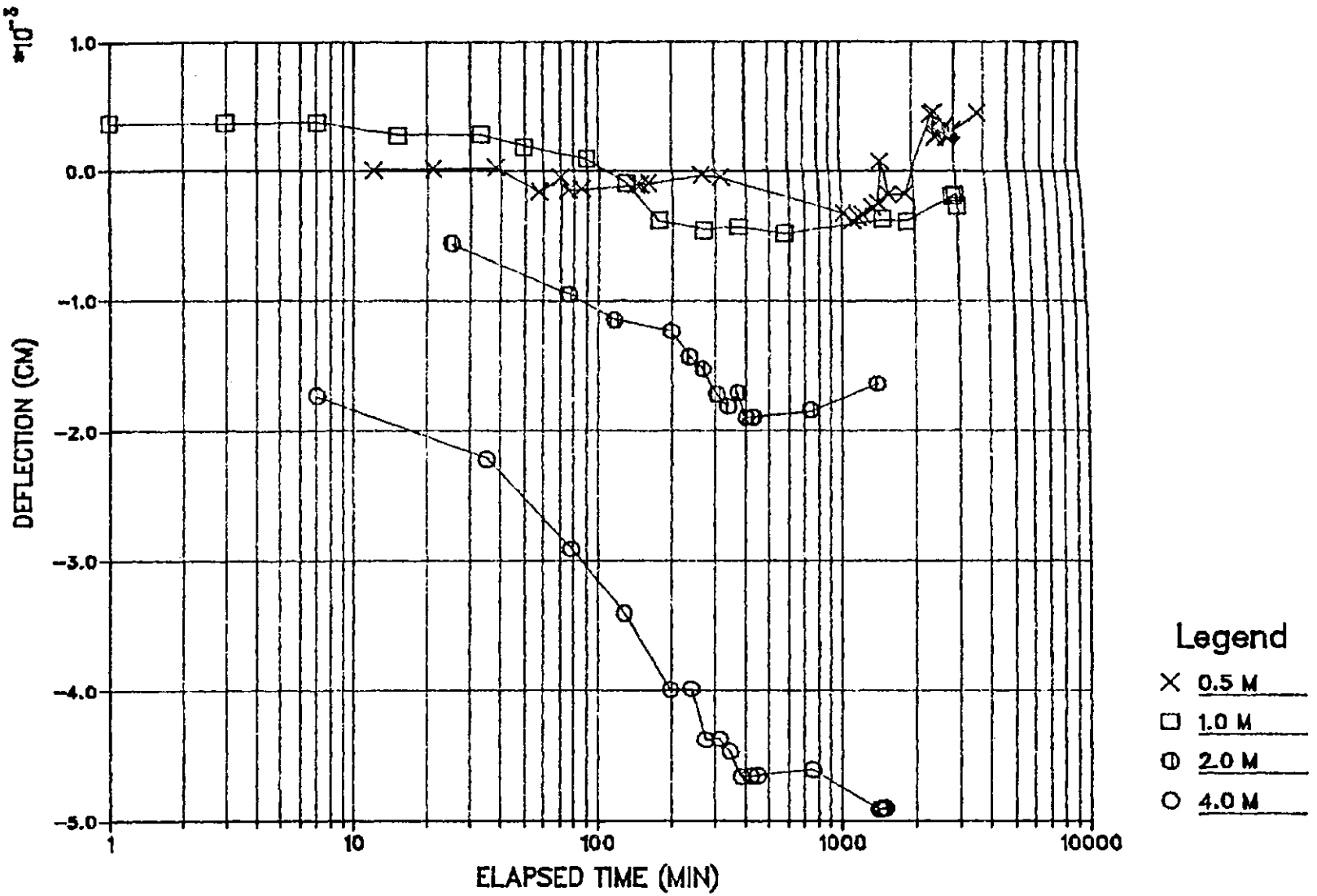
*10^-3
1.0
0.0
-1.0
-2.0
-3.0
-4.0
-5.0
DEFLECTION (CM)
1
10
100
1000
10000
ELAPSED TIME (MIN)
Legend
0.5 M
1.0 M
2.0 M
4.0 M

SAMPLE RC8

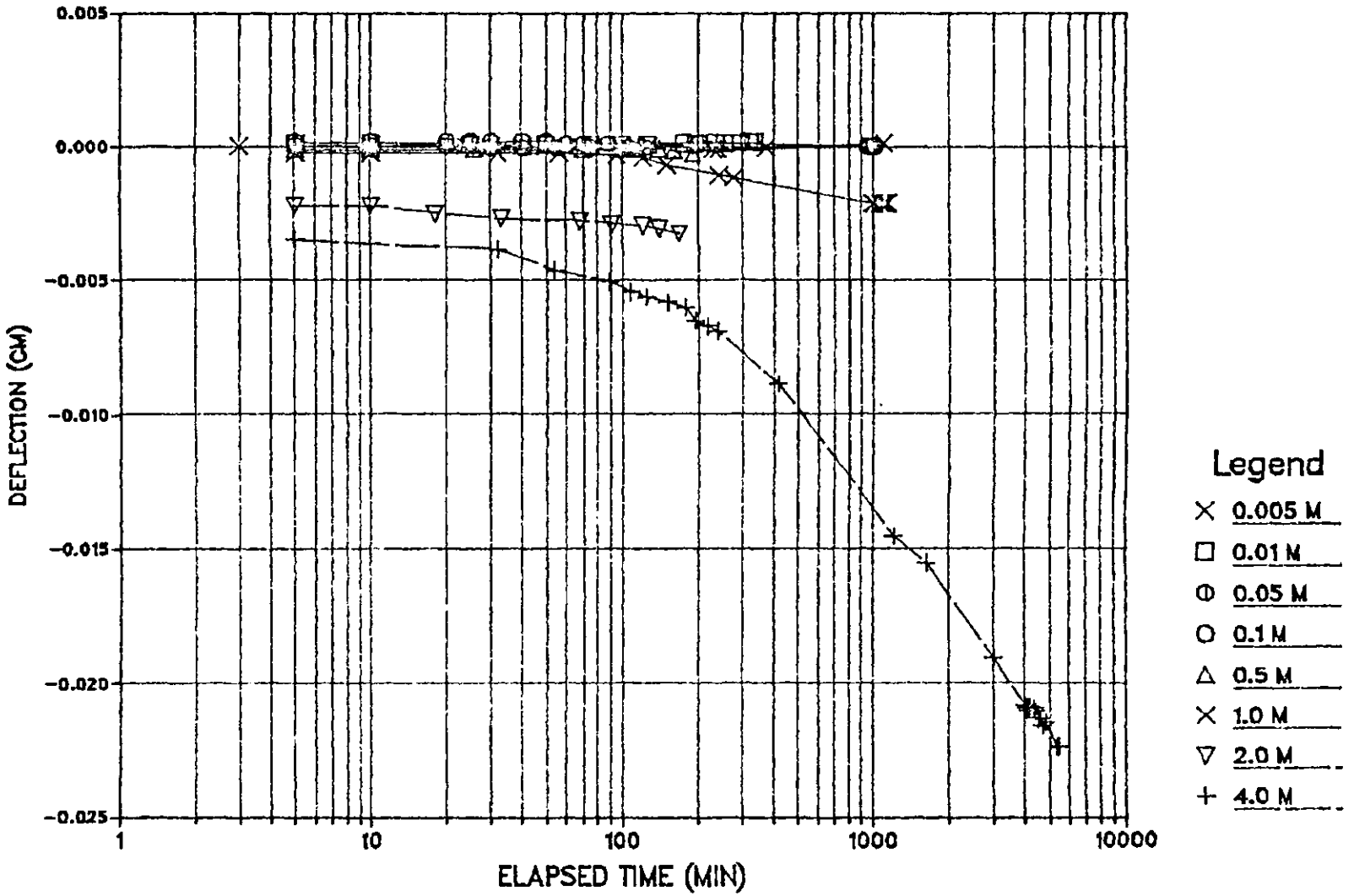
0.005
0.000
-0.005
-0.010
-0.015
-0.020
-0.025
DEFLECTION (CM)
1
10
100
1000
10000
ELAPSED TIME (MIN)
Legend
0.005 M
0.01 M
0.05 M
0.1 M
0.5 M
1.0 M
2.0 M
4.0 M

SAMPLE RC9

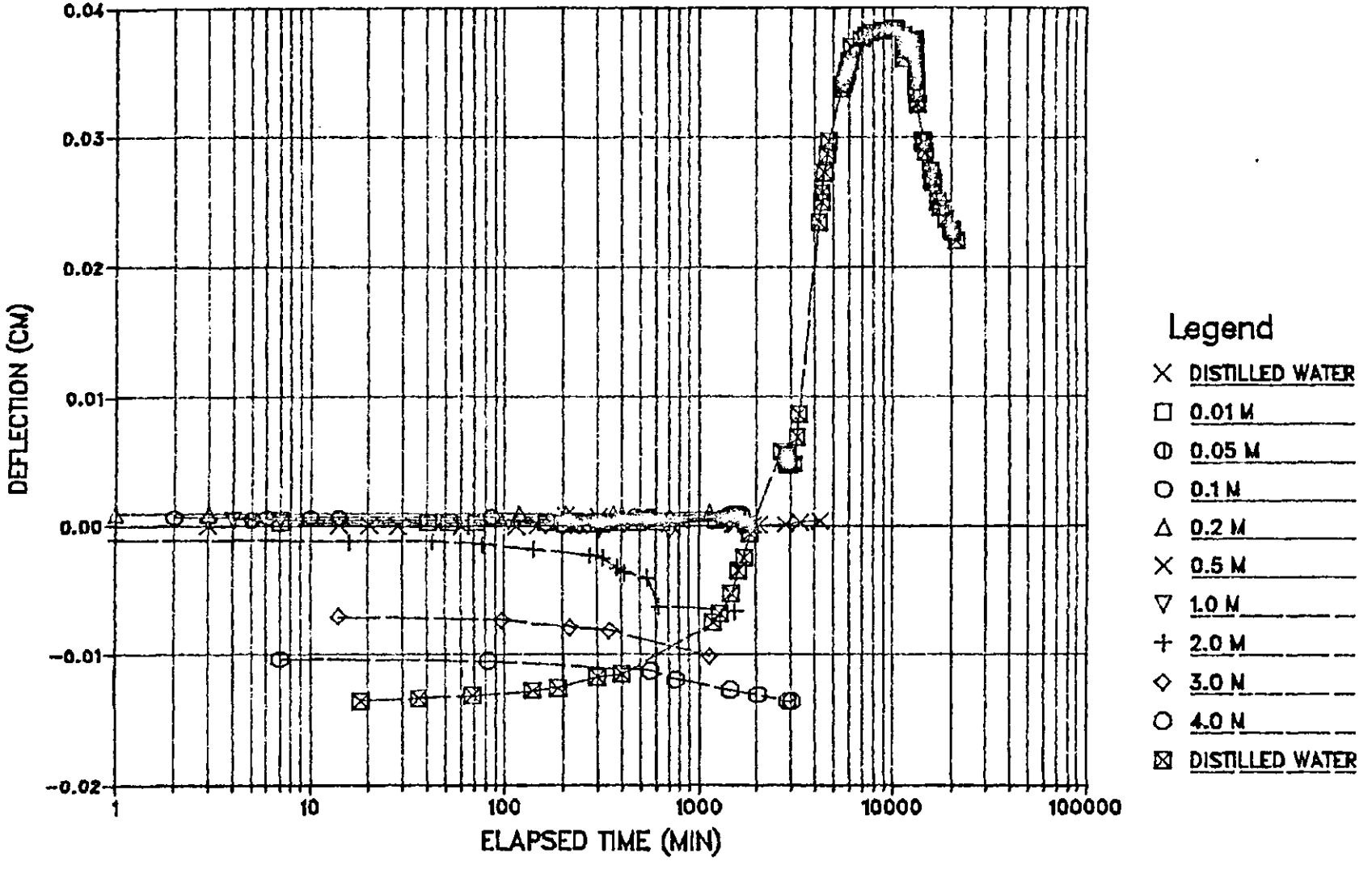
0.04
0.03
0.02
0.01
0.00
-0.01
-0.02
DEFLECTION (CM)
1
10
100
1000
10000
100000
ELAPSED TIME (MIN)
Legend
DISTILLED WATER
0.01 M
0.05 M
0.1 M
0.2 M
0.5 M
1.0 M
2.0 M
3.0 M
4.0 M
DISTILLED WATER

SAMPLE RC10 (4.0 M)

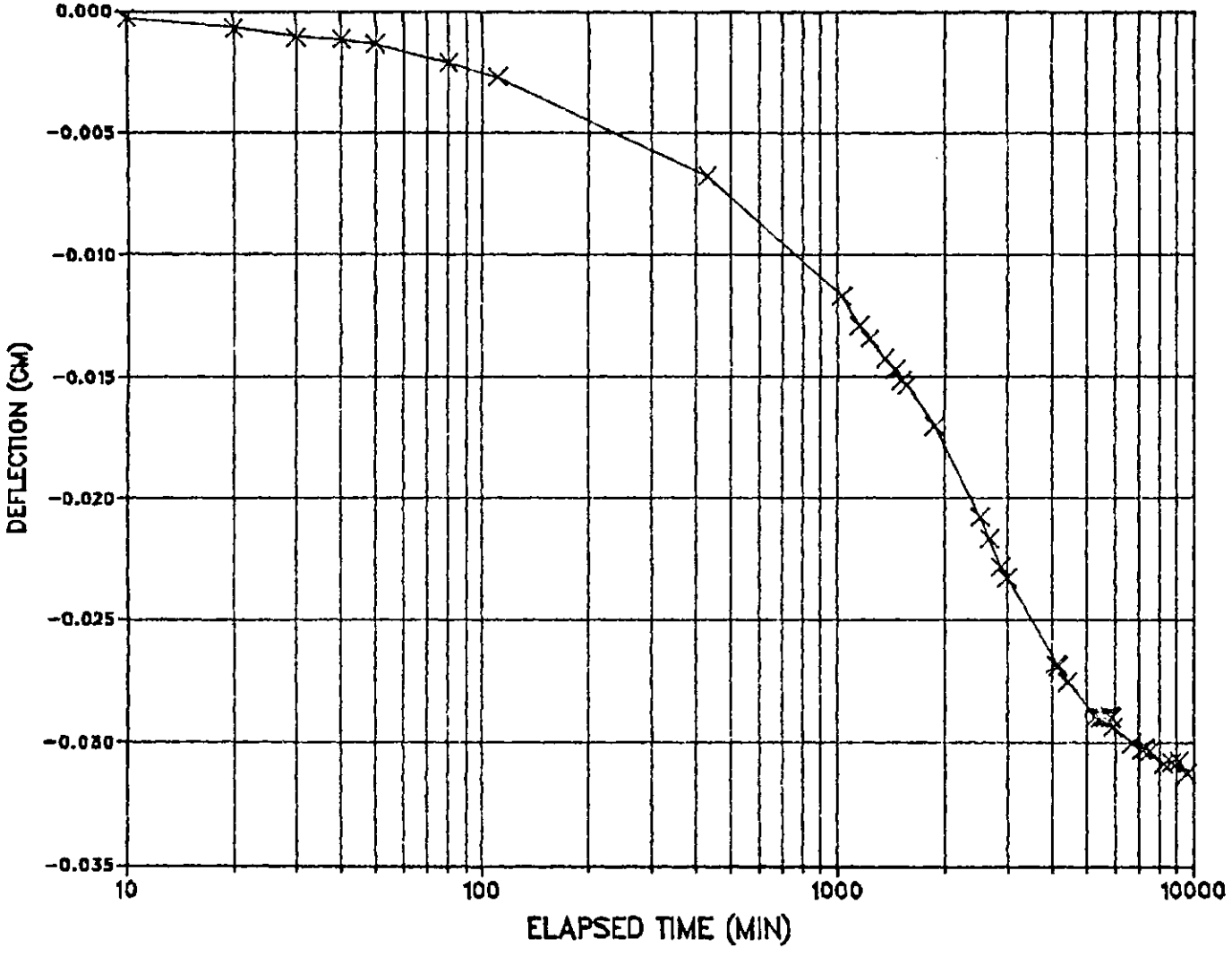

SAMPLE SB1 (4.0 M)

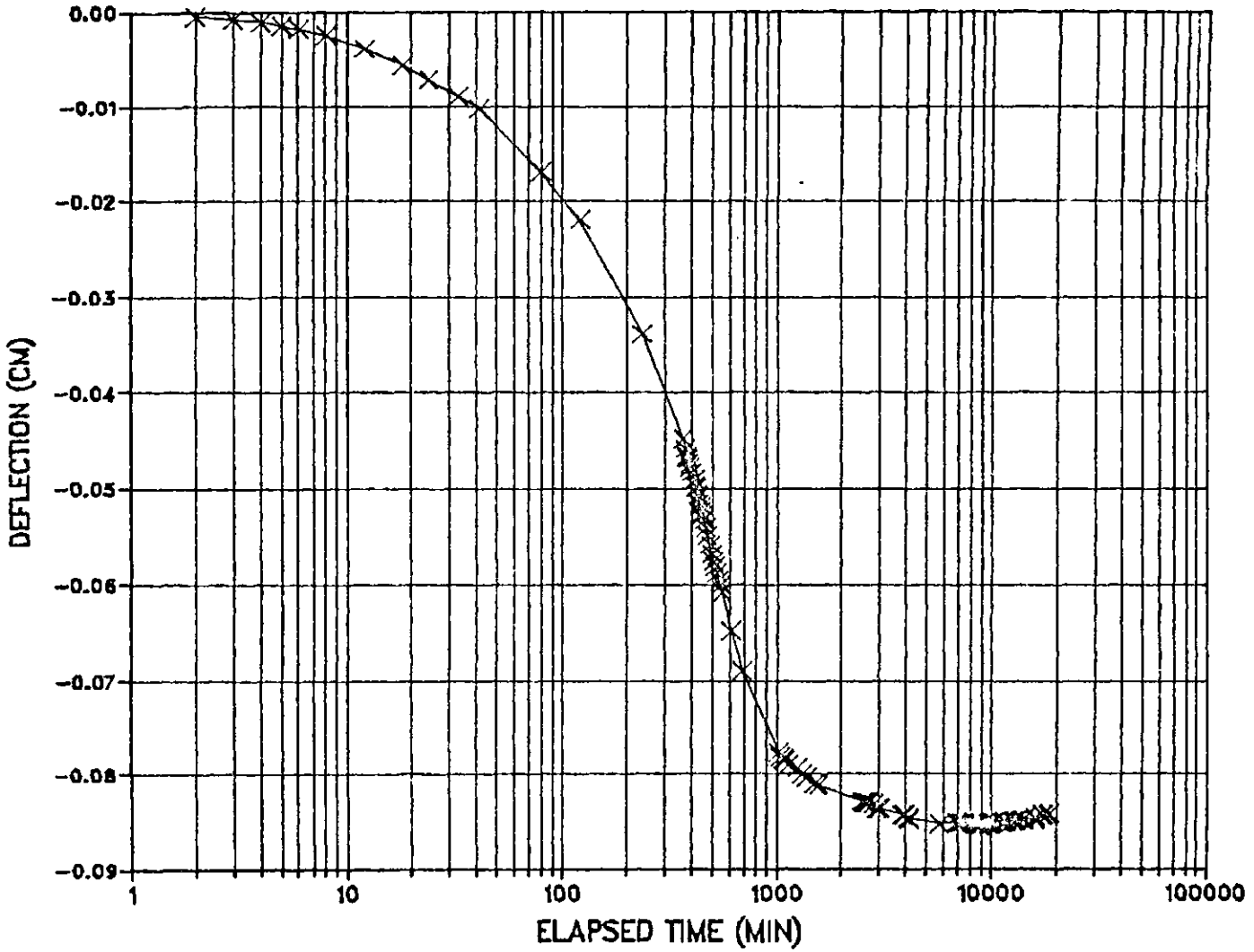

D50

SAMPLE SB2 (4.0 M)

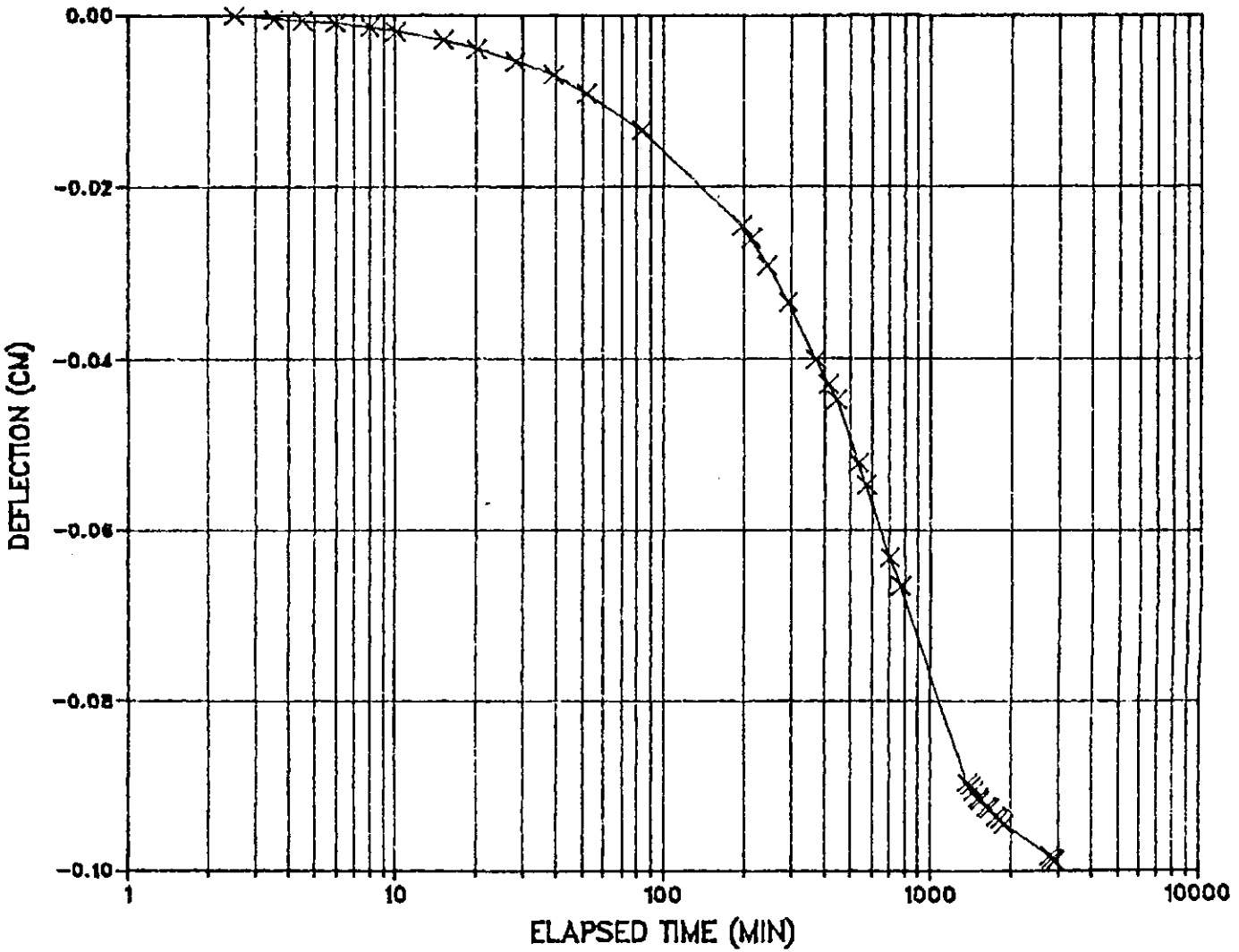

SAMPLE SB3

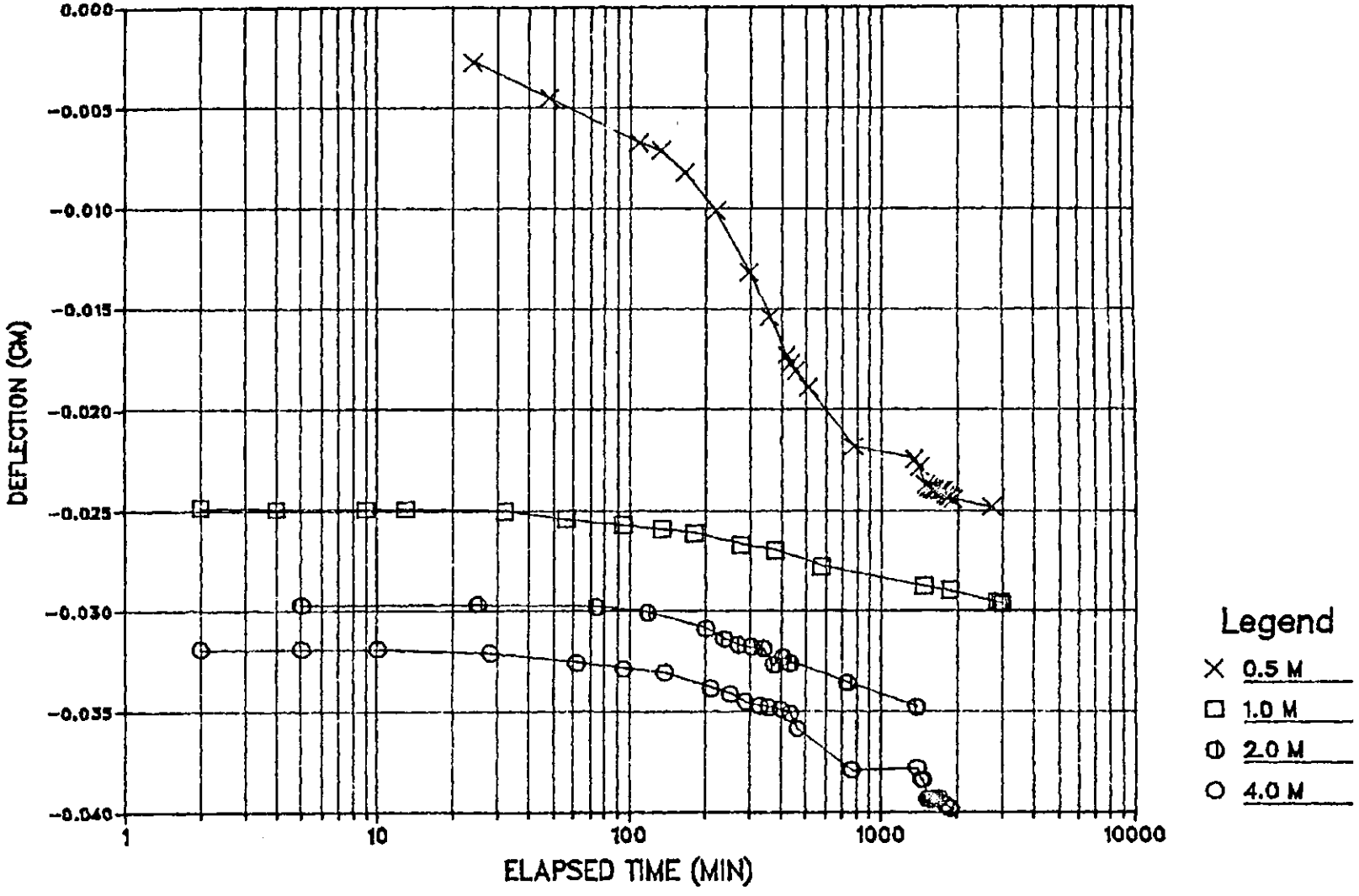
0.000
-0.005
-0.010
-0.015
-0.020
-0.025
-0.030
-0.035
-0.040
DEFLECTION (CM)
1
10
100
1000
10000
ELAPSED TIME (MIN)
Legend
0.5 M
1.0 M
2.0 M
4.0 M

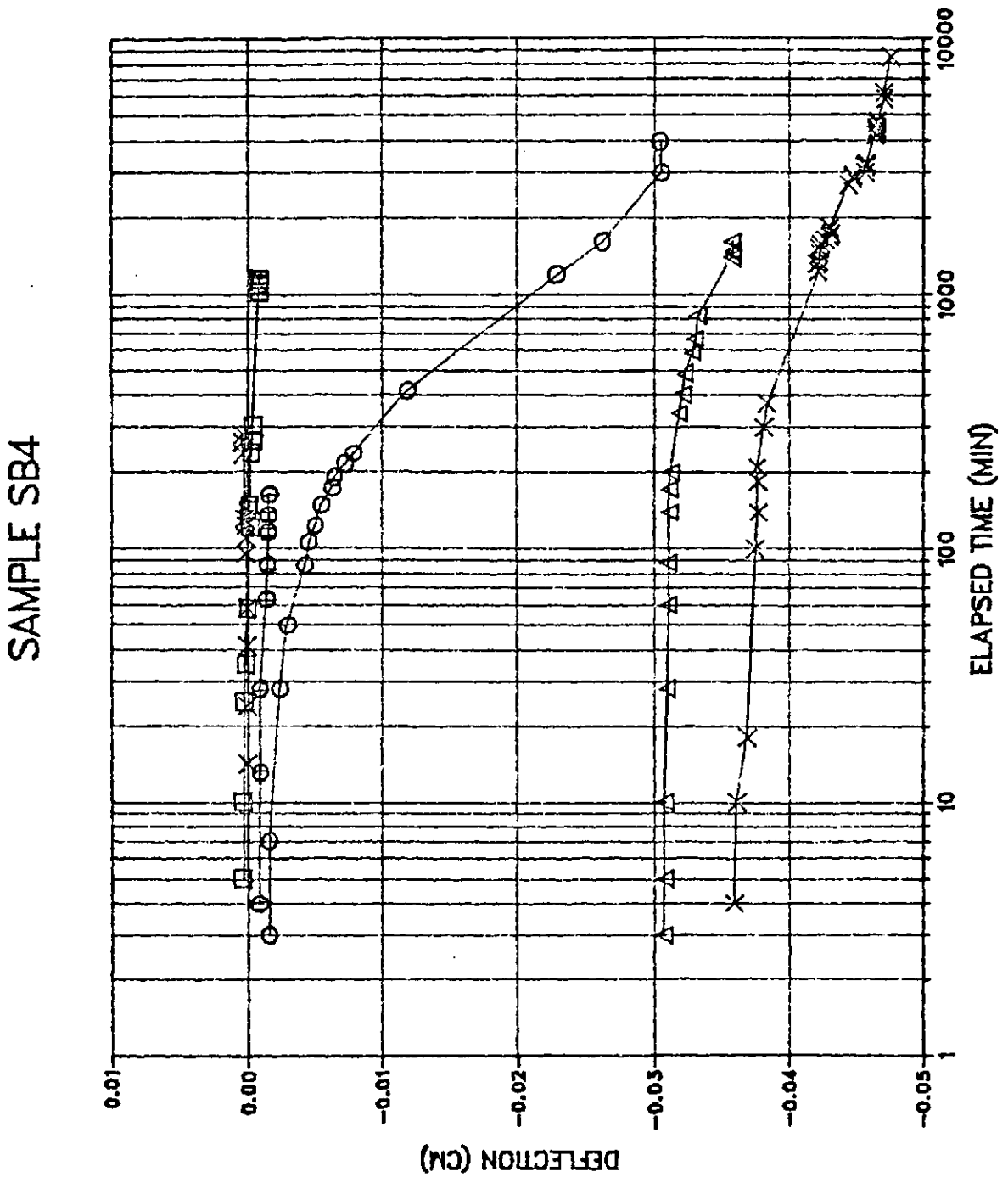
SAMPLE SB4
Legend
DISTILLED WATER
.05 M
0.1 M
0.5 M
1.0 M
2.0 M
DEFLECTION (CM)
0.01
0.00
-0.01
-0.02
-0.03
-0.04
-0.05
ELAPSED TIME (MIN)
1
10
100
1000
10000

SAMPLE SB5

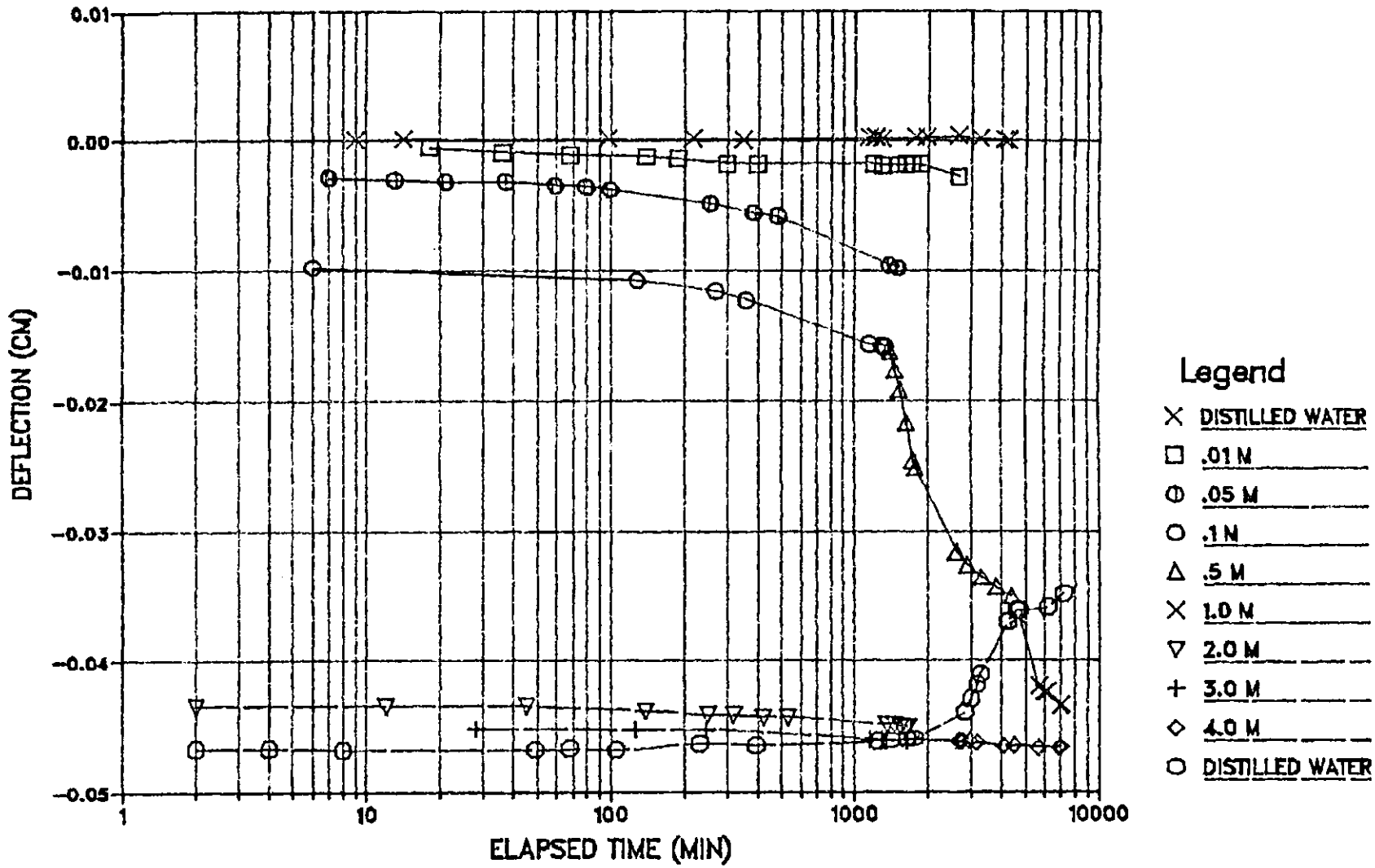
0.01
0.00
-0.01
-0.02
-0.03
-0.04
-0.05
DEFLECTION (CM)
1
10
100
1000
10000
ELAPSED TIME (MIN)
Legend
DISTILLED WATER
.01 M
.05 M
.1 M
.5 M
1.0 M
2.0 M
3.0 M
4.0 M
DISTILLED WATER

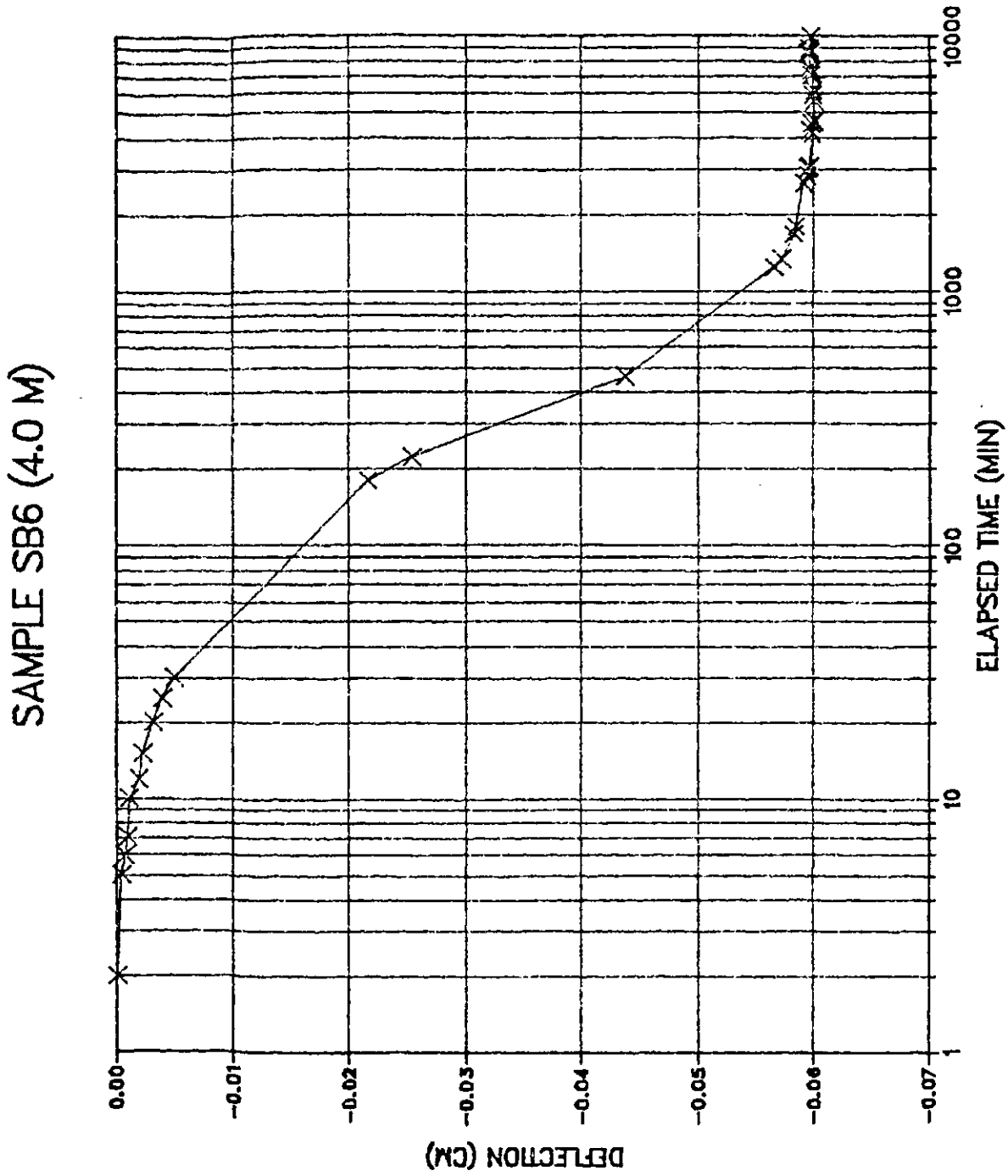
SAMPLE SB6 (4.0 M)
DEFLECTION (CM)
0.00
-0.01
-0.02
-0.03
-0.04
-0.05
-0.06
-0.07
ELAPSED TIME (MIN)
1
10
100
1000
10000

SAMPLE SBOC1

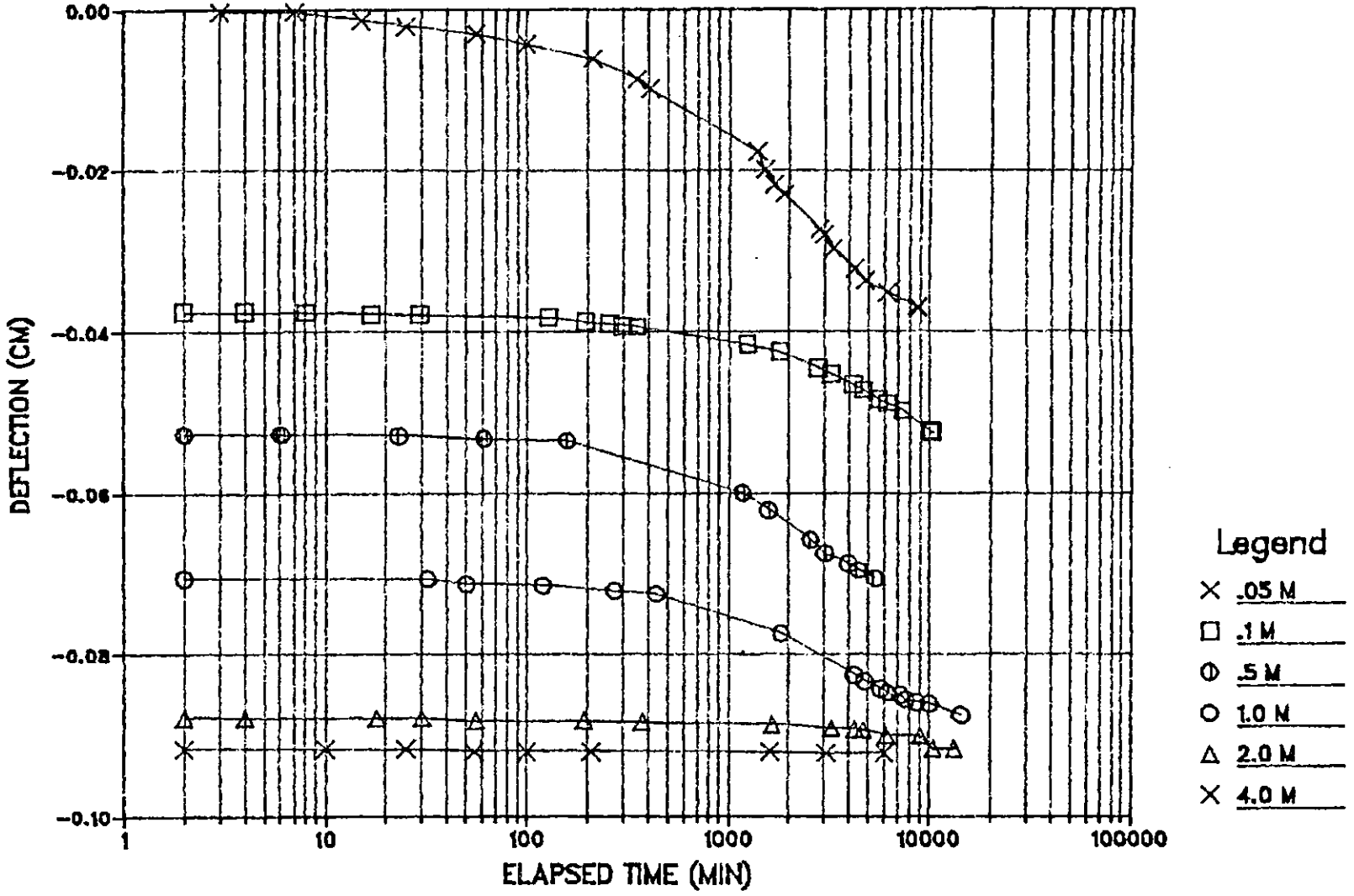

SAMPLE SBOC2

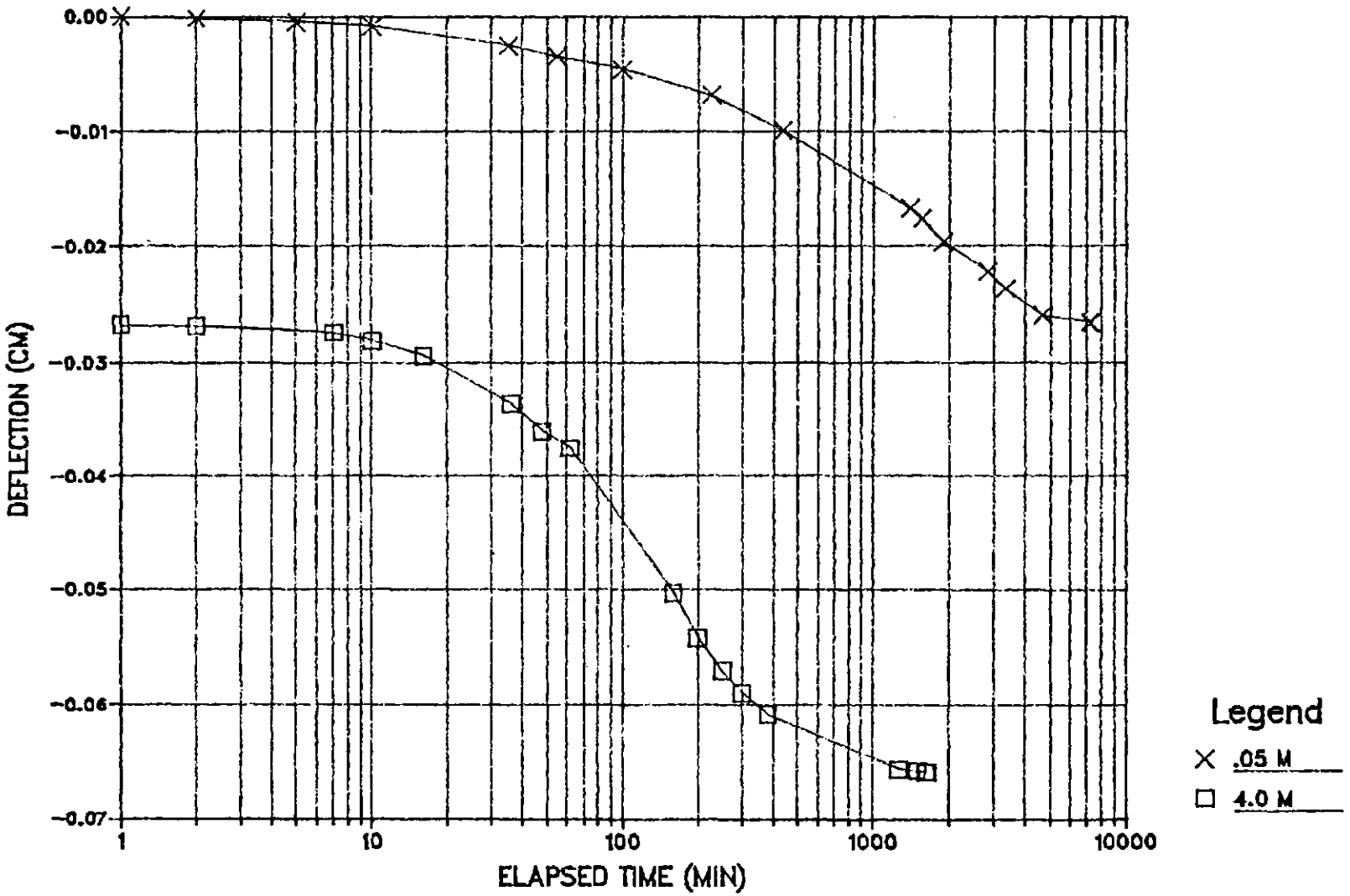

SAMPLE SBOC3

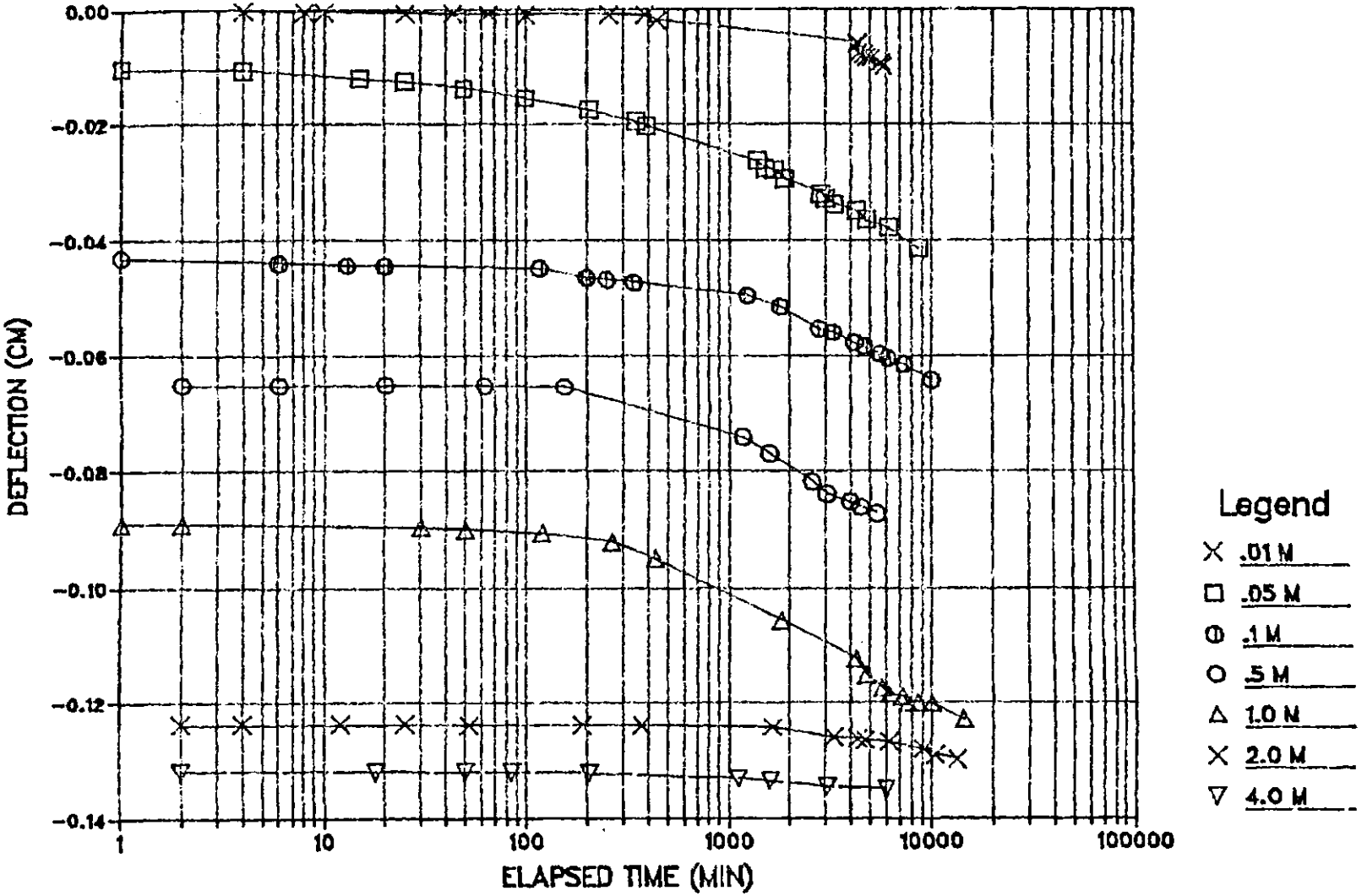

SAMPLE DB1 (4.0 M)

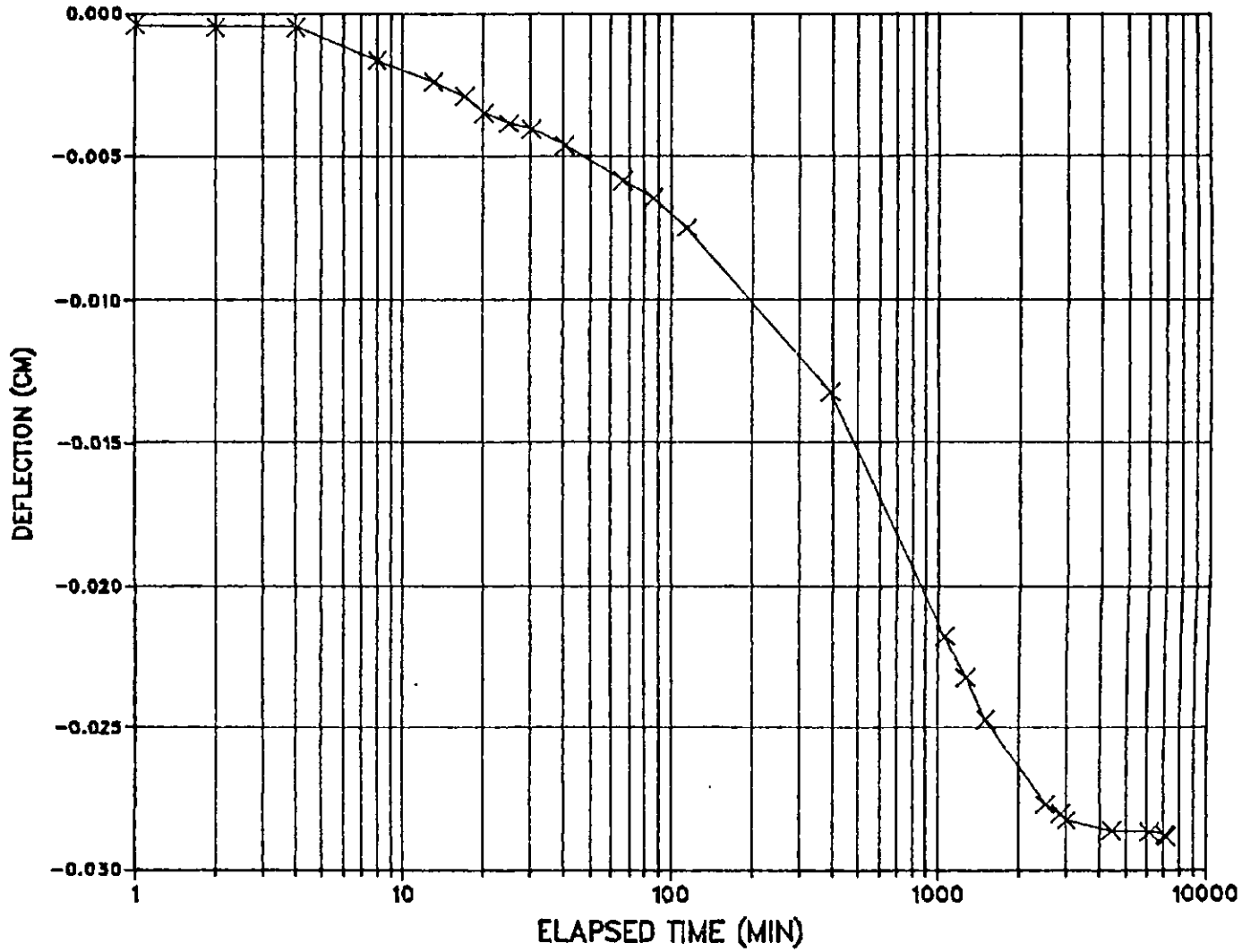

SAMPLE DB2

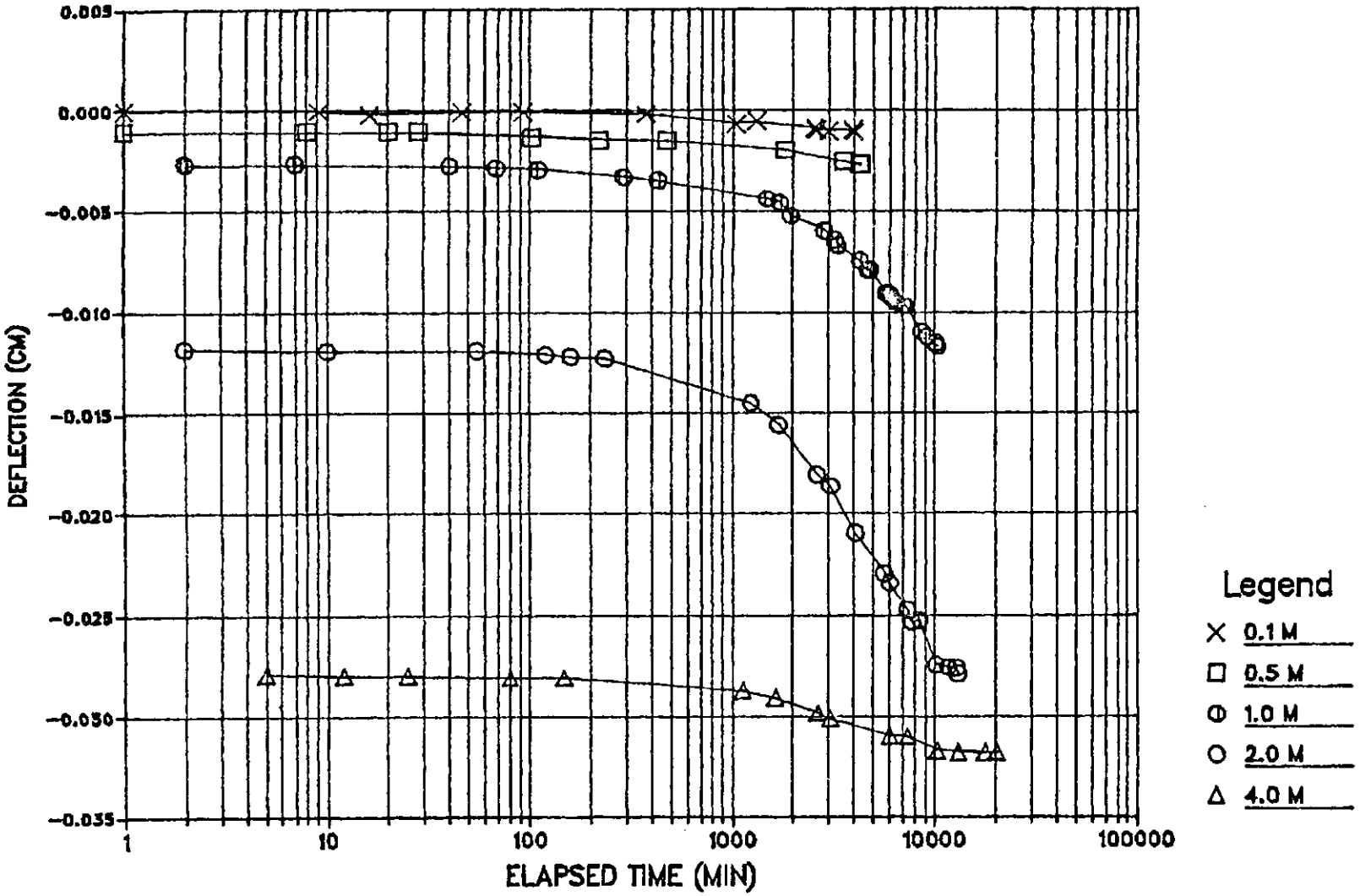

060

SAMPLE DB3 (4.0 M)

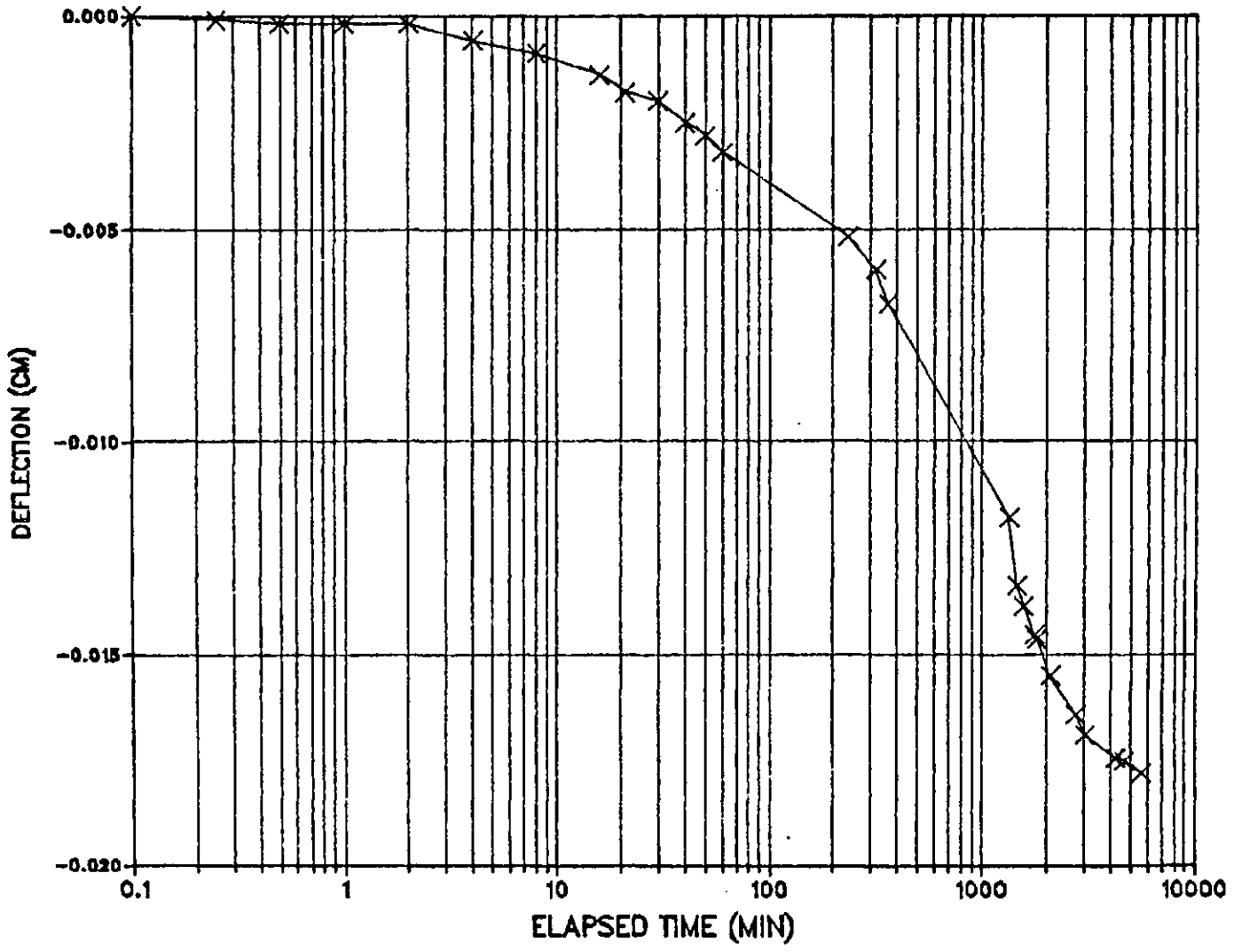

SAMPLE DB4

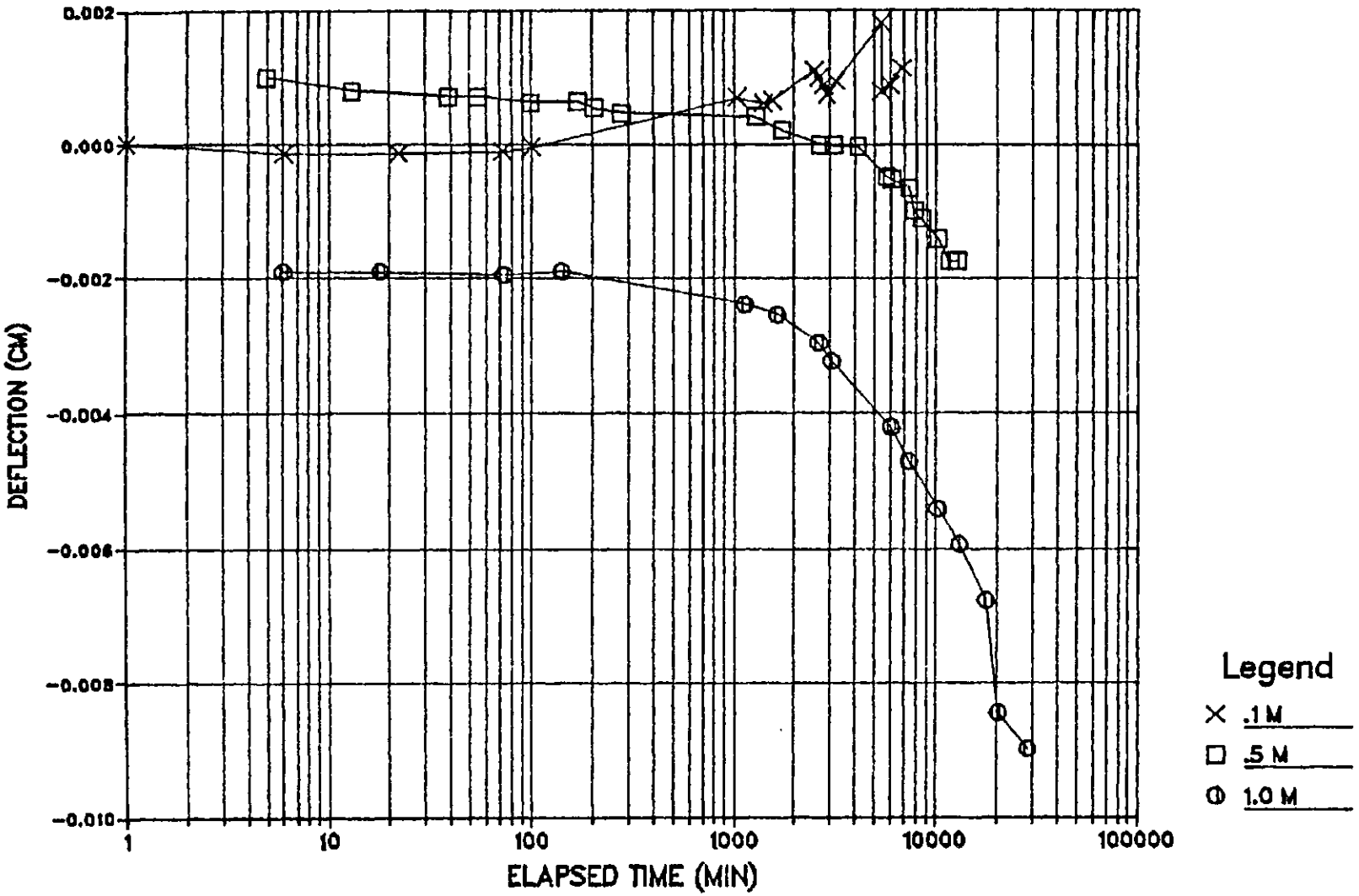
0.002
0.000
-0.002
-0.004
-0.006
-0.008
-0.010
DEFLECTION (CM)
1
10
100
1000
10000
100000
ELAPSED TIME (MIN)
Legend
.1 M
.5 M
1.0 M

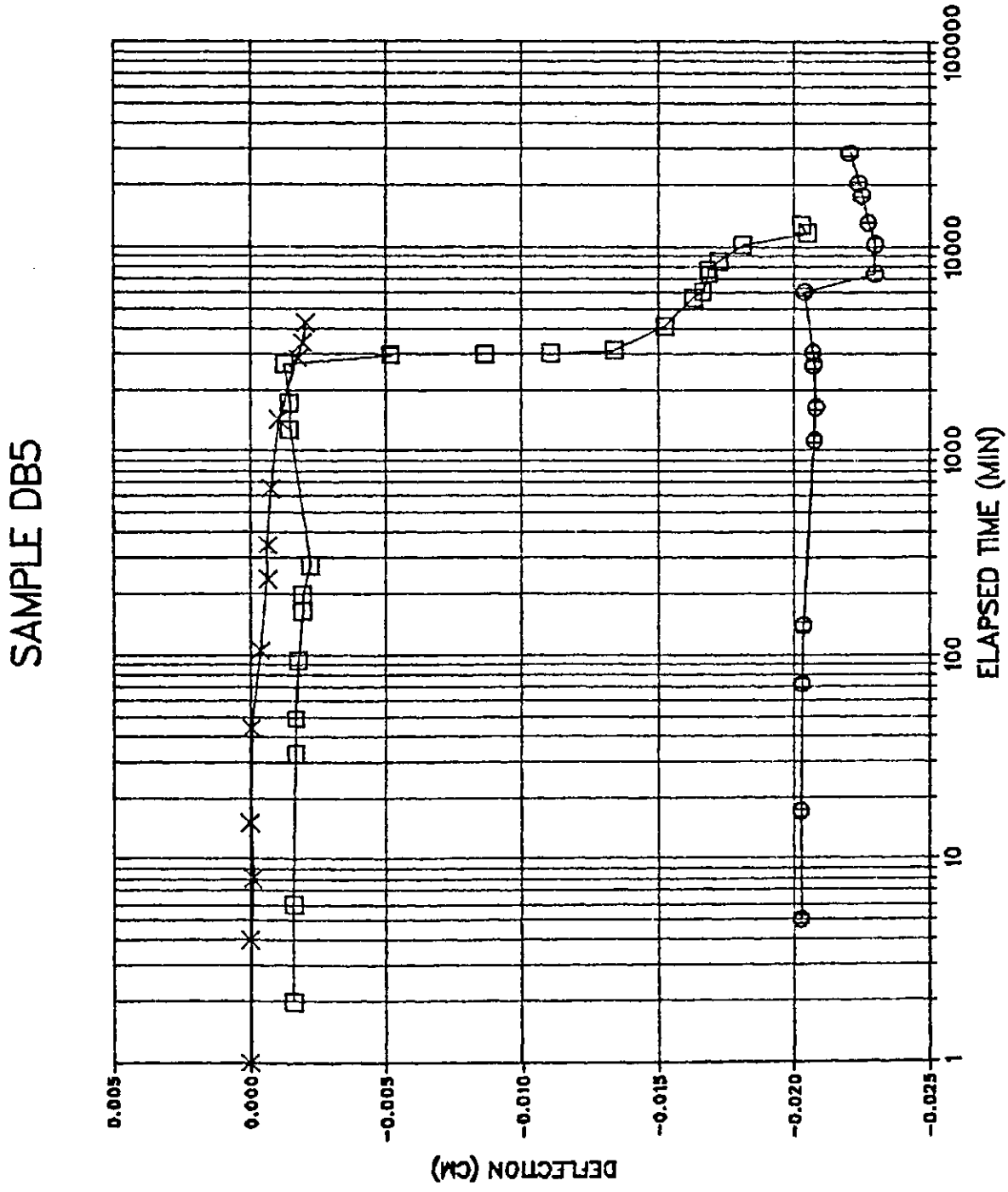
SAMPLE DB5
Legend
0.1 M
.5 M
1.0 M
DEFLECTION (CM)
0.005
0.000
-0.005
-0.010
-0.015
-0.020
-0.025
ELAPSED TIME (MIN)
1
10
100
1000
10000
100000

SAMPLE DB6 (4.0 M)

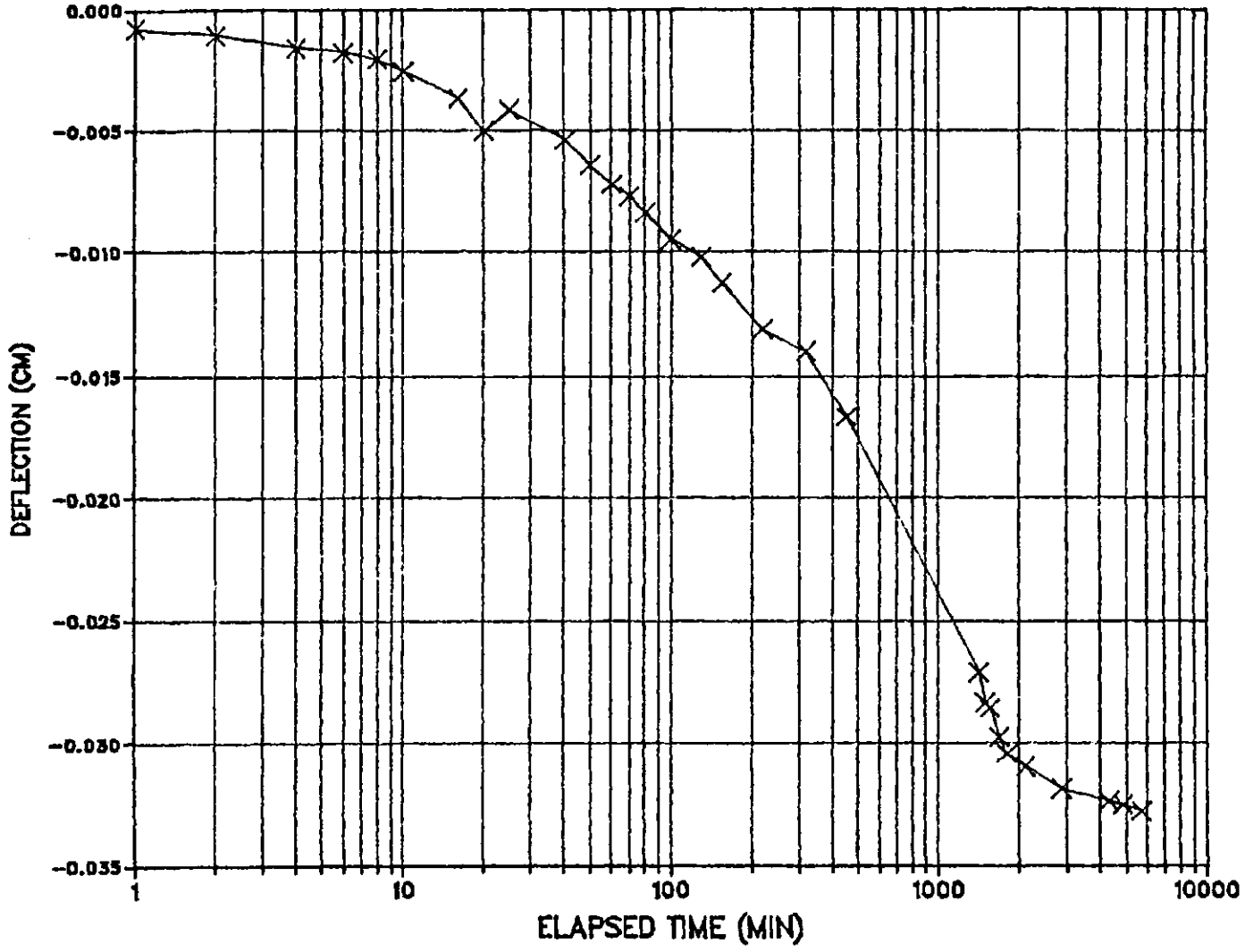

D.4 Cummulative Base Flow versus Time

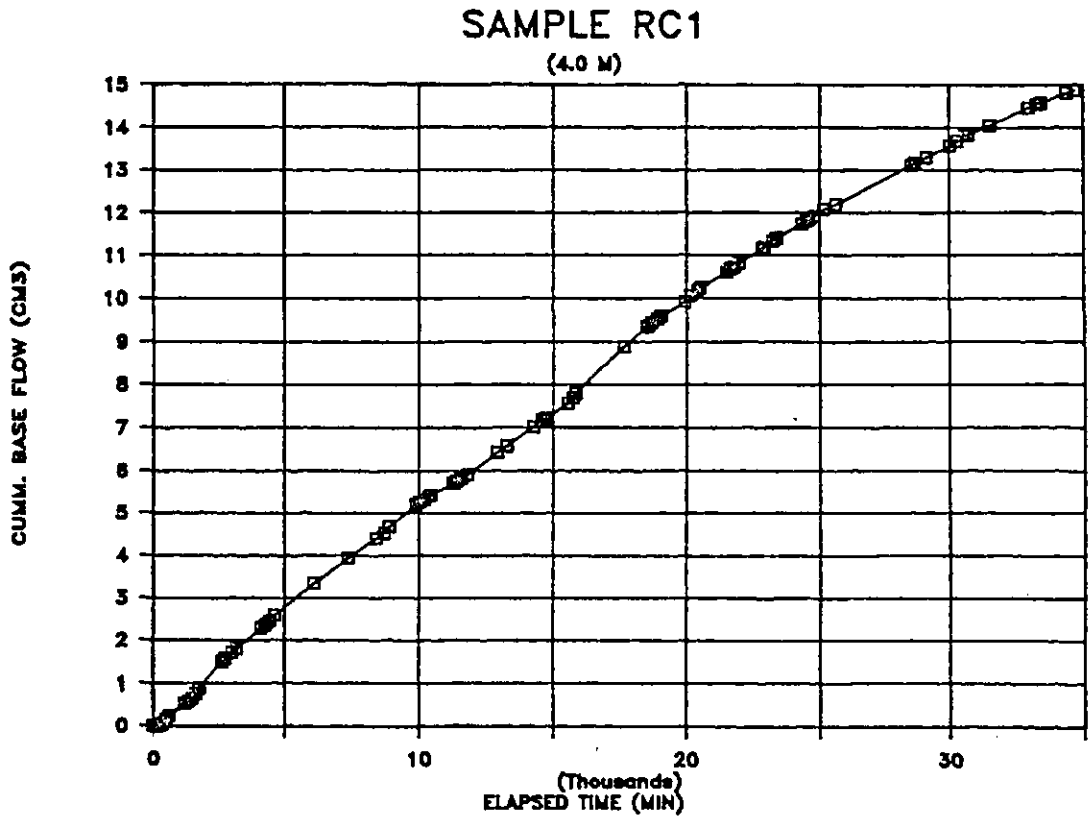

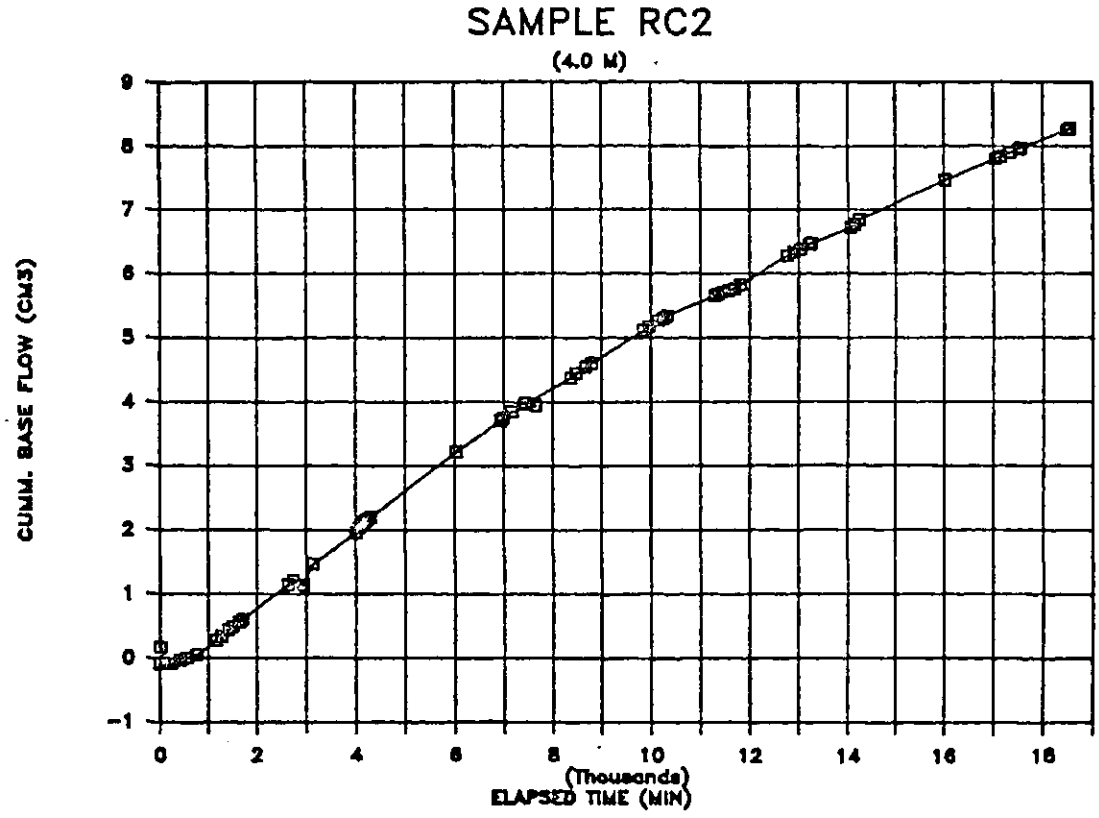

SAMPLE RC3

(4.0 M)

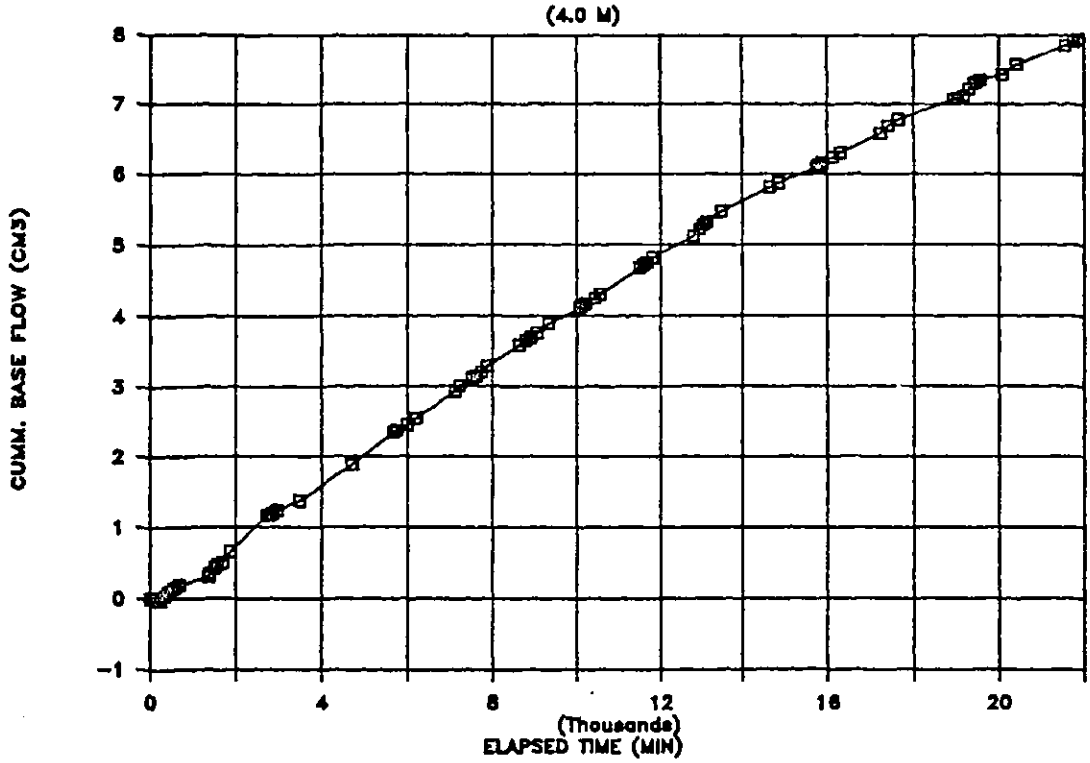

SAMPLE RC4

(0.5 M)

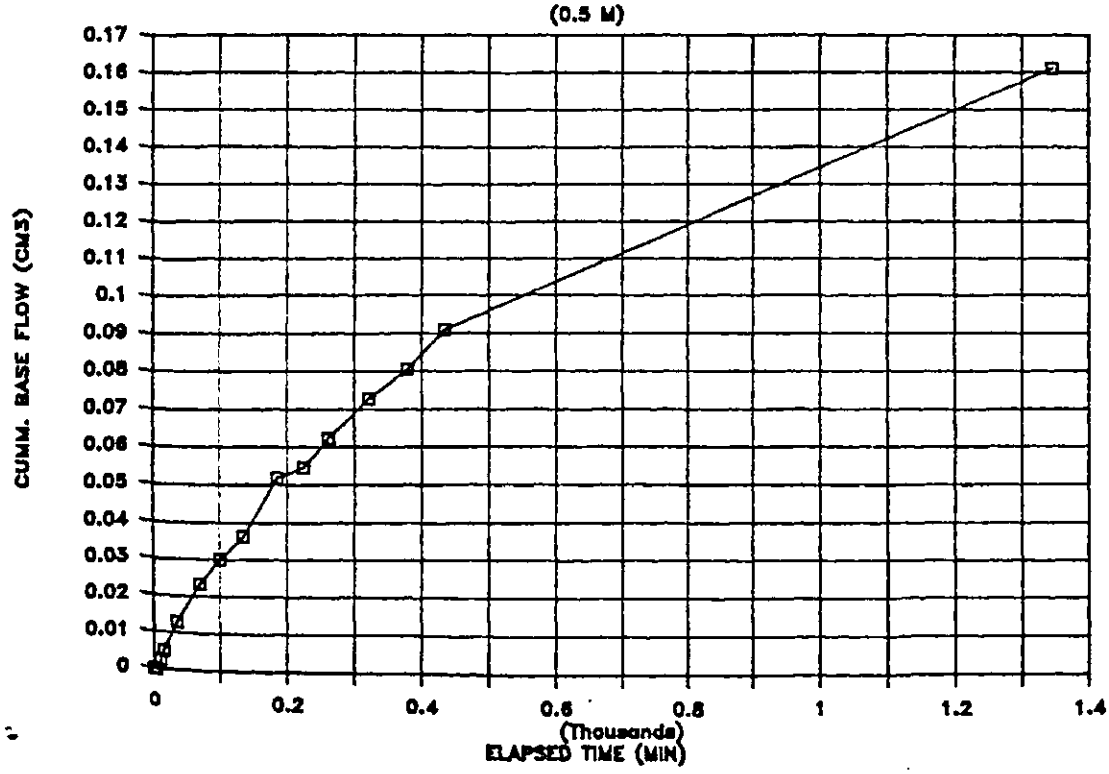

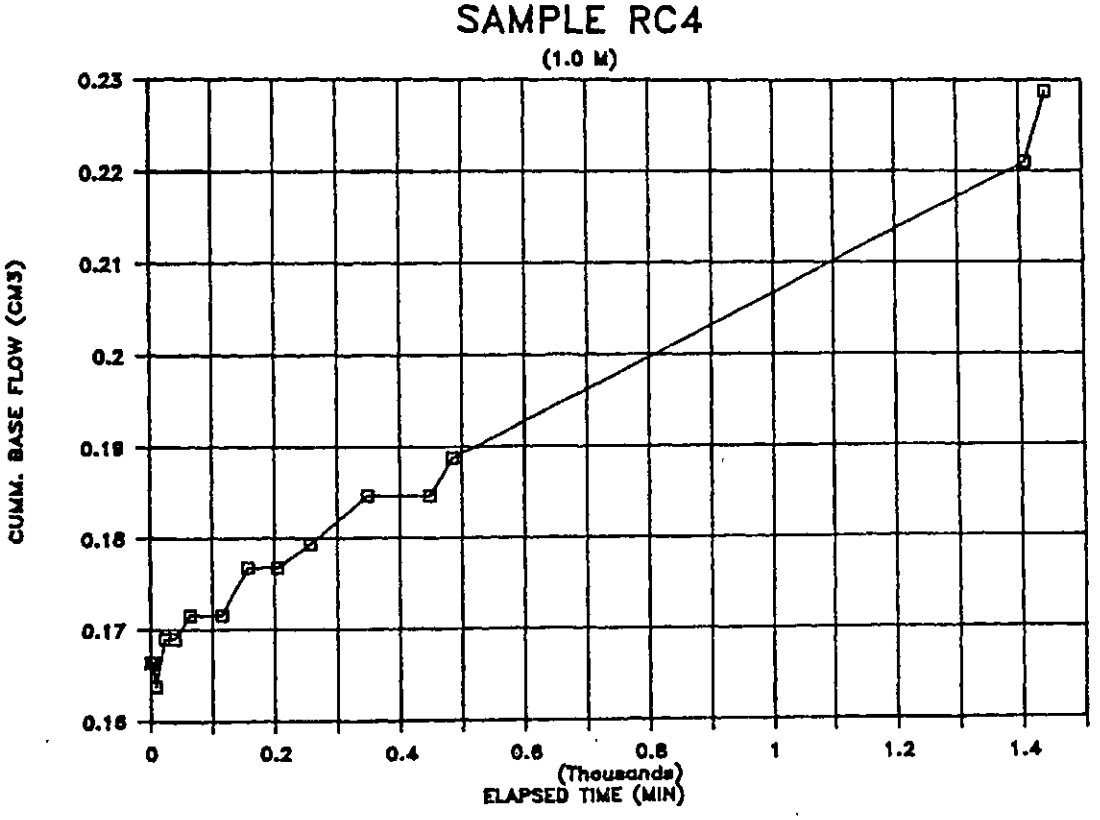
SAMPLE RC4
(1.0 M)
CUMM. BASE FLOW (CM3)
0.23
0.22
0.21
0.2
0.19
0.18
0.17
0.16
0
0.2
0.4
0.6
0.8
1
1.2
1.4
(Thousands)
ELAPSED TIME (MIN)

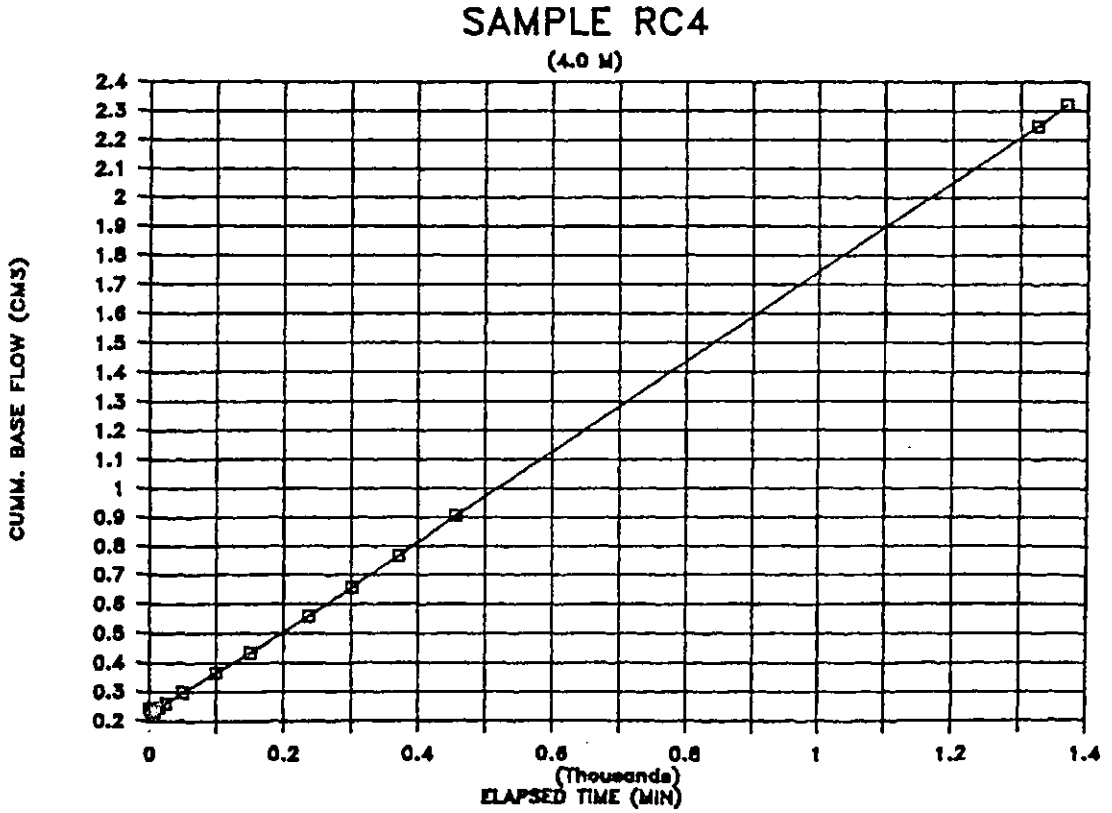
SAMPLE RC4
(4.0 M)
CUMM. BASE FLOW (CM3)
2.4
2.3
2.2
2.1
2
1.9
1.8
1.7
1.6
1.5
1.4
1.3
1.2
1.1
1
0.9
0.8
0.7
0.6
0.5
0.4
0.3
0.2
0
0.2
0.4
0.6
0.8
1
1.2
1.4
(Thousands)
ELAPSED TIME (MIN)

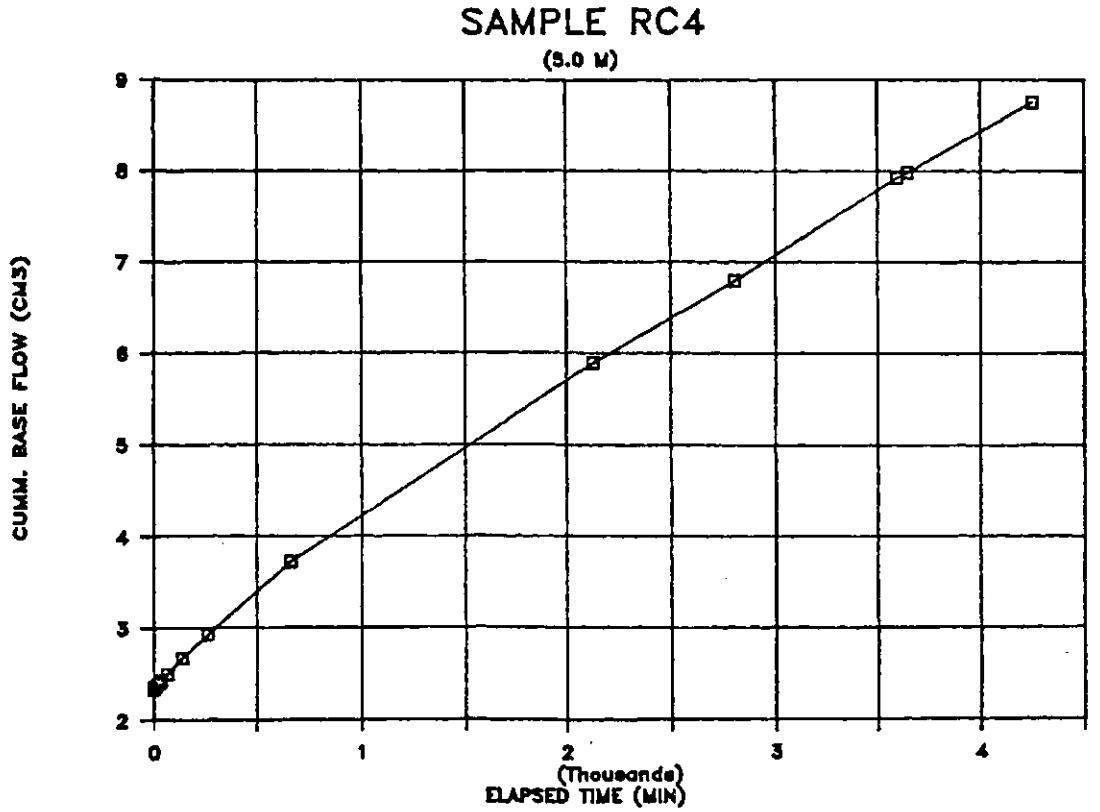
SAMPLE RC4
(5.0 M)
CUMM. BASE FLOW (CM3)
9
8
7
6
5
4
3
2
0
1
2
3
4
(Thousands)
ELAPSED TIME (MIN)

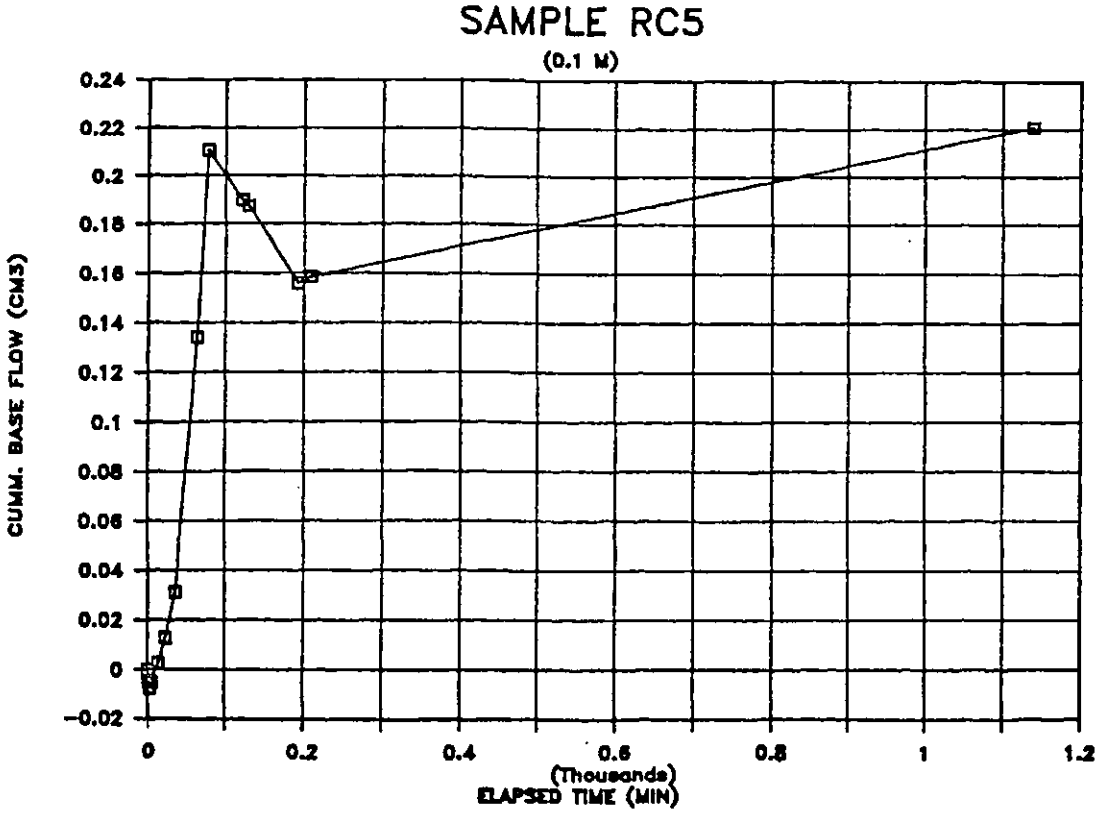
SAMPLE RC5
(0.1 M)
CUMM. BASE FLOW (CM3)
0.24
0.22
0.2
0.18
0.16
0.14
0.12
0.1
0.08
0.06
0.04
0.02
0
-0.02
0
0.2
0.4
0.6
0.8
1
1.2
(Thousands)
ELAPSED TIME (MIN)

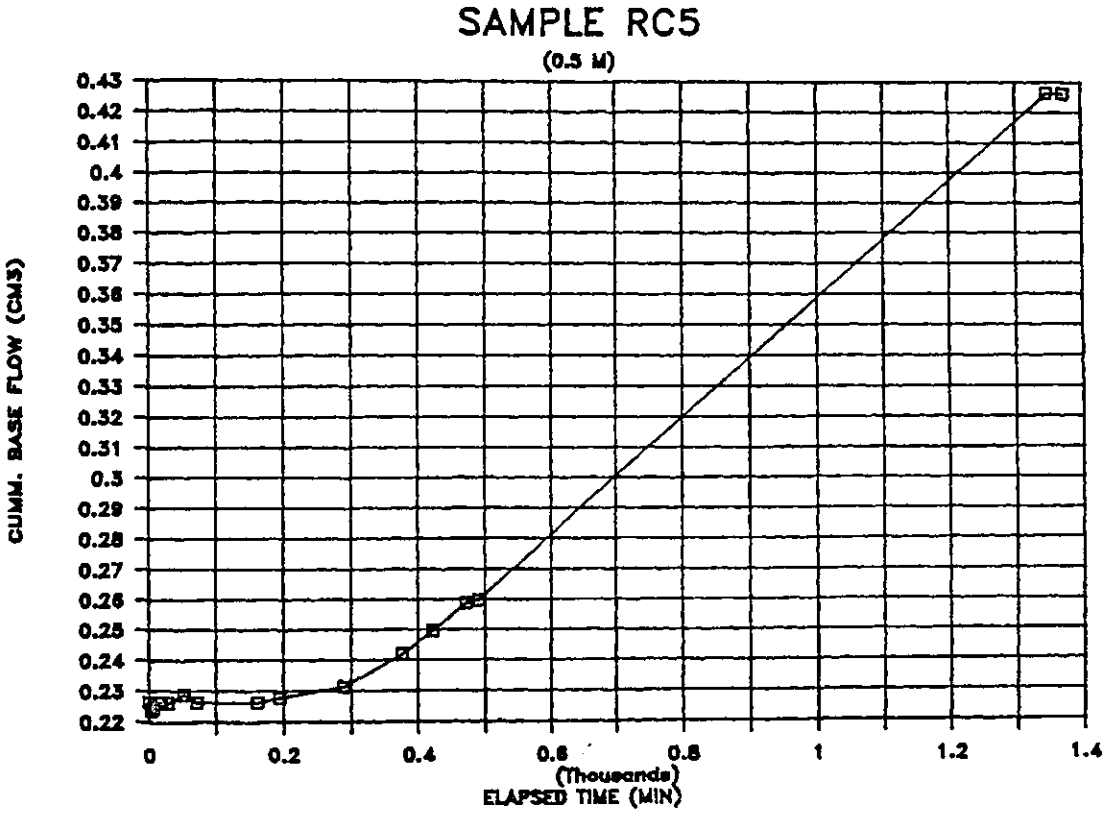
SAMPLE RC5
(0.5 M)
CUMM. BASE FLOW (CM3)
0.43
0.42
0.41
0.4
0.39
0.38
0.37
0.36
0.35
0.34
0.33
0.32
0.31
0.3
0.29
0.28
0.27
0.26
0.25
0.24
0.23
0.22
0
0.2
0.4
0.6
0.8
1
1.2
1.4
(Thousands)
ELAPSED TIME (MIN)

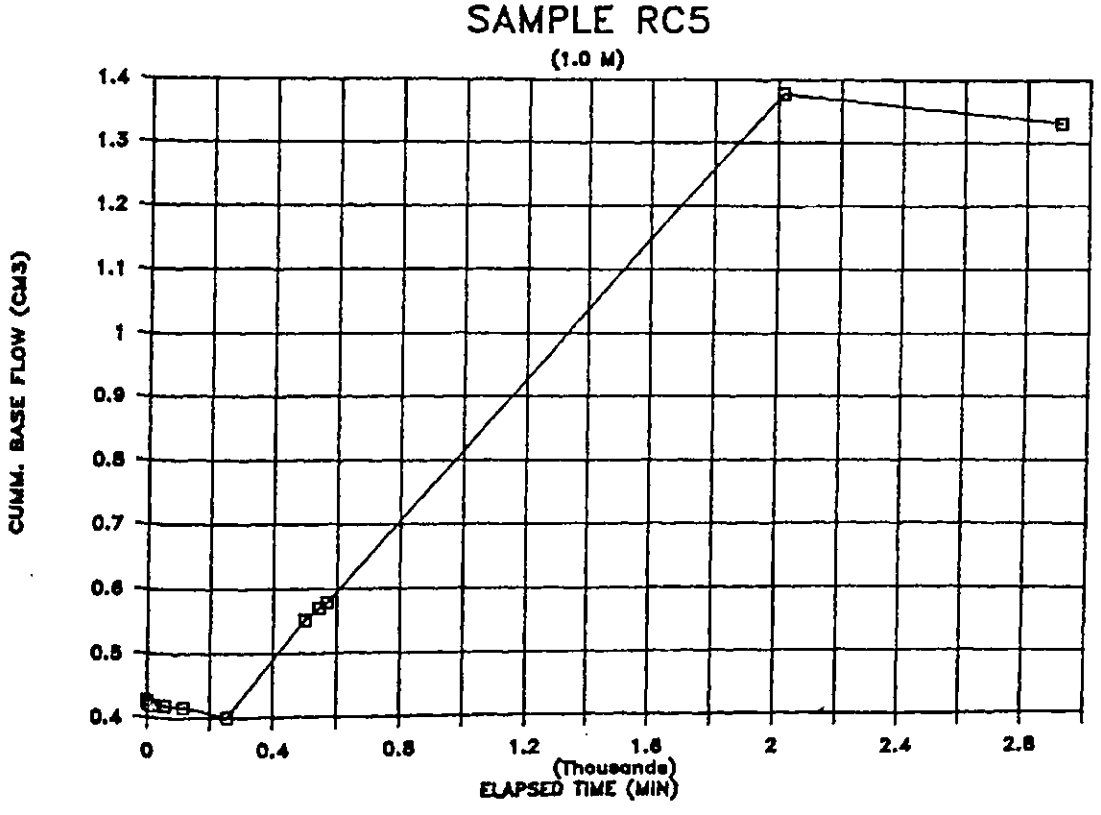
SAMPLE RC5
(1.0 M)
CUMM. BASE FLOW (CM3)
1.4
1.3
1.2
1.1
1
0.9
0.8
0.7
0.6
0.5
0.4
0
0.4
0.8
1.2
1.6
2
2.4
2.8
(Thousands)
ELAPSED TIME (MIN)

SAMPLE RC5

(2.0 M)

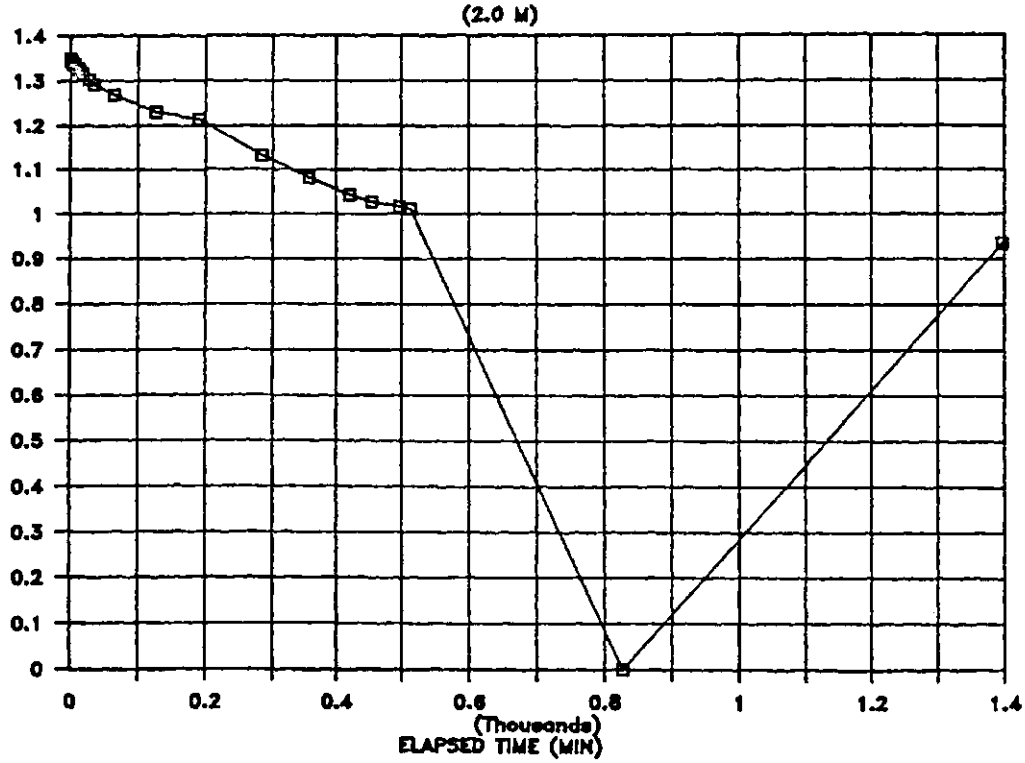

SAMPLE RC5

(4.0 M)

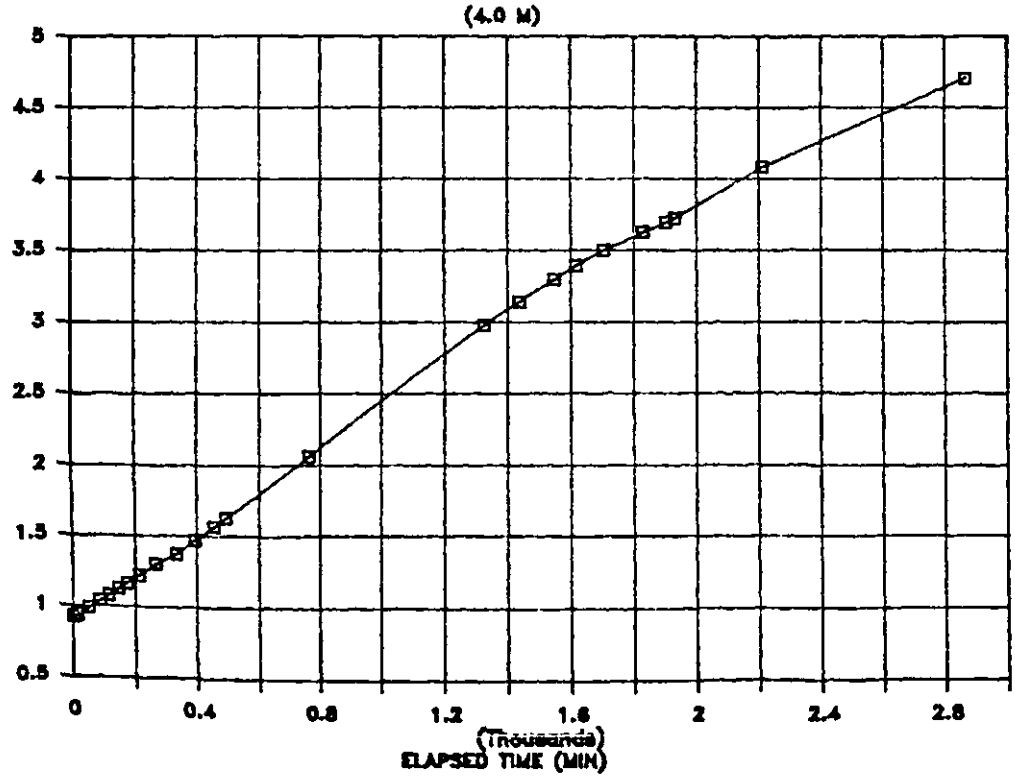

SAMPLE RC5

(5.0 M)

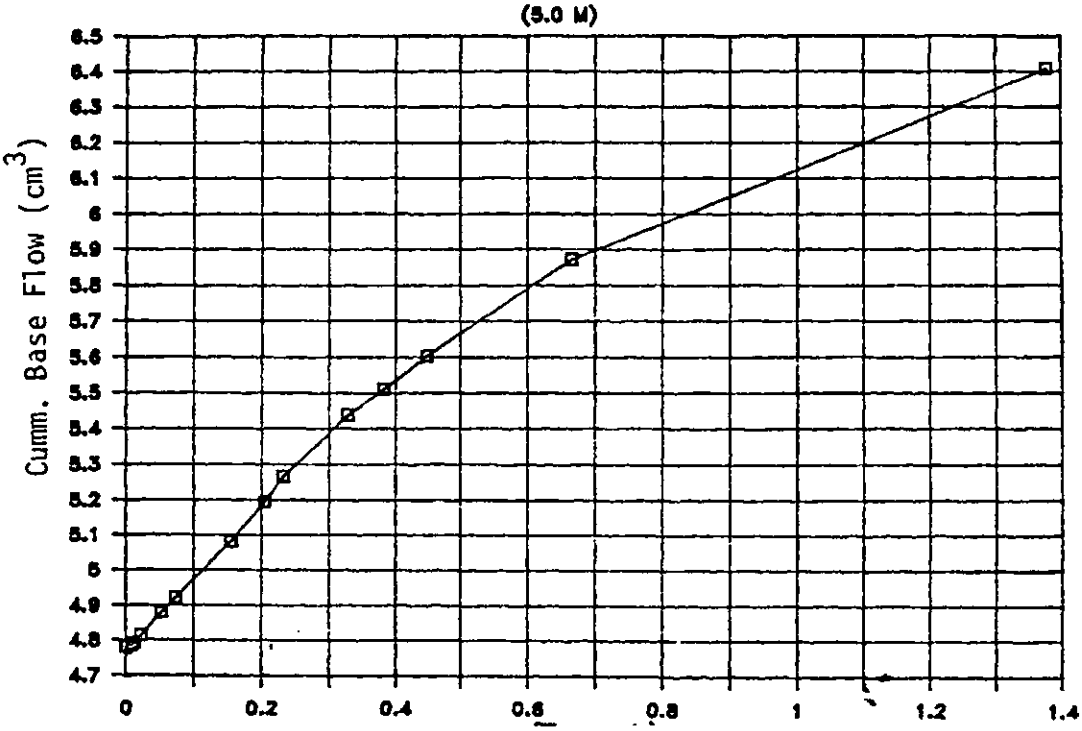

SAMPLE RC6

(0.1 M)

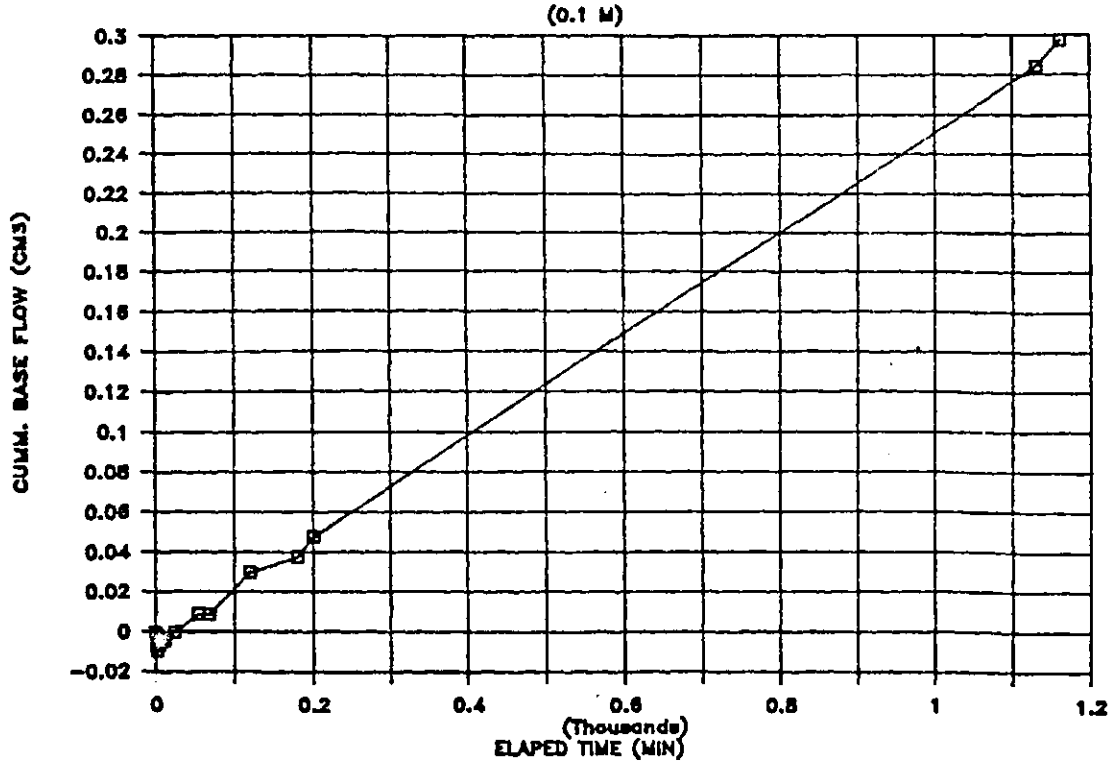

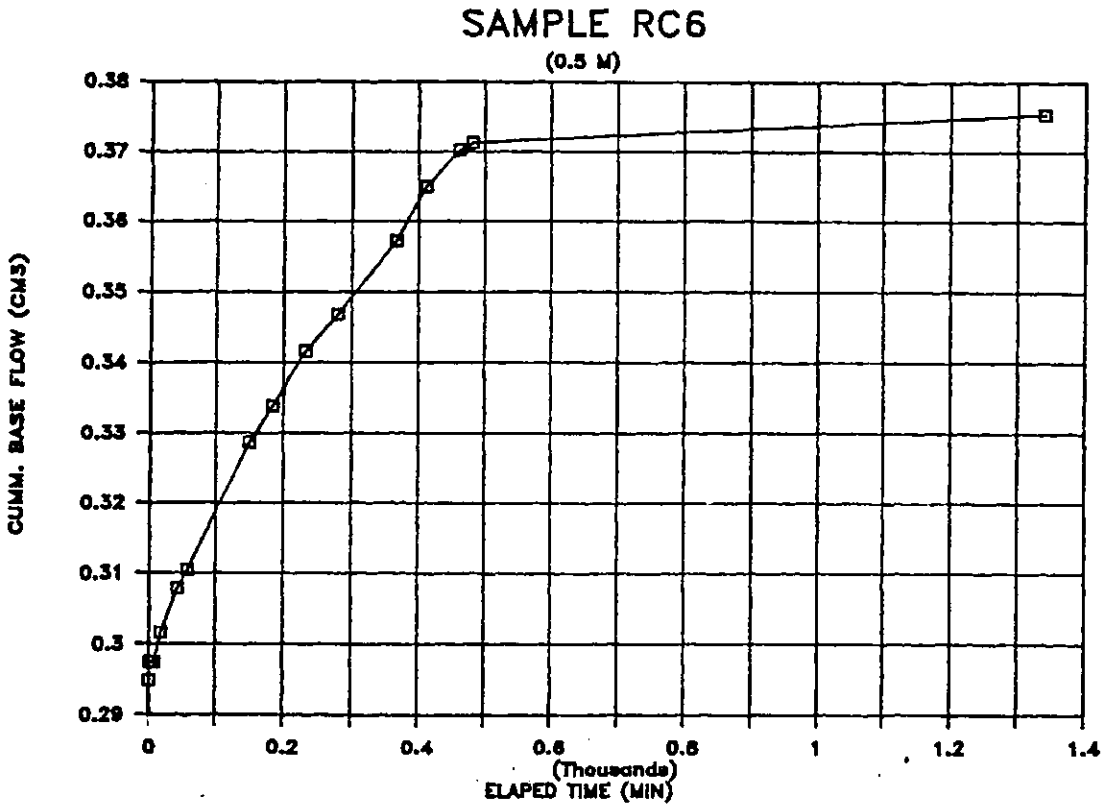
SAMPLE RC6
(0.5 M)
CUMM. BASE FLOW (CM3)
0.38
0.37
0.36
0.35
0.34
0.33
0.32
0.31
0.3
0.29
0
0.2
0.4
0.6
0.8
1
1.2
1.4
(Thousands)
ELAPED TIME (MIN)

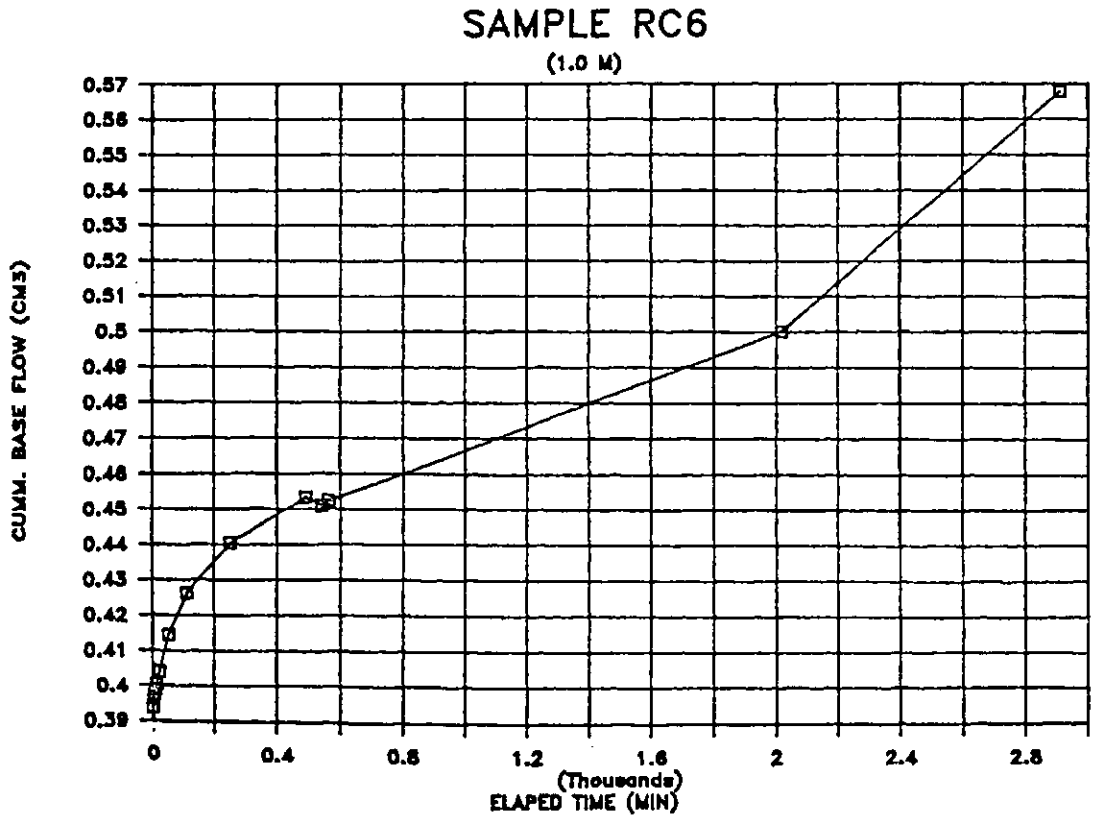
SAMPLE RC6
(1.0 M)
CUMM. BASE FLOW (CM3)
0.57
0.56
0.55
0.54
0.53
0.52
0.51
0.5
0.49
0.48
0.47
0.46
0.45
0.44
0.43
0.42
0.41
0.4
0.39
0
0.4
0.8
1.2
1.6
2
2.4
2.8
(Thousands)
ELAPED TIME (MIN)

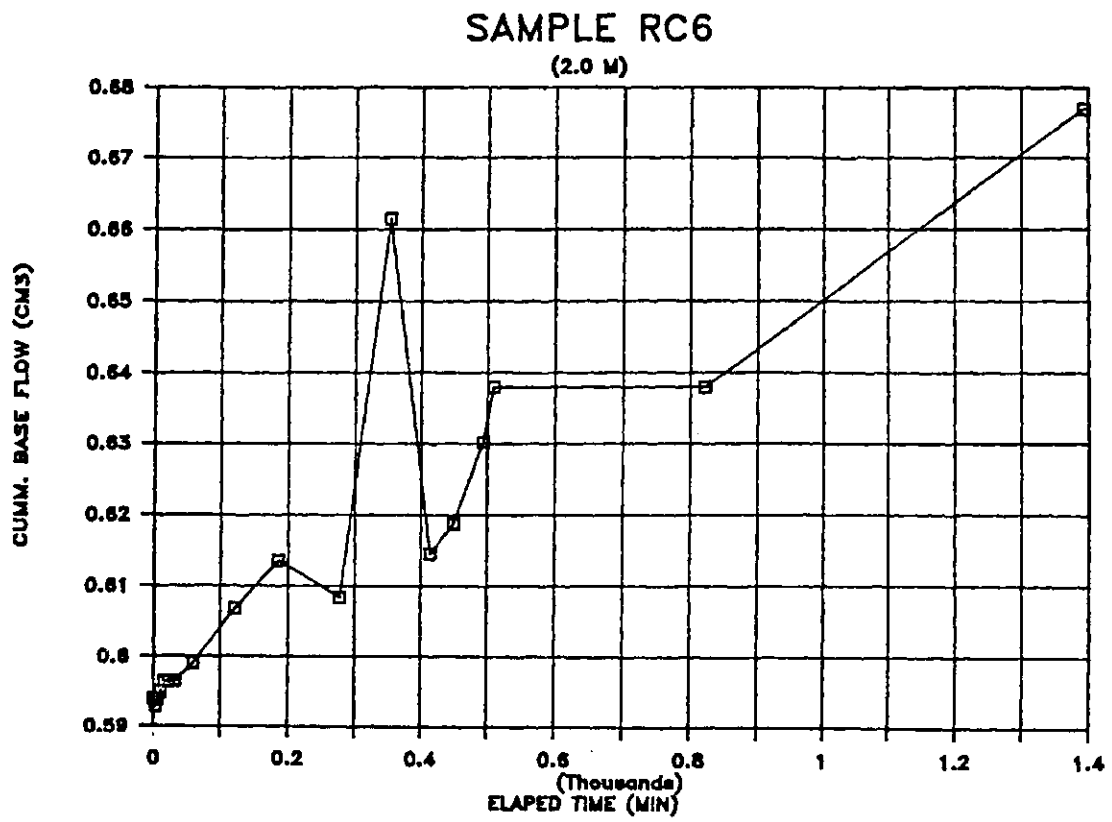
SAMPLE RC6
(2.0 M)
CUMM. BASE FLOW (CM3)
0.68
0.67
0.66
0.65
0.64
0.63
0.62
0.61
0.6
0.59
0
0.2
0.4
0.6
0.8
1
1.2
1.4
(Thousands)
ELAPED TIME (MIN)

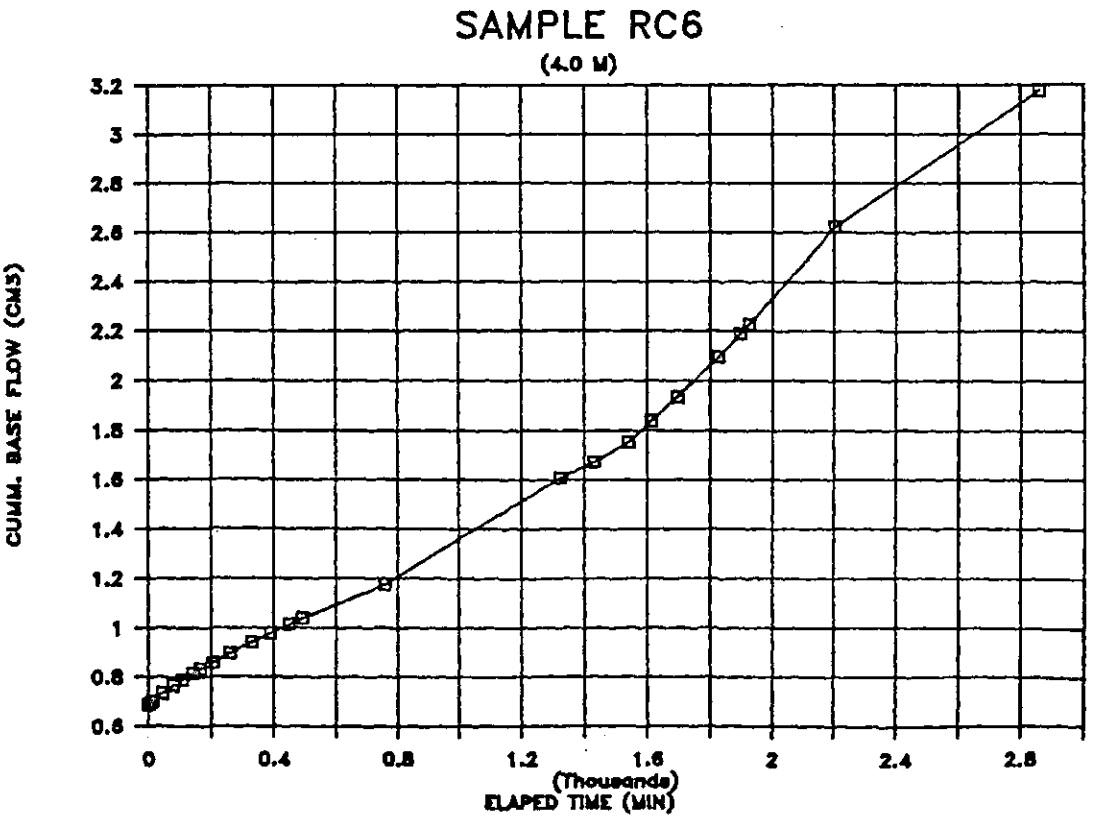
SAMPLE RC6
(4.0 M)
CUMM. BASE FLOW (CM3)
3.2
3
2.8
2.6
2.4
2.2
2
1.8
1.6
1.4
1.2
1
0.8
0.6
0
0.4
0.8
1.2
1.6
2
2.4
2.8
(Thousands)
ELAPED TIME (MIN)

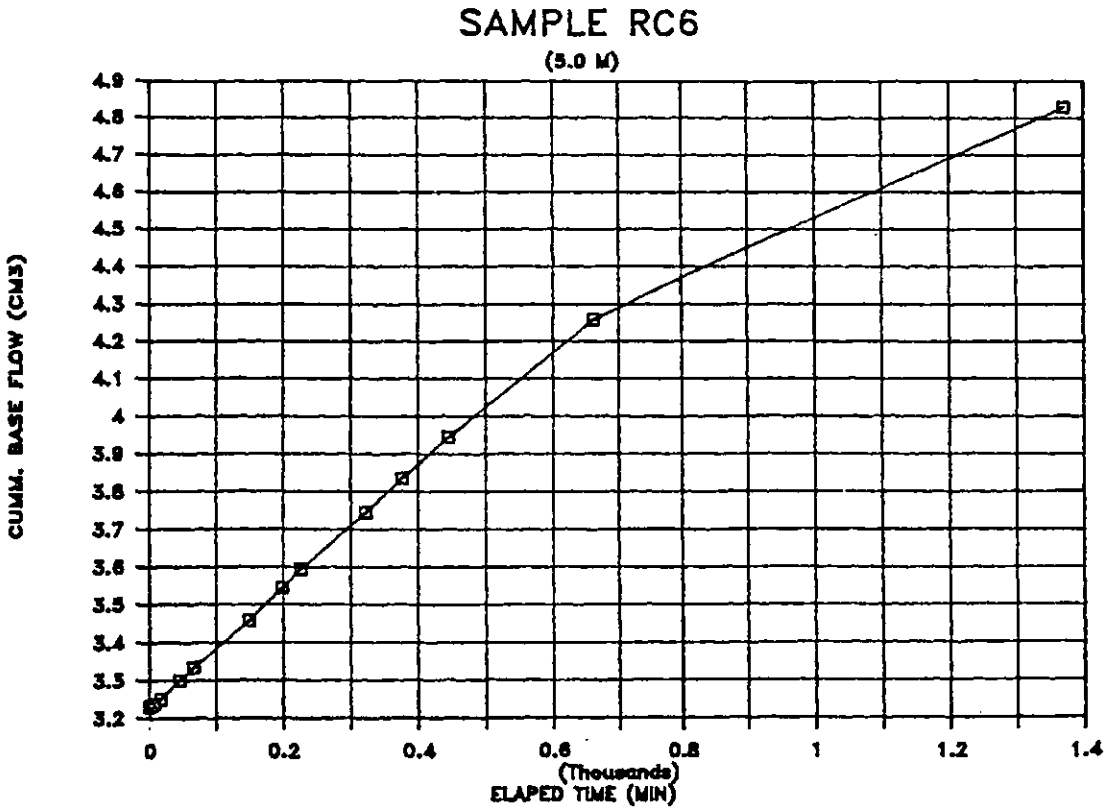
SAMPLE RC6
(5.0 M)
CUMM. BASE FLOW (CM3)
4.9
4.8
4.7
4.6
4.5
4.4
4.3
4.2
4.1
4
3.9
3.8
3.7
3.6
3.5
3.4
3.5
3.2
0
0.2
0.4
0.6
0.8
1
1.2
1.4
(Thousands)
ELAPED TIME (MIN)

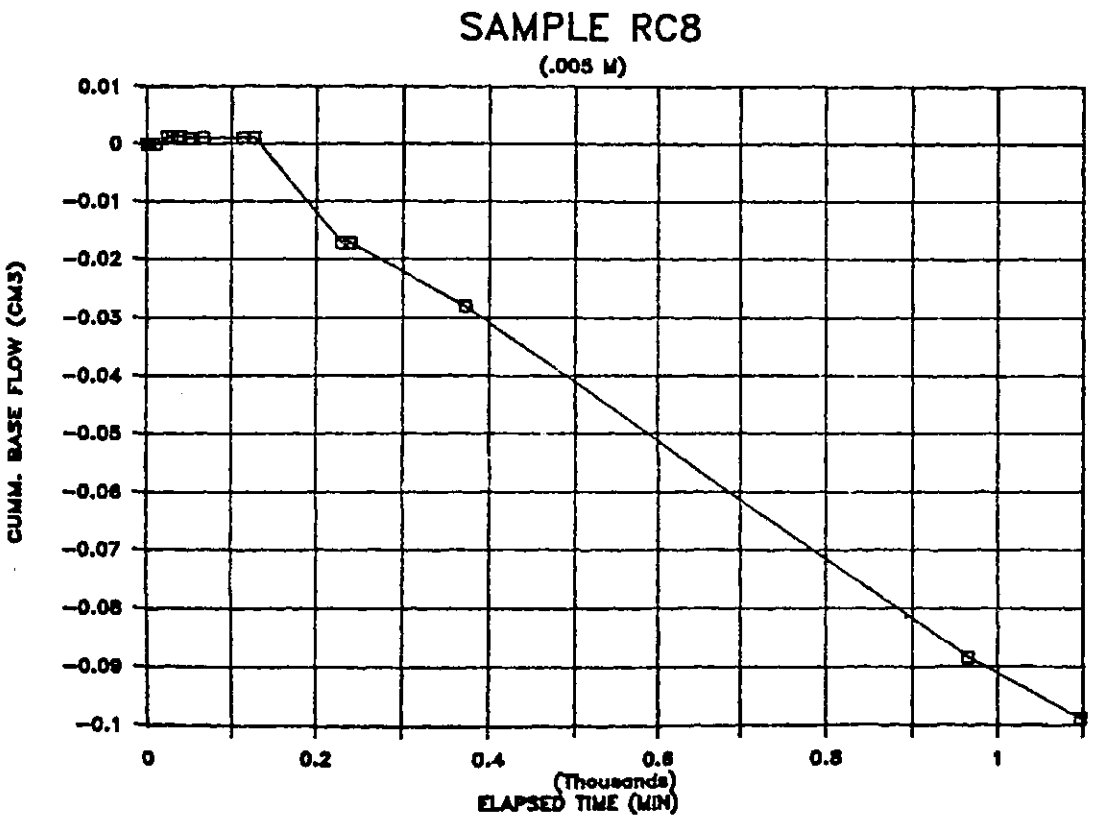
SAMPLE RC8
(.005 M)
CUMM. BASE FLOW (CM3)
0.01
0
-0.01
-0.02
-0.03
-0.04
-0.05
-0.06
-0.07
-0.08
-0.09
-0.1
0
0.2
0.4
0.6
0.8
1
(Thousands)
ELAPSED TIME (MIN)

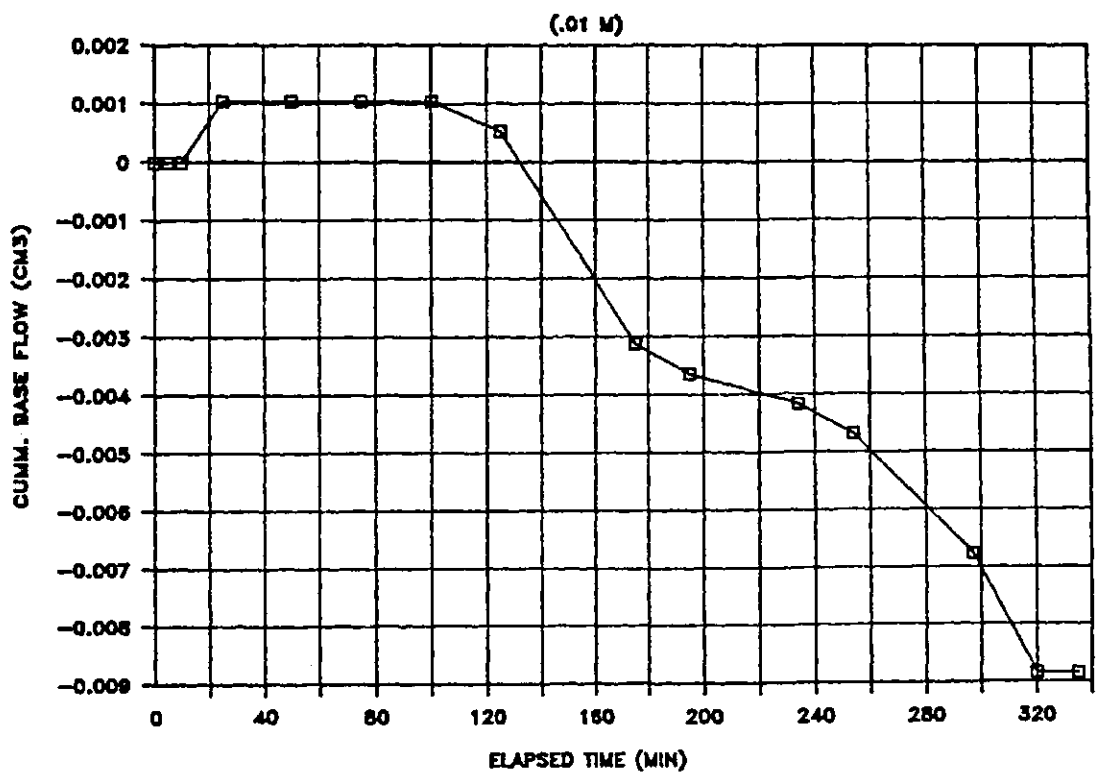
SAMPLE RC8
(.01 M)
CUMM. BASE FLOW (CM3)
0.002
0.001
0
-0.001
-0.002
-0.003
-0.004
-0.005
-0.006
-0.007
-0.008
-0.009
0
40
80
120
160
200
240
280
320
ELAPSED TIME (MIN)

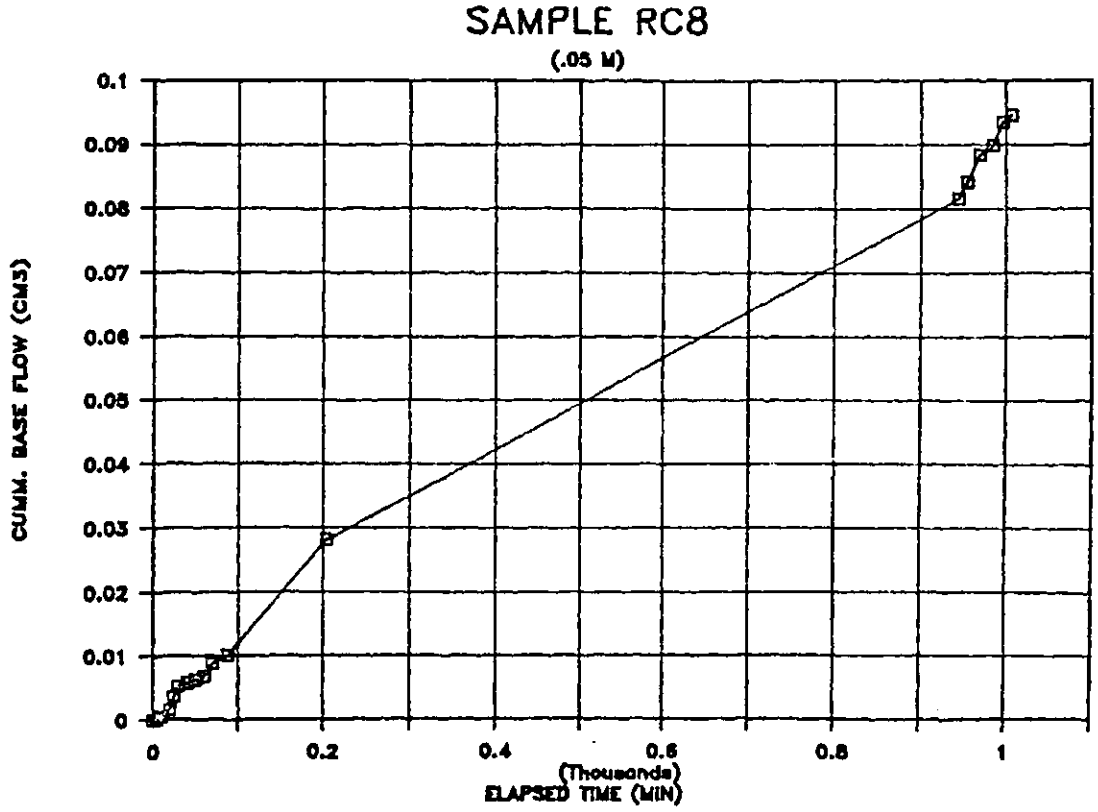
SAMPLE RC8
(.05 M)
CUMM. BASE FLOW (CM3)
0.1
0.09
0.08
0.07
0.06
0.05
0.04
0.03
0.02
0.01
0
0
0.2
0.4
0.6
0.8
1
(Thousands)
ELAPSED TIME (MIN)

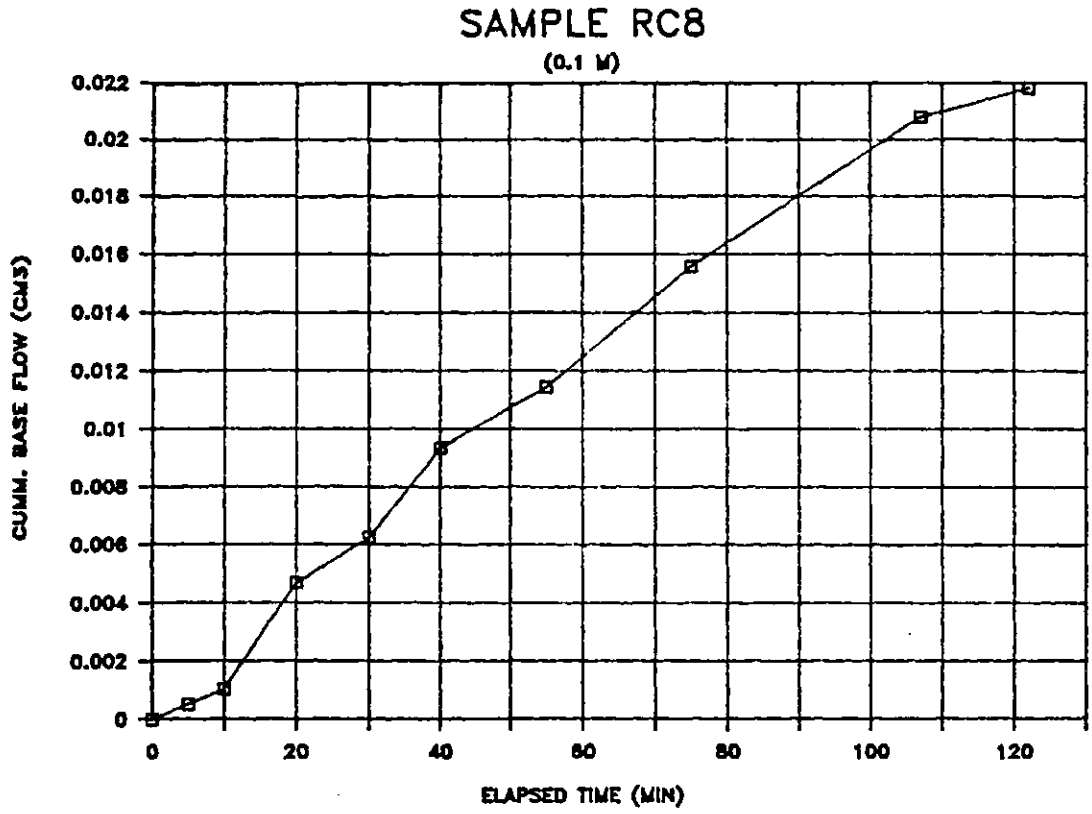
SAMPLE RC8
(0.1 M)
CUMM. BASE FLOW (CMS)
0.022
0.02
0.018
0.016
0.014
0.012
0.01
0.008
0.006
0.004
0.002
0
0
20
40
60
80
100
120
ELAPSED TIME (MIN)

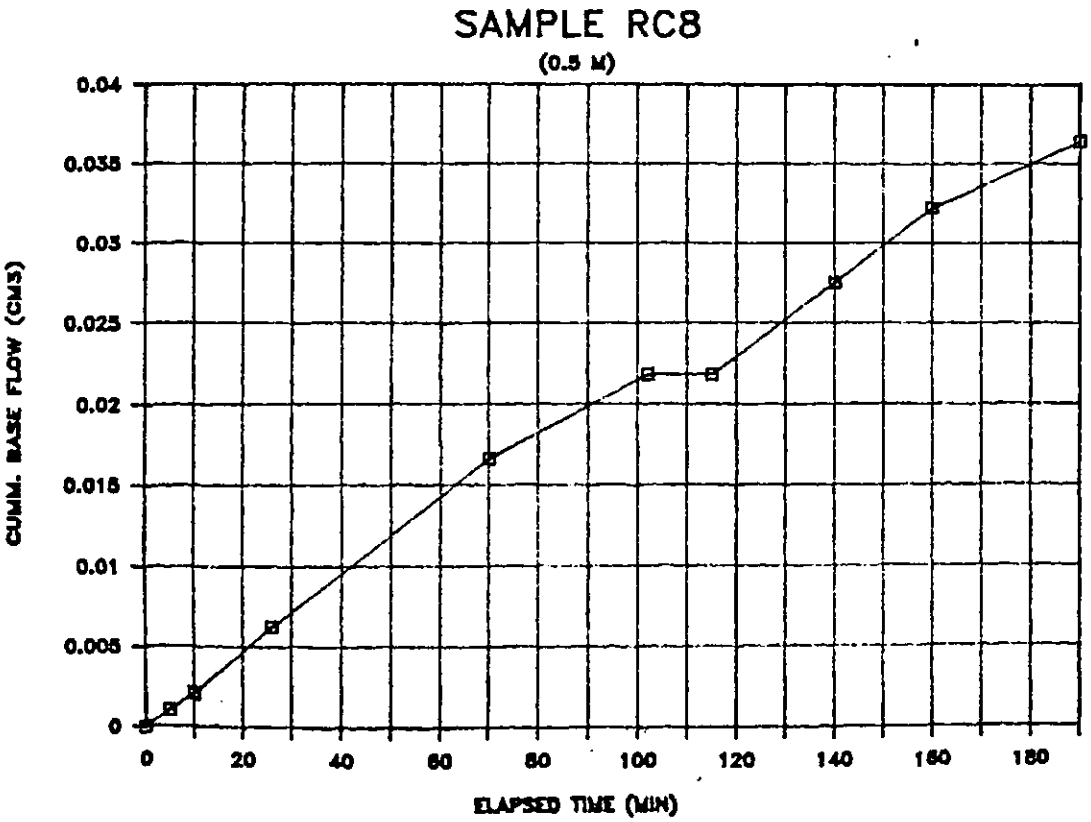
SAMPLE RC8
(0.5 M)
CUMM. BASE FLOW (CMS)
0.04
0.035
0.03
0.025
0.02
0.015
0.01
0.005
0
0
20
40
60
80
100
120
140
160
180
ELAPSED TIME (MIN)

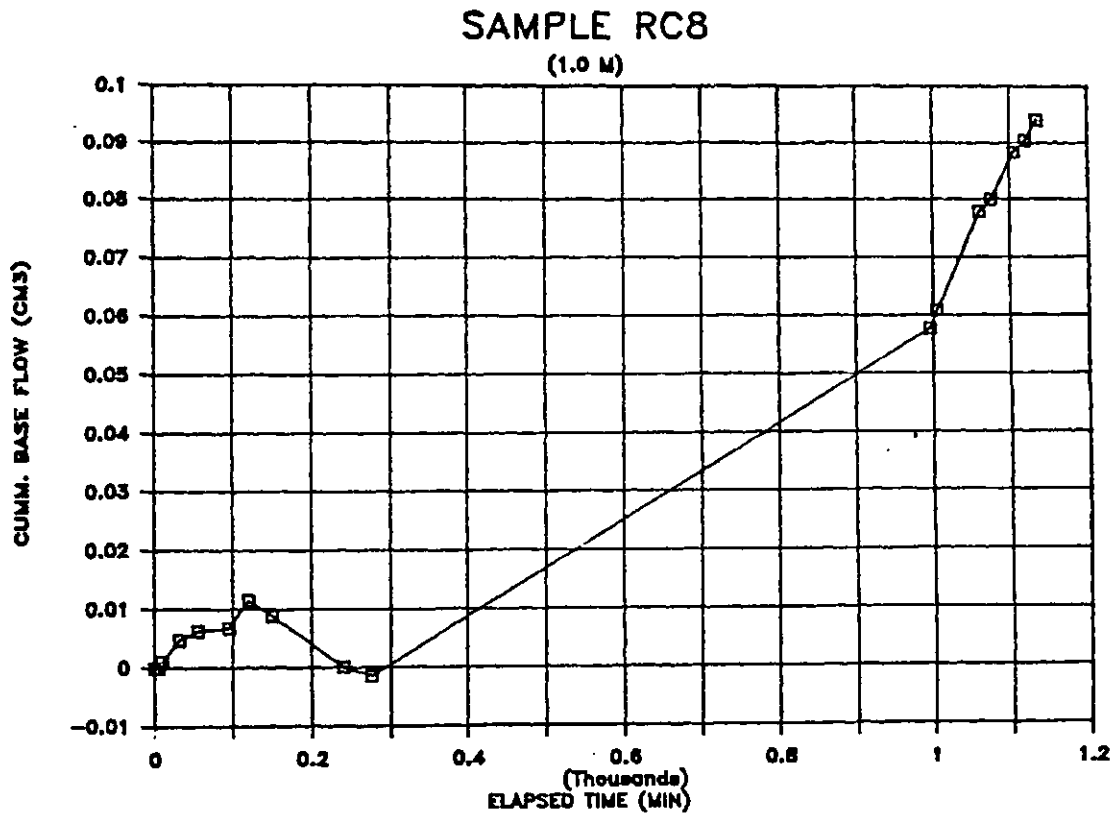
SAMPLE RC8
(1.0 M)
CUMM. BASE FLOW (CM3)
0.1
0.09
0.08
0.07
0.06
0.05
0.04
0.03
0.02
0.01
0
-0.01
0
0.2
0.4
0.6
0.8
1
1.2
(Thousands)
ELAPSED TIME (MIN)

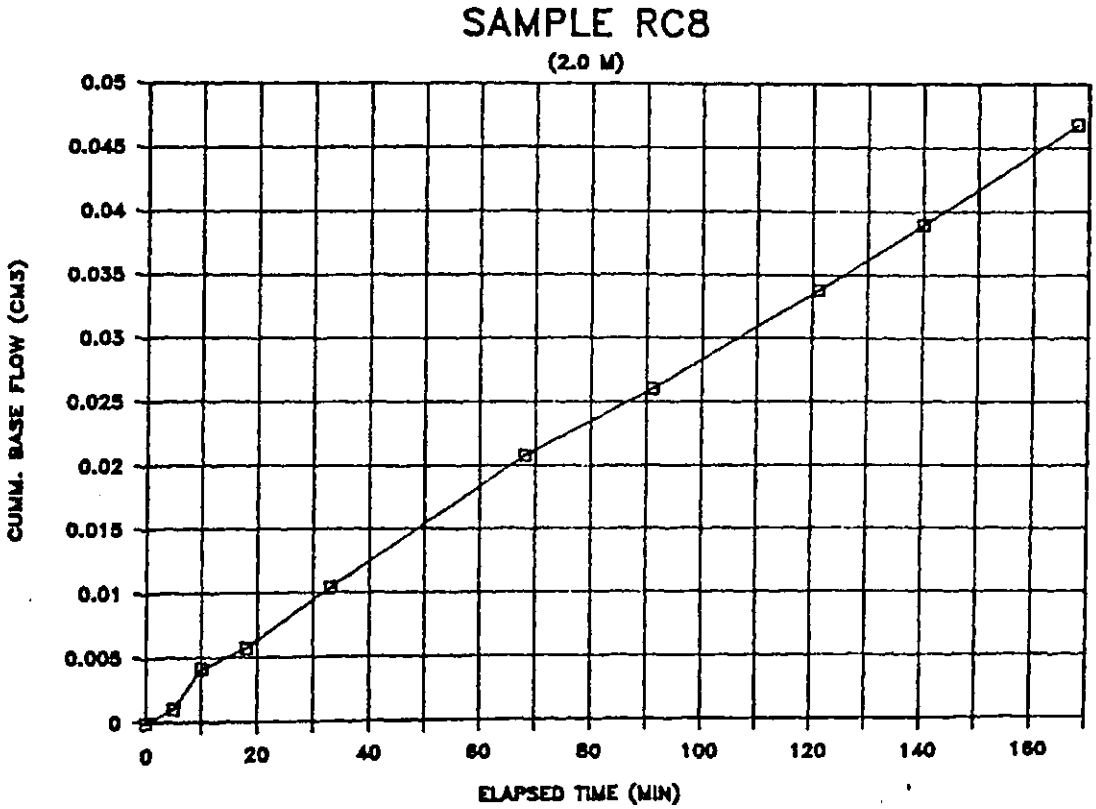
SAMPLE RC8
(2.0 M)
CUMM. BASE FLOW (CM3)
0.05
0.045
0.04
0.035
0.03
0.025
0.02
0.015
0.01
0.005
0
0
20
40
60
80
100
120
140
160
ELAPSED TIME (MIN)

SAMPLE RC8

(4.0 M)

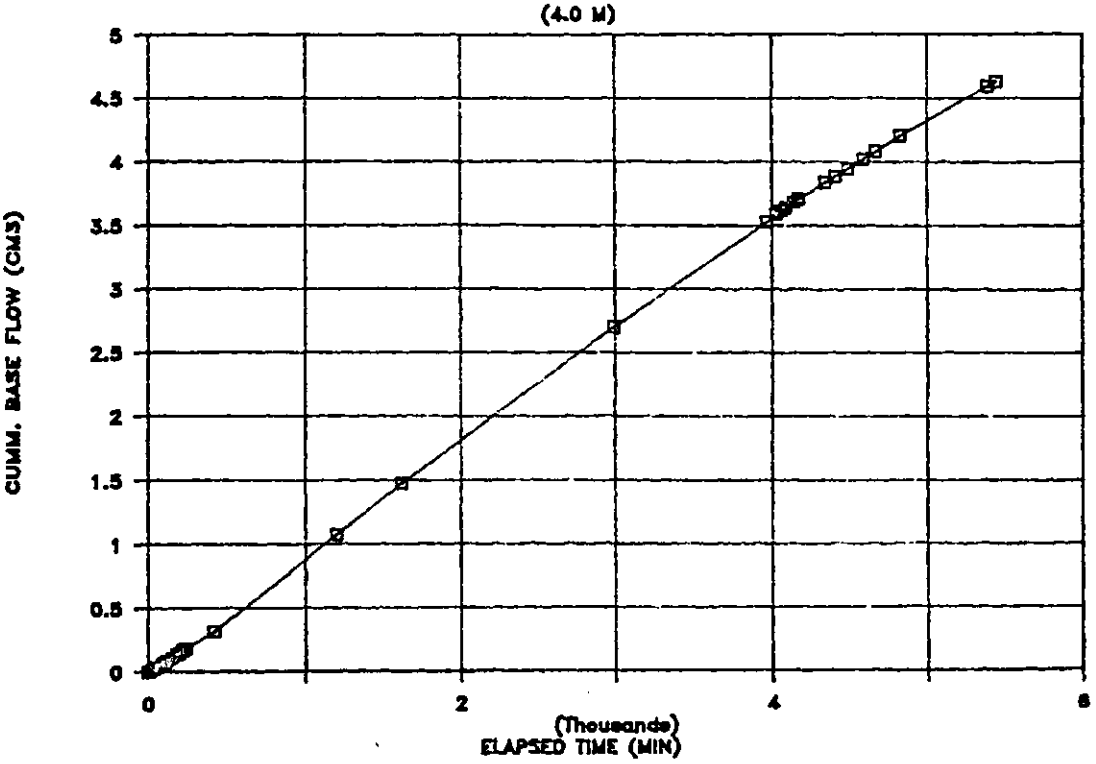

SAMPLE SB1

(4.0 M)

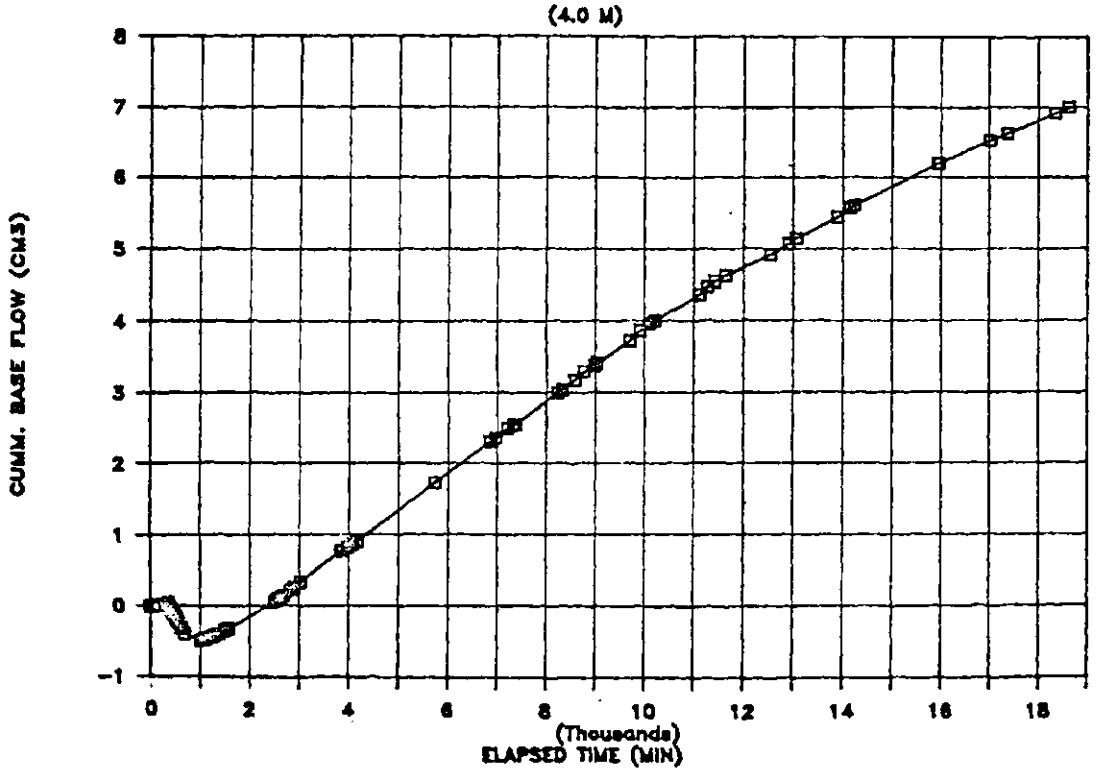

SAMPLE SB2

(4.0 M)

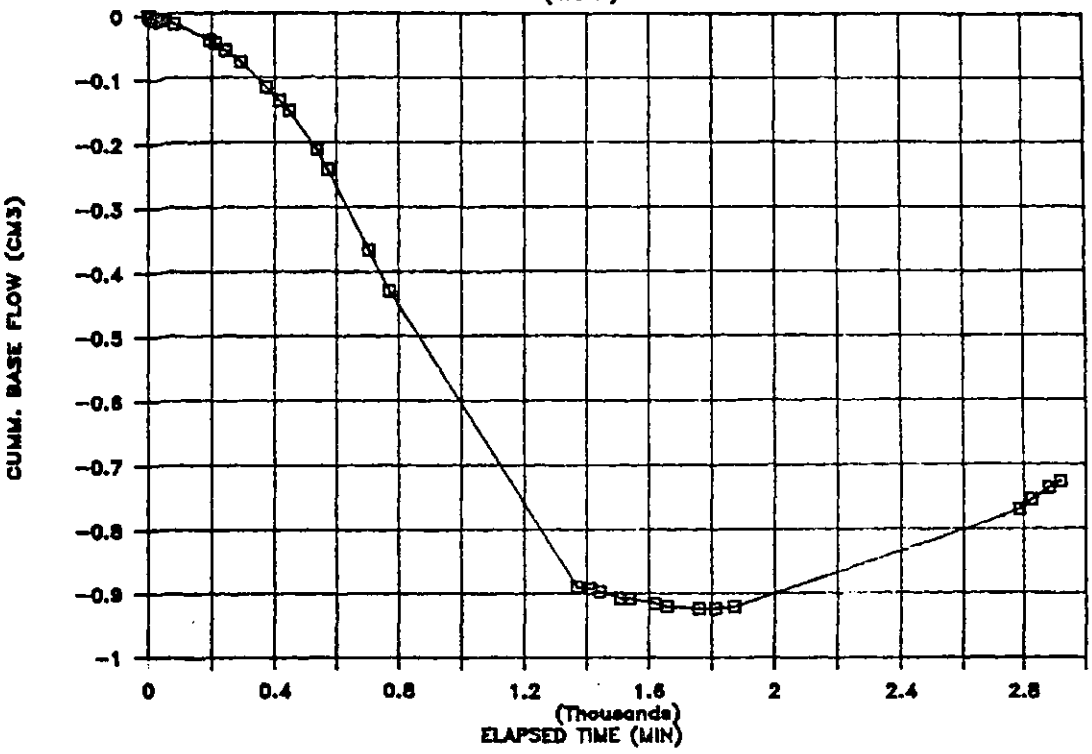

SAMPLE SB4

(D.W)

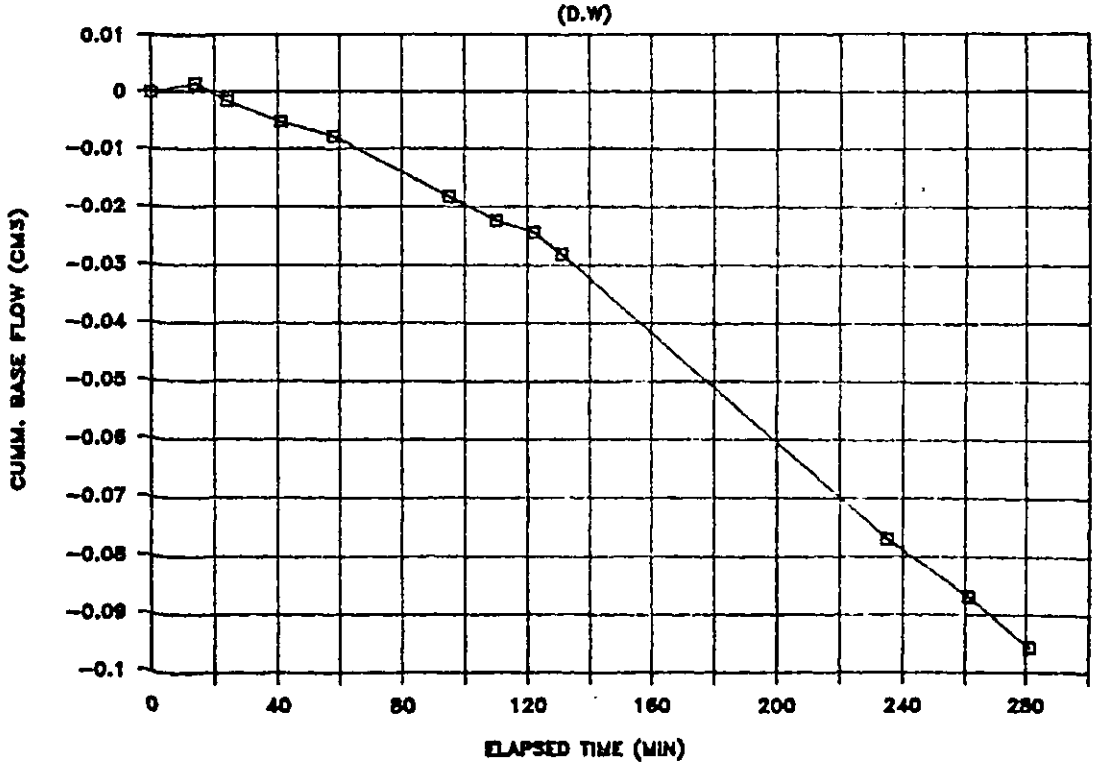

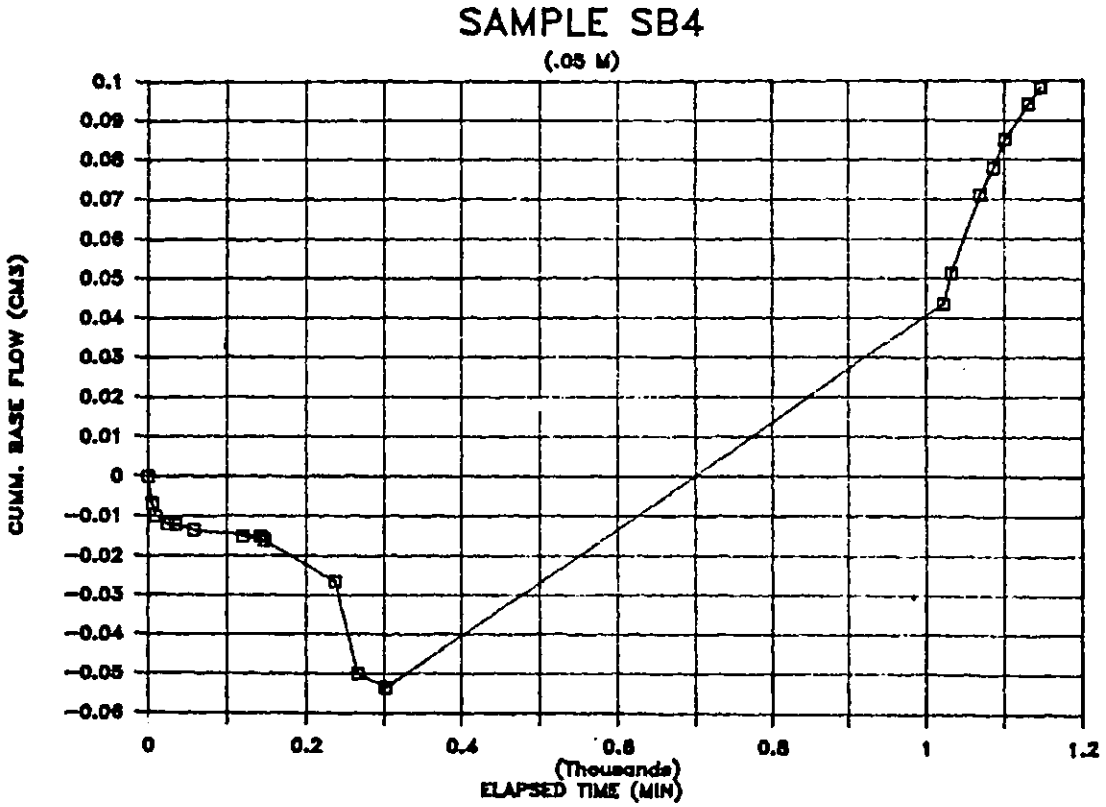
SAMPLE SB4
(.05 M)
CUMM. BASE FLOW (CM3)
0.1
0.09
0.08
0.07
0.06
0.05
0.04
0.03
0.02
0.01
0
-0.01
-0.02
-0.03
-0.04
-0.05
-0.06
0
0.2
0.4
0.6
0.8
1
1.2
(Thousands)
ELAPSED TIME (MIN)

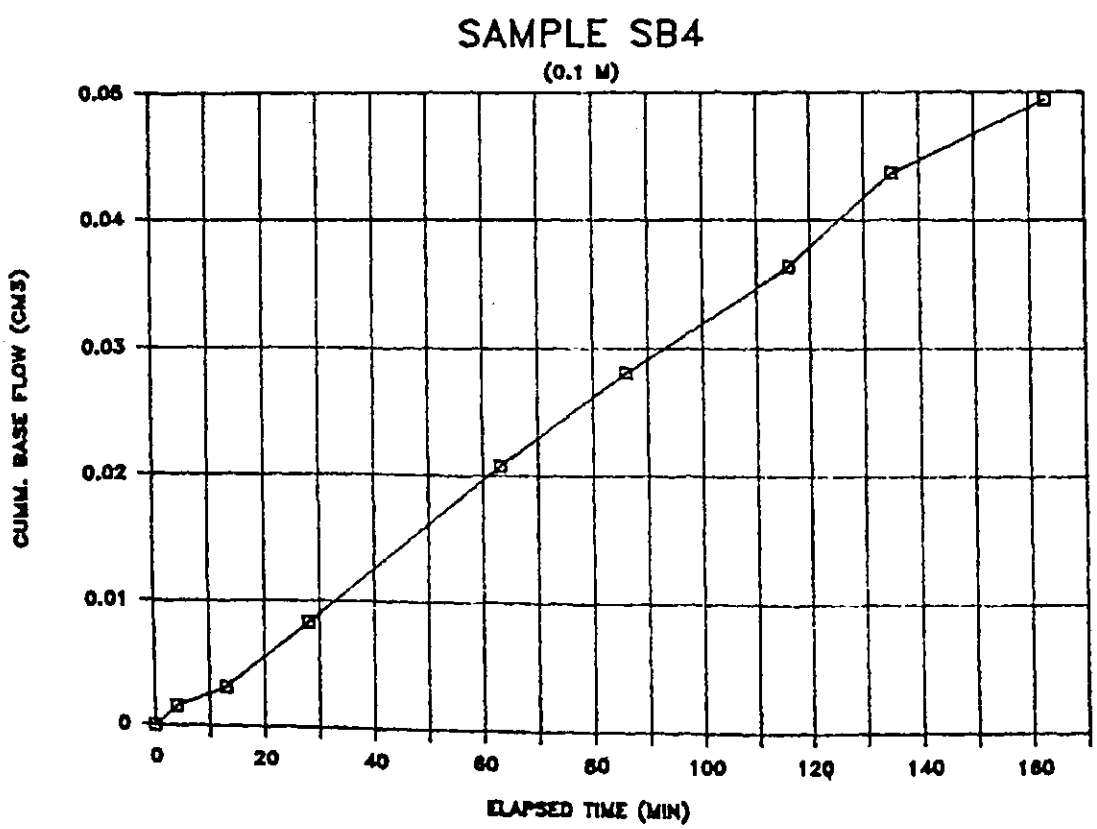
SAMPLE SB4
(0.1 M)
CUMM. BASE FLOW (CM3)
0.05
0.04
0.03
0.02
0.01
0
0
20
40
60
80
100
120
140
160
ELAPSED TIME (MIN)

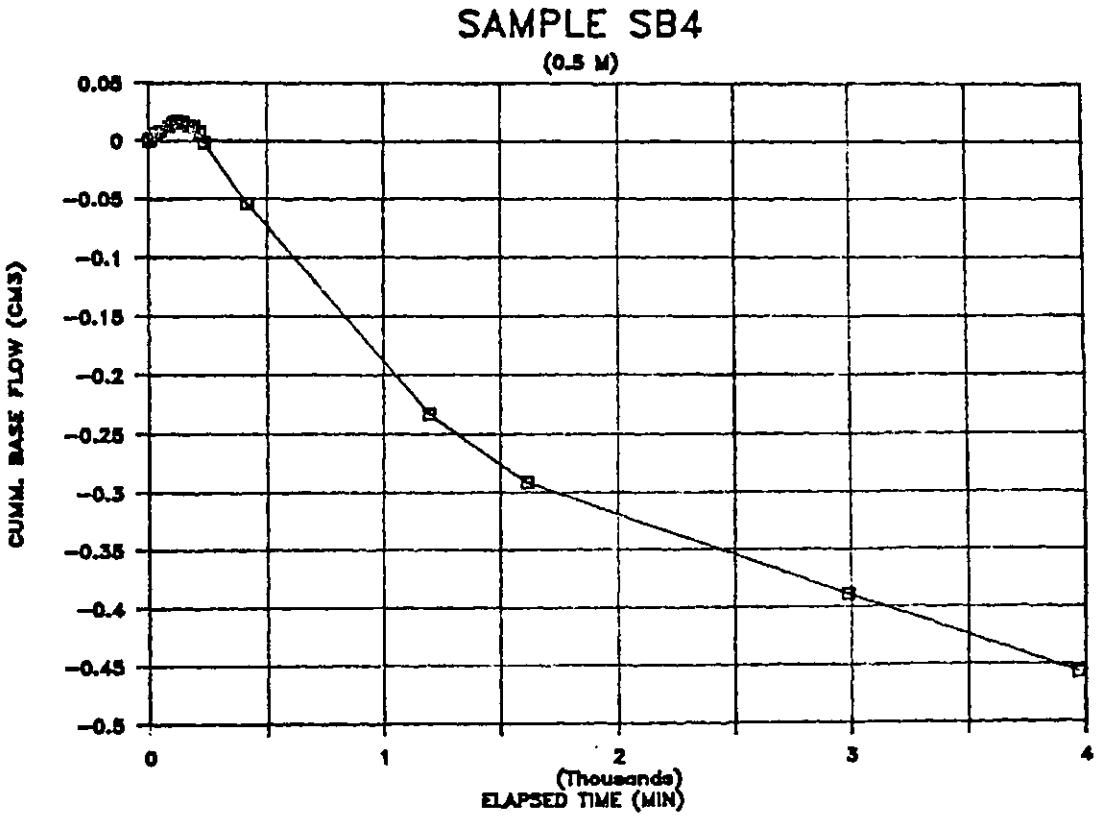
SAMPLE SB4
(0.5 M)
CUMM. BASE FLOW (CM3)
0.05
0
-0.05
-0.1
-0.15
-0.2
-0.25
-0.3
-0.35
-0.4
-0.45
-0.5
0
1
2
3
4
(Thousands)
ELAPSED TIME (MIN)

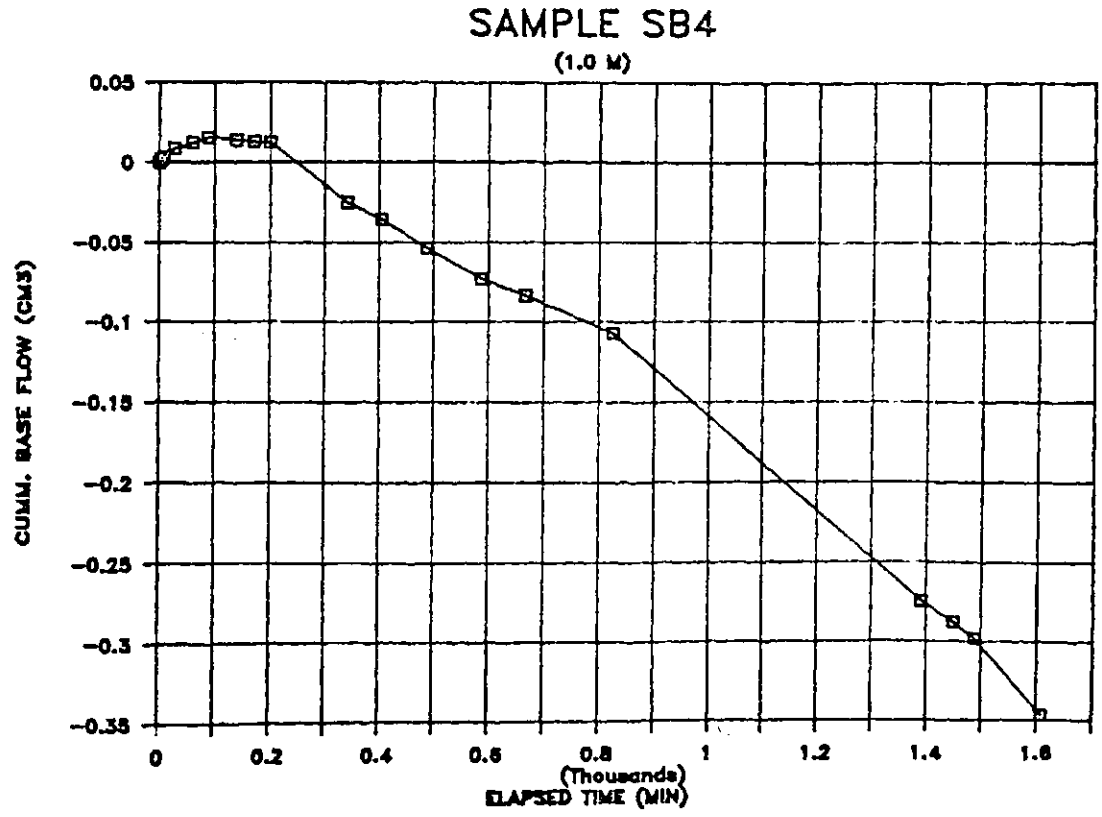
SAMPLE SB4
(1.0 M)
CUMM. BASE FLOW (CM3)
0.05
0
-0.05
-0.1
-0.15
-0.2
-0.25
-0.3
-0.35
0
0.2
0.4
0.6
0.8
1
1.2
1.4
1.6
(Thousands)
ELAPSED TIME (MIN)

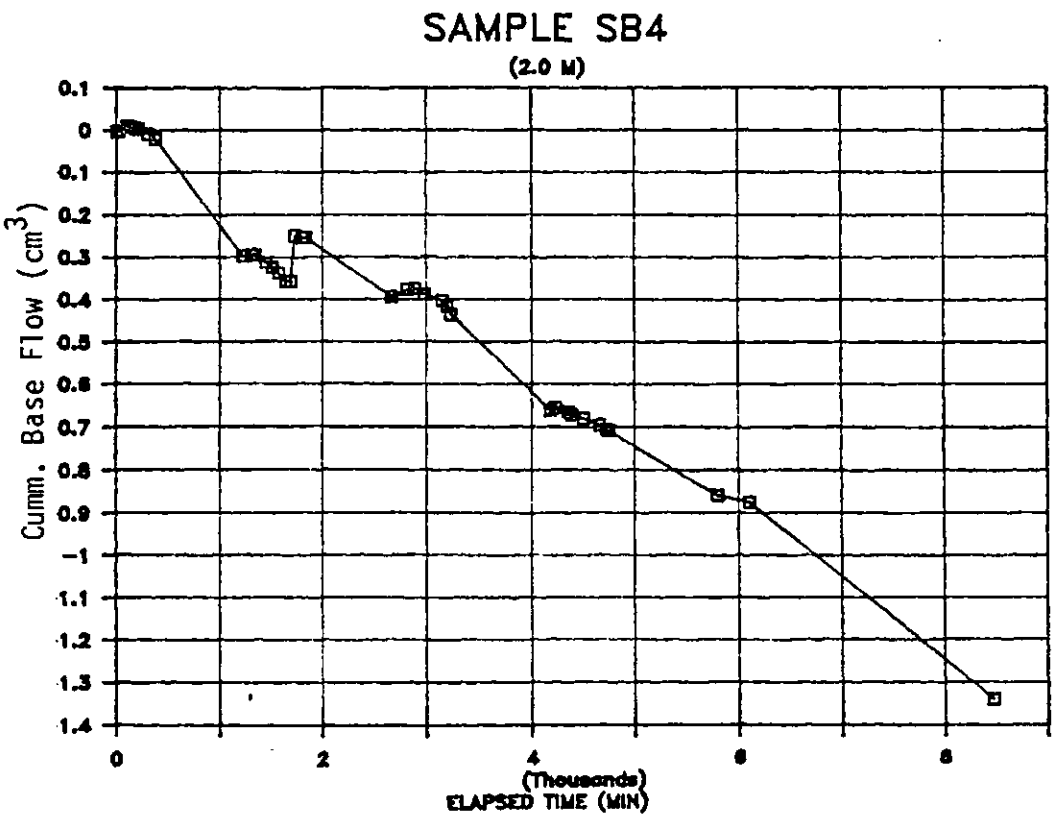
SAMPLE SB4
(2.0 M)
Cumm. Base Flow (cm^3)
0.1
0
-0.1
-0.2
-0.3
-0.4
-0.5
-0.6
-0.7
-0.8
-0.9
-1
-1.1
-1.2
-1.3
-1.4
0
2
4
6
8
(Thousands)
ELAPSED TIME (MIN)

D.5 Base Pressure Responses versus Time

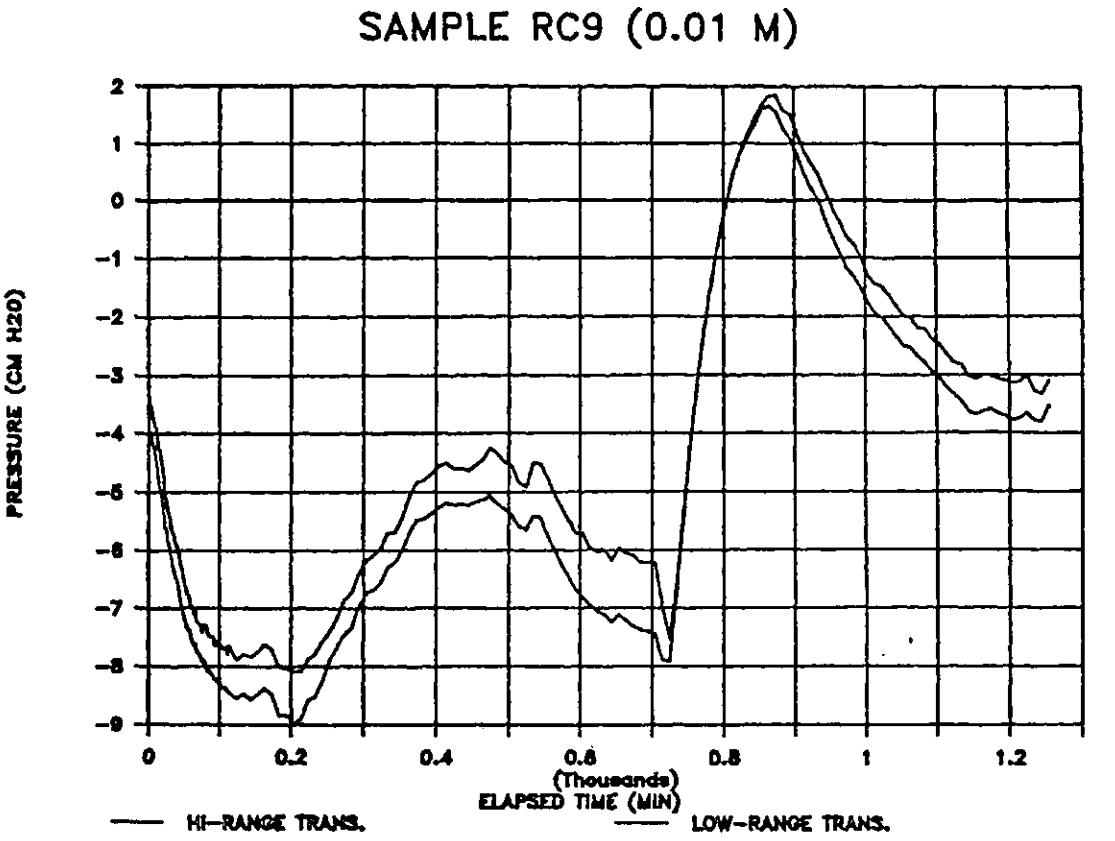

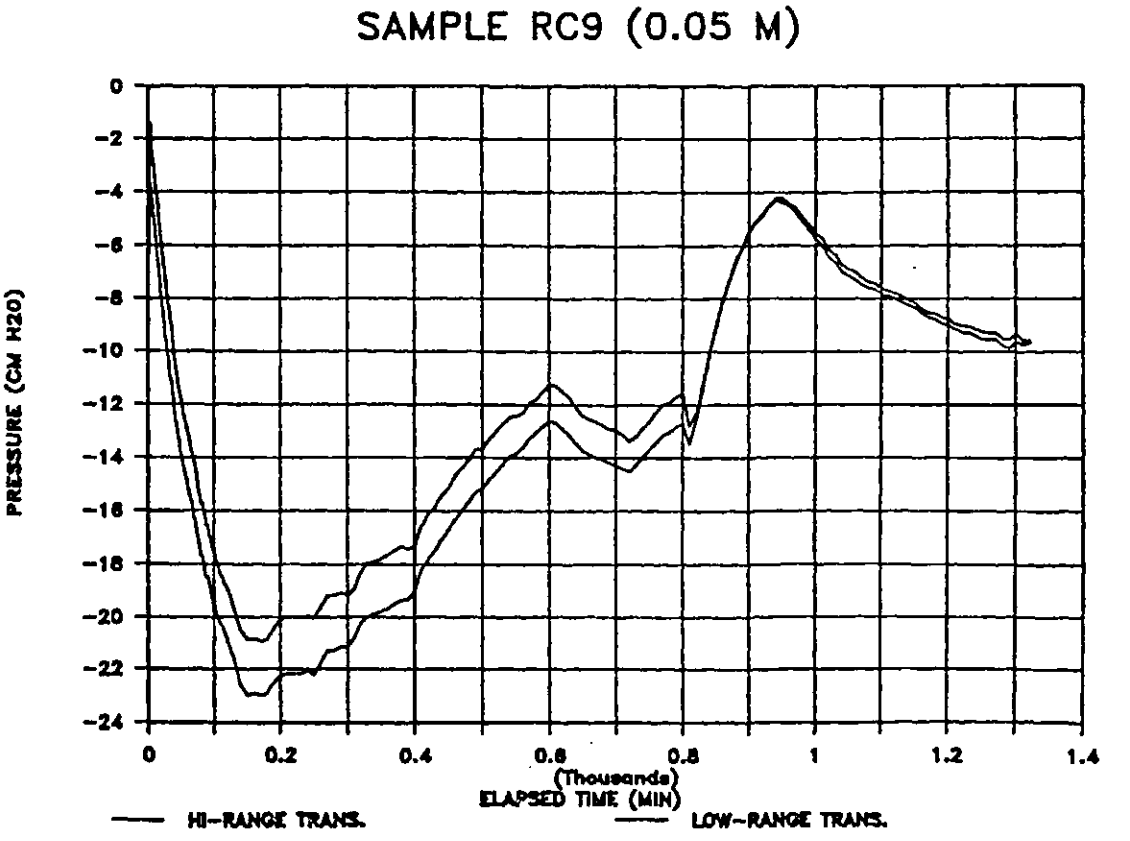

SAMPLE RC9 (0.1 M)

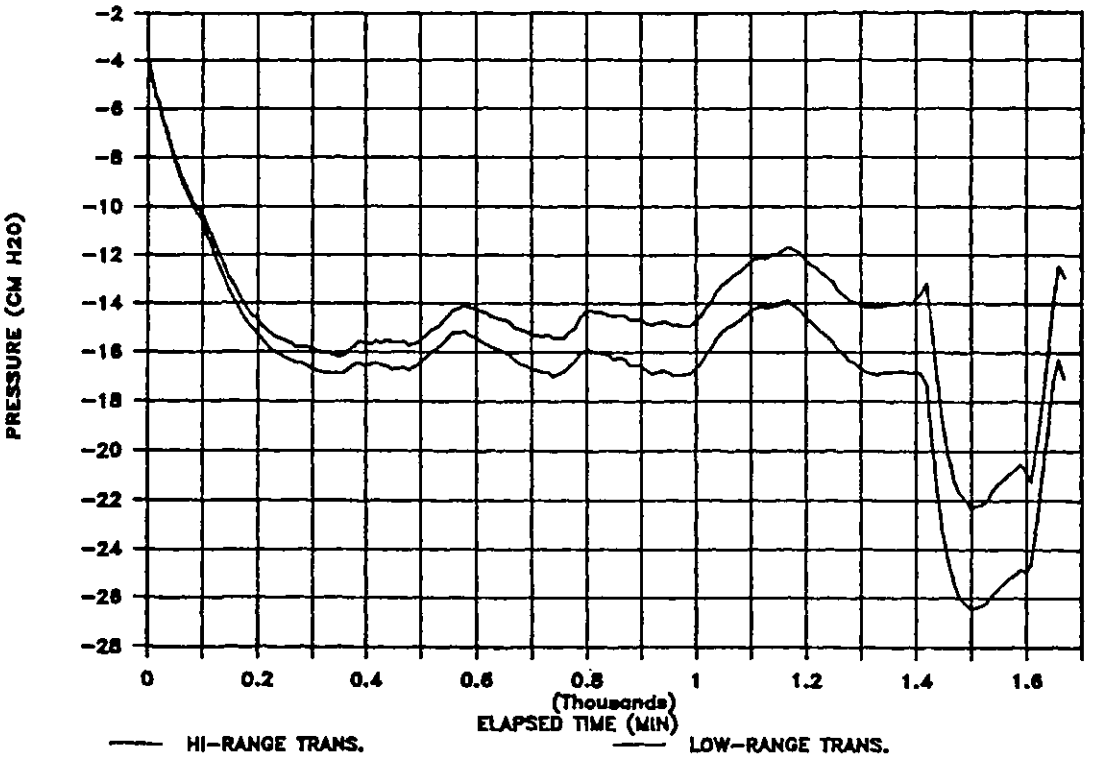

SAMPLE RC9 (0.2 M)

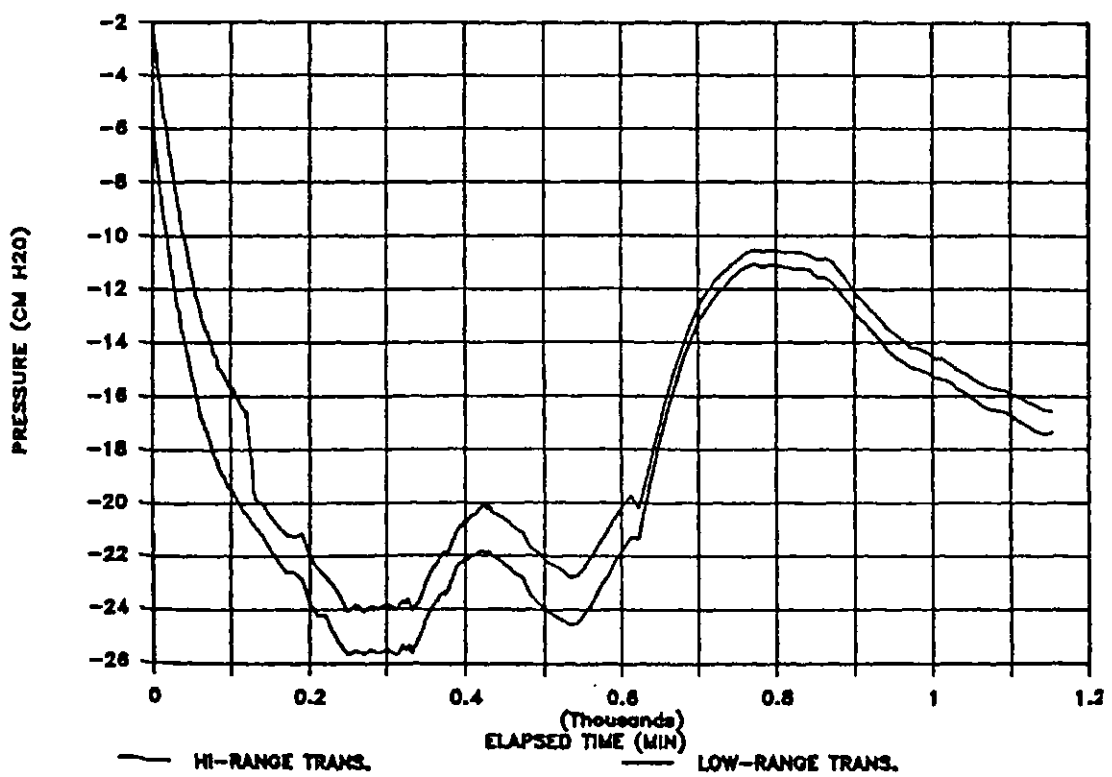

SAMPLE RC9 (0.5 M)

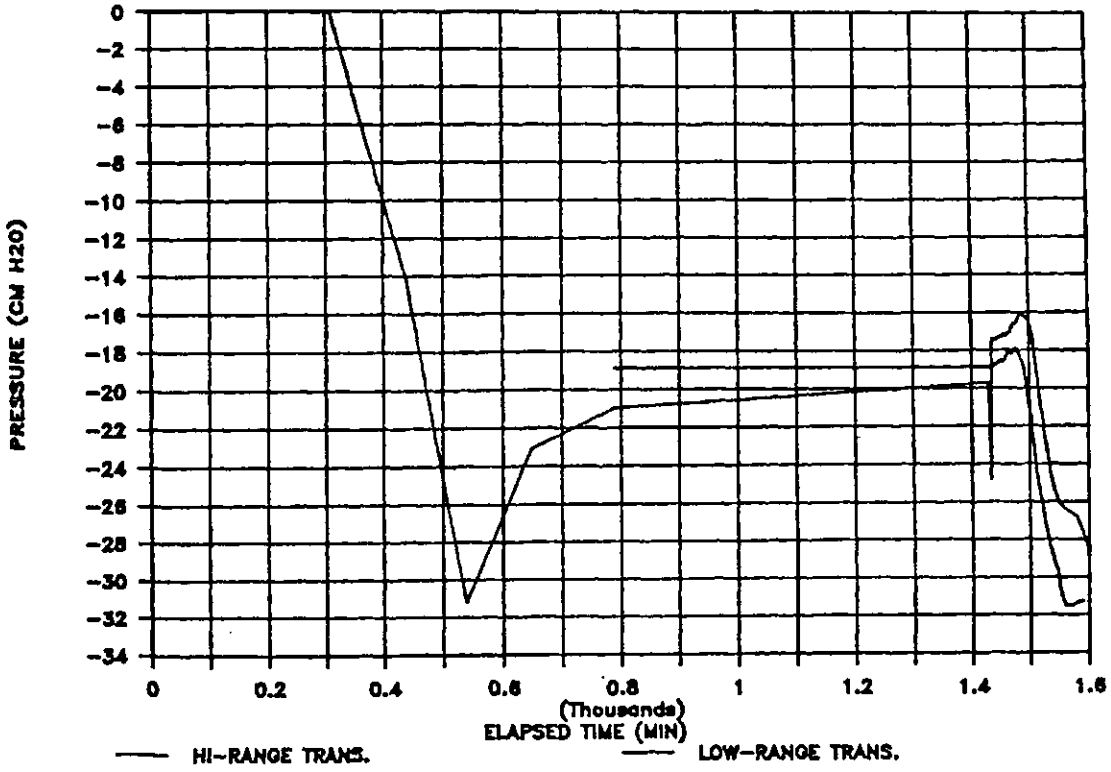

SAMPLE RC9 (1.0 M)

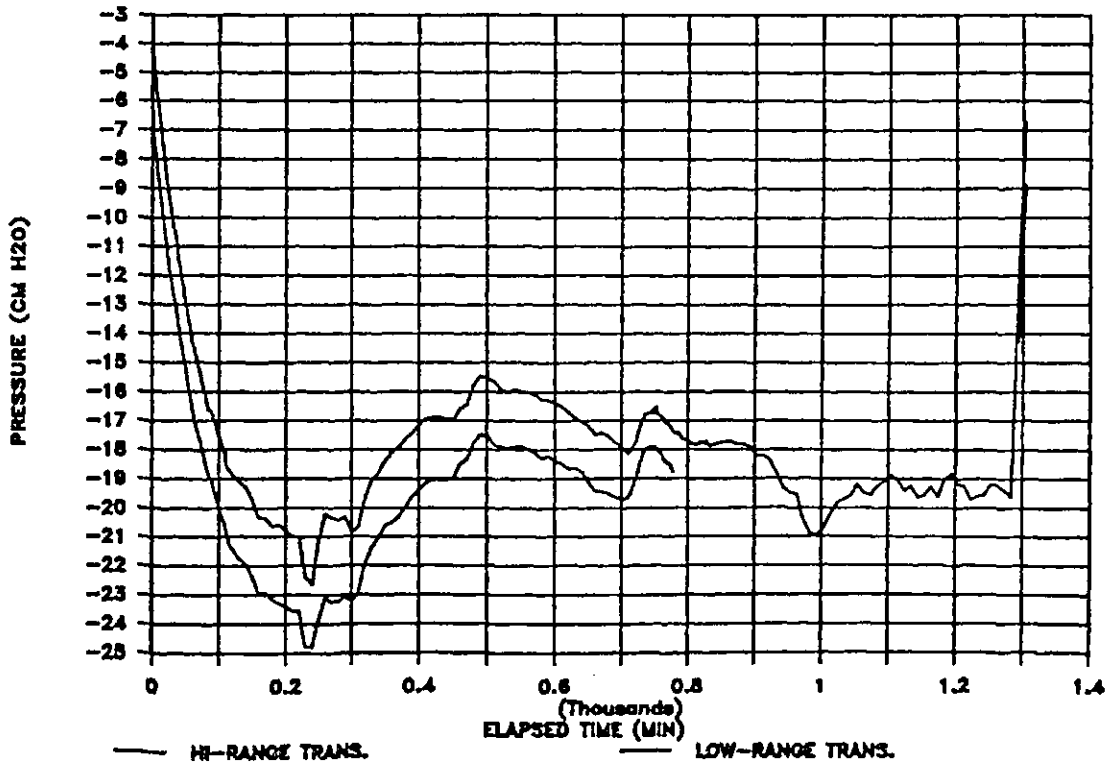

SAMPLE RC9 (2.0 M)

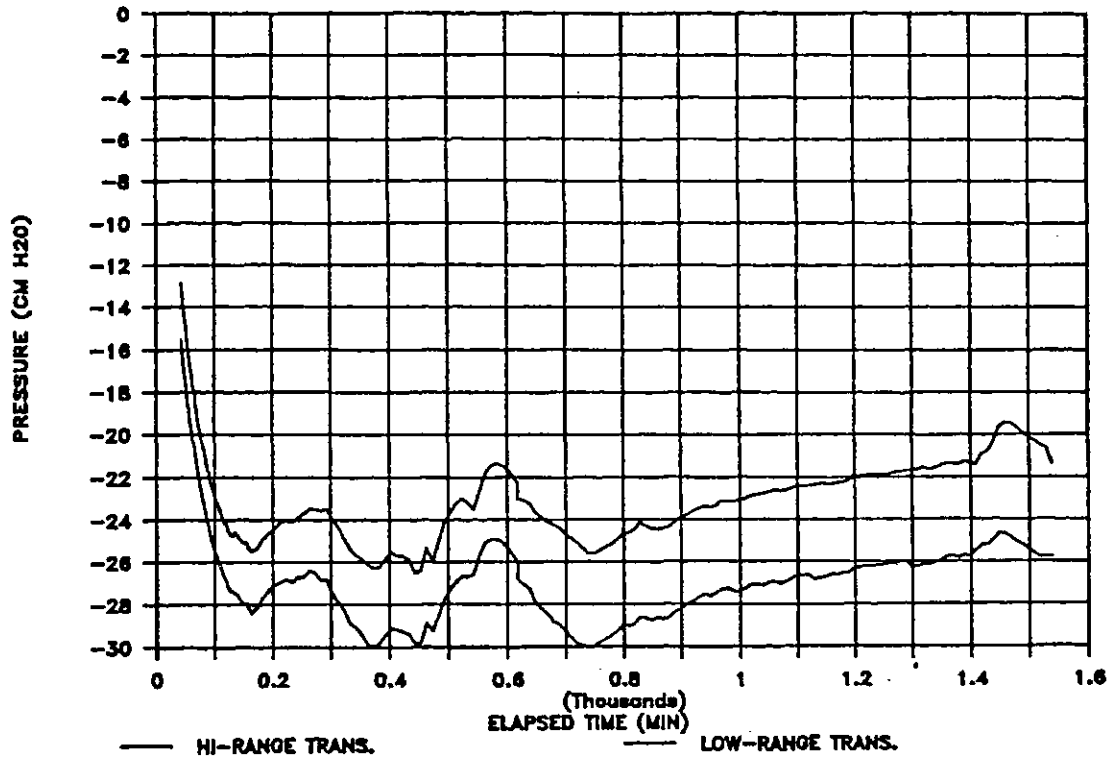

SAMPLE RC9 (3.0 M)

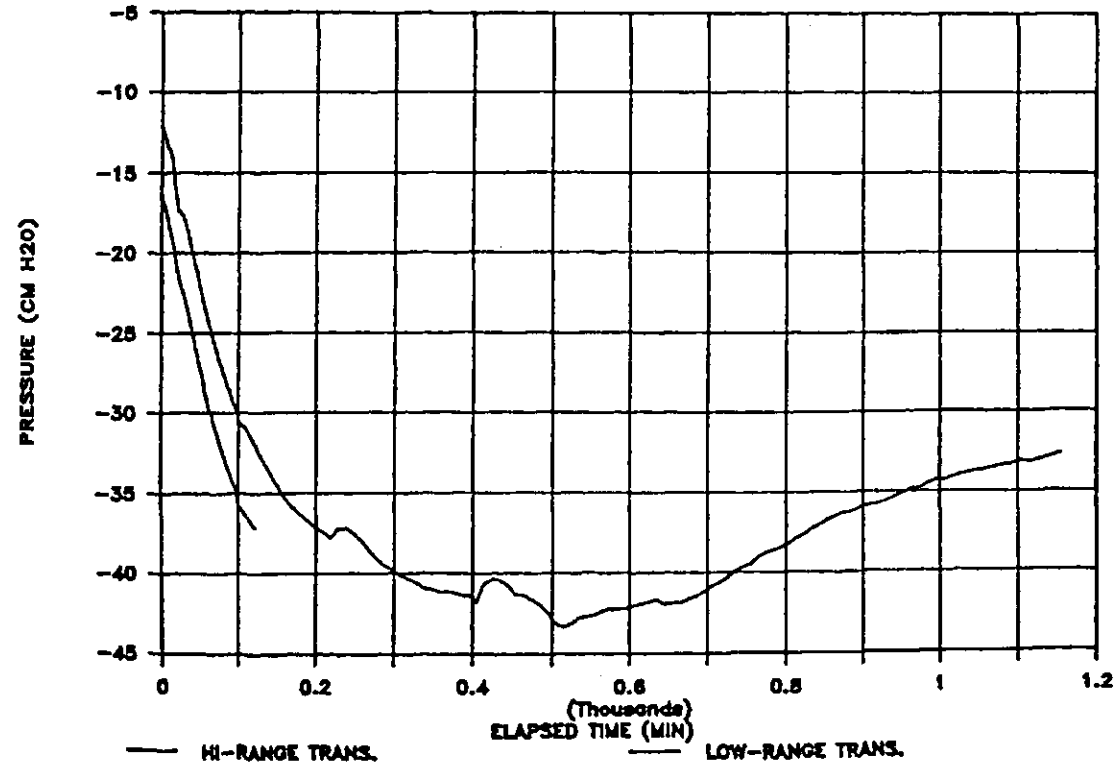

SAMPLE RC9 (4.0 M)

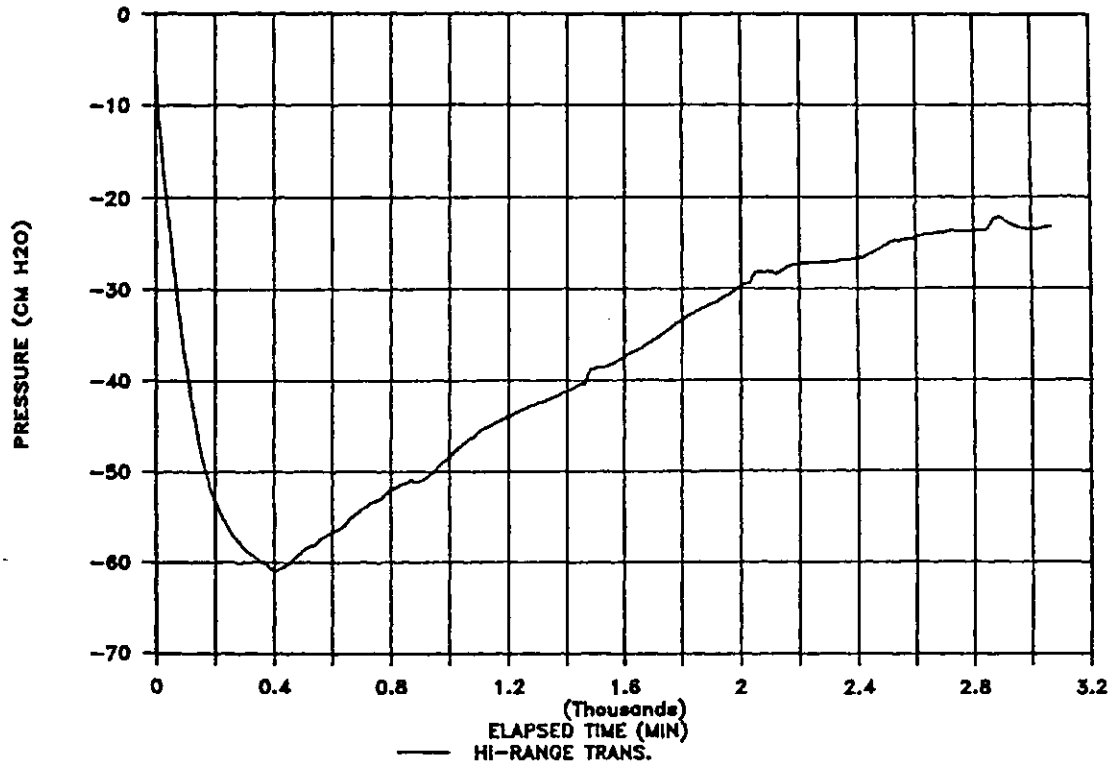

SAMPLE RC9 (DISTILLED WATER - FINAL)

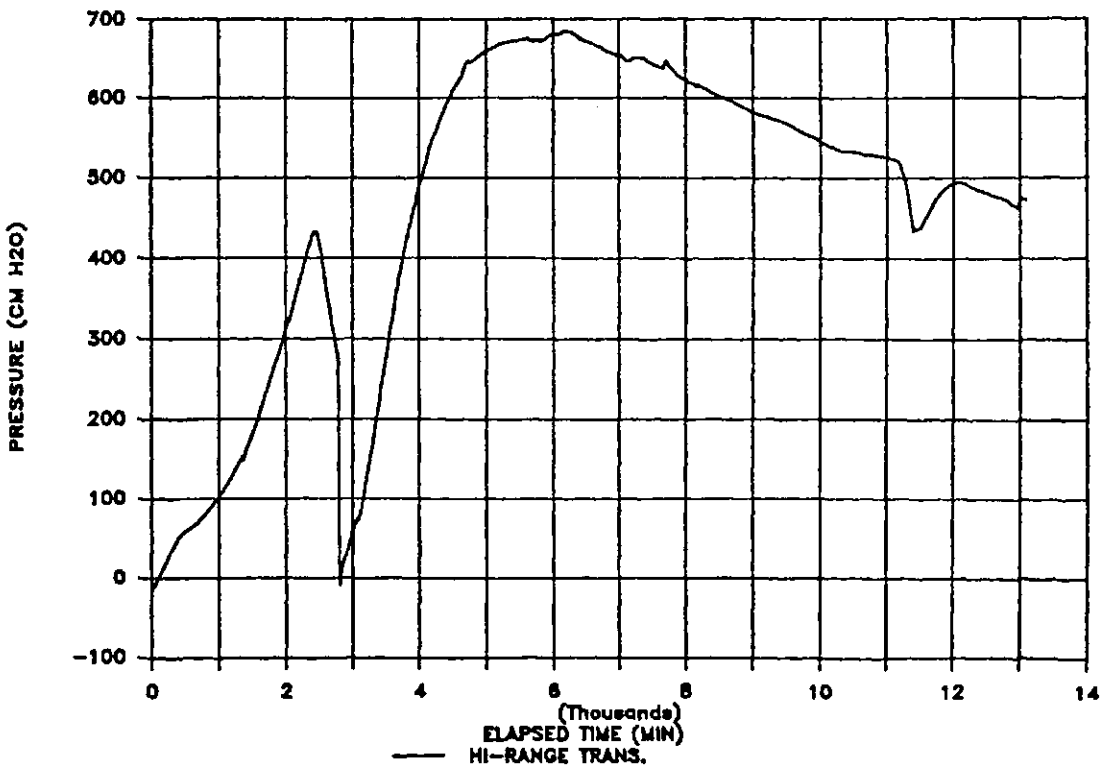

SAMPLE RC10 (4.0 M)

SAMPLE RC10 (4.0 M)

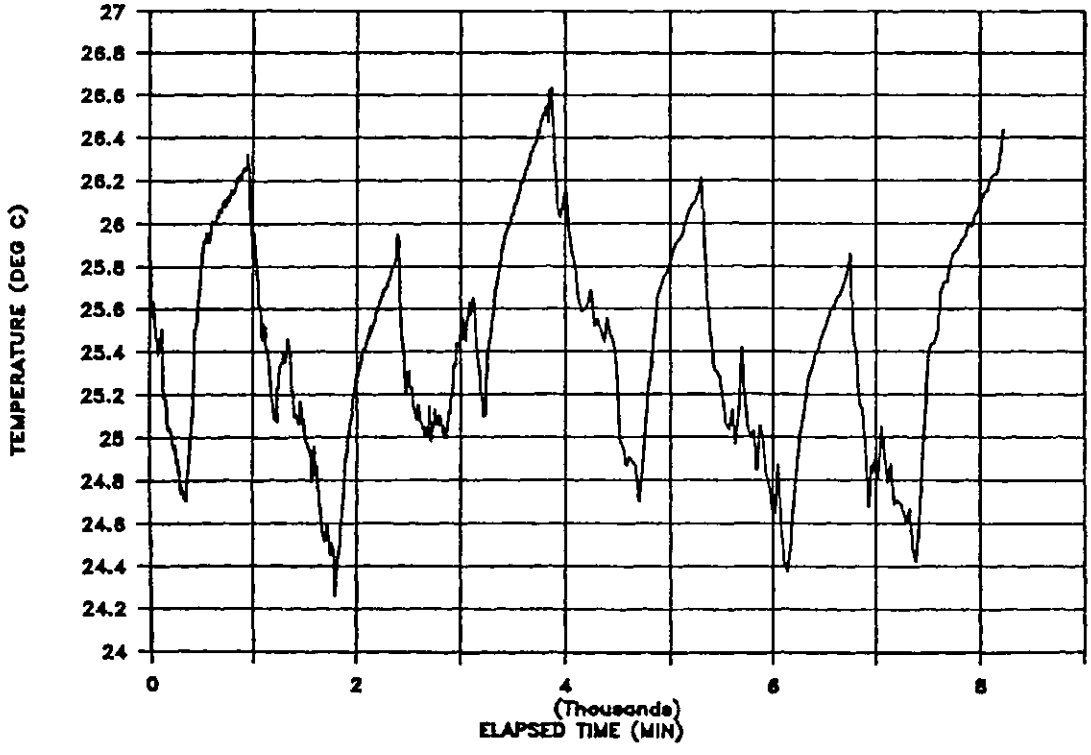

SAMPLE SB5 (DISTILLED WATER – INITIAL)

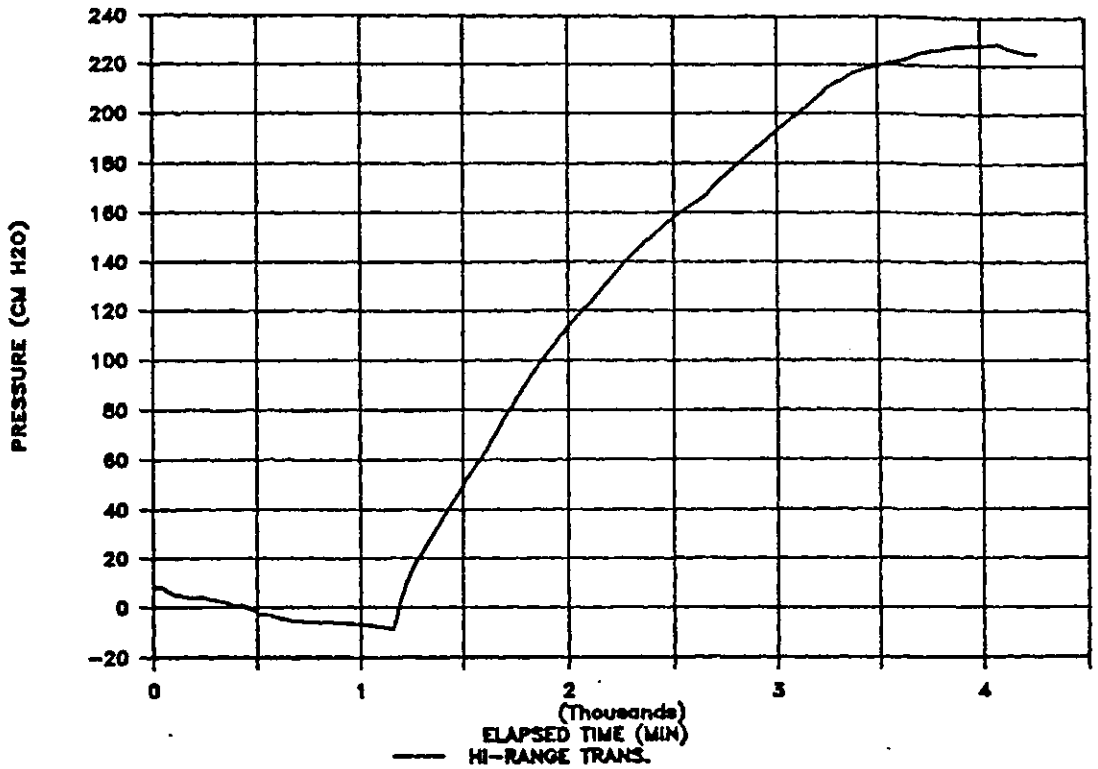

SAMPLE SB5 (.01 M)

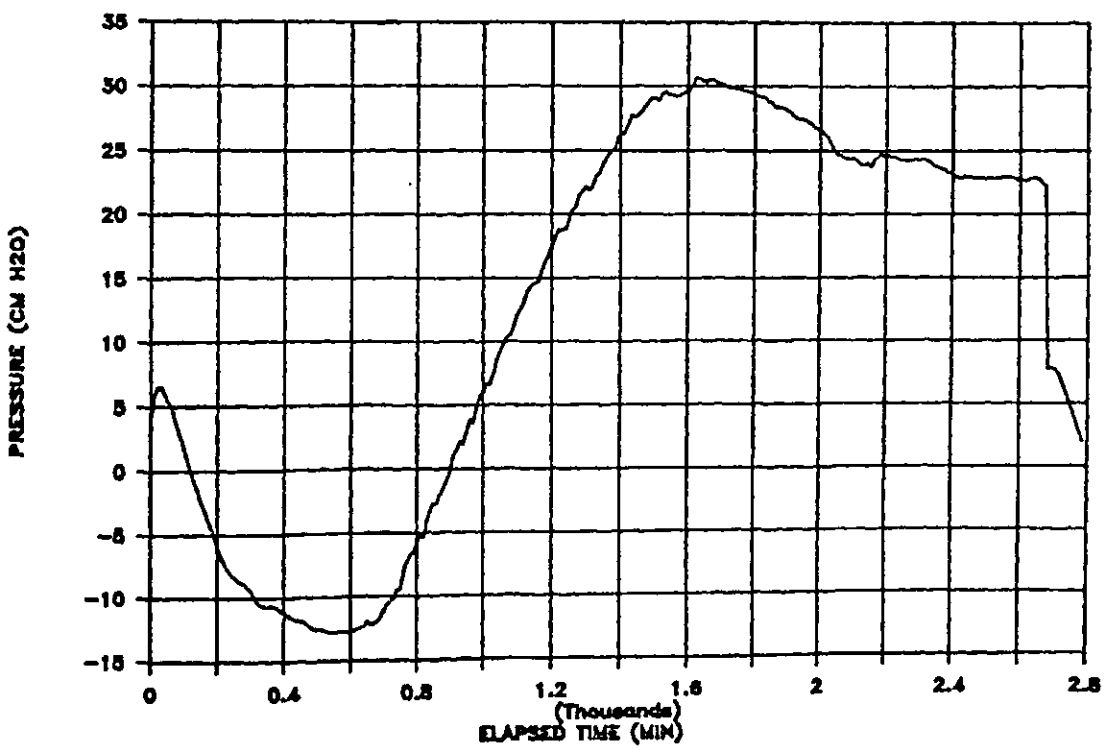

SAMPLE SB5 (0.05 M)

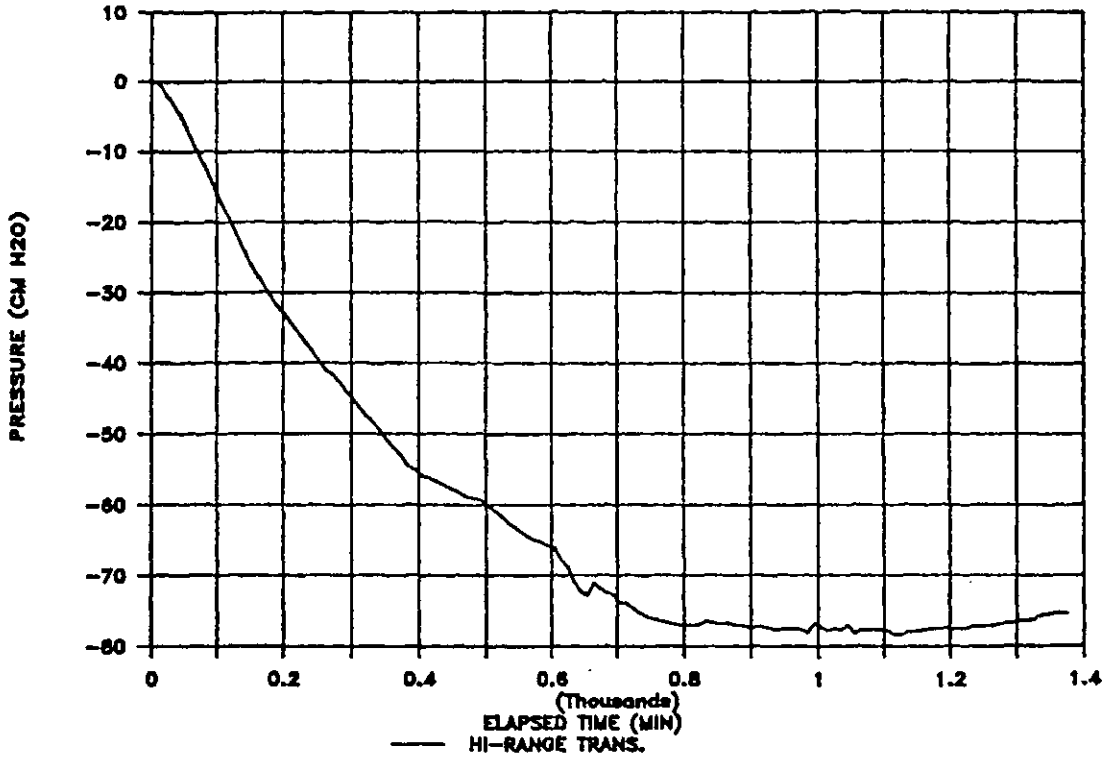

SAMPLE SB5 (0.1 M)

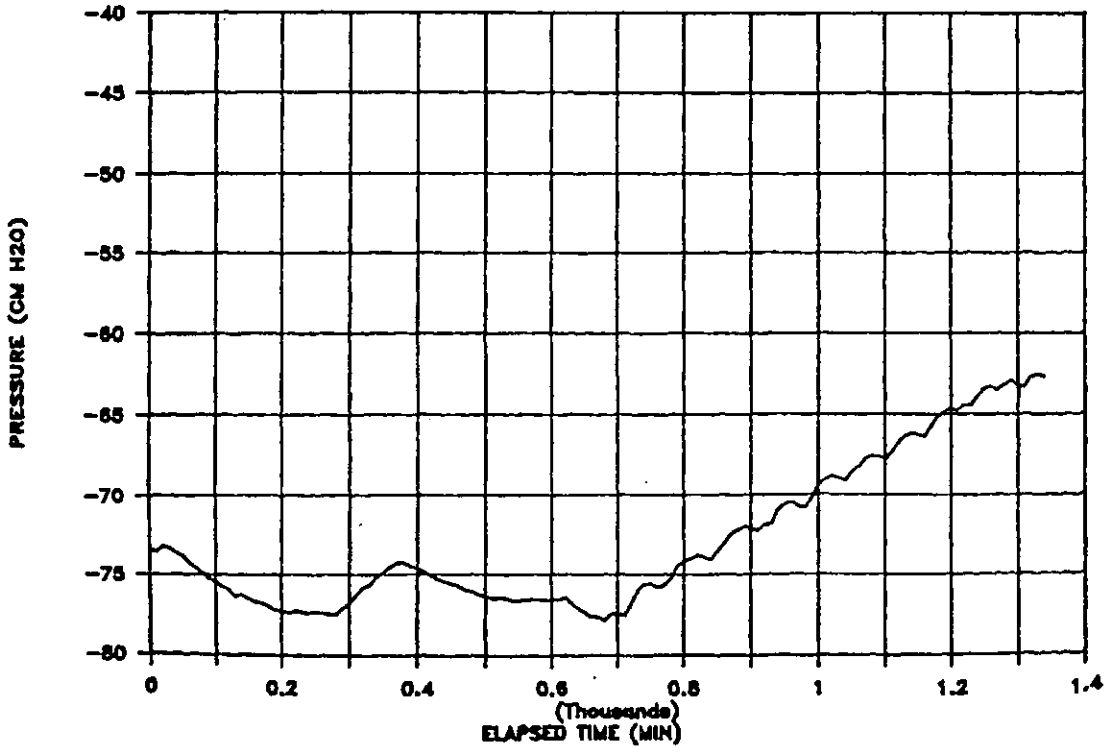

SAMPLE SB5 (0.5 M)

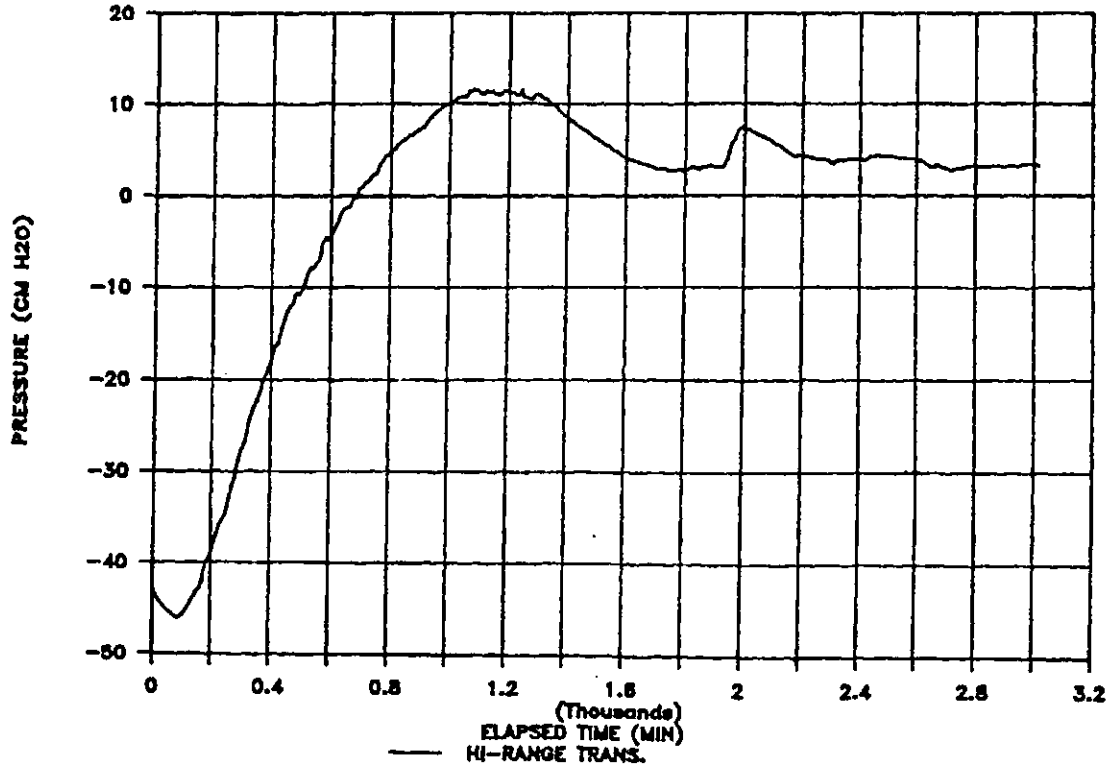

SAMPLE SB5 (1.0 M)

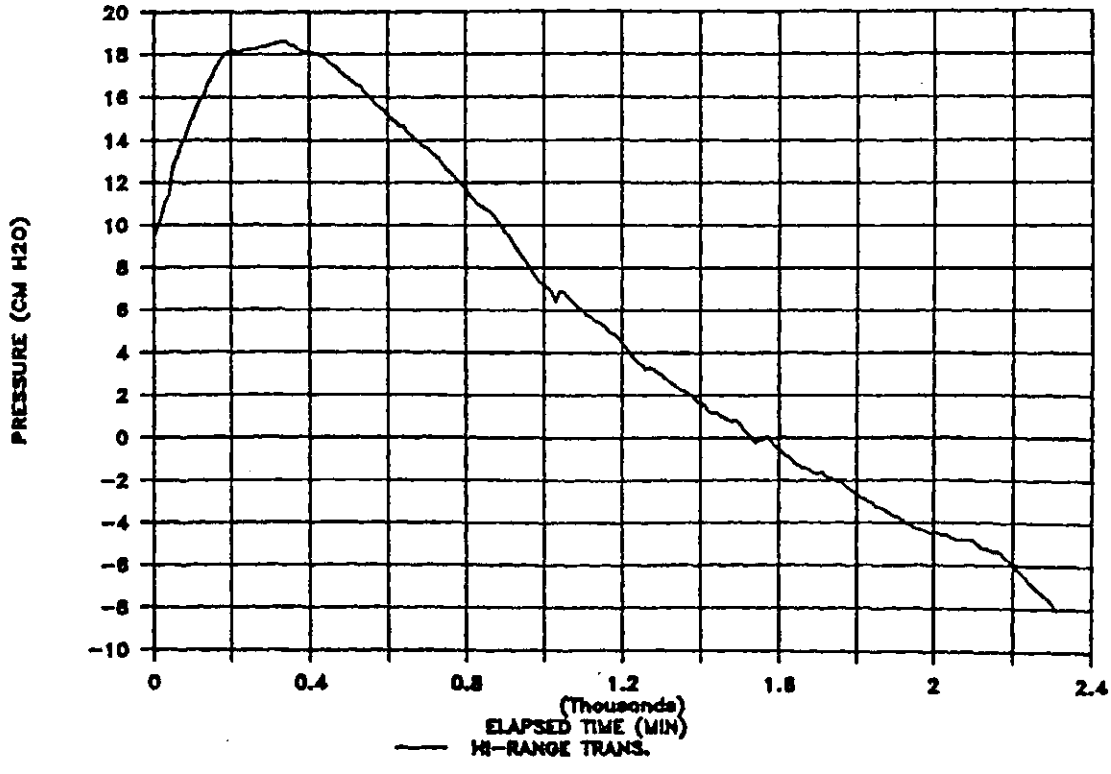

SAMPLE SB5 (2.0 M)

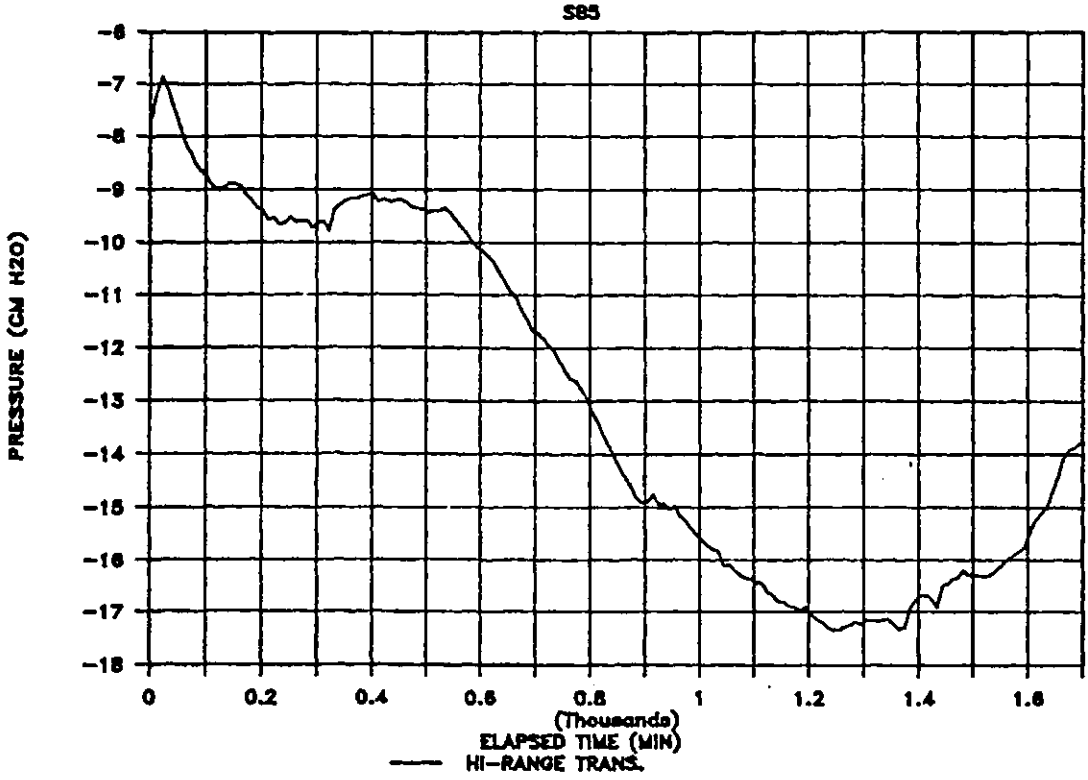

SAMPLE SB5 (3.0 M)

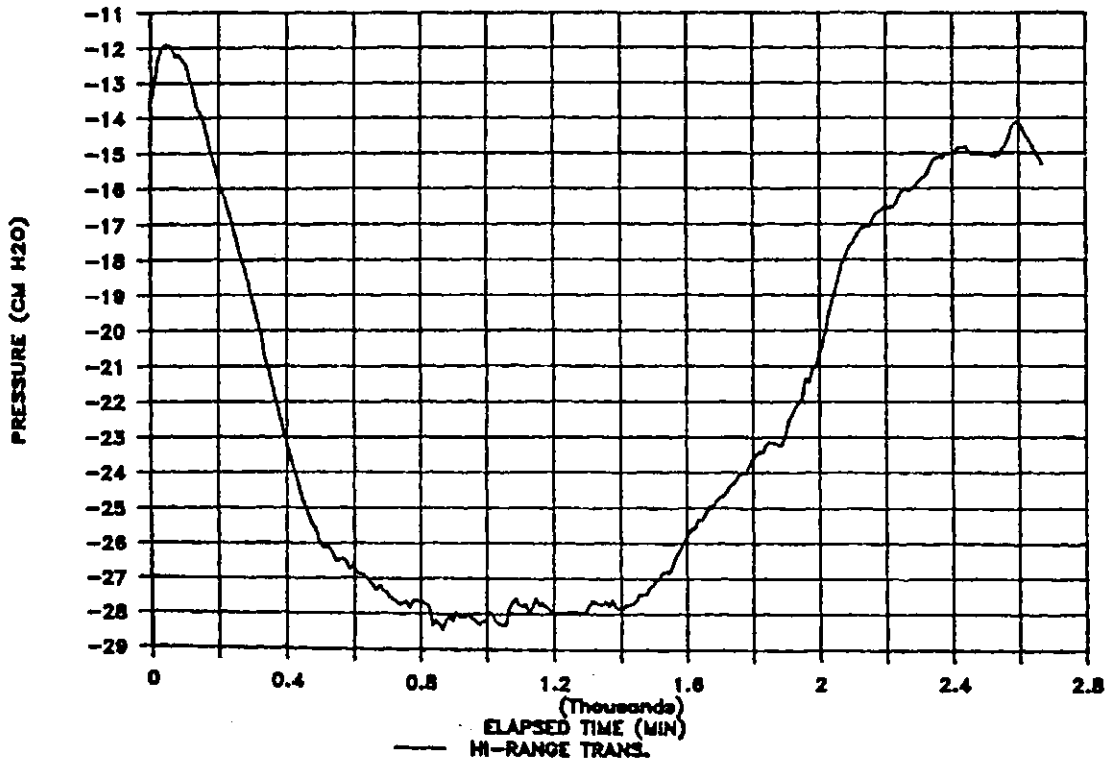

SAMPLE SB5 (4.0 M)

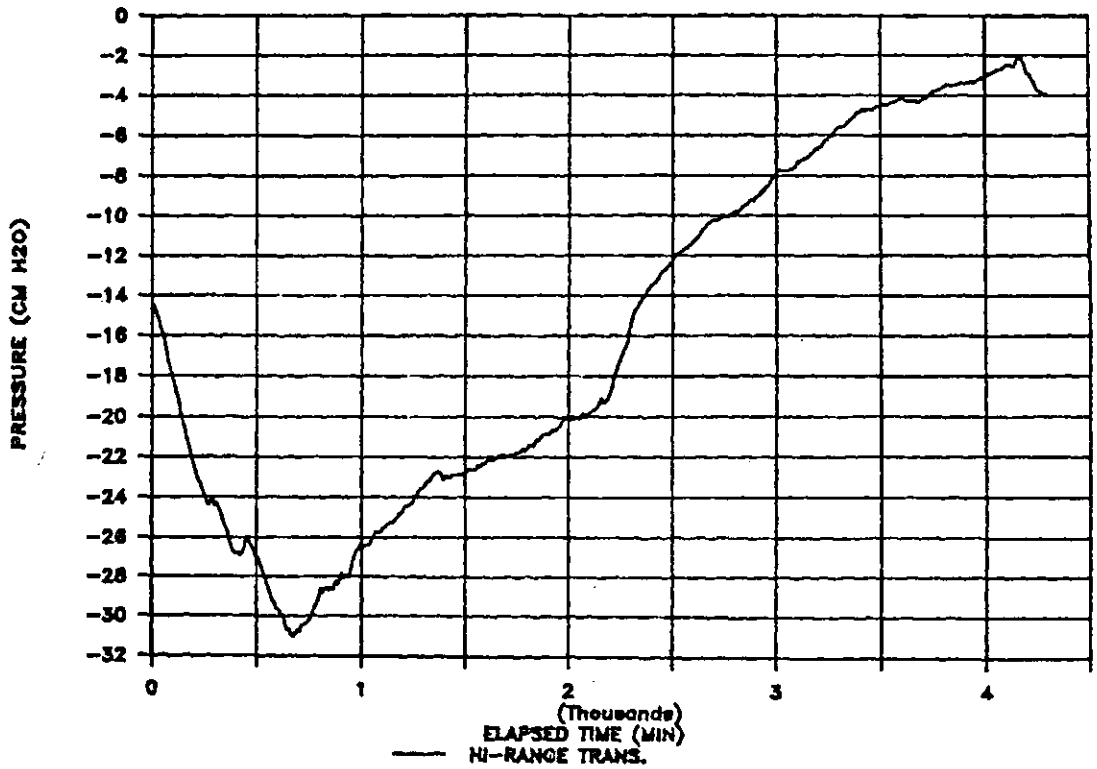

SAMPLE SB5 (DISTILLED WATER – FINAL)

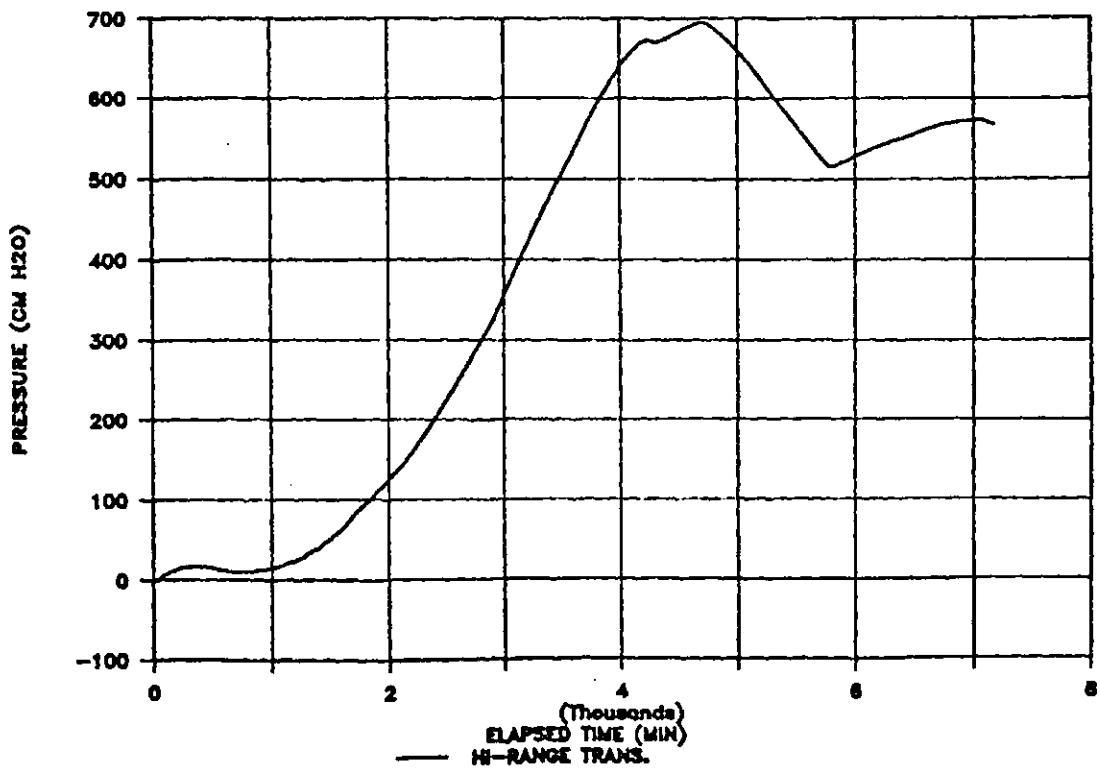

SAMPLE SB6 (4.0 M)

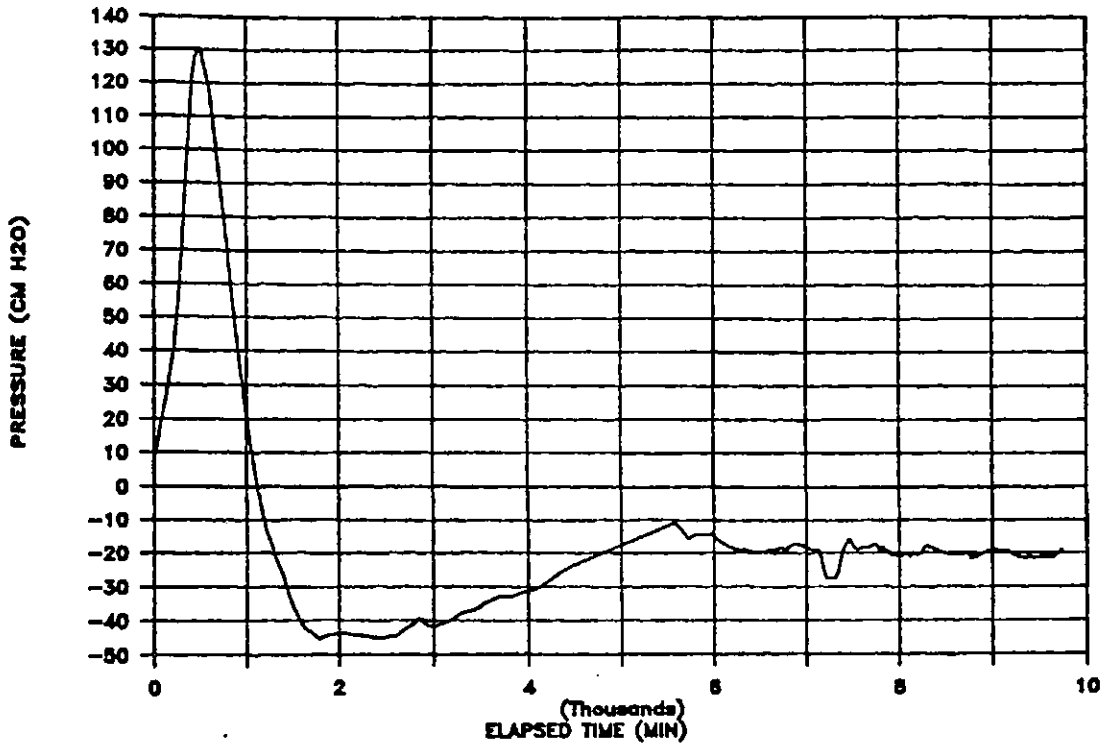

SAMPLE SB6 (4.0 M)

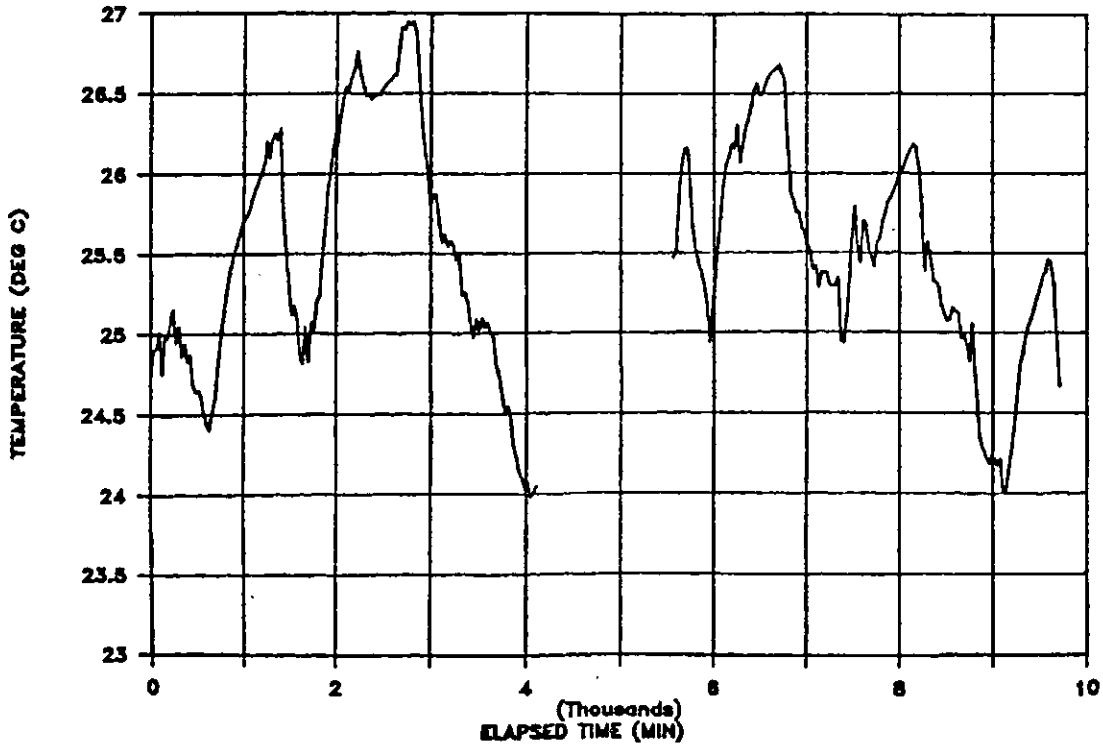

D.6 Diffusion Test Data

D.6.1 Table of Test Measurements

Sample RC7 - Test Data

ELAPSED TIME	BY CONDUCTIVITY SAMPLE VOL (ML)	CONC (GM/L)	SALT FLUX (GM)	CUMM. SALT (GM)	CONC. (GM/L)	SUM COLL VOL	BY TDS SALT FLUX (GM)	CUMM SALT (GM)
0.5M								
0								
75					0.6	7.45	0.00447	0.00447
85					0.93	3.35	0.0031155	0.0075855
265					1.7	3.3	0.00561	0.0131955
315					2.5	3.2	0.008	0.0211955
1107					8.1	3.2	0.02592	0.0471155
1179					9.13	3.35	0.0305855	0.077701
1237					7	3.2	0.0224	0.100101
1295					5.3	3.1	0.01643	0.116531
1485					4.8	6.9	0.03312	0.149651
1548					4.33	3.45	0.0149385	0.1645895
0.5M AFTER								
0						0	0	0
53					2	4.8	0.0096	0.0096
91					1.9	4.28	0.008132	0.017732
203					2.13	8.15	0.0173595	0.0350915
278					2.2	7.9	0.01738	0.0524715
350					1.9	7.75	0.014725	0.0671965
420					2.6	7.6	0.01976	0.0869565
1221					1.23	66	0.08118	0.1681365
1.0M	CONC =		0.0585	POROSITY =	SAMPLE H =		0.582	
0								
18		1.362	0.0153	0.0153				
35		0.852	0.0073	0.0226				
90		0.779	0.0218	0.0444				
129		0.644	0.018	0.0624				
176		0.693	0.028	0.0904				
270		0.699	0.0475	0.1379				
373		0.922	0.0572	0.1951	0.5	62	0.031	0.031
573		0.425	0.0976	0.2927	0.37	218	0.08066	0.11166
1465		2000+			1.75	186	0.3255	0.43716
1857		1.427	0.1998		1.15	140	0.161	0.59816
2870		2000+			1.37	301	0.41237	1.01053
2940		1.299	0.0389				0	1.01053
2994					0.52	62	0.03224	1.04277
2.0M	CONC =		0.117	POROSITY =	SAMPLE H =	0.58		
0								
25		0.756	0.015116	0.015116				
76		1.015	0.03248	0.047596	0.8	62	0.0496	0.0496
116		1.224	0.0204	0.067996	1.01	18	0.01818	0.06778
199		1.438	0.0546	0.122596				0.06778
235		0.808	0.0307	0.153296				0.06778
267		0.615	0.02769	0.180986	0.42	121	0.05082	0.1186
303		0.67	0.03082	0.211806				0.1186
338		0.655	0.02883	0.240636				0.1186

(RC7 Diffusion Test Data cont.)

372			1.1574	0.02546	0.266096		0.89	112	0.09968	0.21828	
402			0.262	0.0345	0.300596					0.21828	
430			0.221	0.02409	0.324686					0.21828	
737			0.378	0.2077	0.532386		0.26	790.8	0.205608	0.423888	
1377			1.367	0.5523	1.084686		1.02	404	0.41208	0.835968	
4.0M		CONC =		0.234	POROSITY =		SAMPLE H =	0.578			
0			0								
35		31	1.045	0.032395	0.032395						
78		48.7	0.6675	0.03250725	0.06490225		0.53	79.7	0.042241	0.042241	
128		52	0.977	0.050804	0.11570625				0	0.042241	
198		64.5	1.308	0.084366	0.20007225				0	0.042241	
241		61	0.9359	0.0570899	0.25716215		0.86	177.5	0.15265	0.194891	
276		90	0.67	0.0603	0.31746215				0	0.194891	
315		90	0.707	0.06363	0.38109215				0	0.194891	
346		73	0.7337	0.0535601	0.43465225		0.53	253	0.13409	0.328981	
386		120	0.578	0.06936	0.50401225				0	0.328981	
421		110	0.552	0.06072	0.56473225				0	0.328981	
451		78	0.663	0.051714	0.61644625		0.44	308	0.13552	0.464501	
753		981	0.5445	0.5341545	1.15060075		0.31	981	0.30411	0.768611	
1408		1088	1.0395	1.130976	2.28157675		0.81	1088	0.88128	1.649891	
1449		92	0.6967	0.0640964	2.34567315				0	1.649891	

Sample SB3 - Test Data

	BY CONDUCTIVITY					BY TDS			
ELAPSED TIME	SAMPLE VOL (ML)	CONC (GM/L)	SALT FLUX (GM)	CUMM. SALT (GM)	CONC. (GM/L)	CUMM SAMP. VOLUME	SALT FLUX (GM)	CUMM SALT (GM)	
0.5M	CONC =	0.02925							
0					0				
48					2.1	3.58	0.007518	0.007518	
108					0.97	3.5	0.003395	0.010913	
165					0.77	3.5	0.002695	0.013608	
296					1.37	3.5	0.004795	0.018403	
348					1.57	3.5	0.005495	0.023898	
418					0.76	3.6	0.002736	0.026634	
776					0.4	3.8	0.00152	0.028154	
1343					0.73	156	0.11388	0.142034	
1480					0.43	3.3	0.001419	0.143453	
1533					1.6	3.6	0.00576	0.149213	
1568					0.43	4.27	0.0018361	0.1510491	
1673					1.5	3.9	0.00585	0.1568991	
1745					1.4	7.8	0.01092	0.1678191	
1821					1.63	7.5	0.012225	0.1800441	
1901					1.46	7.38	0.0107748	0.1908189	
1.0 M	CONC =	0.0585	POROSITY =		SAMPLE H =	0.54			
0									
15		0.547	0.0153	0.0153					
34		0.465	0.0039	0.0192					
94	42	0.39	0.01638	0.03558					
135	36	0.33	0.01188	0.04746					
187	40	0.351	0.01404	0.0615					
276	69	0.46	0.03174	0.09324					
379	68	0.564	0.038352	0.131592	0.167	255	0.042585	0.042585	
577	108	0.682	0.073656	0.205248	0.5	108	0.054	0.096585	
1469	204	2000+	ERR	ERR	1.27	204	0.25908	0.355665	
1862	110	1.389	0.15279	0.00021222	1.12	110	0.1232	0.478865	
2873	332	1.305	0.43326	0.43347222	1.03	332	0.34196	0.820825	
2945	38	0.934	0.035492	0.46896422					
3000					0.45	68.5	0.030825	0.85165	
2.0 M	CONC =	0.117	POROSITY =		SAMPLE H =	0.54			
0		0	0	0					
25	34	0.41	0.01394	0.01394					
74	57	0.36	0.02052	0.03446				0	
118	22	0.719	0.015818	0.050278	0.56	103	0.05768	0.05768	
202	28	1.399	0.039172	0.08945			0	0.05768	
238	28	0.967	0.027076	0.116526			0	0.05768	
270	59	0.477	0.028143	0.144669	0.33	115	0.03795	0.09563	
306	70	0.42	0.0294	0.174069			0	0.09563	
341	64	0.42	0.02688	0.200949			0	0.09563	
374	56	0.467	0.026152	0.227101	0.27	190	0.0513	0.14693	
405	78.2	0.323	0.0252586	0.2523596			0	0.14693	
433	78	0.295	0.02301	0.2753696			0	0.14693	
736	550	0.419	0.23045	0.5058196	0.21	706.2	0.148302	0.295232	
1379	462	1.183	0.546546	1.0523656	0.92	462	0.42504	0.720272	

(SB3 Diffusion Test Data cont.)

4.0 M		CONC =		0.234	POROSITY =	SAMPLE H =		0.53		
0			0		0				0	0
28		32	0.93	0.02976	0.02976				0	0
62		32	0.9065	0.029008	0.058768				0	0
95		37	0.824	0.030488	0.089256		0.64	101	0.06464	0.06464
138		48	0.912	0.043776	0.133032				0	0.06464
211		72	1.116	0.080352	0.213384				0	0.06464
252		56	0.969	0.054264	0.267648		0.72	176	0.12672	0.19136
289		80	0.97	0.0776	0.345248				0	0.19136
329		92	0.635	0.05842	0.403668				0	0.19136
358		60	0.7099	0.042594	0.446262		0.52	232	0.12064	0.312
400		146	0.461	0.067306	0.513568				0	0.312
435		129	0.437	0.056373	0.569941				0	0.312
466		96	0.509	0.048864	0.618805		0.32	371	0.11872	0.43072
768		1055	0.478	0.50429	1.123095		0.33	1055	0.34815	0.77887
1393							1.01	126	0.12726	0.90613
1440		96	+2000				3.41	96	0.32736	1.10623
1465		95	0.785	0.074575	0.074575				0	1.10623
1530		260	0.621	0.16146	0.236035				0	1.10623
1571		155	0.555	0.086025	0.32206		0.4	510	0.204	1.31023
1607		127	0.536	0.068072	0.390132				0	1.31023
1648		136	0.543	0.073848	0.46398				0	1.31023
1701		166.5	0.562	0.093573	0.557553		0.36	429.5	0.15462	1.46485
1795		123.5	1.1151	0.13771485	0.69526785				0	1.46485
1875		97.5		0	0.69526785				0	1.46485

D.6.2 Cummulative Mass Flux versus Time

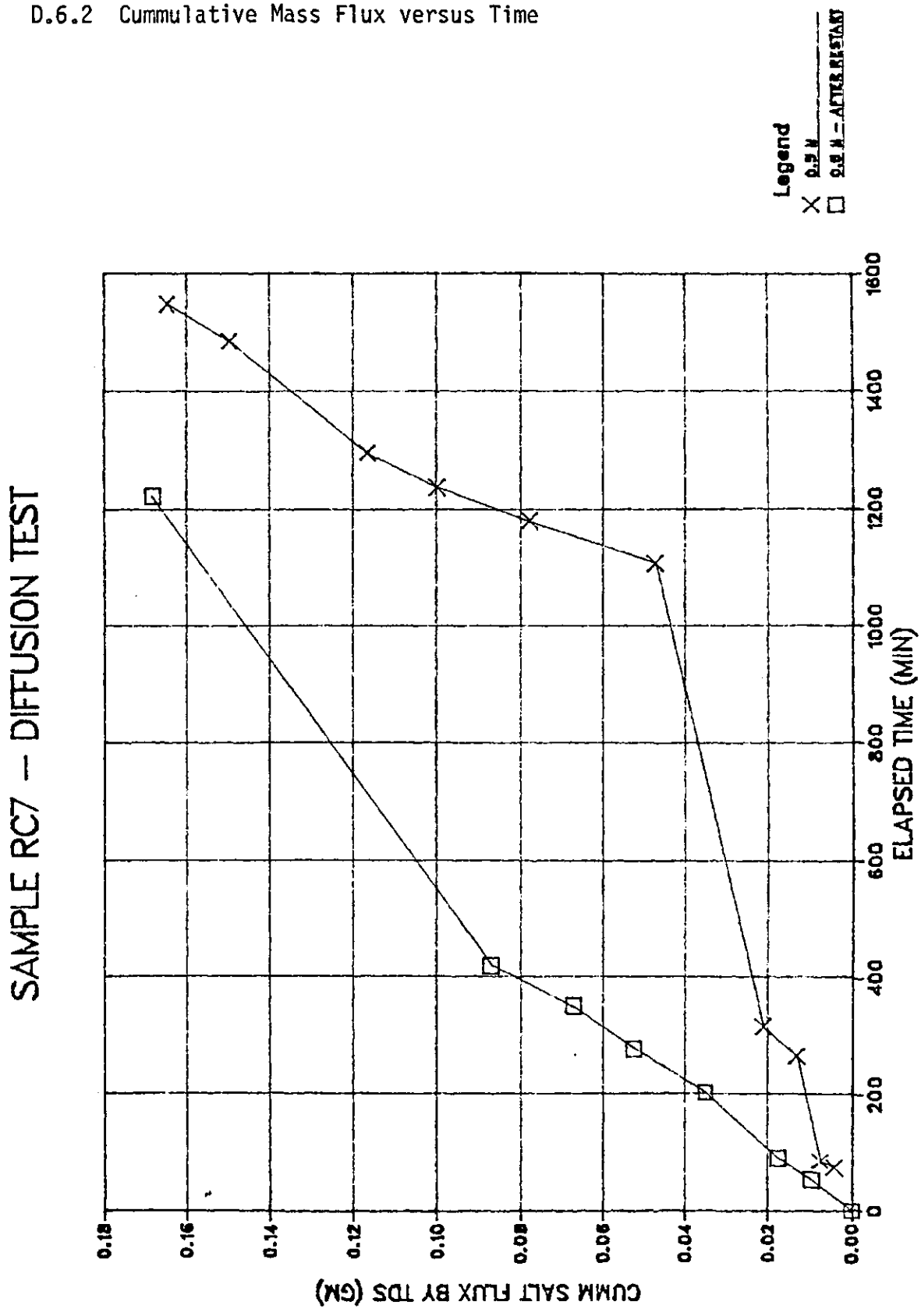

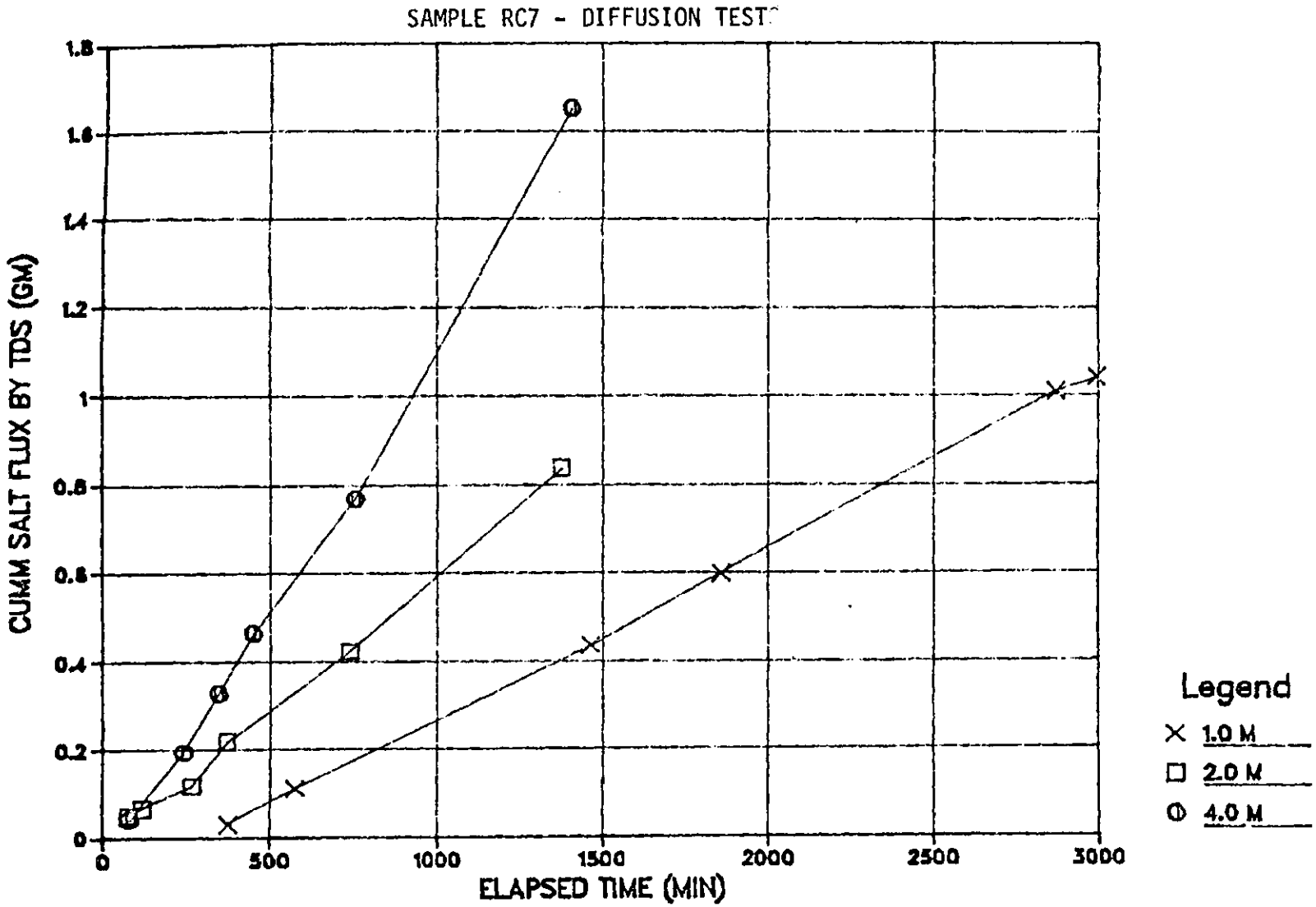
SAMPLE RC7 - DIFFUSION TEST
CUMM SALT FLUX BY TDS (GM)
1.8
1.6
1.4
1.2
1
0.8
0.6
0.4
0.2
0
0
500
1000
1500
2000
2500
3000
ELAPSED TIME (MIN)
Legend
1.0 M
2.0 M
4.0 M

D100

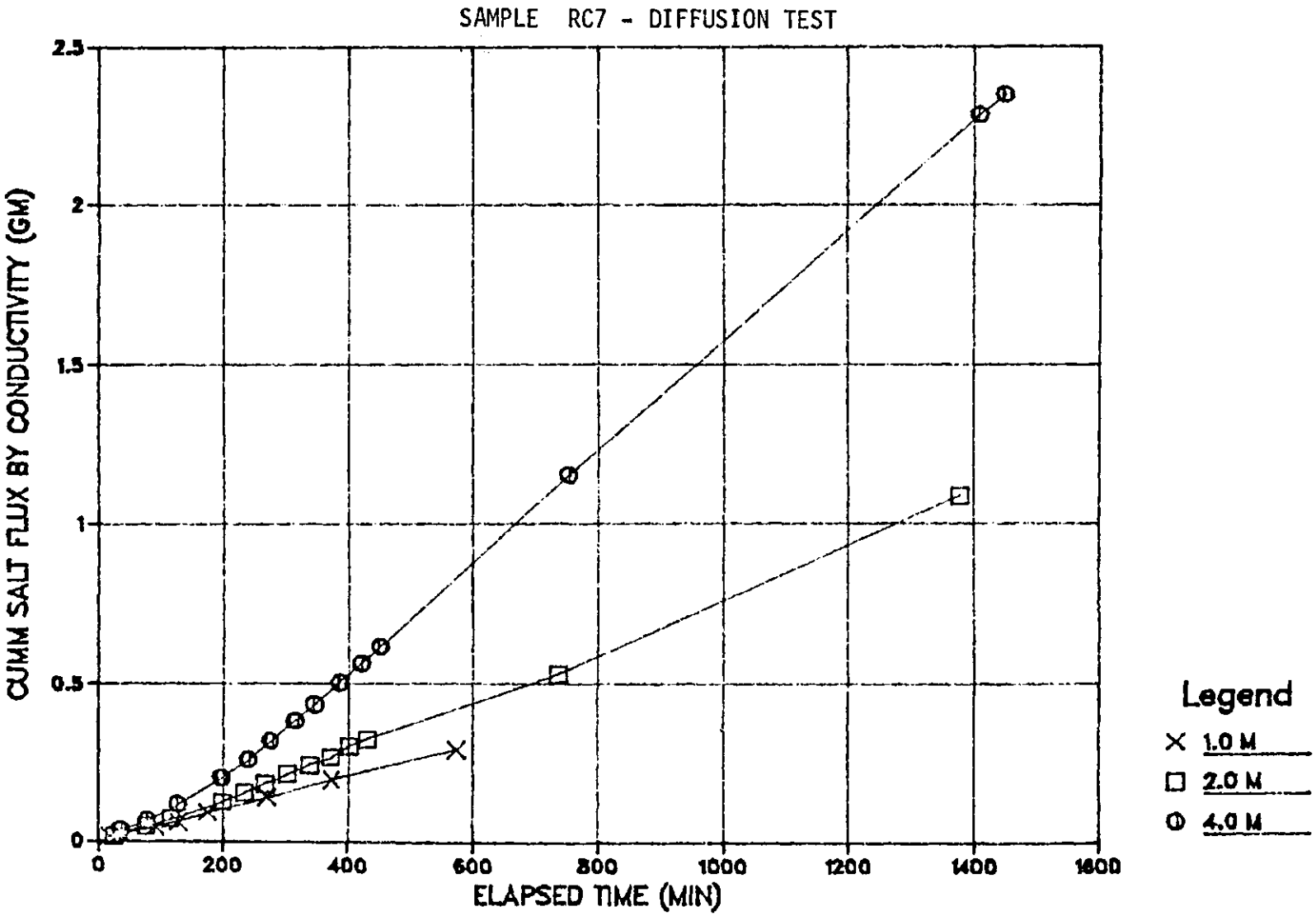
SAMPLE RC7 - DIFFUSION TEST
CUMM SALT FLUX BY CONDUCTIVITY (GM)
ELAPSED TIME (MIN)
0
0.5
1
1.5
2
2.5
0
200
400
600
800
1000
1200
1400
1600
Legend
1.0 M
2.0 M
4.0 M

SAMPLE SB3 – DIFFUSION TEST

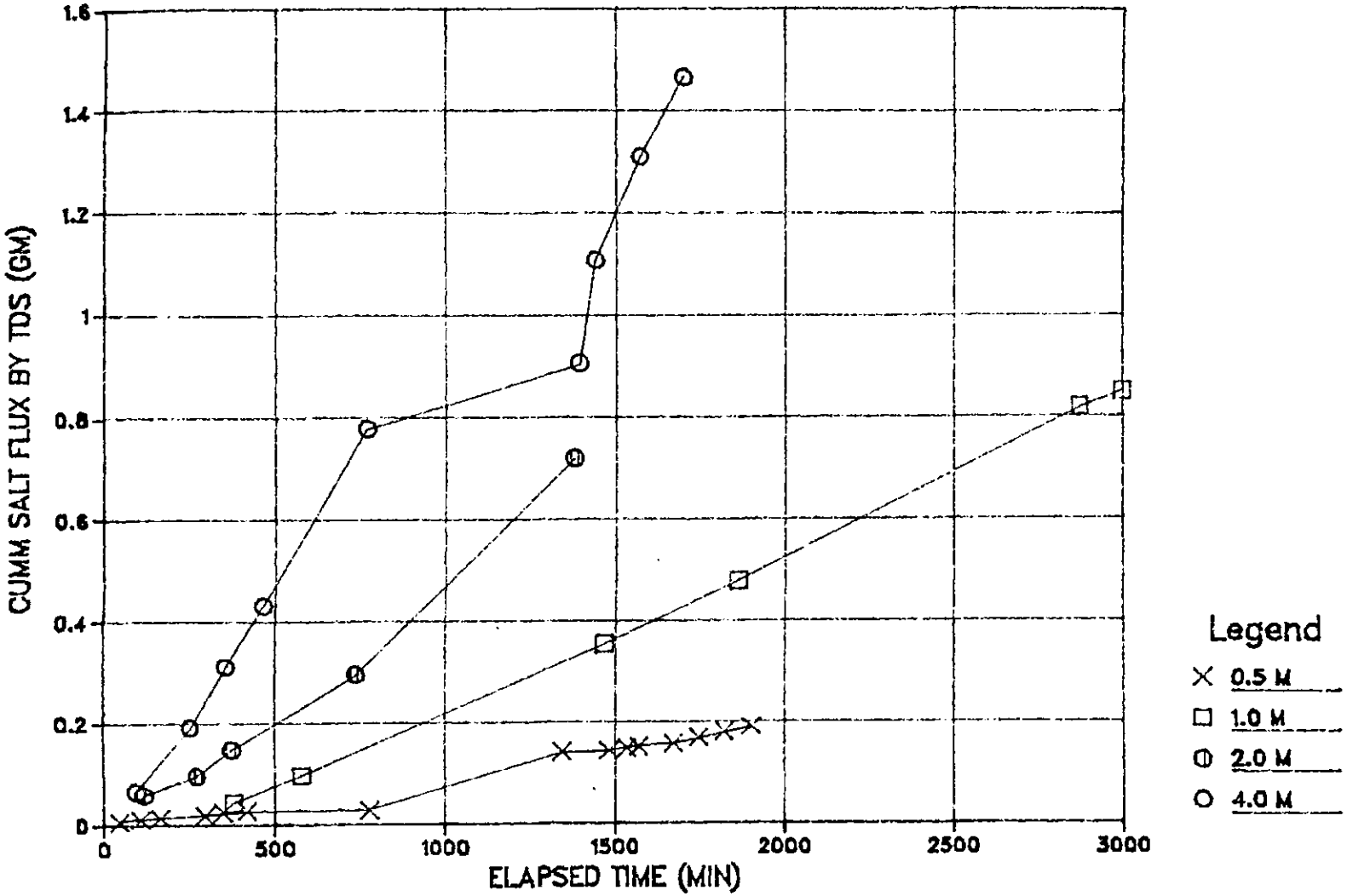

SAMPLE SB3 – DIFFUSION TEST